frontiers | Research Topics

RNA at a breaking point? cytoplasmic cleavage and other post-transcriptional RNA processing in neurodevelopment and disease

Edited by
Catia Andreassi, Monika Piwecka and Raphaëlle Luisier

Published in
Frontiers in Molecular Neuroscience
Frontiers in Cellular Neuroscience

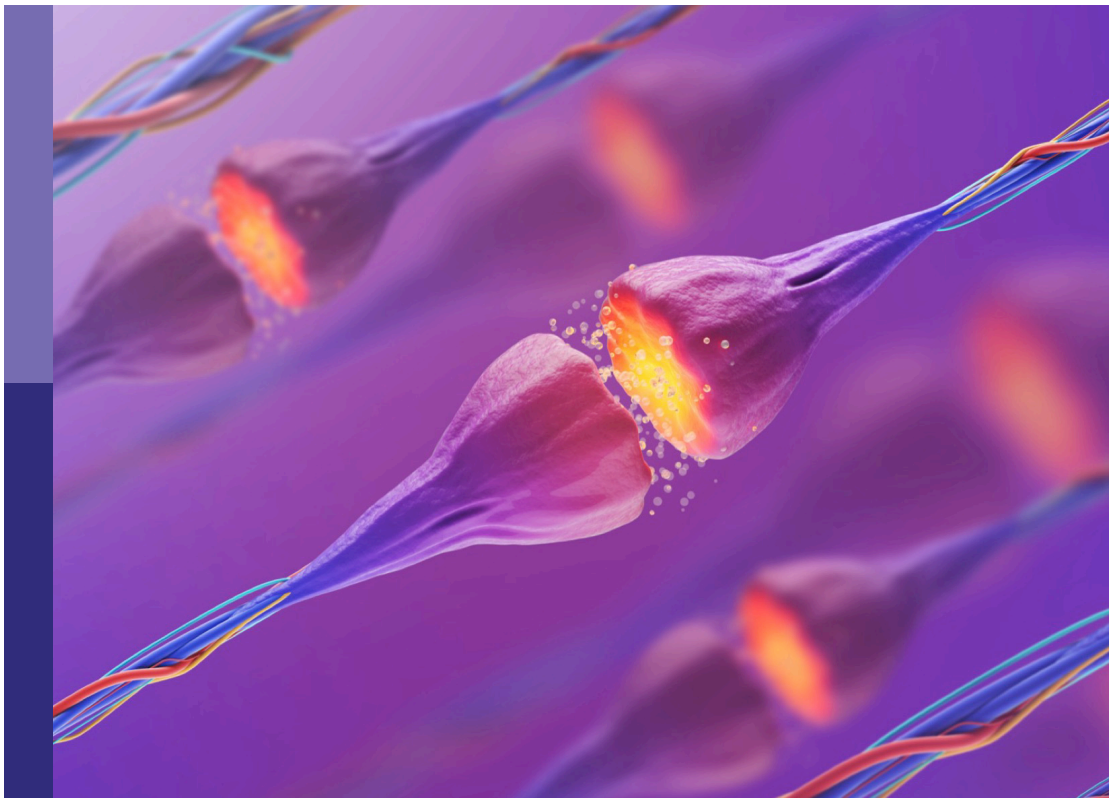

ISSN 1664-8714
ISBN 978-2-8325-2715-3
DOI 10.3389/978-2-8325-2715-3

About Frontiers

Frontiers is more than just an open access publisher of scholarly articles: it is a pioneering approach to the world of academia, radically improving the way scholarly research is managed. The grand vision of Frontiers is a world where all people have an equal opportunity to seek, share and generate knowledge. Frontiers provides immediate and permanent online open access to all its publications, but this alone is not enough to realize our grand goals.

Frontiers journal series

The Frontiers journal series is a multi-tier and interdisciplinary set of open-access, online journals, promising a paradigm shift from the current review, selection and dissemination processes in academic publishing. All Frontiers journals are driven by researchers for researchers; therefore, they constitute a service to the scholarly community. At the same time, the *Frontiers journal series* operates on a revolutionary invention, the tiered publishing system, initially addressing specific communities of scholars, and gradually climbing up to broader public understanding, thus serving the interests of the lay society, too.

Dedication to quality

Each Frontiers article is a landmark of the highest quality, thanks to genuinely collaborative interactions between authors and review editors, who include some of the world's best academicians. Research must be certified by peers before entering a stream of knowledge that may eventually reach the public - and shape society; therefore, Frontiers only applies the most rigorous and unbiased reviews. Frontiers revolutionizes research publishing by freely delivering the most outstanding research, evaluated with no bias from both the academic and social point of view. By applying the most advanced information technologies, Frontiers is catapulting scholarly publishing into a new generation.

What are Frontiers Research Topics?

Frontiers Research Topics are very popular trademarks of the *Frontiers journals series*: they are collections of at least ten articles, all centered on a particular subject. With their unique mix of varied contributions from Original Research to Review Articles, Frontiers Research Topics unify the most influential researchers, the latest key findings and historical advances in a hot research area.

Find out more on how to host your own Frontiers Research Topic or contribute to one as an author by contacting the Frontiers editorial office: frontiersin.org/about/contact

RNA at a breaking point? cytoplasmic cleavage and other post-transcriptional RNA processing in neurodevelopment and disease

Topic editors

Catia Andreassi — University College London, United Kingdom

Monika Piwecka — Institute of Bioorganic Chemistry, Polish Academy of Sciences, Poland

Raphaëlle Luisier — Idiap Research Institute, Switzerland

Citation

Andreassi, C., Piwecka, M., Luisier, R., eds. (2023). *RNA at a breaking point? cytoplasmic cleavage and other post-transcriptional RNA processing in neurodevelopment and disease*. Lausanne: Frontiers Media SA.

doi: 10.3389/978-2-8325-2715-3

Table of contents

frontiers | Frontiers in Molecular Neuroscience

TYPE Editorial
PUBLISHED 30 May 2023
DOI 10.3389/fnmol.2023.1214853

OPEN ACCESS

EDITED AND REVIEWED BY
Clive R. Bramham,
University of Bergen, Norway

*CORRESPONDENCE
Monika Piwecka
✉ monika.piwecka@ibch.poznan.pl

RECEIVED 30 April 2023
ACCEPTED 15 May 2023
PUBLISHED 30 May 2023

CITATION
Piwecka M, Luisier R and Andreassi C (2023) Editorial: RNA at a breaking point? Cytoplasmic cleavage and other post-transcriptional RNA processing in neurodevelopment and disease. *Front. Mol. Neurosci.* 16:1214853. doi: 10.3389/fnmol.2023.1214853

Editorial: RNA at a breaking point? Cytoplasmic cleavage and other post-transcriptional RNA processing in neurodevelopment and disease

Monika Piwecka[1]*, Raphaelle Luisier[2,3] and Catia Andreassi[4]

[1]Department of Non-coding RNAs, Institute of Bioorganic Chemistry, Polish Academy of Sciences, Poznań, Poland, [2]Genomics and Health Informatics Group, Idiap Research Institute, Martigny, Switzerland, [3]SIB Swiss Institute of Bioinformatics, Lausanne, Switzerland, [4]UCL Laboratory for Molecular Cell Biology, University College London, London, United Kingdom

KEYWORDS

non-coding RNA, RNA modification, nerve injury, local mRNA translation, miRNA, lncRNA, circRNA

Editorial on the Research Topic
RNA at a breaking point? Cytoplasmic cleavage and other post-transcriptional RNA processing in neurodevelopment and disease

The nervous system is a complex web of thousands of cell types that require appropriate integration of developmental and mature functions to harmonically respond to both internal and external stimuli. Achieving this feat requires precise coordination of gene expression programs, with alterations in mRNA levels traditionally garnering the most attention. However, recent research has shown that non-coding RNAs, which regulate cellular functions, also play a critical role in the nervous system's function and development. Regulatory RNAs, that include but are not limited to, long non-coding RNAs (lncRNA), microRNAs (miRNA) and circular RNAs (circRNAs), play crucial roles in various biological processes ranging from cell survival to specialized functions like target innervation. Such RNA species are often subjected to modifications, post-transcriptional processing, and are localized to different subcellular compartments, all of which contribute to their biological activity and specificity (Sambandan, 2017; Rajgor, 2020; Keihani et al., 2021; Samaddar and Banerjee, 2021; Zajaczkowski and Bredy, 2021). Lastly, mRNAs or their non-coding portions such as untranslated regions (UTRs) and introns can be bestowed with alternative functions independent of their coding potential and have been shown to modulate protein-protein interactions, intracellular signaling, subcellular localization and time-dependent expression (Nam et al., 2016; Andreassi et al., 2018; Huang, 2021).

The main aim of this Research Topic is to exemplify and review novel and non-canonical functions of coding and non-coding RNAs that may contribute to brain development and functioning of neural cells in homeostasis and disease. Additionally, the Research Topic covers a few distinct aspects of RNA-mediated processes that diversify gene regulatory pathways in neural cells.

This Research Topic includes two research articles and two reviews on miRNA-mediated regulatory pathways. Han et al. investigates the alteration in the expression pattern of exosome-contained miRNAs (exo-miRNAs) isolated from serum of patients suffering from vascular dementia (VaD). The level of miR-154-5p is significantly increased in the serum exosomes of VaD patients compared to healthy individuals. Using a rat model of VaD, the authors also show that the levels of oxidative stress and inflammation are significantly elevated in VaD and that in these animals miR-154-5p is upregulated in the hippocampus, cortex, and bone marrow-endothelial progenitor cells. A study by Griffiths et al. focuses on miR-200c and its known target Sirt1 mRNA. SIRT1 protein plays a central role in maintaining mitochondrial bioenergetics through the regulation of the mitochondrial fission/fusion balance, and ROS production. The authors aim to disentangle miR-200c-Sirt1 contribution to mitochondria imbalance in astrocytes and neurons during ischemic brain injury. NF-kB complex is a known driver and regulator of miRNAs, and both excessive NF-kB and upregulated miRNAs orchestrate a pathogenic gene expression program underlying Alzheimer's disease (AD) onset, and propagation and severity of the disease. The opinion article by Lukiw comprehensively reviews current insights into the pro-inflammatory effects of miRNAs and further explores the potential mechanisms by which NF-kB-regulated miRNA-mediated signaling could be leveraged to develop novel therapeutic interventions for the more effective management of AD and other age-related neurodegenerative disorders. Finally, a mini-review by Wang and Liang summarizes state-of-the-art knowledge on miRNAs involved in T lymphocyte differentiation, activation, and functioning in the context of Multiple Sclerosis (MS). The paper evaluates differentially expressed miRNA as putative diagnostic biomarkers and includes considerations about T lymphocyte-specific miRNAs as therapeutic targets for MS treatment. Two other mini-reviews within our Research Topic provide a summary of the current literature in regard to the role played by lncRNAs in the control of oxidative stress in CNS disorders. Xu and Zhang summarize observations on lncRNAs and the mechanisms they use to regulate oxidative stress, for example by interacting with miRNAs, and the implications of these interactions for CNS disorders, such as AD, Parkinson's disease, spinal cord injury and acute ischemic stroke. Wang J. et al. instead focus on one particular lncRNA called *HOTAIR*. This comprehensive overview of the regulatory functions of *HOTAIR* highlights its contribution to the pathogenesis of ischemic stroke, neurodegenerative disorders, and traumatic brain injury. The authors conclude that *HOTAIR* holds promise to be applied as a diagnostic biomarker of CNS disorders.

Another salient theme explored in this Research Topic is the interrelation between RNA biology and nerve injury and regeneration. Cao et al. report on differentially expressed circRNAs in dorsal root ganglion neurons upon central and peripheral axon injuries in rats. Tian et al. review existing studies showing evidence for altered expression of N6-methyladenosine (m6A) RNA modifiers, and functions of related modified RNAs in CNS injuries, eventually proposing potential directions in m6A research in the context of brain injuries. Another review authored by Zhang et al. delves into the epigenetic mechanisms by which non-coding RNAs and m6A methylation modulate nerve injury-induced neuropathic pain, offering valuable insights into the potential functions and recent advances in this field. The research article by Chernov and Shubayev reveals sex-specific and sexually dimorphic regulation of neurotrophic and immune genes and mRNA axonal transport, as well as differential patterns of CNS-specific microRNA precursors and specific small nucleolar RNAs in response to sciatic nerve axotomy. Regulated neuronal mRNA transport and related local translation are comprehensively reviewed by Triantopoulou and Vidaki. This extensive article elaborates on local mRNA translation in axon outgrowth and guidance, in synapse formation and plasticity, in axon regeneration, and links mRNA transport and local RNA translation to the cytoskeleton (Triantopoulou and Vidaki). Cytoskeletal dynamics and cytoskeleton defects have been also associated and described in the context of the pathogenesis of neurodevelopmental and neurodegenerative diseases. Coordination between local translation and cytoskeletal remodeling is illustrated with multiple examples. Overall, this review article is not only broad but also brings into focus fascinating biology at the interface between the cytoskeleton, RNA-binding proteins (RBPs) and RNA in neuronal cells. More about the fascinating world of RBPs and how their localization can be altered by intrinsic and extrinsic stimuli can be found in this Research Topic. In particular, Nogami et al. describe how FUS mislocalization to cytoplasmic stress granules might result from DNA damage induction, while Wang Y. et al. investigate the alteration in intercellular communications at single-cell level during the early stages of diabetic retinopathy, identifying a new subgroup of Mueller cells and pointing to their potential role in the pathogenesis of this disease.

Our Research Topic also delves into the intricacies of transcription-associated processes that diversify gene regulatory pathways in neural cells. Marshall et al. report on the role of intron-related variable number tandem repeats in promoting disease-related gene expression diversity. Sirp et al. investigate the functional mRNA isoforms of the transcription factor 4-encoding gene (TCF4), which has been associated with several neurocognitive disorders, shedding light on the potential implications of TCF4 in a number of neurocognitive disorders. Wu et al. describe the establishment of a zebrafish model of autism, where the integration of RNA-sequencing data with Gene ontology (GO), Kyoto Encyclopedia of Genes and Genomes (KEGG) and protein–protein interaction (PPI) network analysis points them to the identification of genes that can impact the social behavior deficits observed in the affected zebrafish.

The field of RNA regulation in neurons and glial cells has been flourishing in the past two decades with multiple new discoveries and concepts. Last year (2022), the first edition of NeuroRNA conference "RNA Regulation in Brain Function and Disease" was organized to discuss state-of-the-art research at the interface of RNA biology and neuroscience. A review article by Piwecka et al. summarizes the research insights into the CNS and its dysfunctions from the systems biology perspective to finer molecular and cellular scales that were presented over three days of the conference.

We enjoyed the novel insights and summaries presented in original and review articles within this Research Topic. We hope that the content of this Research Topic will be valuable for the community of researchers that are fascinated with RNA biology and RNA-mediated gene expression regulation in the nervous system, its development, health and disease.

Author contributions

All authors listed have made a substantial, direct, and intellectual contribution to the work and approved it for publication.

Funding

MP would like to acknowledge her funding sources: National Agency for Academic Research, Polish Returns 2019, grant no. PPN/PPO/2019/1/00035, and National Science Centre, Sonata Bis 8, grant no. 2018/30/E/NZ3/00624.

Acknowledgments

We thank all the contributors and reviewers who have participated in this Research Topic.

Conflict of interest

The authors declare that the research was conducted in the absence of any commercial or financial relationships that could be construed as a potential conflict of interest.

Publisher's note

References

Andreassi, C., and Crerar, H., and Riccio, A. (2018). Post-transcriptional processing of mRNA in neurons: the vestiges of the RNA world drive transcriptome diversity. *Front. Mol. Neurosci.* 11, 304. doi: 10.3389/fnmol.2018.00304

Huang, Y, Wang, J, Zhao, Y, Wang, H, Liu, T, Li, Y, et al. (2021). cncRNAdb: a manually curated resource of experimentally supported RNAs with both protein-coding and noncoding function. *Nucleic Acids Res.* 49, D65–D70. doi: 10.1093/nar/gkaa791

Keihani, S., and Kluever, V., and Fornasiero, E. F. (2021). Brain long noncoding rnas: multitask regulators of neuronal differentiation and function. *Molecules.* 26, 3951. doi: 10.3390/molecules26133951

Nam, J. W., and Choi, S-, W., and You, B.-H. (2016). Incredible RNA: dual functions of coding and noncoding. *Mol. Cells.* 39, 367–374. doi: 10.14348/molcells.2016.0039

Rajgor, D, Purkey, A. M, Sanderson, J. L, Welle, T. M, Garcia, J. D, Dell'Acqua, M. L, et al. (2020). Local miRNA-dependent translational control of GABAAR synthesis during inhibitory long-term potentiation. *Cell Rep.* 31, 107785. doi: 10.1016/j.celrep.2020.107785

Samaddar, S., and Banerjee, S. (2021). Far from the nuclear crowd: cytoplasmic lncRNA and their implications in synaptic plasticity and memory. *Neurobiol. Learn. Mem.* 185, 107522. doi: 10.1016/j.nlm.2021.107522

Sambandan, S, Akbalik, G, Kochen, L, Rinne, J, Kahlstatt, J, Glock, C, et al. (2017). Activity-dependent spatially localized miRNA maturation in neuronal dendrites. *Science.* 355, 634–637. doi: 10.1126/science.aaf8995

Zajaczkowski, E. L., and Bredy, T. W. (2021). Circular RNAs in the brain: a possible role in memory? *Neuroscientist.* 27, 473–486. doi: 10.1177/1073858420963028

frontiers | Frontiers in Molecular Neuroscience

MINI REVIEW
published: 25 April 2022
doi: 10.3389/fnmol.2022.865529

MicroRNAs as T Lymphocyte Regulators in Multiple Sclerosis

*Lin Wang and Yuanyuan Liang**

Department of Emergency Medicine, Shengjing Hospital of China Medical University, Shenyang, China

MicroRNA (miRNA) is a class of endogenous non-coding small RNA with regulatory activities, which generally regulates the expression of target genes at the post-transcriptional level. Multiple Sclerosis (MS) is thought to be an autoimmune-mediated chronic inflammatory demyelinating disease of the central nervous system (CNS) that typically affect young adults. T lymphocytes play an important role in the pathogenesis of MS, and studies have suggested that miRNAs are involved in regulating the proliferation, differentiation, and functional maintenance of T lymphocytes in MS. Dysregulated expression of miRNAs may lead to the differentiation balance and dysfunction of T lymphocytes, and they are thus involved in the occurrence and development of MS. In addition, some specific miRNAs, such as miR-155 and miR-326, may have potential diagnostic values for MS or be useful for discriminating subtypes of MS. Moreover, miRNAs may be a promising therapeutic strategy for MS by regulating T lymphocyte function. By summarizing the recent literature, we reviewed the involvement of T lymphocytes in the pathogenesis of MS, the role of miRNAs in the pathogenesis and disease progression of MS by regulating T lymphocytes, the possibility of differentially expressed miRNAs to function as biomarkers for MS diagnosis, and the therapeutic potential of miRNAs in MS by regulating T lymphocytes.

Keywords: MicroRNAs, T lymphocytes, multiple sclerosis, pathogenesis, biomarkers, therapy

OPEN ACCESS

Edited by:
Francesca Fallarino, University of Perugia, Italy

Reviewed by:
Francisco Sanchez-Madrid, Autonomous University of Madrid, Spain
Evgeny Ermakov, Institute of Chemical Biology and Fundamental Medicine (RAS), Russia

***Correspondence:**
Yuanyuan Liang
cmuliangyy@163.com

Specialty section:
This article was submitted to Brain Disease Mechanisms, a section of the journal Frontiers in Molecular Neuroscience

Received: *30 January 2022*
Accepted: *30 March 2022*
Published: *25 April 2022*

Citation:
Wang L and Liang Y (2022) MicroRNAs as T Lymphocyte Regulators in Multiple Sclerosis. Front. Mol. Neurosci. 15:865529. doi: 10.3389/fnmol.2022.865529

INTRODUCTION

Multiple sclerosis (MS), an autoimmune neurological disease of the central nervous system (CNS), which is predominantly characterized by diffuse demyelinating lesions of the white matter (Yamout and Alroughani, 2018), but can also affect the gray matter (Klaver et al., 2013). T lymphocytes play a central role in cell-mediated immunity and can be divided into two main subgroups: (1) CD4 + T helper lymphocytes that regulate the quality and degree of immune response by releasing cytokines and that secrete proteins that can affect cellular functions related to antibacterial responses. In contrast, (2) CD8 + T cytotoxic lymphocytes have the ability to directly recognize and kill infected or transformed cells. The loss of balance between T cell subsets, resulting in attacks on self-antigenic myelin basic protein (MBP), is the most direct known cause of MS, but more details and mechanisms remain to be revealed (Deng et al., 2019; Lückel et al., 2019; Schorer et al., 2019). A large number of studies have demonstrated that CD4 + T cells play an important role in the pathogenesis of MS; helper T cell 1 (Th1) and Th17 cells are involved in the pathogenesis of MS, and regulatory T cells (Tregs) are involved in the pathogenesis of MS in experimental autoimmune encephalomyelitis (EAE) models (Chitnis, 2007; Basak and Majsterek, 2021). Tregs and interleukin-10 (IL-10) are two important negative regulators of disease progression (Ma et al., 2009). In addition, an increase in the number of Th2 cells or the inhibition of Th1/Th17 cells may delay the progression of EAE (Haghmorad et al., 2021; Hou et al., 2021). Thus, at the molecular level, T cell proliferation and function are regulated by a complex network of transcriptional and

post-transcriptional mechanisms, including transcription factors, signaling molecules, epigenetic modifications, and microRNA (miRNA) alterations (Okoye et al., 2014; Kroesen et al., 2015).

MicroRNAs are small non-coding RNAs with the capability of regulating gene expression at the post-transcriptional level either by inhibiting messenger RNA (mRNA) translation or by promoting mRNA degradation (Correia De Sousa et al., 2019). In general, a specific miRNA can regulate several mRNA transcripts, and different transcripts can participate in different cellular programs, while one mRNA transcript may be regulated by multiple miRNAs (Matkovich et al., 2013). In the CNS, miRNAs are abundant and can affect development, proliferation, differentiation, plasticity, and other cellular processes (Iyengar et al., 2014). MiRNAs are also highly expressed in immune cells and are involved in both innate and adaptive immune responses (Zhong et al., 2018). It has been reported that miRNA is a key regulatory factor to maintain immune tolerance (Scalavino et al., 2020). In the process of miRNA synthesis, the deletion of Dicer and Drosha enzymes can lead to T cell dysfunction and autoimmune diseases (Landskroner-Eiger et al., 2013). In different immune cell subgroups, miRNA transcription is different, indicating that the functions of naïve, effector, and memory T cells and regulatory T cells depend on miRNA regulation (Podshivalova and Salomon, 2013; Zhang et al., 2016). Recent studies have found that there is a specific expression pattern of miRNAs in the pathogenesis of MS, and the abnormal expression of miRNAs may be the "priming factor" that leads to the pathogenesis of MS; this pathogenic effect is likely to be achieved by regulating the activation of T cells (De Santis et al., 2010; Wei and Pei, 2010). In addition, miRNAs are histologically specific, can be expressed in paracrine forms, and are detected in many different biological fluids [cerebrospinal fluid (CSF), serum, urine, and saliva] (Jin et al., 2013). Therefore, peripheral circulating miRNAs may be used as biomarkers for the diagnosis of MS, the discrimination of MS subtypes, and the prediction of MS prognosis. Moreover, in-depth studies of miRNA regulation of T lymphocytes involved in the pathogenesis of MS may help to develop new strategies for the treatment of MS at the transcriptional and post-transcriptional levels.

Here, by summarizing recent reports, we discuss the role of T lymphocyte dysfunction in the pathogenesis of MS. Dysregulated expression of miRNAs in T lymphocytes directly or indirectly affects T lymphocyte function and, thus, is involved in the pathogenesis of MS. These miRNAs may be differentially expressed in peripheral circulation; in light of the current data, we further explore the potential of these miRNAs in MS diagnosis and distinguishing MS subtypes and targeting differentially expressed miRNAs to provide novel therapeutic strategies for MS patients.

T LYMPHOCYTE SUBSETS AND PATHOGENESIS OF MULTIPLE SCLEROSIS

T lymphocytes are derived from lymphoid stem cells from the bone marrow. After differentiation and maturation in the thymus, they are distributed to immune organs and tissues of the whole body through lymph and blood circulation to play an immune function (Themeli et al., 2013). Generally, T lymphocytes can be divided into CD4+ and CD8+ subgroups according to the differentiation of antigens on the cell surface. CD4 + T lymphocytes recognize exogenous antigen peptides presented by major histocompatibility complex (MHC)-II molecules and differentiate into Th cells after activation. CD8 + T lymphocytes recognize endogenous antigen peptides presented by MHC-I molecules; after activation, they mainly differentiate into cytotoxic T lymphocytes (Parkhurst et al., 2004; Afridi et al., 2016). Primary CD4 + T lymphocytes have been induced to differentiate into Th1 cells by interferon γ (IFN-γ), and differentiate into Th17 cells by transforming growth factor-β (TGF-β) and interleukin-6 (IL-6) (Van Hamburg et al., 2008).

CD4 + T lymphocytes play a key role in initiating the autoimmune response in MS patients (Kaskow and Baecher-Allan, 2018). It is generally believed that cytokines secreted by Th1 cells, such as IFN-γ and tumor necrosis factor-β (TNF-β), can activate macrophages to destroy oligodendrocytes, resulting in pathological myelination; IFN-γ in turn induces the production of Th1 cells (Merrill, 1992; Næss et al., 2001). TNF-α and IL-12 have proinflammatory effects, and TNF-α can directly produce cytotoxic effects on oligodendrocytes (Dopp et al., 1997). IL-12 is involved in the regulation of T lymphocyte responses and may be associated with the pathogenesis of MS (Gran et al., 2004). In addition, some measures to delay the MS process by inhibiting Th1 cells have also been shown to be effective (Xu et al., 2021). CD4+ Th2 cells are lymphocytes of the anti-inflammatory family and include major secretion immune adjustment factors such as IL-4, IL-5, IL-6, and IL-10 (Bui et al., 2017).

CD8 + T lymphocytes were found to be present in MS plaques, and these cells accumulated over time and were more numerous than CD4 + T lymphocytes (Lassmann, 2018). Human leukocyte antigen (HLA)-E-restricted CD8+ regulatory T lymphocytes can be induced by IFN-γ, which can kill immune cells such as CD4 + T lymphocytes and induce other cells to secrete some inhibitory factors such as TGF-β; IL-10 suppresses immune function and maintains disease stability in MS patients in remission (Frisullo et al., 2010). CD8 + regulatory T cell cloning in the blood and CSF of relapsing-remission MS (RRMS) patients is significantly less than that of convalescent MS patients. In addition, CD94/NKG2A killer suppressor receptors inhibit CD8+ regulatory T cell cloning and killing of other immune cells, exacerbating the disease in RRMS patients (Correale and Villa, 2008; Uemura et al., 2008). All these suggest the role of CD8+ regulatory T lymphocytes in the pathogenesis of MS. Correale et al. suggested the induction of CD8 + CD25 + Foxp3 + cells, CD4+ self-reactive cells, IFN-γ, and IL-17 in the culture plate was inhibited, and the clone of CD8+ regulatory T lymphocytes in the blood and CSF of MS patients in the exacerbation stage is significantly lower than that of patients in the remission stage, indicating that CD8+ regulatory T lymphocytes play a significant regulatory role in MS and may stop the progression of MS (Correale and Villa, 2010). Among MS patients treated with glucocorticoid, Aristimuño et al. (2008) found that the number of CD4+ and CD8+ regulatory T lymphocytes increased, while

the number of CD8+ effector and memory T lymphocytes had a downward trend, indicating that CD8+ regulatory T lymphocytes may play a role in preventing the progression of MS, while CD8+ effector T lymphocytes promote the progression of MS. Effector T lymphocytes may attack the myelin sheath of oligodendrocytes by releasing granzymes, TNF, cytolysin, and other inflammatory mediators and may cause apoptosis of myelin cells (Aristimuño et al., 2008).

Th17 lymphocytes are a newly discovered subgroup of Th lymphocytes, named for their specific secretion of IL-17. Their main function is to prevent the infection of extracellular bacteria by regulating immune cells or non-immune cells, and they also play an important role in the pathogeneses of autoimmune diseases (Miossec and Kolls, 2012). The number of Th17 lymphocytes in the CSF of RRMS patients was found to increase significantly during the relapse stage, suggesting that Th17 lymphocytes may play a pathogenic role in MS (Brucklacher-Waldert et al., 2009). Th17 lymphocytes release proinflammatory mediators including IL-17A, which can downregulate the expression of blood-brain barrier (BBB) connexin, increase the penetration of BBB, and facilitate the entry of soluble inflammatory molecules and other circulating immune molecules into the CNS (Rahman et al., 2018). The level of IL-17 in the BBB of MS patients is associated with the destruction of BBB, suggesting that IL-17 has similar pathogenicity for EAE and MS (Setiadi et al., 2019). In addition, IL-17 inhibits remyelination and repair and promotes oligodendrocyte apoptosis (Pareek et al., 2011).

Treg is another important subgroup derived from the differentiation of CD4 + T lymphocytes under the stimulation of TGF-β. There are at least two types of CD4+ Tregs: CD4 + CD25 + Tregs (nTregs) naturally produced by the thymus, and Tregs produced by peripheral induction (iTregs). NTregs mainly inhibit inflammation in a cell-contact dependent manner, while iTregs play an immunosuppressive role by secreting the inhibitory cytokines IL-10 or TGF-β (Bluestone and Abbas, 2003; Moaaz et al., 2019). The possible mechanisms of Tregs involved in the pathogenesis of MS include the decrease of cell number, the loss of inhibitory ability, and a defect in the ability to migrate to the CNS (Abdolahi et al., 2015). The decrease of FoxP3 expression in Tregs of MS patients suggests that the inhibitory function of Tregs is reduced (Etesam et al., 2016). Studies have shown that increasing the number of Tregs in EAE mice can inhibit the migration and infiltration of mouse autoreactive T lymphocytes into the CNS and significantly improve the symptoms of EAE induced by myelin oligodendrocyte glycoprotein (Yan et al., 2010).

NKT cells are classically described as a subset of T cells sharing characteristics of NK cells and typical αβ T cells (Zarobkiewicz et al., 2021). NKT cells recognize lipid and glycolipid antigens presented in the context of CD1d molecules, a non-classical MHC molecule (Shinjo et al., 1987). Typically, NKT cells are divided into three distinct populations-classical type I NKT (termed also invariant NKT, iNKT), type II (non-classical) NKT, and NKT-like cells (Godfrey et al., 2004). There was a great reduction of iNKT cells in the peripheral blood of MS patients (Illés et al., 2000). After treatment with IFN-β, the number and function of iNKT cells recovered (Gigli et al., 2007). In the remission stage of MS patients, iNKT cells produced more IL-4 and showed Th2-type response polarization, suggesting that iNKT cells may play an immunomodulatory role through Th2 type response in MS patients (Araki et al., 2003). In EAE mice, iNKT cells mainly secreted IL-4 and IL-10 to inhibit EAE (Singh et al., 2001). In addition, iNKT cells can also inhibit the further deterioration of EAE by regulating the polarization of macrophages and the proliferation of myeloid-derived suppressor cells (Condamine and Gabrilovich, 2011).

Innate immune CD16 + γδT lymphocytes also play a role in the pathogenesis of MS. *In vitro* experiments have shown that CD16 + γδT lymphocytes can induce cytotoxicity directly to the CNS. In addition, CD16 + γδT lymphocytes can produce antibody-dependent cytotoxicity to the antibody-coated target cells, thereby damaging the myelin sheath; however, the specific mechanisms have not been fully elucidated (Chen and Freedman, 2008a,b).

Various subtypes of T lymphocytes are involved in the pathogenesis and development of MS. They play damaging, regulatory, or protective roles and even have several simultaneous roles in different disease stages. Further studies of the immune role of T lymphocyte subsets in the pathogenesis of MS may provide new ideas for the treatment of MS. In recent years, as miRNA regulation of the immune system and involvement in the pathogenesis of autoimmune diseases have been reported, people have realized that miRNAs not only have a specific expression pattern in the course of MS, but may also be an important factor leading to the pathogenesis of MS (Wu and Chen, 2016). There are specific distributions of miRNAs transcriptomes in different subtypes of T lymphocytes, and they play a very important regulatory role in the development and differentiation of CD4 + T lymphocytes, the activation of effector T lymphocytes, the maintenance of the immune tolerance function of Treg cells, and the production of memory T lymphocytes. Inhibiting the function of miRNAs or changing the expression of miRNAs can lead to abnormal functions of T lymphocytes, which in turn participates in the pathogenesis and progression of MS.

MicroRNAs ARE INVOLVED IN MULTIPLE SCLEROSIS BY REGULATING T LYMPHOCYTES

MicroRNAs are a newly discovered class of non-coding single-stranded RNA molecules that act mainly at the post-transcriptional level. They bind to target genes and induce complete or partial degradation of mRNAs and thus regulate gene expression (Lindberg et al., 2010). miRNAs play an important regulatory role in maintaining immune homeostasis and normal immune function, and their dysregulated expression may be one of the important reasons for disrupting the immune tolerance balance. The abnormal expression of miRNAs in T lymphocytes of MS patients is key to initiating the autoimmune pathogenesis process of MS, which mainly involves the Th1, Th17, Treg, and CD8+ lymphocytes (Bennett and Stüve, 2009).

Th1 cells mediate autoimmune demyelination in MS. The expression of miR-27b and miR-128 is increased in naïve CD4 + T lymphocytes, and miR-340 expression is increased in memory CD4 + T lymphocytes in MS patients; these increased miRNAs contribute to the proinflammatory Th1 response by inhibiting the expression of IL-4 and B lymphoma Mo-MLV insertion region 1 homolog (BMI1). Downregulation of expression of these miRNAs with oligonucleotide miRNA inhibitors leads to the restoration of Th2 responses and has therapeutic potential in regulating T-cell phenotypes in MS (Guerau-De-Arellano et al., 2011). miR-142-5p expression is increased in the frontal white matter of MS patients; overexpression of miR-142a-5p in activated lymphocytes could shift the pattern of T lymphocyte differentiation toward Th1 lymphocytes. Thus, miR-142-5p may be involved in the pathogenesis of autoimmune neuroinflammation by promoting Th1 lymphocyte differentiation (Talebi et al., 2017). The expression of miR-155 is increased in the serum of MS patients, especially during the relapse period; miR-155 enhances the differentiation of Th17 and Th1 cells by increasing the cytokine production of both IL-17A and IFN-γ, which sustain the inflammation response and aggravate clinical signs of the EAE model (Zhang et al., 2014). miR-140-5p may be involved in the pathogenesis of MS by regulating encephalitogenic T cells. Another mechanism study found that miR-140-5p expression is significantly decreased in MS patients; signal transducer and activator of transcription 1 (STAT1) is a functional target of miR-140-5p, and overexpression of miR-140-5p suppresses phenomenological Th1 differentiation by inhibiting the activation of STAT1 and the expression of its downstream target, T-bet (Guan et al., 2016). miR-92a is one of the substantially upregulated miRNAs in MS. Rezaei et al. (2019) demonstrated that miR-92a expression is significantly enhanced at the peak of EAE, accompanied by decreased expression of DUSP10 or TSC1. Another study found that miR-92a might promote Th1 differentiation, likely owing to downregulation of DUSP10 and TSC1 expression (Rezaei et al., 2019). miR-29b expression is increased in T cells from MS patients and EAE mice. Using mice deficient in miR-29, Wan et al. (2019) suggested that miR-29ab1 is critical in regulating Th1 differentiation through repression of T-bet and IFN-γ (Smith et al., 2012). miR-182 is upregulated in RRMS patients and is correlated with increased numbers of CD4 + Th1 cells and IFN-γ production in the circulation. In EAE mice, overexpression of miR-182 resulted in exacerbation of clinical symptoms and augmentation of Th1 and Th17 differentiation (Wan et al., 2019).

Invasion of Th17 cells into the CNS is an underlying pathogenic mechanism in MS (Abarca-Zabalía et al., 2020). A disturbed Th17/Treg balance contributes to the development of autoimmune diseases, including EAE and MS (Zhou et al., 2016). It was reported that the expression of miR-27a is upregulated, while miR-214 expression is downregulated in relapsing-phase MS patients; the two miRNAs play inhibitory and promoting roles in Th17 differentiation by modulating TGF-β and mTOR signaling, respectively (Ahmadian-Elmi et al., 2016). Li et al. observed that miR-1-3p expression is upregulated in Th17 cells from MS-relapse patients. Overexpression of miR-1-3p in naïve CD4 + T cells promotes Th17 cell differentiation by increasing ETS1 expression (Li et al., 2020). Azimi et al. (2019) demonstrated that miR-326 is involved in the immunopathogenesis of MS by inducing Th17 cell differentiation and maturation. Azimi et al. suggested miR-326 negatively regulates differentiation of naïve T to Th17 cells by targeting Ets-1 (Junker et al., 2009; Azimi et al., 2019).

miR-326 may also target the CD46 molecule, which could increase the degradation of myelin by inhibiting the phagocytic activity of macrophages, thereby increasing the severity of MS and EAE (Junker et al., 2009). miR-155 expression is significantly upregulated in brain-infiltrating myelin-autoreactive CD4 + T lymphocytes, can promote Th17 (but not Th1) development by targeting two heat shock protein genes, *Dnaja2* and *Dnajb1*, and contributes to the development of EAE (Mycko et al., 2015). In *in vitro* cytokine-induced Th17 cells, miR-21 and miR-181c expression is significantly increased, and their upregulation promotes Th17 cell differentiation by targeting Smad7. In miR-21 or miR-181c-deficient mice, Th17 cell differentiation is defective, and EAE progresses slowly. However, because the two miRNAs act on the same target gene, whether their mechanism of promoting Th17 cell differentiation is competitive or synergistic needs to be further verified (Murugaiyan et al., 2015; Zhang et al., 2018; Huang et al., 2021). miR-26a is another important regulator for balancing Th17/Treg differentiation. It was reported the miR-26a expression is downregulated in MS patients and C57BL/6 mice in an EAE model system; decreased miR-26a resulted in increased expression of Th17-related cytokines and vice versa. By contrast, expression of Foxp3, the Treg cell-specific transcription factor, was found to be positively correlated with miR-26a expression. Further study found that overexpression of miR-26a could inhibit Th17 and promote Treg cell function by targeting IL-6 (Zhang et al., 2015). Tob1 is a well-known suppressor of Th17 differentiation and is a direct target of miR-590. Liu Q. et al. (2017) revealed that miR-590 expression is markedly increased in Th17 cells of MS patients and can promote pathogenic Th17 differentiation through inhibiting Tob1 expression. The expression of let-7f-5p is significantly downregulated in CD4 + T lymphocytes from MS patients and during the process of Th17 differentiation. Li et al. suggested that overexpression of let-7f-5p could inhibit Th17 differentiation. Signal transducer and activator of transcription 3 (STAT3) is a direct target of let-7f-5p and also a critical transcription factor of Th17 cells; let-7f-5p may serve as a potential inhibitor of Th17 differentiation in the pathogenesis of MS by targeting STAT3 (Li et al., 2019). Consistent results were obtained by Angelou et al. (2019), who re-emphasized the pivotal roles of let-7 in clonal expansion, and acquisition of the pathogenic Th17 phenotype and suggested that let-7 may directly target the chemokine receptors CCR2 and CCR5 as well as the cytokine receptors IL-1R1 and IL-23R to inhibit pathogenic Th17 differentiation during EAE development.

miR-17 and miR-19b are two miRNAs responsible for promoting Th17 responses. Liu et al. (2014) found miR-17 enhances Th17 polarization by inhibiting Ikaros family zinc finger 4 (IKZF4), whereas miR-19b reduces the expression of phosphatase and tensin homology (PTEN), thereby activating

the PI3K-AKT-mTOR axis crucial for Th17 differentiation. miR-146a deficiency can induce more severe EAE in mice and cause increased differentiation into Th17 cells; a mechanical study suggested that miR-146a is an important molecular brake that blocks the autocrine IL-6- and IL-21-induced Th17 differentiation pathways in autoreactive CD4 T cells (Li et al., 2017). Upregulated let-7e expression was correlated with the development of EAE; inhibiting let-7e *in vivo* reduced the number of encephalitogenic Th1 and Th17 cells and attenuated EAE (Guan et al., 2013). miR-141 and miR-200a are negative regulators of Th17 cell differentiation in RRMS patients; in the relapsing phase of MS, the expression of both miR-141 and miR-200a shows upregulation, which is involved in the pathogenesis of MS by inducing differentiation of Th17 cells and inhibiting differentiation to Treg cells (Naghavian et al., 2015). Wu et al. (2017) showed that miR-448 can enhance Th17 differentiation and aggravate the disease; protein tyrosine phosphatase non-receptor type 2 (PTPN2) is an anti-inflammatory regulator with the capacity to suppress Th17 differentiation and is a direct target of miR-448, which in turn might promote Th17 differentiation in MS by inhibiting PTPN2.

miR-30a expression is greatly decreased during Th17 differentiation in MS patients and EAE mice; IL-21R is a direct target of miR-30a, and overexpression of miR-30a results in fewer Th17 cells and alleviated EAE by targeting IL-21R (Qu et al., 2016). miR-15b is another important miRNA that regulates the differentiation of Th17 cells. miR-15b expression is significantly downregulated in MS patients and EAE mice. By regulating o-GlCNAC transferase activity, miR-15b suppresses Th17 differentiation both *in vivo* and *in vitro* and is involved in the pathogenesis of MS (Liu R. et al., 2017). miR-183c expression is increased in Th17 cells and is induced by the IL-6-STAT3 signal; it can promote pathogenic cytokine production during Th17 cell development and enhances autoimmunity. In fact, miR-183c directly inhibits the expression of the transcription factor Foxo1, which negatively regulates the pathogenicity of Th17 cells by inhibiting the expression of IL-1R1 (Ichiyama et al., 2016).

Tregs dysregulation is a common phenomenon in autoimmune diseases including MS. TGF-β signaling is essential for the development and function of Tregs. The levels of TGF-β signaling components in naïve CD4 T cells of MS patients are reduced (Aram et al., 2020). In an miRNA profile study of naïve CD4 + T lymphocytes in MS patients, Severin et al. (2016) identified 12 differentially expressed miRNAs that were validated using qRT-PCR and predicted to target the TGF-β signaling pathway, including: miR-18a, -27b, -103a, -128, -141, -212, -500a, -628-3p, -708, let-7a, -7b, and -7f. They inferred that miRNAs may be one important reason for Tregs defects observed in MS patients. The increased expression of a variety of TGF-β-targeting miRNAs in naïve CD4 + T cells of MS patients impairs TGF-β signaling and inhibits the development of Tregs, thereby increasing the susceptibility to MS. Another miRNA genome-wide expression profile by microarray analysis on CD4 + T lymphocytes showed the miR-25 and miR-106b expression is downregulated in RRMS patients; these two miRNAs may regulate the TGF-β signaling pathway and Tregs differentiation and maturation by modulating CDKN1A/p21 and BCL2L11/Bim (De Santis et al., 2010). miR-30d expression is increased in feces from EAE mice and untreated MS patients. Liu et al. (2019) showed that synthetic miR-30d can ameliorate EAE through expansion of Tregs. Let-7i expression is upregulated in MS patients; upregulated let-7i expression inhibits CD4 + T lymphocyte differentiation into Treg cells by decreasing the expression of transforming growth factor β receptor 1 (TGFBR1) and insulin-like growth factor 1 receptor (IGF1R) (Kimura et al., 2018). It has been reported the miR-27 expression is highly upregulated in T cells isolated from MS patients. Cruz et al. (2017) showed that miR-27 negatively regulates Treg cells; mechanically, the excessive expression of miR-27 could negatively impact FOXP3 induction and Treg development through targeting of c-Rel (Ruan et al., 2009). Smad7 is also a direct target of miR-181a and -b, and its expression is significantly decreased in brain white matter from MS patients as well as in the spinal cords of EAE mice during the acute and chronic phases of the diseases. Overexpression of miR-181a and -b-inhibited Th1 generation in CD4 + T cells promotes Treg differentiation, providing potential therapeutic options for controlling inflammation in MS (Ghorbani et al., 2017).

Based on our review of recent literature, we believe that miRNAs are involved in the process of T lymphocyte differentiation, activation, and function through a variety of pathways. These mRNAs (**Figure 1** and **Table 1**) are involved in the regulation of T lymphocyte differentiation and transformation, such as the balance between Th1/Th2 and Th17/Tregs. T lymphocytes phenotypic disorders are the main pathological mechanism of a variety of autoimmune diseases, including MS. Importantly, in view of T-cell-specific miRNA expression patterns, evaluation of differential miRNA expression may enable these miRNAs to become diagnostic biomarkers for MS as an important complement to current diagnostic methods (Paul et al., 2019).

MicroRNAs IN T LYMPHOCYTES AS MULTIPLE SCLEROSIS DIAGNOSTIC BIOMARKERS

The dysregulated expression of miRNAs is involved in the pathogenesis of MS through modulating the T lymphocyte phenotype. According to MS complex pathophysiology and innate immunity as well as adaptive immunity contribution to disease, a changed expression profile of miRNAs of a specific T-cell subgroup may provide new potential biomarkers for MS (**Table 2**).

A case-control study was performed by Ghadiri et al., and forty RRSM patients were enrolled (including 20 relapsing and 20 remitting MS patients); they detected the expression levels of several miRNAs in CD4 + T cells using RT-PCR and further evaluated the diagnostic value of these miRNAs for MS. The results showed that the expression levels of miR-30c and miR-34a are elevated significantly in relapsing MS patients compared with those of remitting ones and healthy controls, whereas the miR-199a expression levels were higher in the remitting patients than the relapsing ones and healthy controls. In addition, the

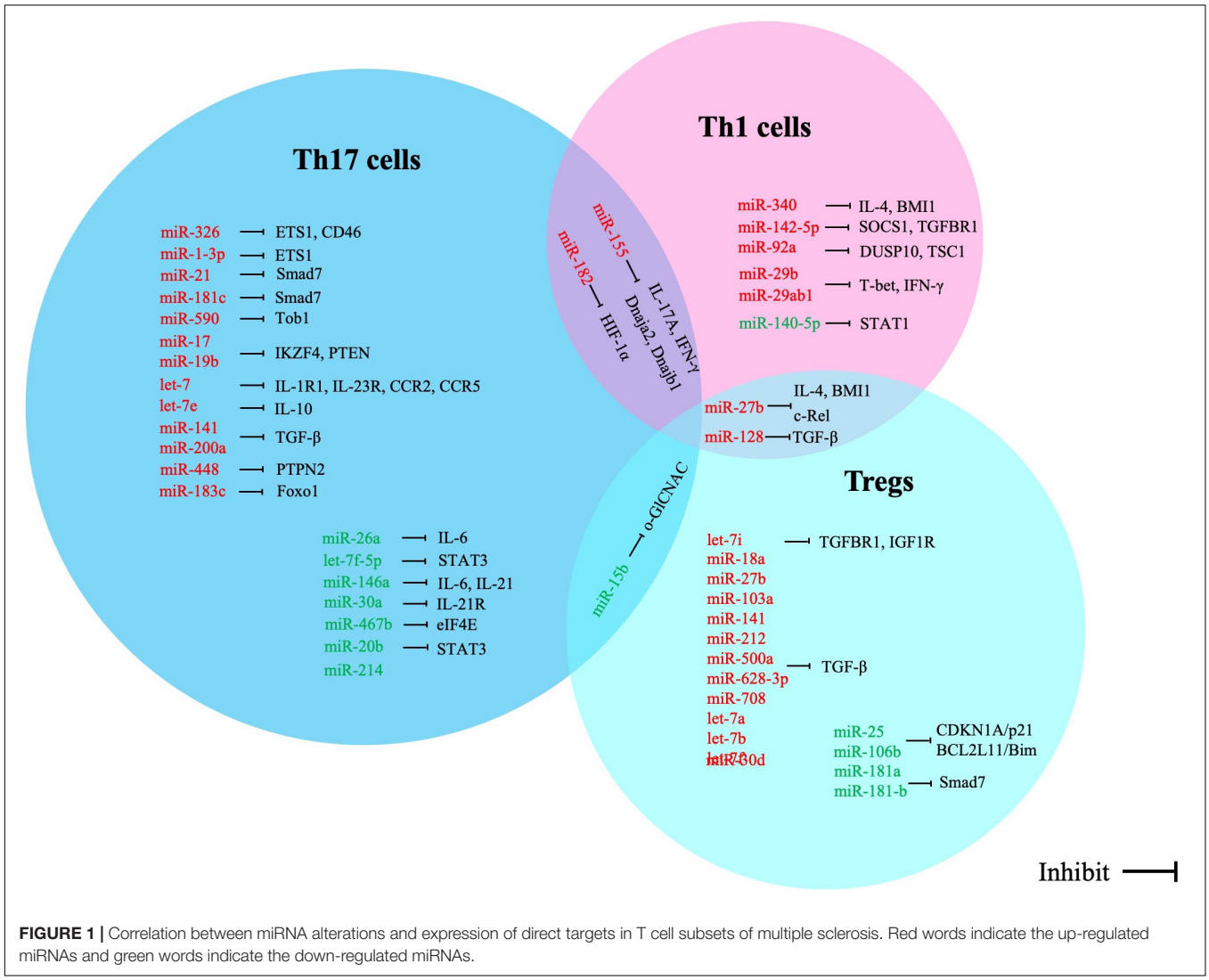

FIGURE 1 | Correlation between miRNA alterations and expression of direct targets in T cell subsets of multiple sclerosis. Red words indicate the up-regulated miRNAs and green words indicate the down-regulated miRNAs.

transcript level of miR-19a was increased in relapsing patients versus remitting patients, but there was no meaningful difference between MS patients and healthy controls. Receiver operating characteristics (ROC) analysis suggested the expression levels of miR-19a, -30c, and -34a have a discriminable value for relapsing and remitting phases in RRMS patients (Ghadiri et al., 2018).

The increase in miR-21 level usually represents an inflammatory response (Loboda et al., 2016). In MS, miR-21 expression was found to be upregulated in RRMS patients in relapse. However, in remitting phase, the expression levels of miR-21 were decreased in CD4 + T cells of RRMS patients, which could be used as a diagnostic biomarker to help distinguish relapsing and remitting phases in RRMS patients. Moreover, Ruhrmann et al. (2018) observed lower expression of miR-21 in RRMS patients than in secondary progressive MS (SPMS) patients and controls, and this difference became significant in a larger independent cohort. miR-155 expression was downregulated in CD8 + T cells of RRMS patients and was associated with the patients' Expanded Disability Status Scale (EDSS), shedding light on the potential use of miR-155 in the diagnosis of MS (Elkhodiry et al., 2021). miR-26a and miR-326 expression was also upregulated in peripheral blood lymphocytes of relapsing phase MS patients when compared with that of the remitting-phase patients and healthy controls. Furthermore, miR-326 was confirmed as a biomarker to discriminate between relapsing and remitting phases of MS with high specificity and sensitivity (100%), as determined by ROC analysis (Honardoost et al., 2014).

Sanders et al. (2016) utilized next-generation sequencing (NGS) for the miRNA expression profile in the CD4 + T cells of SPMS patients; 42 dysregulated miRNAs were identified in the CD4 + T cells of SPMS patients when compared with healthy controls. Five of the miRNAs (miR-21-5p, -26b-5p, -29b-3p, -142-3p, and -155-5p) showed downregulated expression and possessed the potential to be used as a diagnostic SPMS biomarkers (Sanders et al., 2016). miR-1-3p expression is upregulated in Th17 cells in MS-relapse patients and is positively associated with the severity of MS. In addition, overexpression

TABLE 1 | Dysregulation of miRNAs in T sub-typing cells of multiple sclerosis.

Subtypes of T cells	miRNAs	Models/patients	Target	Function	References
Th1 cells	miR-27b, miR-128, miR-340	MS mice/patients	IL-4, BMI1	Contribute to pro-inflammatory Th1 response.	Guerau-De-Arellano et al., 2011
	miR-142-5p	MS patients	SOCS1, TGFBR1	Promote Th1 lymphocytes differentiation	Talebi et al., 2017
	miR-155	MS patients/EAE	IL-17A, IFN-γ	Promote Th1 and Th17 lymphocytes differentiation	Zhang et al., 2014
	miR-140-5p	MS patients	STAT1	Suppress phenomenological Th1 differentiation	Guan et al., 2016
	miR-92a	EAE mice	DUSP10, TSC1	Promote Th1 lymphocytes differentiation	Rezaei et al., 2019
	miR-29b	MS patients/EAE mice	T-bet, IFN-γ	Regulate the Th1 differentiation	Smith et al., 2012
	miR-182	RRMS patients	HIF-1α	Promote Th1 differentiation	Wan et al., 2019
Th17 cells	miR-326	RRMS patients	ETS1, CD46	Regulate differentiation of naïve T to Th17 cells	Junker et al., 2009
	miR-1-3p	MS-relapse patients	ETS1	Promote Th17 cells differentiation	Li et al., 2020
	miR-155	EAE mice	Dnaja2, Dnajb1	Promote Th17 cells development	Mycko et al., 2015
	miR-21	EAE mice/cell models	Smad7	Promote Th17 cells differentiation	Murugaiyan et al., 2015
	miR-181c	EAE mice/cell models	Smad7	Promote Th17 cells differentiation	Zhang et al., 2018
	miR-26a	MS patients/C57BL/6 mice	IL-6	Downregulate Th17 and to upregulate Treg cell function	Zhang et al., 2015
	miR-590	MS patients	Tob1	Promote pathogenic Th17 differentiation in MS and enhance inflammation in CNS	Liu Q. et al., 2017
	let-7f-5p	MS patients	STAT3	Inhibit Th17 differentiation	Li et al., 2019
	miR-17, miR-19b	EAE mice	IKZF4, PTEN	Enhance Th17 polarization and differentiation	Liu et al., 2014
	let-7	EAE mice	Il1r1, Il23r, Ccr2, Ccr5	Inhibit the pathogenic Th17 differentiation	Angelou et al., 2019
	miR-146a	EAE mice	IL-6, IL-21	Regulate Th17 differentiation	Li et al., 2017
	let-7e	EAE mice	IL-10	Promote pathogenic Th17 differentiation	Guan et al., 2013
	miR-141, miR-200a	RRMS patients	TGF-β	Induce differentiation of Th17 cells	Naghavian et al., 2015
	miR-448	MS patients	PTPN2	Promote pathogenic Th17 differentiation	Wu et al., 2017
	miR-30a	MS patients/EAE mice	IL-21R	Inhibit differentiation of Th17 cells	Qu et al., 2016
	miR-467b	EAE mice	eIF4E	Suppress Th17 cell differentiation	Wu et al., 2021
	miR-15b	MS patients/EAE mice	o-GlCNAC	Suppress Th17 cell differentiation	Liu R. et al., 2017
	miR-20b	MS patients/EAE mice	STAT3	Inhibit differentiation of Th17 cells	Zhu et al., 2014
	miR-183c	EAE mice	Foxo1	Promote the pathogenic cytokines production during Th17 cell development	Ichiyama et al., 2016
Tregs	miR-18a, -27b, -103a, -128, -141, -212, -500a, -628-3p, -708, let-7a, -7b, -7f	MS patients	TGF-β	Impair TGF-β signaling and inhibits the development of Tregs.	Severin et al., 2016
	miR-30d	EAE mice	–	Expansion of Tregs	Liu et al., 2019
	let-7i	MS patients	TGFBR1, IGF1R	Inhibited CD4 + T lymphocytes differentiation into Tregs	Kimura et al., 2018
	miR-25, miR-106b	RRMS patients	CDKN1A/p21, BCL2L11/Bim	Disrupt the TGF-β signaling pathway and inhibit Tregs differentiation and maturation	De Santis et al., 2010
	miR-27	MS patients	c-Rel	Inhibit Treg development	Cruz et al., 2017
	miR-181a, 181-b	MS patients/EAE	Smad7	Influence differentiation of Tregs	Ghorbani et al., 2017

of miR-1-3p in naïve CD4 + T cells could promote Th17 cell differentiation by increasing the levels of inflammatory mediators; thus, knockout of miR-1-3p may be a potential therapeutic strategy for MS (Li et al., 2020). miR-590 is another highly expressed miRNA in Th17 cells of MS patients and could also promote Th17 cell differentiation through regulating IL-17A

TABLE 2 | Studies of diagnostic or prognostic biomarkers in patients of multiple sclerosis.

MIRNAs	Expression changes	T cell subtypes	Samples	Biomarker type and indication	References
miR-21-5p, -26b-5p, -29b-3p, -142-3p, -155-5p	Down-regulated	CD4 + T cells	12P/12HC	Diagnosis biomarker for SPMS	Sanders et al., 2016
miR-1-3p	Up-regulated	Th17 cells	36P/33HC	Diagnosis and severity biomarker for MS	Li et al., 2020
miR-590	Up-regulated	Th17 cells	42P/33HC	Diagnosis biomarker for MS	Liu R. et al., 2017
miR-30, -34a	Up-regulated	CD4 + T cells	40P/20HC	Diagnosis biomarker and discriminate for relapsing and remitting phases in RRMS patients	Ghadiri et al., 2018
miR-199a	Down-regulated				
miR-21	Down-regulated	CD4 + T cells	20P/12HC	Discriminate for relapsing and remitting phases in RRMS patients, and SPMS patients	Ruhrmann et al., 2018
miR-26a, miR-326	Up-regulated	Th17 cells	40P/20HC	Discriminate for relapsing and remitting phases in RRMS patients	Honardoost et al., 2014
miR-155	Down-regulated	CD8 + T cells	25P/10HC	Diagnosis biomarker for MS	Elkhodiry et al., 2021
miR-1, -20a, -28, -95, -146a, -335, -625	Down-regulated	PBMC	12 third trimester/12 post-partum/12P	Monitor disease activity of pregnancy in MS patients	Søndergaard et al., 2020

MS, multiple sclerosis; P, Patients; PBMC, peripheral blood mononuclear cells; HC, healthy controls; SPMS, secondary progressive MS, RRMS, remitting relapsing MS.

and RAR-related orphan receptor C expression. miR-590 may serve as a diagnostic biomarker and is a crucial target for potential therapeutic intervention (Liu Q. et al., 2017).

The recurrence rate of pregnant MS patients is 66% less than that of other MS patients (Li et al., 2021). In pregnant MS patients, differentially expressed miRNAs were performed with quantitative real-time PCR on PBMC. Flow cytometry analyzed on PBMC stained with antibodies directed against surface markers of antigen presenting cells (APCs), CD4+ and CD8 + T cells, NK-cells, NKT cells and subsets of these cell types, including programmed cell death 1 ligand 1 (PDL1) and PDL2 expressing subsets. The results showed that the expressions of miR-1, miR-20a, miR-28, miR-95, miR-146a, miR-335, and miR-625 in the PBMC of pregnant MS patients were downregulated, while the levels of PDL1, PDL2 and IL-10 were increased compared with untreated MS patients. The PDL1, PDL2, and IL-10 were the illustrated targets of these miRNAs and there was a negative correlation between them (Søndergaard et al., 2020).

However, miRNAs as diagnostic biomarkers of MS are still a long way from their application in clinical practice. First, miRNAs derived from peripheral T lymphocytes with differential expression rarely overlap; each study has drawn different conclusions, making it impossible to determine the reference value of each miRNA. In addition, there is a lack of international agreement on normalization methods and unified references owing to the different detection methods used in each study. Even if most studies used RT-PCR to detect miRNA expression levels, the results differ owing to different amplification times in RT-PCR detection, and normalization methods may influence the results. Moreover, miRNA from different sources and measured in different moments may also differ (the expression of miRNA in serum could differ from the expression of miRNA in different cell subtypes). Finally, there is a lack of well-designed multicenter studies; for instance, Honardoost et al. (2014) suggested that miR-326 has 100% specificity and sensitivity in MS diagnosis, but this still needs to be validated in a multicenter-controlled study with a larger number of MS patients. Regardless, despite the many shortcomings, the development of miRNAs as biomarkers is critical for future drug development and a better understanding of disease pathogenesis. In addition, miRNAs differentially expressed in peripheral T lymphocytes are non-invasive or minimally invasive; as such, they remain attractive targets for the early application of miRNAs in T lymphocytes as diagnostic biomarkers for MS in clinical practice.

MicroRNAs IN T LYMPHOCYTES AS MULTIPLE SCLEROSIS THERAPEUTIC TARGETS

Studies on the intervention of the MS pathological mechanism by regulating miRNA expression in peripheral T lymphocytes are currently mainly focused on EAE models, in which regulating miRNA expression has a therapeutic effect. For instance, miR-301a expression is upregulated in the T cells of EAE models which promotes Th17 cell differentiation; knockout miR-301a can inhibit Th17 cell development by targeting the IL-6/23-STAT3 pathway, and thus miR-301a expression may be a therapeutic target for controlling autoimmune demyelination (Mycko et al., 2012). Suppression of miR-155 can decrease Th1 and Th17 responses in the CNS, and reduce the clinical severity of EAE, even before the appearance of clinical symptoms (Murugaiyan et al., 2011). In an *in vitro* model of MS, inhibited miR-155 expression reduced the expression of CD4 + T cell effector cytokines IFN-γ and IL-17, contributing to the view that miR-155 might be a valuable target in MS therapy (Jevtić et al., 2015). miR-467b expression was decreased in CD4 + T cells of EAE; silencing miR-467b could inhibit the differentiation and function of Th17 cells by targeting eIF4E, which would alleviate EAE (Wu et al., 2021). Lentiviral vectors for miR-20b overexpression *in vivo* also led to decreased Th17 cells and reduced severity of EAE (Zhu et al., 2014).

In addition to regulating the expression of Th17 cell-related miRNAs to treat MS, modulation of the Th2 to Th1 shift

is also a major research direction. The expression of miR-27b, miR-128, and miR-340 is upregulated in CD4 + T cells from MS patients, which induces the shift from Th2 to Th1 cytokines. Oligonucleotide-miRNA inhibitors of these miRNAs have been shown to induce the restoration of Th2 responses *in vitro*. *In vivo* experiments also suggest that silencing miR-27b, miR-128, and miR-340 could be used to treat MS patients (Guerau-De-Arellano et al., 2011).

However, current studies confirming the potential therapeutic effects of regulating T-cell-associated miRNAs on MS are limited to *in vitro* or in EAE models; there are many challenges in applying this strategy in clinical settings. (i) Although miRNAs are designed to target and regulate specific T-cell-related genes, miRNAs may also target genes unrelated to therapeutic effects and may produce unexpected changes in gene expression levels. Therefore, precise regulation is key to the clinical application of miRNA agomir/antagomir drugs. (ii) As most animal studies of miRNA therapeutic strategies focus on target tissues of interest, it is possible to overlook the off-target effects of miRNA agomir/antagomir in other tissues. How to avoid off-target effect is an important research direction of miRNA therapeutic strategies. (iii) Standardized dosage and schedule, efficacy verification, and prevention of side effects will also be difficulties that need to be overcome in the study of miRNAs as a treatment strategy.

CONCLUSION

MicroRNAs play an important role in fine-tuning the adaptive immune response to inflammatory factors and MS. They can also directly regulate the involvement of T lymphocytes in the pathological mechanism of MS. Although emerging studies have determined the differential expression of miRNAs in a variety of T lymphocytes from MS patients, there is still a lot of work in progress regarding the mechanism of miRNA networks and their targets. Better understanding of how miRNA expression affects T lymphocyte responses would provide clues to the potential relevance of a given miRNA during the disease or allow identification of biomarkers for the discrimination of MS subtypes. However, being able to transform from association to causation is a difficult and challenging task. Only by identifying and verifying the mRNAs specifically targeted by each relevant miRNA can it be determined which miRNAs should be considered as effective options for MS treatment.

AUTHOR CONTRIBUTIONS

LW performed the literature searches and wrote the manuscript. YL critically revised the manuscript. Both authors listed have made a substantial, direct, and intellectual contribution to the work, and approved it for publication.

REFERENCES

Abarca-Zabalía, J., García, M. I., Lozano Ros, A., Marín-Jiménez, I., Martínez-Ginés, M. L., López-Cauce, B., et al. (2020). Differential Expression of SMAD Genes and S1PR1 on Circulating CD4+ T Cells in Multiple Sclerosis and Crohn's Disease. *Int. J. Mol. Sci.* 21:676. doi: 10.3390/ijms21020676

Abdolahi, M., Yavari, P., Honarvar, N. M., Bitarafan, S., Mahmoudi, M., and Saboor-Yaraghi, A. A. (2015). Molecular Mechanisms of the Action of Vitamin A in Th17/Treg Axis in Multiple Sclerosis. *J. Mol. Neurosci.* 57, 605–613. doi: 10.1007/s12031-015-0643-1

Afridi, S., Hoessli, D. C., and Hameed, M. W. (2016). Mechanistic understanding and significance of small peptides interaction with MHC class II molecules for therapeutic applications. *Immunol. Rev.* 272, 151–168. doi: 10.1111/imr.12435

Ahmadian-Elmi, M., Bidmeshki Pour, A., Naghavian, R., Ghaedi, K., Tanhaei, S., Izadi, T., et al. (2016). miR-27a and miR-214 exert opposite regulatory roles in Th17 differentiation *via* mediating different signaling pathways in peripheral blood CD4+ T lymphocytes of patients with relapsing-remitting multiple sclerosis. *Immunogenetics* 68, 43–54. doi: 10.1007/s00251-015-0881-y

Angelou, C. C., Wells, A. C., Vijayaraghavan, J., Dougan, C. E., Lawlor, R., Iverson, E., et al. (2019). Differentiation of Pathogenic Th17 Cells Is Negatively Regulated by Let-7 MicroRNAs in a Mouse Model of Multiple Sclerosis. *Front. Immunol.* 10:3125. doi: 10.3389/fimmu.2019.03125

Araki, M., Kondo, T., Gumperz, J. E., Brenner, M. B., Miyake, S., and Yamamura, T. (2003). Th2 bias of CD4+ NKT cells derived from multiple sclerosis in remission. *Int. Immunol.* 15, 279–288. doi: 10.1093/intimm/dxg029

Aram, J., Frakich, N., Morandi, E., Alrouji, M., Samaraweera, A., Onion, D., et al. (2020). Increased IL-2 and Reduced TGF-β Upon T-Cell Stimulation are Associated with GM-CSF Upregulation in Multiple Immune Cell Types in Multiple Sclerosis. *Biomedicines* 8:226. doi: 10.3390/biomedicines8070226

Aristimuño, C., Navarro, J., De Andrés, C., Martínez-Ginés, L., Giménez-Roldán, S., Fernández-Cruz, E., et al. (2008). Expansion of regulatory CD8+ T-lymphocytes and fall of activated CD8+ T-lymphocytes after i.v. methyl-prednisolone for multiple sclerosis relapse. *J. Neuroimmunol.* 204, 131–135. doi: 10.1016/j.jneuroim.2008.08.009

Azimi, M., Ghabaee, M., Naser Moghadasi, A., and Izad, M. (2019). Altered Expression of miR-326 in T Cell-derived Exosomes of Patients with Relapsing-remitting Multiple Sclerosis. *Iran. J. Allergy Asthma Immunol.* 18, 108–113.

Basak, J., and Majsterek, I. (2021). miRNA-Dependent CD4(+) T Cell Differentiation in the Pathogenesis of Multiple Sclerosis. *Mult. Scler. Int.* 2021:8825588. doi: 10.1155/2021/8825588

Bennett, J. L., and Stüve, O. (2009). Update on inflammation, neurodegeneration, and immunoregulation in multiple sclerosis: therapeutic implications. *Clin. Neuropharmacol.* 32, 121–132. doi: 10.1097/WNF.0b013e3181880359

Bluestone, J. A., and Abbas, A. K. (2003). Natural versus adaptive regulatory T cells. *Nat. Rev. Immunol.* 3, 253–257. doi: 10.1038/nri1032

Brucklacher-Waldert, V., Stuerner, K., Kolster, M., Wolthausen, J., and Tolosa, E. (2009). Phenotypical and functional characterization of T helper 17 cells in multiple sclerosis. *Brain* 132, 3329–3341. doi: 10.1093/brain/awp289

Bui, T. T., Piao, C. H., Song, C. H., Shin, H. S., and Chai, O. H. (2017). Bupleurum chinense extract ameliorates an OVA-induced murine allergic asthma through the reduction of the Th2 and Th17 cytokines production by inactivation of NFκB pathway. *Biomed. Pharmacother.* 91, 1085–1095. doi: 10.1016/j.biopha.2017.04.133

Chen, Z., and Freedman, M. S. (2008a). CD16+ gammadelta T cells mediate antibody dependent cellular cytotoxicity: potential mechanism in the pathogenesis of multiple sclerosis. *Clin. Immunol.* 128, 219–227. doi: 10.1016/j.clim.2008.03.513

Chen, Z., and Freedman, M. S. (2008b). Correlation of specialized CD16(+) gammadelta T cells with disease course and severity in multiple sclerosis. *J. Neuroimmunol.* 194, 147–152. doi: 10.1016/j.jneuroim.2007.11.010

Chitnis, T. (2007). The role of CD4 T cells in the pathogenesis of multiple sclerosis. *Int. Rev. Neurobiol.* 79, 43–72. doi: 10.1016/S0074-7742(07)79003-7

Condamine, T., and Gabrilovich, D. I. (2011). Molecular mechanisms regulating myeloid-derived suppressor cell differentiation and function. *Trends Immunol.* 32, 19–25. doi: 10.1016/j.it.2010.10.002

Correale, J., and Villa, A. (2008). Isolation and characterization of CD8+ regulatory T cells in multiple sclerosis. *J. Neuroimmunol.* 195, 121–134. doi: 10.1016/j.jneuroim.2007.12.004

Correale, J., and Villa, A. (2010). Role of CD8+ CD25+ Foxp3+ regulatory T cells in multiple sclerosis. *Ann. Neurol.* 67, 625–638. doi: 10.1002/ana.21944

Correia De Sousa, M., Gjorgjieva, M., Dolicka, D., Sobolewski, C., and Foti, M. (2019). Deciphering miRNAs' Action through miRNA Editing. *Int. J. Mol. Sci.* 20:6249. doi: 10.3390/ijms20246249

Cruz, L. O., Hashemifar, S. S., Wu, C. J., Cho, S., Nguyen, D. T., et al. (2017). Excessive expression of miR-27 impairs Treg-mediated immunological tolerance. *J. Clin. Invest.* 127, 530–542. doi: 10.1172/JCI88415

De Santis, G., Ferracin, M., Biondani, A., Caniatti, L., Rosaria Tola, M., Castellazzi, M., et al. (2010). Altered miRNA expression in T regulatory cells in course of multiple sclerosis. *J. Neuroimmunol.* 226, 165–171. doi: 10.1016/j.jneuroim.2010.06.009

Deng, Q., Luo, Y., Chang, C., Wu, H., Ding, Y., and Xiao, R. (2019). The Emerging Epigenetic Role of CD8+T Cells in Autoimmune Diseases: A Systematic Review. *Front. Immunol.* 10:856. doi: 10.3389/fimmu.2019.00856

Dopp, J. M., Mackenzie-Graham, A., Otero, G. C., and Merrill, J. E. (1997). Differential expression, cytokine modulation, and specific functions of type-1 and type-2 tumor necrosis factor receptors in rat glia. *J. Neuroimmunol.* 75, 104–112. doi: 10.1016/s0165-5728(97)00009-x

Elkhodiry, A. A., Zamzam, D. A., and El Tayebi, H. M. (2021). miR-155 and functional proteins of CD8+ T cells as potential prognostic biomarkers for relapsing-remitting multiple sclerosis. *Mult. Scler. Relat. Disord.* 53:103078. doi: 10.1016/j.msard.2021.103078

Etesam, Z., Nemati, M., Ebrahimizadeh, M. A., Ebrahimi, H. A., Hajghani, H., Khalili, T., et al. (2016). Altered Expression of Specific Transcription Factors of Th17 (RORγt, RORα) and Treg Lymphocytes (FOXP3) by Peripheral Blood Mononuclear Cells from Patients with Multiple Sclerosis. *J. Mol. Neurosci.* 60, 94–101. doi: 10.1007/s12031-016-0789-5

Frisullo, G., Nociti, V., Iorio, R., Plantone, D., Patanella, A. K., Tonali, P. A., et al. (2010). CD8(+)Foxp3(+) T cells in peripheral blood of relapsing-remitting multiple sclerosis patients. *Hum. Immunol.* 71, 437–441. doi: 10.1016/j.humimm.2010.01.024

Ghadiri, N., Emamnia, N., Ganjalikhani-Hakemi, M., Ghaedi, K., Etemadifar, M., Salehi, M., et al. (2018). Analysis of the expression of mir-34a, mir-199a, mir-30c and mir-19a in peripheral blood CD4+T lymphocytes of relapsing-remitting multiple sclerosis patients. *Gene* 659, 109–117. doi: 10.1016/j.gene.2018.03.035

Ghorbani, S., Talebi, F., Chan, W. F., Masoumi, F., Vojgani, M., Power, C., et al. (2017). MicroRNA-181 Variants Regulate T Cell Phenotype in the Context of Autoimmune Neuroinflammation. *Front. Immunol.* 8:758. doi: 10.3389/fimmu.2017.00758

Gigli, G., Caielli, S., Cutuli, D., and Falcone, M. (2007). Innate immunity modulates autoimmunity: type 1 interferon-beta treatment in multiple sclerosis promotes growth and function of regulatory invariant natural killer T cells through dendritic cell maturation. *Immunology* 122, 409–417. doi: 10.1111/j.1365-2567.2007.02655.x

Godfrey, D. I., Macdonald, H. R., Kronenberg, M., Smyth, M. J., and Van Kaer, L. (2004). NKT cells: what's in a name? *Nat. Rev. Immunol.* 4, 231–237. doi: 10.1038/nri1309

Gran, B., Zhang, G. X., and Rostami, A. (2004). Role of the IL-12/IL-23 system in the regulation of T-cell responses in central nervous system inflammatory demyelination. *Crit. Rev. Immunol.* 24, 111–128. doi: 10.1615/critrevimmunol.v24.i2.20

Guan, H., Fan, D., Mrelashvili, D., Hao, H., Singh, N. P., Singh, U. P., et al. (2013). MicroRNA let-7e is associated with the pathogenesis of experimental autoimmune encephalomyelitis. *Eur. J. Immunol.* 43, 104–114. doi: 10.1002/eji.201242702

Guan, H., Singh, U. P., Rao, R., Mrelashvili, D., Sen, S., Hao, H., et al. (2016). Inverse correlation of expression of microRNA-140-5p with progression of multiple sclerosis and differentiation of encephalitogenic T helper type 1 cells. *Immunology* 147, 488–498. doi: 10.1111/imm.12583

Guerau-De-Arellano, M., Smith, K. M., Godlewski, J., Liu, Y., Winger, R., Lawler, S. E., et al. (2011). Micro-RNA dysregulation in multiple sclerosis favours pro-inflammatory T-cell-mediated autoimmunity. *Brain* 134, 3578–3589. doi: 10.1093/brain/awr262

Haghmorad, D., Yazdanpanah, E., Sadighimoghaddam, B., Yousefi, B., Sahafi, P., Ghorbani, N., et al. (2021). Kombucha ameliorates experimental autoimmune encephalomyelitis through activation of Treg and Th2 cells. *Acta. Neurol. Belg.* 121, 1685–1692. doi: 10.1007/s13760-020-01475-3

Honardoost, M. A., Kiani-Esfahani, A., Ghaedi, K., Etemadifar, M., and Salehi, M. (2014). miR-326 and miR-26a, two potential markers for diagnosis of relapse and remission phases in patient with relapsing-remitting multiple sclerosis. *Gene* 544, 128–133. doi: 10.1016/j.gene.2014.04.069

Hou, H., Sun, Y., Miao, J., Gao, M., Guo, L., and Song, X. (2021). Ponesimod modulates the Th1/Th17/Treg cell balance and ameliorates disease in experimental autoimmune encephalomyelitis. *J. Neuroimmunol.* 356:577583. doi: 10.1016/j.jneuroim.2021.577583

Huang, J., Xu, X., and Yang, J. (2021). miRNAs Alter T Helper 17 Cell Fate in the Pathogenesis of Autoimmune Diseases. *Front. Immunol.* 12:593473. doi: 10.3389/fimmu.2021.593473

Ichiyama, K., Gonzalez-Martin, A., Kim, B. S., Jin, H. Y., Jin, W., Xu, W., et al. (2016). The MicroRNA-183-96-182 Cluster Promotes T Helper 17 Cell Pathogenicity by Negatively Regulating Transcription Factor Foxo1 Expression. *Immunity* 44, 1284–1298. doi: 10.1016/j.immuni.2016.05.015

Illés, Z., Kondo, T., Newcombe, J., Oka, N., Tabira, T., and Yamamura, T. (2000). Differential expression of NK T cell V alpha 24J alpha Q invariant TCR chain in the lesions of multiple sclerosis and chronic inflammatory demyelinating polyneuropathy. *J. Immunol.* 164, 4375–4381. doi: 10.4049/jimmunol.164.8.4375

Iyengar, B. R., Choudhary, A., Sarangdhar, M. A., Venkatesh, K. V., Gadgil, C. J., and Pillai, B. (2014). Non-coding RNA interact to regulate neuronal development and function. *Front. Cell Neurosci.* 8:47. doi: 10.3389/fncel.2014.00047

Jevtić, B., Timotijević, G., Stanisavljević, S., Momèilović, M., Mostarica Stojković, M., and Miljković, D. (2015). Micro RNA-155 participates in re-activation of encephalitogenic T cells. *Biomed. Pharmacother.* 74, 206–210. doi: 10.1016/j.biopha.2015.08.011

Jin, X. F., Wu, N., Wang, L., and Li, J. (2013). Circulating microRNAs: a novel class of potential biomarkers for diagnosing and prognosing central nervous system diseases. *Cell Mol. Neurobiol.* 33, 601–613. doi: 10.1007/s10571-013-9940-9

Junker, A., Krumbholz, M., Eisele, S., Mohan, H., Augstein, F., Bittner, R., et al. (2009). MicroRNA profiling of multiple sclerosis lesions identifies modulators of the regulatory protein CD47. *Brain* 132, 3342–3352. doi: 10.1093/brain/awp300

Kaskow, B. J., and Baecher-Allan, C. (2018). Effector T Cells in Multiple Sclerosis. *Cold Spring Harb. Perspect. Med.* 8:a029025. doi: 10.1101/cshperspect.a029025

Kimura, K., Hohjoh, H., and Yamamura, T. (2018). The Role for Exosomal microRNAs in Disruption of Regulatory T Cell Homeostasis in Multiple Sclerosis. *J. Exp. Neurosci.* 12:1179069518764892. doi: 10.1177/1179069518764892

Klaver, R., De Vries, H. E., Schenk, G. J., and Geurts, J. J. (2013). Grey matter damage in multiple sclerosis: a pathology perspective. *Prion* 7, 66–75. doi: 10.4161/pri.23499

Kroesen, B. J., Teteloshvili, N., Smigielska-Czepiel, K., Brouwer, E., Boots, A. M., Van Den Berg, A., et al. (2015). Immuno-miRs: critical regulators of T-cell development, function and ageing. *Immunology* 144, 1–10. doi: 10.1111/imm.12367

Landskroner-Eiger, S., Moneke, I., and Sessa, W. C. (2013). miRNAs as modulators of angiogenesis. *Cold Spring Harb. Perspect. Med.* 3:a006643. doi: 10.1101/cshperspect.a006643

Lassmann, H. (2018). Pathogenic Mechanisms Associated With Different Clinical Courses of Multiple Sclerosis. *Front. Immunol.* 9:3116. doi: 10.3389/fimmu.2018.03116

Li, B., Wang, X., Choi, I. Y., Wang, Y. C., Liu, S., Pham, A. T., et al. (2017). miR-146a modulates autoreactive Th17 cell differentiation and regulates organ-specific autoimmunity. *J. Clin. Invest.* 127, 3702–3716. doi: 10.1172/JCI94012

Li, H., Zheng, C., Han, J., Zhu, J., Liu, S., and Jin, T. (2021). PD-1/PD-L1 Axis as a Potential Therapeutic Target for Multiple Sclerosis: A T Cell Perspective. *Front. Cell Neurosci.* 15:716747. doi: 10.3389/fncel.2021.716747

Li, L., Ma, X., Zhao, Y. F., and Zhang, C. (2020). MiR-1-3p facilitates Th17 differentiation associating with multiple sclerosis *via* targeting ETS1. *Eur. Rev. Med. Pharmacol. Sci.* 24, 6881–6892. doi: 10.26355/eurrev_202006_21678

Li, Z. H., Wang, Y. F., He, D. D., Zhang, X. M., Zhou, Y. L., Yue, H., et al. (2019). Let-7f-5p suppresses Th17 differentiation *via* targeting STAT3 in multiple sclerosis. *Aging (Albany NY)* 11, 4463–4477. doi: 10.18632/aging.102093

Lindberg, R. L., Hoffmann, F., Mehling, M., Kuhle, J., and Kappos, L. (2010). Altered expression of miR-17-5p in CD4+ lymphocytes of relapsing-remitting

multiple sclerosis patients. *Eur. J. Immunol.* 40, 888–898. doi: 10.1002/eji.200940032

Liu, Q., Gao, Q., Zhang, Y., Li, Z., and Mei, X. (2017). MicroRNA-590 promotes pathogenic Th17 cell differentiation through targeting Tob1 and is associated with multiple sclerosis. *Biochem. Biophys. Res. Commun.* 493, 901–908. doi: 10.1016/j.bbrc.2017.09.123

Liu, R., Ma, X., Chen, L., Yang, Y., Zeng, Y., Gao, J., et al. (2017). MicroRNA-15b Suppresses Th17 Differentiation and Is Associated with Pathogenesis of Multiple Sclerosis by Targeting O-GlcNAc Transferase. *J. Immunol.* 198, 2626–2639. doi: 10.4049/jimmunol.1601727

Liu, S., Rezende, R. M., Moreira, T. G., Tankou, S. K., Cox, L. M., Wu, M., et al. (2019). Oral Administration of miR-30d from Feces of MS Patients Suppresses MS-like Symptoms in Mice by Expanding Akkermansia muciniphila. *Cell Host Microb.* 26, 779.e–794.e. doi: 10.1016/j.chom.2019.10.008

Liu, S. Q., Jiang, S., Li, C., Zhang, B., and Li, Q. J. (2014). miR-17-92 cluster targets phosphatase and tensin homology and Ikaros Family Zinc Finger 4 to promote TH17-mediated inflammation. *J. Biol. Chem.* 289, 12446–12456. doi: 10.1074/jbc.M114.550723

Loboda, A., Sobczak, M., Jozkowicz, A., and Dulak, J. (2016). TGF-β1/Smads and miR-21 in Renal Fibrosis and Inflammation. *Mediators Inflamm.* 2016:8319283.

Lückel, C., Picard, F., Raifer, H., Campos Carrascosa, L., Guralnik, A., Zhang, Y., et al. (2019). IL-17(+) CD8(+) T cell suppression by dimethyl fumarate associates with clinical response in multiple sclerosis. *Nat. Commun.* 10:5722. doi: 10.1038/s41467-019-13731-z

Ma, A., Xiong, Z., Hu, Y., Qi, S., Song, L., Dun, H., et al. (2009). Dysfunction of IL-10-producing type 1 regulatory T cells and CD4(+)CD25(+) regulatory T cells in a mimic model of human multiple sclerosis in Cynomolgus monkeys. *Int. Immunopharmacol.* 9, 599–608. doi: 10.1016/j.intimp.2009.01.034

Matkovich, S. J., Hu, Y., and Dorn, G. W. II (2013). Regulation of cardiac microRNAs by cardiac microRNAs. *Circ. Res.* 113, 62–71. doi: 10.1161/CIRCRESAHA.113.300975

Merrill, J. E. (1992). Proinflammatory and antiinflammatory cytokines in multiple sclerosis and central nervous system acquired immunodeficiency syndrome. *J. Immunother.* 12, 167–170. doi: 10.1097/00002371-199210000-00004

Miossec, P., and Kolls, J. K. (2012). Targeting IL-17 and TH17 cells in chronic inflammation. *Nat. Rev. Drug. Discov.* 11, 763–776. doi: 10.1038/nrd3794

Moaaz, M., Youssry, S., Elfatatry, A., and El Rahman, M. A. (2019). Th17/Treg cells imbalance and their related cytokines (IL-17, IL-10 and TGF-β) in children with autism spectrum disorder. *J. Neuroimmunol.* 337:577071. doi: 10.1016/j.jneuroim.2019.577071

Murugaiyan, G., Beynon, V., Mittal, A., Joller, N., and Weiner, H. L. (2011). Silencing microRNA-155 ameliorates experimental autoimmune encephalomyelitis. *J. Immunol.* 187, 2213–2221. doi: 10.4049/jimmunol.1003952

Murugaiyan, G., Da Cunha, A. P., Ajay, A. K., Joller, N., Garo, L. P., Kumaradevan, S., et al. (2015). MicroRNA-21 promotes Th17 differentiation and mediates experimental autoimmune encephalomyelitis. *J. Clin. Invest.* 125, 1069–1080. doi: 10.1172/JCI74347

Mycko, M. P., Cichalewska, M., Cwiklinska, H., and Selmaj, K. W. (2015). miR-155-3p Drives the Development of Autoimmune Demyelination by Regulation of Heat Shock Protein 40. *J. Neurosci.* 35, 16504–16515. doi: 10.1523/JNEUROSCI.2830-15.2015

Mycko, M. P., Cichalewska, M., Machlanska, A., Cwiklinska, H., Mariasiewicz, M., and Selmaj, K. W. (2012). MicroRNA-301a regulation of a T-helper 17 immune response controls autoimmune demyelination. *Proc. Natl. Acad. Sci. U S A* 109, E1248–E1257. doi: 10.1073/pnas.1114325109

Naghavian, R., Ghaedi, K., Kiani-Esfahani, A., Ganjalikhani-Hakemi, M., Etemadifar, M., and Nasr-Esfahani, M. H. (2015). miR-141 and miR-200a, Revelation of New Possible Players in Modulation of Th17/Treg Differentiation and Pathogenesis of Multiple Sclerosis. *PLoS One* 10:e0124555. doi: 10.1371/journal.pone.0124555

Næss, L. M., Oftung, F., Aase, A., Michaelsen, T. E., and Pollard, A. J. (2001). T-cell responses against meningococcal antigens. *Methods Mol. Med.* 66, 339–348. doi: 10.1385/1-59259-148-5:339

Okoye, I. S., Coomes, S. M., Pelly, V. S., Czieso, S., Papayannopoulos, V., Tolmachova, T., et al. (2014). MicroRNA-containing T-regulatory-cell-derived exosomes suppress pathogenic T helper 1 cells. *Immunity* 41, 89–103. doi: 10.1016/j.immuni.2014.05.019

Pareek, T. K., Belkadi, A., Kesavapany, S., Zaremba, A., Loh, S. L., Bai, L., et al. (2011). Triterpenoid modulation of IL-17 and Nrf-2 expression ameliorates neuroinflammation and promotes remyelination in autoimmune encephalomyelitis. *Sci. Rep.* 1:201. doi: 10.1038/srep00201

Parkhurst, M. R., Riley, J. P., Robbins, P. F., and Rosenberg, S. A. (2004). Induction of CD4+ Th1 lymphocytes that recognize known and novel class II MHC restricted epitopes from the melanoma antigen gp100 by stimulation with recombinant protein. *J. Immunother.* 27, 79–91. doi: 10.1097/00002371-200403000-00001

Paul, A., Comabella, M., and Gandhi, R. (2019). Biomarkers in Multiple Sclerosis. *Cold Spring Harb. Perspect. Med.* 9:a029058.

Podshivalova, K., and Salomon, D. R. (2013). MicroRNA regulation of T-lymphocyte immunity: modulation of molecular networks responsible for T-cell activation, differentiation, and development. *Crit. Rev. Immunol.* 33, 435–476. doi: 10.1615/critrevimmunol.2013006858

Qu, X., Zhou, J., Wang, T., Han, J., Ma, L., Yu, H., et al. (2016). MiR-30a inhibits Th17 differentiation and demyelination of EAE mice by targeting the IL-21R. *Brain Behav. Immun.* 57, 193–199. doi: 10.1016/j.bbi.2016.03.016

Rahman, M. T., Ghosh, C., Hossain, M., Linfield, D., Rezaee, F., Janigro, D., et al. (2018). IFN-γ, IL-17A, or zonulin rapidly increase the permeability of the blood-brain and small intestinal epithelial barriers: Relevance for neuro-inflammatory diseases. *Biochem. Biophys. Res. Commun.* 507, 274–279. doi: 10.1016/j.bbrc.2018.11.021

Rezaei, N., Talebi, F., Ghorbani, S., Rezaei, A., Esmaeili, A., Noorbakhsh, F., et al. (2019). MicroRNA-92a Drives Th1 Responses in the Experimental Autoimmune Encephalomyelitis. *Inflammation* 42, 235–245. doi: 10.1007/s10753-018-0887-3

Ruan, Q., Kameswaran, V., Tone, Y., Li, L., Liou, H. C., Greene, M. I., et al. (2009). Development of Foxp3(+) regulatory t cells is driven by the c-Rel enhanceosome. *Immunity* 31, 932–940. doi: 10.1016/j.immuni.2009.10.006

Ruhrmann, S., Ewing, E., Piket, E., Kular, L., Cetrulo Lorenzi, J. C., Fernandes, S. J., et al. (2018). Hypermethylation of MIR21 in CD4+ T cells from patients with relapsing-remitting multiple sclerosis associates with lower miRNA-21 levels and concomitant up-regulation of its target genes. *Mult. Scler.* 24, 1288–1300. doi: 10.1177/1352458517721356

Sanders, K. A., Benton, M. C., Lea, R. A., Maltby, V. E., Agland, S., Griffin, N., et al. (2016). Next-generation sequencing reveals broad down-regulation of microRNAs in secondary progressive multiple sclerosis CD4+ T cells. *Clin. Epigenet.* 8:87. doi: 10.1186/s13148-016-0253-y

Scalavino, V., Liso, M., and Serino, G. (2020). Role of microRNAs in the Regulation of Dendritic Cell Generation and Function. *Int. J. Mol. Sci.* 21:1319. doi: 10.3390/ijms21041319

Schorer, M., Kuchroo, V. K., and Joller, N. (2019). Role of Co-stimulatory Molecules in T Helper Cell Differentiation. *Adv. Exp. Med. Biol.* 1189, 153–177. doi: 10.1007/978-981-32-9717-3_6

Setiadi, A. F., Abbas, A. R., Jeet, S., Wong, K., Bischof, A., Peng, I., et al. (2019). IL-17A is associated with the breakdown of the blood-brain barrier in relapsing-remitting multiple sclerosis. *J. Neuroimmunol.* 332, 147–154. doi: 10.1016/j.jneuroim.2019.04.011

Severin, M. E., Lee, P. W., Liu, Y., Selhorst, A. J., Gormley, M. G., Pei, W., et al. (2016). MicroRNAs targeting TGFβ signalling underlie the regulatory T cell defect in multiple sclerosis. *Brain* 139, 1747–1761. doi: 10.1093/brain/aww084

Shinjo, K., Makiyama, T., Asai, T., Saito, S., Miyake, M., and Tuboi, S. (1987). [Total femur replacement in osteogenic sarcoma of the femur]. *Gan No Rinsho* 33, 993–1000.

Singh, A. K., Wilson, M. T., Hong, S., Olivares-Villagómez, D., Du, C., Stanic, A. K., et al. (2001). Natural killer T cell activation protects mice against experimental autoimmune encephalomyelitis. *J. Exp. Med.* 194, 1801–1811. doi: 10.1084/jem.194.12.1801

Smith, K. M., Guerau-De-Arellano, M., Costinean, S., Williams, J. L., Bottoni, A., Mavrikis Cox, G., et al. (2012). miR-29ab1 deficiency identifies a negative feedback loop controlling Th1 bias that is dysregulated in multiple sclerosis. *J. Immunol.* 189, 1567–1576. doi: 10.4049/jimmunol.1103171

Søndergaard, H. B., Airas, L., Christensen, J. R., Nielsen, B. R., Börnsen, L., Oturai, A., et al. (2020). Pregnancy-Induced Changes in microRNA Expression in Multiple Sclerosis. *Front. Immunol.* 11:552101. doi: 10.3389/fimmu.2020.552101

Talebi, F., Ghorbani, S., Chan, W. F., Boghozian, R., Masoumi, F., Ghasemi, S., et al. (2017). MicroRNA-142 regulates inflammation and T cell differentiation in an animal model of multiple sclerosis. *J. Neuroinflamm.* 14:55. doi: 10.1186/s12974-017-0832-7

Themeli, M., Kloss, C. C., Ciriello, G., Fedorov, V. D., Perna, F., Gonen, M., et al. (2013). Generation of tumor-targeted human T lymphocytes from induced pluripotent stem cells for cancer therapy. *Nat. Biotechnol.* 31, 928–933. doi: 10.1038/nbt.2678

Uemura, Y., Ohno, H., Ohzeki, Y., Takanashi, H., Murooka, H., Kubo, K., et al. (2008). The selective M-CSF receptor tyrosine kinase inhibitor Ki20227 suppresses experimental autoimmune encephalomyelitis. *J. Neuroimmunol.* 195, 73–80. doi: 10.1016/j.jneuroim.2008.01.015

Van Hamburg, J. P., De Bruijn, M. J., Ribeiro De Almeida, C., Van Zwam, M., Van Meurs, M., De Haas, E., et al. (2008). Enforced expression of GATA3 allows differentiation of IL-17-producing cells, but constrains Th17-mediated pathology. *Eur. J. Immunol.* 38, 2573–2586. doi: 10.1002/eji.200737840

Wan, C., Bi, W., Lin, P., Zhang, Y., Tian, J., Fang, S., et al. (2019). MicroRNA 182 promotes T helper 1 cell by repressing hypoxia induced factor 1 alpha in experimental autoimmune encephalomyelitis. *Eur. J. Immunol.* 49, 2184–2194. doi: 10.1002/eji.201948111

Wei, B., and Pei, G. (2010). microRNAs: critical regulators in Th17 cells and players in diseases. *Cell Mol. Immunol.* 7, 175–181. doi: 10.1038/cmi.2010.19

Wu, R., He, Q., Chen, H., Xu, M., Zhao, N., Xiao, Y., et al. (2017). MicroRNA-448 promotes multiple sclerosis development through induction of Th17 response through targeting protein tyrosine phosphatase non-receptor type 2 (PTPN2). *Biochem. Biophys. Res. Commun.* 486, 759–766. doi: 10.1016/j.bbrc.2017.03.115

Wu, T., and Chen, G. (2016). miRNAs Participate in MS Pathological Processes and Its Therapeutic Response. *Mediat. Inflamm.* 2016:4578230. doi: 10.1155/2016/4578230

Wu, T., Lei, Y., Jin, S., Zhao, Q., Cheng, W., Xi, Y., et al. (2021). miRNA-467b inhibits Th17 differentiation by targeting eIF4E in experimental autoimmune encephalomyelitis. *Mol. Immunol.* 133, 23–33. doi: 10.1016/j.molimm.2021.02.008

Xu, Z., Lin, C. C., Ho, S., Vlad, G., and Suciu-Foca, N. (2021). Suppression of Experimental Autoimmune Encephalomyelitis by ILT3.Fc. *J. Immunol.* 206, 554–565. doi: 10.4049/jimmunol.2000265

Yamout, B. I., and Alroughani, R. (2018). Multiple Sclerosis. *Semin. Neurol.* 38, 212–225.

Yan, Y., Zhang, G. X., Gran, B., Fallarino, F., Yu, S., Li, H., et al. (2010). IDO upregulates regulatory T cells *via* tryptophan catabolite and suppresses encephalitogenic T cell responses in experimental autoimmune encephalomyelitis. *J. Immunol.* 185, 5953–5961. doi: 10.4049/jimmunol.1001628

Zarobkiewicz, M. K., Morawska, I., Michalski, A., Roliński, J., and Bojarska-Junak, A. (2021). NKT and. *Int. J. Mol. Sci.* 22:9520.

Zhang, J., Cheng, Y., Cui, W., Li, M., Li, B., and Guo, L. (2014). MicroRNA-155 modulates Th1 and Th17 cell differentiation and is associated with multiple sclerosis and experimental autoimmune encephalomyelitis. *J. Neuroimmunol.* 266, 56–63. doi: 10.1016/j.jneuroim.2013.09.019

Zhang, R., Tian, A., Wang, J., Shen, X., Qi, G., and Tang, Y. (2015). miR26a modulates Th17/T reg balance in the EAE model of multiple sclerosis by targeting IL6. *Neuromol. Med.* 17, 24–34. doi: 10.1007/s12017-014-8335-5

Zhang, Y., Feng, Z. P., Naselli, G., Bell, F., Wettenhall, J., Auyeung, P., et al. (2016). MicroRNAs in CD4(+) T cell subsets are markers of disease risk and T cell dysfunction in individuals at risk for type 1 diabetes. *J. Autoimmun.* 68, 52–61. doi: 10.1016/j.jaut.2015.12.006

Zhang, Z., Xue, Z., Liu, Y., Liu, H., Guo, X., Li, Y., et al. (2018). MicroRNA-181c promotes Th17 cell differentiation and mediates experimental autoimmune encephalomyelitis. *Brain Behav. Immun.* 70, 305–314. doi: 10.1016/j.bbi.2018.03.011

Zhong, H., Ma, M., Liang, T., and Guo, L. (2018). Role of MicroRNAs in Obesity-Induced Metabolic Disorder and Immune Response. *J. Immunol. Res.* 2018:2835761. doi: 10.1155/2018/2835761

Zhou, Y., Leng, X., Luo, S., Su, Z., Luo, X., Guo, H., et al. (2016). Tolerogenic Dendritic Cells Generated with Tofacitinib Ameliorate Experimental Autoimmune Encephalomyelitis through Modulation of Th17/Treg Balance. *J. Immunol. Res.* 2016:5021537. doi: 10.1155/2016/5021537

Zhu, E., Wang, X., Zheng, B., Wang, Q., Hao, J., Chen, S., et al. (2014). miR-20b suppresses Th17 differentiation and the pathogenesis of experimental autoimmune encephalomyelitis by targeting RORγt and STAT3. *J. Immunol.* 192, 5599–5609. doi: 10.4049/jimmunol.1303488

Conflict of Interest: The authors declare that the research was conducted in the absence of any commercial or financial relationships that could be construed as a potential conflict of interest.

Publisher's Note: All claims expressed in this article are solely those of the authors and do not necessarily represent those of their affiliated organizations, or those of the publisher, the editors and the reviewers. Any product that may be evaluated in this article, or claim that may be made by its manufacturer, is not guaranteed or endorsed by the publisher.

frontiers | Frontiers in Molecular Neuroscience

MINI REVIEW
published: 15 June 2022
doi: 10.3389/fnmol.2022.931704

Regulation of Oxidative Stress by Long Non-coding RNAs in Central Nervous System Disorders

Xiaoman Xu[1] *and Yi Zhang*[2]*

[1] Department of Pulmonary and Critical Care Medicine, Shengjing Hospital of China Medical University, Shenyang, China,
[2] Department of Gerontology and Geriatrics, Shengjing Hospital of China Medical University, Shenyang, China

Central nervous system (CNS) disorders, such as ischemic stroke, Alzheimer's disease, Parkinson's disease, spinal cord injury, glioma, and epilepsy, involve oxidative stress and neuronal apoptosis, often leading to long-term disability or death. Emerging studies suggest that oxidative stress may induce epigenetic modifications that contribute to CNS disorders. Non-coding RNAs are epigenetic regulators involved in CNS disorders and have attracted extensive attention. Long non-coding RNAs (lncRNAs) are non-coding RNAs more than 200 nucleotides long and have no protein-coding function. However, these molecules exert regulatory functions at the transcriptional, post-transcriptional, and epigenetic levels. However, the major role of lncRNAs in the pathophysiology of CNS disorders, especially related to oxidative stress, remains unclear. Here, we review the molecular functions of lncRNAs in oxidative stress and highlight lncRNAs that exert positive or negative roles in oxidation/antioxidant systems. This review provides novel insights into the therapeutic potential of lncRNAs that mediate oxidative stress in CNS disorders.

Keywords: long non-coding RNAs, oxidative stress, therapeutic target, central nervous system, pathogenesis

OPEN ACCESS

Edited by:
Andrei Surguchov, University of Kansas Medical Center, United States

Reviewed by:
Irina G. Sourgoutcheva, University of Kansas Medical Center, United States
Marco Venturin, University of Milan, Italy

***Correspondence:**
Yi Zhang
cmuzhangyi@163.com

Specialty section:
This article was submitted to Brain Disease Mechanisms, a section of the journal Frontiers in Molecular Neuroscience

Received: *29 April 2022*
Accepted: *24 May 2022*
Published: *15 June 2022*

Citation:
Xu X and Zhang Y (2022) Regulation of Oxidative Stress by Long Non-coding RNAs in Central Nervous System Disorders. Front. Mol. Neurosci. 15:931704. doi: 10.3389/fnmol.2022.931704

INTRODUCTION

Central nervous system (CNS) disorders, such as acute ischemic stroke (AIS), Alzheimer's disease (AD), Parkinson's disease (PD), spinal cord injury (SCI), glioma, and epilepsy, usually lead to serious clinical consequences, long-term disability, or death (Xu et al., 2021). Several pathological processes involved in CNS disorders, including neuroinflammation, mitochondrial dysfunction, apoptosis, oxidative stress, and autophagy result in impaired CNS structure and dysfunction (Anderson et al., 2016; Khoshnam et al., 2017). In these pathological processes, oxidative stress plays a pivotal role in each disease (Scannevin et al., 2012). Oxidative stress refers to a pathological state in which free radicals in the body exceed its antioxidant capacity. Due to the redox imbalance, excessive reactive oxygen species (ROS) and reactive nitrogen (RNS) are generated, leading to Fenton reactions occurring *via* the action of metal ions to form hydroxyl radicals (·OH) (Sies, 2015; Sinha and Dabla, 2015). Excessive ROS induces lipid peroxidation and DNA, RNA, and protein oxidation, leading to neuronal dysfunction and death (Chen et al., 2011; Ouyang et al., 2015). Previous studies suggest that patients with higher concentrations of lipid peroxidation mediators have worse prognosis in CNS disorders, such as in AIS and AD (Klimiuk et al., 2019; Maciejczyk et al., 2020). Therefore, considering that hyperactive oxidative stress responses arise after the occurrence of CNS disorders, finding effective strategies to modulate oxidative stress

in the CNS is important for restricting oxidative injuries and protecting neurological function (Costa et al., 2016).

Emerging studies suggest that oxidative stress may induce epigenetic modifications that ultimately lead to CNS disorders (Zhao et al., 2016). Non-coding RNAs have attracted extensive attention as epigenetic regulators involved in CNS disorders (Wu and Kuo, 2020). Long non-coding RNAs (LncRNAs) are a class of RNAs more than 200 nucleotides long but have no protein-coding function. These molecules were initially considered as a transcription by-product without important biological functions. However, numerous studies found that lncRNAs serve as an important "medium" in cells (Hombach and Kretz, 2016). LncRNAs are involved in the regulation of cell proliferation, differentiation, the cell cycle, and apoptosis at the transcriptional, post-transcriptional, and epigenetic levels. Furthermore, a few annotated lncRNAs play an important role in oxidative stress-related diseases and CNS disorders (Chu et al., 2022). For instance, elevated levels of the lncRNA rhabdomyosarcoma 2 related transcript (RMST) augment AIS by reducing microRNA (miR)-221-3p-mediated regulation of phosphoinositide-3-kinase regulatory subunit 1 (PIK3R1) and activating the transforming growth factor-β (TGF-β) pathway (Li et al., 2022). In contrast, knocking down lncRNA Gm11974 attenuates neuronal injury in AIS by modulating the miR-122-5p/semaphorin 3A (SEMA3A) signaling pathway (Yang et al., 2021). These results reveal that lncRNAs exert a positive or negative role in oxidative stress responses and suggest that lncRNAs may be key molecules involved in oxidative stress.

Despite recent advances, the role of lncRNAs and their downstream regulatory networks in regulating oxidative stress remains unclear. In this review, we collect existing evidence and discuss the characteristics of lncRNAs and their involvement in the oxidative/antioxidant system in different CNS disorders including AIS, neurodegenerative diseases, traumatic diseases, epilepsy, and glioma. Moreover, we discuss the potential molecular mechanisms involved in the regulation of oxidative stress, which may provide new insights into potential therapeutic lncRNA targets in CNS disorders that mediate oxidative stress.

OXIDATIVE STRESS AND THE NRF2/KEAP1/ARE PATHWAY

Oxidative stress occurs when the physiological balance between oxidants and antioxidants is disrupted, which shifts the balance to favor oxidants and results in potential damage to the body (Sies et al., 2017). Oxidative stress and the related inflammatory responses, autophagy and apoptosis, are key factors involved in CNS disorders (Hybertson et al., 2011). ROS are continuously produced by all aerobic organisms through both enzymatic and non-enzymatic reactions. The most common ROS include superoxide anion radicals ($O_2 \cdot^-$), hydroxyl radicals (·OH), hydrogen peroxide (H_2O_2), nitric oxide (NO), and nitrite peroxide ($ONOO^-$). In humans, the major ROS sources are mitochondria and various ROS-producing enzymes, including nicotinamide adenine dinucleotide phosphate (NADPH) oxidase (NOX), xanthine oxidase (XO), nitric oxide synthase (NOS), and myeloperoxidase (MPO) (Pizzino et al., 2017; Jakubczyk et al., 2020). The CNS has a relatively poor antioxidant defense due to its high oxygen consumption and high polyunsaturated fatty acid levels. At the physiological level, neurons are repaired through their own antioxidant defense system, which prevents neuronal oxidative damage (Salim, 2017). When excessive ROS production exceeds the repair capacity of the endogenous antioxidant system, biological macromolecules (such as lipids, proteins, and nucleic acids) undergo oxidative damage and can even activate apoptosis. Endogenous antioxidant enzymes such as superoxide dismutase (SOD), catalase (CAT) and glutathione peroxidase (GPx), and non-enzymatic antioxidants such as glutathione, ubiquinone, and ascorbic acid (vitamin C) help maintain cellular redox homeostasis (**Figure 1**; Rodrigo et al., 2013; Salim, 2017).

Among the antioxidant defense mechanisms, nuclear factor-erythroid related factor-2 (Nrf2) is a master regulator of transcriptional activation in antioxidant effects and can balance ROS production. Under oxidative stress, Nrf2 dissociates from Kelch-like Ech-associated protein 1 (Keap1) and translocates into the nucleus, where it binds to antioxidant response elements (ARE) (Silva-Palacios et al., 2018), thereby activating downstream antioxidant defense enzymes such as NAD(P)H quinone dehydrogenase 1 (NQO1), heme oxygenase 1 (HO-1), glutathione S-transferase (GST), and enzymes involved in glutathione synthesis and metabolism (γ-glutamyl cysteine synthetase) (Yamamoto et al., 2018; Baird and Yamamoto, 2020). Unfortunately, decreased antioxidant proteins have been found in many CNS disorders. Recent findings on the association of lncRNAs with oxidative stress may provide new ideas for explaining this phenomenon.

LNCRNA CLASSIFICATION

LncRNAs account for 80–90% of all ncRNAs. Compared with other ncRNAs such as microRNAs (miRs) and circular RNAs, lncRNAs have longer sequences, more complex spatial structures, and more diverse and complex mechanisms involved in the regulation of gene expression (Esteller, 2011). LncRNAs generally have similar characteristics to protein-coding genes, but tend to contain only one intron and have a low tendency for co-transcriptional splicing. Similar to mRNA, lncRNAs are alternately spliced and are primarily transcribed by RNA polymerase II, with about half having 5′-Cap and 3′-polyadenosine structures. LncRNAs also have a special secondary structure that provides several protein and DNA/RNA binding sites (Wei et al., 2018). Thus, lncRNAs regulate gene expression in various ways: (i) by interfering with transcription factor binding to target genes; (ii) interacting with small RNA; (iii) binding to proteins and acting as ribonuclein scaffolds; (iv) binding to chromatin to regulate chromatin remodeling; (v) and binding mRNA and affecting translation, shearing, and degradation (Shi et al., 2013; Deniz and Erman, 2017). LncRNAs have differences in size, molecular partners, and mechanism of action. According to their relative position and host protein-coding genes, lncRNAs can be divided into exons, introns, overlapping lncRNAs, and intergenic lncRNAs (**Figure 2**; Tan et al., 2021).

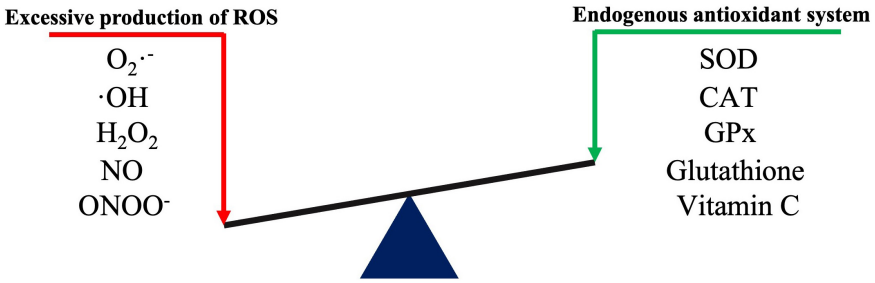

FIGURE 1 | Schematic diagram of redox reactions.

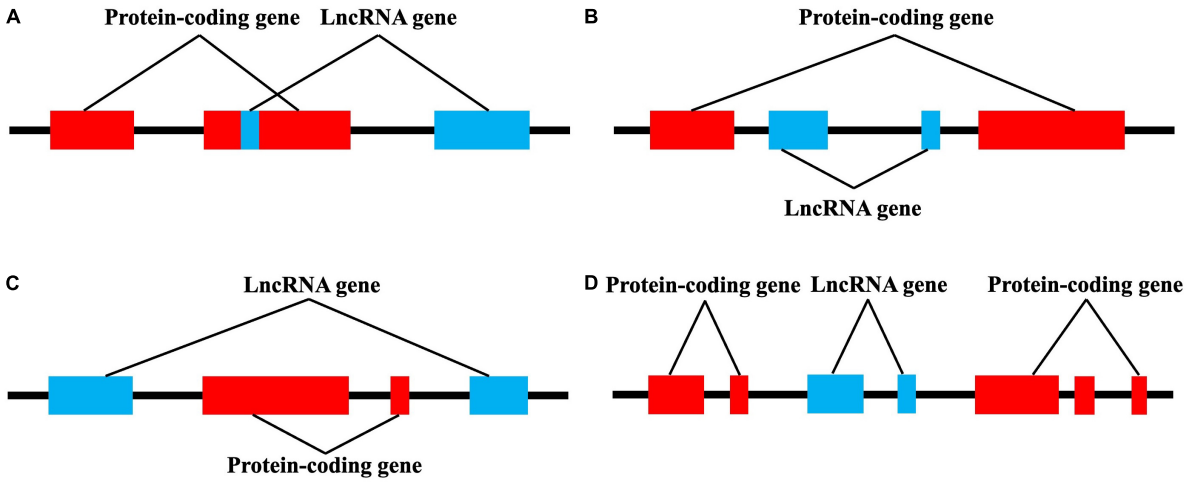

FIGURE 2 | lncRNAs are classified into four categories by their location relative to neighboring protein-coding genes. **(A)** Exon lncRNAs, **(B)** intron lncRNAs, **(C)** overlapping lncRNAs, and **(D)** intergenic lncRNAs.

There is no clear, unified standard for lncRNA classification. Indeed, lncRNA can be basically divided into the following categories based on their relative positions with encoding genes: intergenic lncRNA (lincRNA), sense lncRNA, antisense lncRNA, untranslated lncRNA, promoter-related lncRNA (pancRNA), introns lncRNA (intronic RNA), and enhancing lncRNA. The position of the lncRNA in the genome often determines its regulating mechanism and related functions (Chen et al., 2021a). In addition, lncRNAs are roughly classified into four categories according to their roles: signal molecules, decoy molecules, guide molecules, and scaffold molecules (**Figure 3**; Wang and Chang, 2011). As signal molecules, lncRNAs participate in the conduction of some signal pathways. Some lncRNAs regulate the transcription of downstream genes and reflect their spatiotemporal expression. As decoy molecules, lncRNAs can combine with and remove some transcription factors to regulate gene expression. As guide molecules, lncRNAs can recruit *cis*- or *trans*- genes for chromatin modification enzymes. As scaffold molecules, lncRNAs can bind various proteins to form complexes and modify histones on chromatin (Dahariya et al., 2019; He et al., 2021).

The functions of lncRNAs are well known and numerous abnormal lncRNAs are observed in CNS disorders. However, research on the mechanism and possible consequences of abnormal lncRNAs in CNS disorders remains limited, especially for CNS disorders involving oxidative stress. In this review, we specifically focus on how lncRNAs regulate oxidative stress in CNS disorders (**Table 1**). By mediating oxidative stress, lncRNAs may provide new potential targets for the treatment of CNS disorders.

LNCRNAS MEDIATING OXIDATIVE STRESS IN CENTRAL NERVOUS SYSTEM DISORDERS

LncRNAs Mediating Oxidative Stress in Acute Ischemic Stroke

During AIS, the sudden reduction or interruption of glucose and oxygen supply rapidly disturbs energy metabolism in brain tissue, which leads to the generation of abundant ROS and oxidative intermediates, resulting in severe oxidative damage in a short period of time (Wang et al., 2018a). In early AIS, cellular metabolism shifts to anaerobic glycolysis, resulting in decreased NADPH, increased O_2^-, and dysregulated neuronal

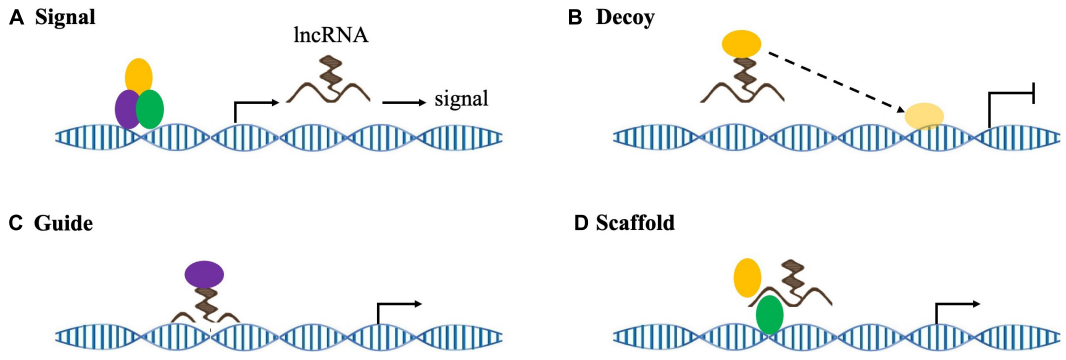

FIGURE 3 | lncRNA mechanisms of action. **(A)** As signaling molecules, lncRNAs convey specific cell development and spatiotemporal information to regulate corresponding gene expression. **(B)** As decoy molecules, lncRNAs sequester target molecules, which inhibits downstream functions. **(C)** As guide molecules, lncRNAs recruit chromatin modification complexes to target genes in either *cis* or *trans*. **(D)** As scaffold molecules, lncRNAs form functional complexes to participate in histone modification and/or stabilize nuclear structures.

energy metabolism (Burmistrova et al., 2019). This also causes neuronal ion channels to malfunction and cell membranes to depolarize, leading to excessive release of excitatory transmitters and subsequent excitatory toxicity (Amantea and Bagetta, 2017). Excessive glutamate release causes Na^{+}–Ca^{2+} exchanger (NCX) dysfunction and mitochondrial depolarization, resulting in calcium overload and increased ROS production (Shi et al., 2018). Additionally, phospholipase is activated, which leads to polyunsaturated fatty acid (PUFA) release and ROS generation as PUFAs are metabolized into inflammatory mediators such as prostaglandins (Chuang et al., 2015; **Figure 4**).

Nuclear paraspeckle assembly transcript 1 (NEAT1) is a lncRNA that is dysregulated in various human cancers (Li et al., 2021a). NEAT1 plays a protective role in oxygen-glucose deprivation/reoxygenation (OGD/R)-activated brain microvascular endothelial cells (Zhou et al., 2019). As an activator of the antioxidant pathway, NEAT1 overexpression stabilizes Mfn2 mRNA by recruiting Nova, thereby increasing Mfn2 expression and alleviating ischemia-reperfusion-induced oxidative stress and apoptosis *via* the Mfn2/Sirt3 pathway (Zhou et al., 2022).

The lncRNA rhabdomyosarcoma 2-associated transcript (RMST) has pivotal roles in regulating AIS through multiple pathophysiological mechanisms, including oxidative stress. In OGD/R-induced AIS, increased RMST was observed. Downregulating RMST ameliorated increased MDA and ROS while decreasing SOD and NO levels. The effect of RMST downregulation abrogates OGD/R-triggered oxidative stress, likely by downregulating SEMA3A expression *via* sponging miR-377 (Zhao et al., 2021).

Previous studies reported that the lncRNA AK139328 is associated with ischemia/reperfusion injury (IRI) in various organs (Chen et al., 2015; Yu et al., 2018). AK139328 is increased in PC12 cells activated by OGD/R. However, AK139328 silencing decreases ROS production and upregulates endothelial nitric oxide synthase (eNOS) protein expression, which suggests that knocking down AK139328 may alleviate OGD/R-induced oxidative stress in PC12 cells (Liu et al., 2021).

OGD could upregulate lncRNA small nucleolar RNA host gene 14 (SNHG14) and downregulate its derived miR-199b in BV2 cells. SNHG14-derived miR-199b targets the 3′ UTR of aquaporin 4 (AQP4) to increase SOD activity and markedly decrease MDA levels (Liu et al., 2021).

MACC1-AS1 is the antisense lncRNA of MACC1 and has been identified as an oncogene in multiple cancers (Zhao et al., 2018; Guo et al., 2020). miR-6867-5p suppresses the proliferation of endometriosis (Park et al., 2019); MACC1-AS1, the endogenous competitor of miR-6867-5p, exerts anti-apoptosis effects, maintains cell barrier function, and reduces anti-oxidative stress in hypoxia-induced human brain microvascular endothelial cells (HBMECs) under hypoxic conditions by regulating miR-6867-5p/TWIST1 (Yan et al., 2020).

Opa-interacting protein 5 antisense RNA 1 (OIP5-AS1) is involved in the development of multiple human cancers (Deng et al., 2018; Wang et al., 2019). OIP5-AS1 could also function through miRNAs. Overexpressing OIP5-AS1 attenuates oxidative stress and inflammation in a middle cerebral artery occlusion/reperfusion (MCAO/R) rat model, possibly *via* antioxidant functions activated by targeting miR-186-5p to increase C1q/TNF-related protein 3 (CTRP3) and Nrf2 (Chen et al., 2021b). Similarly, neuroprotective effects were observed from the lncRNA CCAAT enhancer binding protein α antisense RNA 1 (CEBPA-AS1).

OGD/R upregulates CEBPA-AS1 expression in SH-SY5Y cells, while CEBPA-AS1 silencing antagonizes the effects of OGD/R on oxidative stress by decreasing ROS levels and increasing SOD and GSH levels. These results indicate that CEBPA-AS1 knockdown reduces OGD/R-induced oxidative stress in neurons (Di et al., 2021).

The lncRNA potassium voltage-gated channel subfamily Q member 1 opposite strand 1 (KCNQ1OT1) aggravates oxidative stresses and inflammation during hypoxia. KCNQ1OT1 could target miRNAs to alter oxidative stress. For example, KCNQ1OT1 is upregulated in blood samples from patients with AIS. In OGD/R model PC12 cells, the cells were protected from oxidative

TABLE 1 | The molecular targets, downstream pathways and oxidative stress regulation of lncRNAs in central nervous system (CNS) disorders.

CNS disorders	lncRNAs	Expression	Intermediate molecule	Downstream pathway	Animals or Cells	Models	Observed oxidative stress indicators	References
AIS	NEAT1	Decreased	Mfn2	Sirt3	BV-2/N2a cells	OGD/R	ROS, SOD, MDA	Zhou et al., 2022
	RMST	Increased	miR-377	SEMA3A	N2a cells	OGD/R	ROS, MDA, SOD, NO	Zhao et al., 2021
	AK139328	Increased	Netrin-1	NA	PC12 cells	OGD/R	ROS, eNOS	Liu et al., 2021
	SNHG14	Increased	miR-199b	AQP4	BV-2 cells	OGD/R	SOD, MDA	Liu et al., 2021
	MACC1-AS1	Decreased	miR-6867-5p	TWIST1	HBMECs	Hypoxia	ROS, SOD, MDA, CAT	Yan et al., 2020
	OIP5-AS1	Decreased	miR-186-5p	CTRP3	Rats/BV-2 cells	MCAO/R	MDA, SOD, GSH-Px	Chen et al., 2021b
	CEBPA-AS1	Increased	miR-24-3p	BOK	SH-SY5Y cells	OGD/R	ROS, SOD, GSH	Di et al., 2021
	KCNQ1OT1	Increased	miR-140-3p	HIF-1α	PC12 cells	OGD/R	ROS, SOD, MDA, LDH	Yi et al., 2020
	ZFAS1	Decreased	miR-582-3p	NOS3	PC12 cells	OGD/R	MDA, LDH, GSH-px, SOD, NO, eNOS	Zhang and Zhang, 2020
	SNHG16	Decreased	miR-421	XIAP	SK-N-SH cells	OGD/R	ROS, SOD, MDA, LDH	Cao et al., 2022
	GAS5	Increased	miR-455-5p	PTEN	Rats/PC12 cells	OGD/R, MCAO/R	CAT, SOD, GSH-Px	Wu et al., 2021
	Gm11974	Increased	miR-122-5p	SEMA3A	Mice/N2a cells	OGD/MCAO	MDA, LDH, NO, CAT, H2O2	Yang et al., 2021
	SNHG7	Decreased	miR-134-5p	FGF9	N2a cells	OGD	ROS, SOD, MDA, CAT, LDH	Sun et al., 2021
	AK046177	Increased	miR-134	CREB	Rats/Primary cortical cells	OGD/R/MCAO	SOD, GSH-Px, MDA, NADPH, Nrf2	Wang et al., 2020a
AD	XIST	Increased	miR-132	NA	Hippocampal neurons	$A\beta_{25-35}$	SOD, GSH-Px, MDA	Wang et al., 2018b
	H19	Increased	miR-129	HMGB1	PC12 cells	$A\beta_{25-35}$	SOD, MDA, CAT	Zhang et al., 2021
	BDNF-AS	Increased	NA	BDNF	PC12 cells	$A\beta_{25-35}$	SOD, MDA, CAT, ROS	Guo et al., 2018

(Continued)

TABLE 1 | (Continued)

CNS disorders	lncRNAs	Expression	Intermediate molecule	Downstream pathway	Animals or Cells	Models	Observed oxidative stress indicators	References
	WT1-AS	Decreased	WT1	miR-375/SIX4	SH-SY5Y cells	$A\beta_{25-35}$	ROS, MDA, LDH, SOD, GSH-Px	Wang et al., 2020b
	TUG1	Increased	miR-15a	ROCK1	Mice/Hippocampal neurons	$A\beta_{25-35}$	MDA, SOD	Li et al., 2020
PD	MIAT	Increased	miR-221-3p	TGF-β1/Nrf2 axis	Mice/MN9D dopaminergic neuronal cells	MPTP	SOD, GSH, MDA	Lang et al., 2022
	NORAD	Decreased	miR-204-5p	SLC5A3	Neuroblastoma/SK-N-SH/-N-AS cells	MPP^+	SOD, LDH	Zhou et al., 2020
	RMST	Increased	NA	TLR/NF-κB signaling	Rats	MPTP	SOD, CAT, GSH-Px, NOS, MDA, NO	Ma et al., 2021
	AL049437	Increased	miR-205-5p	MAPK1	Mouse/SH-SY5Y cells	MPTP/ MPP^+	ROS	Zhang et al., 2020a
	MALAT1	Increased	EZH2	Nrf2	C57BL/6 mice	MPTP	SOD, CAT	Cai et al., 2020
	Lnc-p21	Increased	miR-625	TRPM2	SH-SY5Y	MPP^+	SOD	Ding et al., 2019
	T199678	Decreased	miR-101-3p	α-Syn	SH-SY5Y cells	α-Syn	ROS	Bu et al., 2020
SCI	CASC9	Decreased	miR-383-5p	LDHA	Rats/PC12 cells	LPS/Pentobarbital	LDH, MDA	Guan and Wang, 2021
	GAS5	Increased	CELF2	VAV1	RN-Sc cells	OGD/R	GSH-Px, SOD, MDA	Wang et al., 2021a
	TCTN2	Decreased	miR-329-3p	IGF1R	Rats/PC12 cells	LPS	SOD, MDA	Liu et al., 2022
	SOX2OT	Increased	miR-331-3p	Neurod1	Rats/PC12 cells	LPS	SOD, MDA	Li et al., 2021b
Glioma	H19	Increased	NA	NA	U251/LN229 cells	H_2O_2	NA	Duan et al., 2018
TLE	MEG3	Decreased	NA	PI3K/AKT/mTOR pathway	Rats	LiCl/Pilocarpine	SOD, MDA	Zhang et al., 2020a

α-Syn, α-synuclein; AD, Alzheimer's disease; AIS, acute ischemic stroke; CAT, catalase; eNOS, endothelial nitric oxide synthase; EZH2, enhancer of zeste homolog 2; GSH-PX, glutathione peroxidase; HBMECs, hypoxia-induced human brain microvascular endothelial cells; LDH, lactate dehydrogenase; LPS, lipopolysaccharide; MCAO/R, middle cerebral artery occlusion/reperfusion; MDA, malondialdehyde; MPP^+, 1-Methyl-4-phenylpyridinium ion; MPTP, 1-methyl-4-phenyl-1,2,3,6-tetrahydropyridine; NADPH, nicotinamide adenine dinucleotide phosphate; NF-κB, nuclear factor kappa B; NO, nitric oxide; NOS3, nitric oxide synthase 3; Nrf2, nuclear factor E2-related factor 2; OGD/R, oxygen-glucose deprivation/reoxygenation; PD, Parkinson's disease; RN-Sc, rat neurons-spinal cord; ROS, reactive oxygen species; SCI, spinal cord injury; SOD, superoxide dismutase; TGF-β1, transforming growth factor-β1; TLE, temporal lobe epilepsy; TLR, Toll-like receptor.

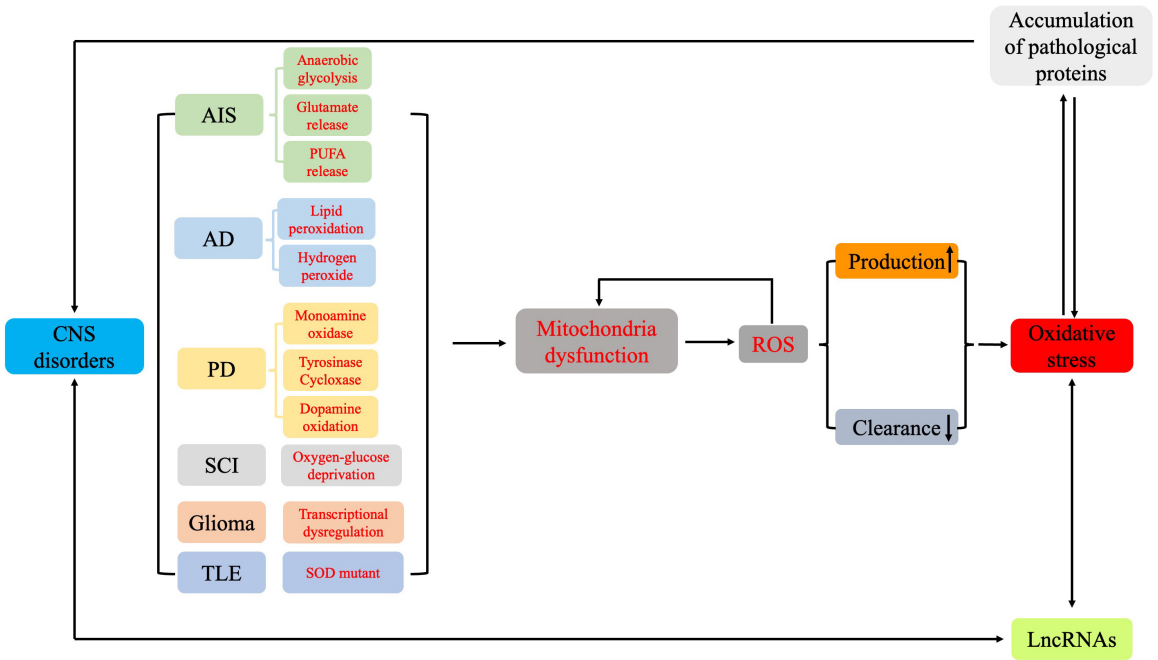

FIGURE 4 | The pathways involved in oxidative stress and in the formation of reactive oxygen species in the different pathologies of central nervous system disorders.

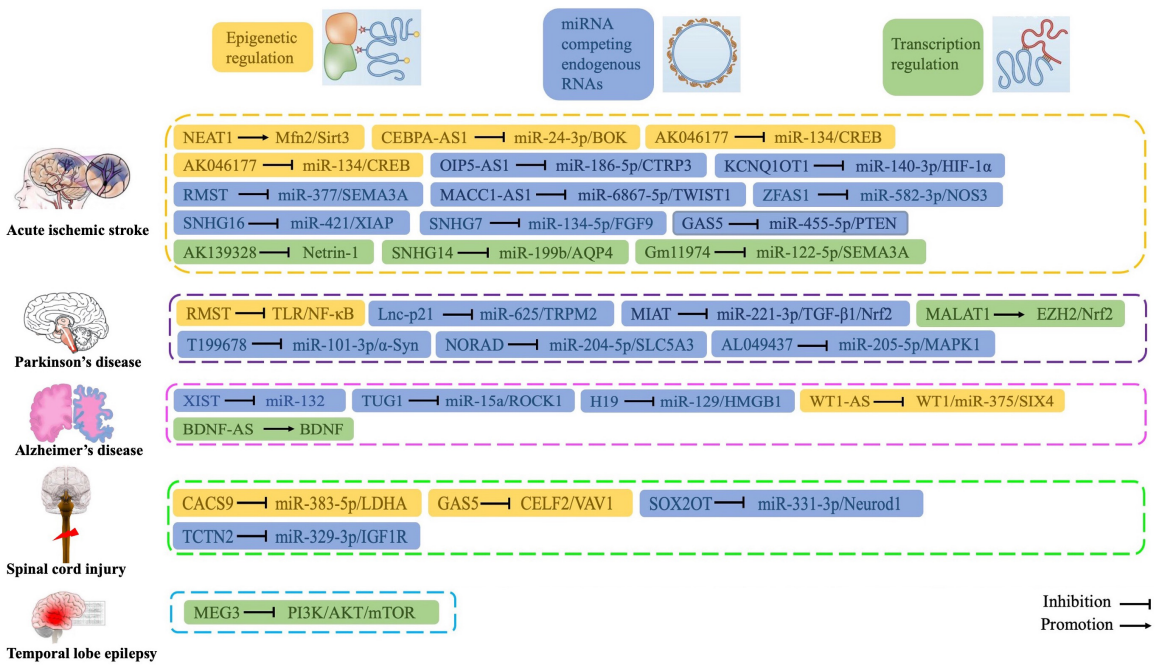

FIGURE 5 | Roles and functions of lncRNAs in regulating oxidative stress during central nervous system disorders.

stress injury. KCNQ1OT1 might target miR-140-3p to enhance hypoxia-inducible factor-1α (HIF-1α) expression (Yi et al., 2020).

The lncRNA ZFAS1 is significantly downregulated in patients with AIS. Mechanistically, lncRNA ZFAS1 acts as a "sponge" for miR-582-3p, which upregulates nitric oxide synthase 3 (NOS3) expression and associated antioxidant functions (Zhang and Zhang, 2020).

LncRNA small nucleolar RNA host gene16 (SNHG16) has been well-documented for oncogenic properties in various malignancies (Gong et al., 2020). X-linked inhibitor-of-apoptosis

protein (XIAP) suppresses neurological dysfunction and neuronal apoptosis, thereby relating to preconditioning treatment for cerebral I/R injury (Wang et al., 2021b). Overexpressing SNHG16 enhances cell proliferation and inhibits apoptosis. SNHG16 might enhance XIAP expression by sponging miR-421 to attenuate cell inflammation and oxidative stress in an OGD/R-induced SK-N-SH cell model (Cao et al., 2022).

The lncRNA growth-arrest-specific transcript 5 (GAS5) is widely reported as a tumor suppressor gene (Saussez et al., 1998). Suppressing GAS5 exerts anti-oxidative stress effects in MCAO rats, downregulates GAS5-impaired NOS activity, reduces MDA and protein carbonyl content, and enhances SOD, CAT, and glutathione peroxidase (GSH-Px) activities. Additionally, GAS5 increases cell viability and decreases apoptosis in OGD/R-induced PC12 cells and MCAO rats (Wu et al., 2021).

Previous studies indicate that some antioxidants (CAT and SOD) and pro-oxidants (LDH, MDA, and NO) could be potential endogenous targets for stroke therapy (Chen et al., 2011). In MCAO mice, silencing lncRNA Gm11974 contributes to the recovery of neurological function. In addition, depleting Gm11974 suppresses neuronal apoptosis in OGD-stimulated N2a cells, These neuroprotective effects may occur because Gm11974 silencing increases SOD and CAT activity while decreasing MDA, LDH, and NO levels (Yang et al., 2021).

Cyclic AMP response element binding protein (CREB), a leucine zipper transcription factor, inhibits ROS production and inhibits severe ischemic injury by upregulating brain-derived neurotrophic factor (BDNF) and Bcl-2 (Kitagawa, 2007). The role of lncRNA AK046177 has not been elucidated, though in MCAO rats, inhibiting AK046177 expression significantly alleviates I/R- or OGD/R-mediated neuronal injury. This neuroprotective effect after cerebral ischemia injury occurs *via* AK046177 inhibition, while increases cAMP synthesis, promotes CREB expression and phosphorylation, stimulates Nrf2 activation, and attenuates I/R- or OGD/R- mediated injury (Wang et al., 2020a).

The lncRNA SNHG7 is downregulated in OGD-treated neurons. SNHG7 expression reduces OGD-induced cell damage. Increased SNHG7 expression reverses N2a cell viability during OGD, promotes SOD and CAT activity, and decreases OGD-triggered MDA and ROS production. FGF9, a target of miR-134-5p, represses OGD/R-induced cell damage by promoting cell viability and repressing cell apoptosis (Gao et al., 2020). SNHG7 overexpression protects against OGD-induced neuronal damage by modulating cytotoxicity, cell viability, apoptosis, and oxidative stress. The underlying molecular mechanism is that SNHG7 stimulates FGF9 expression by associating with miR-134-5p (Sun et al., 2021).

In summary, multiple lncRNAs are involved in the pathogenesis of AIS through oxidative stress. Regulating lncRNAs expression has neuroprotective effects in AIS cells and animal models. In addition, most of these lncRNAs regulate the expression of their downstream mRNAs by sponging their target miRNAs, which regulates oxidative stress (Zhang et al., 2020c). These recent studies provide a new mechanism for lncRNAs to participate in AIS pathogenesis and suggest potential novel therapeutic strategies for AIS.

LncRNAs Mediating Oxidative Stress in Alzheimer's Disease

Oxidative stress plays an important role in AD pathogenesis. Excessive oxidative stress causes lipid peroxidation, protein nitrification, and nucleic acid destruction, which affects the synaptic capacity of neurons and even leads to apoptosis (Jiang et al., 2016a). When amyloid (Aβ) is irreversibly deposited in brain tissue, oxygen free radicals are produced, which causes oxidative stress, resulting in neuronal dysfunction, metabolic disorder, and a significant decline in learning, cognition, and memory (Cheignon et al., 2018). Aβ activates *N*-methyl-D-aspartic acid receptors to promote oxygen free radical production, thereby inducing neuronal damage (Shelat et al., 2008). *In vitro* cultured neurons exposed to Aβ have increased lipid peroxidation and hydrogen peroxide levels. Antioxidants may inhibit Aβ aggregation (Meske et al., 2008). In addition, Aβ can inactivate antioxidant enzymes, which induces ROS generation and forms a positive feedback pathway to aggravate oxidative stress in the nervous system (Dessalew et al., 2007). Moreover, oxidative stress activates glycogen synthetic kinase (GSK-3), which is an isomer of Tau protein kinase. Therefore, oxidative stress also promotes Tau protein phosphorylation, resulting in neurological impairment (Rönnemaa et al., 2008).

LncRNAs may antagonize Aβ neurotoxicity through various mechanisms, including antioxidant activity. In hippocampal neurons, Aβ25-35 treatment induces oxidative stress, which is indicated by significantly decreased SOD and GSH-Px activity and increased MDA levels. XIST knockdown alleviates the effects of Aβ25-35 treatment on SOD, GSH-Px, and MDA levels. Studies investigating the underlying mechanism by which XIST functions suggest that XIST exerts regulatory functions by binding to miR-132 and upregulating its expression. Importantly, miR-132 has been reported to play a neuroprotective role against oxidative stress (Wong et al., 2013; Wang et al., 2018b).

Aβ25-35 upregulates H19 and downregulates miR-129 in PC12 cells. Further, silencing H19 and upregulating miR-129 improves cell viability and represses apoptosis in PC12 cells stimulated by Aβ25-35 in AD. This protective effect was partly achieved by two ncRNAs, elevated SOD and CAT expression, and decreased MDA expression (Zhang et al., 2021).

The lncRNA BDNF-AS, a natural antisense transcript to BDNF, negatively modulates BDNF *in vitro* and *in vivo* (Modarresi et al., 2012). In Aβ25-35-induced PC12 cells, ROS production is significantly increased, MDA activity is substantially elevated, and SOD and CAT activity are dramatically decreased. Silencing BDNF-AS reverses the Aβ25-35 induced oxidative stress response, suggesting that BDNF-AS may participate in AD development and progression *via* oxidative stress (Guo et al., 2018). A previous study suggests that BDNF protects neurons against 3-nitropropionic acid-induced oxidative stress by increasing sestrin2 expression and decreasing ROS

formation (Wu et al., 2016). Therefore, silencing BDNF-AS may exert anti-oxidative effects by increasing BDNF expression.

Wilms' tumor suppressor (WT1) is highly expressed in AD and promote apoptosis, which leads to neurological failure (Lovell et al., 2003). The lncRNA WT1-AS, a natural antisense transcript to WT1, negatively modulates WT1. In Aβ25-35-induced SH-SY5Y cells, WT1-AS is downregulated. In contrast, overexpressing WT1-AS significantly decreases ROS, MDA, and LDH levels in SH-SY5Y cells, while SOD and GSH-Px are markedly elevated. miR-375, which is a target of WT1, targets the 3′ UTR of SIX4. Overexpressing WT1-AS inhibits miR-375 expression by suppressing WT1, which prevents AD occurrence and development (Wang et al., 2020b).

LncRNA taurine upregulated gene 1 (TUG1) functions by regulating miRNA expression. TUG1 silencing strengthens antioxidant ability and depresses neuronal apoptosis in an Aβ25-35-induced AD mouse model. Further, TUG1 might perform antioxidant functions by targeting miR-15a to inhibit Rho-associated protein kinase 1 (ROCK1) (Li et al., 2020).

Although several studies confirm that oxidative stress is an important mechanism of AD pathogenesis, the number of studies on lncRNAs that regulate oxidative stress during AD pathogenesis is limited. In Aβ25-35-induced AD cells and animal models, XIST, H19, BDNF-As, WT1-As, and TUG1 regulate oxidative stress by modulating target miRNA or *via* other pathways. By investigating the regulatory mechanism of these lncRNAs, we will further understand the role of lncRNAs in AD pathogenesis and identify potential therapeutic strategies for AD.

LncRNAs Mediating Oxidative Stress in Parkinson's Disease

Parkinson's disease is a progressive age-related neurodegenerative disease (Andrei Surguchov, 2022). The main pathological features of PD are the loss of dopaminergic neurons in the substantia nigra dense region and the formation of Lewy bodies (Samii et al., 2004). The main clinical manifestations of PD are static tremor, myotonia, bradykinesia, and abnormal posture and gait. These symptoms are often accompanied by non-motor symptoms such as anxiety, depression, and cognitive decline (Khoo et al., 2013; Lopiano et al., 2016). The pathogenesis of PD is still unclear. Recent studies have confirmed that oxidative stress plays an important role in PD occurrence and development (Gaki and Papavassiliou, 2014). Oxidative stress damages neurons through free radicals. Substantia nigra dopaminergic neurons are particularly susceptible to oxidative stress (Rodriguez-Pallares et al., 2012). ROS target mitochondria, resulting in dysfunction and reduced energy production. Dopaminergic neurons in the substantia nigra have super-long unmyelinated axons and high energy consumption (Pissadaki and Bolam, 2013). In patients with PD, substantia nigra dopamine neurons under oxidative stress have energy demands that exceeds the energy supply, which eventually kills the damaged neurons. In the remaining dopaminergic neurons, cellular metabolism is accelerated due to compensatory dopamine synthesis, which produces more free radicals and further increases oxidative stress (Dias et al., 2013). Furthermore, oxidative deamination of dopamine by monoamine oxidase (MAO) produces H_2O_2 as a by-product, while enzymatic oxidation of the electron-rich catechin portion of dopamine by tyrosinase, cycloxase, and other enzymes produces O_2^- (Muñoz et al., 2012). Spontaneous dopamine oxidation can also occur through interactions with unstable iron and other biomaterials, thereby producing ROS (H_2O_2, O_2^-, and OH) (Sun et al., 2018). Considering the significant role of oxidative stress in PD pathogenesis, ameliorating oxidative stress by regulating lncRNAs can deepen our understanding of PD pathogenesis and elucidate new treatments.

LncRNA myocardial infarction-associated transcript (MIAT) was originally isolated as a candidate gene for myocardial infarction. The over-expanding role of MIAT in various human diseases has been recently revealed, including PD (Shen et al., 2021). MIAT is highly expressed in 1-methyl-4-phenyl-1,2,3,6-tetrahydropyridine (MPTP)-treated mice and 1-methyl-4-phenylpyridinium ion (MPP +)-treated cells. Downregulating MIAT promotes SOD and GSH production, but inhibits MDA in MPP + -treated cells. Blocking MIAT increases cell viability and inhibits cell apoptosis. Additionally, MIAT enhances Nrf2 expression by modulating its target, miR-221-3p (Lang et al., 2022).

The lncRNA non-coding RNA activated by DNA damage (NORAD) is a highly conserved lncRNA that is necessary for genome stability. Dysregulated NORAD is present in various cancer types (Soghli et al., 2021). In MPP + -induced neuroblastoma cells, reduced NORAD expression is observed. Interestingly, NORAD overexpression relieves cytotoxicity and inflammatory responses of neuroblastoma cells after MPP + treatment. NORAD upregulation also inhibits MPP + -induced LDH increase, reduces increased ROS activity, and suppresses SOD activity in SK-N-SH and SK-N-AS cells. The inhibition of oxidative stress by NORAD upregulation is partly achieved by regulating the miR-204-5p/solute carrier family 5-member 3 (SLC5A3) axis (Zhou et al., 2020).

In MPTP-induced PD rat models, silencing RMST also has anti-oxidative stress effects. Silencing RMST could reduce inflammatory responses and suppress neuron apoptosis in the substantia nigra of PD rats. In addition, silencing RMST increases SOD, CAT, and GSH-Px activity, reduces NOS activity, and decreases MDA and NO content. These results suggest that RMST could be neuroprotective against dopamine neurons injury caused by oxidative stress (Ma et al., 2021).

miR-205-5p plays a protective role during PD. Upregulation miR-205-5p inhibits the expression of leucine-rich repeat kinase 2 (LRRK2) and prevents neurite outgrowth defects induced by the R1441G LRRK2 mutation, which indicates a major role of miR-205-5p in neuron survival (Cho et al., 2013). AL049437 is a "sponge" or an endogenous competitor of miR-205-5p. Silencing AL049437 promotes the protective function of miR-205-5p, suppresses apoptosis of SH-SY5Y cells, and reduces oxidative stress (Zhang et al., 2020b).

As an activator of the antioxidant pathway, overexpression of MALAT1 was observed in MPTP-treated PD mice. MALAT1

contributes to inflammasome activation in microglial cells, which triggers neuronal injury by interacting with enhancer of zeste homolog 2 (EZH2) to regulate Nrf2-mediated antioxidative responses. Reducing MALAT1 increases antioxidant capacity and attenuates oxidative stress damage (Cai et al., 2020).

Long non-coding RNA-p21 (lnc-p21) regulates mRNA translation, gene expression, protein stability, and p53-dependent apoptosis (Hall et al., 2015). Lnc-p21 is upregulated in PD and remains overexpressed during PD progression (Kraus et al., 2017). In human neuroblastoma SH-SY5Y cells treated with MPP +, lnc-p21 is highly expressed. Knocking down lnc-p21 mitigates MPP +-induced oxidative stress and neuroinflammation, as evidenced by decreased ROS generation, increased SOD activity, and decreased interleukin 6 (IL-6), tumor necrosis factor α (TNF-α) and IL-1β levels. TRPM2 is activated by oxidative stress, resulting in elevated intracellular Ca^{2+} concentrations (Nazıroğlu, 2011). Mechanistically, lnc-p21 knockdown exerts anti-oxidative function by downregulating TRPM2 expression *via* sponging miR-625, the target of lnc-p21 (Ding et al., 2019).

Gene microarray analysis revealed decreased lncRNA-T199678 expression in an exogenous α-synuclein-induced SH-SY5Y cellular model of PD (Lin et al., 2018). In α-synuclein-induced SH-SY5Y cellular PD models, ROS levels are significantly increased, while overexpressing lncRNA-T199678 reverses intracellular oxidative stress induced by exogenous α-synuclein. miR-101-3p is a potential target for lncRNA-T199678 and binds with α-synuclein at a specific 3′ UTR binding site. Therefore, overexpressing lncRNA-T199678 inhibits α-synuclein-induced neuronal damage *via* regulating intracellular oxidative stress, cell cycle dysfunction, and apoptosis by targeting miR-101-3p (Bu et al., 2020).

In vitro and *in vivo* studies of PD suggest that lncRNAs regulate miRNA participation in oxidative stress through endogenous competition mechanisms and directly regulate SOD and LDH levels. Moreover, Nrf2 is a main target of lncRNA regulation. Therefore, lncRNAs may be involved in regulating oxidative stress in PD through various mechanisms and may become a potential target for PD treatment.

LncRNAs Mediating Oxidative Stress in Spinal Cord Injury

Spinal cord injury is a common CNS disorder that is characterized by different degrees of sensorimotor dysfunction, which often leads to paraplegia, quadriplegia, and other pathological changes that seriously affect the quality of life in a patient (James et al., 2019). Oxidative stress plays an important role in SCI pathogenesis. Previous studies showed that abundant ROS are generated immediately after SCI, which can induce oxidative stress not neutralized in time. More importantly, oxidative stress is involved in secondary events, such as excitatory toxicity, inflammatory responses, and neuronal and glial apoptosis (Fatima et al., 2015). Taking effective measures to prevent or decrease oxidative stress after injury is an effective measure to intervene in SCI. For each link of free radical chain reactions, an appropriate inhibitor or free radical scavenger can achieve effective anti-oxidation (Kikuchi et al., 2013). At present, various antioxidants have been studied. Some results suggest that lncRNAs may affect oxidative stress through various mechanisms and play a therapeutic role in SCI.

LncRNA cancer susceptibility candidate 9 (CASC9) has been extensively studied in various cancers and functions as an oncogene in bladder cancer and esophageal squamous cell carcinoma (Huo et al., 2020; Zhao et al., 2020). Lipopolysaccharide (LPS) downregulates CASC9 and upregulates its derived miR-383-5p in LPS-induced PC12 cells. CASC9-derived miR-383-5p targets the 3′ UTR of LDHA to downregulate Nrf2 and HO-1 proteins. CASC9 also exert functions through miRNAs. Overexpressing CASC9 attenuates oxidative stress and inflammation in an SCI rat model. This antioxidant function may occur by targeting miR-383-5p to inhibit Nrf2/HO-1 signaling (Guan and Wang, 2021).

lncRNA growth arrest specific transcript 5 (GAS5) regulates the development of some CNS disorders. For instance, GAS5 was identified as a potential tumor suppressor in glioma (Zhao et al., 2015). Overexpressing GAS5 facilitates cell apoptosis induced by OGD in MCAO mouse models by reducing mitogen activated protein kinase 4 (MAP4K4) expression (Deng et al., 2020). The CELF2/VAV1 pathway might coordinate with GAS5 to enhance OGD-triggered oxidative stress and cell injury. GAS5 knockdown downregulates VAV1 expression by recruiting CELF2 to the coding region of VAV1 mRNA, which mitigates SCI by reducing oxidative stress and caspase-3 activity in rat models (Wang et al., 2021a).

LncRNA tectonic family member 2 (TCTN2) is a functional RNA that is involved in autophagy in neurons, thereby modulating neuronal apoptosis and improving SCI (Ren et al., 2019). Insulin-like growth factor 1 receptor (IGF1R) has an active role in neural stem cell-mediated motor recovery after spinal cord transection (Hwang et al., 2018). In the spinal cord of SCI model rats and LPS-stimulated PC12 cells, increased miR-329-3p levels are observed. Inhibiting miR-329-3p reverses LPS-induced neuronal apoptosis, oxidative stress, and inflammation by upregulating IGF1R. miR-329-3p is a target of TCTN2. Thus, exosomes derived from TCTN2-modified mesenchymal stem cells may improve SCI *via* the miR-329-3p/IGF1R axis (Liu et al., 2022).

LncRNA SOX2 overlapping transcript (SOX2OT) is linked to the development of multiple human cancers (Zhang et al., 2016; Zhan et al., 2020). Neurod1 is involved in SCI-stimulated oxidative stress and inflammatory damage (Fu et al., 2018). SOX2OT was identified as a miR-331-3p sponge that positively regulates Neurod1 expression. SOX2OT knockdown ameliorates LPS-mediated inflammation, improves cell viability, reduces apoptosis, and inhibits oxidative stress in PC12 cells by modulating the miR-331-3p/Neurod1 axis and activating Janus kinase signaling (Li et al., 2021b).

LncRNAs Mediating Oxidative Stress in Other Disorders

Oxidative stress is closely related to cancer cell survival and the development of glioma (Gilbert et al., 2014). Excessive ROS

levels produced by oxidative stress can affect cell function and change gene expression, which may promote glioma progression (Kim et al., 2014). LncRNA H19 encodes a 2.3-kb long transcript and is a carcinogenic lncRNA in several cancers, including glioma (Jiang et al., 2016b). Overexpressing H19 in gliomas can contribute to malignant transformation, promote tumor proliferation, invasion, infiltration, and chemoresistance (Jia et al., 2016). In glioma cell models, H19 levels are induced by oxidative stress and are increased in U251 and LN229 cells. Meanwhile, overexpressing H19 in U251 and LN229 cells causes temozolomide resistance, which indicates that H19 confers temozolomide resistance to glioma cells (Duan et al., 2018).

Epilepsy is a disease in which epigenetic mechanisms play an important role in the pathogenesis (Surguchov et al., 2017). Temporal lobe epilepsy (TLE) is a common CNS disorder that is characterized by recurrent seizures (Chen et al., 2016). LncRNA maternally expressed gene 3 (MEG3) is a well-known tumor suppressor gene (Wang et al., 2012). In TLE rat models, MEG3 expression is downregulated along with high MDA content and decreased SOD activity. Upregulating MEG3 enhances cell viability, reverses oxidative stress, and inhibits apoptosis through activating the PI3K/AKT/mTOR pathway in TLE. These findings may contribute to developing new therapeutic targets for epilepsy (Zhang et al., 2020a).

CONCLUSION

The cellular and molecular changes underlying CNS injuries provide a wealth of potential biomarkers and therapeutic targets. Oxidative stress plays an important role in the occurrence and development of CNS disorders. In addition, secondary pathological damage caused by oxidative stress, including neuroinflammatory responses, mitochondrial damage, and increased apoptosis, are the main cause of exacerbated CNS disorders. Therefore, regulating oxidative stress in CNS disorders may help alleviate neurological damage and provide a new therapeutic strategy for CNS disorders.

In recent years, accumulating studies show that lncRNAs, which were originally considered "junk" and "noise," are widely involved in multiple human diseases, including CNS disorders and are associated with oxidative stress. We demonstrate that many lncRNAs regulate oxidative stress by interacting with miRNAs, thereby regulating SOD activity, MDA expression levels, and other functions. In addition, some lncRNAs directly regulate antioxidant pathways (such as Nrf2/HO-1 signaling) to regulate the pathogenesis of CNS disorders. These oxidative stress-related lncRNAs may be potential key biomarkers and therapeutic targets of CNS disorders (**Figure 5**). Further, these lncRNAs may provide a novel strategy for disease diagnosis and treatment. Future studies will elucidate the precise mechanisms by which lncRNAs regulate oxidative stress in CNS disorders.

AUTHOR CONTRIBUTIONS

YZ and XX wrote the manuscript. YZ produced the figures. XX edited and revised the review. Both authors have read and approved the final manuscript.

REFERENCES

Amantea, D., and Bagetta, G. (2017). Excitatory and inhibitory amino acid neurotransmitters in stroke: from neurotoxicity to ischemic tolerance. *Curr. Opin. Pharmacol.* 35, 111–119. doi: 10.1016/j.coph.2017.07.014

Anderson, M. A., Burda, J. E., Ren, Y., Ao, Y., O'shea, T. M., Kawaguchi, R., et al. (2016). Astrocyte scar formation aids central nervous system axon regeneration. *Nature* 532, 195–200. doi: 10.1038/nature17623

Andrei Surguchov (2022). "Biomarkers in Parkinson's disease," in *Neurodegenerative Diseases Biomarkers*, eds P. V. Peplow, B. Martinez, and T. A. Gennarelli (Berlin: Springer), 155–180. doi: 10.1016/j.nicl.2017.09.009

Baird, L., and Yamamoto, M. (2020). The molecular mechanisms regulating the KEAP1-NRF2 Pathway. *Mol. Cell. Biol.* 40:e00099–20. doi: 10.1128/MCB.00099-20

Bu, L. L., Xie, Y. Y., Lin, D. Y., Chen, Y., Jing, X. N., Liang, Y. R., et al. (2020). LncRNA-T199678 mitigates α-synuclein-induced dopaminergic neuron injury via miR-101-3p. *Front. Aging Neurosci.* 12:599246. doi: 10.3389/fnagi.2020.599246

Burmistrova, O., Olias-Arjona, A., Lapresa, R., Jimenez-Blasco, D., Eremeeva, T., Shishov, D., et al. (2019). Targeting PFKFB3 alleviates cerebral ischemia-reperfusion injury in mice. *Sci. Rep.* 9:11670. doi: 10.1038/s41598-019-48196-z

Cai, L. J., Tu, L., Huang, X. M., Huang, J., Qiu, N., Xie, G. H., et al. (2020). LncRNA MALAT1 facilitates inflammasome activation via epigenetic suppression of Nrf2 in Parkinson's disease. *Mol. Brain* 13, 130. doi: 10.1186/s13041-020-00656-8

Cao, X., Ma, J., and Li, S. (2022). Mechanism of lncRNA SNHG16 in oxidative stress and inflammation in oxygen-glucose deprivation and reoxygenation-induced SK-N-SH cells. *Bioengineered* 13, 5021–5034. doi: 10.1080/21655979.2022.2026861

Cheignon, C., Tomas, M., Bonnefont-Rousselot, D., Faller, P., Hureau, C., and Collin, F. (2018). Oxidative stress and the amyloid beta peptide in Alzheimer's disease. *Redox Biol.* 14, 450–464. doi: 10.1016/j.redox.2017.10.014

Chen, H., Yoshioka, H., Kim, G. S., Jung, J. E., Okami, N., Sakata, H., et al. (2011). Oxidative stress in ischemic brain damage: mechanisms of cell death and potential molecular targets for neuroprotection. *Antioxid. Redox Signal.* 14, 1505–1517. doi: 10.1089/ars.2010.3576

Chen, J., Liu, X. M., Yue, X., and Chen, S. Z. (2016). The clinical efficacy and safety of levetiracetam add-on therapy for child refractory epilepsy. *Eur. Rev. Med. Pharmacol. Sci.* 20, 2689–2694.

Chen, Y., Li, Z., Chen, X., and Zhang, S. (2021a). Long non-coding RNAs: from disease code to drug role. *Acta Pharm Sin B* 11, 340–354. doi: 10.1016/j.apsb.2020.10.001

Chen, Y., Liu, W., Chen, M., Sun, Q., Chen, H., and Li, Y. (2021b). Up-regulating lncRNA OIP5-AS1 protects neuron injury against cerebral hypoxia-ischemia induced inflammation and oxidative stress in microglia/macrophage through activating CTRP3 via sponging miR-186-5p. *Int. Immunopharmacol.* 92:107339. doi: 10.1016/j.intimp.2020.107339

Chen, Z., Luo, Y., Yang, W., Ding, L., Wang, J., Tu, J., et al. (2015). Comparison analysis of dysregulated LncRNA profile in mouse plasma and liver after hepatic ischemia/reperfusion injury. *PLoS One* 10:e0133462. doi: 10.1371/journal.pone.0133462

Cho, H. J., Liu, G., Jin, S. M., Parisiadou, L., Xie, C., Yu, J., et al. (2013). MicroRNA-205 regulates the expression of Parkinson's disease-related leucine-rich repeat kinase 2 protein. *Hum. Mol. Genet.* 22, 608–620. doi: 10.1093/hmg/dds470

Chu, P. M., Yu, C. C., Tsai, K. L., and Hsieh, P. L. (2022). Regulation of oxidative stress by long non-coding RNAs in vascular complications of diabetes. *Life (Basel)* 12, 274. doi: 10.3390/life12020274

Chuang, D. Y., Simonyi, A., Kotzbauer, P. T., Gu, Z., and Sun, G. Y. (2015). Cytosolic phospholipase A2 plays a crucial role in ROS/NO signaling during microglial activation through the lipoxygenase pathway. *J. Neuroinflamm.* 12, 199. doi: 10.1186/s12974-015-0419-0

Costa, L. G., Garrick, J. M., Roquè, P. J., and Pellacani, C. (2016). Mechanisms of neuroprotection by quercetin: counteracting oxidative stress and more. *Oxid. Med. Cell. Longev.* 2016, 2986796. doi: 10.1155/2016/2986796

Dahariya, S., Paddibhatla, I., Kumar, S., Raghuwanshi, S., Pallepati, A., and Gutti, R. K. (2019). Long non-coding RNA: classification, biogenesis and functions in blood cells. *Mol. Immunol.* 112, 82–92. doi: 10.1016/j.molimm.2019.04.011

Deng, J., Deng, H., Liu, C., Liang, Y., and Wang, S. (2018). Long non-coding RNA OIP5-AS1 functions as an oncogene in lung adenocarcinoma through targeting miR-448/Bcl-2. *Biomed. Pharmacother.* 98, 102–110. doi: 10.1016/j.biopha.2017.12.031

Deng, Y., Chen, D., Gao, F., Lv, H., Zhang, G., Sun, X., et al. (2020). Silencing of long non-coding RNA GAS5 suppresses neuron cell apoptosis and nerve injury in ischemic stroke through inhibiting DNMT3B-dependent MAP4K4 methylation. *Transl. Stroke Res.* 11, 950–966. doi: 10.1007/s12975-019-00770-3

Deniz, E., and Erman, B. (2017). Long noncoding RNA (lincRNA), a new paradigm in gene expression control. *Funct. Integr. Genomics* 17, 135–143. doi: 10.1007/s10142-016-0524-x

Dessalew, N., Patel, D. S., and Bharatam, P. V. (2007). 3D-QSAR and molecular docking studies on pyrazolopyrimidine derivatives as glycogen synthase kinase-3beta inhibitors. *J. Mol. Graph. Model.* 25, 885–895. doi: 10.1016/j.jmgm.2006.08.009

Di, G., Yang, X., Cheng, F., Liu, H., and Xu, M. (2021). CEBPA-AS1 knockdown alleviates oxygen-glucose deprivation/reperfusion-induced neuron cell damage by the MicroRNA 24-3p/BOK axis. *Mol. Cell. Biol.* 41, e0006521. doi: 10.1128/MCB.00065-21

Dias, V., Junn, E., and Mouradian, M. M. (2013). The role of oxidative stress in Parkinson's disease. *J. Parkinsons Dis.* 3, 461–491.

Ding, X. M., Zhao, L. J., Qiao, H. Y., Wu, S. L., and Wang, X. H. (2019). Long non-coding RNA-p21 regulates MPP(+)-induced neuronal injury by targeting miR-625 and derepressing TRPM2 in SH-SY5Y cells. *Chem. Biol. Interact.* 307, 73–81. doi: 10.1016/j.cbi.2019.04.017

Duan, S., Li, M., Wang, Z., Wang, L., and Liu, Y. (2018). H19 induced by oxidative stress confers temozolomide resistance in human glioma cells via activating NF-κB signaling. *Onco Targets Ther.* 11, 6395–6404.

Esteller, M. (2011). Non-coding RNAs in human disease. *Nat. Rev. Genet.* 12, 861–874.

Fatima, G., Sharma, V. P., Das, S. K., and Mahdi, A. A. (2015). Oxidative stress and antioxidative parameters in patients with spinal cord injury: implications in the pathogenesis of disease. *Spinal Cord* 53, 3–6. doi: 10.1038/sc.2014.178

Fu, X., Shen, Y., Wang, W., and Li, X. (2018). MiR-30a-5p ameliorates spinal cord injury-induced inflammatory responses and oxidative stress by targeting neurod 1 through MAPK/ERK signalling. *Clin. Exp. Pharmacol. Physiol.* 45, 68–74. doi: 10.1111/1440-1681.12856

Gaki, G. S., and Papavassiliou, A. G. (2014). Oxidative stress-induced signaling pathways implicated in the pathogenesis of Parkinson's disease. *Neuromolecular Med.* 16, 217–230. doi: 10.1007/s12017-014-8294-x

Gao, X. Z., Ma, R. H., and Zhang, Z. X. (2020). miR-339 promotes hypoxia-induced neuronal apoptosis and impairs cell viability by targeting FGF9/CACNG2 and mediating MAPK pathway in ischemic stroke. *Front. Neurol.* 11:436. doi: 10.3389/fneur.2020.00436

Gilbert, M. R., Liu, Y., Neltner, J., Pu, H., Morris, A., Sunkara, M., et al. (2014). Autophagy and oxidative stress in gliomas with IDH1 mutations. *Acta Neuropathol.* 127, 221–233. doi: 10.1007/s00401-013-1194-6

Gong, C. Y., Tang, R., Nan, W., Zhou, K. S., and Zhang, H. H. (2020). Role of SNHG16 in human cancer. *Clin. Chim. Acta* 503, 175–180. doi: 10.1016/j.cca.2019.12.023

Guan, C., and Wang, Y. (2021). LncRNA CASC9 attenuates lactate dehydrogenase-mediated oxidative stress and inflammation in spinal cord injury via sponging miR-383-5p. *Inflammation* 44, 923–933. doi: 10.1007/s10753-020-01387-7

Guo, C. C., Jiao, C. H., and Gao, Z. M. (2018). Silencing of LncRNA BDNF-AS attenuates Aβ(25-35)-induced neurotoxicity in PC12 cells by suppressing cell apoptosis and oxidative stress. *Neurol. Res.* 40, 795–804. doi: 10.1080/01616412.2018.1480921

Guo, Y., Zhong, J., Wu, F., and Zhan, Z. (2020). Long noncoding RNA MACC1-AS1 promotes the stemness of hepatocellular carcinoma cells by antagonizing miR-145. *J. Int. Med. Res.* 48, 300060520920411. doi: 10.1177/0300060520920411

Hall, J. R., Messenger, Z. J., Tam, H. W., Phillips, S. L., Recio, L., and Smart, R. C. (2015). Long noncoding RNA lincRNA-p21 is the major mediator of UVB-induced and p53-dependent apoptosis in keratinocytes. *Cell Death Dis.* 6, e1700. doi: 10.1038/cddis.2015.67

He, C., Wang, K., Gao, Y., Wang, C., Li, L., Liao, Y., et al. (2021). Roles of noncoding RNA in reproduction. *Front. Genet.* 12:777510. doi: 10.3389/fgene.2021.777510

Hombach, S., and Kretz, M. (2016). Non-coding RNAs: classification, biology and functioning. *Adv. Exp. Med. Biol.* 937, 3–17. doi: 10.1007/978-3-319-42059-2_1

Huo, W., Tan, D., and Chen, Q. (2020). CASC9 facilitates cell proliferation in bladder cancer by regulating CBX2 expression. *Nephron* 144, 388–399. doi: 10.1159/000507828

Hwang, D. H., Park, H. H., Shin, H. Y., Cui, Y., and Kim, B. G. (2018). Insulin-like growth factor-1 receptor dictates beneficial effects of treadmill training by regulating survival and migration of neural stem cell grafts in the injured spinal cord. *Exp. Neurobiol.* 27, 489–507. doi: 10.5607/en.2018.27.6.489

Hybertson, B. M., Gao, B., Bose, S. K., and Mccord, J. M. (2011). Oxidative stress in health and disease: the therapeutic potential of Nrf2 activation. *Mol. Aspects Med.* 32, 234–246. doi: 10.1016/j.mam.2011.10.006

James, S. L., Theadom, A., Ellenbogen, R. G., Bannick, M. S., Montjoy-Venning, W., Lucchesi, L. R., et al. (2019). Global, regional, and national burden of traumatic brain injury and spinal cord injury, 1990-2016: a systematic analysis for the global burden of disease study 2016. *Lancet Neurol.* 18, 56–87. doi: 10.1016/S1474-4422(18)30415-0

Jakubczyk, K., Dec, K., Kałduńska, J., Kawczuga, D., Kochman, J., and Janda, K. (2020). Reactive oxygen species - sources, functions, oxidative damage. *Pol. Merkur. Lekarski.* 48, 124–127.

Jia, P., Cai, H., Liu, X., Chen, J., Ma, J., Wang, P., et al. (2016). Long non-coding RNA H19 regulates glioma angiogenesis and the biological behavior of glioma-associated endothelial cells by inhibiting microRNA-29a. *Cancer Lett.* 381, 359–369. doi: 10.1016/j.canlet.2016.08.009

Jiang, T., Sun, Q., and Chen, S. (2016a). Oxidative stress: a major pathogenesis and potential therapeutic target of antioxidative agents in Parkinson's disease and Alzheimer's disease. *Prog. Neurobiol.* 147, 1–19. doi: 10.1016/j.pneurobio.2016.07.005

Jiang, X., Yan, Y., Hu, M., Chen, X., Wang, Y., Dai, Y., et al. (2016b). Increased level of H19 long noncoding RNA promotes invasion, angiogenesis, and stemness of glioblastoma cells. *J. Neurosurg.* 124, 129–136.

Khoo, T. K., Yarnall, A. J., Duncan, G. W., Coleman, S., O'brien, J. T., Brooks, D. J., et al. (2013). The spectrum of nonmotor symptoms in early Parkinson disease. *Neurology* 80, 276–281. doi: 10.1212/WNL.0b013e31827deb74

Khoshnam, S. E., Winlow, W., Farzaneh, M., Farbood, Y., and Moghaddam, H. F. (2017). Pathogenic mechanisms following ischemic stroke. *Neurol. Sci.* 38, 1167–1186. doi: 10.1007/s10072-017-2938-1

Kikuchi, K., Tancharoen, S., Takeshige, N., Yoshitomi, M., Morioka, M., Murai, Y., et al. (2013). The efficacy of edaravone (radicut), a free radical scavenger, for cardiovascular disease. *Int. J. Mol. Sci.* 14, 13909–13930. doi: 10.3390/ijms140713909

Kim, S. H., Kwon, C. H., and Nakano, I. (2014). Detoxification of oxidative stress in glioma stem cells: mechanism, clinical relevance, and therapeutic development. *J. Neurosci. Res.* 92, 1419–1424. doi: 10.1002/jnr.23431

Kitagawa, K. (2007). CREB and cAMP response element-mediated gene expression in the ischemic brain. *FEBS J.* 274, 3210–3217. doi: 10.1111/j.1742-4658.2007.05890.x

Klimiuk, A., Maciejczyk, M., Choromańska, M., Fejfer, K., Waszkiewicz, N., and Zalewska, A. (2019). Salivary redox biomarkers in different stages of dementia severity. *J. Clin. Med.* 8, 840. doi: 10.3390/jcm8060840

Kraus, T. F. J., Haider, M., Spanner, J., Steinmaurer, M., Dietinger, V., and Kretzschmar, H. A. (2017). Altered long noncoding RNA expression precedes

the course of Parkinson's disease-a preliminary report. *Mol. Neurobiol.* 54, 2869–2877. doi: 10.1007/s12035-016-9854-x

Lang, Y., Zhang, H., Yu, H., Li, Y., Liu, X., and Li, M. (2022). Long non-coding RNA myocardial infarction-associated transcript promotes 1-Methyl-4-phenylpyridinium ion-induced neuronal inflammation and oxidative stress in Parkinson's disease through regulating microRNA-221-3p/ transforming growth factor /nuclear factor E2-related factor 2 axis. *Bioengineered* 13, 930–940. doi: 10.1080/21655979.2021.2015527

Li, J., Wang, N., Nie, H., Wang, S., Jiang, T., Ma, X., et al. (2022). Long non-coding RNA RMST worsens ischemic stroke via MicroRNA-221-3p/PIK3R1/TGF-β Signaling pathway. *Mol. Neurobiol.* 59, 2808–2821. doi: 10.1007/s12035-021-02632-2

Li, K., Yao, T., Zhang, Y., Li, W., and Wang, Z. (2021a). NEAT1 as a competing endogenous RNA in tumorigenesis of various cancers: role, mechanism and therapeutic potential. *Int. J. Biol. Sci.* 17, 3428–3440. doi: 10.7150/ijbs.62728

Li, R., Li, X., Huang, Y., Qiu, H., Li, L., and Bi, Z. (2021b). LncRNA SOX2OT knockdown alleviates lipopolysaccharide-induced damage of PC12 cells by regulating miR-331-3p/Neurod1 axis. *World Neurosurg.* 147, e293–e305. doi: 10.1016/j.wneu.2020.12.049

Li, X., Wang, S. W., Li, X. L., Yu, F. Y., and Cong, H. M. (2020). Knockdown of long non-coding RNA TUG1 depresses apoptosis of hippocampal neurons in Alzheimer's disease by elevating microRNA-15a and repressing ROCK1 expression. *Inflamm. Res.* 69, 897–910. doi: 10.1007/s00011-020-01364-8

Lin, D., Liang, Y., Jing, X., Chen, Y., Lei, M., Zeng, Z., et al. (2018). Microarray analysis of an synthetic α-synuclein induced cellular model reveals the expression profile of long non-coding RNA in Parkinson's disease. *Brain Res.* 1678, 384–396. doi: 10.1016/j.brainres.2017.11.007

Liu, J., Lin, M., Qiao, F., and Zhang, C. (2022). Exosomes derived from lncRNA TCTN2-modified mesenchymal stem cells improve spinal cord injury by miR-329-3p/IGF1R axis. *J. Mol. Neurosci.* 72, 482–495. doi: 10.1007/s12031-021-01914-7

Liu, L., Zheng, B., and Wang, Z. (2021). Protective effects of the knockdown of lncRNA AK139328 against oxygen glucose deprivation/reoxygenation-induced injury in PC12 cells. *Mol. Med. Rep.* 24, 621. doi: 10.3892/mmr.2021.12260

Lopiano, L., Modugno, N., Marano, P., Sensi, M., Meco, G., Cannas, A., et al. (2016). Motor outcomes in patients with advanced Parkinson's disease treated with levodopa/carbidopa intestinal gel in Italy: an interim analysis from the GREENFIELD observational study. *Neurol. Sci.* 37, 1785–1792. doi: 10.1007/s10072-016-2664-0

Lovell, M. A., Xie, C., Xiong, S., and Markesbery, W. R. (2003). Wilms' tumor suppressor (WT1) is a mediator of neuronal degeneration associated with the pathogenesis of Alzheimer:s disease. *Brain Res.* 983, 84–96. doi: 10.1016/s0006-8993(03)03032-4

Ma, X., Wang, Y., Yin, H., Hua, L., Zhang, X., Xiao, J., et al. (2021). Down-regulated long non-coding RNA RMST ameliorates dopaminergic neuron damage in Parkinson's disease rats via regulation of TLR/NF-κB signaling pathway. *Brain Res. Bull.* 174, 22–30. doi: 10.1016/j.brainresbull.2021.04.026

Maciejczyk, M., Zalewska, A., and Gerreth, A. K. (2020). Salivary redox biomarkers in selected neurodegenerative diseases. *J. Clin. Med.* 9:97. doi: 10.3390/jcm9020497

Meske, V., Albert, F., and Ohm, T. G. (2008). Coupling of mammalian target of rapamycin with phosphoinositide 3-kinase signaling pathway regulates protein phosphatase 2A– and glycogen synthase kinase-3 -dependent phosphorylation of Tau. *J. Biol. Chem.* 283, 100–109. doi: 10.1074/jbc.M704292200

Modarresi, F., Faghihi, M. A., Lopez-Toledano, M. A., Fatemi, R. P., Magistri, M., Brothers, S. P., et al. (2012). Inhibition of natural antisense transcripts in vivo results in gene-specific transcriptional upregulation. *Nat. Biotechnol.* 30, 453–459. doi: 10.1038/nbt.2158

Muñoz, P., Huenchuguala, S., Paris, I., and Segura-Aguilar, J. (2012). Dopamine oxidation and autophagy. *Parkinsons Dis.* 2012:920953. doi: 10.1155/2012/920953

Nazıroğlu, M. (2011). TRPM2 cation channels, oxidative stress and neurological diseases: where are we now? *Neurochem. Res.* 36, 355–366. doi: 10.1007/s11064-010-0347-4

Ouyang, Y. B., Stary, C. M., White, R. E., and Giffard, R. G. (2015). The use of microRNAs to modulate redox and immune response to stroke. *Antioxid. Redox Signal.* 22, 187–202. doi: 10.1089/ars.2013.5757

Park, S., Lim, W., Bazer, F. W., Whang, K. Y., and Song, G. (2019). Quercetin inhibits proliferation of endometriosis regulating cyclin D1 and its target microRNAs in vitro and in vivo. *J. Nutr. Biochem.* 63, 87–100. doi: 10.1016/j.jnutbio.2018.09.024

Pissadaki, E. K., and Bolam, J. P. (2013). The energy cost of action potential propagation in dopamine neurons: clues to susceptibility in Parkinson's disease. *Front. Comput. Neurosci.* 7:13. doi: 10.3389/fncom.2013.00013

Pizzino, G., Irrera, N., Cucinotta, M., Pallio, G., Mannino, F., Arcoraci, V., et al. (2017). Oxidative stress: harms and benefits for human health. *Oxid. Med. Cell. Longev.* 2017, 8416763. doi: 10.1155/2017/8416763

Ren, X. D., Wan, C. X., and Niu, Y. L. (2019). Overexpression of lncRNA TCTN2 protects neurons from apoptosis by enhancing cell autophagy in spinal cord injury. *FEBS Open Bio* 9, 1223–1231. doi: 10.1002/2211-5463.12651

Rodrigo, R., Fernández-Gajardo, R., Gutiérrez, R., Matamala, J. M., Carrasco, R., Miranda-Merchak, A., et al. (2013). Oxidative stress and pathophysiology of ischemic stroke: novel therapeutic opportunities. *CNS Neurol. Disord. Drug Targets* 12, 698–714. doi: 10.2174/18715273113120500015

Rodriguez-Pallares, J., Parga, J. A., Joglar, B., Guerra, M. J., and Labandeira-Garcia, J. L. (2012). Mitochondrial ATP-sensitive potassium channels enhance angiotensin-induced oxidative damage and dopaminergic neuron degeneration. Relevance for aging-associated susceptibility to Parkinson's disease. *Age (Dordr)* 34, 863–880. doi: 10.1007/s11357-011-9284-7

Rönnemaa, E., Zethelius, B., Sundelöf, J., Sundström, J., Degerman-Gunnarsson, M., Berne, C., et al. (2008). Impaired insulin secretion increases the risk of Alzheimer disease. *Neurology* 71, 1065–1071. doi: 10.1212/01.wnl.0000310646.32212.3a

Salim, S. (2017). Oxidative stress and the central nervous system. *J. Pharmacol. Exp. Ther.* 360, 201–205.

Samii, A., Nutt, J. G., and Ransom, B. R. (2004). Parkinson's disease. *Lancet* 363, 1783–1793.

Saussez, S., Marchant, H., Nagy, N., Decaestecker, C., Hassid, S., Jortay, A., et al. (1998). Quantitative glycohistochemistry defines new prognostic markers for cancers of the oral cavity. *Cancer* 82, 252–260.

Scannevin, R. H., Chollate, S., Jung, M. Y., Shackett, M., Patel, H., Bista, P., et al. (2012). Fumarates promote cytoprotection of central nervous system cells against oxidative stress via the nuclear factor (erythroid-derived 2)-like 2 pathway. *J. Pharmacol. Exp. Ther.* 341, 274–284. doi: 10.1124/jpet.111.190132

Shelat, P. B., Chalimoniuk, M., Wang, J. H., Strosznajder, J. B., Lee, J. C., Sun, A. Y., et al. (2008). Amyloid beta peptide and NMDA induce ROS from NADPH oxidase and AA release from cytosolic phospholipase A2 in cortical neurons. *J. Neurochem.* 106, 45–55. doi: 10.1111/j.1471-4159.2008.05347.x

Shen, Y., Cui, X., Hu, Y., Zhang, Z., and Zhang, Z. (2021). LncRNA-MIAT regulates the growth of SHSY5Y cells by regulating the miR-34-5p-SYT1 axis and exerts a neuroprotective effect in a mouse model of Parkinson's disease. *Am. J. Transl. Res.* 13, 9993–10013.

Shi, M., Cao, L., Cao, X., Zhu, M., Zhang, X., Wu, Z., et al. (2018). DR-region of Na(+)/K(+) ATPase is a target to treat excitotoxicity and stroke. *Cell Death Dis.* 10:6. doi: 10.1038/s41419-018-1230-5

Shi, X., Sun, M., Liu, H., Yao, Y., and Song, Y. (2013). Long non-coding RNAs: a new Frontier in the study of human diseases. *Cancer Lett.* 339, 159–166. doi: 10.1016/j.canlet.2013.06.013

Sies, H. (2015). Oxidative stress: a concept in redox biology and medicine. *Redox Biol.* 4, 180–183. doi: 10.1016/j.redox.2015.01.002

Sies, H., Berndt, C., and Jones, D. P. (2017). Oxidative stress. *Annu. Rev. Biochem.* 86, 715–748.

Silva-Palacios, A., Ostolga-Chavarría, M., Zazueta, C., and Königsberg, M. (2018). Nrf2: Molecular and epigenetic regulation during aging. *Ageing Res. Rev.* 47, 31–40. doi: 10.1016/j.arr.2018.06.003

Sinha, N., and Dabla, P. K. (2015). Oxidative stress and antioxidants in hypertension-a current review. *Curr. Hypertens. Rev.* 11, 132–142. doi: 10.2174/1573402111666150529130922

Soghli, N., Yousefi, T., Abolghasemi, M., and Qujeq, D. (2021). NORAD, a critical long non-coding RNA in human cancers. *Life Sci.* 264:118665. doi: 10.1016/j.lfs.2020.118665

Sun, W., Sun, L., Sun, X., and Ma, S. (2021). Long non-coding RNA SNHG7 upregulates FGF9 to alleviate oxygen and glucose deprivation-induced neuron cell injury in a miR-134-5p-dependent manner. *Metab. Brain Dis.* 36, 2483–2494.

Sun, Y., Pham, A. N., Hare, D. J., and Waite, T. D. (2018). Kinetic modeling of pH-dependent oxidation of dopamine by iron and its relevance to Parkinson's disease. *Front. Neurosci.* 12:859. doi: 10.3389/fnins.2018.00859

Surguchov, A., Surgucheva, I., Sharma, M., Sharma, R., and Singh, V. (2017). Pore-forming proteins as mediators of novel epigenetic mechanism of epilepsy. *Front. Neurol.* 8:3. doi: 10.3389/fneur.2017.00003

Tan, X., Liu, Y., Liu, Y., Zhang, T., and Cong, S. (2021). Dysregulation of long non-coding RNAs and their mechanisms in Huntington's disease. *J. Neurosci. Res.* 99, 2074–2090. doi: 10.1002/jnr.24825

Wang, C., Wan, H., Wang, Q., Sun, H., Sun, Y., Wang, K., et al. (2020a). Safflor Yellow B Attenuates Ischemic Brain Injury via Downregulation of Long Noncoding AK046177 and Inhibition of MicroRNA-134 Expression in Rats. *Oxid. Med. Cell Longev.* 2020:4586839. doi: 10.1155/2020/4586839

Wang, Q., Ge, X., Zhang, J., and Chen, L. (2020b). Effect of lncRNA WT1-AS regulating WT1 on oxidative stress injury and apoptosis of neurons in Alzheimer's disease via inhibition of the miR-375/SIX4 axis. *Aging (Albany NY)* 12, 23974–23995. doi: 10.18632/aging.104079

Wang, S. D., Fu, Y. Y., Han, X. Y., Yong, Z. J., Li, Q., Hu, Z., et al. (2021b). Hyperbaric oxygen preconditioning protects against cerebral ischemia/reperfusion injury by inhibiting mitochondrial apoptosis and energy metabolism disturbance. *Neurochem. Res.* 46, 866–877. doi: 10.1007/s11064-020-03219-4

Wang, D., Xu, X., Pan, J., Zhao, S., Li, Y., Wang, Z., et al. (2021a). GAS5 knockdown alleviates spinal cord injury by reducing VAV1 expression via RNA binding protein CELF2. *Sci. Rep.* 11:3628. doi: 10.1038/s41598-021-83145-9

Wang, K. C., and Chang, H. Y. (2011). Molecular mechanisms of long noncoding RNAs. *Mol. Cell* 43, 904–914.

Wang, L. W., Li, X. B., Liu, Z., Zhao, L. H., Wang, Y., and Yue, L. (2019). Long non-coding RNA OIP5-AS1 promotes proliferation of gastric cancer cells by targeting miR-641. *Eur. Rev. Med. Pharmacol. Sci.* 23, 10776–10784. doi: 10.26355/eurrev_201912_19780

Wang, P., Ren, Z., and Sun, P. (2012). Overexpression of the long non-coding RNA MEG3 impairs in vitro glioma cell proliferation. *J. Cell Biochem.* 113, 1868–1874. doi: 10.1002/jcb.24055

Wang, S. W., Liu, Z., and Shi, Z. S. (2018a). Non-coding RNA in acute ischemic stroke: mechanisms, biomarkers and therapeutic targets. *Cell Transplant* 27, 1763–1777. doi: 10.1177/0963689718806818

Wang, X., Wang, C., Geng, C., and Zhao, K. (2018b). LncRNA XIST knockdown attenuates Aβ(25-35)-induced toxicity, oxidative stress, and apoptosis in primary cultured rat hippocampal neurons by targeting miR-132. *Int. J. Clin. Exp. Pathol.* 11, 3915–3924.

Wei, C. W., Luo, T., Zou, S. S., and Wu, A. S. (2018). The role of long noncoding RNAs in central nervous system and neurodegenerative diseases. *Front. Behav. Neurosci.* 12:175. doi: 10.3389/fnbeh.2018.00175

Wong, H. K., Veremeyko, T., Patel, N., Lemere, C. A., Walsh, D. M., Esau, C., et al. (2013). De-repression of FOXO3a death axis by microRNA-132 and -212 causes neuronal apoptosis in Alzheimer's disease. *Hum. Mol. Genet.* 22, 3077–3092. doi: 10.1093/hmg/ddt164

Wu, C. L., Chen, S. D., Yin, J. H., Hwang, C. S., and Yang, D. I. (2016). Nuclear factor-kappaB-dependent sestrin2 induction mediates the antioxidant effects of BDNF against mitochondrial inhibition in rat cortical neurons. *Mol. Neurobiol.* 53, 4126–4142. doi: 10.1007/s12035-015-9357-1

Wu, R., Yun, Q., Zhang, J., and Bao, J. (2021). Long non-coding RNA GAS5 retards neural functional recovery in cerebral ischemic stroke through modulation of the microRNA-455-5p/PTEN axis. *Brain Res. Bull.* 167, 80–88. doi: 10.1016/j.brainresbull.2020.12.002

Wu, Y. Y., and Kuo, H. C. (2020). Functional roles and networks of non-coding RNAs in the pathogenesis of neurodegenerative diseases. *J. Biomed. Sci.* 27:49. doi: 10.1186/s12929-020-00636-z

Xu, J., Zheng, Y., Wang, L., Liu, Y., Wang, X., Li, Y., et al. (2021). miR-124: a promising therapeutic target for central nervous system injuries and diseases. *Cell. Mol. Neurobiol.* doi: 10.1007/s10571-021-01091-6 [Epub ahead of print].

Yamamoto, M., Kensler, T. W., and Motohashi, H. (2018). The KEAP1-NRF2 system: a thiol-based sensor-effector apparatus for maintaining redox homeostasis. *Physiol. Rev.* 98, 1169–1203. doi: 10.1152/physrev.00023.2017

Yan, G., Zhao, H., and Hong, X. (2020). LncRNA MACC1-AS1 attenuates microvascular endothelial cell injury and promotes angiogenesis under hypoxic conditions via modulating miR-6867-5p/TWIST1 in human brain microvascular endothelial cells. *Ann. Transl. Med.* 8:876. doi: 10.21037/atm-20-4915

Yang, L., Wang, L., Wang, J., and Liu, P. (2021). Long non-coding RNA Gm11974 aggravates oxygen-glucose deprivation-induced injury via miR-122-5p/SEMA3A axis in ischaemic stroke. *Metab. Brain Dis.* 36, 2059–2069. doi: 10.1007/s11011-021-00792-7

Yi, M., Li, Y., Wang, D., Zhang, Q., Yang, L., and Yang, C. (2020). KCNQ1OT1 exacerbates ischemia-reperfusion injury through targeted inhibition of miR-140-3P. *Inflammation* 43, 1832–1845.

Yu, S. Y., Dong, B., Fang, Z. F., Hu, X. Q., Tang, L., and Zhou, S. H. (2018). Knockdown of lncRNA AK139328 alleviates myocardial ischaemia/reperfusion injury in diabetic mice via modulating miR-204-3p and inhibiting autophagy. *J. Cell. Mol. Med.* 22, 4886–4898. doi: 10.1111/jcmm.13754

Zhan, Y., Chen, Z., He, S., Gong, Y., He, A., Li, Y., et al. (2020). Long non-coding RNA SOX2OT promotes the stemness phenotype of bladder cancer cells by modulating SOX2. *Mol. Cancer* 19:25. doi: 10.1186/s12943-020-1143-7

Zhang, R., Wang, J., Liu, B., Wang, W., Fan, X., Zheng, B., et al. (2020c). Differentially expressed lncRNAs, miRNAs and mRNAs with associated ceRNA networks in a mouse model of myocardial ischemia/reperfusion injury. *Mol. Med. Rep.* 22, 2487–2495. doi: 10.3892/mmr.2020.11300

Zhang, L., Wang, J., Liu, Q., Xiao, Z., and Dai, Q. (2020b). Knockdown of long non-coding RNA AL049437 mitigates MPP+-induced neuronal injury in SH-SY5Y cells via the microRNA-205-5p/MAPK1 axis. *Neurotoxicology* 78, 29–35. doi: 10.1016/j.neuro.2020.02.004

Zhang, H., Tao, J., Zhang, S., and Lv, X. (2020a). LncRNA MEG3 reduces hippocampal neuron apoptosis via the PI3K/AKT/mTOR pathway in a rat model of temporal lobe epilepsy. *Neuropsychiatr. Dis. Treat.* 16, 2519–2528. doi: 10.2147/NDT.S270614

Zhang, Y. Y., Bao, H. L., Dong, L. X., Liu, Y., Zhang, G. W., and An, F. M. (2021). Silenced lncRNA H19 and up-regulated microRNA-129 accelerates viability and restrains apoptosis of PC12 cells induced by Aβ(25-35) in a cellular model of Alzheimer's disease. *Cell. Cycle* 20, 112–125. doi: 10.1080/15384101.2020.1863681

Zhang, Y., and Zhang, Y. (2020). lncRNA ZFAS1 improves neuronal injury and inhibits inflammation, oxidative stress, and apoptosis by sponging mir-582 and upregulating NOS3 expression in cerebral ischemia/reperfusion injury. *Inflammation* 43, 1337–1350. doi: 10.1007/s10753-020-01212-1

Zhang, Y., Yang, R., Lian, J., and Xu, H. (2016). LncRNA Sox2ot overexpression serves as a poor prognostic biomarker in gastric cancer. *Am J. Transl. Res.* 8, 5035–5043.

Zhao, H., Han, Z., Ji, X., and Luo, Y. (2016). Epigenetic regulation of oxidative stress in ischemic stroke. *Aging Dis.* 7, 295–306. doi: 10.14336/AD.2015.1009

Zhao, L., Zhang, M., Yan, F., and Cong, Y. (2021). Knockdown of RMST impedes neuronal apoptosis and oxidative stress in OGD/R-induced ischemic stroke via depending on the miR-377/SEMA3A signal network. *Neurochem. Res.* 46, 584–594. doi: 10.1007/s11064-020-03194-w

Zhao, W., Chen, T., and Zhao, Y. (2020). Upregulated lncRNA CASC9 contributes to progression of non-small cell lung cancer through inhibition of miR-335-3p and activation S100A14 expression. *Onco Targets Ther.* 13, 6027–6036. doi: 10.2147/OTT.S249973

Zhao, X., Wang, P., Liu, J., Zheng, J., Liu, Y., Chen, J., et al. (2015). Gas5 exerts tumor-suppressive functions in human glioma cells by targeting miR-222. *Mol. Ther.* 23, 1899–1911. doi: 10.1038/mt.2015.170

Zhao, Y., Liu, Y., Lin, L., Huang, Q., He, W., Zhang, S., et al. (2018). The lncRNA MACC1-AS1 promotes gastric cancer cell metabolic plasticity via AMPK/Lin28 mediated mRNA stability of MACC1. *Mol. Cancer* 17:69. doi: 10.1186/s12943-018-0820-2

Zhou, S., Zhang, D., Guo, J., Chen, Z., Chen, Y., and Zhang, J. (2020). Long non-coding RNA NORAD functions as a microRNA-204-5p sponge to repress the progression of Parkinson's disease in vitro by increasing the solute carrier family 5 member 3 expression. *IUBMB Life* 72, 2045–2055. doi: 10.1002/iub.2344

Zhou, Z. W., Ren, X., Zheng, L. J., Li, A. P., and Zhou, W. S. (2022). LncRNA NEAT1 ameliorate ischemic stroke via promoting Mfn2 expression through binding to Nova and activates Sirt3. *Metab. Brain Dis.* 37, 653–664. doi: 10.1007/s11011-021-00895-1

Zhou, Z. W., Zheng, L. J., Ren, X., Li, A. P., and Zhou, W. S. (2019). LncRNA NEAT1 facilitates survival and angiogenesis in oxygen-glucose deprivation (OGD)-induced brain microvascular endothelial cells (BMECs) via targeting miR-377 and upregulating SIRT1, VEGFA, and BCL-XL. *Brain Res.* 1707, 90–98. doi: 10.1016/j.brainres.2018.10.031

Conflict of Interest: The authors declare that the research was conducted in the absence of any commercial or financial relationships that could be construed as a potential conflict of interest.

Publisher's Note: All claims expressed in this article are solely those of the authors and do not necessarily represent those of their affiliated organizations, or those of the publisher, the editors and the reviewers. Any product that may be evaluated in this article, or claim that may be made by its manufacturer, is not guaranteed or endorsed by the publisher.

frontiers | Frontiers in Molecular Neuroscience

MINI REVIEW
published: 23 June 2022
doi: 10.3389/fnmol.2022.949095

Long Non-coding RNA HOTAIR in Central Nervous System Disorders: New Insights in Pathogenesis, Diagnosis, and Therapeutic Potential

*Jialu Wang[1], Jiuhan Zhao[1], Pan Hu[1], Lianbo Gao[2], Shen Tian[2] and Zhenwei He[2]**

[1] Department of Neurology, The First Affiliated Hospital of China Medical University, Shenyang, China, [2] Department of Neurology, The Fourth Affiliated Hospital of China Medical University, Shenyang, China

Central nervous system (CNS) disorders, such as ischemic stroke, neurodegenerative diseases, multiple sclerosis, traumatic brain injury, and corresponding neuropathological changes, often lead to death or long-term disability. Long non-coding RNA (lncRNA) is a class of non-coding RNA with a transcription length over 200 nt and transcriptional regulation. lncRNA is extensively involved in physiological and pathological processes through epigenetic, transcription, and post-transcriptional regulation. Further, dysregulated lncRNA is closely related to the occurrence and development of human diseases, including CNS disorders. HOX Transcript antisense RNA (HOTAIR) is the first discovered lncRNA with *trans*-transcriptional regulation. Recent studies have shown that HOTAIR may participate in the regulation of the occurrence and development of CNS disorders. In addition, HOTAIR has the potential to become a new biomarker for the diagnosis and prognosis assessment of CNS disorders and even provide a new therapeutic target for CNS disorders. Here, we reviewed the research results of HOTAIR in CNS disorders to provide new insights into the pathogenesis, diagnostic value, and therapeutic target potential of HOTAIR in human CNS disorders.

Keywords: long non-coding RNAs, central nervous system disorders, HOTAIR, pathogenesis, diagnostic value, therapeutic target

OPEN ACCESS

Edited by:
Andrei Surguchov, University of Kansas Medical Center, United States

Reviewed by:
Irina G. Sourgoutcheva, University of Kansas Medical Center, United States

****Correspondence:***
Zhenwei He
zwhe@cmu.edu.cn

Specialty section:
This article was submitted to Brain Disease Mechanisms, a section of the journal Frontiers in Molecular Neuroscience

Received: *20 May 2022*
Accepted: *07 June 2022*
Published: *23 June 2022*

Citation:
Wang J, Zhao J, Hu P, Gao L, Tian S and He Z (2022) Long Non-coding RNA HOTAIR in Central Nervous System Disorders: New Insights in Pathogenesis, Diagnosis, and Therapeutic Potential. Front. Mol. Neurosci. 15:949095. doi: 10.3389/fnmol.2022.949095

INTRODUCTION

Central nervous system (CNS) disorders, including ischemic stroke, neurodegenerative diseases (NDDs), multiple sclerosis (MS), traumatic brain injury (TBI) and the subsequent neuropathic injuries, are the main causes of morbidity and mortality (Hong et al., 2019; Khellaf et al., 2019; Herpich and Rincon, 2020). However, due to the lack of beneficial treatments for these complex neuropathologies, CNS disorders are often accompanied by acute and chronic cellular damage (Shang et al., 2020; Troshev et al., 2021). Therefore, there is an urgent need for effective therapeutic methods to prevent secondary injury caused by treatment and to successfully treat CNS disorders (Marehbian et al., 2017; Esechie et al., 2019).

Long non-coding RNA (LncRNA) is a class of non-coding RNA with a transcription length over 200 nt and transcriptional regulation. Most lncRNAs are transcribed and spliced by RNA polymerase II, and some lncRNAs have both 5′ end caps and 3′ poly(A) tails (Derrien et al., 2012). Similar to protein-coding genes, some epigenetic modifications of lncRNAs are visible throughout the genome, but they usually have no functional open reading frame (Tan et al., 2021). Importantly, lncRNAs participate in the occurrence and development of many diseases (Riva et al., 2016; Bao et al., 2018). Accordingly, they can be used as a molecular sponge, modulator of signal pathways, epigenetic regulator, and molecular scaffold to extensively regulate various important biological activities, including cell proliferation, differentiation, growth and development, and cell apoptosis. Specifically, lncRNAs participate in various signal transduction regulation processes and play the following roles: (i) scaffold: binding to two or more proteins to play a regulatory role; (ii) decoy: inducing and combining with a series of regulatory factors to hinder its combination with the corresponding functional sites; (iii) guide: recruiting specific proteins and combining with them to form complexes; (iv) signal: lncRNA can reflect the regulation of genes by transcription factors or signal pathways in space and time (Wang and Chang, 2011).

lncRNAs interact with other biomolecules (e.g., DNA, RNA and proteins) and play an important role in biological processes through several mechanisms, such as acting as inhibitory sponges for microRNAs (miRNAs), participating in chromatin remodeling and affecting protein stability (Jalali et al., 2017). lncRNAs can be expressed in multiple tissues, but the highest expression levels are found in the CNS (Policarpo et al., 2021). Several lncRNAs have been shown to play important roles in the regulation of CNS development, and the ability of lncRNAs to participate in the regulation of hundreds of transcriptomes against CNS injury and disorder makes them candidates for stabilizing transcriptomic homeostasis and as promising therapeutic targets (Wu et al., 2013). HOTAIR is one of the most extensively studied lncRNAs found dysregulated in human tumors. Although it does not encode proteins, it is involved in RNA processing, gene regulation, chromatin modification, gene transcription, and post-transcriptional regulation.

HOTAIR expression level can well reflect the disease state and can be used as a potential biomarker (Liu et al., 2020). Studies have shown that HOTAIR can competitively inhibit some target miRNAs to act as its molecular sponge to release miRNA inhibition on target messenger RNA (mRNA) and play specific biological functions (Rajagopal et al., 2020; Chi et al., 2021). HOTAIR plays an indispensable role in many pathophysiological processes through epigenetic regulation (Tsai et al., 2010). Accordingly, HOTAIR has been extensively studied in various types of tumors, and results have shown that it is widely involved in tumor cell proliferation, apoptosis, angiogenesis, invasion, and metastasis (Gupta et al., 2010; Yang et al., 2018; Zhang J. et al., 2020). Moreover, emerging evidence confirms that HOTAIR is also widely involved in the pathogenesis of CNS disorders and can be a potential diagnostic marker and therapeutic target of CNS disorders. It has a broad clinical application prospect in the early diagnosis, efficacy judgment, prognosis prediction, and gene therapy of CNS disorders (Jin Z. L. et al., 2021; Momtazmanesh and Rezaei, 2021).

In this review, we outline the mechanisms by which HOTAIR exerts its regulatory function and summarize its role in the pathogenesis of ischemic stroke, NDDs, MS, and TBI. Finally, the potential of HOTAIR as a disease diagnostic biomarker of CNS disorders is highlighted.

LNCRNA HOTAIR

Human homeobox (HOX) is a 2,158-nt, single-strand gene transcribed in an antisense manner from the HOXC locus on chromosome 12q13.13, one of the chromosomal loci of the clustered HOX genes (HOXA, B, C, and D) (Gupta et al., 2010). HOTAIR was first discovered by Rinn et al. (2007) as a special lncRNA that regulates gene expression by *trans*-silencing chromatin. The human HOTAIR gene is located in the intergenic region between HOXC11 and HOXC12 in the HOXC cluster on chromosome 12 (Li et al., 2017). HOTAIR can recruit polyclonal repressor complex 2 (PRC2) at the 5′ end to inhibit the expression of homeobox gene cluster D (Hung and Chang, 2010). Histone modifications are essential for transcriptional activation, and PRC2 contains the enhancer of Zeste homolog 2 (EZH2), a histone methyltransferase that marks transcriptionally repressed genes by trimethylation at lysine 27 of histone H3 (H3K27me3) (Duan et al., 2020). HOTAIR binds to GA-rich motifs in the genome to form a broad domain occupied by PRC2 and subsequently H3K27me3 (Song et al., 2019).

Lysine-specific demethylase 1 (LSD1), a member of the amine oxidase family, forms a complex with repressor element 1 silencing transcription factor (REST) corepressor 1 (CoREST1), which acts as a bridge to link LSD1 to REST to form LSD1/CoREST/REST complex. LSD1/CoREST/REST complex mediates histone H3 lysine-4 dimethylation (H3K4me2) demethylation to regulate the transcriptional activity of target genes. The 3′ end of HOTAIR binds to a compound containing LSD1 to inactivate gene expression *via* H3K4me2 (**Figure 1**). Overall, HOTAIR has specific bidirectional binding ability, that is, the 5′-end domain binds to the PRC2 complex, while its 3′-end domain binds to the LSD1/REST/CoREST complex. In addition, HOTAIR can act as a scaffold to guide PRC2, and LSD1 forms a complex and mediates the complex to a specific genomic locus to demethylate the chromosomes H3K27me3 and H3K4me2. Thus, the chromosome is maintained in a closed state maintaining, and the corresponding downstream genes are silenced (Tsai et al., 2010).

MECHANISMS OF HOTAIR FUNCTION

HOTAIR plays an important role in the development of CNS disorders (**Table 1**). It is closely associated with inflammatory response, cell apoptosis, oxidative stress, and autophagy. However, the relevant molecular mechanisms are still unclear. Here, we summarize the molecular mechanisms related to the function of HOTAIR.

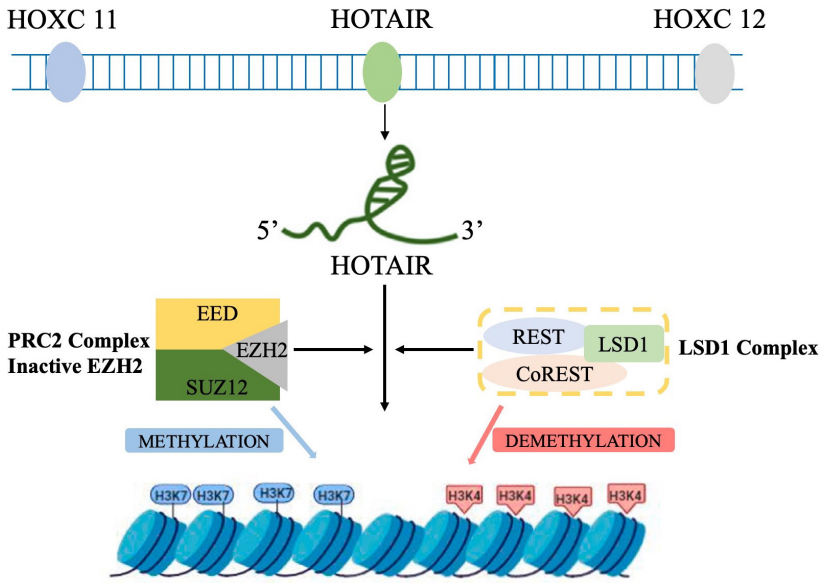

FIGURE 1 | Schematic representation of HOTAIR-mediated gene silencing. HOTAIR acts as a molecular scaffold, bridging PRC2 and LSD1 complexes and altering gene expression by promoting H3K27me3 and H3K4 demethylation (by PRC2 and LDS1, respectively) at the target genes.

AS Competitive Endogenous RNA

Competing endogenous RNAs (ceRNA) hypothesis reveals a novel mechanism of RNA interaction. MiRNAs are known to cause gene silencing by binding mRNAs, while ceRNA can competitively bind miRNAs to regulate gene expression (Thomson and Dinger, 2016). ceRNA can bind to miRNAs through miRNA response elements (MREs) to affect miRNA-induced gene silencing. Recent studies have shown that ceRNA is an important mechanism for the occurrence and development of various CNS disorders (Moreno-García et al., 2020; Luo et al., 2021). Interaction with target sites in the mRNA 3′ UTR can lead to reduced mRNA stability and translational repression, thereby regulating RNA gene expression (Amort et al., 2013). Several studies have shown that HOTAIR is an important ceRNA that mainly serves as a miRNA sponge in the body (Xu et al., 2016). In breast cancer (BC), HOTAIR upregulates HMGA2 expression by competitively binding to miR-20a-5p, resulting in cell growth, metastasis, and apoptosis (Zhao et al., 2018). HOTAIR also promotes BC progression and metastasis by serving as a sponge for miR-129-5p to upregulate FZD7 expression (Wu et al., 2021). In a rat model of myocardial ischemia-reperfusion injury, HOTAIR upregulation promoted STAT3 expression, positively regulating the HOTAIR/miR-17-5p/STAT3 axis (Chen et al., 2021). In addition, HOTAIR also serves as ceRNA in multiple CNS disorders, such as Parkinson's disease (PD) (Zhao et al., 2020), MS, and TBI (Duan et al., 2018). However, the specific role of miRNA expression regulation in the pathogenesis of CNS disorders remains to be further elaborated.

Regulating Inflammatory Response

Sequencing analysis of the HOTAIR-related proteome showed that HOTAIR activates various proteins containing protein kinase domains and promotes the enrichment of important inflammatory signaling pathway proteins and their complexes, such as I-kappa B kinase complex, tumor necrosis factor alpha (TNF-α)/nuclear transcription factor-κB (NF-κB) signaling protein complex and the IKKα-IKKβ complex (Zhao et al., 2021). In addition, HOTAIR also upregulates the expression of multiple inflammatory signaling proteins, such as TNF-α and mitogen-activated protein kinase (Zhuang et al., 2015). For example, in ox-LDL induction in Raw264.7 cells (*in vitro* atherosclerosis model), HOTAIR overexpression reduced the inflammatory response and by NF-κB pathway by regulating FXR1. This indicated that HOTAIR may serve as a treatment target for preventing and treating atherosclerosis (Pang et al., 2018). HOTAIR knockdown reduced NF-κB target gene expression by inhibiting NF-κB and related cofactor recruitment at the target gene promoter in lipopolysaccharide-induced inflammatory response in macrophages (Obaid et al., 2018). Moreover, HOTAIR may regulate the gene transcription of key repressors of the NF-κB activation pathway through epigenetic regulation, thus participating in the immune escape of glioma cells (Wang et al., 2021). Therefore, HOTAIR expression may be involved in the development of CNS disorders by inhibition of inflammatory responses and release of inflammatory factors.

Regulating Multiple Signaling Pathways

HOTAIR is involved in the regulation of multiple signaling pathways, especially in tumors. Guo et al. (2018) reported that upregulated HOTAIR expression activated the Wnt/β-catenin pathway, an important pathway related to tumor genesis and development. Further, it promoted cisplatin resistance *via* suppression-expression and alters intercellular signal transduction in lung cancer (Guo et al., 2018). In colorectal

TABLE 1 | Role of HOTAIR in CNS disorders.

Neurological disorders	Animal models/Cell employed	Regulation	Target genes/Pathway	Potential therapeutic effect	References
Ischemic stroke	pMCAO C57BL/6 mice/ OGD-injured N2a	Upregulated	KLF6/miR-148a-3p/KLF6 axis and STAT3 pathway	Inhibit neural cell inflammatory response and apoptosis, increase cell viability, decrease infarcted area and neurological deficits.	Huang et al., 2021
	OGD/R-induced hBMVECs	Upregulated	EZH2, Bax, caspase-3, Bcl-2, occludin, claudin-5, ZO-1, VE-cadherin	Maintain BBB permeability and anti-apoptosis	Wang et al., 2022a
	pMCAO ICR mice/ hypoxia induced HT22 cells	Upregulated	NOX2	Inhibit cell apoptosis	Yang and Lu, 2016
AD	HeLa cells/ brain tissue samples of AD patients	Downregulated	CDK5R1/miR-15/107	Reduce Aβ production and Tau protein hyperphosphorylation	Spreafico et al., 2018
	APP/PS1 mice	Upregulated	miR-130a-3p	Anti-inflammation	Lu et al., 2022
	Sevoflurane-mediated SD rats	Upregulated	*Bdnf*	Increase BDNF expression in hippocampus	Wang J. Y. et al., 2018
	ISO-evoked SD rats/HT22 cells	Upregulated	miR-129-5p	Reverse the injury of ISO on cell viability, inflammation, apoptosis, and oxidative stress	Wang et al., 2022b
PD	MPTP induced C57BL/6J mice/MPP^+ induced SH-SY5Y	Upregulated	miR-221-3p/α-synuclein	Increase cell viability, reduce cell apoptosis, inhibit inflammatory cytokines secretion and oxidative stress reaction	Sun et al., 2022
	MPP^+ induced SK-N-SH cells	Upregulated	miR-874-5p/ATG10	Anti-autophagy	Zhao et al., 2020
	MPTP induced C57BL/6J mice/MPP^+ induced SH-SY5Y	Upregulated	miR-326	Inhibit NLRP3 mediated pyroptosis activation	Zhang Q. et al., 2021
	MPTP induced C57BL/6J mice/MPP^+ induced SH-SY5Y	Upregulated	miR-126-5p/RAB3IP	Inhibit autophagy and cell apoptosis	Lin et al., 2019
	MPTP-induced C57BL/6/MPP^+-induced MN9D	Upregulated	miR-221-3p/NPTX2	Inhibit autophagy in the substantia nigra compacta	Lang et al., 2020
	MPTP-induced C57BL/6/MPP^+-induced MN9D	Upregulated	SSTR1	Inhibit dopaminergic neuron apoptosis	Cai et al., 2020
	MPTP induced C57BL/6 mice/MPP^+ induced SH-SY5Y	Upregulated	LRRK2	Inhibit dopamine neuronal apoptosis by suppressing caspase 3 activity	Wang S. et al., 2017
	MPTP induced C57BL/6 mice/MPP^+ induced SH-SY5Y	Upregulated	LRRK2	Anti-apoptosis	Liu S. et al., 2016
MS	MOG_{35-55} induced C57BL/6 mice	Upregulated (VD deficiency)	NA	Immunomodulatory effects	Pahlevan Kakhki et al., 2018
	Cuprizone induced C57BL/6 mice/	Upregulated	miR-136-5p	Inhibit microglia activation promote myelin regeneration	Duan et al., 2018
TBI	Craniotomy C57BL/6 mice	Upregulated	MYD88	Inhibit microglia overactivation and inflammatory factor release after TBI	Cheng et al., 2021

AD, Alzheimer's disease; ATG10, autophagy-related 10; BBB, blood-brain barrier; Bdnf, brain-derived neurotrophic factor; CDK5R1, cyclin-dependent kinase 5 regulatory subunit 1; EZH2, enhancer of Zeste homolog 2; hBMVECs, human brain microvascular endothelial cells; ISO, isoflurane; LRRK2, leucine-rich repeat kinase 2; MOG, myelin oligodendrocyte glycoprotein; MS, multiple sclerosis; MYD88, myeloid differentiation factor-88 adaptor protein; NLRP3, NOD-like receptor (NLR) family pyrin domain-containing protein 3; NOX2, nicotinamide adenine dinucleotide phosphate oxidase oxidases 2; NPTX2, neuronal pentraxin II; OGD, Oxygen–glucose deprivation; PD, Parkinson's disease; pMCAO, permanent middle cerebral artery occlusion; RAB3IP, Rab3a interacting protein; SD, Sprague–Dawley; SSTR1, somatostatin receptor 1; TBI, Traumatic Brain Injury; VE, vascular endothelial; ZO-1, zonula occludens-1.

cancer (CRC), knockdown of HOTAIR inhibited the activation of Wnt/β-catenin pathway, resulting in inhibited proliferation and invasion of CRC cells and chemoresistance, suggesting that the HOTAIR/Wnt/β-catenin pathway may be a potential therapeutic target in CRC (Xiao et al., 2018).

Meanwhile, although the Wnt/β-catenin pathway was also found to be involved in the progression and, thus, the poor prognosis of glioma patients (Kaur et al., 2013), it is unknown whether HOTAIR plays a role in glioma pathogenesis by regulating the Wnt/β-catenin pathway. The phosphoinositide-3-kinase (PI3K)/AKT/mammalian target of rapamycin (mTOR) pathway plays a crucial role in the malignant transformation of human tumors and their subsequent proliferation and metastasis (Mabuchi et al., 2015). HOTAIR upregulation was identified in an ovarian cancer cell model, and it was found to increase tumor progression and promote tumor aggressiveness and metastasis *via* activation of the PI3K/AKT/mTOR pathway (Dong and Hui, 2016). Moreover, HOTAIR promoted the development of glioma and the expression of fibroblast growth factor 1 (FGF1), which promotes tumorigenesis by activating the PT3K/AKT pathway tumorigenic function (Hadari et al., 2001). However, aside from glioma, the role of HOTAIR in the pathogenesis, development, and prognosis of other CNS disorders through the regulation of more signaling pathways has not been clearly explained.

Cell Cycle–Associated Gene Regulation

Studies have shown that HOTAIR knockdown in different tumor cells could affect EZH2-dependent cell cycle expression and induce cell cycle arrest (Kogo et al., 2011; Zhou et al., 2015). Gupta et al. (2010) was the first to report that in BC, two tumor suppressor genes (i.e., p21 and p16), which blocked cell cycle transition from G1 phase to S phase, are direct target genes of HOTAIR by chromatin immunoprecipitation. In glioblastoma studies, interference of HOTAIR expression in U87 and U87 VIII cells induced G1 phase arrest and increased expression of RB and dephosphorylated RB (Zhou et al., 2015). As RB is at the core of the G1 cell cycle regulation network, several growth factors (e.g., platelet-derived growth factor and epidermal growth factor) bind with their corresponding receptors to promote cyclin transcription. Activated cyclin and cyclin-dependent kinases (CDKs) form a complex to dephosphorylate RB, which can affect the transcription activity of the E2F family. The downstream transcription target genes of the E2F family, including B-Myb, c-Myc, and CDC2, are all essential proteins for the G1/S phase transition of cell cycle (Ertosun et al., 2016). The above results show that p16/P21 is activated after HOTAIR expression, and the regulatory network of cyclin D1→RB→E2F1 in tumor cells is blocked individually. Further, rapid passage of cell cycle from the G1 phase is eliminated, resulting in cell cycle arrest. Therefore, HOTAIR can be used as a candidate target for inhibiting the tumor cell cycle evolution. However, whether HOTAIR plays a role in CNS disorders by regulating cell cycle remains to be further determined.

Regulating Protein Ubiquitination

HOTAIR acts as a platform for protein ubiquitination, helping assemble E3 ubiquitin ligases to bind to their respective substrates, promoting ubiquitination of the complex and accelerating its degradation. Mex3b and Dzip3 are E3 ubiquitin ligases with specific RNA-binding domains that bind HOTAIR. Mex3b exists in the nucleus and cytoplasm, and the corresponding ubiquitination substrate is Snurportin-1 protein. Dzip3, however, exists only in cytoplasmic vesicles and promotes the ubiquitination of Ataxin-1 protein (Yoon et al., 2013). Mex3b acts as E3 ubiquitin ligase in HOTAIR-induced degradation of Runt-related transcription factor 3 (Runx3), and silencing HOTAIR or Mex3b attenuates Runx3 degradation. Therefore, the interaction between HOTAIR and Mex3b can induce the ubiquitination of Runx3 protein and enhance the invasion ability of gastric cancer cells, and providing a potential therapeutic target for gastric cancer metastasis (Xue et al., 2018). HOTAIR binds to the androgen receptor (AR) protein to block its interaction with the E3 ubiquitin ligase murine double minute 2, thereby preventing AR ubiquitination and protein degradation and contributing to castration-resistant prostate cancer (Zhang et al., 2015). However, there are few studies on HOTAIR regulation of protein ubiquitination, and the role of HOTAIR in the ubiquitination process of different proteins in CNS disorders still needs to be further studied.

HOTAIR INVOLVEMENT IN PATHOGENESIS OF CENTRAL NERVOUS SYSTEM DISORDERS

Dysregulated HOTAIR expression has been found in various pathological processes, including in CNS disorders (**Figure 2**). However, the specific mechanism of HORAIR involvement in the pathogenesis of CNS disorders is still controversial. HOTAIR may exert diverse functions in modulating pathological processes in different types of CNS disorders. In this part, we elucidated important evidence for understanding the crucial roles of the HOTAIR functional network in signaling pathways and identifying new diagnostic biomarkers, as well as therapeutic targets for CNS disorders (e.g., ischemic stroke, Alzheimer's disease (AD), PD, MS, and TBI).

HOTAIR in Ischemic Stroke

Stroke is one of the leading causes of death and disability worldwide, with ischemic stroke accounting for approximately 87% of all strokes (Bao et al., 2018). An ischemic stroke is mainly caused by a sudden stop of blood flow to the brain, which reduces the supply of oxygen and glucose to brain cells (Wang S. W. et al., 2018). Patients with ischemic stroke may present with varying neurological deficits, such as limb paralysis, language impairment, ataxia, and paresthesia (Balch et al., 2020). Diabetes, hypertension, high cholesterol, smoking, alcohol abuse, atrial fibrillation, and other factors are contribute to the risk of ischemic stroke (Koh and Park, 2017). However, current measures to protect the brain from ischemic stroke remain suboptimal (Satani and Savitz, 2016). Therefore, studies on the underlying mechanisms of ischemic brain injury are urgently needed.

HOTAIR expression is significantly elevated in permanent middle cerebral artery occlusion (pMCAO) mice, and this

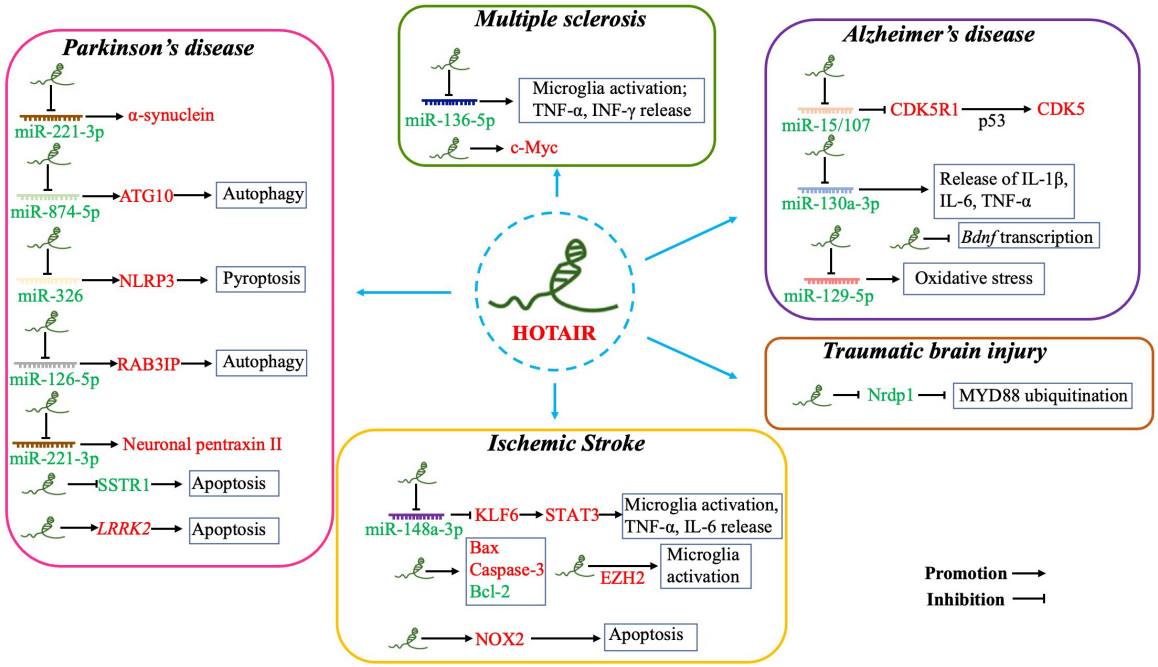

FIGURE 2 | Overexpressed HOTAIR is involved in the pathogenesis of CNS disorders by sponging miRNAs, inducing apoptosis, promoting microglia activation and neuroinflammation, enhancing oxidative stress, and inhibiting *Bdnf* transcription. (i) Parkinson's disease: HOTAIR acts as competing endogenous RNA by sponging miR-211-3p, miR-874-5p, miR-326, and miR-126-5p. HOTAIR also induces apoptosis by inhibiting SSTR1 or promoting LRRK2 expression. (ii) Ischemic stroke: Overexpressed HOTAIR acts as competing endogenous RNA by sponging miR-148a-3p to upregulate STAT3; promoting microglia activation and the release of pro-inflammatory factors; and upregulating EZH2, also a pathway regulated by HOTAIR to activate microglia. HOTAIR promotes apoptosis by upregulating Bax, Caspase-3, and NOX2, as well as by downregulating Bcl-2 expression. (iii) Alzheimer's disease: Overexpressed HOTAIR acts as competing endogenous RNA by sponging miR-15/107, miR-130a-3p, and miR-129-5p to promote apoptosis, oxidative stress, and neuroinflammation. HOTAIR is also involved in the pathogenesis of AD by inhibiting *Bdnf* transcription. (iv) Multiple sclerosis: Overexpressed HOTAIR sponges miR-136-5p to promote microglia activation, release of TNF-α and IFN-γ, and upregulate c-Myc expression. (v) Traumatic brain injury: Overexpressed HOTAIR inhibits MYD88 ubiquitination to repress microglial activation. Red and green fonts represent high and low expression, respectively.

is accompanied with increased infarcted area, apoptosis of neural cells, and exacerbation of neurological deficits (Huang et al., 2021). Silencing HOTAIR expression reversed the above ischemic injury induced by cerebral artery occlusion, decreased pro-inflammatory factors (TNF-α and IL-6), and inhibited the apoptosis of neural cells. Increased HOTAIR expression was also observed in oxygen–glucose deprivation (OGD)-injured N2a cells. In addition, HOTAIR silencing markedly increased cell viability and reduced apoptosis rate and pro-inflammatory factors, indicating that HOTAIR suppression may exert protective roles in ischemic and hypoxic neural cells *via* anti-inflammation and anti-apoptosis. HOTAIR may also act as a ceRNA to impose posttranscriptional regulation (Liu et al., 2014).

miR-148a-3p was downregulated in OGD-injured N2a cells. In addition, as a target of HOTAIR, KLF6 is important in modulating inflammation and immune responses (Syafruddin et al., 2020). Upregulated KLF6 expression was found in ischemia/reperfusion (I/R) injury (Zhang Y. et al., 2020). Downregulated KLF6 expression promoted cell viability, decreased apoptosis, and repressed inflammatory response. HOTAIR silencing downregulated KLF6 expression by sponging miR-148a-3p; thus, modulating HOTAIR expression may protect I/R injured cells *via* the miR-148a-3p/KLF6 axis. KLF6 inhibited the expression of anti-inflammatory genes by suppressing STAT3 signaling (Chen et al., 2018). Activation of the STAT3 pathway promoted microglia/macrophage polarization toward an anti-inflammatory phenotype and ameliorated brain damage (Liu et al., 2019). HOTAIR silencing could activate the STAT3 pathway to protect against cerebral I/R injury and promote neurological recovery after ischemic stroke by downregulating KLF6 expression (Huang et al., 2021).

HOTAIR expression was also upregulated in an *in vitro* model of OGD/R injury. HOTAIR silencing reduced endothelial cell permeability and increased the expression of occludin, claudin-5, zonula occludens-1, and VE-cadherin in OGD/R-treated human brain microvascular endothelial cells. Moreover, HOTAIR knockdown significantly decreased the expression levels of the apoptosis-related proteins Bax and cleaved caspase-3 and significantly increased those of Bcl-2. Therefore, maintenance of the blood-brain barrier (BBB) structure and anti-apoptosis effects were the main cytoprotective mechanism of HOTAIR. EZH2 is a histone methyltransferase that has been shown to be involved in I/R injury (Jin D. et al., 2021). Inhibition of microglia activation and inflammatory response by EZH2 knockdown was one of the mechanisms by which it exerted its neuroprotective effect in hypoxic-ischemic brain injury (Xue et al., 2019). HOTAIR has

been documented to be an EZH2-binding lncRNA, regulating EZH2 expression and recruiting EZH2 to MYC promoter sites (Wang Y. et al., 2018). EZH2 expression was significantly upregulated in OGD/R-treated cells, and EZH2 overexpression attenuated the effects of HOTAIR knockdown on cell viability, BBB permeability, and cell apoptosis. Wang et al. (2022a) reported that a positive association between HOTAIR and EZH2 expression could be an underlying mechanism in the pathology of I/R injury, and HOTAIR mediated OGD/R-induced cell injury in an EZH2-dependent manner (Wang et al., 2022a).

Similar conclusions were obtained by Yang et al., showing that HOTAIR expression was significantly increased in pMCAO mice. In addition, high HOTAIR expression promoted the onset of ischemic infarct and cell apoptosis, whereas HOTAIR silencing attenuated hypoxia-induced apoptosis of HT22 cells. Further study on the specific mechanisms suggested that the expression of nicotinamide adenine dinucleotide phosphate oxidase oxidase 2 (NOX2) might be involved in the apoptosis regulated by HOTAIR. NOX2, as a key part of the electron transport chain, plays an important role in the plasma membrane (Lambeth et al., 2000). NOX2 has been shown to be a major inducer of stroke, and deletion of the Nox2 gene significantly reduced infarct size after I/R treatment in mice (Kahles et al., 2007). In pMCAO mice, NOX2 expression was obviously increased, and NOX2 overexpression promoted HT22 cell apoptosis, but this was reversed by HOTAIR knockdown. Thus, it is speculated that HOTAIR may bind to NOX2, and HOTAIR silencing may be a treatment approach in ischemic stroke by downregulating NOX2 expression (Yang and Lu, 2016).

Altogether, these findings suggest that elevated HOTAIR expression may be involved in the pathogenesis of ischemic stroke, and silencing HOTAIR may play a therapeutic role in ischemic stroke through anti-inflammatory, anti-apoptotic, ceRNA, and other mechanisms. However, the exact mechanism of HOTAIR involvement in ischemic stroke needs to be further clarified to develop targeted therapies for ischemic stroke.

HOTAIR in Alzheimer's Disease

Alzheimer's disease is the leading cause of dementia worldwide, inducing progressive impairment of cognitive function that seriously affects daily life (Liu, 2022). After age 65 years, the incidence of AD approximately doubles every 5 years, and 50% of the population aged $\geq$ 85 years has AD (Winblad et al., 2016). Currently, more than 30 million people worldwide have AD (Saez-Atienzar and Masliah, 2020). AD is often associated with other human pathologies making the treatment difficult (Surguchov, 2020). Multiple mechanisms are involved in the pathogenesis of AD, but it is characterized by two hallmark pathological features: β-amyloid (Aβ) plaque deposition and neurofibrillary tangle accumulation. However, because the etiology and pathogenesis of AD are yet to be fully elucidated, there is currently no effective treatment modality (Hou et al., 2019). Therefore, new therapeutic strategies need to be explored in both preclinical and clinical studies.

Cyclin-dependent kinase 5 (CDK5) is a proline-directed serine/threonine kinase involved in several developmental and physiological processes in the CNS (McLinden et al., 2012). Abnormal kinase activity is thought to play an important role in AD pathogenesis (Wang J. Z. et al., 2007). Particularly, CDK5 has been thought to exacerbate the development of two major pathological features of AD by inducing Aβ production and mediating Tau protein hyperphosphorylation (Liu S. L. et al., 2016). CDK5 activity depends on the activation of the p35 regulatory subunit and is related to its activation quantity. P35 is encoded by the cyclin-dependent kinase 5 regulatory subunit 1 (CDK5R1) gene, which has a highly conserved 3′ UTR. This indicates that post-transcriptional regulation plays a crucial role in controlling CDK5R1 expression (Zuccotti et al., 2014). miR-15/107 expression is downregulated, while CDK5R1 mRNA expression is upregulated in the hippocampus and cerebral cortex of AD patients, suggesting that miR-15/107 may be involved in the negative regulation of CDK5R1 expression (Moncini et al., 2017). lncRNAs may be provide another layer of complexity in the regulation of CDK5R1 expression associated with AD pathogenesis, a hypothesis proposed by Spreafico et al. (2018) In a HeLa cell model, the researchers identified that HOTAIR negatively regulated CDK5R1 expression through a positive action on miR-15/107. The result was also confirmed in AD patients, that is, HOTAIR is downregulated in the hippocampus and cerebellum. Therefore, upregulated HOTAIR expression may inhibit AD pathogenesis by regulating the p35/CDK5R1/CDK5 axis and reducing Aβ production and Tau protein hyperphosphorylation (Spreafico et al., 2018).

Regular physical exercise is confirmed to inhibit cognitive degeneration in AD patients (Lu et al., 2022). In APP/PS1 mice, voluntary exercise (VE) improves cognitive function evaluated using the Morris water maze test. In addition, VE reduced the level of HOTAIR in hippocampal tissues of APP/PS1 mice and helped inhibit inflammation. Conversely, HOTAIR overexpression counteracted the protective effect of VE on cognitive function and promoted the release of inflammatory factors (IL-1β, IL-6, and TNF-α), suggesting that HOTAIR may promote AD by promoting inflammatory response. Therefore, the HOTAIR/miR-130a-3p axis may be involved in the pathological mechanism of AD through the inflammatory response, and thus, inhibiting HOTAIR expression may be a feasible therapeutic strategy for AD. Further exploration of the mechanisms by which HOTAIR regulates the inflammatory response *via* miR-130a-3p sponging is needed.

Inhibition of HOTAIR expression also rescued sevoflurane-mediated brain function impairment in rats. Sevoflurane induces neuronal apoptosis, and the resulting neurotoxicity is thought to be one of the causes of cognitive impairment and AD in elderly patients (Brosnan and Bickler, 2013). A possible mechanism by which sevoflurane causes cognitive impairment is through impaired transcription of mRNA encoding brain-derived neurotrophic factor (*Bdnf*) (Stiegler and Tung, 2014). *Bdnf* mRNA levels in the hippocampus of rats were significantly reduced after sevoflurane treatment. In the study by Wang et al., decreased *Bdnf* expression after sevoflurane treatment was mediated by HOTAIR lncRNA, as indicated by *Bdnf* expression coming close to normal after siRNA intervention for HOTAIR. Thus, HOTAIR inhibition may exert a role in the treatment of AD through upregulation of *Bdnf* transcription

(Wang J. Y. et al., 2018). Similar conclusions were found by Wang et al.; in their isoflurane (ISO)-evoked HT22 cell model, downregulated HOTAIR expression contributed to the recovery from abnormal viability, apoptosis, inflammation, and oxidative stress through miR-129-5p regulation. miR-129-5p as a ceRNA of HOTAIR mediated its impact on cognition and oxidative stress in the ISO-injured SD rat model (Wang et al., 2022b).

Collectively, *in vitro* and *in vivo* studies reported that HOTAIR was highly expressed in AD models. Inhibition of HOTAIR expression may exert anti-AD effects through various mechanisms, including anti-inflammatory response, anti-apoptosis, and oxidative stress. In-depth studies on the mechanism of HOTAIR in the pathogenesis of AD are needed to develop therapeutic strategies for AD.

HOTAIR in Parkinson's Disease

As the second most common neurodegenerative disease after AD, PD has a high incidence rate (Spatola and Wider, 2014). In Europe, the prevalence and incidence rates of PD are approximately 108-257/100 000 and 11-19/100 000 per year, respectively (Balestrino and Schapira, 2020). Further, PD is prevalent in 1.37% of people aged over 60 years. In China, the incidence of PD is as high as 3.62 million (Qi et al., 2021). With the aging of the population, the incidence of PD is expected to double in the next 20 years (Chen, 2010). PD is characterized by static tremor, bradykinesia, stiffness, and other symptoms that reduce quality of life, culminating in severe disability due to inability to control motor function (Ma C. L. et al., 2014). PD is mainly caused by the degeneration and loss of dopaminergic neurons in the substantia nigra and the significant decrease of dopamine content in the striatum (Zhang W. S. et al., 2021). Studies have shown that the pathogenesis of PD includes α-synuclein misfolding and aggregation, mitochondrial dysfunction, protein clearance disorder, neuroinflammation, and oxidative stress (Jankovic and Tan, 2020). In addition, genetic factors such as mutations in genes encoding leucine-rich repeat kinase 2 (LRRK2) and GBA are common genetic risk factors for familial and sporadic PD (Riboldi and Di Fonzo, 2019; Jeong and Lee, 2020).

The complex etiology of PD poses an urgent need to identify a useful therapeutic target (Surguchov, 2022). HOTAIR was highly expressed in *in vitro* and *in vivo* models of PD, and downregulated HOTAIR increased cell viability and reduced cell apoptosis and inhibited the secretion of inflammatory cytokines and oxidative stress reaction. As a presynaptic neuronal protein, α-synuclein is a key factor in the pathogenesis of PD (Shahnawaz et al., 2020). Prevention of α-synuclein aggregation and reduction of its neurotoxicity could be a potential approach to improve the pathogenesis of PD (Fayyad et al., 2019). Sun et al. (2022) found a HOTAIR/miR-221-3p/α-synuclein signaling axis in a 1-methyl-4-phenyl-1,2,3,6-tetrahydropyridine-hydrochloride (MPTP)-induced mouse model of PD. Further, miR-221-3p can directly bind to HOTAIR and α-synuclein. As a ceRNA, HOTAIR regulates α-synuclein expression by sponging miR-221-3p (Sun et al., 2022). Therefore, overexpressed HOTAIR may be a pathogenic factor of PD, and HOTAIR inhibition reduced α-synuclein aggregation and toxicity in PD models, suggesting the potential therapeutic value of HOTAIR in PD.

Similarly, high HOTAIR expression was also observed in MPP^+-induced SK-N-SH cell models. Impairment of autophagy has been reported to be involved in the pathogenesis of PD (Lu et al., 2020). Autophagy initiation requires the expression of autophagy-related 10 (ATG10) (Song et al., 2017). Zhao et al. (2020) identified a regulatory axis in HOTAIR/miR-874-5p/ATG10, and highly expressed HOTAIR increased ATG10 expression by sponging miR-874-5p, indicating the HOTAIR was involved in PD by enhancing autophagy. miR-326 has been reported to suppress inducible nitric oxide synthase expression and promote autophagy of dopaminergic neurons (Zhao et al., 2019) in PD. In addition, it was also a target of HOTAIR. In a mice model of PD, HOTAIR silencing repressed neuronal damage by inhibiting NOD-like receptor family pyrin domain-containing protein 3-mediated pyroptosis activation *via* regulation of miR-326 (Zhang Q. et al., 2021).

The *Rab3a* interacting protein (RAB3IP) regulates neurite growth and spinal cord development, suggesting that RAB3IP plays a regulatory role in neurons (Ren et al., 2018). RAB3IP has been confirmed to inhibit the autophagy of mammalian cells through its non-conservative C-terminal region, and autophagy impairment leads to the loss of age-related dopaminergic neurons, corresponding to the loss of dopamine in the striatal body and the accumulation of α-synuclein (Amagai et al., 2015). Lin et al. (2019) found that RAB3IP expression was upregulated in a PD mouse model, and downregulated RAB3IP expression suppressed autophagy and cell apoptosis. They further suggested that HOTAIR knockdown inhibited RAB3IP expression by acting as a ceRNA for miR-126-5p (Lin et al., 2019). Furthermore, HOTAIR downregulation also potentially inhibited the autophagy of dopaminergic neurons in the substantia nigra compacta. Mechanistically, HOTAIR can affect the expression of neuronal pentraxin II by sponging miR-221-3p (Lang et al., 2020). Therefore, HOTAIR may serve as a potential therapeutic target in PD.

High HOTAIR expression can accelerate the progression of dyskinesia in PD. In a PD cell model, HOTAIR bound to the promoter region of somatostatin receptor 1 (SSTR1), leading to increased methylation of SSTR1 by recruiting DNA methyltransferases. Notably, in a MPTP-induced PD mouse model, overexpressed HOTAIR stimulated DNA methylation of SSTR1 to reduce SSTR1 expression, thereby accelerating dyskinesia and facilitating dopaminergic neuron apoptosis (Cai et al., 2020). *LRRK2* gene mutations have been widely recognized as the most common cause of dominantly inherited PD and one of the risk factors for sporadic PD (Tolosa et al., 2020). Several studies demonstrated that repression of LRRK2 kinase activity was a potential therapeutic strategy for the treatment of PD (Blanca Ramírez et al., 2017). A regulatory relationship between HOTAIR and *LRRK2* mRNA was observed in a PD cell model, and Liu S. et al. (2016) found HOTAIR overexpression increased the stability of *LRRK2* mRNA and upregulated its expression in MPP^+-induced SH-SY5Y. In addition, HOTAIR knockdown provided protection against MPP^+-induced dopamine neuronal apoptosis by suppressing caspase 3 activity (Wang S. et al., 2017).

In summary, *in vivo* and *in vitro* models of PD showed enhanced expression of HOTAIR, and high HOTAIR expression promoted the occurrence and development of PD. Inhibited HOTAIR expression mainly exerted a therapeutic effect on PD by regulating the expression of target miRNAs and downstream genes at the post-transcriptional level. The possible neuroprotective mechanisms included anti-inflammatory, anti-oxidant stress, inhibition of autophagy, and anti-apoptotic effects. Moreover, the direct regulation of key pathogenic genes of PD (*LRRK2*) was also one of the important mechanisms by which HOTAIR was involved in the pathogenesis of PD. Therefore, inhibition of HOTAIR levels may be an effective disease-modifying strategy in PD.

HOTAIR in Multiple Sclerosis

Multiple sclerosis (MS) is an autoimmune disease with an increasing incidence worldwide (Browne et al., 2014). Complex gene-environment interactions play an important role in the pathogenesis of MS, but the underlying causes and mechanisms behind the increase in MS incidence remain unclear (Lemus et al., 2018). The current results suggest that adverse lifestyle and changes in the human body environment can lead to the activation of peripheral immune cells. These cells secrete inflammatory factors to infiltrate the CNS, leading to glial proliferation, myelin demyelination, and secondary axonal injury (Dobson and Giovannoni, 2019). Epidemiological studies on MS suggest that low serum vitamin D (VD) level, smoking, childhood obesity, and Epstein-Barr virus infection may be involved in the occurrence of the disease (Wang et al., 2020). Clinically, MS is primarily manifested as sensory disturbances, autonomic nervous dysfunction, and ataxia (Kamińska et al., 2017).

Clinical studies have shown that microglia activation is associated with disease severity in MS patients (Rothhammer et al., 2018). Microglia is directly involved in cuprizone-induced demyelination by producing pro-inflammatory cytokines including TNF-α and interferon-γ (Klein et al., 2018). In cuprizone-induced demyelination, HOTAIR expression was upregulated, and this promoted microglia transformation into a pro-inflammatory M1-like phenotype and release of pro-inflammatory factors by regulation of miR-136-5p expression. Duan et al. (2018) proved that sulfasalazine inhibited M1 polarization of microglia and release of inflammatory factors by inhibiting HOTAIR expression, promoting myelin regeneration. This suggests that inhibition of HOTAIR expression is a potential approach in the treatment of MS (Duan et al., 2018).

MS is a complex disease that may be caused by the interaction between genetic and environmental risk factors, with VD deficiency considered to be the main cause (Hernández-Ledesma et al., 2021). Although the molecular mechanisms of VD protection in MS are not fully understood, the immunomodulatory properties of VD may be crucial in mediating its effects. For example, VD supplementation in patients with MS has been shown to regulate cytokine production and T-cell proliferation (Shirvani-Farsani et al., 2017). VD has also been reported to regulate HOTAIR expression (Jiang and Bikle, 2014; Riege et al., 2017). The exact mechanism by which VD regulates HOTAIR expression in MS remains unclear. However, a possible mediator is the c-Myc factor, which has been shown to regulate the effects of VD (Piek et al., 2010) and activate HOTAIR expression (Ma M. Z. et al., 2014). Pahlevan Kakhki et al. (2018) found that HOTAIR expression was dysregulated in both MS patients and animal models and was correlated with immune-activated sites. The role of HOTAIR in the pathogenesis of MS is still unclear, but it is speculated that HOTAIR might play a role in CNS-related processes (e.g., myelination) through various epigenetic mechanisms, including histone modification, chromatin remodeling, and miRNA regulation. These speculated mechanisms are consistent with the known immunomodulatory and neuroprotective effects of VD (Pahlevan Kakhki et al., 2018).

HOTAIR in Traumatic Brain Injury

Traumatic brain injury is characterized by high disability and mortality; however, there is currently no effective treatment modality for TBI (Stein et al., 2010). It can usually be divided into primary and secondary injuries (Najem et al., 2018). Neuroinflammation is a hallmark of TBI and includes activation of resident glial cells (microglia and astrocytes), recruitment of immune cells, and release of inflammatory mediators in the brain (Simon et al., 2017). Abnormal activation of microglia and excessive release of inflammatory factors play an important role in secondary injury of TBI, and these mechanisms hinder nerve injury repair post-TBI (Lee et al., 2019). Many studies have shown that inhibition of TBI-induced microglial activation and neuroinflammatory response is beneficial for improving TBI (Corrigan et al., 2016; Kumar et al., 2017). Therefore, it is important to explore strategies to alleviate TBI by inhibiting microglial activation and inflammatory factor release.

HOTAIR is significantly upregulated in activated microglia of TBI mice, and silencing HOTAIR could inhibit microglial activation and reduce the release of IL-1β, IL-6, and TNF-α. Cheng et al. (2021) further explored the regulatory mechanism of HOTAIR on microglia activity and found that HOTAIR may directly inhibit microglia activation by binding myeloid differentiation factor-88 adaptor protein (MYD88). MYD88 is a crucial linker molecule in the toll-like receptor signaling pathway, and its expression is significantly upregulated in TBI mice. Downregulated MYD88 expression can improve TBI by reducing microglial activation (Zhu et al., 2014; Leite et al., 2015). Nrdp1, a member of the E3 ubiquitin ligase family, can downregulate the protein level of MYD88 by mediating MYD88 ubiquitination (Wang et al., 2009). Cheng et al. (2021) explored the effect of HOTAIR on microglia activation in TBI mice and found that overexpression of HOTAIR stabilized MYD88 by inhibiting Nrdp1-mediated MYD88 ubiquitination, preventing microglia overactivation and inflammatory factor release after TBI and improving prognosis (Cheng et al., 2021).

DIAGNOSTIC AND PROGNOSTIC SIGNIFICANCE OF HOTAIR IN CENTRAL NERVOUS SYSTEM DISORDERS

Early diagnosis is crucial for the treatment and prognosis of CNS disorders, but current diagnostic methods are inadequate

for early diagnosis of CNS disorders. Therefore, it is important to improve diagnostic methods and develop highly specific and sensitivity biomarkers. lncRNA is expressed in various tissues; although the expression level is lower than that of protein-coding genes, its tissue specificity is much higher (Pan et al., 2018). This gives it potential advantages as a biological marker with highly specific diagnostic functions. Abnormal expression of lncRNAs not only exist in tissues and cells, but also in various body fluids, including blood, urine, saliva, and gastric juice (Sartori and Chan, 2014). In addition, lncRNAs remain stable in circulating plasma even in the presence of ribonuclease (Ren et al., 2013). However, the mechanism by which circulating lncRNAs are secreted into the blood and stably exists has not been fully elucidated. Exosomes can better protect plasma lncRNAs against the degradation of ribonucleases. Under pathological conditions, cells can selectively load lncRNAs into exosomes, resulting in high specificity for disease diagnosis (Gezer et al., 2014).

HOTAIR has been reported to contribute to the pathogenesis of MS both in animal models and in human studies. In addition, it might also be a risk locus of MS. Taheri et al. (2020) genotyped three single-nucleotide polymorphisms (SNPs) in HOTAIR, namely, rs12826786, rs1899663, and rs4759314, in Iranian MS patients and healthy subjects and found that rs4759314 SNP was associated with the risk of MS in an allelic model [OR (95% CI) = 1.34 (1.08–1.67)]. This suggested that HOTAIR might be a risk locus for MS in the Iranian population (Taheri et al., 2020). Soltanmoradi et al. (2021) enrolled 60 RRMS patients (30 patients with relapse, 30 patients with remission) to evaluate the diagnostic value of HOTAIR in MS patients. The results showed higher levels of HOTAIR in relapse patients than in remission patients. Moreover, there was a positive correlation between high HOTAIR expression and increased levels of matrix metalloproteinases 9 in peripheral blood mononuclear cells of MS patients with relapse. Further, the receiver operating characteristic analysis showed the potential of HOTAIR (area under the curve: 0.87; sensitivity: 83%; specificity: 80%) as biomarkers for distinguishing between relapse and remission phases of RRMS (Soltanmoradi et al., 2021).

Currently, there are only few studies on HOTAIR as a diagnostic marker of CNS disorders, and these studies remain at the level of HOTAIR expression. Research on its regulation mechanism is limited, and thus, HOTAIR cannot be directly applied in clinical practice. However, with the development of body fluid detection, in the context of precision medicine, lncRNA measurement has become a conducive method for accurate diagnosis and development of individualized prevention and treatment plans (Kumar and Goyal, 2017; He et al., 2021). Compared with traditional diagnostic markers of CNS disorders, lncRNA has higher specificity and sensitivity (Chandra Gupta and Nandan Tripathi, 2017), and thus, it is expected to become a new biological indicator for the diagnosis of CNS disorders.

CONCLUSION

In conclusion, recent studies have shown that HOTAIR is involved in the occurrence and development of several CNS disorders and may be a potential biomarker for disease diagnosis and prognosis. *In vitro* and *in vivo* studies have shown that inhibition of HOTAIR expression can play a therapeutic role in CNS disorders through multiple mechanisms, suggesting it may be a potential therapeutic target for CNS disorders.

AUTHOR CONTRIBUTIONS

JW and JZ wrote the manuscript. PH, LG, and ST produced the figures. ZH edited and revised the review. All authors have read and approved the final manuscript.

FUNDING

This work was supported by China Postdoctoral Science Foundation (No. 2020M681011) and Natural Science Foundation of Liaoning Province (No. 2020-MS-09).

REFERENCES

Amagai, Y., Itoh, T., Fukuda, M., and Mizuno, K. (2015). Rabin8 suppresses autophagosome formation independently of its guanine nucleotide-exchange activity towards Rab8. *J. Biochem.* 158, 139–153. doi: 10.1093/jb/mvv032

Amort, T., Soulière, M. F., Wille, A., Jia, X. Y., Fiegl, H., Wörle, H., et al. (2013). Long non-coding RNAs as targets for cytosine methylation. *RNA Biol.* 10, 1003–1008. doi: 10.4161/rna.24454

Balch, M. H. H., Nimjee, S. M., Rink, C., and Hannawi, Y. (2020). Beyond the brain: the systemic pathophysiological response to acute ischemic stroke. *J. Stroke* 22, 159–172.

Balestrino, R., and Schapira, A. H. V. (2020). Parkinson disease. *Eur. J. Neurol.* 27, 27–42.

Bao, M. H., Szeto, V., Yang, B. B., Zhu, S. Z., Sun, H. S., and Feng, Z. P. (2018). Long non-coding RNAs in ischemic stroke. *Cell Death Dis.*9:281.

Blanca Ramírez, M., Madero-Perez, J., Rivero-Rios, P., Martinez-Salvador, M., Lara Ordonez, A. J., Fernandez, B., et al. (2017). LRRK2 and parkinson's disease: from lack of structure to gain of function. *Curr. Protein Pept. Sci.* 18, 677–686. doi: 10.2174/1389203717666160311121748

Brosnan, H., and Bickler, P. E. (2013). Xenon neurotoxicity in rat hippocampal slice cultures is similar to isoflurane and sevoflurane. *Anesthesiology* 119, 335–344. doi: 10.1097/ALN.0b013e31829417f0

Browne, P., Chandraratna, D., Angood, C., Tremlett, H., Baker, C., Taylor, B. V., et al. (2014). Atlas of Multiple Sclerosis 2013: a growing global problem with widespread inequity. *Neurology* 83, 1022–1024. doi: 10.1212/WNL.0000000000000768

Cai, L., Tu, L., Yang, X., Zhang, Q., Tian, T., Gu, R., et al. (2020). HOTAIR accelerates dyskinesia in a MPTP-lesioned mouse model of PD via SSTR1 methylation-mediated ERK1/2 axis. *Mol. Ther. Nucleic Acids* 22, 140–152.

Chandra Gupta, S., and Nandan Tripathi, Y. (2017). Potential of long non-coding RNAs in cancer patients: from biomarkers to therapeutic targets. *Int. J. Cancer* 140, 1955–1967. doi: 10.1002/ijc.30546

Chen, D., Wei, L., Liu, Z. R., Yang, J. J., Gu, X., Wei, Z. Z., et al. (2018). Pyruvate kinase M2 increases angiogenesis, neurogenesis, and functional recovery mediated by upregulation of STAT3 and focal adhesion kinase activities after ischemic stroke in adult mice. *Neurotherapeutics* 15, 770–784.

Chen, J. J. (2010). Parkinson's disease: health-related quality of life, economic cost, and implications of early treatment. *Am. J. Manag. Care* 16 Suppl Implications, S87–S93.

Chen, J., Li, X., Zhao, F., and Hu, Y. (2021). HOTAIR/miR-17-5p axis is involved in the propofol-mediated cardioprotection against ischemia/reperfusion injury. *Clin. Interv. Aging* 16, 621–632. doi: 10.2147/CIA.S286429

Cheng, S., Zhang, Y., Chen, S., and Zhou, Y. (2021). LncRNA HOTAIR participates in microglia activation and inflammatory factor release by regulating the ubiquitination of MYD88 in traumatic brain injury. *J. Mol. Neurosci.* 71, 169–177. doi: 10.1007/s12031-020-01623-7

Chi, K., Geng, X., Liu, C., Zhang, Y., Cui, J., Cai, G., et al. (2021). LncRNA-HOTAIR promotes endothelial cell pyroptosis by regulating the miR-22/NLRP3 axis in hyperuricaemia. *J. Cell Mol. Med.* 25, 8504–8521. doi: 10.1111/jcmm.16812

Corrigan, F., Mander, K. A., Leonard, A. V., and Vink, R. (2016). Neurogenic inflammation after traumatic brain injury and its potentiation of classical inflammation. *J. Neuroinflammation* 13:264. doi: 10.1186/s12974-016-0738-9

Derrien, T., Johnson, R., Bussotti, G., Tanzer, A., Djebali, S., Tilgner, H., et al. (2012). The GENCODE v7 catalog of human long noncoding RNAs: analysis of their gene structure, evolution, and expression. *Genome Res.* 22, 1775–1789. doi: 10.1101/gr.132159.111

Dobson, R., and Giovannoni, G. (2019). Multiple sclerosis – a review. *Eur. J. Neurol.* 26, 27–40.

Dong, L., and Hui, L. (2016). HOTAIR promotes proliferation, migration, and invasion of ovarian cancer SKOV3 cells through regulating PIK3R3. *Med. Sci. Monit.* 22, 325–331. doi: 10.12659/msm.894913

Duan, C., Liu, Y., Li, Y., Chen, H., Liu, X., Chen, X., et al. (2018). Sulfasalazine alters microglia phenotype by competing endogenous RNA effect of miR-136-5p and long non-coding RNA HOTAIR in cuprizone-induced demyelination. *Biochem. Pharmacol.* 155, 110–123. doi: 10.1016/j.bcp.2018.06.028

Duan, R., Du, W., and Guo, W. (2020). EZH2: a novel target for cancer treatment. *J. Hematol. Oncol.* 13:104. doi: 10.1186/s13045-020-00937-8

Ertosun, M. G., Hapil, F. Z., and Osman Nidai, O. (2016). E2F1 transcription factor and its impact on growth factor and cytokine signaling. *Cytokine Growth Factor Rev.* 31, 17–25. doi: 10.1016/j.cytogfr.2016.02.001

Esechie, A., Bhardwaj, A., Masel, T., and Raji, M. (2019). Neurocognitive sequela of burn injury in the elderly. *J. Clin. Neurosci.* 59, 1–5. doi: 10.1016/j.jocn.2018.10.089

Fayyad, M., Salim, S., Majbour, N., Erskine, D., Stoops, E., Mollenhauer, B., et al. (2019). Parkinson's disease biomarkers based on α-synuclein. *J. Neurochem.* 150, 626–636. doi: 10.1111/jnc.14809

Gezer, U., Özgür, E., Cetinkaya, M., Isin, M., and Dalay, N. (2014). Long non-coding RNAs with low expression levels in cells are enriched in secreted exosomes. *Cell Biol. Int.* 38, 1076–1079. doi: 10.1002/cbin.10301

Guo, F., Cao, Z., Guo, H., and Li, S. (2018). The action mechanism of lncRNA-HOTAIR on the drug resistance of non-small cell lung cancer by regulating Wnt signaling pathway. *Exp. Ther. Med.* 15, 4885–4889. doi: 10.3892/etm.2018.6052

Gupta, R. A., Shah, N., Wang, K. C., Kim, J., Horlings, H. M., Wong, D. J., et al. (2010). Long non-coding RNA HOTAIR reprograms chromatin state to promote cancer metastasis. *Nature* 464, 1071–1076. doi: 10.1038/nature08975

Hadari, Y. R., Gotoh, N., Kouhara, H., Lax, I., and Schlessinger, J. (2001). Critical role for the docking-protein FRS2 alpha in FGF receptor-mediated signal transduction pathways. *Proc. Natl. Acad. Sci. U.S.A.* 98, 8578–8583. doi: 10.1073/pnas.161259898

He, J., Wu, F., Han, Z., Hu, M., Lin, W., Li, Y., et al. (2021). Biomarkers (mRNAs and Non-Coding RNAs) for the diagnosis and prognosis of colorectal cancer – from the body fluid to tissue level. *Front. Oncol.* 11:632834. doi: 10.3389/fonc.2021.632834

Hernández-Ledesma, A. L., Rodríguez-Méndez, A. J., Gallardo-Vidal, L. S., Robles-Osorio, M. L., Villagrán-Herrera, M. E., Martínez-Peña, M. G., et al. (2021). Vitamin D status, proinflammatory cytokines and bone mineral density in Mexican people with multiple sclerosis. *Mult. Scler Relat. Disord.* 56:103265. doi: 10.1016/j.msard.2021.103265

Herpich, F., and Rincon, F. (2020). Management of acute ischemic stroke. *Crit. Care Med.* 48, 1654–1663.

Hong, Y., Tang, H. R., Ma, M., Chen, N., Xie, X., and He, L. (2019). Multiple sclerosis and stroke: a systematic review and meta-analysis. *BMC Neurol.* 19:139.

Hou, Y., Dan, X., Babbar, M., Wei, Y., Hasselbalch, S. G., Croteau, D. L., et al. (2019). Ageing as a risk factor for neurodegenerative disease. *Nat. Rev. Neurol.* 15, 565–581. doi: 10.1038/s41582-019-0244-7

Huang, Y., Wang, Y., Liu, X., and Ouyang, Y. (2021). Silencing lncRNA HOTAIR improves the recovery of neurological function in ischemic stroke via the miR-148a-3p/KLF6 axis. *Brain Res. Bull.* 176, 43–53. doi: 10.1016/j.brainresbull.2021.08.003

Hung, T., and Chang, H. Y. (2010). Long noncoding RNA in genome regulation: prospects and mechanisms. *RNA Biol.* 7, 582–585. doi: 10.4161/rna.7.5.13216

Jalali, S., Singh, A., Maiti, S., and Scaria, V. (2017). Genome-wide computational analysis of potential long noncoding RNA mediated DNA:DNA:RNA triplexes in the human genome. *J. Transl. Med.* 15:186.

Jankovic, J., and Tan, E. K. (2020). Parkinson's disease: etiopathogenesis and treatment. *J Neurol Neurosurg Psychiatry* 91, 795–808.

Jeong, G. R., and Lee, B. D. (2020). Pathological functions of LRRK2 in Parkinson's disease. *Cells* 9:2565. doi: 10.3390/cells9122565

Jiang, Y. J., and Bikle, D. D. (2014). LncRNA profiling reveals new mechanism for VDR protection against skin cancer formation. *J. Steroid Biochem. Mol. Biol.* 144 (Pt A), 87–90. doi: 10.1016/j.jsbmb.2013.11.018

Jin, D., Wei, W., Song, C., Han, P., and Leng, X. (2021). Knockdown EZH2 attenuates cerebral ischemia-reperfusion injury via regulating microRNA-30d-3p methylation and USP22. *Brain Res. Bull.* 169, 25–34. doi: 10.1016/j.brainresbull.2020.12.019

Jin, Z. L., Gao, W. Y., Liao, S. J., Yu, T., Shi, Q., Yu, S. Z., et al. (2021). Paeonol inhibits the progression of intracerebral haemorrhage by mediating the HOTAIR/UPF1/ACSL4 axis. *ASN Neuro* 13:17590914211010647. doi: 10.1177/17590914211010647

Kahles, T., Luedike, P., Endres, M., Galla, H. J., Steinmetz, H., Busse, R., et al. (2007). NADPH oxidase plays a central role in blood-brain barrier damage in experimental stroke. *Stroke* 38, 3000–3006. doi: 10.1161/STROKEAHA.107.489765

Kamińska, J., Koper, O. M., Piechal, K., and Kemona, H. (2017). Multiple sclerosis – etiology and diagnostic potential. *Postepy. High. Med. Dosw (Online)* 71, 551–563. doi: 10.5604/01.3001.0010.3836

Kaur, N., Chettiar, S., Rathod, S., Rath, P., Muzumdar, D., Shaikh, M. L., et al. (2013). Wnt3a mediated activation of Wnt/β-catenin signaling promotes tumor progression in glioblastoma. *Mol. Cell Neurosci.* 54, 44–57. doi: 10.1016/j.mcn.2013.01.001

Khellaf, A., Khan, D. Z., and Helmy, A. (2019). Recent advances in traumatic brain injury. *J. Neurol.* 266, 2878–2889. doi: 10.1007/s00415-019-09541-4

Klein, B., Mrowetz, H., Barker, C. M., Lange, S., Rivera, F. J., and Aigner, L. (2018). Age influences microglial activation after cuprizone-induced demyelination. *Front. Aging Neurosci.* 10:278. doi: 10.3389/fnagi.2018.00278

Kogo, R., Shimamura, T., Mimori, K., Kawahara, K., Imoto, S., Sudo, T., et al. (2011). Long noncoding RNA HOTAIR regulates polycomb-dependent chromatin modification and is associated with poor prognosis in colorectal cancers. *Cancer Res.* 71, 6320–6326. doi: 10.1158/0008-5472.CAN-11-1021

Koh, S. H., and Park, H. H. (2017). Neurogenesis in stroke recovery. *Transl. Stroke Res.* 8, 3–13.

Kumar, A., Stoica, B. A., Loane, D. J., Yang, M., Abulwerdi, G., Khan, N., et al. (2017). Microglial-derived microparticles mediate neuroinflammation after traumatic brain injury. *J. Neuroinflammation* 14:47. doi: 10.1186/s12974-017-0819-4

Kumar, M. M., and Goyal, R. (2017). LncRNA as a therapeutic target for angiogenesis. *Curr. Top. Med. Chem.* 17, 1750–1757. doi: 10.2174/1568026617666161116144744

Lambeth, J. D., Cheng, G., Arnold, R. S., and Edens, W. A. (2000). Novel homologs of gp91phox. *Trends Biochem. Sci.* 25, 459–461. doi: 10.1016/s0968-0004(00)01658-3

Lang, Y., Li, Y., Yu, H., Lin, L., Chen, X., Wang, S., et al. (2020). HOTAIR drives autophagy in midbrain dopaminergic neurons in the *Substantia nigra* compacta in a mouse model of Parkinson's disease by elevating NPTX2 via miR-221-3p binding. *Aging (Albany NY)* 12, 7660–7678. doi: 10.18632/aging.103028

Lee, S. W., De Rivero Vaccari, J. P., Truettner, J. S., Dietrich, W. D., and Keane, R. W. (2019). The role of microglial inflammasome activation in pyroptotic cell death following penetrating traumatic brain injury. *J. Neuroinflammation* 16:27. doi: 10.1186/s12974-019-1423-6

Leite, F. R., De Aquino, S. G., Guimarães, M. R., Cirelli, J. A., Zamboni, D. S., Silva, J. S., et al. (2015). Relevance of the myeloid differentiation factor 88 (MyD88) on RANKL, OPG, and nod expressions induced by TLR and IL-1R signaling

in bone marrow stromal cells. *Inflammation* 38, 1–8. doi: 10.1007/s10753-014-0001-4

Lemus, H. N., Warrington, A. E., and Rodriguez, M. (2018). Multiple sclerosis: mechanisms of disease and strategies for myelin and axonal repair. *Neurol. Clin.* 36, 1–11. doi: 10.1016/j.ncl.2017.08.002

Li, J., Wang, J., Zhong, Y., Guo, R., Chu, D., Qiu, H., et al. (2017). HOTAIR: a key regulator in gynecologic cancers. *Cancer Cell Int.* 17:65. doi: 10.1186/s12935-017-0434-6

Lin, Q., Hou, S., Dai, Y., Jiang, N., and Lin, Y. (2019). LncRNA HOTAIR targets miR-126-5p to promote the progression of Parkinson's disease through RAB3IP. *Biol. Chem.* 400, 1217–1228. doi: 10.1515/hsz-2018-0431

Liu, R. M. (2022). Aging, cellular senescence, and Alzheimer's disease. *Int. J. Mol. Sci.* 23:1989.

Liu, S. L., Wang, C., Jiang, T., Tan, L., Xing, A., and Yu, J. T. (2016). The role of Cdk5 in Alzheimer's disease. *Mol. Neurobiol.* 53, 4328–4342.

Liu, S., Cao, Q., An, G., Yan, B., and Lei, L. (2020). Identification of the 3-lncRNA signature as a prognostic biomarker for colorectal cancer. *Int. J. Mol. Sci.* 21:9359. doi: 10.3390/ijms21249359

Liu, S., Cui, B., Dai, Z. X., Shi, P. K., Wang, Z. H., and Guo, Y. Y. (2016). Long Non-coding RNA HOTAIR Promotes Parkinson's Disease Induced by MPTP Through up-regulating the expression of LRRK2. *Curr. Neurovasc. Res.* 13, 115–120. doi: 10.2174/1567202613666160316155228

Liu, X. H., Sun, M., Nie, F. Q., Ge, Y. B., Zhang, E. B., Yin, D. D., et al. (2014). Lnc RNA HOTAIR functions as a competing endogenous RNA to regulate HER2 expression by sponging miR-331-3p in gastric cancer. *Mol. Cancer* 13:92. doi: 10.1186/1476-4598-13-92

Liu, Z. J., Ran, Y. Y., Qie, S. Y., Gong, W. J., Gao, F. H., Ding, Z. T., et al. (2019). Melatonin protects against ischemic stroke by modulating microglia/macrophage polarization toward anti-inflammatory phenotype through STAT3 pathway. *CNS Neurosci. Ther.* 25, 1353–1362. doi: 10.1111/cns.13261

Lu, J., Liu, L., Chen, J., Zhi, J., Li, J., Li, L., et al. (2022). The involvement of lncRNA HOTAIR/miR-130a-3p axis in the regulation of voluntary exercise on cognition and inflammation of Alzheimer's disease. *Am. J. Alzheimers Dis. Other Dement.* 37:15333175221091424. doi: 10.1177/15333175221091424

Lu, J., Wu, M., and Yue, Z. (2020). Autophagy and Parkinson's disease. *Adv. Exp. Med. Biol.* 1207, 21–51.

Luo, X., Tu, T., Zhong, Y., Xu, S., Chen, X., Chen, L., et al. (2021). ceRNA network analysis shows that lncRNA CRNDE promotes progression of glioblastoma through sponge mir-9-5p. *Front. Genet.* 12:617350. doi: 10.3389/fgene.2021.617350

Ma, C. L., Su, L., Xie, J. J., Long, J. X., Wu, P., and Gu, L. (2014). The prevalence and incidence of Parkinson's disease in China: a systematic review and meta-analysis. *J. Neural Transm. (Vienna)* 121, 123–134. doi: 10.1007/s00702-013-1092-z

Ma, M. Z., Li, C. X., Zhang, Y., Weng, M. Z., Zhang, M. D., Qin, Y. Y., et al. (2014). Long non-coding RNA HOTAIR, a c-Myc activated driver of malignancy, negatively regulates miRNA-130a in gallbladder cancer. *Mol. Cancer* 13:156. doi: 10.1186/1476-4598-13-156

Mabuchi, S., Kuroda, H., Takahashi, R., and Sasano, T. (2015). The PI3K/AKT/mTOR pathway as a therapeutic target in ovarian cancer. *Gynecol. Oncol.* 137, 173–179.

Marehbian, J., Muehlschlegel, S., Edlow, B. L., Hinson, H. E., and Hwang, D. Y. (2017). Medical management of the severe traumatic brain injury patient. *Neurocrit. Care* 27, 430–446.

McLinden, K. A., Trunova, S., and Giniger, E. (2012). At the fulcrum in health and disease: Cdk5 and the balancing acts of neuronal structure and physiology. *Brain Disord. Ther.* 2012(Suppl 1):001. doi: 10.4172/2168-975X.S1-001

Momtazmanesh, S., and Rezaei, N. (2021). Long non-coding RNAs in diagnosis, treatment, prognosis, and progression of glioma: a state-of-the-art review. *Front. Oncol.* 11:712786. doi: 10.3389/fonc.2021.712786

Moncini, S., Lunghi, M., Valmadre, A., Grasso, M., Del Vescovo, V., Riva, P., et al. (2017). The miR-15/107 Family of microRNA genes regulates CDK5R1/p35 with implications for Alzheimer's disease pathogenesis. *Mol. Neurobiol.* 54, 4329–4342. doi: 10.1007/s12035-016-0002-4

Moreno-García, L., López-Royo, T., Calvo, A. C., Toivonen, J. M., De La Torre, M., Moreno-Martínez, L., et al. (2020). Competing endogenous RNA networks as biomarkers in neurodegenerative diseases. *Int. J. Mol. Sci.* 21:9582. doi: 10.3390/ijms21249582

Najem, D., Rennie, K., Ribecco-Lutkiewicz, M., Ly, D., Haukenfrers, J., Liu, Q., et al. (2018). Traumatic brain injury: classification, models, and markers. *Biochem. Cell Biol.* 96, 391–406. doi: 10.1139/bcb-2016-0160

Obaid, M., Udden, S. M. N., Deb, P., Shihabeddin, N., Zaki, M. H., and Mandal, S. S. (2018). LncRNA HOTAIR regulates lipopolysaccharide-induced cytokine expression and inflammatory response in macrophages. *Sci. Rep.* 8:15670. doi: 10.1038/s41598-018-33722-2

Pahlevan Kakhki, M., Nikravesh, A., Shirvani Farsani, Z., Sahraian, M. A., and Behmanesh, M. (2018). HOTAIR but not ANRIL long non-coding RNA contributes to the pathogenesis of multiple sclerosis. *Immunology* 153, 479–487. doi: 10.1111/imm.12850

Pan, X., Zheng, G., and Gao, C. (2018). LncRNA PVT1: a novel therapeutic target for cancers. *Clin. Lab.* 64, 655–662. doi: 10.7754/Clin.Lab.2018.171216

Pang, J. L., Wang, J. W., Hu, P. Y., Jiang, J. S., and Yu, C. (2018). HOTAIR alleviates ox-LDL-induced inflammatory response in Raw264.7 cells via inhibiting NF-κB pathway. *Eur. Rev. Med. Pharmacol. Sci.* 22, 6991–6998. doi: 10.26355/eurrev_201810_16170

Piek, E., Sleumer, L. S., Van Someren, E. P., Heuver, L., De Haan, J. R., De Grijs, I., et al. (2010). Osteo-transcriptomics of human mesenchymal stem cells: accelerated gene expression and osteoblast differentiation induced by vitamin D reveals c-MYC as an enhancer of BMP2-induced osteogenesis. *Bone* 46, 613–627. doi: 10.1016/j.bone.2009.10.024

Policarpo, R., Sierksma, A., De Strooper, B., and D'ydewalle, C. (2021). From junk to function: LncRNAs in CNS health and disease. *Front. Mol. Neurosci.* 14:714768. doi: 10.3389/fnmol.2021.714768

Qi, S., Yin, P., Wang, L., Qu, M., Kan, G. L., Zhang, H., et al. (2021). Prevalence of Parkinson's disease: a community-based study in China. *Mov. Disord.* 36, 2940–2944. doi: 10.1002/mds.28762

Rajagopal, T., Talluri, S., Akshaya, R. L., and Dunna, N. R. (2020). HOTAIR LncRNA: A novel oncogenic propellant in human cancer. *Clin. Chim. Acta* 503, 1–18. doi: 10.1016/j.cca.2019.12.028

Ren, H., Xu, Z., Guo, W., Deng, Z., and Yu, X. (2018). Rab3IP interacts with SSX2 and enhances the invasiveness of gastric cancer cells. *Biochem. Biophys. Res. Commun.* 503, 2563–2568. doi: 10.1016/j.bbrc.2018.07.016

Ren, S., Wang, F., Shen, J., Sun, Y., Xu, W., Lu, J., et al. (2013). Long non-coding RNA metastasis associated in lung adenocarcinoma transcript 1 derived miniRNA as a novel plasma-based biomarker for diagnosing prostate cancer. *Eur. J. Cancer* 49, 2949–2959. doi: 10.1016/j.ejca.2013.04.026

Riboldi, G. M., and Di Fonzo, A. B. (2019). GBA, gaucher disease, and Parkinson's disease: from genetic to clinic to new therapeutic approaches. *Cells* 8:364. doi: 10.3390/cells8040364

Riege, K., Hölzer, M., Klassert, T. E., Barth, E., Bräuer, J., Collatz, M., et al. (2017). Massive effect on LncRNAs in human monocytes during fungal and bacterial infections and in response to vitamins A and D. *Sci. Rep.* 7:40598. doi: 10.1038/srep40598

Rinn, J. L., Kertesz, M., Wang, J. K., Squazzo, S. L., Xu, X., Brugmann, S. A., et al. (2007). Functional demarcation of active and silent chromatin domains in human HOX loci by noncoding RNAs. *Cell* 129, 1311–1323. doi: 10.1016/j.cell.2007.05.022

Riva, P., Ratti, A., and Venturin, M. (2016). The long non-coding RNAs in neurodegenerative diseases: novel mechanisms of pathogenesis. *Curr. Alzheimer Res.* 13, 1219–1231. doi: 10.2174/1567205013666160622112234

Rothhammer, V., Borucki, D. M., Tjon, E. C., Takenaka, M. C., Chao, C. C., Ardura-Fabregat, A., et al. (2018). Microglial control of astrocytes in response to microbial metabolites. *Nature* 557, 724–728. doi: 10.1038/s41586-018-0119-x

Saez-Atienzar, S., and Masliah, E. (2020). Cellular senescence and Alzheimer disease: the egg and the chicken scenario. *Nat. Rev. Neurosci.* 21, 433–444.

Sartori, D. A., and Chan, D. W. (2014). Biomarkers in prostate cancer: what's new? *Curr. Opin. Oncol.* 26, 259–264. doi: 10.1097/CCO.0000000000000065

Satani, N., and Savitz, S. I. (2016). Is immunomodulation a principal mechanism underlying how cell-based therapies enhance stroke recovery? *Neurotherapeutics* 13, 775–782. doi: 10.1007/s13311-016-0468-9

Shahnawaz, M., Mukherjee, A., Pritzkow, S., Mendez, N., Rabadia, P., Liu, X., et al. (2020). Discriminating α-synuclein strains in Parkinson's disease and multiple system atrophy. *Nature* 578, 273–277.

Shang, K., He, J., Zou, J., Qin, C., Lin, L., Zhou, L. Q., et al. (2020). Fingolimod promotes angiogenesis and attenuates ischemic brain damage via modulating microglial polarization. *Brain Res.* 1726:146509. doi: 10.1016/j.brainres.2019.146509

Shirvani-Farsani, Z., Kakhki, M. P., Gargari, B. N., Doosti, R., Moghadasi, A. N., Azimi, A. R., et al. (2017). The expression of VDR mRNA but not NF-κB surprisingly decreased after vitamin D treatment in multiple sclerosis patients. *Neurosci. Lett.* 653, 258–263.

Simon, D. W., Mcgeachy, M. J., Bayır, H., Clark, R. S., Loane, D. J., and Kochanek, P. M. (2017). The far-reaching scope of neuroinflammation after traumatic brain injury. *Nat. Rev. Neurol.* 13, 171–191.

Soltanmoradi, S., Tavakolpour, V., Moghadasi, A. N., and Kouhkan, F. (2021). Expression analysis of NF-κB-associated long noncoding RNAs in peripheral blood mononuclear cells from relapsing-remitting multiple sclerosis patients. *J. Neuroimmunol.* 356:577602. doi: 10.1016/j.jneuroim.2021.577602

Song, C., Mitter, S. K., Qi, X., Beli, E., Rao, H. V., Ding, J., et al. (2017). Oxidative stress-mediated NFκB phosphorylation upregulates p62/SQSTM1 and promotes retinal pigmented epithelial cell survival through increased autophagy. *PLoS One* 12:e0171940. doi: 10.1371/journal.pone.0171940

Song, Y., Wang, R., Li, L. W., Liu, X., Wang, Y. F., Wang, Q. X., et al. (2019). Long non-coding RNA HOTAIR mediates the switching of histone H3 lysine 27 acetylation to methylation to promote epithelial-to-mesenchymal transition in gastric cancer. *Int. J. Oncol.* 54, 77–86. doi: 10.3892/ijo.2018.4625

Spatola, M., and Wider, C. (2014). Genetics of Parkinson's disease: the yield. *Parkinsonism Relat. Disord.* 20(Suppl. 1), S35–S38. doi: 10.1016/S1353-8020(13)70011-7

Spreafico, M., Grillo, B., Rusconi, F., Battaglioli, E., and Venturin, M. (2018). Multiple layers of CDK5R1 regulation in Alzheimer's disease implicate long non-coding RNAs. *Int. J. Mol. Sci.* 19:2022. doi: 10.3390/ijms19072022

Stein, S. C., Georgoff, P., Meghan, S., Mizra, K., and Sonnad, S. S. (2010). 150 years of treating severe traumatic brain injury: a systematic review of progress in mortality. *J. Neurotrauma* 27, 1343–1353. doi: 10.1089/neu.2009.1206

Stiegler, M. P., and Tung, A. (2014). Cognitive processes in anesthesiology decision making. *Anesthesiology* 120, 204–217. doi: 10.1097/ALN.0000000000000073

Sun, Q., Zhang, Y., Wang, Y., Wang, S., Yang, F., Cai, H., et al. (2022). LncRNA HOTAIR promotes α-synuclein aggregation and apoptosis of SH-SY5Y cells by regulating miR-221-3p in Parkinson's disease. *Exp. Cell Res.* 417:113132. doi: 10.1016/j.yexcr.2022.113132

Surguchov, A. (2020). Caveolin: a new link between diabetes and AD. *Cell Mol. Neurobiol.* 40, 1059–1066. doi: 10.1007/s10571-020-00796-4

Surguchov, A. (2022). "Biomarkers in Parkinson's disease," in *Neurodegenerative Diseases Biomarkers. Neuromethods*, Vol. 173, eds P. V. Peplow, B. Martinez, and T. A. Gennarelli (New York, NY: Humana). doi: 10.1016/j.nicl.2017.09.009

Syafruddin, S. E., Mohtar, M. A., Wan Mohamad Nazarie, W. F., and Low, T. Y. (2020). Two sides of the same coin: the roles of KLF6 in physiology and pathophysiology. *Biomolecules* 10:1378. doi: 10.3390/biom10101378

Taheri, M., Noroozi, R., Sadeghpour, S., Omrani, M. D., and Ghafouri-Fard, S. (2020). The rs4759314 SNP within Hotair lncRNA is associated with risk of multiple sclerosis. *Mult. Scler. Relat. Disord.* 40:101986. doi: 10.1016/j.msard.2020.101986

Tan, Y. T., Lin, J. F., Li, T., Li, J. J., Xu, R. H., and Ju, H. Q. (2021). LncRNA-mediated posttranslational modifications and reprogramming of energy metabolism in cancer. *Cancer Commun. (Lond)* 41, 109–120. doi: 10.1002/cac2.12108

Thomson, D. W., and Dinger, M. E. (2016). Endogenous microRNA sponges: evidence and controversy. *Nat. Rev. Genet.* 17, 272–283. doi: 10.1038/nrg.2016.20

Tolosa, E., Vila, M., Klein, C., and Rascol, O. (2020). LRRK2 in Parkinson disease: challenges of clinical trials. *Nat. Rev. Neurol.* 16, 97–107. doi: 10.1038/s41582-019-0301-2

Troshev, D., Berezhnoy, D., Kulikova, O., Abaimov, D., Muzychuk, O., Nalobin, D., et al. (2021). The dynamics of nigrostriatal system damage and neurobehavioral changes in the rotenone rat model of Parkinson's disease. *Brain Res. Bull.* 173, 1–13. doi: 10.1016/j.brainresbull.2021.04.006

Tsai, M. C., Manor, O., Wan, Y., Mosammaparast, N., Wang, J. K., Lan, F., et al. (2010). Long noncoding RNA as modular scaffold of histone modification complexes. *Science* 329, 689–693. doi: 10.1126/science.1192002

Wang, C., Chen, T., Zhang, J., Yang, M., Li, N., Xu, X., et al. (2009). The E3 ubiquitin ligase Nrdp1 'preferentially' promotes TLR-mediated production of type I interferon. *Nat. Immunol.* 10, 744–752. doi: 10.1038/ni.1742

Wang, J. Y., Feng, Y., Fu, Y. H., and Liu, G. L. (2018). Effect of sevoflurane anesthesia on brain is mediated by lncRNA HOTAIR. *J. Mol. Neurosci.* 64, 346–351. doi: 10.1007/s12031-018-1029-y

Wang, J. Z., Grundke-Iqbal, I., and Iqbal, K. (2007). Kinases and phosphatases and tau sites involved in Alzheimer neurofibrillary degeneration. *Eur. J. Neurosci.* 25, 59–68. doi: 10.1111/j.1460-9568.2006.05226.x

Wang, K. C., and Chang, H. Y. (2011). Molecular mechanisms of long noncoding RNAs. *Mol. Cell* 43, 904–914.

Wang, S. W., Liu, Z., and Shi, Z. S. (2018). Non-coding RNA in acute ischemic stroke: mechanisms, biomarkers and therapeutic targets. *Cell Transplant.* 27, 1763–1777. doi: 10.1177/0963689718806818

Wang, S., Zhang, X., Guo, Y., Rong, H., and Liu, T. (2017). The long noncoding RNA HOTAIR promotes Parkinson's disease by upregulating LRRK2 expression. *Oncotarget* 8, 24449–24456.

Wang, T., Li, H., Han, Y., Wang, Y., Gong, J., Gao, K., et al. (2020). A rapid and high-throughput approach to quantify non-esterified oxylipins for epidemiological studies using online SPE-LC-MS/MS. *Anal. Bioanal. Chem.* 412, 7989–8001. doi: 10.1007/s00216-020-02931-y

Wang, Y., Mao, J., Li, X., Wang, B., and Zhou, X. (2022a). lncRNA HOTAIR mediates OGD/R-induced cell injury and angiogenesis in a EZH2-dependent manner. *Exp. Ther. Med.* 23:99. doi: 10.3892/etm.2021.11022

Wang, Y., Xie, Y., Li, L., He, Y., Zheng, D., Yu, P., et al. (2018). EZH2 RIP-seq Identifies tissue-specific long non-coding RNAs. *Curr. Gene Ther.* 18, 275–285. doi: 10.2174/1566523218666181008125010

Wang, Y., Yi, K., Liu, X., Tan, Y., Jin, W., Li, Y., et al. (2021). HOTAIR Up-regulation activates NF-κB to induce immunoescape in gliomas. *Front. Immunol.* 12:785463. doi: 10.3389/fimmu.2021.785463

Wang, Y., Zhao, S., Li, G., Wang, D., and Jin, Y. (2022b). Neuroprotective effect of HOTAIR silencing on isoflurane-induced cognitive dysfunction via sponging microRNA-129-5p and inhibiting neuroinflammation. *Neuroimmunomodulation* 13, 1–11. doi: 10.1159/000521014

Winblad, B., Amouyel, P., Andrieu, S., Ballard, C., Brayne, C., Brodaty, H., et al. (2016). Defeating Alzheimer's disease and other dementias: a priority for European science and society. *Lancet Neurol.* 15, 455–532. doi: 10.1016/S1474-4422(16)00062-4

Wu, D., Zhu, J., Fu, Y., Li, C., and Wu, B. (2021). LncRNA HOTAIR promotes breast cancer progression through regulating the miR-129-5p/FZD7 axis. *Cancer Biomark.* 30, 203–212. doi: 10.3233/CBM-190913

Wu, P., Zuo, X., Deng, H., Liu, X., Liu, L., and Ji, A. (2013). Roles of long noncoding RNAs in brain development, functional diversification and neurodegenerative diseases. *Brain Res. Bull.* 97, 69–80. doi: 10.1016/j.brainresbull.2013.06.001

Xiao, Z., Qu, Z., Chen, Z., Fang, Z., Zhou, K., Huang, Z., et al. (2018). LncRNA HOTAIR is a prognostic biomarker for the proliferation and chemoresistance of colorectal cancer via MiR-203a-3p-mediated Wnt/ß-catenin signaling pathway. *Cell Physiol. Biochem.* 46, 1275–1285. doi: 10.1159/000489110

Xu, C. Z., Jiang, C., Wu, Q., Liu, L., Yan, X., and Shi, R. (2016). A feed-forward regulatory loop between HuR and the long noncoding RNA HOTAIR promotes head and neck squamous cell carcinoma progression and metastasis. *Cell Physiol. Biochem.* 40, 1039–1051. doi: 10.1159/000453160

Xue, H., Xu, Y., Wang, S., Wu, Z. Y., Li, X. Y., Zhang, Y. H., et al. (2019). Sevoflurane post-conditioning alleviates neonatal rat hypoxic-ischemic cerebral injury via Ezh2-regulated autophagy. *Drug Des. Devel. Ther.* 13, 1691–1706. doi: 10.2147/DDDT.S197325

Xue, M., Chen, L. Y., Wang, W. J., Su, T. T., Shi, L. H., Wang, L., et al. (2018). HOTAIR induces the ubiquitination of Runx3 by interacting with Mex3b and enhances the invasion of gastric cancer cells. *Gastric. Cancer* 21, 756–764. doi: 10.1007/s10120-018-0801-6

Yang, G., Fu, Y., Lu, X., Wang, M., Dong, H., and Li, Q. (2018). LncRNA HOTAIR/miR-613/c-met axis modulated epithelial-mesenchymal transition of retinoblastoma cells. *J. Cell Mol. Med.* 22, 5083–5096. doi: 10.1111/jcmm.13796

Yang, L., and Lu, Z. N. (2016). Long non-coding RNA HOTAIR promotes ischemic infarct induced by hypoxia through up-regulating the expression of NOX2. *Biochem. Biophys. Res. Commun.* 479, 186–191. doi: 10.1016/j.bbrc.2016.09.023

Yoon, J. H., Abdelmohsen, K., Kim, J., Yang, X., Martindale, J. L., Tominaga-Yamanaka, K., et al. (2013). Scaffold function of long non-coding RNA HOTAIR in protein ubiquitination. *Nat. Commun.* 4:2939. doi: 10.1038/ncomms3939

Zhang, A., Zhao, J. C., Kim, J., Fong, K. W., Yang, Y. A., Chakravarti, D., et al. (2015). LncRNA HOTAIR enhances the androgen-receptor-mediated transcriptional program and drives castration-resistant prostate cancer. *Cell Rep.* 13, 209–221. doi: 10.1016/j.celrep.2015.08.069

Zhang, J., Chen, G., Gao, Y., and Liang, H. (2020). HOTAIR/miR-125 axis-mediated Hexokinase 2 expression promotes chemoresistance in human glioblastoma. *J. Cell Mol. Med.* 24, 5707–5717. doi: 10.1111/jcmm.15233

Zhang, Q., Huang, X. M., Liao, J. X., Dong, Y. K., Zhu, J. L., He, C. C., et al. (2021). LncRNA HOTAIR promotes neuronal damage through facilitating NLRP3 mediated-pyroptosis activation in parkinson's disease via regulation of miR-326/ELAVL1 axis. *Cell Mol. Neurobiol.* 41, 1773–1786. doi: 10.1007/s10571-020-00946-8

Zhang, W. S., Gao, C., Tan, Y. Y., and Chen, S. D. (2021). Prevalence of freezing of gait in Parkinson's disease: a systematic review and meta-analysis. *J. Neurol.* 268, 4138–4150.

Zhang, Y., Li, C., Guan, C., Zhou, B., Wang, L., Yang, C., et al. (2020). MiR-181d-5p targets KLF6 to improve ischemia/reperfusion-induced AKI through effects on renal function, apoptosis, and inflammation. *Front. Physiol.* 11:510. doi: 10.3389/fphys.2020.00510

Zhao, J., Jin, W., Yi, K., Wang, Q., Zhou, J., Tan, Y., et al. (2021). Combination LSD1 and HOTAIR-EZH2 inhibition disrupts cell cycle processes and induces apoptosis in glioblastoma cells. *Pharmacol. Res.* 171:105764. doi: 10.1016/j.phrs.2021.105764

Zhao, J., Li, H., and Chang, N. (2020). LncRNA HOTAIR promotes MPP+-induced neuronal injury in Parkinson's disease by regulating the miR-874-5p/ATG10 axis. *Excli J.* 19, 1141–1153. doi: 10.17179/excli2020-2286

Zhao, W., Geng, D., Li, S., Chen, Z., and Sun, M. (2018). LncRNA HOTAIR influences cell growth, migration, invasion, and apoptosis via the miR-20a-5p/HMGA2 axis in breast cancer. *Cancer Med.* 7, 842–855. doi: 10.1002/cam4.1353

Zhao, X. H., Wang, Y. B., Yang, J., Liu, H. Q., and Wang, L. L. (2019). MicroRNA-326 suppresses iNOS expression and promotes autophagy of dopaminergic neurons through the JNK signaling by targeting XBP1 in a mouse model of Parkinson's disease. *J. Cell Biochem.* 120, 14995–15006. doi: 10.1002/jcb.28761

Zhou, X., Ren, Y., Zhang, J., Zhang, C., Zhang, K., Han, L., et al. (2015). HOTAIR is a therapeutic target in glioblastoma. *Oncotarget* 6, 8353–8365. doi: 10.18632/oncotarget.3229

Zhu, H. T., Bian, C., Yuan, J. C., Chu, W. H., Xiang, X., Chen, F., et al. (2014). Curcumin attenuates acute inflammatory injury by inhibiting the TLR4/MyD88/NF-κB signaling pathway in experimental traumatic brain injury. *J. Neuroinflammation* 11:59. doi: 10.1186/1742-2094-11-59

Zhuang, Y., Nguyen, H. T., Burow, M. E., Zhuo, Y., El-Dahr, S. S., Yao, X., et al. (2015). Elevated expression of long intergenic non-coding RNA HOTAIR in a basal-like variant of MCF-7 breast cancer cells. *Mol .Carcinog.* 54, 1656–1667. doi: 10.1002/mc.22237

Zuccotti, P., Colombrita, C., Moncini, S., Barbieri, A., Lunghi, M., Gelfi, C., et al. (2014). hnRNPA2/B1 and nELAV proteins bind to a specific U-rich element in CDK5R1 3'-UTR and oppositely regulate its expression. *Biochim. Biophys. Acta* 1839, 506516 doi: 10.1016/j.bbagrm.2014.04.018

Conflict of Interest: The authors declare that the research was conducted in the absence of any commercial or financial relationships that could be construed as a potential conflict of interest.

Publisher's Note: All claims expressed in this article are solely those of the authors and do not necessarily represent those of their affiliated organizations, or those of the publisher, the editors and the reviewers. Any product that may be evaluated in this article, or claim that may be made by its manufacturer, is not guaranteed or endorsed by the publisher.

frontiers | Frontiers in Molecular Neuroscience

OPINION
published: 28 June 2022
doi: 10.3389/fnmol.2022.943492

NF-kB (p50/p65)-Mediated Pro-Inflammatory microRNA (miRNA) Signaling in Alzheimer's Disease (AD)

Walter J. Lukiw [1,2,3]*

[1] LSU Neuroscience Center, Louisiana State University Health Science Center, New Orleans, LA, United States, [2] Department of Ophthalmology, Louisiana State University Health Science Center, New Orleans, LA, United States, [3] Department Neurology, Louisiana State University Health Science Center, New Orleans, LA, United States

Keywords: Alzheimer's disease (AD), microRNA, NF-kB (p50/p65), reactive oxygen species (ROS), lipopolysaccharide, miRNA-based therapy, miRNA-9/miRNA-30b/miRNA-34a/miRNA-146a/miRNA-155, anti-NF-kB therapy

OPEN ACCESS

Edited by:
Jun Yan,
The University of Queensland, Australia

Reviewed by:
Uwe Beffert,
Boston University, United States

***Correspondence:**
Walter J. Lukiw
wlukiw@lsuhsc.edu

Specialty section:
This article was submitted to Molecular Signalling and Pathways, a section of the journal Frontiers in Molecular Neuroscience

Received: *13 May 2022*
Accepted: *27 May 2022*
Published: *28 June 2022*

Citation:
Lukiw WJ (2022) NF-kB (p50/p65)-Mediated Pro-Inflammatory microRNA (miRNA) Signaling in Alzheimer's Disease (AD). Front. Mol. Neurosci. 15:943492. doi: 10.3389/fnmol.2022.943492

INTRODUCTION

A small family of NF-kB (p50/p65)-regulated microRNAs (miRNAs) has been identified and partially characterized in Alzheimer's disease (AD) brain in the hippocampal CA1 and temporal lobe neocortical regions, and in reactive oxygen species (ROS)-, cytokine interleukin 1-beta (IL-1β)-, amyloid beta 42 (Aβ42) peptide- and/or lipopolysaccharide (LPS)-stressed human neuronal-glial (HNG) cells in primary co-culture. This microRNA family currently includes miRNA-9, miRNA-30b, miRNA-34a, miRNA-125b, miRNA-146a and miRNA-155. Other brain-enriched miRNA species may be involved. Experimental evidence suggests that in neurological diseases, the upregulation of this small pro-inflammatory miRNA family orchestrates a pathogenic gene expression program that can explain many aspects of AD onset, and propagation and severity of the disease including failure of microglial-mediated clearance of amyloid-beta (Aβ) and other end-stage peptides from brain cells, amyloidogenesis, astrogliosis, deficits in neurotropism, neuronal cell atrophy, and downregulation in the production of essential cytoskeletal components and synaptic signaling elements. This opinion article will contribute to the interpretation of the most recent findings in the current research area involving NF-kB-regulated miRNA-mediated signaling pathways, and how this information may aid in the advancement of therapeutic strategies for more effective clinical management of AD and other progressive age-related and lethal neurodegenerative disorders.

ALZHEIMER'S DISEASE (AD): EPIDEMIOLOGY AND BASIC FEATURES

AD is a slowly developing, irreversible, progressive, and inflammatory neurodegeneration of the human brain, central nervous system (CNS), and neural vasculature (Alzheimer et al., 1995; Lane et al., 2018; Trejo-Lopez et al., 2021). Due in part to the aging population and demographics, the global incidence and prevalence of AD are sharply increasing, and AD currently represents the largest single cause of age-related memory impairment and behavioral and cognitive decline in Westernized societies. Current estimates put the global incidence of AD at about ∼55 million, and this number is expected to reach epidemic proportions and rise to about ∼150 million cases by the

year 2050 (Tahami Monfared et al., 2022; https://alz-journals.onlinelibrary.wiley.com/doi/full/10.1002/alz.12638; https://www.alz.org/media/documents/Alzheimers-facts-and-figures.pdf; https://www.Alzint.org/about/dementia-facts-figures/dementia-statistics/last accessed 13 June 2022). AD places a tremendous socioeconomic burden on caregivers and on the healthcare system as a whole. Despite ∼115 years of intense and directed research, no effective treatment or cure for AD exists, although many insights into the molecular-genetic nature of this age-related disease have been established (Alzheimer et al., 1995; Kaur et al., 2015; Lane et al., 2018; Dong et al., 2021; Hermans et al., 2021; Trejo-Lopez et al., 2021; Liu et al., 2022; Olufunmilayo and Holsinger, 2022; Pogue et al., 2022; Rastegar-Moghaddam et al., 2022; Singh et al., 2022; Tahami Monfared et al., 2022; Yoon et al., 2022). As a devastating, inflammatory, and terminal neurodegenerative disorder, one molecular genetic component that has emerged at the forefront of current AD research is the DNA-binding element NF-kB, probably the single most important transcription factor yet identified in the complex neuropathology of AD. This opinion article will address some recently described effects of NF-kB on a small family of regulatory miRNAs observed to be significantly altered in abundance, complexity and speciation in AD-affected brain.

NF-κB-SENSITIVE microRNAS AND INFLAMMATORY SIGNALING IN ALZHEIMER'S DISEASE (AD)

Discovered about ∼36 years ago, the heterodimeric transcription factor NF-kB (p50/p65) was first described as a rapidly inducible nuclear factor κ-light-chain transcription enhancer of activated B cell lymphocytes in part responsible for the humoral immunity component of the immune system (Sen and Baltimore, 1986; Kaltschmidt et al., 1993; Taganov et al., 2006). Since then, recognition sites for this redox-controlled transcriptional activator and DNA-binding protein have been found to occur in multiple gene promoters, and it is now known to drive a broad range of gene expression patterns in diverse cellular types involved in host innate- and adaptive-immune functions with important roles in the clearance of waste molecules from the cytoplasm, inflammatory signaling, differentiation, cell growth, tumorigenesis and neurodegeneration (Taganov et al., 2006; Zhang et al., 2017; Baltimore, 2019). In resting cells the pre-formed NF-kB (p50/p65; 115 kDa) heterodimer is bound to a hydrophobic inhibitory kappa B protein (IkB, 36 kDa) that prevents free NF-kB from promoter-DNA-binding and gene transactivation. However NF-κB can be rapidly induced in all cell types by treating them with pro-inflammatory mediators that include interleukin-1beta (IL-1β), interleukin 6 (IL-6), tumor necrosis factor alpha (TNFα), and endotoxins such as lipopolysaccharides (LPS), an intensely inflammatory lipoprotein produced exclusively by Gram-negative bacteria, Aβ peptides, viral gene products, ultraviolet and other ionizing irradiation, and reactive oxygen species (ROS)-generating and/or oxidizing compounds. Exposure to these factors induces IkB decomposition triggered through a site-specific phosphorylation of an IκB kinase (IKK) complex, followed by degradation via the ubiquitin-proteasome system, and then rapid NF-kB-activated transcription by multiple pro-inflammatory NF-kB-sensitive gene promoters. The human brain and CNS contain a very active, pleiotropic NF-kB-signaling system that has a function in both neurological health and disease (Kaltschmidt and Kaltschmidt, 2009; Christian et al., 2016; Liu et al., 2022; Yoon et al., 2022). While the NF-kB (p50/p65; also known as p50/RelA) heterodimer is especially abundant in nervous tissues, other homo- or hetero-dimeric NF-kB transcription factor complexes containing at least 5 other molecular components that include RelA, RelB, c-Rel, p50, p52, and NFKB1 (p105) form at least 12 different identified NF-kB complexes. All share the conserved Rel homology domain (RHD) responsible for DNA binding, dimerization, and association with the repressor protein IκB (Zhang et al., 2017; Pires et al., 2018; Baltimore, 2019; https://www.genecards.org/cgi-bin/carddisp.pl?gene=RELA; last accessed 25 May 2022). It has been repeatedly demonstrated: (i) that activated NF-kB subsequently upregulates a select sub-group of disease-associated miRNAs comprising a well-characterized NF-kB-sensitive *Homo sapiens*-enriched family of potentially pathogenic miRNAs that include miRNA-9, miRNA-30b, miRNA-34a, miRNA-146a, and miRNA-155 normally involved in immunity, inflammation, and brain cell genetic function in the CNS (Lukiw, 2012, 2020; Brennan et al., 2019; Juźwik et al., 2019; Barnabei et al., 2021; Song et al., 2021; Yoon et al., 2022); (ii) that the same miRNAs are upregulated in AD brain; (iii) that this group of significantly over-expressed miRNAs are abundant in progressive and often lethal viral and prion-mediated and/or related neurological syndromes associated with progressive inflammatory neurodegeneration; and (iv) that all of these NF-kB-sensitive endotoxin-responsive miRNA genes have as many as three tandem, functional NF-kB binding sites stacked in their immediate 5'-promoter region, making this miRNA gene family exceptionally sensitive to NF-kB activation and NF-kB-mediated transcriptional upregulation (Taganov et al., 2006; Lukiw et al., 2008; Alexandrov et al., 2019; Jauhari et al., 2020; **Table 1**). Interestingly, there is also abundant recent evidence (i) that endotoxins such as LPS and other biophysical-barrier-penetrating glycolipids and lipoproteins specifically induce neurodegeneration by promoting neuro-inflammatory signaling by stimulation of Toll-like receptors (TLRs) present on the outer membranes of glial cells of the CNS (Kumar, 2019; Singh et al., 2022); (ii) that extremely potent pro-inflammatory species of LPSs have been found by many independent groups to be localized in human brain neurons in AD brain (Zhan et al., 2018, 2021; Alexandrov et al., 2019; Zhao et al., 2019a; Singh et al., 2022); and (iii) that a life-long supply of microbiome-abundant Gram-negative bacteria-derived LPS would be available over the long-term to chronically upregulate NF-kB in the brain and CNS, as is observed in LPS-treated human neurons in primary culture and in AD temporal lobe neocortex, the latter an anatomical area targeted by the AD process (Lukiw and Bazan, 1998; Zhang et al., 2017; Zhan et al., 2018, 2021; Zhao and Lukiw, 2018; Alexandrov et al., 2019; Zhao et al., 2019a; Singh et al., 2022).

TABLE 1 | NF-kB-induced microRNAs (miRNAs), their mRNA targets, functions, and pathways in Alzheimer's disease (AD)-affected brain; all miRNAs listed show: (i) significant upregulation following NF-kB (p50/p65) activation; (ii) are potentially pathogenic and are upregulated in AD brain, AD cell culture, and transgenic murine models of AD (TgAD); and (iii) have been shown to interactively contribute to the AD process; some closely related work on the functions these miRNAs in neuronal cell culture, TgAD models, and other human neurodegenerative diseases have also been included in the References.

Human miRNA	mRNA target(s)	mRNA function	Result of mRNA and gene expression deficit	Reference
miRNA-9	CFH	complement factor H; repressor of activation of the innate immune response in brain and retina at the C3 to C3b transition	CFH deficits in disease are pro-inflammatory; excessive activation of the innate-immune response, altered immune-signaling, neuroinflammation	Clement et al. (2016), Recabarren and Alarcón (2017), Chen et al. (2018), Natoli and Fernando (2018)
	TREM2	triggering receptor expressed in myeloid and microglial cells; surface receptor essential in removing cellular debris; viral infection	deficits in phagocytosis and clearance of end-stage metabolic products from cells including amyloid beta (Aβ) peptides	Lukiw et al. (2008), Zhao and Lukiw (2013, 2018), Bhattacharjee et al. (2016), Chen et al. (2021)
	TSPAN-7	transmembrane spanning superfamily member 7; regulator of surface receptor signal transduction; activates ADAM10-dependent cleavage activity of βAPP; tau seeding activity; viral infection	amyloidogenesis; impairment of autophagic activity and promotion of amyloid plaque formation; inhibition of autophagy; supports the formation of neurofibrillary tangles (NFT)	Jaber et al. (2019), Perot and Ménager (2020), Chen et al. (2021), Turk et al. (2021)
miRNA-30b	NF-L (NEFL)	neurofilament light chain protein; neuron-specific; supports neuronal cytoarchitecture, radial diameter of axons and synaptic signaling	loss of neuronal cytoarchitecture and signaling capacity; neuronal atrophy; synaptic structural deficits; general biomarker for neurodegeneration	McLachlan et al. (1990), Kittur et al. (1994), Brennan et al. (2019), Xu et al. (2021), Zhao et al. (2021)
miRNA-34a	SHANK3	SH3 proline-rich and multiple-ankyrin-repeat domain (SHANK3) cytoskeletal anchoring protein; gene directional gene expression effects; associated with viral infection	Disruption of the cytoskeleton and post-synaptic structure and scaffolding network; deficits in synaptic organization, dendritic spine maturation and synaptic vesicle release	Lu et al. (2010), Choi et al. (2015), Jaber et al. (2017), Lee et al. (2017), Jin et al. (2018), Zhao et al. (2019b)
	TREM2	triggering receptor expressed in myeloid and microglial cells; surface receptor essential in removing cellular debris; associated with viral (SARS-CoV-2) infection	deficits in phagocytosis and clearance of end-stage metabolic products from cells including amyloid beta (Aβ) peptides- deficits in AD and AMD	Zhao and Lukiw (2013), Zhao et al. (2013), Hermans et al. (2021), Wu et al. (2021), Olufunmilayo and Holsinger (2022)
miRNA-125b	CDKN2A	cyclin-dependent kinase inhibitor 2A cell cycle inhibitor; induces cell cycle arrest; viral (SARS-CoV-2) infection	downregulation of cell cycle control: astrogliosis and glial cell proliferation	Pogue et al. (2010), Czapski et al. (2021), Valeri et al. (2021)
	SYN-2	synapsin-2: neuron-specific; neuronal synaptic phosphoprotein; coats synaptic vesicles; functions in the regulation of neurotransmitter release	impairment of neurotransmitter release and trans-synaptic signaling; synaptic signaling deficits observed in AD brain and in TgAD murine models	Ferreira and Rapoport (2002), Mirza and Zahid (2018), Zhao et al. (2019a, 2021), Jeśko et al. (2021)
	15-LOX-1	ALOX15; arachidonate 15-lipoxygenase; essential in the conversion of docosahexaenoic acid to neuro-protectin D1 (NPD1)	lack of NPD1; lack of neurotrophic support; deficiency of neurotrophic omega-3 fatty acid derivatives in the human brain neocortex	Lukiw et al. (2005), Zhao et al. (2014), Sun et al. (2018), Al-Fadly et al. (2019)
miRNA-146a	CFH	complement factor H; complement control glycoprotein; deficits in disease are pro-inflammatory to the host; viral (SARS-CoV-2) infection; see above	defective control and stimulation of the innate- immune response; and pro-inflammatory signaling; role in neuro-pathological signaling in AD and prion disease	Alexandrov et al. (2019), Slota and Booth (2019), Fan et al. (2020), Yu et al. (2020), Aslani et al. (2021), Pogue and Lukiw (2021), Wu et al. (2021)
	IRAK-1	interleukin-1 receptor-associated kinase 1; initiation and sustenance of the innate immune response and NF-κB signaling	compensatory surge in IRAK-2 and chronic stimulation of NF-κB signaling in the brain; neuroinflammation	Cui et al. (2010), Arena et al. (2017), Aslani et al. (2021)
	TSPAN12	transmembrane superfamily member 12; cell surface receptor involved in signal transduction; activates ADAM10-dependent cleavage of βAPP and tau seeding activity	pathological shift from neurotrophic (sAPPα) to amyloidogenic (beta- and gamma-secretase cleavage); processing of βAPP into neurotoxic Aβ42 peptides	Li et al. (2011), Jaber et al. (2017), Aslani et al. (2021), Miyoshi et al. (2021)
miRNA-155	CFH	complement factor H; see above	defective regulation of the innate-immune response (see above)	Chen et al. (2018), Zingale et al. (2021), Rastegar-Moghaddam et al. (2022)

THERAPEUTIC STRATEGIES DIRECTED AGAINST NF-kB AND/OR PRO-INFLAMMATORY miRNA SIGNALING

Because NF-kB signaling pathways appear to be centrally involved in a great many immune- and inflammation-linked human diseases from carcinogenesis to neurodegeneration, a large number of natural and synthetic NF-kB inhibitors have been designed and tested, and are under very active investigation to limit the extent of NF-kB activation in the cellular environment. The evolution of one single high-potency gene-activating transcription factor in overlapping signaling pathways has made it challenging to find biologically active inhibitory molecules that can interfere with and/or block specific signaling pathways that lead to NF-κB activation without multiple off-target effects or other complicating factors. Even so, a number of NF-kB modulator and blocking strategies have been adopted or are undergoing rigorous evaluation in both research laboratories and in clinical settings. In general, therapeutic NF-kB inhibition can occur *via* four basic mechanistic strategies: (i) by blockage of the original physiological stimulating signals that drive NF-kB activation; (ii) by targeting phosphorylation pathways associated with NF-kB activation because NF-κB phosphorylation controls transcription in a gene-specific manner; (iii) by modulation or activation of the IkB complex or other NF-kB subunits; and/or (iv) by blockage of NF-kB translocation, DNA sequence recognition, and binding and/or modification of NF-kB that affects its activity or target specificity. These approaches include but are not limited to the following strategies, most of which are under very active research and therapeutic development: (i) antioxidant approaches that neutralize the primary NF-kB activation signals such as quenching of reactive oxygen species (ROS) and other oxidizing and/or redox compounds (Kaur et al., 2015; Barnabei et al., 2021; Jover-Mengual et al., 2021; Pogue and Lukiw, 2021); (ii) alteration of multiple phosphorylation events that disrupt the activation of the multi-subunit NF-kB transcription complex and alter the interaction of these phosphorylation sites that ultimately determines the selectivity of NF-κB effects on transcriptional activity (by advanced investigation of these highly interactive phosphorylation sites and mechanisms it should be possible to modulate or block many aspects of phosphorylation-mediated NF-kB activation; Christian et al., 2016; https://360researchreports.com/global-nf-kb-inhibitors-market-20149725); (iii) as previously pointed out, because active NF-kB complexes are assembled from various combinations of RelA, RelB, c-Rel, p50, p52, NFKB1 (p105) etc., it may be possible to specifically block the generation and/or assembly of a single monomeric species of NF-kB by limiting the abundance of one of the subunits of NF-kB by genome editing, including knock-out technologies and/or the Cas9/CRISPR editing system (Wang et al., 2018; Dai et al., 2020; Katti et al., 2022); (iv) NF-kB is directed to bind to its genomic targets by topological features located in certain promoter DNA sequences; therefore, these highly specific promoter DNA binding sites can be masked, blocked, or modulated using genome blocking technologies involving small non-coding RNA (sncRNA), NF-kB decoy sequence, and/or Cas9/CRISPR editing strategies (Taganov et al., 2006; Christian et al., 2016; Zhang et al., 2017; Baltimore, 2019; Dai et al., 2020; Katti et al., 2022; Yoon et al., 2022); (v) specific upregulated miRNA abundance and speciation may be blocked or modulated using chemically stabilized anti-miRNA strategies or by targeting miRNA processing enzymes, thus preventing the creation of a fully active and/or biologically available miRNA species; (vi) directed delivery systems to the brain and/or CNS or other tissue and/or organ systems to minimize unwarranted off-target effects; (vii) long-term systemic ingestion of low-dose NF-κB inhibitors including dietary-administered flavonoids, lignans, diterpenes and sesquiterpenes, saponins, polysaccharides, polyphenols, biological fiber, and other natural products that may have general beneficial effects on reducing pro-inflammatory signaling, carcinogenesis, and neurodegeneration by chronic dampening of NF-κB activities. These have been used for millennia in the pharmacopeia associated with ethnic biomedical-treatment approaches (Gilmore and Herscovitch, 2006; Li et al., 2020a,b; Olajide and Sarker, 2020; Uddin et al., 2021; Al-Khayri et al., 2022; Das et al., 2022); and/or (viii) any combination of these therapeutic strategies. Regarding the creation and testing of synthetic NF-kB modulatory or blocking compounds, about ∼80 pharmaceutical companies are currently in the pursuit of more effective, directed and specifically targeted NF-kB inhibitors for clinical application in human diseases involving excessive NF-kB activation and signaling (https://www.futuremarketinsights.com/reports/nf-kb-inhibitors-market; https://www.Globenewswire.com/news-release/2020/12/08/2141 093/0/en/NF-kappa-B-Inhibitors-Therapeutics-pipeline-analysis-of-80-Companies.html; https://360researchreports.com/global-nf-kb-inhibitors-market- 20149725; last accessed 25 May 2022).

DISCUSSION

The pleiotropic homo- or hetero-dimeric transcription factor NF-kB is a master regulator of the innate immune system, inflammatory responses, and neurotropic, cytoskeletal, synaptic, phagocytic, and synaptic deficit characteristics of the AD-affected brain and related neurodegenerative disorders. One critically important regulatory action of the NF-kB complex is to upregulate a small family of pathogenic miRNAs in the brain and CNS, which in turn targets and downregulates a group of mRNAs whose downregulation is decisive in driving the neuropathology of AD (**Table 1**). It is our opinion that these NF-kB-regulated miRNA-mRNA linked pathological interactions will provide a wealth of targets for therapeutics and disease intervention. The merging of experimental and human clinical trials will be decisive in the strategic design and application of NF-kB and NF-kB-miRNA-induced modulatory agents and drugs useful in the more efficacious treatment of the current AD epidemic.

AUTHOR CONTRIBUTIONS

WL researched, compiled data, and wrote the paper. WL approved and submitted the final version.

FUNDING

Research involving small non-coding RNA (sncRNA) and miRNA signaling, including NF-kB (p50/p65)-mediated miRNA signaling, the innate-immune response, amyloidogenesis and neuro-inflammation in AD and prion disease, contributions of the microbiome-derived neurotoxins such as lipopolysaccharide (LPS), reactive oxygen species (ROS), anti-NF-kB and/or anti-miRNA therapeutic strategies was supported through the Louisiana Biotechnology Research Network (LBRN), an unrestricted grant to the LSU Eye Center from Research to Prevent Blindness (RPB), The Brown Foundation, Joe and Dorothy Dorsett Innovation in Science Healthy Aging Award; and National Institutes of Health (NIH) NIA Grants AG18031 and AG038834.

REFERENCES

Alexandrov, P., Zhao, Y., Li, W., and Lukiw, W. J. (2019). Lipopolysaccharide-stimulated, NF-kB-, miRNA-146a- and miRNA-155-mediated molecular-genetic communication between the human gastrointestinal tract microbiome and the brain. *Folia Neuropathol.* 57, 211–219. doi: 10.5114/fn.2019.88449

Al-Fadly, E. D., Elzahhar, P. A., Tramarin, A., Elkazaz, S., Shaltout, H., Abu-Serie, M. M., et al. (2019). Tackling neuroinflammation and cholinergic deficit in Alzheimer's disease: multi-target inhibitors of cholinesterases, cyclooxygenase-2 and 15-lipoxygenase. *Eur. J. Med. Chem.* 167, 161–186. doi: 10.1016/j.ejmech.2019.02.012

Al-Khayri, J. M., Sahana, G. R., Nagella, P., Joseph, B. V., Alessa, F. M., and Al-Mssallem, M. Q. (2022). Flavonoids as potential anti-inflammatory molecules: a review. *Molecules.* 27, 2901. doi: 10.3390/molecules27092901

Alzheimer, A., Stelzmann, R. A., Schnitzlein, H. N., and Murtagh, F. R. (1995). An English translation of Alzheimer's 1907 paper, "Uber eine eigenartige Erkankung der Hirnrinde". *Clin. Anat.* 8, 429–431. doi: 10.1002/ca. 980080612

Arena, A., Iyer, A. M., Milenkovic, I., Kovacs, G. G., Ferrer, I., Perluigi, M., et al. (2017). Developmental expression and dysregulation of miRNA-146a and miRNA-155 in Down's syndrome and mouse models of down's syndrome and Alzheimer's disease. *Curr. Alzheimer's Res.* 14, 1305–1317. doi: 10.2174/1567205014666 170706112701

Aslani, M., Mortazavi-Jahromi, S. S., and Mirshafiey, A. (2021). Efficient roles of miRNA-146a in cellular and molecular mechanisms of neuroinflammatory disorders: An effectual review in neuroimmunology. *Immunol. Lett.* 238, 1–20. doi: 10.1016/j.imlet.2021.07.004

Baltimore, D. (2019). Sixty years of discovery. *Annu. Rev. Immunol.* 37, 1–17. doi: 10.1146/annurev-immunol-042718-041210

Barnabei, L., Laplantine, E., Mbongo, W., Rieux-Laucat, F., and Weil, R. (2021). NF-κB: at the borders of autoimmunity and inflammation. *Front. Immunol.* 12, 716469. doi: 10.3389/fimmu.2021.716469

Bhattacharjee, S., Zhao, Y., Dua, P., Rogaev, E. I., and Lukiw, W. J. (2016). microRNA-34a-mediated down-regulation of the microglial-enriched triggering receptor and phagocytosis-sensor TREM2 in age-related macular degeneration. *PLoS One.* 11, e0150211. doi: 10.1371/journal.pone.0150211

Brennan, S., Keon, M., Liu, B., Su, Z., and Saksena, N. K. (2019). Panoramic visualization of circulating microRNAs across neurodegenerative diseases in humans. *Mol. Neurobiol.* 56, 7380–7407. doi: 10.1007/s12035-019-1615-1

Chen, J., Qi, Y., Liu, C. F., Lu, J. M., Shi, J., and Shi, Y. (2018). microRNA expression data analysis to identify key miRNAs associated with Alzheimer's disease. *J. Gene Med.* 20, e3014. doi: 10.1002/jgm.3014

Chen, M. L., Hong, C. G., Yue, T., Li, H. M., Duan, R., Hu, W. B., et al. (2021). Inhibition of miR-331-3p and miR-9-5p ameliorates Alzheimer's disease by enhancing autophagy. *Theranostics* 11, 2395–2409. doi: 10.7150/thno.47408

Choi, S. Y., Pang, K., Kim, J. Y., Ryu, J. R., Kang, H., and Liu, Z. (2015). Post-transcriptional regulation of SHANK3 expression by microRNAs related to multiple neuropsychiatric disorders. *Mol. Brain.* 8, 74. doi: 10.1186/s13041-015-0165-3

Christian, F., Smith, E. L., and Carmody, R. J. (2016). The regulation of NF-κB subunits by phosphorylation. *Cells* 5, 12. doi: 10.3390/cells5010012

Clement, C., Hill, J. M., Dua, P., Culicchia, F., and Lukiw, W. J. (2016). Analysis of RNA from Alzheimer's disease post-mortem brain tissues. *Mol. Neurobiol.* 53, 1322–1328. doi: 10.1007/s12035-015-9105-6

Cui, J. G., Li, Y. Y., Zhao, Y., Bhattacharjee, S., and Lukiw, W. J. (2010). Differential regulation of interleukin-1 receptor-associated kinase-1 (IRAK-1) and IRAK-2 by microRNA-146a and NF-kB in stressed human astroglial cells and in Alzheimer disease. *J. Biol. Chem.* 285, 38951–38960. doi: 10.1074/jbc.M110.178848

Czapski, G. A., Cieślik, M., Białopiotrowicz, E., Lukiw, W. J., and Strosznajder, J. B. (2021). Down-regulation of cyclin D2 in amyloid β toxicity, inflammation, and Alzheimer's disease. *PLoS ONE* 16, e0259740. doi: 10.1371/journal.pone.0259740

Dai, W., Wu, J., Wang, D., and Wang, J. (2020). Cancer gene therapy by NF-κB-activated cancer cell-specific expression of CRISPR/Cas9 targeting telomeres. *Gene Ther.* 27, 266–280. doi: 10.1038/s41434-020-0128-x

Das, R., Mehta, D. K., and Dhanawat, M. (2022). Medicinal plants in cancer treatment: contribution of nuclear factor-kappa B (NF-kB) inhibitors. *Mini. Rev. Med. Chem.* doi: 10.2174/1389557522666220307170126

Dong, Z., Gu, H., Guo, Q., Liang, S., Xue, J., Yao, F., et al. (2021). Profiling of serum exosome miRNA reveals the potential of a miRNA panel as diagnostic biomarker for Alzheimer's disease. *Mol. Neurobiol.* 58, 3084–3094. doi: 10.1007/s12035-021-02323-y

Fan, W., Liang, C., Ou, M., Zou, T., Sun, F., Zhou, H., et al. (2020). microRNA-146a Is a wide-reaching neuroinflammatory regulator and potential treatment target in neurological diseases. *Front. Mol. Neurosci.* 13, 90. doi: 10.3389/fnmol.2020.00090

Ferreira, A., and Rapoport, M. (2002). The synapsins: beyond the regulation of neurotransmitter release. *Cell. Mol. Life Sci.* 59, 589–595. doi: 10.1007/s00018-002-8451-5

Gilmore, T. D., and Herscovitch, M. (2006). Inhibitors of NF-kappaB signaling: 785 and counting. *Oncogene.* 25, 6887–6899. doi: 10.1038/sj.onc

Hermans, S. J., Nero, T. L., Morton, C. J., Gooi, J. H., Crespi, G. A. N., Hancock, N. C., et al. (2021). Structural biology of cell surface receptors implicated in Alzheimer's disease. *Biophys. Rev.* 14, 233–255. doi: 10.1007/s12551-021-00903-9

Jaber, V., Zhao, Y., and Lukiw, W. J. (2017). Alterations in micro RNA-messenger RNA (miRNA-mRNA) coupled signaling networks in sporadic Alzheimer's disease (AD) hippocampal CA1. *J. Alzheimer's Dis. Parkinsonism.* 7, 312. doi: 10.4172/2161-0460.1000312

Jaber, V. R., Zhao, Y., Sharfman, N. M., Li, W., and Lukiw, W. J. (2019). Addressing Alzheimer's disease (AD) neuropathology using anti-microRNA (AM) strategies. *Mol. Neurobiol.* 56, 8101–8108. doi: 10.1007/s12035-019-1632-0

Jauhari, A., Singh, T., Mishra, S., Shankar, J., and Yadav, S. (2020). Coordinated action of miRNA-146a and parkin gene regulate rotenone-induced neurodegeneration. *Toxicol. Sci.* 176, 433–445. doi: 10.1093/toxsci/kfaa066

Jeśko, H., Wieczorek, I., Wencel, P. L., Gassowska-Dobrowolska, M., Lukiw, W. J., and Strosznajder, R. P. (2021). Age-related transcriptional deregulation of genes coding synaptic proteins in Alzheimer's disease murine model: potential neuroprotective effect of fingolimod. *Front. Mol. Neurosci.* 14, 660104. doi: 10.3389/fnmol.2021.660104

Jin, C., Kang, H., Ryu, J. R., Kim, S., Zhang, Y., Lee, Y., et al. (2018). Integrative brain transcriptome analysis reveals region-specific and broad molecular changes in SHANK3-overexpressing mice. *Front. Mol. Neurosci.* 11, 250. doi: 10.3389/fnmol.2018.00250

Jover-Mengual, T., Hwang, J. Y., Byun, H. R., Court-Vazquez, B. L., Centeno, J. M., Burguete, M. C., et al. (2021). The role of NF-κB triggered

inflammation in cerebral ischemia. *Front. Cell. Neurosci.* 15, 633610. doi: 10.3389/fncel.2021.633610

Juźwik, C. A., S Drake S., Zhang, Y., Paradis-Isler, N., Sylvester, A., Amar-Zifkin, A., et al. (2019). microRNA dysregulation in neurodegenerative diseases: A systematic review. *Prog. Neurobiol.* 182, 101664. doi: 10.1016/j.pneurobio.2019.101664

Kaltschmidt, B., Baeuerle, P. A., and Kaltschmidt, C. (1993). Potential involvement of the transcription factor NF-kappa B in neurological disorders. *Mol Aspects Med.* 14, 171–190. doi: 10.1016/0098-2997(93)90004-w

Kaltschmidt, B., and Kaltschmidt, C. (2009). NF-kappaB in the nervous system. *Cold Spring Harb. Perspect. Biol.* 1, a001271. doi: 10.1101/cshperspect.a001271

Katti, A., Diaz, B. J., Caragine, C. M., Sanjana, N. E., and Dow, L. E. (2022). CRISPR in cancer biology and therapy. *Nat. Rev. Cancer*. 22, 259–279. doi: 10.1038/s41568-022-00441-w

Kaur, U., Banerjee, P., Bir, A., Sinha, M., Biswas, A., and Chakrabarti, S. (2015). Reactive oxygen species, redox signaling and neuroinflammation in Alzheimer's disease: the NF-κB connection. *Curr. Top Med. Chem.* 15, 446–457. doi: 10.2174/1568026615666150114160543

Kittur, S., Hoh, J., Endo, H., Tourtellotte, W., Weeks, B. S., Markesbery, W., et al. (1994). Cytoskeletal neurofilament gene expression in brain tissue from Alzheimer's disease patients. Decrease in NF-L and NF-M message. *J. Geriatr. Psychiatry Neurol.* 7, 153–158. doi: 10.1177/089198879400700305

Kumar, V. (2019). Toll-like receptors in the pathogenesis of neuroinflammation. *J. Neuroimmunol.* 332, 16–30. doi: 10.1016/j.jneuroim.2019.03.012

Lane, C. A., Hardy, J., and Schot, J. M. (2018). Alzheimer's disease. *Eur. J. Neurol.* 25, 59–70. doi: 10.1111/ene.13439

Lee, Y., Kang, H., Lee, B., Zhang, Y., Kim, Y., Kim, S., et al. (2017). Integrative analysis of brain region-specific SHANK3 interactomes for understanding the heterogeneity of neuronal pathophysiology related to SHANK3 mutations. *Front. Mol. Neurosci.* 10, 110. doi: 10.3389/fnmol.2017.00110

Li, C. L., Liu, X. H., Qiao, Y., Ning, L. N., Li, W. J., and Sun, Y. S. (2020a). Allicin alleviates inflammation of diabetic macroangiopathy via the Nrf2 and NF-kB pathway. *Eur. J. Pharmacol.* 876, 173052. doi: 10.1016/j.ejphar.2020.173052

Li, L., Xu, Y., Zhao, M., and Gao, Z. (2020b). Neuro-protective roles of long non-coding RNA MALAT1 in Alzheimer's disease with the involvement of the microRNA-30b/CNR1 network and the following PI3K/AKT activation. *Exp. Mol. Pathol.* 117, 104545. doi: 10.1016/j.yexmp.2020.104545

Li, Y. Y., Cui, J. G., Dua, P., Pogue, A. I., Bhattacharjee, S., and Lukiw, W. J. (2011). Differential expression of miRNA-146a-regulated inflammatory genes in human primary neural, astroglial and microglial cells. *Neurosci. Lett.* 499, 109–113. doi: 10.1016/j.neulet.2011.05.044

Liu, S., Fan, M., Zheng, Q., Hao, S., Yang, L., Xia, Q., et al. (2022). microRNAs in Alzheimer's disease: Potential diagnostic markers and therapeutic targets. *Biomed. Pharmacother.* 148, 112681. doi: 10.1016/j.biopha.2022.112681

Lu, B., Guo, H., Zhao, J., Wang, C., Wu, G., Pang, M., et al. (2010). Increased expression of iASPP, regulated by hepatitis B virus X protein-mediated NF-κB activation, in hepatocellular carcinoma. *Gastroenterology*. 139, 2183–2194.e5. doi: 10.1053/j.gastro.2010.06.049

Lukiw, W. J. (2012). NF-κB-regulated micro RNAs (miRNAs) in primary human brain cells. *Exp. Neurol.* 235, 484–490. doi: 10.1016/j.expneurol.2011.11.022

Lukiw, W. J. (2020). microRNA-146a signaling in Alzheimer's disease (AD) and prion disease (PrD). *Front. Neurol.* 11, 462. doi: 10.3389/fneur.2020.00462

Lukiw, W. J., and Bazan, N. G. (1998). Strong nuclear factor-kappaB-DNA binding parallels cyclooxygenase-2 gene transcription in aging and in sporadic Alzheimer's disease superior temporal lobe neocortex. *J. Neurosci. Res.* 53, 583–592. doi: 10.1002/(SICI)1097-4547(19980901)53:5<583:AID-JNR8>3.0.CO;2-5.

Lukiw, W. J., Cui, J. G., Marcheselli, V. L., Bodker, M., Botkjaer, A., Gotlinger, K., et al. (2005). A role for docosahexaenoic acid-derived neuroprotectin D1 in neural cell survival and Alzheimer disease. *J. Clin. Invest.* 115, 2774–2783. doi: 10.1172/JCI25420

Lukiw, W. J., Zhao, Y., Cui, J. G. (2008). An NF-kB-sensitive micro RNA-146a-mediated inflammatory circuit in Alzheimer disease and in stressed human brain cells. *J. Biol. Chem.* 283, 31315–31322. doi: 10.1074/jbc.M805371200

McLachlan, D. R. C., Lukiw, W. J., and Kruck, T. P. (1990). Aluminum, altered transcription, and the pathogenesis of Alzheimer's disease. *Environ. Geochem. Health*. 12, 103–114. doi: 10.1007/BF01734059

Mirza, F. J., and Zahid, S. (2018). The role of synapsins in neurological disorders. *Neurosci. Bull.* 34, 349–358. doi: 10.1007/s12264-017-0201-7

Miyoshi, E., Bilousova, T., Melnik, M., Fakhrutdinov, D., Poon, W. W., Vinters, H. V., et al. (2021). Exosomal tau with seeding activity is released from Alzheimer's disease synapses, and seeding potential is associated with amyloid beta. *Lab Invest.* 101, 1605–1617. doi: 10.1038/s41374-021-00644-z

Natoli, R., and Fernando, N. (2018). microRNA as therapeutics for age-related macular degeneration. *Adv. Exp. Med. Biol.* 1074, 37–43. doi: 10.1007/978-3-319-75402-4_5

Olajide, O. A., and Sarker, S. D. (2020). Alzheimer's disease: natural products as inhibitors of neuroinflammation. *Inflammopharmacology*. 28, 1439–1455. doi: 10.1007/s10787-020-00751-1

Olufunmilayo, E. O., and Holsinger, R. M. D. (2022). Variant TREM2 signaling in Alzheimer's disease. *J. Mol. Biol.* 434, 167470. doi: 10.1016/j.jmb.2022.167470

Perot, B. P., and Ménager, M. M. (2020). Tetraspanin 7 and its closest paralog tetraspanin 6: membrane organizers with key functions in brain development, viral infection, innate immunity, diabetes and cancer. *Med. Microbiol. Immunol.* 209, 427–436. doi: 10.1007/s00430-020-00681-3

Pires, B. R. B., Binato, R., Ferreira, G. M., Cecchini, R., Panis, C., and Abdelhay, E. (2018). NF-kappaB regulates redox status in breast cancer subtypes. *Genes (Basel).*9, 320. doi: 10.3390/genes9070320

Pogue, A. I., Cui, J. G., Li, Y. Y., Zhao, Y., Culicchia, F., and Lukiw, W. J. (2010). Micro RNA-125b (miRNA-125b) function in astrogliosis and glial cell proliferation. *Neurosci. Lett.* 476, 18–22. doi: 10.1016/j.neulet.2010.03.054

Pogue, A. I., and Lukiw, W. J. (2021). microRNA-146a-5p, neurotropic viral infection and prion disease (PrD). *Int. J. Mol. Sci.* 22, 9198. doi: 10.3390/ijms22179198

Pogue, A. I., Zhao, Y., and Lukiw, W. J. (2022). microRNA-146a as a biomarker for transmissible spongiform encephalopathy. *Folia Neuropathol.* 60, 24–34. doi: 10.5114/fn.2022.113561

Rastegar-Moghaddam, S. H., Ebrahimzadeh-Bideskan, A., Shahba, S., Malvandi, A. M., and Mohammadipour, A. (2022). Roles of the miR-155 in neuroinflammation and neurological disorders: a potent biological and therapeutic target. *Cell. Mol. Neurobiol.* doi: 10.1007/s10571-022-01200-z

Recabarren, D., and Alarcón, M. (2017). Gene networks in neurodegenerative disorders. *Life Sci.* 183, 83–97. doi: 10.1016/j.lfs.2017.06.009

Sen, R., and Baltimore, D. (1986). Multiple nuclear factors interact with the immunoglobulin enhancer sequences. *Cell.* 46, 705–716. doi: 10.1016/0092-8674(86)90346-6

Singh, S., Sahu, K., Singh, C., and Singh, A. (2022). Lipopolysaccharide induced altered signaling pathways in various neurological disorders. *Naunyn Schmiedebergs Arch. Pharmacol.* 395, 285–294. doi: 10.1007/s00210-021-02198-9

Slota, J. A., and Booth, S. A. (2019). MicroRNAs in neuroinflammation: implications in disease pathogenesis, biomarker discovery and therapeutic applications. *Noncoding RNA*. 5, 35. doi: 10.3390/ncrna5020035

Song, Y., Hu, M., Zhang, J., Teng, Z. Q., and Chen, C. (2021). A novel mechanism of synaptic and cognitive impairments mediated via microRNA-30b in Alzheimer's disease. *EBioMedicine*. 39, 409–421. doi: 10.1016/j.ebiom.2018.11.059

Sun, G. Y., Simonyi, A., Fritsche, K. L., Chuang, D. Y., Hannink, M., Gu, Z., et al., (2018). Docosahexaenoic acid (DHA): an essential nutrient and a nutraceutical for brain health and diseases. *Prostaglandins Leukot. Essent. Fatty Acids*. 136, 3–13. doi: 10.1016/j.plefa.2017.03.006

Taganov, K. D., Boldin, M. P., Chang, K. J., and Baltimore, D. (2006). NF-kappaB-dependent induction of microRNA miRNA-146a, an inhibitor targeted to signaling proteins of innate immune responses. *Proc. Natl. Acad. Sci. USA*. 103, 12481–12486. doi: 10.1073/pnas.0605298103

Tahami Monfared, A. A., Byrnes, M. J., White, L. A., and Zhang, Q. (2022). Alzheimer's disease: epidemiology and clinical progression. *Neurol. Ther.* 11, 553–569. doi: 10.1007/s40120-022-00338-8

Trejo-Lopez, J. A., Yachnis, A. T., and Prokop, S. (2021). Neuropathology of Alzheimer's disease. *Neurotherapeutics*. doi: 10.1007/s13311-021-01146-y

Turk, A., Kunej, T., and Peterlin, B. (2021). microRNA-target interaction regulatory network in Alzheimer's disease. *J. Pers. Med.* 11, 1275. doi: 10.3390/jpm11121275

Uddin, M. S., Hasana, S., Ahmad, J., Hossain, M. F., Rahman, M. M., Behl, T., et al. (2021). Anti-Neuroinflammatory potential of polyphenols by

inhibiting NF-κB to halt Alzheimer's disease. *Curr. Pharm. Des.* 27, 402–414. doi: 10.2174/1381612826666201118092422

Valeri, A., Chiricosta, L., Calcaterra, V., Biasin, M., Cappelletti, G., Carelli, S., et al. (2021). Transcriptomic analysis of HCN-2 cells suggests connection among oxidative stress, senescence, and neuron death after SARS-CoV-2 infection. *Cells*. 10, 2189. doi: 10.3390/cells10092189

Wang, P., Liu, Z., Zhang, X., Li, J., Sun, L., Ju, Z., et al. (2018). CRISPR/Cas9-mediated gene knockout reveals a guardian role of NF-κB/RelA in maintaining the homeostasis of human vascular cells. *Protein Cell*. 9, 945–965. doi: 10.1007/s13238-018-0560-5

Wu, Y., Wang, M., Yin, H., Ming, S., Li, X., Jiang, G., et al. (2021). TREM-2 is a sensor and activator of T cell response in SARS-CoV-2 infection. *Sci Adv*. 7, eabi6802. doi: 10.1126/sciadv.abi6802

Xu, H., Zhang, J., Shi, X., Li, X., and Zheng, C. (2021). NF-κB inducible miR-30b-5p aggravates joint pain and loss of articular cartilage via targeting SIRT1-FoxO3a-mediated NLRP3 inflammasome. *Aging*. 13, 20774–20792. doi: 10.18632/aging.203466

Yoon, S., Kim, S. E., Ko, Y., Jeong, G. H., Lee, K. H., Lee, J., et al. (2022). Differential expression of microRNAs in Alzheimer's disease: a systematic review and meta-analysis. *Mol. Psychiatry*. 27, 2405–2413. doi: 10.1038/s41380-022-01476-z

Yu, J., Yuan, X., Chen, H., Chaturvedi, S., Braunstein, E. M., and Brodsky, R. A. (2020). Direct activation of the alternative complement pathway by SARS-CoV-2 spike proteins is blocked by factor D inhibition. *Blood*. 136, 2080–2089. doi: 10.1182/blood.2020008248

Zhan, X., Hakoupian, M., Jin, L. W., and Sharp, F. R. (2021). Lipopolysaccharide, identified using an antibody and by PAS Staining, is associated with corpora amylacea and white matter injury in Alzheimer's disease and aging brain. *Front. Aging Neurosci.* 13, 705594. doi: 10.3389/fnagi.2021.705594

Zhan, X., Stamova, B., and Sharp, F. R. (2018). Lipopolysaccharide associates with amyloid plaques, neurons and oligodendrocytes in Alzheimer's disease brain: a review. *Front. Aging Neurosci.* 10, 42. doi: 10.3389/fnagi.2018.00042

Zhang, Q., Lenardo, M. J., and Baltimore, D. (2017). 30 Years of NF-κB: a blossoming of relevance to human pathobiology. *Cell*. 168, 37–57. doi: 10.1016/j.cell.2016.12.012

Zhao, Y., Arceneaux, L., Culicchia, F., and Lukiw, W. J. (2021). Neurofilament Light (NF-L) chain protein from a highly polymerized structural component of the neuronal cytoskeleton to a neurodegenerative disease biomarker in the periphery. *HSOA J. Alzheimer's Neurodegener Dis.* 7, 056. doi: 10.24966/AND-9608/100056 Epub 2021 Oct 13.

Zhao, Y., Bhattacharjee, S., Jones, B. M., Dua, P., Alexandrov, P. N., Hill, J. M., et al. (2013). Regulation of TREM2 expression by an NF-κB-sensitive miRNA-34a. *Neuroreport* 24, 318–323. doi: 10.1097/WNR.0b013e32835fb6b0

Zhao, Y., Bhattacharjee, S., Jones, B. M., Hill, J. M., Dua, P., and Lukiw, W. J. (2014). Regulation of neurotropic signaling by the inducible, NF-kB-sensitive miRNA-125b in Alzheimer's disease (AD) and in primary human neuronal-glial (HNG) cells. *Mol. Neurobiol.* 50, 97–106. doi: 10.1007/s12035-013-8595-3

Zhao, Y., Jaber, V. R., LeBeauf, A., Sharfman, N. M., and Lukiw, W. J. (2019b). microRNA-34a (miRNA-34a) mediated down-regulation of the post-synaptic cytoskeletal element SHANK3 in sporadic Alzheimer's disease (AD). *Front. Neurol.* 10:28. doi: 10.3389/fneur.2019.00028

Zhao, Y., and Lukiw, W. J. (2013). TREM2 signaling, miRNA-34a and the extinction of phagocytosis. *Front. Cell. Neurosci.* 7, 131. doi: 10.3389/fncel.2013.00131

Zhao, Y., and Lukiw, W. J. (2018). Bacteroidetes neurotoxins and inflammatory neurodegeneration. *Mol. Neurobiol.* 55, 9100–9107. doi: 10.1007/s12035-018-1015-y

Zhao, Y., Sharfman, N. M., Jaber, V. R., and Lukiw, W. J. (2019a). Down-regulation of essential synaptic components by GI-tract microbiome-derived lipopolysaccharide (LPS) in LPS-treated human neuronal-glial (HNG) cells in primary culture: relevance to Alzheimer's disease (AD). *Front. Cell. Neurosci.* 13, 314. doi: 10.3389/fncel.2019.00314

Zingale, V. D., Gugliandolo, A., and Mazzon, E. (2021). miRNA-155: an important regulator of neuroinflammation. *Int. J. Mol. Sci.* 23, 90. doi: 10.3390/ijms23010090

Conflict of Interest: The author declares that the research was conducted in the absence of any commercial or financial relationships that could be construed as a potential conflict of interest.

Publisher's Note: All claims expressed in this article are solely those of the authors and do not necessarily represent those of their affiliated organizations, or those of the publisher, the editors and the reviewers. Any product that may be evaluated in this article, or claim that may be made by its manufacturer, is not guaranteed or endorsed by the publisher.

frontiers | Frontiers in Cellular Neuroscience

TYPE Original Research
PUBLISHED 29 July 2022
DOI 10.3389/fncel.2022.881175

OPEN ACCESS

EDITED BY
Ulises Gomez-Pinedo,
Health Research Institute of Hospital Clínico San Carlos, Spain

REVIEWED BY
Md A. Hakim,
Loma Linda University, United States
Hyeong-Geug Kim,
Indiana University-Purdue University Indianapolis, United States

*CORRESPONDENCE
Huazhong Ying
yhz0101@126.com
Qiaojuan Shi
shiqiaojuan@163.com

†These authors have contributed equally to this work

SPECIALTY SECTION
This article was submitted to Cellular Neuropathology, a section of the journal Frontiers in Cellular Neuroscience

RECEIVED 28 April 2022
ACCEPTED 01 July 2022
PUBLISHED 29 July 2022

CITATION
Han X, Zhou L, Tu Y, Wei J, Zhang J, Jiang G, Shi Q and Ying H (2022) Circulating exo-miR-154-5p regulates vascular dementia through endothelial progenitor cell-mediated angiogenesis.
Front. Cell. Neurosci. 16:881175.
doi: 10.3389/fncel.2022.881175

Circulating exo-miR-154-5p regulates vascular dementia through endothelial progenitor cell-mediated angiogenesis

Xue Han[1†], Li Zhou[2†], Yu Tu[1], Jiajia Wei[1], Jiajia Zhang[1], Guojun Jiang[3], Qiaojuan Shi[1*] and Huazhong Ying[1,2*]

[1]Zhejiang Provincial Key Laboratory of Laboratory Animals and Safety Research, Hangzhou Medical College, Hangzhou, China, [2]School of Pharmaceutical Sciences, Zhejiang Chinese Medical University, Hangzhou, China, [3]Department of Pharmacy, Affiliated Xiaoshan Hospital, Hangzhou Normal University, Hangzhou, China

Background: Vascular dementia (VaD) mainly results from cerebral vascular lesions and tissue changes, which contribute to neurodegenerative processes. Effective therapeutic approaches to targeting angiogenesis may reduce mortality of VaD. Endothelial progenitor cells (EPCs) play a key role in postnatal angiogenesis. Many exosomal microRNAs (exo-miRNAs) have been reported to involve in the development of dementia. The present study was designed to investigate whether the expression profile of the exo-miRNAs is significantly altered in patients with VaD and to reveal the function of differentially expressed miRNAs and the relevant mechanisms in EPC-mediated angiogenesis in VaD rat model.

Results: Exosomes isolated from serum of patients with VaD (n = 7) and age-matched control subjects (n = 7), and miRNA sequencing and bioinformatics analysis found that circulating exosome miRNA-155-5p, miRNA-154-5p, miR-132-5p, and miR-1294 were upregulated in patients with VaD. The expression of miRNA-154-5p was further verified to be upregulated in clinical samples (n = 23) and 2-vessel occlusion-induced VaD rat model by reverse transcription quantitative PCR (RT-qPCR). Notably, miRNA-154-5p inhibition in bone marrow-EPCs (BM-EPCs) from VaD rats improved EPC functions, including tube formation, migration, and adhesion, and elevated concentrations of vascular endothelial growth factor (VEGF) and stromal cell-derived factor-1α (SDF-1α). The mRNA levels of ICAM-1, VCAM-1, and MCP-1 were reduced in miRNA-154-5p-inhibited EPCs. In addition, miRNA-154-5p inhibition increased the level of superoxide dismutase (SOD), and decreased reactive oxygen species (ROS) in EPCs. PRKAA2 was chosen as a promising target gene of miR-154-5p, and miRNA-154-5p inhibition upregulated the protein expression of AMPKα2. Furthermore, upregulation of miR-154-5p markedly diminished EPC functions and inhibited angiogenesis following EPC transplantation in VaD rats.

Conclusion: Circulating exo-miR-154-5p was upregulated in patients with VaD, and miR-154-5p upregulation was associated with impaired EPC functions and angiogenesis in VaD rat model. Therefore, miR-154-5p is a promising biomarker and therapeutic strategy for VaD.

KEYWORDS

vascular dementia, miR-154-5p, exosome, endothelial progenitor cells, angiogenesis

Introduction

Vascular dementia (VaD) accounts for roughly 15–30% of dementia cases worldwide and increases linearly with age (Terracciano et al., 2021). VaD is characterized by progressive cognitive impairment, neurodegeneration, and memory difficulty, which is mainly attributed to cerebrovascular pathologies (Ghassab-Abdollahi et al., 2021). VaD is becoming the second most common cause of dementia next only to Alzheimer's disease (AD). Although numerous studies have been made on the elucidation of mechanisms for VaD in recent years, the treatment approaches still focus on controlling the associated cardiovascular and cerebrovascular symptoms (Librizzi et al., 2021). There is still a lack of effective strategies against VaD. Therefore, investigation of the mechanism underlying cerebrovascular pathologies and further exploration of the novel therapeutic strategies have become a pivotal medical issue.

Emerging evidence suggests that exosomes play a vital role in the pathogenesis of neurodegeneration (Beatriz et al., 2021). Exosomes are generated and secreted through exocytosis of microvesicles (MVs) by mass of cell types, including stem cells (Fayazi et al., 2021). They are released into the extracellular space and exist in most body fluids, including saliva, plasma, urine, and even breast milk. These MVs can transfer nucleic acids and proteins to nearby cells, thereby affecting the activation of the recipient cells (Li et al., 2021). MicroRNAs (miRNAs) are conserved, endogenous, and small non-coding RNAs (22 nucleotides in length) that anneal to the 3′-UTR of their target mRNAs to negatively regulate the translation (Kong et al., 2021). Importantly, abnormal expression of miRNAs is associated with a wide range of disorders. It has been shown that miRNA expression pattern in exosome from peripheral blood implies a diagnostic biomarker for the stage and grade of liver diseases (Murakami et al., 2012). Moreover, exosomal miRNAs (exo-miRNAs) in cerebrospinal fluid has been reported to be specific and sensitive biomarkers for differentiating Parkinson's disease (PD) from healthy and AD (Gui et al., 2015). However, alterations of miRNA content in serum exosome from patients with VaD have not yet been described.

It is well-established that VaD is featured in cerebrovascular dysfunction, which precedes neurodegeneration. Structural and functional lesion of cerebral blood vessels results in cerebral blood flow regulation disturbance, vascular reserve consumption, and a decrease in brain repair ability (Raz et al., 2016). Chronic cerebral hypoperfusion (CCH) begins with such cerebrovascular damage that will further disrupt the homeostasis, such as oxidative stress, inflammation, mitochondrial and neurotransmitter dysfunction, and apoptosis (Du et al., 2017). In recent years, studies suggest that endothelial progenitor cells (EPCs) have a potential therapeutic application for vascular diseases (Han et al., 2017a; Zhou et al., 2019). EPCs possess the properties of migrating and homing to the injury area to promote angiogenesis and vasculogenesis (Han et al., 2017b). In addition, EPCs can derive from bone marrow and release pro-angiogenic growth factors liking vascular endothelial growth factor (VEGF). Clinical research has reported that a reduction of circulating EPCs was positive correlated with the cognitive dysfunction in patients with AD (Kong et al., 2011). Transplantation of EPCs can prolong the lifespan in stroke-prone spontaneously hypertensive rats (SHR-SP) and promote local angiogenesis in ischemic brain (Peng et al., 2018). Notably, EPC-derived MVs were able to trigger neoangiogenesis *via* a horizontal transfer of mRNA to endothelial cells of micro-/macro-vasculature (Deregibus et al., 2007). In short, EPCs have promising therapeutic potential against vascular brain diseases. Nevertheless, the relation between EPC bioactivity and CCH-induced cognitive impairment remains unclear.

In the present study, we established a bilateral common carotid artery occlusion (BCCAO) rat model, which could imitate the pathogenesis of VaD (Jiwa et al., 2010). We aimed to explore the effect of differentially expressed exo-miRNAs on EPC-mediated angiogenesis in BCCAO rats.

Materials and methods

Clinical samples

This research was approved by the Ethics Committee of Zhejiang Xiaoshan Hospital (Hangzhou, China). A cohort of 30 patients with VaD at the Department of Neurology,

Zhejiang Xiaoshan Hospital, and 12 healthy young and 22 healthy elder controls at the Department of Physical Examination Center, Zhejiang Xiaoshan Hospital were enrolled. All patients were Han Chinese and were recruited from November 2019 to January 2020. The patients with VaD were diagnosed by a neurologist based on the National Institute of Neurological Disorders and Stroke (NINDS)-Association Internationale pour la Recherche et l'Enseignement en Neurosciences (AIREN) clinical criteria (Román et al., 1993). Patients with VaD were scored with the clinical dementia rating (CDR), the Minimum Mental State Examination (MMSE) criteria and the Hachinski criteria (**Table 1**). The exclusion criteria were a history of a head injury with loss of consciousness, physical abnormalities, and meeting Diagnostic and Statistical Manual of Mental Disorders, the fourth edition (DSM-IV) criteria for substance dependence or current mood or anxiety disorders. In addition, patients administrated with anti-angiogenic medications for any indication were also excluded. All participants signed written informed consent.

Blood sampling

Due to the time of blood drawing needed to accommodate the clinic and laboratory, all sample collection in this study were conducted between 9 a.m. and 11 a.m. Peripheral blood from all subjects was placed in a serum tube for 1 h, and the tubes were centrifuged at 3,000 × *g* for 10 min at 4°C. The supernatant was regarded as serum and stored at −80°C until detection.

TABLE 1 Primers used for RT-PCR analysis.

Gene	Species	Forward primer	Reverse primer
miR-155-5p	Human	5′-GTGTTAATGCTAA TCGTGATAGGGG-3′	5′-CAGTGCAGGG TCCGAGGTATT-3′
miR-154-5p	Human	5′-CCAGCGTGTAGG TTATCCGTG-3′	5′-CAGTGCAGGGTC CGAGGTATT-3′
miR-132-5p	Human	5′-CCGTGGCTTTC GATTGTTACT-3′	5′-CAGTGCAGGGTCC GAGGTATT-3′
miR-1294	Human	5′-AGCGTGTGTG AGGTTGGCAT-3′	5′-CAGTGCAGGG TCCGAGGTATT-3′
miR-154-5p	Rat	5′-AGGTTATCCGT GTTGCCT-3′	5′-GAACATGTCTG CGTATCTC-3′
ICAM-1	Rat	5′-AGATCATACGGGTT TGGGCTTC-3′	5′-TATGACTCGTGAAA GAAATCAGCTC-3′
VCAM-1	Rat	5′-TTTGCAAGAAA AGCCAACATGAAAG-3′	5′-TCTCCAACAGTT CAGACGTTAGC-3′
MCP-1	Rat	5′-GTCACCAAGCTC AAGAGAGAGA-3′	5′-AGTGGATGCAT TAGCTTCAGA-3′
β-actin	Rat	5′-AAGTCCCTCAC CCTCCCAAAAG-3′	5′-AAGCAATG CTGTCACCTTCCC-3′

Exosome preparation

The procedure of exosome preparation as described before with minor modification (Li et al., 2017). In brief, serum was melted in 37°C water bath and supplemented with 10 times the volume of phosphate-buffered saline (PBS) buffer. After filtration with 0.22 μm filter membrane, the supernatant was centrifuged at 100,000 × *g* overnight at 4°C (Optima-L80XP, Beckman Coulter, CA, United States). The supernatant was discarded carefully, then appropriate amount of PBS was added and centrifuged at 100,000 × *g* for 2 h. The obtained precipitate was exosome. The exosome samples were suspended in 20–30 μl PBS, and the morphology was observed using the Tecnai transmission electron microscopy (FEI, OR, United States) under 80 kV. The particle size of exosomes was detected with a ZetaView Nanoparticle Tracking Analysis (Particle Metrix, Meerbusch, Germany).

RNA sequencing

Differential gene expression was analyzed with RNA-sequencing assay. Exosome samples from healthy control and patients with VaD (n = 7 per condition) were used to isolate less than 200 nt RNA with miRNeasy Mini Kit (QIAGEN, Hilden, Germany). Sequencing libraries were built and transcriptome sequenced using a HiSeq 2000 (Illumina, San Diego, CA, United States). Agilent 2100 Bioanalyzer was chosen to analyze insert sizes in complementary DNA (cDNA) libraries. Gene expression data were evaluated on Dr. Tom system (BGI, Wuhan, China). Raw sequencing data are available in **Supplementary material**.

Real-time quantitative PCR analysis

Total RNA from exosomes and tissues was extracted using TRIZOL reagent according to the manufacturer's instruction (Takara) and was reverse-transcribed with a PrimeScript™ RT Reagent Kit (Takara). Real-time PCR was performed using SYBR Premix Ex Taq™ (Takara) with the LightCycler 480 System (Roche Diagnostics, Basel, Switzerland). Primer sequences were synthesized in Sangon Biotech (Shanghai, China) and listed in **Table 1**.

Animals

Male Sprague-Dawley rats were 18-month-old supplied by the Laboratory Animal Center of Hangzhou Medical College (SPF grade; Hangzhou, China). All animals were housed at 22–25°C and 40–60% humidity under a 12-h light/dark cycle. Rats were with free access to food and water. Efforts were made to

minimize their suffering. The study procedures were carried out according to the National Institutes of Health Guidelines for the Care and Use of Laboratory Animals. The study protocol was approved by the Ethics Committee of Laboratory Animal Care and Welfare, Hangzhou Medical College. After adaptive feeding for a week, rats were randomly divided into sham group and VaD group.

Establishing of vascular dementia rat model

The bilateral common carotid artery occlusion (BCCAO) rat model has been widely accepted as an experimental model of VaD (Leardini-Tristão et al., 2017, 2020). The procedures were carried out as previously reported (Leardini-Tristão et al., 2017, 2020). In brief, after rats were anesthetized with phenobarbital sodium (40 mg/kg, *i.p.*), the bilateral common carotid arteries were carefully isolated from the peripheral vagus nerve through a midline incision and double-ligated with surgical silk. Sham group was subjected to the same procedure, except that the bilateral common carotid artery was not ligated. The rats were kept on a heating pad at 38°C until recovery from anesthesia.

Cerebral blood flow monitoring

For cerebral blood flow monitoring, a laser speckle blood flow imaging system (SIM BFI-WF; SIM Opto-Technology Co., Ltd., Wuhan, China) was employed. The skin of the head was cut to expose the subdermal blood vessels. A thin circle of glass was inserted into the window frame, and cerebral blood flow velocity was detected before and after establishing of VaD rat model.

Morris water maze

The Morris water maze (MWM) test was used to evaluate the spatial learning and memory of rats as previously reported with minor alteration (Xu et al., 2016). After 3 months of BCCAO operation, the rats began to place navigation test for 4 consecutive days. The pool was 1.2 m in diameter and height 0.6 m, and filled with water and opaque liquid maintained 24–26°C inside. The external visual reminder around the pool were kept constant, which helped for rats to spatial orientation. A platform (12 cm in diameter) was submerged 2.5 cm below the water surface in the northeaster quadrant. The animals received four trials per day. In each trial, rats were softly released into the water facing the tank wall at one of the four starting positions. The rats were permitted a maximum of 60 s to find the hidden platform. If the rats failed to find the hidden platform within the specified time, they were guided to the platform and allowed to stay for 15 s, and a score of 60 s was assigned. The escape latency was recorded to analyze the spatial learning. On the fifth day, a probe trial was carried out to assess spatial memory. Briefly, the rats were allowed to freely swim for 60 s in the pool from which the platform was removed, and the time spent in the target quadrant were recorded. The path taken by animals were monitored using a computer-based video camera, and the data was analyzed with the MT-200 image analyzing software (Taimeng Co., Chengdu, China).

Nissl staining and immunofluorescence staining

Rats in both groups were sacrificed after the MWM test, and brain tissues were collected for pathological observation. Brain samples were incubated with 4% paraformaldehyde for 24 h at room temperature and were embedded in paraffin. After that, embedded brain paraffin sections were sliced into 5 μm section, then de-paraffinized with xylene and dehydrated with a graded concentration of ethanol. Nissl-stained sections were used to stain the section for 5 min. Representative pictures of Nissl-stained sections in the CA1, CA3, DG, and cortex regions were taken under a high-power optical microscope (Leica Microsystems, Wetzlar, Germany). The number of neurons was counted using ImageJ software (National Institutes of Health, Bethesda, MD, United States).

For immunofluorescence stain, angiogenesis in the brain tissues was detected using a monoclonal antibody CD31 (diluted 1:300; R&D System; Minneapolis, MN, United States), and Iba-1-positive microglial cells were evaluated using a rat antibody (diluted 1:200; Abcam, ab178846) followed by immunofluorescence staining using AlexaFluor 488 IgG antibody (Jackson ImmunoResearch; West Groove, PA, United States). Dapi (diluted 1:300; Beyotime, Shanghai, China) was used for nuclei staining. CD31-positive or Iba-1-positive stain were observed using a fluorescence microscope (Leica Microsystems, Wetzlar, Germany).

TUNEL assay

Apoptotic neurons were measured using a TUNEL Assay Kit (Wuhan Boster Biological Technology, Ltd., Wuhan, China) according to the manufacturer's instructions. Briefly, brain samples were incubated with anti-neuronal nuclei antibody overnight at 4°C. Sections were then washed three times with PBS and incubated with TUNEL reaction mixture for 1 h at room temperature. Images of TUNEL-stained sections in the

cortex were captured using a fluorescence microscope. TUNEL-positive neurons were quantitated using ImageJ software.

Activity of malondialdehyde, superoxide dismutase, and glutathione peroxidase

Serum from sham and VaD groups were collected for the measurement of oxidative stress-related biological parameters. The activities of malondialdehyde (MDA), superoxide dismutase (SOD), and glutathione peroxidase (GSH-PX) were determined with commercial kits according to the manufacturer's instructions (Nanjing Jiancheng Bioengineering Institute, Nanjing, China). The samples were analyzed in duplicate.

Measurement of inflammatory factors and myeloperoxidase

Brain tissue samples were analyzed for interleukin (IL)-1β, tumor-necrosis factor (TNF)-α, and myeloperoxidase (MPO) with commercial ELISA kits according to the manufacturer's instructions (Anogen, Mississauga, ON, Canada). All readings were made from an ELISA plate reader. The samples were analyzed in duplicate.

Estimation of bone marrow-endothelial progenitor cell functions

Isolation and culturing of BM-EPCs were performed as previously described (Han et al., 2017a). To evaluate the ability of angiogenesis, Matrigel tube formation assay was performed. After 7 days of culture, BM-EPCs were replated into a 96-well plate, which was precoated with Matrigel (BD Biosciences; Bedford, MA, United States) with a concentration of 30,000 per 100 μl. Plate was incubated for 4–6 h at 37°C, images of tube morphology were captured using a microscope. Tube formation was assessed by counting tube numbers.

The ability of migration was estimated using a modified Boyden chamber assay as previously reported (Yu et al., 2016). Briefly, BM-EPCs were plated with a concentration of 30,000 per 100 μl on the upper chamber (8 μm pores), and cell-free medium containing 50 ng/ml VEGF (Sigma-Aldrich, Darmstadt, Germany) was added to the lower chamber of a 24-well Transwell plate (Corning; Lowell, MA, United States). The plate was incubated for 24 h at 37°C, and cells were then fixed with 2% paraformaldehyde and stained with Hoechst 33258 (Beyotime). The images were taken with a microscope. The migrated cells were counted using ImageJ software.

The adhesion assay was applied to assess the EPC function. A total of 30,000 cells were plated into a 96-well plate per well, which was precoated with the mouse vitronectin (1 μg/ml; Sigma). Cells were incubated for 2 h at 37°C, and non-adherent cells were carefully removed with PBS. Adherent cells were fixed with 2% paraformaldehyde and stained with Hoechst 33258. The stained cells were then assessed using a fluorescence microscope and counted with ImageJ software.

Measurement of vascular endothelial growth factor, stromal cell-derived factor-1α, and superoxide dismutase concentrations

The concentrations of VEGF and stromal cell-derived factor-1α (SDF-1α) in culture medium were detected using commercial ELSA Kits (R&D System). The level of SOD was measured using a SOD Quantification Kit (Beyotime). The procedures were performed according to the manufacturers' protocols. All samples were measured in duplicate.

Determination of reactive oxygen species generation

Intracellular reactive oxygen species (ROS) level was measured with the membrane-permeable dye dihydroethidium (DHE; Invitrogen; Carlsbad, CA, United States). After 7 days cultivation, BM-EPCs were plated into 96-well plate and stained with DHE (2 μM) for 1 h at room temperature. Cells were gently washed with PBS twice to remove excess probe, and images were taken with a fluorescence microscope.

Treatment of bone marrow-endothelial progenitor cells *in vitro*

After 7 days of culture, BM-EPCs were transferred with adenovirus or Lipofectamine 3000 (Invitrogen) in M199 medium supplemented with 1% FBS for 36 h. The sequences of miR-154-5p inhibitor, negative control, and miR-154-5p mimics (GenePharma; Shanghai, China) were as follows (5′-3′): miR-154-5p inhibitor, CGAAGGCAACACGGAUAACCUA; negative control sense, UUCUCCGAA CGUGUCACGUTT; negative control antisense, ACGUGACACGUUCGG AGAATT; miR-154-5p mimics sense, UAGGUUAUCCGUGUUGCCUUCG; and miR-154-5p mimics antisense, AAGGCAACACGGAUAACCUAUU.

After 36 h of quiescent culture, cells were used to functions assay and EPC transplantation assay.

Endothelial progenitor cell transplantation assay

After 5 days of culturing, BM-EPCs were labeled with 5-bromo-2′-deoxyuridine (BrdU; Thermo Fisher Scientific; Waltham, MA, United States) as previously described (Peng et al., 2018). In brief, endothelial growth medium-2 (EGM-2; Cambrex Corp; East Rutherford, NJ, United States) was used to dilute BrdU-labeled reagent (1:100), and the mixture was filtered with a 0.2 μm filter and heated to 37°C. A total of 2 ml of EGM-2 containing BrdU was added to cells that were plated in a six-well plate. On day 7, cells were washed with PBS for three times and harvested with 0.125% trypsin. Sprague-Dawley rat EPCs (400,000 cells) were transplanted into VaD rat *via* the tail vein. After 7 days of a single injection of EPCs, rats were sacrificed, and brain tissues were collected for immunofluorescence staining.

Statistical analysis

Data are expressed as mean ± SD. Statistical analysis was performed using one-way analysis of variance (ANOVA) with the Newman–Keuls multiple comparison test, and Student's *t*-test for two group analysis. A value of $p < 0.05$ was considered to be statistically significant.

Results

Characterization of extracellular vesicles extracted from serum

There were 52 participants included in this study, consisting of 30 (58%) patients with VaD and 22 (42%) healthy controls. The demographic and identity of these participators were summarized in **Table 2**. The extracellular vesicles derived from human serum were characterized using transmission electron microscopy, Nanoparticle Tracking Analysis, and Western blot assay. As shown in **Figures 1A,B**, the EVs were in the classical cup morphology of exosomes, and the particle size was in the range of 70–150 nm. Western blot analysis showed that the EVs expressed positive marker proteins of exosome, including Alix, CD63, and CD9, and did not express the glyceraldehyde-3-phosphate dehydrogenase (GAPDH), a negative marker of exosome (**Figure 1C**). The results indicate that the EVs purified from human serum are qualified exosomes.

TABLE 2 The demographic and identity of clinical samples.

Variables		Healthy controls	VaD	*P*
No of subjects		22	30	
Age		72.3 ± 11.7	75.3 ± 5.7	0.2241
Sex (M/F)		10/12	14/16	
Clinical characteristics				
CDR (%)	0.5–1	N/A	33.3%	
	2	N/A	40.0%	
	3	N/A	26.7%	
MMSE (%)	0–10	N/A	0.0%	
	10–24	N/A	100.0%	
Hachinski (%)	0–7	N/A	0.0%	
	≥7	N/A	100.0%	
Body Mass Index (kg/m^2)		26.3 ± 2.5	26.6 ± 2.4	0.6956
Hypertension		8 (36.4%)	17 (56.7%)	0.1536
Diabetes		2 (9.1%)	7 (23.3%)	0.1868
Cardiovascular disease		3 (13.6%)	8 (26.7%)	0.2644

miRNAs are differentially expressed in serum exosomes of patients with vascular dementia

To explore whether the contents of exosomes were changed between patients with VaD and healthy controls, purify exosomes from seven normal subjects and seven patients with VaD who met the inclusion and exclusion criteria were selected to conduct miRNA library sequencing. Transcriptome analysis of miRNAs showed that a total of 598 mature miRNAs were detected, of which 33% were upregulated and 19% were downregulated both twice and more than twice high in VaD group compared with the control group (**Figure 2A**). Kyoto Encyclopedia of Genes and Genomes (KEGG) analysis showed that the genes targeted by these differentially expressed miRNAs were mainly enriched in blood vessel development, cellular migration, and cell adhesion signaling pathways (**Figure 2B**). This result indicates that the differentially expressed miRNAs may be involved in the regulation of cells, which possessed these biological functions. The miRNAs in VaD group that were upregulated by two times or more with statistical differences ($p < 0.05$) were chosen as the objects of study (**Figure 2C**), and specific change multiple is shown in **Table 3**. These 4 miRNAs were further verified in 15 normal subjects and 23 patients with VaD, and reverse transcription polymerase chain reaction (RT-PCR) results showed that miR-154-5p were significantly upregulated in the VaD group compared with the control group ($p < 0.05$, **Figure 2D**). Although there were no significant differences between control group and VaD group of miR-1294, miR-132-5p, and miR-155-5p ($p > 0.05$, **Figures 2E–G**). To further study the influence of aging on levels of miRNAs, 12 healthy young were recruited. The demographic

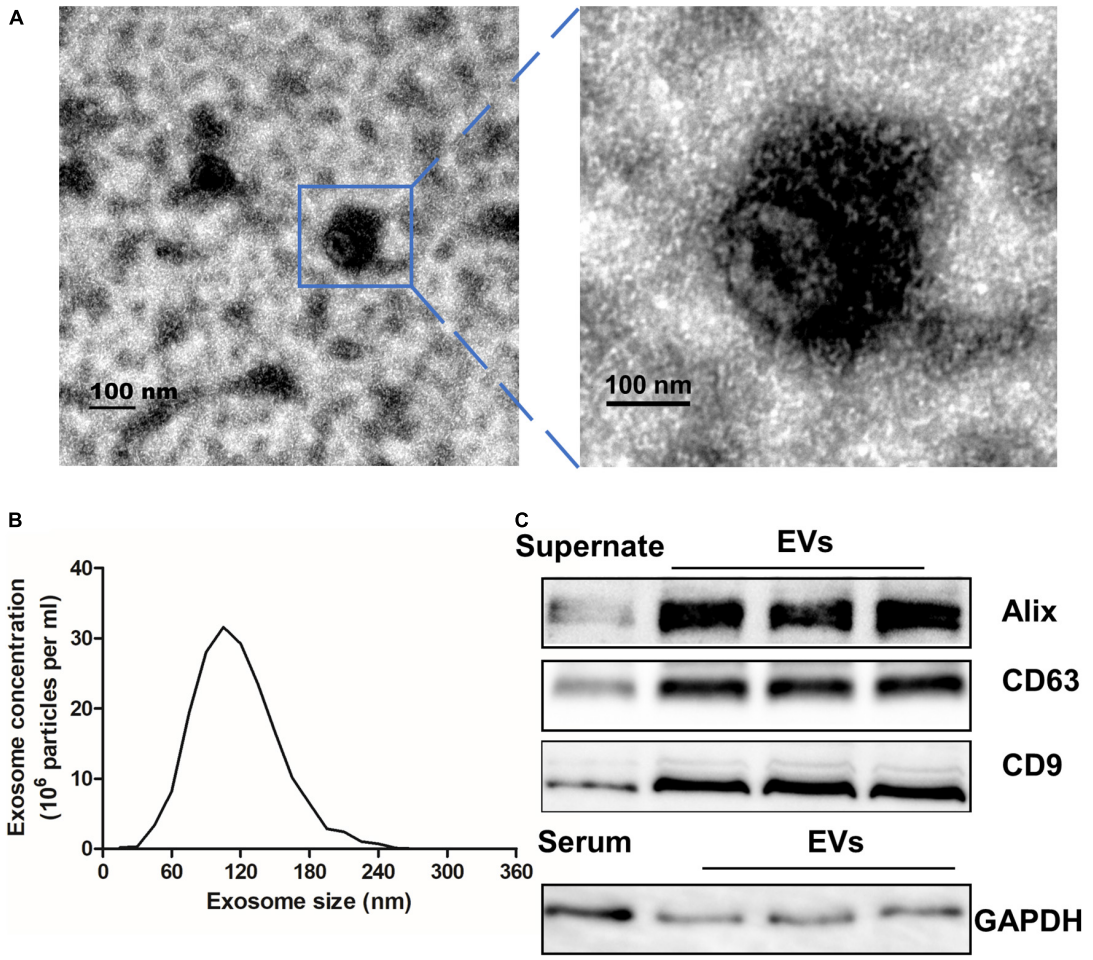

FIGURE 1
Characterization of EVs extracted from serum. **(A)** Transmission electron microscope was used to analyze extracted exosomes which were zoomed indicated by the blue frame. Scale bar = 100 nm. **(B)** The particle size of serum EVs was measured with a Nanoparticle Tracking Analysis. **(C)** EVs and Supernate or serum were detected by Western blot for the exosome-riched markers Alix, CD63, and CD9, and the negative marker GAPDH. EVs, extracellular vesicles; GAPDH, glyceraldehyde-3-phosphate dehydrogenase.

and identity of healthy young and elder participators were summarized in Supplementary Table 1. There were no significant differences between young group and elder group for miR-154-5p, miR-1294, miR-132-5p, and miR-155-5p ($p > 0.05$, Supplementary Figure 1). These results suggest that miR-154-5p is confirmed to be significantly increased in serum exosomes of patients with VaD.

Establishing of vascular dementia rat model and upregulation of oxidative stress and inflammation in vascular dementia rats

To evaluate the influence of miR-154-5p on VaD in brain tissue, BCCAO surgery was performed to induce VaD model. After 3 months of surgery, spatial memory was assessed by the MWM test, and TUNEL stain and Nissl stain were used to evaluate pathologic changes in the cerebral tissues of VaD rats. In the acquisition trials, VaD rats exhibited an obvious impairment in spatial learning, which was evidenced by longer latency time to reach the platform compared with sham group ($p < 0.05$, Figure 3A). In the probe trial, the trajectory chart showed decreased times in platform site crossings in VaD rats (Figure 3B). The analysis showed that the time spent in the target quadrant was greatly reduced in VaD rats compared with sham group ($p < 0.05$, Figure 3C). Moreover, as showed in Figures 3D,E, the number of TUNEL-positive cells was significantly increased in the cortex region of the VaD rats compared with sham rats ($p < 0.05$). Nissl staining revealed a marked neuronal injure evidenced by the disappeared Nissl bodies, and shrunken and deepened staining of cell bodies in the CA1, CA3, DG,

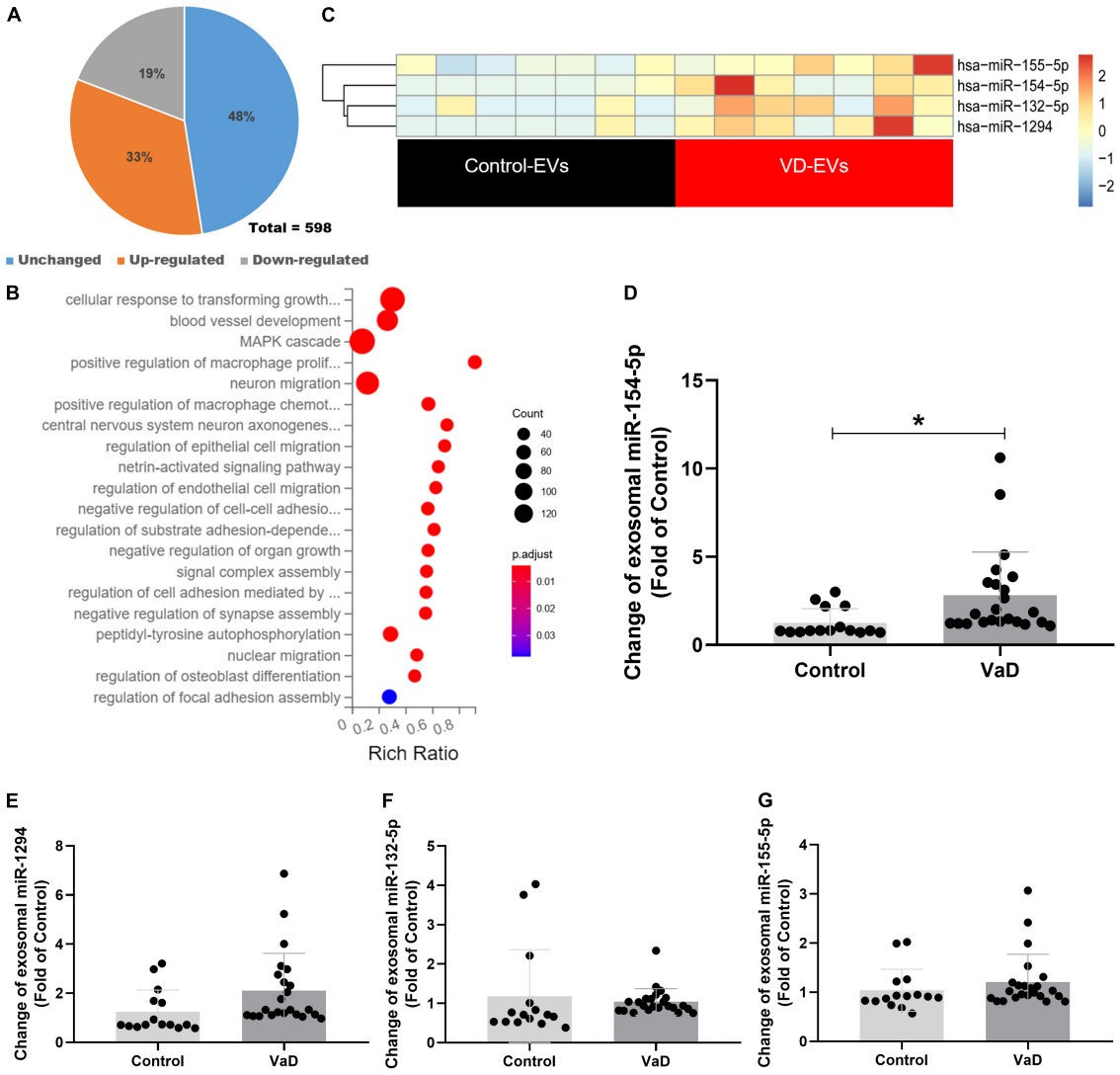

FIGURE 2
Bioinformatics analysis of miRNAs expression profiles in serum exosomes of patients with VaD. **(A)** Pie chart of differentially expressed miRNAs. The Jacinth part presented upregulated miRNAs; the gray part indicated downregulated miRNAs; the blue part presented unchanged miRNAs. **(B)** Heat map of differentially expressed miRNAs from patients with VaD and control group. **(C)** The KEGG analysis of the pathways enriched by the differentially expressed miRNAs from patients with VaD. **(D–G)** The upregulated miRNAs were further verified using RT-PCR in patients with VaD and control group (Control: $n = 13$, VaD: $n = 23$). *$p < 0.05$. Data are shown as mean ± SD. KEGG, Kyoto Encyclopedia of Genes and Genomes; RT-PCR, reverse transcription polymerase chain reaction; VaD, vascular dementia.

and cortex region of VaD rats when compared to sham rats ($p < 0.05$, Figures 3F,G). In addition, representative images of cerebral blood flow before and after establishment of VaD model are showed in Figure 3H. The redder the color, the faster the blood flow, and the blue color indicates slow blood flow. The cerebral blood velocity decreased by 46.8% following BCCAO surgery was compared with before surgery (Figure 3I). The above results indicating a VaD rat model successfully established.

Levels of oxidative stress and inflammation in VaD rats were evaluated. VaD rats showed significantly higher serum MDA level, and lower SOD and GSH-PX levels than sham group ($p < 0.05$, Supplementary Figures 2A–C). Furthermore, the VaD rats exhibited more remarkable elevation of IL-1β, TNF-α, and MPO in cerebral tissues than sham rats ($p < 0.05$,

TABLE 3 The up-regulated miRNAs.

Name	Fold change (VaD/Ctrl)	*P*
Has-miR-154-5p	11.91	0.03
Has-miR-1294	8.76	0.02
Has-miR-132-5p	4.44	0.02
Has-miR-155-5p	2.81	0.02

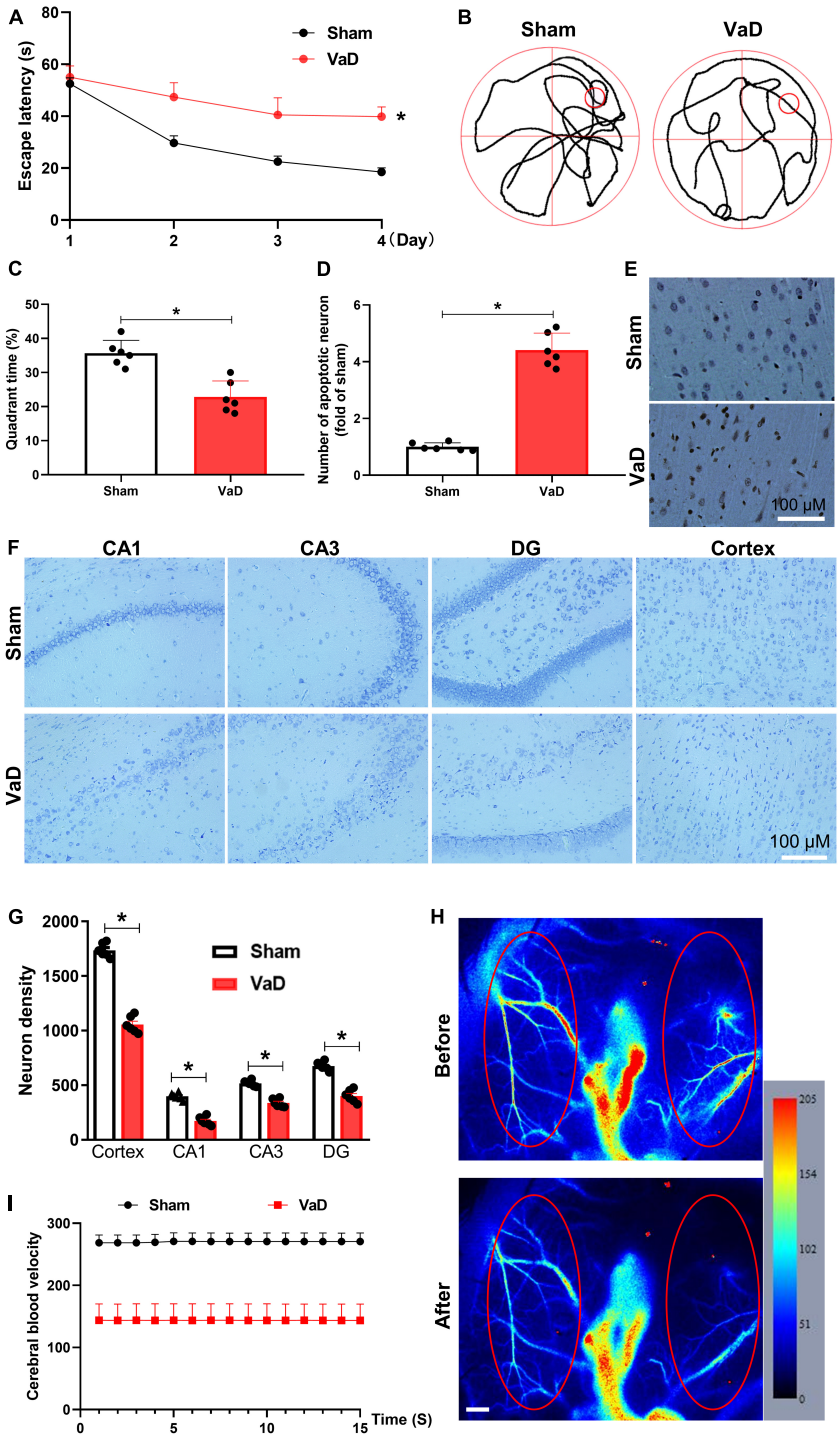

FIGURE 3
Establishing of VaD rat model. Sprague-Dawley rats were subjected to bilateral common carotid artery occlusion surgery to induce VaD rat model. Three months later, the Morris water maze (MWM) test was performed, then brains were collected for histopathological analysis. **(A)** The trajectory chart. **(B)** The latency time of rats to reach a hidden platform from day 1 to day 4 were recorded. **(C)** The percentage of time spent in the platform quadrant was calculated. **(D)** The statistical chart for TUNEL-positive cells. **(E)** Representative images of TUNEL staining in the cortex region. Representative images of Nissl staining in the CA1, CA3, DG, and cortex regions **(F)**, and neuron density **(G)**. **(H)** Cerebral blood velocity before and after surgery. Red ellipse represents region of interest. Scale bar, 0.5 mm. **(I)** The cerebral blood velocity was measured in regions of interest. [**(A–G)**: $n = 6$; **(H,I)**: $n = 3$]. *$p < 0.05$. Data are shown as mean ± SD.

Supplementary Figures 2D–F). Meanwhile, increased Iba-1-positive cells were confirmed by immunofluorescence staining of cortex sections from VaD rats ($p < 0.05$, Supplementary Figures 2G,H). These results suggest that levels of oxidative stress and inflammation are significantly increased in VaD rats.

miR-154-5p is upregulated in the hippocampus, cortex, and bone marrow-endothelial progenitor cell from vascular dementia rats

To examine the expression of miR-154-5p in brain tissues and cellular, RT-PCR was performed. The expression of miR-154-5p was significantly increased in the hippocampus, cortex, and BM-EPC from VaD rats ($p < 0.05$, Supplementary Figure 2I), whereas there were no significant differences in microglia and astrocyte ($p > 0.05$, Supplementary Figure 2I), suggesting that miR-154-5p is likely involved in the development of VaD *via* endothelium.

Inhibition of miR-154-5p improves vascular dementia-induced endothelial progenitor cell dysfunction and excessive oxidative stress in bone marrow-endothelial progenitor cells

Strong evidence demonstrates that cerebrovascular dysfunction links with VaD (Kalaria, 2018). Prior studies have reported that EPCs contribute to cerebral vascular repair disorders, such as AD and stroke (Bai et al., 2015; Zhang et al., 2018). To define the effect of miR-154-5p on EPC function in VaD rats, miR-154-5p inhibitor was used to knock down its expression. BM-EPCs were isolated from the VaD rats, and tube formation, migration, and adhesion ability were evaluated *in vitro*. BM-EPCs from VaD rats resulted in a significant decrease in the number of tubes ($p < 0.05$, Figures 4A,B), migration cells ($p < 0.05$, Figures 4C,D), and adhesion ability ($p < 0.05$, Figures 4E,F) compared with EPCs from sham group. miR-154-5p inhibitor significantly elevated tube formation, migration, and adhesion ($p < 0.05$, Figures 4A–F). In notice, miR-154-5p inhibitor markedly attenuated VaD-induced reduction of VEGF and SDF-1α concentrations in EPC from VaD rats ($p < 0.05$, Figures 4G,H).

Interestingly, miR-154-5p also potentially regulated adhesion molecules and oxidative stress. RT-PCR analysis revealed upregulated gene level expression of adhesion molecules, including ICAM-1, VCAM-1, and MCP-1, in BM-EPCs from VaD rats, whereas the miR-154-5p inhibitor significantly blunted the levels of these genes in BM-EPCs ($p < 0.05$, Figures 4I–K). Moreover, EPC from VaD rats showed a significant decrease of SOD, and miR-154-5p inhibitor dramatically increased the concentration of SOD in BM-EPCs ($p < 0.05$, Figure 4L). In agreement with this result, the miR-154-5p inhibitor effectively reduced production of ROS, as shown by DHE staining in EPC from VaD rats ($p < 0.05$, Figures 4M,N). In addition, we speculated the promising targets of miR-154-5p using miRDB, TargetScan 8.0, and miRNA.org PRKAA2, which could encode AMPKα2 was chosen as a potential target gene of miR-154-5p (Figure 4O). To prove that miR-154-5p could target AMPKα2, the protein expression of AMPKα2 was measured with Western blot. As shown in Figure 4P, the protein expression of AMPKα2 was remarkedly decreased in BM-EPCs from VaD rats compared with EPCs from sham group. The miR-154-5p inhibitor increased expression of AMPKα2 in BM-EPCs (Figure 4P). Taken together, these data indicate that inhibition of miR-154-5p was able to ameliorate EPC dysfunction in VaD rats, which may be associated with downregulated levels of adhesion molecules, oxidative stress, and AMPKα 2 expression.

Overexpression of miR-154-5p impairs endothelial progenitor cell functions and inhibits angiogenesis following endothelial progenitor cell transplantation in vascular dementia rats

To further clarify the function of miR-154-5p on angiogenesis in VaD rats, we overexpressed miR-154-5p with RNA mimics in BM-EPCs. The overexpression of miR-154-5p alone markedly worsened EPC functions, reflected by reduced number of tubes, migration cells, and adhesion cells in rats compared with normal control group ($p < 0.05$, Figures 5A–F). Later, VaD rats were transplanted with BrdU-labeled EPCs, which were pretreated with miR-154-5p mimics or negative control, and immunofluorescent staining for endothelial cell-specific marker CD31 (green), followed by BrdU (red) were performed in the cortex of brain tissues. As shown in Figure 5G, some BrdU-positive cells were integrated into CD31-positive vessels in the cortex of VaD rats that received NC-EPC transplantation. However, the miR-154-5p-EPC transplantation showed little incorporation into cerebral angiogenesis of VaD rats (Figure 5G). Based on these results, miR-154-5p was sufficient to trigger poor angiogenesis in the brain of VaD rats.

Discussion

The primary findings of the current study were as follows. First, miR-154-5p was significantly increased in serum exosomes

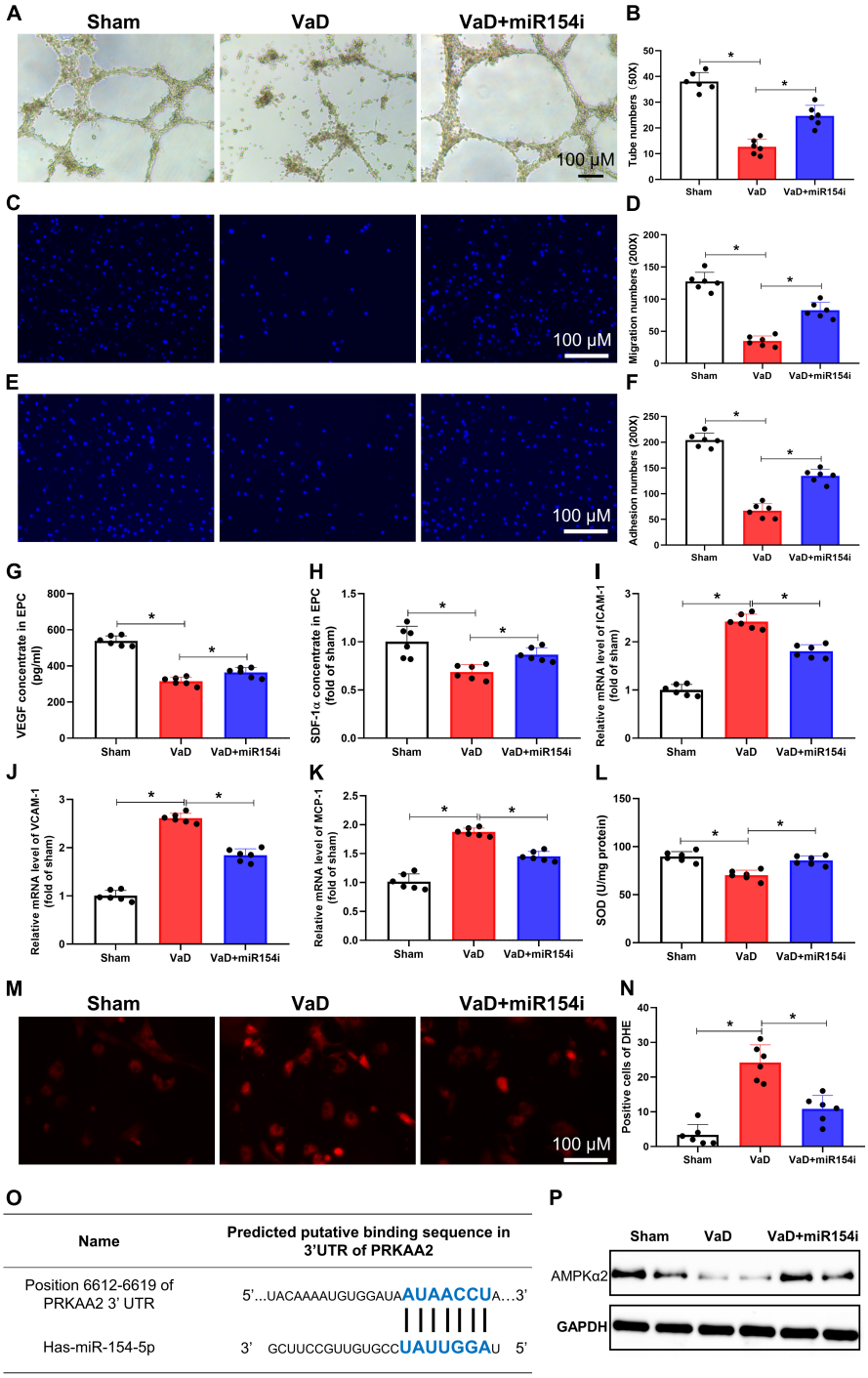

FIGURE 4

Inhibition of miR-154-5p improves VaD-induced EPC dysfunction and reduces oxidative stress in BM-EPCs. After 3 months of bilateral common carotid artery occlusion surgery, rats were euthanized, and BM-EPCs were harvested for functional tests. BM-EPC function was estimated by tube formation assay **(A,B)**, migration ability **(C,D)**, and adhesion capacity **(E,F)**. MiR-154-5p inhibitor significantly improved VaD-induced EPC dysfunction. The levels of VEGF **(G)** and SDF-1α **(H)** in culture medium were detected by ELISA kits. Results from the real-time PCR experiments for analysis the expression of ICAM-1 **(I)**, VCAM-1 **(J)**, and MCP-1 **(K)** in BM-EPCs. **(L)** SOD level in BM-EPCs was measured with a kit. Images of DHE staining **(M)** and quantitative analysis of DHE-positive cells **(N)**. **(O)** The predicted miR-154-5p-binding sites in PRKAA2 mRNA 3′-UTR were confirmed. **(P)** The downregulated level of AMPKα2 was increased by miR-154-5p inhibitor in BM-EPCs. 50×: scale bar, 100 μm; 200×: scale bar, 100 μm [**(A–N)**: $n = 6$; **(P)**: $n = 3$]. *$p < 0.05$. Data are shown as mean ± SD. BM-EPC, bone marrow-endothelial progenitor cell; SDF, stromal cell-derived factor; SOD, superoxide dismutase; VaD, vascular dementia.

10.3389/fncel.2022.881175

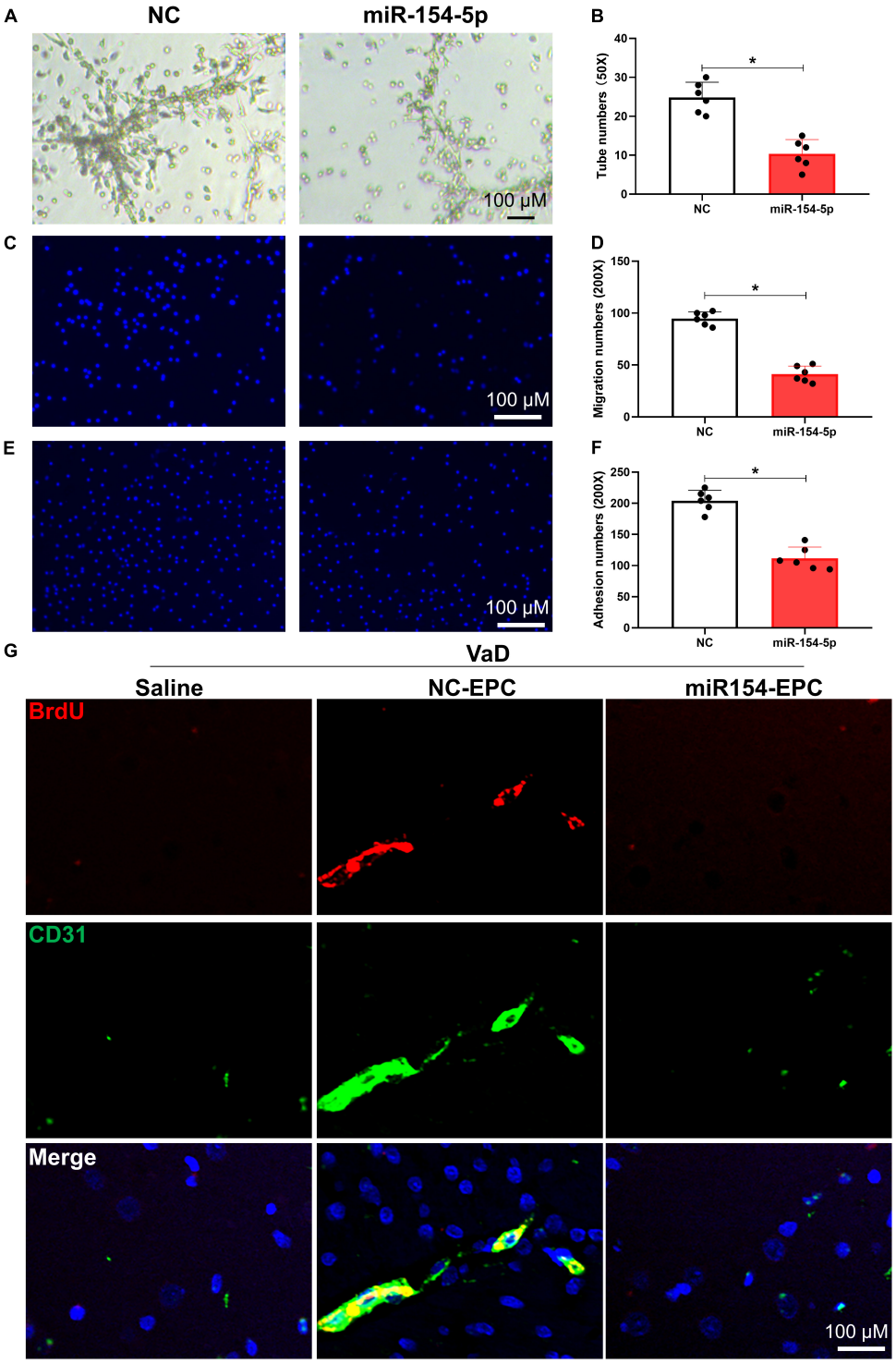

FIGURE 5

Overexpression of miR-154-5p impairs EPC functions and inhibits angiogenesis following EPC transplantation in VaD rats. After 7 days culture, BM-EPCs were transfected with normal control (NC) scrambled RNA or miR-154-5p mimics, and EPC functions were then evaluated using tube formation assay **(A,B)**, migration ability **(C,D)**, and adhesion capacity **(E,F)**. **(A)**: 50×: scale bar, 100 μm; **(C,E)**: 200×: scale bar, 100 μm. VaD rats were subjected to a single injection of saline or BrdU-labeled EPCs, which were transfected with NC RNA and miR-154-5p mimics. Seven days later, brain samples were harvested and stained with CD31 (green) and BrdU (red). **(G)** Representative images in the cortex region of VaD rats. 200×: scale bar, 100 μm [**(A–F)**: $n = 6$; **(G)**: $n = 3$]. *$p < 0.05$. Data are shown as mean ± SD. BrdU, 5-bromo-2′-deoxyuridine; EPC, endothelial progenitor cell; VaD, vascular dementia.

from patients with VaD. Second, the expression of miR-154-5p was also upregulated both in brain tissues and in BM-EPCs, and inhibition of miR-154-5p markedly ameliorated EPC dysfunction, evidenced by reduced expression of adhesion molecule and diminished oxidative stress in BCCAO-induced VaD rats. Finally, we showed that upregulation of miR-154-5p obviously worsened EPC function and inhibited angiogenesis following EPC transplantation in VaD rats. Our results confirmed that miR-154-5p may be one of the important regulators of EPC-mediated angiogenesis participating in the development of VaD.

Vascular dementia is proposed to be a chronic cerebrovascular syndrome resulted from diverse etiologies, with cerebral vascular damage being the key pathological manifestation. The pathogenesis of VaD has not yet been elucidated and mainly includes injury of the cholinergic system, neuroinflammation, synaptic plasticity, and the toxicity of excitatory amino acids and free radicals (Kalaria et al., 2016). Majority of patients with VaD do not have any symptoms in the stage of onset, thus effectively diagnostic biomarker and therapeutic prevention seem to be quite important. Recently, many exciting evidences indicate that exosomal contents, which cause dramatically changes under neurological damage condition, represent a possibility for the diagnosis and treatment of neurodegenerative disorders (Yuyama and Igarashi, 2017; Hamlett Ledreux et al., 2018). In general, exosomes are a kind of secreted bilayer-enclosed MVs with a size range of 50–150 nm diameter (Hamlett Ledreux et al., 2018). In this study, our results showed that isolated MVs from human serum corresponded to properties of exosomes in morphology and size.

Exosomes can deliver important proteins, miRNAs, and short-interfering RNA during intercellular communication. They are considered as carriers for functional miRNAs binding to the enzyme Argonaute 2 and transferring to the surrounding cells, including neurons and astrocytes (Hamlett Goetzl et al., 2017). Notably, altered miRNAs profiles in CSF or blood exosomes were closely associated with neurodegenerative disorders. It has reported that decreased miR-193b in CSF exosomes could function in the progression of AD (Liu et al., 2014). Besides, Application of low-level IFNγ released exosomes containing miRNAs species is able to increase myelination, reduce oxidative stress, and improve remyelination in acute lysolecithin-induced demyelination (Pusic et al., 2014). However, the alteration in exosome-mediated miRNA signature in VaD remains further research to clarify, and it may be a possible disease pathology. Our results showed that miR-154-5p was significantly elevated in serum exosomes of patients with VaD compared with healthy control *via* bioinformatics analysis. Meanwhile, this increment was further conformed in the brain tissues and BM-EPC of VaD rats, implying miR-154-5p involved in the development of VaD.

For the Kyoto Encyclopedia of Genes and Genomes (KEGG) analysis, the different genes were mainly enriched in blood vessel development, cellular migration, and cell adhesion signaling pathways. Numerous studies have revealed that recruitment EPCs into damaged tissues is one of the key events in neovascularization (Bai et al., 2015; Pías-Peleteiro et al., 2017). Due to their distinct capabilities, EPCs possess a promising potential in treatment of vascular diseases. In a diabetic ischemic stroke model, transplanted EPCs contribute to improve stroke outcome, promote angiogenesis, and elevate VEGF expression (Bai et al., 2015). Unfortunately, EPC function was significantly undermined in patients with AD and VaD (Kong et al., 2011). In line with these results, we found that EPC functions, including tube formation, migration ability, and adhesion capacity, were impaired, and pro-angiogenic growth factors VEGF and SDF-1α were reduced in BCCAO induced for 3 months model. Moreover, EPCs have been shown to provide an abundant source of exosomes suggesting one of the pivotal components modifying the bioactivity. The exosomes-mediated transfer of miR-126 has been shown to prevent microvascular dysfunction and effectively ameliorate sepsis outcomes in mice (Zhou et al., 2018). miR-154-5p, as a conserved miRNA in mammal, is associated with cell proliferation, cardiac fibroblasts, cardiomyocyte hypertrophy, and oxidant stress (Sun et al., 2016; Wang et al., 2019). However, the role of miR-154-5p in cerebrovascular remains unknown. Here, we found that inhibition of miR-154-5p improved the BCCAO-induced EPC dysfunction, upregulation of adhesion molecule, and excessive oxidative stress level. As expected, overexpression of miR-154-5p could worsen the EPC functions *in vitro*.

The EPC transplantation has a powerful potential in vascular repair and revascularization in neurological disorders besides AD (Peng et al., 2018; Zhang et al., 2018). It is also a broad-spectrum method, and patients with different risk factors of neurodegeneration, including aging, diabetes, hypertension, etc., may be applicable. In APP/PS1 transgenic mice, the EPC transplantation markedly improved spatial learning and memory functions, repaired blood–brain barrier tight junction function, and stimulated angiogenesis (Zhang et al., 2018). The EPC delivery might also represent an advanced strategy for interventional treatment of VaD. In this study, the EPC transplantation in CCH-induced rats was helpful for angiogenesis in the cortex tissues. While transplanted the EPCs which were overexpressed miR-154-5p reversed the angiogenesis effect.

There is a limitation in this study. The mechanism that related to miR-154-5p regulation of EPC-mediated angiogenesis under pathological condition of VaD mainly confirmed in VaD rats, we did not verify in patients with VaD. This limitation could cause bias in our study. Nonetheless, these data on the upregulation of circulating exo-miR-154-5p in patients with VaD are intriguing. Obviously, the results need to be further evaluated in patients with VaD in the future.

Conclusion

In conclusion, in the current study, we show that exosomal miR-154-5p expression is significantly increased in VaD individuals. The upregulation of miR-154-5p is sufficient to trigger the EPC dysfunction and impairment of angiogenesis. Inhibition of miR-154-5p has beneficial effects on ameliorating EPC functions implying the clinical potential of miR-154-5p inhibition during VaD therapy.

Data availability statement

The datasets presented in this study can be found in online repositories. The name of the repository and accession number can be found below: National Center for Biotechnology Information (NCBI) BioProject, https://www.ncbi.nlm.nih.gov/bioproject/, PRJNA833586.

Ethics statement

The studies involving human participants were reviewed and approved by the Ethics Committee of Zhejiang Xiaoshan Hospital. The patients/participants provided their written informed consent to participate in this study. The animal study was reviewed and approved by the Ethics Committee of Laboratory Animal Care and Welfare, Hangzhou Medical College.

Author contributions

HY, XH, and QJS contributed to the literature search and study design. XH participated in the drafting of the manuscript. XH, LZ, YT, JW, and JZ carried out the experiments. XH and LZ contributed to data collection and analysis. All authors contributed to the article and approved the submitted version.

Funding

This study was supported by the National Natural Science Foundation of China (31900381 to XH), the Natural Science Foundation of Zhejiang Province (LGJ18H310002 to XH and LY18H310009 to GJJ), the Medical Health Science and Technology Funding of Zhejiang (2018KY653 to GJJ), and the Basic Scientific Research Project of Hangzhou Medical College (KYZD202102 to QJS and KYYB202114 to XH).

Conflict of interest

The authors declare that the research was conducted in the absence of any commercial or financial relationships that could be construed as a potential conflict of interest.

Publisher's note

All claims expressed in this article are solely those of the authors and do not necessarily represent those of their affiliated organizations, or those of the publisher, the editors and the reviewers. Any product that may be evaluated in this article, or claim that may be made by its manufacturer, is not guaranteed or endorsed by the publisher.

Supplementary material

The Supplementary Material for this article can be found online at: https://www.frontiersin.org/articles/10.3389/fncel.2022.881175/full#supplementary-material

References

Bai, Y.-Y., Wang, L., Chang, D., Zhao, Z., Lu, C.-Q., Wang, G., et al. (2015). Synergistic effects of transplanted endothelial progenitor cells and rwj 67657 in diabetic ischemic stroke models. *Stroke* 46, 1938–1946. doi: 10.1161/STROKEAHA.114.008495

Beatriz, M., Vilaça, R., and Lopes, C. (2021). Exosomes: innocent bystanders or critical culprits in neurodegenerative diseases. *Front. Cell Dev. Biol.* 9:635104. doi: 10.3389/fcell.2021.635104

Deregibus, M. C., Cantaluppi, V., Calogero, R., Lo Iacono, M., Tetta, C., Biancone, L., et al. (2007). Endothelial progenitor cell derived microvesicles activate an angiogenic program in endothelial cells by a horizontal transfer of mrna. *Blood* 110, 2440–2448.

Du, S.-Q., Wang, X.-R., Xiao, L.-Y., Tu, J.-F., Zhu, W., He, T., et al. (2017). Molecular mechanisms of vascular dementia: what can be learned from animal models of chronic cerebral hypoperfusion? *Mole. Neurobiol.* 54, 3670–3682. doi: 10.1007/s12035-016-9915-1

Fayazi, N., Sheykhhasan, M., Soleimani Asl, S., and Najafi, R. (2021). Stem cell-derived exosomes: a new strategy of neurodegenerative disease treatment. *Mole. Neurobiol.* 58, 3494–3514. doi: 10.1007/s12035-021-02324-x

Ghassab-Abdollahi, N., Mobasseri, K., Dehghani Ahmadabad, A., Nadrian, H., and Mirghafourvand, M. (2021). The effects of huperzine a on dementia and mild cognitive impairment: an overview of systematic reviews. *Phytother. Res.* 35, 4971–4987. doi: 10.1002/ptr.7126

Gui, Y., Liu, H., Zhang, L., Lv, W., and Hu, X. (2015). Altered microrna profiles in cerebrospinal fluid exosome in parkinson disease and alzheimer disease. *Oncotarget* 6, 37043–37053. doi: 10.18632/oncotarget.6158

Hamlett Goetzl, E. J., Ledreux, A., Vasilevko, V., Boger, H. A., LaRosa, A., et al. (2017). Neuronal exosomes reveal alzheimer's disease biomarkers in down syndrome. *Alzheimer's Dementia* 13, 541–549. doi: 10.1016/j.jalz.2016.08.012

Hamlett Ledreux, A., Potter, H., Chial, H. J., Patterson, D., Espinosa, J. M., et al. (2018). Exosomal biomarkers in down syndrome and alzheimer's disease. *Free Rad. Biol. Med.* 114, 110–121. doi: 10.1016/j.freeradbiomed.2017.08.028

Han, X., Deng, Y., Yu, J., Sun, Y., Ren, G., Cai, J., et al. (2017a). Acarbose accelerates wound healing via akt/enos signaling in mice. *Oxidat. Med. Cell. Longev.* 2017:7809581. doi: 10.1155/2017/7809581

Han, X., Tao, Y., Deng, Y., Yu, J., Sun, Y., and Jiang, G. (2017b). Metformin accelerates wound healing in type 2 diabetic db/db mice. *Mole. Med. Rep.* 16, 8691–8698. doi: 10.3892/mmr.2017.7707

Jiwa, N. S., Garrard, P., and Hainsworth, A. H. (2010). Experimental models of vascular dementia and vascular cognitive impairment: a systematic review. *J. Neurochem.* 115, 814–828. doi: 10.1111/j.1471-4159.2010.06958.x

Kalaria, R. N. (2018). The pathology and pathophysiology of vascular dementia. *Neuropharmacology* 134(Pt B), 226–239. doi: 10.1016/j.neuropharm.2017.12.030

Kalaria, R. N., Akinyemi, R., and Ihara, M. (2016). Stroke injury, cognitive impairment and vascular dementia. *Biochimica et biophysica acta* 1862, 915–925. doi: 10.1016/j.bbadis.2016.01.015

Kong, X.-D., Zhang, Y., Liu, L., Sun, N., Zhang, M.-Y., and Zhang, J.-N. (2011). Endothelial progenitor cells with alzheimer's disease. *Chin. Med. J.* 124, 901–906.

Kong, Y., Tian, X., He, R., Li, C., Xu, H., Tian, L., et al. (2021). The accumulation of exosome-associated microrna-1246 and microrna-150-3p in human red blood cell suspensions. *J. Transl. Med.* 19:225. doi: 10.1186/s12967-021-02887-2

Leardini-Tristão, M., Andrade, G., Garcia, C., Reis, P. A., Lourenço, M., Moreira, E. T. S., et al. (2020). Physical exercise promotes astrocyte coverage of microvessels in a model of chronic cerebral hypoperfusion. *J. Neuroinflam.* 17:117. doi: 10.1186/s12974-020-01771-y

Leardini-Tristão, M., Borges, J. P., Freitas, F., Rangel, R., Daliry, A., Tibiriçá, E., et al. (2017). The impact of early aerobic exercise on brain microvascular alterations induced by cerebral hypoperfusion. *Brain Res.* 1657, 43–51. doi: 10.1016/j.brainres.2016.11.030

Li, P., Kaslan, M., Lee, S. H., Yao, J., and Gao, Z. (2017). Progress in exosome isolation techniques. *Theranostics* 7, 789–804. doi: 10.7150/thno.18133

Li, Y., Feng, W., Kong, M., Liu, R., Wu, A., Shen, L., et al. (2021). Exosomal circrnas: a new star in cancer. *Life Sci.* 269:119039. doi: 10.1016/j.lfs.2021.119039

Librizzi, D., Cabanel, N., Zavorotnyy, M., Riehl, E., Kircher, T., Luster, M., et al. (2021). Clinical Relevance of [F]Florbetaben and [F]Fdg Pet/Ct Imaging on the Management of Patients with Dementia. *Molecules* 26:5. doi: 10.3390/molecules26051282

Liu, C.-G., Song, J., Zhang, Y.-Q., and Wang, P.-C. (2014). Microrna-193b is a regulator of amyloid precursor protein in the blood and cerebrospinal fluid derived exosomal microrna-193b is a biomarker of alzheimer's disease. *Mole. Med. Rep.* 10, 2395–2400. doi: 10.3892/mmr.2014.2484

Murakami, Y., Toyoda, H., Tanahashi, T., Tanaka, J., Kumada, T., Yoshioka, Y., et al. (2012). Comprehensive mirna expression analysis in peripheral blood can diagnose liver disease. *PLoS One* 7:e48366. doi: 10.1371/journal.pone.0048366

Peng, C., Dong, X.-H., Liu, J.-L., Tao, Y.-L., Xu, C.-F., Wang, L.-P., et al. (2018). A preventive injection of endothelial progenitor cells prolongs lifespan in stroke-prone spontaneously hypertensive rats. *Clin. Sci.* 132, 1797–1810. doi: 10.1042/CS20180360

Pías-Peleteiro, J., Campos, F., Castillo, J., and Sobrino, T. (2017). Endothelial progenitor cells as a therapeutic option in intracerebral hemorrhage. *Neur. Regen. Res.* 12, 558–561. doi: 10.4103/1673-5374.205085

Pusic, A. D., Pusic, K. M., Clayton, B. L. L., and Kraig, R. P. (2014). Ifnγ-stimulated dendritic cell exosomes as a potential therapeutic for remyelination. *J. Neuroimmunol.* 266, 12–23. doi: 10.1016/j.jneuroim.2013.10.014

Raz, L., Knoefel, J., and Bhaskar, K. (2016). The Neuropathology and Cerebrovascular Mechanisms of Dementia. *J. Cereb. Blood Flow Metabol.* 36, 172–186.

Román, G. C., Tatemichi, T. K., Erkinjuntti, T., Cummings, J. L., Masdeu, J. C., Garcia, J. H., et al. (1993). Vascular dementia: diagnostic criteria for research studies. report of the ninds-airen international workshop. *Neurology* 43, 250–260.

Sun, L.-Y., Bie, Z.-D., Zhang, C.-H., Li, H., Li, L.-D., and Yang, J. (2016). Mir-154 directly suppresses Dkk2 to activate wnt signaling pathway and enhance activation of cardiac fibroblasts. *Cell Biol. Internat.* 40, 1271–1279. doi: 10.1002/cbin.10655

Terracciano, A., Aschwanden, D., Passamonti, L., Toschi, N., Stephan, Y., Luchetti, M., et al. (2021). Is neuroticism differentially associated with risk of alzheimer's disease, vascular dementia, and frontotemporal dementia? *J. Psychiat. Res.* 138, 34–40. doi: 10.1016/j.jpsychires.2021.03.039

Wang, Q., Yu, X., Dou, L., Huang, X., Zhu, K., Guo, J., et al. (2019). Mir-154-5p functions as an important regulator of angiotensin ii-mediated heart remodeling. *Oxidat. Med. Cell. Long.* 2019:8768164. doi: 10.1155/2019/8768164

Xu, X., Zhang, B., Lu, K., Deng, J., Zhao, F., Zhao, B.-Q., et al. (2016). Prevention of hippocampal neuronal damage and cognitive function deficits in vascular dementia by dextromethorphan. *Mole. Neurobiol.* 53, 3494–3502. doi: 10.1007/s12035-016-9786-5

Yu, J.-W., Deng, Y.-P., Han, X., Ren, G.-F., Cai, J., and Jiang, G.-J. (2016). Metformin improves the angiogenic functions of endothelial progenitor cells via activating ampk/enos pathway in diabetic mice. *Cardiovasc. Diabetol.* 15:88. doi: 10.1186/s12933-016-0408-3

Yuyama, K., and Igarashi, Y. (2017). Exosomes as carriers of alzheimer's amyloid-ß. *Front. Neurosci.* 11:229. doi: 10.3389/fnins.2017.00229

Zhang, S., Zhi, Y., Li, F., Huang, S., Gao, H., Han, Z., et al. (2018). Transplantation of in vitro cultured endothelial progenitor cells repairs the blood-brain barrier and improves cognitive function of app/ps1 transgenic ad mice. *J. Neurolog. Sci.* 2018:387. doi: 10.1016/j.jns.2018.01.019

Zhou, G., Han, X., Wu, Z., Shi, Q., and Bao, X. (2019). Rosiglitazone accelerates wound healing by improving endothelial precursor cell function and angiogenesis in mice. *PeerJ* 7:e7815. doi: 10.7717/peerj.7815

Zhou, Y., Li, P., Goodwin, A. J., Cook, J. A., Halushka, P. V., Chang, E., et al. (2018). Exosomes from endothelial progenitor cells improve the outcome of a murine model of sepsis. *Mol. Ther.* 26, 1375–1384. doi: 10.1016/j.ymthe.2018.02.020

frontiers | Frontiers in Molecular Neuroscience

TYPE Review
PUBLISHED 01 August 2022
DOI 10.3389/fnmol.2022.949096

OPEN ACCESS

EDITED BY
Catia Andreassi,
University College London,
United Kingdom

REVIEWED BY
Susana Cohen-Cory,
University of California, Irvine,
United States
Yoshiyuki Konishi,
University of Fukui, Japan

*CORRESPONDENCE
Marina Vidaki
marina.vidaki@uoc.gr

SPECIALTY SECTION
This article was submitted to Neuroplasticity and Development, a section of the journal Frontiers in Molecular Neuroscience

RECEIVED 20 May 2022
ACCEPTED 07 July 2022
PUBLISHED 01 August 2022

CITATION
Triantopoulou N and Vidaki M (2022) Local mRNA translation and cytoskeletal reorganization: Mechanisms that tune neuronal responses.
Front. Mol. Neurosci. 15:949096.
doi: 10.3389/fnmol.2022.949096

Local mRNA translation and cytoskeletal reorganization: Mechanisms that tune neuronal responses

Nikoletta Triantopoulou[1,2] and Marina Vidaki[1,2]*

[1]Division of Basic Sciences, Medical School, University of Crete, Heraklion, Greece, [2]Institute of Molecular Biology and Biotechnology, Foundation for Research and Technology Hellas (IMBB-FORTH), Heraklion, Greece

Neurons are highly polarized cells with significantly long axonal and dendritic extensions that can reach distances up to hundreds of centimeters away from the cell bodies in higher vertebrates. Their successful formation, maintenance, and proper function highly depend on the coordination of intricate molecular networks that allow axons and dendrites to quickly process information, and respond to a continuous and diverse cascade of environmental stimuli, often without enough time for communication with the soma. Two seemingly unrelated processes, essential for these rapid responses, and thus neuronal homeostasis and plasticity, are local mRNA translation and cytoskeletal reorganization. The axonal cytoskeleton is characterized by high stability and great plasticity; two contradictory attributes that emerge from the powerful cytoskeletal rearrangement dynamics. Cytoskeletal reorganization is crucial during nervous system development and in adulthood, ensuring the establishment of proper neuronal shape and polarity, as well as regulating intracellular transport and synaptic functions. Local mRNA translation is another mechanism with a well-established role in the developing and adult nervous system. It is pivotal for axonal guidance and arborization, synaptic formation, and function and seems to be a key player in processes activated after neuronal damage. Perturbations in the regulatory pathways of local translation and cytoskeletal reorganization contribute to various pathologies with diverse clinical manifestations, ranging from intellectual disabilities (ID) to autism spectrum disorders (ASD) and schizophrenia (SCZ). Despite the fact that both processes are essential for the orchestration of pathways critical for proper axonal and dendritic function, the interplay between them remains elusive. Here we review our current knowledge on the molecular mechanisms and specific interaction networks that regulate and potentially coordinate these interconnected processes.

KEYWORDS

local mRNA translation, cytoskeleton reorganization, neuronal development, axon elongation and regeneration, synaptogenesis, ribonucleoprotein complexes

Introduction

Neurons are the "foundation stones" of the nervous system (NS), relentlessly processing and conveying information crucial for the orchestration of all the necessary functions of life. They are among the most structurally sophisticated cells, consisting of a cell body (soma) with two molecularly and functionally distinct types of cytoplasmic protrusions: the dendrites and the axon (Kevenaar and Hoogenraad, 2015). The significantly extended axons of higher vertebrates are often required to quickly integrate and process multiple incoming signals, independently of the soma. Thus, it is easy to envisage that the proper development, maintenance, and function of the NS depends on a certain degree of axonal autonomy, as in most cases there is simply not enough time for communication with the soma (Mofatteh, 2020). This semi-autonomous activity of axons strongly relies on two processes: Local mRNA translation and dynamic cytoskeleton reorganization.

Neurons possess free ribosomes in their distal compartments and are thus capable of regulating protein synthesis locally and on-demand, using mRNA molecules that are trafficked to various subcellular locations and maintained in a dormant state unto specific stimulation (Cajigas et al., 2012; Buxbaum et al., 2014; Zappulo et al., 2017; Glock et al., 2021). Since the translation of a single mRNA molecule can generate multiple proteins, localized protein synthesis is considered an energetically favorable mechanism over transport of individual proteins to distal axonal compartments, allowing for drastic alteration of the local proteome and subsequent rapid responses upon receipt of microenvironmental signaling (Gasparski et al., 2022). On the other hand, the neuronal cytoskeleton, composed of actin filaments (filamentous actin or F-actin), neurofilaments, and microtubules (MTs), acts as a key regulator of crucial molecular and cellular events related to the establishment and maintenance of neuronal polarity, morphology, structural integrity, and plasticity (Luo, 2002; Barnes and Polleux, 2009). Even though its name implies a static nature, the cytoskeleton is actually exceptionally dynamic, capable of undergoing rapid rearrangements in order to adjust to emerging cellular needs in response to several stimuli.

Local mRNA translation is highly linked to the cytoskeleton, as the latter not only serves as a platform for mRNA trafficking but also acts as a scaffold for the organization of the translational machinery components (Venticinque et al., 2011; Kevenaar and Hoogenraad, 2015; Piper et al., 2015). Meanwhile, successful cytoskeleton reorganization is accomplished by a cycle of polymerization and depolymerization of filaments, based on monomers that are locally synthesized (Grantham et al., 2002; Buxbaum et al., 2014; Preitner et al., 2014). Despite the obvious interrelation of the two processes, and their well-established roles in the regulation of crucial cellular events during development and adulthood, little is known about the potential molecular mechanisms and complexes that are involved in their coordination. Here, we aim to provide an overview of the current literature on the co-orchestrated regulation of local protein synthesis and cytoskeletal reorganization, both in the developing and adult NS. Our goal is to summarize our knowledge and highlight potential missing information that would help us understand the pivotal interplay between these processes, necessary for proper NS structure and function.

Importance and regulation of local mRNA translation in neurons

De novo protein synthesis localized to specific subcellular regions, a process known as local mRNA translation, can be achieved via targeted mRNA transport and allows for the spatiotemporal control of a cell's protein repertoire (Holt and Schuman, 2013). Localized protein synthesis has been studied extensively in model organisms, where the specific subcellular localization of cytosolic mRNA molecules (e.g., *bicoid*, *oscar*, *nanos*) is crucial for development and cell fate determination (Forrest and Gavis, 2003; Weil et al., 2008; Zimyanin et al., 2008). For example, due to its large size and polarity, the normal development and function of an oocyte in *Drosophila melanogaster* or *Xenopus laevis*, depends on the targeted transport of translationally silent mRNAs, and the subsequent activation of protein synthesis at a specific developmental stage or location (Besse and Ephrussi, 2008). This differential subcellular localization of mRNAs in different systems of various species serves as an evolutionarily conserved mechanism for the asymmetrical distribution of proteins among each cell compartment (Mofatteh, 2020). Interestingly, the localized mRNAs often times undergo differential cleavage of their untranslated regions (UTRs) that generates compartment-specific protein isoforms (Andreassi et al., 2021). In addition, due to differences in their post-translational modifications (PTMs), newly synthesized proteins resulting from local mRNA translation are also functionally different than their already existing counterparts. For instance, locally synthesized β-actin is critical for cell polarity and directional movement of fibroblasts (Liao et al., 2008).

In the sublimely complex NS, formation of functional neuronal networks necessitates precise axonal and dendritic positioning, which in turn require spatiotemporal regulation of gene expression. Neuronal local translation is an elegant mechanism, key to this regulation; specific mRNAs that are transported in a dormant state in distal neuronal compartments, are translated on-demand, thus providing axons with a level of autonomy that is crucial for their proper development and function (Mofatteh, 2020).

Local mRNA translation in axon outgrowth and guidance

Several studies highlight the role of local translation in neurodevelopmental processes, such as growth cone formation, axon pathfinding and branching, and formation of synapses, while at the same time numerous neurodevelopmental disorders have been correlated with disrupted local protein synthesis (Sasaki et al., 2010; Zivraj et al., 2010; Spillane et al., 2012; Gkogkas et al., 2013; Santini et al., 2013). After extensive research in the last couple of decades, we now know that developing axons exhibit high capacity for local translation, which provides them with such remarkable autonomy, that they can grow and navigate independently of the neuronal soma. Indeed, a series of elegant *in vitro* experiments initially unraveled that *Xenopus* retinal axon pathfinding remains unaffected by the removal of the soma (Harris et al., 1987). This observation, along with previous pioneer studies that uncovered the presence of ribosomes in the axonal compartment, led to the conclusion that the basic translation machinery is available in axons, allowing them to tune their proteome and respond to their environment as needed (Harris et al., 1987; Mofatteh, 2020). However, the cellular mechanisms that regulate precise positioning of ribonucleoprotein particles (RNPs) in axons remain largely unknown. Recent work in *X. laevis* has shown that axonal mRNAs and RNPs are co-transported with late endosomes, with the latter ones also serving as docks for local translation of proteins responsible for axon survival and integrity (Cioni et al., 2019). Interestingly, mitochondria reside in the endosome hotspots for local translation and numerous of the translated mRNAs correspond to proteins that regulate or maintain mitochondrial functions (Cioni et al., 2019). These observations in good agreement with previous work unraveling the importance of mitochondria in local translation and axon branching downstream of nerve growth factor (NGF) (Spillane et al., 2013), underline a remarkable mechanism that axons display, in order to self-sustain their protein homeostasis and the energy required to do so.

On top of the ability to maintain their integrity, axons need to respond to a multitude of extracellular signals. Especially in the mammalian NS the neuronal microenvironment is rather complex. Axons and their growth cones receive and integrate a plethora of constant chemoattractive and chemorepulsive cues *in vivo*. Successful guidance to their synaptic targets is then achieved via intracellular signal transduction and subsequent directed movement along the correct pathway (Dickson, 2002; Erskine and Herrera, 2007). This directional steering strongly depends on local mRNA translation and several axon guidance molecules and growth factors are responsible for eliciting rapid axonal protein synthesis. For instance, the Slits and Semaphorins serve as extracellular cues that promote local translation of mRNA molecules and induce repulsive turning of axons. Notably, blocking local translation can inhibit repulsive turning in response to these molecules (Piper et al., 2006). On the other hand, attractive cues like Netrin-1 also require local protein synthesis to exert their effect on growing axons. The Netrin-1 receptor DCC has been previously shown to directly interact with the translation machinery in developing axons, thereby promoting translation of specific mRNAs and *de novo* synthesis of proteins necessary for Netrin-1 signaling (Tcherkezian et al., 2021). Notably, one of the best characterized mRNAs that are asymmetrically translated in response to Netrin-1 signaling is that of β-*actin*, thereby providing the growth cone with blocks for rapid cytoskeletal remodeling, and directional steering toward the chemoattractant source (Leung et al., 2006, 2018).

Local mRNA translation in synapse formation and plasticity

Apart from its evident role in axon development, local protein synthesis is pivotal for synapses. Many studies have shown that the ability of synapses to synthesize proteins in response to specific local demands is necessary for the developing nerve terminal to sense and respond to extrinsic signals. Therefore, it is essential for synaptogenesis, synapse strengthening, and elimination, and even for relaying signals to the cell soma and influencing neuronal survival (Batista and Hengst, 2016). Notably, local translation has been found to be indispensable at both the pre- and post-synaptic sites (Agrawal and Welshhans, 2021). In the post-synaptic compartment, where polyribosomes were first visualized by electron microscopy (EM), a lot of work has been focused on the function of local mRNA translation, which appears as a highly dynamic modulator of the local proteome (Steward and Levy, 1982; Ostroff et al., 2012, 2018). A number of studies highlight a potential similar role of mRNA translation in the pre-synaptic compartment (Koenig, 1967; Autilio et al., 1968; Morgan and Austin, 1968; Koenig et al., 2000; Scarnati et al., 2018). Although initial EM studies were unable to detect ribosomes, or ribosomal RNA (Bartlett and Banker, 1984), recent work has revealed clusters of ribosomes associated with actin in mature axons, as well as a particularly diverse pool of pre-synaptic axonal and dendritic mRNAs (Koenig et al., 2000; Cajigas et al., 2012; Hafner et al., 2019).

A very-well studied signal that induces axon terminal branching and synaptogenesis is the Brain Derived Neurotrophic Factor (BDNF) (Wang et al., 2022). BDNF initiates local translation via activation of tropomyosin receptor kinase B (TrkB) receptors and mTOR signaling, as well as via stimulation of the group I metabotropic glutamate receptors (mGluRs) and ERK-MAPK signaling, regulating synapse formation, plasticity, and maintenance (Steward and Schuman, 2003; Schratt et al., 2004; Napoli et al., 2008). BDNF is secreted both pre- and post-synaptically and affects TrkB receptors

localized on both pre- and post-synaptic membranes (Gomes et al., 2006; Mohajerani et al., 2007; Song et al., 2017). Therefore, BDNF activates both pre- and post-synaptic pathways and elicits local protein synthesis and rapid effects on membrane excitability and synaptic transmission (Pradhan et al., 2019). At the pre-synaptic compartment, BDNF-induced activation of TrkB potentiates the release of neurotransmitters such as GABA and glutamate, via the TrkB-ERK pathway (Kang and Schuman, 1995; Levine et al., 1995; Kang et al., 1997; Jovanovic et al., 2000). Post-synaptically, BDNF-induced activation of TrkB generates fast dendritic calcium transients and induces several intracellular signaling pathways (Lang et al., 2007) that may further support structural changes, such as spine density increase and dendritic growth (Segal and Greenberg, 1996; Alonso et al., 2004; Mohajerani et al., 2007). Additional studies have demonstrated that BDNF can induce local synthesis of the transcription factors SMAD1/5/8 followed by their retrograde transport, providing an example of tight signal regulation and relay (Ji and Jaffrey, 2012). In the neuromuscular junction (NMJ) of *D. melanogaster*, a well-investigated invertebrate synaptic system, SMAD proteins are involved in synapse function both in pre- and in post-synaptic cells (Ueberham and Thomas, 2013).

Based on all of the aforementioned observations and a plethora of additional studies, it is unassailable that synaptic plasticity is greatly affected by the levels of local protein synthesis (Biever et al., 2019), and that activity-dependent local translation is essential for the formation and maintenance of long-term memories. For example, it was recently demonstrated that long-term plasticity of GABA release in established synapses requires local translation (Cioni et al., 2018). Concomitantly, an elegant study that perturbed synaptic translation by local depletion of mitochondrial energy compartments, uncovered severe impairment of spine morphological alterations, highlighting the necessity of both protein synthesis and mitochondria during plasticity in hippocampal neurons (Rangaraju et al., 2019).

The significance of local protein synthesis for synapse formation, function, and plasticity is further underlined by the fact that genetic alterations of the pathways that regulate local mRNA translation are associated with the emergence of synaptopathies, the clinical manifestations of which range from mild intellectual disabilities (ID) to autism spectrum disorders (ASD) and schizophrenia (SCZ) (Ehninger and Silva, 2009; De Rubeis et al., 2013). A common anatomical feature of synaptopathies is the dysgenesis of dendritic spines (Penzes et al., 2011; De Rubeis et al., 2013). For instance, Fragile X Syndrome is an inherited synaptopathy characterized by dendritic spine defects which result in neurodevelopmental delays and autistic-like phenotypes (Irwin et al., 2002; Jacquemont et al., 2007; De Rubeis et al., 2013). It is caused by loss of function of FMRP, an RNA-binding protein (RBP) that regulates local mRNA translation and degradation in neurons, and is responsible for the dendritic targeting of mRNAs (Dictenberg et al., 2008; De Rubeis et al., 2013). In addition, defective assembly of RNPs has been associated with the emergence of neurological diseases such as spinal muscular atrophy (SMA) and amyotrophic lateral sclerosis (ALS) (Sanchez et al., 2013; Mofatteh, 2020).

Local mRNA translation in axon regeneration

Increasing evidence indicates that axonal mRNA translation continues to play roles in mature axons, especially during plastic responses such as injury-induced axon regeneration (Verma et al., 2005; Jung et al., 2012; Kalinski et al., 2015). Interestingly, axonal regeneration following injury encompasses cellular processes that are very similar to physiological axon growth during development, namely axon elongation and the formation of a new growth cone, which is receptive to developmental cues that guide it toward its lost synaptic targets to restore connectivity (Verma et al., 2005; Giger et al., 2010). All these processes require local mRNA translation. And while mature axons of the peripheral nervous system (PNS) maintain the capacity for mRNA trafficking and translation, which is necessary for regeneration after injury, mature axons of the central nervous system (CNS) lose this intrinsic ability (Gumy et al., 2010). This is primarily because the transition from development to maturity in the CNS is marked by gene expression changes that favor synaptic functions and block growth, therefore limiting the capacity of axons for local translation (Jung et al., 2012). *In vitro* as well as *in vivo* studies have shown that the enhancement of protein synthesis in injured axons promotes regeneration, while on the other hand, axonal regeneration is attenuated when mRNA translation is blocked after injury (Verma et al., 2005; Christie et al., 2010; Donnelly et al., 2011; Saxton and Sabatini, 2017). These observations suggest that there is a strong correlation between local mRNA translation and the intrinsic ability of axons to regenerate.

Structure and functions of the neuronal cytoskeleton

As implied by its name, the main role of the cytoskeleton is not only to provide a structural scaffold, establishing and maintaining the mechanical properties, morphology, polarity, and integrity of neurons but also to contribute to neuronal plasticity (Kevenaar and Hoogenraad, 2015). It is an incredibly dynamic structure, undergoing rapid remodeling in order to meet emerging cellular needs in response to constant environmental stimuli and intrinsic homeostatic processes. Several key cellular and molecular events, including protrusion, motility, macromolecule, and organelle positioning, as well as vesicular trafficking, strongly depend on the cytoskeleton,

its dynamic flux and ability to serve as a signaling platform (Kim and Coulombe, 2010).

Major components of the neuronal cytoskeleton

The neuronal cytoskeleton is built up from three distinct but integrated fibrous polymers: MTs, F-actin, and neurofilaments. MTs are cylindrical polymers comprised of α- and β-tubulin heterodimers, actin filaments are polymers built up from globular actin (G-actin) and neurofilaments are a family of neuronal intermediate filaments (Kevenaar and Hoogenraad, 2015). F-actin and MTs can serve as rails for long- and short-range axonal transport and can influence axon growth and specification (Kevenaar and Hoogenraad, 2015). Neurofilaments are found mostly in axons and serve as regulators of their diameter and conductance (Yuan et al., 2017).

MTs are characterized by their highly dynamic nature, and their continuous growth and shrinkage constitute the main driving forces for rapid cytoskeletal remodeling (Kevenaar and Hoogenraad, 2015). The filaments can exist in a stable state, marked by PTMs, or they can be dynamically unstable, stochastically switching between polymerization and depolymerization (Mitchison and Kirschner, 1984; Janke, 2014). This is regulated by a wide array of factors, among which are the microtubule-associated proteins (MAPs), with various MAPs, such as MAP1B and Tau, influencing MT dynamics by inducing their stabilization (Drechsel et al., 1992; Tortosa et al., 2013; Derisbourg et al., 2015). One major characteristic of axonal MTs in particular is their unipolar organization, with their plus-end (fast-growing) oriented toward the axon tip and the minus-end (more stable) located in the opposite direction, toward the soma (Baas et al., 1988; Stepanova et al., 2003; Stone et al., 2008). Interestingly though, MTs are excluded from dendritic spines and can only be found in dendritic shafts with mixed orientation (Baas et al., 1988; Stone et al., 2008; Kapitein et al., 2010).

F-actin is another actively dynamic structure, rapidly switching between polymerization and depolymerization, due to the weak interaction forces of actin monomers. Actin monomers are added to the growing end of the protrusion, while actin subunits dissociate in the opposite end (Letourneau, 2009). They are also highly polarized due to the orientation of the actin monomers in the filament (Kevenaar and Hoogenraad, 2015). Many actin-binding proteins (ABPs) influence actin dynamics through different mechanisms, such as the promotion of polymerization/depolymerization of G-actin, as well as the crosslinking and anchoring of F-actin to other cellular components (Letourneau, 2009). Axonal actin is organized along the axon in ring-like structures, comprised of short actin filaments connected by spectrin tetramers and caped by adducin (Xu et al., 2013; Lukinavièius et al., 2014; D'Este et al., 2015). Concomitantly, the cytoskeleton of the dendritic spines is composed of a highly branched network of long- and short-branched actin filaments, connected by many ABPs (Nakahata and Yasuda, 2018). Rearrangements of the actin cytoskeleton, such as actin polymerization/depolymerization, branching, cross-linking, and trafficking, are regulated by multiple ABPs and small GTPase proteins and influence the formation, shape, motility, and stability of dendritic spines (Harvey et al., 2008; Murakoshi et al., 2011; Bosch et al., 2014; Hedrick et al., 2016).

The cytoskeleton during axon outgrowth and guidance

It has become clear that the cytoskeleton enacts a central role during neuronal development, acting as a signaling platform and generating intracellular forces which regulate the speed and direction of outgrowth (Tanaka and Sabry, 1995). Localized cyclic polymerization and depolymerization of F-actin, in combination with MTs stabilization, and chaperoning events like Kinesin1-mediated sliding of MTs contribute to the generation of the mechanical forces needed for the induction of neurite outgrowth (Flynn et al., 2012). The initial exploration stage is characterized by the rapid multidirectional extension and retraction of actin protrusions in response to microenvironmental cues (Tanaka and Sabry, 1995). In particular, in the growth cones that are the distal tips of growing axons, highly dynamic actin filaments that originate from a meshed actin network in the leading edge (lamellipodium), generate filopodial protrusions that serve as cellular antennae, sampling the microenvironment for numerous attractive and repellent extracellular signals (Kolodkin and Tessier-Lavigne, 2011). This plethora of external cues promotes the activation of intracellular cascades, which ultimately converge on the cytoskeleton and induce local rearrangements that contribute to the overall neuronal response and guidance toward the correct direction (Vitriol and Zheng, 2012). Following actin protrusions and signaling, the MTs explore the new growth cone intracellular environment, in order to stabilize the navigating axons and promote proper directionality (Pinto-Costa et al., 2020). Signal transduction in the growth cones depends on factors such as the Rho subfamily of Ras-related GTPases (Tanaka and Sabry, 1995), while numerous ABPs such as Cofilin 1 (Cfl1), Profilins, and Ena/VASP family members are essential for actin reorganization (Dent et al., 2011).

The cytoskeleton during synapse formation and plasticity

Upon reaching the appropriate synaptic target, axonal growth cones cease to explore the environment and axons

attenuate their growth, initiating the formation of branches and ultimately presynaptic sites, with crucial cytoskeletal rearrangements (Kevenaar and Hoogenraad, 2015). Specifically, NGF-mediated localized debundling of MTs promotes the formation of axon branches, whereas actin assembly contributes to the stabilization of the branch (Ketschek et al., 2015). Cytoskeletal rearrangements are also pivotal in dendritic spines, although the proper function of neuronal circuits strongly depends on the capacity of spines to remain in a stable state for long periods of time. Numerous studies point to the significance of dynamic molecular and subsequent structural reorganization of spines for circuit plasticity during learning (Grutzendler et al., 2002; Trachtenberg et al., 2002; Yang et al., 2009; Hayashi-Takagi et al., 2015; Li et al., 2017). Synaptic activity regulates dendritic spine morphology by influencing the reorganization of MTs and F-actin in both the developing and adult NS (Gordon-Weeks and Fournier, 2014). The balance between polymerization and depolymerization of actin networks is essential in synaptic plasticity, inducing activity-dependent structural alterations in dendritic spines (Hotulainen and Hoogenraad, 2010). On the other hand, MTs in the dendritic shafts also undergo rapid structural changes that are necessary for spine plasticity and maintenance of proper spine structure (Jaworski et al., 2009; Merriam et al., 2011, 2013). On top of their structural role though, both actin and microtubule filaments have been shown to be of utmost importance for the tethering and stabilization of dendritic mitochondrial compartments, which provide spines with the fuel required for synaptic local translation and plastic responses (Rangaraju et al., 2019).

The cytoskeleton during axon regeneration

Successful axon regeneration, following trauma induced by mechanical injury or a neurodegenerative disease, strongly relies on the capacity of the cytoskeleton for rapid and coordinated rearrangements (Kevenaar and Hoogenraad, 2015). One of the reasons why adult CNS axons fail to regenerate after injury is the inhibitory microenvironmental cues that ultimately suppress cytoskeletal reorganizations, required for axon regrowth (Gordon-Weeks and Fournier, 2014). Upon CNS injury, the retraction bulbs that are formed at the tips of the injured neurons are dystrophic and growth-incompetent, comprised of a severely disorganized cytoskeleton (Ertürk et al., 2007). Conversely, the bulbs that are formed at the tips of injured PNS neurons consist of a highly organized and appropriately bundled network of MTs and dynamic actin structures, which resemble a developmental growth cone and can promote axon regrowth and regeneration (Gordon-Weeks and Fournier, 2014). Inhibitory molecules converge upon the neuronal cytoskeleton by initiating intracellular signaling cascades that hinder axonal regrowth. The small GTPase RhoA, as well as its downstream effector Rho Kinase (ROCK), are central mediators of the actin cytoskeleton, regulating inhibitory signaling pathways that limit regeneration (Alabed et al., 2006; McKerracher and Higuchi, 2006). Various inhibitory ligands activate RhoA-mediated cascades, therefore blocking axonal repair. Several studies have indicated that RhoA or ROCK inhibition improves axonal regeneration by enhancing the *in vitro* and *in vivo* regrowth of injured CNS neurons on repellent substrates (Wahl et al., 2000; Dergham et al., 2002; Borisoff et al., 2003; Fournier et al., 2003; Yukawa et al., 2005; Alabed et al., 2006). Therefore, RhoA inhibitors display therapeutic potential and are currently used in clinical trials aiming to enhance axonal regeneration after spinal cord injury (Fehlings et al., 2011; Pinto-Costa et al., 2020).

The cytoskeleton in transport

Besides its crucial aforementioned roles, the cytoskeleton is an essential element for the active transport of a plethora of molecular cargoes along the significantly extended projections of neurons. Neuronal homeostasis, axonal polarization and outgrowth, synaptic function, and regeneration of axons after injury are all processes that rely on cytoskeleton-dependent transport. Conserved mechanisms of active motor protein-mediated transport are crucial for the proper distribution of various types of cargoes, such as axonal proteins, mRNAs, signaling molecules, vesicles, and organelles, at specific locations within the axons and dendrites (Broix et al., 2021). Three types of motor proteins mediate the cytoskeletal transport of the aforementioned cargoes: Myosins, kinesins, and dyneins. Kinesin is responsible for the anterograde long-range transport (from the soma to the synapse) of cargoes along the MTs, while dynein is involved in the retrograde long-range transport (from the synapse to the soma) (Hirokawa et al., 2010). In contrast to the previous motor proteins, myosin moves along the actin filaments of the cytoskeleton and facilitates short-range transport (Vale, 2003). Notably, dynein-dependent retrograde axonal transport is one of the first cellular processes activated after NS injury, in order for neurons to induce a regenerative response (Broix et al., 2021).

Coordination between local translation and cytoskeletal remodeling

It is more than evident that cytoskeletal dynamics are crucial for proper architecture, function, and regeneration of the NS, and indeed, numerous studies have linked cytoskeletal defects to the emergence of neurodevelopmental and neurodegenerative diseases (Kevenaar and Hoogenraad, 2015). Concomitantly, local protein synthesis is pivotal for neuronal homeostasis, with

an increasing number of studies unraveling its role during development, plasticity, and regeneration. The two processes are essentially interrelated and it has been recently demonstrated that cytoskeletally-tethered mitochondria exist in dendrites, as local energy booths that fuel local translation in synapses and potentially other neuronal compartments (Rangaraju et al., 2019). However, what remains poorly understood up to date, are the molecular mechanisms neurons utilize to co-regulate local protein synthesis and cytoskeletal remodeling, when rapidly responding to stimuli.

The CYFIP1 complexes

The FMRP-CYFIP1 ribonucleoprotein complex

One of the best-characterized mechanisms that coordinate cytoskeletal remodeling and local translation involves the FMRP-CYFIP1 RNP complex. The cytoplasmic fragile X mental retardation protein (FMRP) interacts with the Cytoplasmic FMRP Interacting Protein (CYFIP1), also known as Specific Rac1-Activated protein (SRA1), forming a heterodimer ribonucleoparticle that represses protein synthesis (Kobayashi et al., 1998; Schenck et al., 2001, 2003; Napoli et al., 2008). FMRP is an RBP implicated in mRNA translation, localization, and stability (Bagni and Greenough, 2005; Zalfa et al., 2007; Zhang et al., 2007). It is the encoded protein product of the X-linked fragile X mental retardation 1 (*fmr1*) gene. FMRP interacts with specific mRNA molecules by recognizing domains such as G quartets and/or U-rich sequences, or via small non-coding RNA adaptors and miRNAs (Napoli et al., 2008). It influences the dendritic targeting of mRNAs and regulates mRNA translation and decay in the neuronal soma and at synapses (Bassell and Warren, 2008; Dictenberg et al., 2008). The other crucial partner of the FMRP-CYFIP1 RNP complex is CYFIP1, a protein that regulates both cytoskeletal dynamics and protein translation. FMRP tethers specific mRNAs to CYFIP1, which in turn interacts and binds to the cap-binding eukaryotic initiation factor 4E (eIF4E) and inhibits the initiation of translation (Napoli et al., 2008; De Rubeis et al., 2013). Extracellular cues, like BDNF, and synaptic activity result in the release of CYFIP1 from eIF4E and from bound mRNAs, promoting the initiation of mRNA translation (Napoli et al., 2008). Protein synthesis can then begin after the eukaryotic initiation factor 4G (eIF4G) binds to eIF4E, promoting the recruitment of other initiation factors and ribosomal proteins (Santini et al., 2017). Several mRNAs have been identified to be translationally inhibited by the FMRP-CYFIP1 complex in the mammalian brain, including *map1b*, *camkII*, *arc,* and *app*. Indeed, the absence of any of the two, CYFIP1 or FMRP, has been associated with increased translation levels of the aforementioned mRNAs (Zhang et al., 2001; Zalfa et al., 2003; Lu et al., 2004; Hou et al., 2006; Westmark and Malter, 2007; Napoli et al., 2008). In dendrites and synapses, BDNF promotes the FMRP-CYFIP1-mediated translation of *arc/arg3.1* and *camkII* (Aakalu et al., 2001; Yin et al., 2002; Zalfa et al., 2003; Schratt et al., 2004; Napoli et al., 2008).

The CYFIP1-WRC complex

Besides the FMRP-CYFIP1-eIF4E complex, CYFIP1 has also been identified as part of the WAVE Regulatory Complex (WRC). WRC is implicated in actin polymerization by regulating the actin-nucleating activity of the Arp2/3 complex (Schenck et al., 2001; Kunda et al., 2003; Napoli et al., 2008; De Rubeis et al., 2013). It is a heteropentamer, containing WAVE1/2/3, ABI1/2, NCKAP1, and HPSC300, and can be activated through kinases and phospholipids, as well as through the small Rho GTPase Rac1, which induces a CYFIP1-mediated activation of WRC (Kobayashi et al., 1998; Eden et al., 2002; Takenawa and Suetsugu, 2007; Chen et al., 2010).

Both CYFIP1 complexes are crucial for proper synaptic function, since they establish a fine balance between cytoskeletal reorganization and mRNA translation. The incorporation of CYFIP1 in each complex relies on the capacity of CYFIP1 to undergo conformational changes. Specifically, a more globular CYFIP1 conformation is required for the assembly of the FMRP-CYFIP1-eIF4E complex, while a planar form is suitable for the recruitment of CYFIP1 to the WRC (Chen et al., 2010; De Rubeis et al., 2013). This conformational change of CYFIP1 is promoted by factors such as BDNF. BDNF administration results in a Rac1 signaling-mediated conformational transition of CYFIP1 from globular to planar (De Rubeis et al., 2013). This reduces the amount of CYFIP1 interacting with FMRP and, as a result, enhances protein synthesis of key regulators of synaptic plasticity, such as ARC (De Rubeis et al., 2013). Concomitantly, it increases the pool of CYFIP1 recruited on the WRC, promoting actin cytoskeleton rearrangements, necessary for proper spine morphology and function (De Rubeis et al., 2013).

Perturbations in the balance of these two CYFIP1 interconnected pathways are associated with spine dysmorphogenesis, a recurrent feature of several neuropsychiatric disorders (Penzes et al., 2011; De Rubeis et al., 2013). In particular, loss of function of FMRP causes the Fragile X Syndrome (FXS), a common inherited ID, also implicated in the emergence of ASD (Hatton et al., 2006; Jacquemont et al., 2007; Bassell and Warren, 2008). At the cellular level, FXS is characterized by deficient synaptic maturation, while patients with FXS display dendritic spine defects, autistic-like phenotypes, and neurodevelopmental delays (Irwin et al., 2002; Jacquemont et al., 2007). A model proposed by Napoli et al. (2008) suggests that in the absence of FMRP, there would be decreased binding of CYFIP1 to FMRP target mRNAs and subsequent alleviation of translational inhibition. This would result in abnormally high levels of proteins whose synthesis

undergoes FMRP regulation (Napoli et al., 2008). Since a wide array of mRNAs is regulated by FMRP, the simultaneous dysregulation of numerous proteins may contribute to the emergence of FXS (Brown et al., 2001; Miyashiro et al., 2003; Liao et al., 2008; Darnell et al., 2011; Klemmer et al., 2011).

cyfip1 is located at the 15q11.2 chromosomal locus, a hot-spot for ASD. Mutations that lead to downregulation of *cyfip1* mRNA levels have been associated with cognitive disabilities and ASD (Doornbos et al., 2009; van der Zwaag et al., 2010; Cooper et al., 2011; von der Lippe et al., 2011). In addition, downregulation of the *cyfip1* mRNA has been observed in a subgroup of FXS patients who display a Prader-Willi-like phenotype, severe ASD, and obsessive-compulsive behavior (Nowicki et al., 2007; De Rubeis et al., 2013). CYFIP1 has also been linked to SCZ (Tam et al., 2010; Zhao et al., 2013). Depletion of CYFIP1 negatively influences ARC synthesis and actin polymerization, severely affecting spine morphology (De Rubeis et al., 2013). Not only CYFIP1 but also a plethora of CYFIP1 interactors, among which NCKAP1 and eIF4E, are implicated in disorders with a broad range of clinical manifestations, such as ID, ASD, and SCZ (Nowicki et al., 2007; Doornbos et al., 2009; Neves-Pereira et al., 2009; Tam et al., 2010; Cooper et al., 2011; Zhao et al., 2013).

Genetic ablation of the WRC components is also associated with defective rearrangements of the actin cytoskeleton, which negatively influence dendritic spine homeostasis, morphology, and excitability (Grove et al., 2004; Wiens et al., 2005; Kim et al., 2006; Soderling et al., 2007). Regarding the potential therapeutic strategies for these synaptopathies, Santini et al. (2017) proposed an interesting viewpoint related to the treatment of FXS. Particularly, they showed that treating FXS mice with 4EGI-1, which blocks interactions between eIF4E and eIF4G that are required for protein synthesis, reverses defects in hippocampus-dependent memory and spine morphology (Santini et al., 2017). Since the aberrant increase in the levels of many proteins is associated with the emergence of FXS, the targeting of translation initiation factors may be a promising therapeutic plan.

The mena-ribonucleoprotein complex

Another important player involved in cytoskeletal dynamics and local translation is the Enabled/Vasodilator-Stimulated Phosphoprotein (Ena/VASP) family. Three Ena/VASP family members are found in vertebrates: Mena (Mammalian-Enabled), VASP (Vasodilator-Stimulated Phosphoprotein), and EVL (Ena-VASP like). The Ena/VASP proteins contain two conserved domains: the N-terminus EVH1 (Ena-VASP Homology 1) and the C-terminus EVH2. The EVH1 domain binds to proteins with FPPPP (FP4) repeats and is crucial for cellular localization (Bilancia et al., 2014; Harker et al., 2019). EVH2 is composed of an F-actin binding domain (FAB), a G-actin binding domain (GAB), and a C-terminal coiled-coil tetramerization domain (Bachmann et al., 1999; Walders-Harbeck et al., 2002). Between EVH1 and EVH2, there is a central poly-proline region that binds the monomer-binding protein profilin 1 (PFN1) (Ferron et al., 2007; Hansen and Mullins, 2010; Harker et al., 2019), which is necessary for both Arp2/3 and Ena/VASP function (Skruber et al., 2020). All Ena/VASP members display actin filament anti-capping and barbed-end elongation enhancement activity (Barzik et al., 2005; Hansen and Mullins, 2010; Breitsprecher et al., 2011; Winkelman et al., 2014; Havrylenko et al., 2015), which renders them crucial for lamellipodia-based motility and the assembly of filopodia (Grevengoed and Peifer, 2003; Gates et al., 2007; Kwiatkowski et al., 2007; Tucker et al., 2011; Havrylenko et al., 2015). At the initial stage of filopodia assembly, Ena/VASP proteins localize at the edge of the lamellipodia protrusions and facilitate the formation of straight, long actin filaments (Bear et al., 2002; Svitkina et al., 2003; Barzik et al., 2005; Applewhite et al., 2007; Bear and Gertler, 2009; Winkelman et al., 2014; Harker et al., 2019). Their localization at the tips of newly formed and mature filopodia promotes the subsequent assembly of fascin-bundled filaments of the same length (Svitkina et al., 2003; Winkelman et al., 2014; Harker et al., 2019). The capacity of Ena/VASP proteins to bind G-actin, F-actin, and profilin and, hence, deliver monomers from the actin-binding sites to the growing barbed ends of actin filaments, is crucial during these processes and enhances motility and protrusion (Chereau and Dominguez, 2006; Ferron et al., 2007; Hansen and Mullins, 2010; Breitsprecher et al., 2011).

Given their pivotal roles in actin-remodeling, Ena/VASP proteins are key players during cell movement and adhesion. Especially in the NS, numerous genetic studies have shown that the Ena/VASP family members are critical factors for neurulation, neuritogenesis, migration, axon guidance and branching, and synapse formation (Lanier et al., 1999; Lebrand et al., 2004; Menzies et al., 2004; Li et al., 2005; Dwivedy et al., 2007; Kwiatkowski et al., 2007; Lin et al., 2007; McConnell et al., 2016). Neurons deficient for Ena/VASP proteins fail to respond to axon guidance cues that elicit both local translation and actin reorganization in axons, such as Netrin and Slit (Lanier et al., 1999; Lebrand et al., 2004; Menzies et al., 2004; McConnell et al., 2016).

Regarding the role of the Ena/VASP family in local mRNA translation, recent findings point to a Mena-dependent regulation. Mena (ENAH), being an actin-regulatory protein, has been implicated in integrin-mediated signaling, cell motility, and adhesion in the developing and adult NS (Drees and Gertler, 2008; Gupton and Gertler, 2010; Gupton et al., 2012). A recent study by Vidaki et al. (2017) revealed an additional

role of Mena as a regulator of both steady-state and BDNF-induced local translation in axons. Mena was found to associate with multiple RBPs and is a main component of a novel RNP complex involved in localized mRNA translation in axons (Vidaki et al., 2017). This complex contains known regulators of translation, like HnrnpK, Pcbp1, and additional RBPs, as well as specific cytosolic mRNAs involved in NS development and function, such as *dyrk1a* (Vidaki et al., 2017). Notably, Dyrk1a is a dosage-sensitive, dual-specificity kinase important in neuronal development and implicated in the emergence of ASD, ID, Down syndrome, and Parkinson's disease (Tejedor and Hämmerle, 2011; O'Roak et al., 2012; Qian et al., 2013; Krumm et al., 2014; Coutadeur et al., 2015; Di Vona et al., 2015; van Bon et al., 2016). Although the localization, and thus axonal transport of *dyrk1a* mRNA is not affected in the absence of Mena, translation of the mRNA is Mena-dependent, and the study revealed a significant decrease in Dyrk1a protein levels, both locally in axons, and globally in Mena-null developing brains (Vidaki et al., 2017). HnrnpK and PCBP1 can form complexes that bind to the 3′-UTRs of target mRNAs, inhibiting the initiation of translation, therefore Mena could be required for the disassembly of the RNP and de-repression of translation (Gebauer and Hentze, 2004; Vidaki et al., 2017). This hypothesis, combined with the facts that both Mena and HnrnpK are implicated in synapse formation and plasticity and that Mena-deficient mice exhibit severe axon guidance defects, highlights the significance of Mena in NS formation and function. Mena's capability of binding to different growth cone receptors, and its dual role in regulating actin rearrangements and local proteins synthesis, could act as a balancing force between the two processes, coupling and coordinating them on spatiotemporal demand (Lanier et al., 1999; Giesemann et al., 2003; Li et al., 2005; Folci et al., 2014; McConnell et al., 2016; Vidaki et al., 2017).

The DCC cell-surface receptor

The DCC (Deleted in colorectal cancer) receptor is another example of a molecule that could coordinate local mRNA translation and cytoskeletal reorganization, downstream of Netrin-1 signaling. DCC is a ∼185 kD protein encoded by the *DCC* gene, which is located on chromosome 18q (Keino-Masu et al., 1996). It is a single-pass transmembrane receptor for the extracellular factor Netrin-1, facilitating important functions related to axonal and dendritic growth, guidance, and targeting during development (Keino-Masu et al., 1996; Fazeli et al., 1997; Parent et al., 2005; Tcherkezian et al., 2021). Its extracellular portion contains six fibronectin type III (FN1-FN6) domains and four immunoglobulin-like domains, whereas its intracellular part is comprised of three domains, P1, P2, and P3 (Kolodziej et al., 1996; Finci et al., 2017). DCC can be found in various neuronal populations, expressed across the lifespan of many species, including humans, but its levels decrease dramatically following the transition from embryonic life to adulthood (Manitt et al., 2011; Horn et al., 2013; Reyes et al., 2013; Torres-Berrio et al., 2020). This decrease is accompanied by a change in the role of DCC-mediated signaling, which henceforth is crucial for neuronal survival, and the organization and refinement of large neuronal circuits (Torres-Berrio et al., 2020). Netrin-1, a member of the laminin superfamily, is a secreted protein that binds to the FN4 and FN5 domains of DCC and promotes local protein synthesis and reorganization of the actin cytoskeleton (Torres-Berrio et al., 2020; Tcherkezian et al., 2021). Upon Netrin-1 binding, DCC serves as a platform for the assembly of a multicomponent complex, where numerous intracellular components associated with the translation initiation machinery are recruited (Torres-Berrio et al., 2020; Tcherkezian et al., 2021). Regulation of local translation is mediated by factors such as the Nck-1 adaptor protein and the ribosomal protein L5, which link DCC to the large and small ribosomal subunits (Tcherkezian et al., 2021). Nck-1 activates Src family kinases and Rho GTPases, enhancing the release of Ca^{2+} and initiating local translation and actin cytoskeleton rearrangements (Torres-Berrio et al., 2020). The cytoplasmic domain of DCC also interacts with eukaryotic initiation factors (eIFs) such as eIF4E, which facilitates the recruitment of mRNAs in the preinitiation translation complex, 80S ribosomes, ribosomal subunits 40S and 60S, and various signal transduction proteins implicated in translational control (Tcherkezian et al., 2021). In parallel, Netrin-1-binding to DCC activates PKA that leads to Ena/VASP-dependent actin polymerization, and initiates a signaling cascade that results in Wave-Arp2/3-dependent actin filament branching (Lebrand et al., 2004; Bouchard et al., 2008; Boyer and Gupton, 2018). Therefore, DCC poses as a compelling molecule that coordinates cytoskeletal remodeling and local mRNA translation downstream of Netrin-1, leading to tightly regulated neuronal responses.

Additional guidance receptors, like Robo2/3 that binds Slit2 and Nrp1 that binds Sema3A, elicit local translation during axon development, as well as cytoskeletal reorganization (Piper et al., 2006; Leung et al., 2013; Bellon et al., 2017; Russell and Bashaw, 2018). However, their mechanism of function is either indirect, or elusive, with respect to the immediate coordination of the two processes, and thus they will not be discussed further.

The APC-ribonucleoprotein complex

An additional molecular network that appears to co-regulate and interrelate local protein synthesis and MT filaments, is the APC-RNP complex. Adenomatus Polyposis Coli (APC) was

initially identified as a tumor suppressor, mutated in numerous human colon carcinomas and brain tumors (Powell et al., 1992; Sieber et al., 2002; Green and Kaplan, 2003; Kawasaki et al., 2003; Attard et al., 2007). Structurally, APC is a large scaffold protein with binding domains for several protein targets (Preitner et al., 2014). It is also an MT plus-end tracking protein (+ TIP), involved in the regulation of MT dynamics, playing important roles in cell polarity, adhesion, axon migration, and regulation of the cytoskeleteon (Shi et al., 2004; Watanabe et al., 2004; Etienne-Manneville et al., 2005; Kita et al., 2006; Koester et al., 2007; Purro et al., 2008). In migrating cells, APC has been observed at the ends of detyrosinated MTs (Glu-MTs), where it associates with a minority of MTs toward the leading edge of growing cellular protrusions, promoting MT assembly (Näthke et al., 1996; Mimori-Kiyosue et al., 2000; Wen et al., 2004; Mili et al., 2008).

Apart from regulating MT dynamics, APC associates with both mRNAs and RBPs and forms APC-RNPs involved in local mRNA translation (Mili et al., 2008; Preitner et al., 2014). A genome-wide study by Mili et al. (2008) in migrating fibroblasts revealed a function of APC in RNA localization, as well as a novel RNA anchoring mechanism. They specifically proposed that APC is a component of RNP complexes that contain localized RNAs, *pabp1* and *fmrp*, and is required for accumulation and anchoring of mRNA transcripts in pseudopodial protrusions (Mili et al., 2008). These transcripts are anchored in granules located at the plus ends of Glu-MTs via their 3′-UTRs (Mili et al., 2008). Another genome-wide study by Preitner et al. (2014) in native brain tissue identified APC as an RBP, which serves as a binding platform for a wide array of functionally related protein and mRNA targets. Among these molecular targets are β-*catenin*,β-*actin,* and *importin*-β, which are known to be locally translated in axons and in the leading edge of migrating cells, as well as β*2B-tubulin* (Hanz et al., 2003; Condeelis and Singer, 2005; Jones et al., 2008; Preitner et al., 2014). β2B-tubulin (Tubb2b) is a tubulin isotype implicated in cortical neuron migration and axon tract formation in humans (Jaglin et al., 2009; Cederquist et al., 2012; Romaniello et al., 2012; Preitner et al., 2014). Preitner et al. (2014) suggested a model where APC can induce MT polymerization partially by directing the local protein synthesis of β2B-tubulin in the periphery of MT growing ends. To do so, APC initally binds to the 3′-UTR of β*2B-tubulin* mRNA in order to facilitate its translocation to the dynamic MTs, located in the axonal growth cone's periphery (Preitner et al., 2014). Subsequently, APC acts as a positive regulator of local translation, promoting β2B-tubulin protein synthesis (Preitner et al., 2014). This axonal enrichment of β2B-tubulin protein at the periphery influences MT dynamics by promoting their further extension and thus contributing to the formation of the axonal growth cone's expanded structure (Preitner et al., 2014). APC functions have also been implicated in the canonical Wnt/β-catenin signaling pathway, which is known to regulate gene transcription (Rubinfeld et al., 1993; Zeng et al., 2005; Clevers and Nusse, 2012). In accordance with this fact, Preitner et al. (2014) showed that APC binds β-*catenin* mRNA, as well as the mRNAs of several other proteins involved in Wnt/β-catenin signaling, supporting the notion that APC might significantly influence this specific pathway. An additional study from Yasuda et al. (2013) further specifies the way APC mediates local translation. The group showed that Fus is a component of APC-RNPs that preferentially affects protein synthesis within cellular protrusions, and they specifically revealed that local protein synthesis from APC-RNPs can take place within cytoplasmic Fus granules (Yasuda et al., 2013).

In accordance with its roles in MT dynamics and translation, and therefore in numerous aspects of neuronal cell biology, disruption or loss of APC function has been associated with impaired polarization and cell migration, and has also been implicated in neurological disorders, such as SCZ and autism (Etienne-Manneville and Hall, 2003; Watanabe et al., 2004; Kroboth et al., 2007; Kalkman, 2012).

Zipcode binding protein

Zipcode binding protein (ZBP1) is an oncofetal protein that belongs to a family of highly conserved RBPs and is crucial for proper NS development (Nicastro et al., 2017). Three paralogs are found in vertebrates: IMP1/ZBP1, IMP2, and IMP3/VgRBP (Yisraeli, 2005). In neurons, ZBP1 and VgRBP are localized in growth cones and associate with β-*actin* transcripts (Zhang et al., 2001; Leung et al., 2006; Yao et al., 2006; Welshhans and Bassell, 2011). ZBP1 contains four hnRNP K-homology domains and two RNA recognition motifs (Nielsen et al., 1999; Yisraeli, 2005). Normally, ZBP1 is highly expressed in embryos, and reduced levels, or impaired protein function hinders embryonic development and results in a smaller cerebral cortex (Nishino et al., 2013). In developing neurons, ZBP1 regulates dendritic morphology, growth cone guidance, and axonal remodeling (Eom et al., 2003; Leung et al., 2006; Sasaki et al., 2010; Welshhans and Bassell, 2011; Medioni et al., 2014). To do so, ZBP1 interacts with a wide array of mRNAs (Jønson et al., 2007; Hansen and Mullins, 2010; Patel et al., 2012; Conway et al., 2016; Hafner et al., 2019). This interaction is required for translational regulation, transport, and maintenance of mRNAs, with the most-studied one being that of β-*actin* (Leeds et al., 1997; Hüttelmaier et al., 2005; Leung et al., 2006; Weidensdorfer et al., 2009; Conway et al., 2016). Despite the fact that ZBP1 does not directly associate with the cytoskeleton, its role in the precise localization and translation of β-actin renders it worth mentioning herein.

β-actin is a crucial factor during neuronal development, favoring actin polymerization, cellular remodeling, and migration (Jung et al., 2014; Nicastro et al., 2017). For

instance, in the growth cones of developing axons, local β-actin synthesis is essential in steering (Welshhans and Bassell, 2011). Localization of β-*actin* mRNA to subcellular sites of actin polymerization requires ZBP1 (Lawrence and Singer, 1986). ZBP1 binds to "zipcode," a conserved 54-nucleotide element in the 3′-UTR of the β-*actin* mRNA and facilitates its translocation to actin-rich protrusions, such as the developing neuronal growth cone (Farina et al., 2003; Hüttelmaier et al., 2005). A study of Hüttelmaier et al. (2005) in NG108-15 neuroblastoma cells describes the best characterized mechanism of ZBP1-regulated translation of the β-*actin* mRNA. In particular, they proposed that ZBP1 associates with the β-*actin* transcript through the assembly of a localized mRNA-protein complex in the nucleus. Subsequently, ZBP1 mediates transport of the β-*actin* mRNA to the cytoplasm in a translationally repressed state (Hüttelmaier et al., 2005). This ZBP1-mediated inhibition of translation prevents premature protein synthesis. Translation can then occur when the ZBP1-RNA complex reaches its destination at the cell edge. Once at the periphery of the cell and in response to extracellular cues, ZBP1 can be phosphorylated by the protein kinase Src in a key tyrosine residue necessary for ZBP1's RNA binding capacity (Hüttelmaier et al., 2005). This phosphorylation interferes with RNA binding and alleviates translational repression by decreasing ZBP1's affinity to β-*actin* mRNA. Consequently, the β-actin mRNA can then be released and translated. The local increase in β-actin protein levels favors actin polymerization, cellular remodeling, and migration (Jung et al., 2014; Nicastro et al., 2017).

Another study by Welshhans and Bassell (2011), in ZBP1 deficient (ZBP1-/-) cortical neurons, demonstrates a genetic requirement for ZBP1 in local translation of β-*actin* and axon guidance. Especially following stimulation with cues like Netrin-1 and BDNF that elicit local mRNA translation and cytoskeletal rearrangements, the axonal growth cones of ZBP1-/- neurons exhibit attenuated localization of β-*actin* transcripts, as well as impaired β-actin local protein synthesis (Welshhans and Bassell, 2011). Furthermore, both filopodial dynamics and axon guidance are impaired in ZBP1-/- cortical neurons (Welshhans and Bassell, 2011). This is not a surprising consequence of ZBP1's depletion (and subsequent β-actin translation impairment) since β-actin is mostly involved in filopodial dynamics (Suter and Forscher, 2000). Improper enrichment of β-actin protein in the growth cone is associated with impaired filopodial dynamics and axon guidance defects (Welshhans and Bassell, 2011).

Notably, ZBP1 has also been identified as a downstream mediator of non-canonical Sonic hedgehog (Shh) signaling during commissural axon guidance and providing the first link between Shh and growth cone cytoskeleton rearrangements (Lepelletier et al., 2017). Shh guides spinal cord commissural axons by attracting them toward the floorplate (Lepelletier et al., 2017). Local protein synthesis in response to Shh is the main driving force during this process. A study of Lepelletier et al. (2017) in rat commissural axons revealed that upon Shh stimulation, phospho-ZBP1 levels are increased in the growth cones. They also observed that Shh stimulation of axons that have been removed from the cell bodies results in increased β-actin protein levels in the growth cones (Lepelletier et al., 2017). On the other hand, depletion of ZBP1 *in vivo* results in commissural axon guidance defects (Lepelletier et al., 2017). Therefore, they suggest a model where stimulation of growth cones by Shh gradients induces ZBP1 phosphorylation and subsequent translation of its mRNA cargo, thereby allowing the growth cones to respond to Shh in a spatially defined manner (Lepelletier et al., 2017). Taking everything into account and considering the fact that ZBP1 can also bind to other mRNA molecules, such as the actin-related proteins (Arp) mRNAs which are involved in actin polymerization, ZBP1 seems to be a crucial factor for cytoskeleton dynamics by regulating local protein synthesis of specific cytoskeletal components and mediators (Jønson et al., 2007).

The Shot-Kra complex

A study by Lee et al. (2007) highlights a new mechanism of how local mRNA translation can be coupled with cytoskeletal reorganization in the commissural neurons of *Drosophila melanogaster*. Short stop (Shot) is a neuronally expressed protein that constitutes a member of the cytoskeleton-associated plakin family in *D. melanogaster* (Lee and Kolodziej, 2002). Shot binds to, cross-links, and organizes both MTs and F-actin, thereby linking cytoskeletal structures together (Lee and Kolodziej, 2002; Sonnenberg and Liem, 2007). Krasavietz (KRA; also known as Extra bases) on the other hand is a novel Shot interactor identified in *D. melanogaster* (Lee et al., 2007). It contains a W2 motif which is also found in eIF5 and eIF2Bε, two translation initiation factors that regulate the activity of the heterotrimeric GTP-binding protein eIF2 (Lee et al., 2007). In its GTP-bound form, eIF2 is required for the recruitment of the initiator tRNA to the small (40S) ribosomal subunit (Howe and Hershey, 1984; Gavrilova et al., 1987). eIF2Bε and eIF5 regulate the activity of eIF2 by mediating GDP-GTP exchange and GTP hydrolysis (Chakrabarti and Maitra, 1991; Huang et al., 1997; Gomez et al., 2002; Kershaw et al., 2021).

Lee et al. (2007) conducted genetic complementation assays in *D. melanogaster* to highlight the crucial roles of Shot and Kra in midline axon guidance, a process highly dependent on Slit signaling via the Robo receptor. Based on their proposed model, Shot could serve as a cytoskeleton-localized platform for

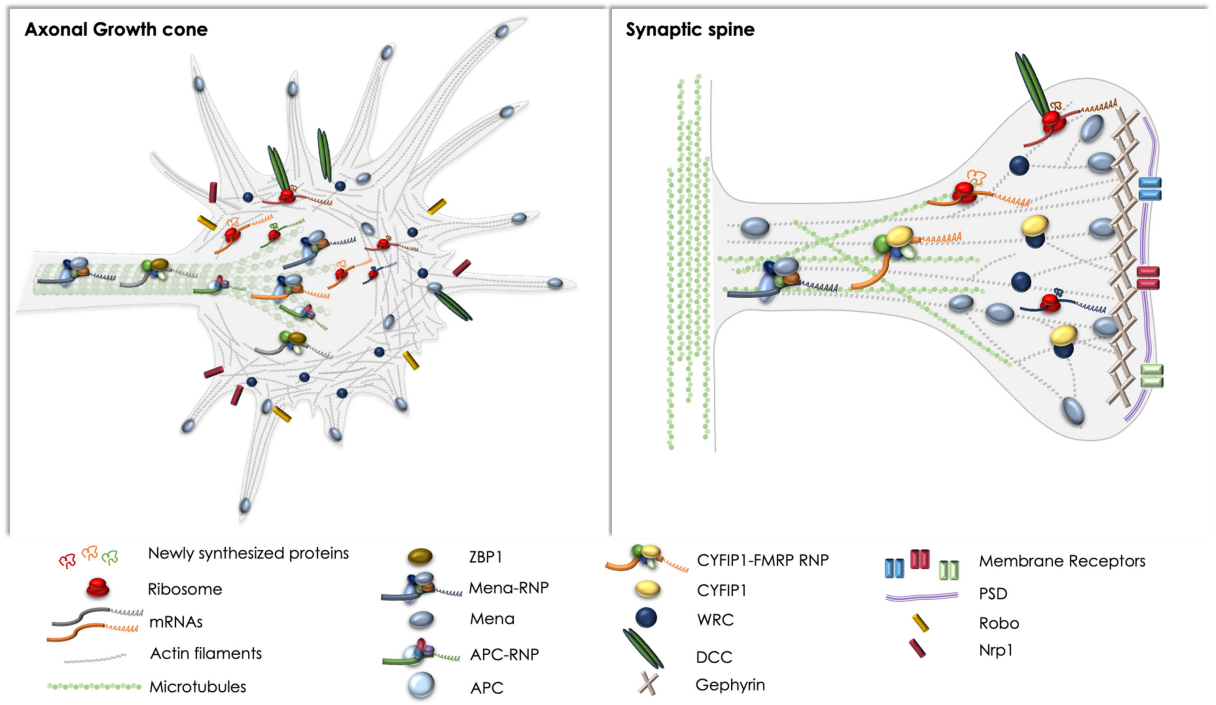

FIGURE 1
Schematic representation of the complexes discussed herein, with respect to basic components and spatial distribution in axonal growth cones (left) and synaptic spines (right). Note the regulatory complexes that have been reported and could potentially affect local protein synthesis and cytoskeletal rearrangements in both compartments, like the DCC receptor and the Mena-RNP. ZBP1 and the APC-RNP have been extensively studied in axons, whereas the CYFIP1-FMRP-RNP has been primarily examined in synapses. Potential crosstalk between the pathways remains elusive, although the direct or indirect association of receptors like DCC and Robo with Mena, or the WRC has been previously reported (Menzies et al., 2004; McConnell et al., 2016; Zou et al., 2018).

eIF2β and Kra, blocking eIF2β-mediated translation initiation in growth cones upon Slit-Robo repulsive signaling (Lee et al., 2007). They specifically found that Kra binds to the β-subunit of eIF2 through its W2 domain and associates with the growth cone cytoskeleton by physically interacting with Shot (Lee et al., 2007). *In vitro*, Kra inhibits global translation, suggesting a potential competition with eIF2Bε or eIF5 or both, for binding to eIF2β and blocking the initiation of translation by inhibiting the recruitment of the initiator tRNA to the 40S ribosomal subunit (Lee et al., 2007). Additionally, ectopic midline crossing defects due to loss of function mutations showed that eIF2β, as well as the W2 domain of Kra and the F-actin binding domain of Shot are crucial for proper midline axon guidance (Lee et al., 2007). Taken together, their study revealed that Slit-mediated midline repulsion requires the assembly of a functional, inhibitory, Shot-Kra-eIF2β translation complex that needs to be connected to the F-actin network to ensure proper function in the neuronal growth cone (Lee et al., 2007). Therefore, Shot can serve both as a cytoskeleton organizer and as a scaffold for translation regulators involved in midline axon guidance.

Although the Shot-Kra-eIF2β complex inhibits protein synthesis, it could have an alternative role in activating the translation of specific mRNAs. An interesting viewpoint regarding this potential additional function was described by Van Horck and Holt (2008). Based on the aforementioned model, Slit-induced repulsion would promote the translational activation of mRNAs that influence cytoskeletal disassembly, as well as the translational repression of mRNAs involved in cytoskeletal assembly. Thus, they hypothesized that the Shot-Kra-eIF2β complex could contribute to fine-tuning the balance between local mRNA translation repression and activation during midline axon guidance (Van Horck and Holt, 2008).

Interestingly, the mammalian homologs of Shot, namely, MACF1 and dystonin, are strongly expressed in the NS where they execute essential functions during development, as well as during maintenance/aging (Voelzmann et al., 2017). They interact with all cytoskeletal elements and affect important regulators of axonal MT, such as Tau and Map2. Although their function has not been studied with respect to mRNA translation, dystonin loss was reported to reduce levels of Tau and Map2 proteins, but not mRNAs, which could imply a potential role

in translational control, alongside with their well-characterized function in cytoskeletal organization (Voelzmann et al., 2017).

Concluding remarks

The highly polarized morphology and function of neurons is tightly bound to extremely complex, yet finely tuned intracellular processes, and precisely coordinated molecular mechanisms. Local mRNA translation, namely the ability of neurons to synthesize their proteins *in situ* and independently of the soma, is an astounding example of such sophisticated mechanisms. It enables remote axonal and dendritic subcellular compartments to remodel their proteome promptly and in response to local demand, allowing immediate responses to changes in the extracellular environment. It is not surprising therefore, that aberrant local translation in neuronal distal compartments has been correlated with numerous neurodevelopmental and neurodegenerative disorders, as well as the ability of axons to regenerate after injury. However, our current understanding of the mechanisms that regulate local mRNA translation is quite limited. On the other hand, the cytoskeleton is intrinsically linked to all aspects of NS development, maintenance, and function. Rapid rearrangements of cytoskeletal elements are required for neurons to be able to migrate, navigate their axons to synaptic targets, form and maintain synapses, and recover from traumatic injury. Therefore, it is not surprising that the regulation of the cytoskeleton has been extensively studied throughout the years, and numerous works have contributed to our understanding of filament formation, elongation, branching, and stability, as well as their implication to motility, guidance, synaptogenesis, and plasticity in the NS.

Given the innate connection of local mRNA translation and cytoskeletal reorganization, especially for prompt plastic responses to environmental stimuli, it is self-evident for neurons to retain common regulatory mechanisms for the sake of time and energy consumption. Yet, our current knowledge on those mechanisms and their coordination is very limited. A lot of effort has been put into uncovering specific mRNAs that are locally translated in different neuronal compartments, in an attempt to understand the molecular basis of axon development, synapse formation, and plasticity, as well as axonal response to injury. This has resulted in an extensive cataloging of transcripts that are specifically localized in subneuronal compartments, and are locally translated under different conditions. Notably, a large number of those transcripts encode cytoskeletal elements, like actin and tubulin, as well as cytoskeleton-associated proteins that bind to and stabilize cytoskeletal filaments. However, the proteins and protein complexes that regulate translation of those mRNAs in a precise spatiotemporal manner remain elusive, and so does our understanding of their crosstalk with the cytoskeleton. Herein, we have included protein complexes that appear to co-regulate mRNA translation and cytoskeletal remodeling, potentially connecting and balancing the two processes in the developing and adult NS (**Figure 1**). Nonetheless, a lot of research is still required, in order for us to fully apprehend the elegant means neurons possess to tune their molecular repertoires and intracellular procedures, in order to achieve prompt responses and precise function, both at the cellular and organismal level. Such knowledge could uncover novel therapeutic targets for neuronal disorders, and strategies based on the modulation of specific molecules with dual roles, tuning distinct processes toward the same outcome.

Author contributions

MV conceptualized the manuscript. NT and MV wrote and edited the manuscript. Both authors contributed to the article and approved the submitted version.

Funding

Research in MV lab was supported by grants from the Hellenic Foundation for Research and Innovation (HFRI #2343 to MV), the Stavros Niarchos Foundation (SNF & HFRI #01442 to MV), and Fondation Santé (to MV).

Acknowledgments

We thank A. Tatarakis for the comments on the manuscript.

Conflict of interest

The authors declare that the research was conducted in the absence of any commercial or financial relationships that could be construed as a potential conflict of interest.

Publisher's note

References

Aakalu, G., Smith, W. B., Nguyen, N., Jiang, C., and Schuman, E. M. (2001). Dynamic visualization of local protein synthesis in hippocampal neurons. *Neuron* 30, 489–502. doi: 10.1016/s0896-6273(01)00295-1

Agrawal, M., and Welshhans, K. (2021). Local translation across neural development: a focus on radial glial cells, axons, and synaptogenesis. *Front. Mol. Neurosci.* 14:717170. doi: 10.3389/fnmol.2021.717170

Alabed, Y. Z., Grados-Munro, E., Ferraro, G. B., Hsieh, S. H.-K., and Fournier, A. E. (2006). Neuronal responses to myelin are mediated by rho kinase. *J. Neurochem.* 96, 1616–1625. doi: 10.1111/j.1471-4159.2006.03670.x

Alonso, M., Medina, J. H., and Pozzo-Miller, L. (2004). ERK1/2 activation is necessary for BDNF to increase dendritic spine density in hippocampal CA1 pyramidal neurons. *Learn. Mem.* 11, 172–178. doi: 10.1101/lm.67804

Andreassi, C., Luisier, R., Crerar, H., Darsinou, M., Blokzijl-Franke, S., Lenn, T., et al. (2021). Cytoplasmic cleavage of IMPA1 3'UTR is necessary for maintaining axon integrity. *Cell Rep.* 34:108778. doi: 10.1016/j.celrep.2021.108778

Applewhite, D. A., Barzik, M., Kojima, S.-I., Svitkina, T. M., Gertler, F. B., and Borisy, G. G. (2007). Ena/VASP proteins have an anti-capping independent function in filopodia formation. *Mol. Biol. Cell* 18, 2579–2591. doi: 10.1091/mbc.e06-11-0990

Attard, T. M., Giglio, P., Koppula, S., Snyder, C., and Lynch, H. T. (2007). Brain tumors in individuals with familial adenomatous polyposis: a cancer registry experience and pooled case report analysis. *Cancer* 109, 761–766. doi: 10.1002/cncr.22475

Autilio, L. A., Appel, S. H., Pettis, P., and Gambetti, P. L. (1968). Biochemical studies of synapses *in vitro*. I. Protein synthesis. *Biochemistry* 7, 2615–2622. doi: 10.1021/bi00847a025

Baas, P. W., Deitch, J. S., Black, M. M., and Banker, G. A. (1988). Polarity orientation of microtubules in hippocampal neurons: uniformity in the axon and nonuniformity in the dendrite. *Proc. Natl. Acad. Sci. U.S.A.* 85, 8335–8339. doi: 10.1073/pnas.85.21.8335

Bachmann, C., Fischer, L., Walter, U., and Reinhard, M. (1999). The EVH2 domain of the vasodilator-stimulated phosphoprotein mediates tetramerization, F-actin binding, and actin bundle formation. *J. Biol. Chem.* 274, 23549–23557. doi: 10.1074/jbc.274.33.23549

Bagni, C., and Greenough, W. T. (2005). From mRNP trafficking to spine dysmorphogenesis: the roots of fragile X syndrome. *Nat. Rev. Neurosci.* 6, 376–387. doi: 10.1038/nrn1667

Barnes, A. P., and Polleux, F. (2009). Establishment of axon-dendrite polarity in developing neurons. *Annu. Rev. Neurosci.* 32, 347–381. doi: 10.1146/annurev.neuro.31.060407.125536

Bartlett, W. P., and Banker, G. A. (1984). An electron microscopic study of the development of axons and dendrites by hippocampal neurons in culture. II. Synaptic relationships. *J. Neurosci.* 4, 1954–1965. doi: 10.1523/JNEUROSCI.04-08-01954.1984

Barzik, M., Kotova, T. I., Higgs, H. N., Hazelwood, L., Hanein, D., Gertler, F. B., et al. (2005). Ena/VASP proteins enhance actin polymerization in the presence of barbed end capping proteins. *J. Biol. Chem.* 280, 28653–28662. doi: 10.1074/jbc.M503957200

Bassell, G. J., and Warren, S. T. (2008). Fragile X syndrome: loss of local mRNA regulation alters synaptic development and function. *Neuron* 60, 201–214. doi: 10.1016/j.neuron.2008.10.004

Batista, A. F. R., and Hengst, U. (2016). Intra-axonal protein synthesis in development and beyond. *Int. J. Dev. Neurosci.* 55, 140–149. doi: 10.1016/j.ijdevneu.2016.03.004

Bear, J. E., and Gertler, F. B. (2009). Ena/VASP: towards resolving a pointed controversy at the barbed end. *J. Cell Sci.* 122, 1947–1953. doi: 10.1242/jcs.038125

Bear, J. E., Svitkina, T. M., Krause, M., Schafer, D. A., Loureiro, J. J., Strasser, G. A., et al. (2002). Antagonism between Ena/VASP proteins and actin filament capping regulates fibroblast motility. *Cell* 109, 509–521. doi: 10.1016/s0092-8674(02)00731-6

Bellon, A., Iyer, A., Bridi, S., Lee, F. C. Y., Ovando-Vázquez, C., Corradi, E., et al. (2017). miR-182 regulates Slit2-mediated axon guidance by modulating the local translation of a specific mRNA. *Cell Rep.* 18, 1171–1186. doi: 10.1016/j.celrep.2016.12.093

Besse, F., and Ephrussi, A. (2008). Translational control of localized mRNAs: restricting protein synthesis in space and time. *Nat. Rev. Mol. Cell Biol.* 9, 971–980. doi: 10.1038/nrm2548

Biever, A., Donlin-Asp, P. G., and Schuman, E. M. (2019). Local translation in neuronal processes. *Curr. Opin. Neurobiol.* 57, 141–148. doi: 10.1016/j.conb.2019.02.008

Bilancia, C. G., Winkelman, J. D., Tsygankov, D., Nowotarski, S. H., Sees, J. A., Comber, K., et al. (2014). Enabled negatively regulates diaphanous-driven actin dynamics *in vitro* and *in vivo*. *Dev. Cell* 28, 394–408. doi: 10.1016/j.devcel.2014.01.015

Borisoff, J. F., Chan, C. C. M., Hiebert, G. W., Oschipok, L., Robertson, G. S., Zamboni, R., et al. (2003). Suppression of Rho-kinase activity promotes axonal growth on inhibitory CNS substrates. *Mol. Cell. Neurosci.* 22, 405–416. doi: 10.1016/s1044-7431(02)00032-5

Bosch, M., Castro, J., Saneyoshi, T., Matsuno, H., Sur, M., and Hayashi, Y. (2014). Structural and molecular remodeling of dendritic spine substructures during long-term potentiation. *Neuron* 82, 444–459. doi: 10.1016/j.neuron.2014.03.021

Bouchard, J.-F., Horn, K. E., Stroh, T., and Kennedy, T. E. (2008). Depolarization recruits DCC to the plasma membrane of embryonic cortical neurons and enhances axon extension in response to netrin-1. *J. Neurochem.* 107, 398–417. doi: 10.1111/j.1471-4159.2008.05609.x

Boyer, N. P., and Gupton, S. L. (2018). Revisiting Netrin-1: one who guides (Axons). *Front. Cell. Neurosci.* 12:221. doi: 10.3389/fncel.2018.00221

Breitsprecher, D., Kiesewetter, A. K., Linkner, J., Vinzenz, M., Stradal, T. E. B., Small, J. V., et al. (2011). Molecular mechanism of Ena/VASP-mediated actin-filament elongation. *EMBO J.* 30, 456–467. doi: 10.1038/emboj.2010.348

Broix, L., Turchetto, S., and Nguyen, L. (2021). Coordination between Transport and Local Translation in Neurons. *Trends Cell Biol.* 31, 372–386. doi: 10.1016/j.tcb.2021.01.001

Brown, V., Jin, P., Ceman, S., Darnell, J. C., O'Donnell, W. T., Tenenbaum, S. A., et al. (2001). Microarray identification of FMRP-associated brain mRNAs and altered mRNA translational profiles in fragile X syndrome. *Cell* 107, 477–487. doi: 10.1016/s0092-8674(01)00568-2

Buxbaum, A. R., Wu, B., and Signer, R. H. (2014). Single β-actin mRNA detection in neurons reveals a mechanism for regulating its translatability. *Science* 343, 419–422. doi: 10.1126/science.1242939

Cajigas, I. J., Tushev, G., Will, T. J., tom Dieck, S., Fuerst, N., and Schuman, E. M. (2012). The local transcriptome in the synaptic neuropil revealed by deep sequencing and high-resolution imaging. *Neuron* 74, 453–466. doi: 10.1016/j.neuron.2012.02.036

Cederquist, G. Y., Luchniak, A., Tischfield, M. A., Peeva, M., Song, Y., Menezes, M. P., et al. (2012). An inherited TUBB2B mutation alters a kinesin-binding site and causes polymicrogyria, CFEOM and axon dysinnervation. *Hum. Mol. Genet.* 21, 5484–5499. doi: 10.1093/hmg/dds393

Chakrabarti, A., and Maitra, U. (1991). Function of eukaryotic initiation factor 5 in the formation of an 80 S ribosomal polypeptide chain initiation complex. *J. Biol. Chem.* 266, 14039–14045.

Chen, Z., Borek, D., Padrick, S. B., Gomez, T. S., Metlagel, Z., Ismail, A. M., et al. (2010). Structure and control of the actin regulatory WAVE complex. *Nature* 468, 533–538. doi: 10.1038/nature09623

Chereau, D., and Dominguez, R. (2006). Understanding the role of the G-actin-binding domain of Ena/VASP in actin assembly. *J. Struct. Biol.* 155, 195–201. doi: 10.1016/j.jsb.2006.01.012

Christie, K. J., Webber, C. A., Martinez, J. A., Singh, B., and Zochodne, D. W. (2010). PTEN inhibition to facilitate intrinsic regenerative outgrowth of adult peripheral axons. *J. Neurosci.* 30, 9306–9315. doi: 10.1523/JNEUROSCI.6271-09.2010

Cioni, J.-M., Koppers, M., and Holt, C. E. (2018). Molecular control of local translation in axon development and maintenance. *Curr. Opin. Neurobiol.* 51, 86–94. doi: 10.1016/j.conb.2018.02.025

Cioni, J.-M., Lin, J. Q., Holtermann, A. V., Koppers, M., Jakobs, M. A. H., Azizi, A., et al. (2019). Late endosomes act as mRNA translation platforms and sustain mitochondria in axons. *Cell* 176, 56–72.e15 doi: 10.1016/j.cell.2018.11.030

Clevers, H., and Nusse, R. (2012). Wnt/β-catenin signaling and disease. *Cell* 149, 1192–1205. doi: 10.1016/j.cell.2012.05.012

Condeelis, J., and Singer, R. H. (2005). How and why does beta-actin mRNA target? *Biol. Cell* 97, 97–110. doi: 10.1042/BC20040063

Conway, A. E., Van Nostrand, E. L., Pratt, G. A., Aigner, S., Wilbert, M. L., Sundararaman, B., et al. (2016). Enhanced CLIP uncovers IMP Protein-RNA targets in human pluripotent stem cells important for cell adhesion and survival. *Cell Rep.* 15, 666–679. doi: 10.1016/j.celrep.2016.03.052

Cooper, G. M., Coe, B. P., Girirajan, S., Rosenfeld, J. A., Vu, T. H., Baker, C., et al. (2011). A copy number variation morbidity map of developmental delay. *Nat. Genet.* 43, 838–846. doi: 10.1038/ng.909

Coutadeur, S., Benyamine, H., Delalonde, L., de Oliveira, C., Leblond, B., Foucourt, A., et al. (2015). A novel DYRK1A (dual specificity tyrosine phosphorylation-regulated kinase 1A) inhibitor for the treatment of Alzheimer's disease: effect on Tau and amyloid pathologies *in vitro*. *J. Neurochem.* 133, 440–451. doi: 10.1111/jnc.13018

Darnell, J. C., Van Driesche, S. J., Zhang, C., Hung, K. Y. S., Mele, A., Fraser, C. E., et al. (2011). FMRP stalls ribosomal translocation on mRNAs linked to synaptic function and autism. *Cell* 146, 247–261. doi: 10.1016/j.cell.2011.06.013

De Rubeis, S., Pasciuto, E., Li, K. W., Fernández, E., Di Marino, D., Buzzi, A., et al. (2013). CYFIP1 coordinates mRNA translation and cytoskeleton remodeling to ensure proper dendritic spine formation. *Neuron* 79, 1169–1182. doi: 10.1016/j.neuron.2013.06.039

Dent, E. W., Gupton, S. L., and Gertler, F. B. (2011). The growth cone cytoskeleton in axon outgrowth and guidance. *Cold Spring Harb. Perspect. Biol.* 3:a001800. doi: 10.1101/cshperspect.a001800

Dergham, P., Ellezam, B., Essagian, C., Avedissian, H., Lubell, W. D., and McKerracher, L. (2002). Rho signaling pathway targeted to promote spinal cord repair. *J. Neurosci.* 22, 6570–6577.

Derisbourg, M., Leghay, C., Chiappetta, G., Fernandez-Gomez, F.-J., Laurent, C., Demeyer, D., et al. (2015). Role of the Tau N-terminal region in microtubule stabilization revealed by new endogenous truncated forms. *Sci. Rep.* 5:9659. doi: 10.1038/srep09659

D'Este, E., Kamin, D., Göttfert, F., El-Hady, A., and Hell, S. W. (2015). STED nanoscopy reveals the ubiquity of subcortical cytoskeleton periodicity in living neurons. *Cell Rep.* 10, 1246–1251. doi: 10.1016/j.celrep.2015.02.007

Di Vona, C., Bezdan, D., Islam, A. B. M. M. K., Salichs, E., López-Bigas, N., Ossowski, S., et al. (2015). Chromatin-wide profiling of DYRK1A reveals a role as a gene-specific RNA polymerase II CTD kinase. *Mol. Cell* 57, 506–520. doi: 10.1016/j.molcel.2014.12.026

Dickson, B. J. (2002). Molecular mechanisms of axon guidance. *Science* 298, 1959–1964. doi: 10.1126/science.1072165

Dictenberg, J. B., Swanger, S. A., Antar, L. N., Singer, R. H., and Bassell, G. J. (2008). A direct role for FMRP in activity-dependent dendritic mRNA transport links filopodial-spine morphogenesis to fragile X syndrome. *Dev. Cell* 14, 926–939. doi: 10.1016/j.devcel.2008.04.003

Donnelly, C. J., Willis, D. E., Xu, M., Tep, C., Jiang, C., Yoo, S., et al. (2011). Limited availability of ZBP1 restricts axonal mRNA localization and nerve regeneration capacity. *EMBO J.* 30, 4665–4677. doi: 10.1038/emboj.2011.347

Doornbos, M., Sikkema-Raddatz, B., Ruijvenkamp, C. A. L., Dijkhuizen, T., Bijlsma, E. K., and Gijsbers, A. C. J. (2009). Nine patients with a microdeletion 15q11.2 between breakpoints 1 and 2 of the Prader-Willi critical region, possibly associated with behavioural disturbances. *Eur. J. Med. Genet.* 52, 108–115. doi: 10.1016/j.ejmg.2009.03.010

Drechsel, D. N., Hyman, A. A., Cobb, M. H., and Kirschner, M. W. (1992). Modulation of the dynamic instability of tubulin assembly by the microtubule-associated protein tau. *Mol. Biol. Cell* 3, 1141–1154. doi: 10.1091/mbc.3.10.1141

Drees, F., and Gertler, F. B. (2008). Ena/VASP: proteins at the tip of the nervous system. *Curr. Opin. Neurobiol.* 18, 53–59. doi: 10.1016/j.conb.2008.05.007

Dwivedy, A., Gertler, F. B., Miller, J., Holt, C. E., and Lebrand, C. (2007). Ena/VASP function in retinal axons is required for terminal arborization but not pathway navigation. *Development* 134, 2137–2146. doi: 10.1242/dev.002345

Eden, S., Rohatgi, R., Podtelejnikov, A. V., Mann, M., and Kirschner, M. W. (2002). Mechanism of regulation of WAVE1-induced actin nucleation by Rac1 and Nck. *Nature* 418, 790–793. doi: 10.1038/nature00859

Ehninger, D., and Silva, A. J. (2009). Genetics and neuropsychiatric disorders: treatment during adulthood. *Nat. Med.* 15, 849–850. doi: 10.1038/nm0809-849

Eom, T., Antar, L. N., Singer, R. H., and Bassell, G. J. (2003). Localization of a beta-actin messenger ribonucleoprotein complex with zipcode-binding protein modulates the density of dendritic filopodia and filopodial synapses. *J. Neurosci.* 23, 10433–10444. doi: 10.1523/JNEUROSCI.23-32-10433.2003

Erskine, L., and Herrera, E. (2007). The retinal ganglion cell axon's journey: insights into molecular mechanisms of axon guidance. *Dev. Biol.* 308, 1–14. doi: 10.1016/j.ydbio.2007.05.013

Ertürk, A., Hellal, F., Enes, J., and Bradke, F. (2007). Disorganized microtubules underlie the formation of retraction bulbs and the failure of axonal regeneration. *J. Neurosci.* 27, 9169–9180. doi: 10.1523/JNEUROSCI.0612-07.2007

Etienne-Manneville, S., and Hall, A. (2003). Cdc42 regulates GSK-3beta and adenomatous polyposis coli to control cell polarity. *Nature* 421, 753–756. doi: 10.1038/nature01423

Etienne-Manneville, S., Manneville, J.-B., Nicholls, S., Ferenczi, M. A., and Hall, A. (2005). Cdc42 and Par6-PKCzeta regulate the spatially localized association of Dlg1 and APC to control cell polarization. *J. Cell Biol.* 170, 895–901. doi: 10.1083/jcb.200412172

Farina, K. L., Huttelmaier, S., Musunuru, K., Darnell, R., and Singer, R. H. (2003). Two ZBP1 KH domains facilitate beta-actin mRNA localization, granule formation, and cytoskeletal attachment. *J. Cell Biol.* 160, 77–87. doi: 10.1083/jcb.200206003

Fazeli, A., Dickinson, S. L., Hermiston, M. L., Tighe, R. V., Steen, R. G., Small, C. G., et al. (1997). Phenotype of mice lacking functional Deleted in colorectal cancer (Dcc) gene. *Nature* 386, 796–804. doi: 10.1038/386796a0

Fehlings, M. G., Theodore, N., Harrop, J., Maurais, G., Kuntz, C., Shaffrey, C. I., et al. (2011). A phase I/IIa clinical trial of a recombinant Rho protein antagonist in acute spinal cord injury. *J. Neurotrauma* 28, 787–796. doi: 10.1089/neu.2011.1765

Ferron, F., Rebowski, G., Lee, S. H., and Dominguez, R. (2007). Structural basis for the recruitment of profilin-actin complexes during filament elongation by Ena/VASP. *EMBO J.* 26, 4597–4606. doi: 10.1038/sj.emboj.7601874

Finci, L. I., Zhang, J., Sun, X., Smock, R. G., Meijers, R., Zhang, Y., et al. (2017). Structure of unliganded membrane-proximal domains FN4-FN5-FN6 of DCC. *Protein Cell* 8, 701–705. doi: 10.1007/s13238-017-0439-x

Flynn, K. C., Hellal, F., Neukirchen, D., Jacob, S., Tahirovic, S., Dupraz, S., et al. (2012). ADF/cofilin-mediated actin retrograde flow directs neurite formation in the developing brain. *Neuron* 76, 1091–1107. doi: 10.1016/j.neuron.2012.09.038

Folci, A., Mapelli, L., Sassone, J., Prestori, F., D'Angelo, E., Bassani, S., et al. (2014). Loss of hnRNP K impairs synaptic plasticity in hippocampal neurons. *J. Neurosci.* 34, 9088–9095. doi: 10.1523/JNEUROSCI.0303-14.2014

Forrest, K. M., and Gavis, E. R. (2003). Live imaging of endogenous RNA reveals a diffusion and entrapment mechanism for nanos mRNA localization in *Drosophila*. *Curr. Biol.* 13, 1159–1168. doi: 10.1016/s0960-9822(03)00451-2

Fournier, A. E., Takizawa, B. T., and Strittmatter, S. M. (2003). Rho kinase inhibition enhances axonal regeneration in the injured CNS. *J. Neurosci.* 23, 1416–1423.

Gasparski, A. N., Mason, D. E., Moissoglu, K., and Mili, S. (2022). Regulation and outcomes of localized RNA translation. *Wiley Interdiscip. Rev. RNA*. [Epub ahead of print]. doi: 10.1002/wrna.1721

Gates, J., Mahaffey, J. P., Rogers, S. L., Emerson, M., Rogers, E. M., Sottile, S. L., et al. (2007). Enabled plays key roles in embryonic epithelial morphogenesis in *Drosophila*. *Development* 134, 2027–2039. doi: 10.1242/dev.02849

Gavrilova, L. P., Rutkevitch, N. M., Gelfand, V. I., Motuz, L. P., Stahl, J., Bommer, U. A., et al. (1987). Immunofluorescent localization of protein synthesis components in mouse embryo fibroblasts. *Cell Biol. Int. Rep.* 11, 745–753. doi: 10.1016/0309-1651(87)90134-2

Gebauer, F., and Hentze, M. W. (2004). Molecular mechanisms of translational control. *Nat. Rev. Mol. Cell Biol.* 5, 827–835. doi: 10.1038/nrm1488

Giesemann, T., Schwarz, G., Nawrotzki, R., Berhörster, K., Rothkegel, M., Schlüter, K., et al. (2003). Complex formation between the postsynaptic scaffolding protein gephyrin, profilin, and Mena: a possible link to the microfilament system. *J. Neurosci.* 23, 8330–8339. doi: 10.1523/JNEUROSCI.23-23-08330.2003

Giger, R. J., Hollis, E. R., and Tuszynski, M. H. (2010). Guidance molecules in axon regeneration. *Cold Spring Harb. Perspect. Biol.* 2:a001867. doi: 10.1101/cshperspect.a001867

Gkogkas, C. G., Khoutorsky, A., Ran, I., Rampakakis, E., Nevarko, T., Weatherill, D. B., et al. (2013). Autism-related deficits via dysregulated eIF4E-dependent translational control. *Nature* 493, 371–377. doi: 10.1038/nature11628

Glock, C., Biever, A., Tushev, G., Nassim-Assir, B., Kao, A., Bartnik, I., et al. (2021). The translatome of neuronal cell bodies, dendrites, and axons. *Proc. Natl. Acad. Sci. U.S.A.* 118:e2113929118. doi: 10.1073/pnas.2113929118

Gomes, R. A., Hampton, C., El-Sabeawy, F., Sabo, S. L., and McAllister, A. K. (2006). The dynamic distribution of TrkB receptors before, during, and after synapse formation between cortical neurons. *J. Neurosci.* 26, 11487–11500. doi: 10.1523/JNEUROSCI.2364-06.2006

Gomez, E., Mohammad, S. S., and Pavitt, G. D. (2002). Characterization of the minimal catalytic domain within eIF2B: the guanine-nucleotide exchange factor for translation initiation. *EMBO J.* 21, 5292–5301. doi: 10.1093/emboj/cdf515

Gordon-Weeks, P. R., and Fournier, A. E. (2014). Neuronal cytoskeleton in synaptic plasticity and regeneration. *J. Neurochem.* 129, 206–212. doi: 10.1111/jnc.12502

Grantham, J., Ruddock, L. W., Roobol, A., and Carden, M. J. (2002). Eukaryotic chaperonin containing T-complex polypeptide 1 interacts with filamentous actin and reduces the initial rate of actin polymerization *in vitro*. *Cell Stress Chaperones* 7, 235–242. doi: 10.1379/1466-1268(2002)007<0235:ecctcp>2.0.co;2

Green, R. A., and Kaplan, K. B. (2003). Chromosome instability in colorectal tumor cells is associated with defects in microtubule plus-end attachments caused by a dominant mutation in APC. *J. Cell Biol.* 163, 949–961. doi: 10.1083/jcb.200307070

Grevengoed, E. E., and Peifer, M. (2003). Cytoskeletal connections: building strong cells in new ways. *Curr. Biol.* 13, R568–R570. doi: 10.1016/s0960-9822(03)00476-7

Grove, M., Demyanenko, G., Echarri, A., Zipfel, P. A., Quiroz, M. E., Rodriguiz, R. M., et al. (2004). ABI2-deficient mice exhibit defective cell migration, aberrant dendritic spine morphogenesis, and deficits in learning and memory. *Mol. Cell. Biol.* 24, 10905–10922. doi: 10.1128/MCB.24.24.10905-10922.2004

Grutzendler, J., Kasthuri, N., and Gan, W.-B. (2002). Long-term dendritic spine stability in the adult cortex. *Nature* 420, 812–816. doi: 10.1038/nature01276

Gumy, L. F., Tan, C. L., and Fawcett, J. W. (2010). The role of local protein synthesis and degradation in axon regeneration. *Exp. Neurol.* 223, 28–37. doi: 10.1016/j.expneurol.2009.06.004

Gupton, S. L., and Gertler, F. B. (2010). Integrin signaling switches the cytoskeletal and exocytic machinery that drives neuritogenesis. *Dev. Cell* 18, 725–736. doi: 10.1016/j.devcel.2010.02.017

Gupton, S. L., Riquelme, D., Hughes-Alford, S. K., Tadros, J., Rudina, S. S., Hynes, R. O., et al. (2012). Mena binds α5 integrin directly and modulates α5β1 function. *J. Cell Biol.* 198, 657–676. doi: 10.1083/jcb.201202079

Hafner, A.-S., Donlin-Asp, P. G., Leitch, B., Herzog, E., and Schuman, E. M. (2019). Local protein synthesis is a ubiquitous feature of neuronal pre- and postsynaptic compartments. *Science* 364:eaau3644. doi: 10.1126/science.aau3644

Hansen, S. D., and Mullins, R. D. (2010). VASP is a processive actin polymerase that requires monomeric actin for barbed end association. *J. Cell Biol.* 191, 571–584. doi: 10.1083/jcb.201003014

Hanz, S., Perlson, E., Willis, D., Zheng, J.-Q., Massarwa, R., Huerta, J. J., et al. (2003). Axoplasmic importins enable retrograde injury signaling in lesioned nerve. *Neuron* 40, 1095–1104. doi: 10.1016/s0896-6273(03)00770-0

Harker, A. J., Katkar, H. H., Bidone, T. C., Aydin, F., Voth, G. A., Applewhite, D. A., et al. (2019). Ena/VASP processive elongation is modulated by avidity on actin filaments bundled by the filopodia cross-linker fascin. *Mol. Biol. Cell* 30, 851–862. doi: 10.1091/mbc.E18-08-0500

Harris, W. A., Holt, C. E., and Bonhoeffer, F. (1987). Retinal axons with and without their somata, growing to and arborizing in the tectum of Xenopus embryos: a time-lapse video study of single fibres *in vivo*. *Development* 101, 123–133. doi: 10.1242/dev.101.1.123

Harvey, C. D., Yasuda, R., Zhong, H., and Svoboda, K. (2008). The spread of Ras activity triggered by activation of a single dendritic spine. *Science* 321, 136–140. doi: 10.1126/science.1159675

Hatton, D. D., Sideris, J., Skinner, M., Mankowski, J., Bailey, D. B., Roberts, J., et al. (2006). Autistic behavior in children with fragile X syndrome: prevalence, stability, and the impact of FMRP. *Am. J. Med. Genet. A* 140A, 1804–1813. doi: 10.1002/ajmg.a.31286

Havrylenko, S., Noguera, P., Abou-Ghali, M., Manzi, J., Faqir, F., Lamora, A., et al. (2015). WAVE binds Ena/VASP for enhanced Arp2/3 complex-based actin assembly. *Mol. Biol. Cell* 26, 55–65. doi: 10.1091/mbc.E14-07-1200

Hayashi-Takagi, A., Yagishita, S., Nakamura, M., Shirai, F., Wu, Y. I., Loshbaugh, A. L., et al. (2015). Labelling and optical erasure of synaptic memory traces in the motor cortex. *Nature* 525, 333–338. doi: 10.1038/nature15257

Hedrick, N. G., Harward, S. C., Hall, C. E., Murakoshi, H., McNamara, J. O., and Yasuda, R. (2016). Rho GTPase complementation underlies BDNF-dependent homo- and heterosynaptic plasticity. *Nature* 538, 104–108. doi: 10.1038/nature19784

Hirokawa, N., Niwa, S., and Tanaka, Y. (2010). Molecular motors in neurons: transport mechanisms and roles in brain function, development, and disease. *Neuron* 68, 610–638. doi: 10.1016/j.neuron.2010.09.039

Holt, C. E., and Schuman, E. M. (2013). The central dogma decentralized: new perspectives on RNA function and local translation in neurons. *Neuron* 80, 648–657. doi: 10.1016/j.neuron.2013.10.036

Horn, K. E., Glasgow, S. D., Gobert, D., Bull, S.-J., Luk, T., Girgis, J., et al. (2013). DCC expression by neurons regulates synaptic plasticity in the adult brain. *Cell Rep.* 3, 173–185. doi: 10.1016/j.celrep.2012.12.005

Hotulainen, P., and Hoogenraad, C. C. (2010). Actin in dendritic spines: connecting dynamics to function. *J. Cell Biol.* 189, 619–629. doi: 10.1083/jcb.201003008

Hou, L., Antion, M. D., Hu, D., Spencer, C. M., Paylor, R., and Klann, E. (2006). Dynamic translational and proteasomal regulation of fragile X mental retardation protein controls mGluR-dependent long-term depression. *Neuron* 51, 441–454. doi: 10.1016/j.neuron.2006.07.005

Howe, J. G., and Hershey, J. W. (1984). Translational initiation factor and ribosome association with the cytoskeletal framework fraction from HeLa cells. *Cell* 37, 85–93. doi: 10.1016/0092-8674(84)90303-9

Huang, H. K., Yoon, H., Hannig, E. M., and Donahue, T. F. (1997). GTP hydrolysis controls stringent selection of the AUG start codon during translation initiation in Saccharomyces cerevisiae. *Genes Dev.* 11, 2396–2413. doi: 10.1101/gad.11.18.2396

Hüttelmaier, S., Zenklusen, D., Lederer, M., Dictenberg, J., Lorenz, M., Meng, X., et al. (2005). Spatial regulation of beta-actin translation by Src-dependent phosphorylation of ZBP1. *Nature* 438, 512–515. doi: 10.1038/nature04115

Irwin, S. A., Idupulapati, M., Gilbert, M. E., Harris, J. B., Chakravarti, A. B., Rogers, E. J., et al. (2002). Dendritic spine and dendritic field characteristics of layer V pyramidal neurons in the visual cortex of fragile-X knockout mice. *Am. J. Med. Genet.* 111, 140–146. doi: 10.1002/ajmg.10500

Jacquemont, S., Hagerman, R. J., Hagerman, P. J., and Leehey, M. A. (2007). Fragile-X syndrome and fragile X-associated tremor/ataxia syndrome: two faces of FMR1. *Lancet Neurol.* 6, 45–55. doi: 10.1016/S1474-4422(06)70676-7

Jaglin, X. H., Poirier, K., Saillour, Y., Buhler, E., Tian, G., Bahi-Buisson, N., et al. (2009). Mutations in the beta-tubulin gene TUBB2B result in asymmetrical polymicrogyria. *Nat. Genet.* 41, 746–752. doi: 10.1038/ng.380

Janke, C. (2014). The tubulin code: molecular components, readout mechanisms, and functions. *J. Cell Biol.* 206, 461–472. doi: 10.1083/jcb.201406055

Jaworski, J., Kapitein, L. C., Gouveia, S. M., Dortland, B. R., Wulf, P. S., Grigoriev, I., et al. (2009). Dynamic microtubules regulate dendritic spine morphology and synaptic plasticity. *Neuron* 61, 85–100. doi: 10.1016/j.neuron.2008.11.013

Ji, S.-J., and Jaffrey, S. R. (2012). Intra-axonal translation of SMAD1/5/8 mediates retrograde regulation of trigeminal ganglia subtype specification. *Neuron* 74, 95–107. doi: 10.1016/j.neuron.2012.02.022

Jones, K. J., Korb, E., Kundel, M. A., Kochanek, A. R., Kabraji, S., McEvoy, M., et al. (2008). CPEB1 regulates beta-catenin mRNA translation and cell migration in astrocytes. *Glia* 56, 1401–1413. doi: 10.1002/glia.20707

Jønson, L., Vikesaa, J., Krogh, A., Nielsen, L. K., Hansen, T. V., Borup, R., et al. (2007). Molecular composition of IMP1 ribonucleoprotein granules. *Mol. Cell. Proteomics* 6, 798–811. doi: 10.1074/mcp.M600346-MCP200

Jovanovic, J. N., Czernik, A. J., Fienberg, A. A., Greengard, P., and Sihra, T. S. (2000). Synapsins as mediators of BDNF-enhanced neurotransmitter release. *Nat. Neurosci.* 3, 323–329. doi: 10.1038/73888

Jung, H., Gkogkas, C. G., Sonenberg, N., and Holt, C. E. (2014). Remote control of gene function by local translation. *Cell* 157, 26–40. doi: 10.1016/j.cell.2014.03.005

Jung, H., Yoon, B. C., and Holt, C. E. (2012). Axonal mRNA localization and local protein synthesis in nervous system assembly, maintenance and repair. *Nat. Rev. Neurosci.* 13, 308–324. doi: 10.1038/nrn3210

Kalinski, A. L., Sachdeva, R., Gomes, C., Lee, S. J., Shah, Z., Houle, J. D., et al. (2015). mRNAs and protein synthetic machinery localize into regenerating spinal cord axons when they are provided a substrate that supports growth. *J. Neurosci.* 35, 10357–10370. doi: 10.1523/JNEUROSCI.1249-15.2015

Kalkman, H. O. (2012). A review of the evidence for the canonical Wnt pathway in autism spectrum disorders. *Mol. Autism* 3:10. doi: 10.1186/2040-2392-3-10

Kang, H., and Schuman, E. M. (1995). Long-lasting neurotrophin-induced enhancement of synaptic transmission in the adult hippocampus. *Science* 267, 1658–1662. doi: 10.1126/science.7886457

Kang, H., Welcher, A. A., Shelton, D., and Schuman, E. M. (1997). Neurotrophins and time: different roles for TrkB signaling in hippocampal long-term potentiation. *Neuron* 19, 653–664. doi: 10.1016/s0896-6273(00)80378-5

Kapitein, L. C., Schlager, M. A., Kuijpers, M., Wulf, P. S., van Spronsen, M., MacKintosh, F. C., et al. (2010). Mixed microtubules steer dynein-driven cargo transport into dendrites. *Curr. Biol.* 20, 290–299. doi: 10.1016/j.cub.2009.12.052

Kawasaki, Y., Sato, R., and Akiyama, T. (2003). Mutated APC and Asef are involved in the migration of colorectal tumour cells. *Nat. Cell Biol.* 5, 211–215. doi: 10.1038/ncb937

Keino-Masu, K., Masu, M., Hinck, L., Leonardo, E. D., Chan, S. S., Culotti, J. G., et al. (1996). Deleted in Colorectal Cancer (DCC) encodes a netrin receptor. *Cell* 87, 175–185. doi: 10.1016/s0092-8674(00)81336-7

Kershaw, C. J., Jennings, M. D., Cortopassi, F., Guaita, M., Al-Ghafli, H., and Pavitt, G. D. (2021). GTP binding to translation factor eIF2B stimulates its guanine nucleotide exchange activity. *iScience* 24:103454. doi: 10.1016/j.isci.2021.103454

Ketschek, A., Jones, S., Spillane, M., Korobova, F., Svitkina, T., and Gallo, G. (2015). Nerve growth factor promotes reorganization of the axonal microtubule array at sites of axon collateral branching. *Dev. Neurobiol.* 75, 1441–1461. doi: 10.1002/dneu.22294

Kevenaar, J. T., and Hoogenraad, C. C. (2015). The axonal cytoskeleton: from organization to function. *Front. Mol. Neurosci.* 8:44. doi: 10.3389/fnmol.2015.00044

Kim, S., and Coulombe, P. A. (2010). Emerging role for the cytoskeleton as an organizer and regulator of translation. *Nat. Rev. Mol. Cell Biol.* 11, 75–81. doi: 10.1038/nrm2818

Kim, Y., Sung, J. Y., Ceglia, I., Lee, K.-W., Ahn, J.-H., Halford, J. M., et al. (2006). Phosphorylation of WAVE1 regulates actin polymerization and dendritic spine morphology. *Nature* 442, 814–817. doi: 10.1038/nature04976

Kita, K., Wittmann, T., Näthke, I. S., and Waterman-Storer, C. M. (2006). Adenomatous polyposis coli on microtubule plus ends in cell extensions can promote microtubule net growth with or without EB1. *Mol. Biol. Cell* 17, 2331–2345. doi: 10.1091/mbc.e05-06-0498

Klemmer, P., Meredith, R. M., Holmgren, C. D., Klychnikov, O. I., Stahl-Zeng, J., Loos, M., et al. (2011). Proteomics, ultrastructure, and physiology of hippocampal synapses in a fragile X syndrome mouse model reveal presynaptic phenotype. *J. Biol. Chem.* 286, 25495–25504. doi: 10.1074/jbc.M110.210260

Kobayashi, K., Kuroda, S., Fukata, M., Nakamura, T., Nagase, T., Nomura, N., et al. (1998). p140Sra-1 (specifically Rac1-associated protein) is a novel specific target for Rac1 small GTPase. *J. Biol. Chem.* 273, 291–295. doi: 10.1074/jbc.273.1.291

Koenig, E. (1967). Synthetic mechanisms in the axon. IV. *In vitro* incorporation of [3H]precursors into axonal protein and RNA. *J. Neurochem.* 14, 437–446. doi: 10.1111/j.1471-4159.1967.tb09542.x

Koenig, E., Martin, R., Titmus, M., and Sotelo-Silveira, J. R. (2000). Cryptic peripheral ribosomal domains distributed intermittently along mammalian myelinated axons. *J. Neurosci.* 20, 8390–8400. doi: 10.1523/JNEUROSCI.20-22-08390.2000

Koester, M. P., Müller, O., and Pollerberg, G. E. (2007). Adenomatous polyposis coli is differentially distributed in growth cones and modulates their steering. *J. Neurosci.* 27, 12590–12600. doi: 10.1523/JNEUROSCI.2250-07.2007

Kolodkin, A. L., and Tessier-Lavigne, M. (2011). Mechanisms and molecules of neuronal wiring: a primer. *Cold Spring Harb. Perspect. Biol.* 3:a001727. doi: 10.1101/cshperspect.a001727

Kolodziej, P. A., Timpe, L. C., Mitchell, K. J., Fried, S. R., Goodman, C. S., Jan, L. Y., et al. (1996). frazzled encodes a Drosophila member of the DCC immunoglobulin subfamily and is required for CNS and motor axon guidance. *Cell* 87, 197–204. doi: 10.1016/s0092-8674(00)81338-0

Kroboth, K., Newton, I. P., Kita, K., Dikovskaya, D., Zumbrunn, J., Waterman-Storer, C. M., et al. (2007). Lack of adenomatous polyposis coli protein correlates with a decrease in cell migration and overall changes in microtubule stability. *Mol. Biol. Cell* 18, 910–918. doi: 10.1091/mbc.e06-03-0179

Krumm, N., O'Roak, B. J., Shendure, J., and Eichler, E. E. (2014). A de novo convergence of autism genetics and molecular neuroscience. *Trends Neurosci.* 37, 95–105. doi: 10.1016/j.tins.2013.11.005

Kunda, P., Craig, G., Dominguez, V., and Baum, B. (2003). Abi, Sra1, and Kette control the stability and localization of SCAR/WAVE to regulate the formation of actin-based protrusions. *Curr. Biol.* 13, 1867–1875. doi: 10.1016/j.cub.2003.10.005

Kwiatkowski, A. V., Rubinson, D. A., Dent, E. W., Edward van Veen, J., Leslie, J. D., Zhang, J., et al. (2007). Ena/VASP Is Required for neuritogenesis in the developing cortex. *Neuron* 56, 441–455. doi: 10.1016/j.neuron.2007.09.008

Lang, S. B., Stein, V., Bonhoeffer, T., and Lohmann, C. (2007). Endogenous brain-derived neurotrophic factor triggers fast calcium transients at synapses in developing dendrites. *J. Neurosci.* 27, 1097–1105. doi: 10.1523/JNEUROSCI.3590-06.2007

Lanier, L. M., Gates, M. A., Witke, W., Menzies, A. S., Wehman, A. M., Macklis, J. D., et al. (1999). Mena is required for neurulation and commissure formation. *Neuron* 22, 313–325. doi: 10.1016/s0896-6273(00)81092-2

Lawrence, J. B., and Singer, R. H. (1986). Intracellular localization of messenger RNAs for cytoskeletal proteins. *Cell* 45, 407–415. doi: 10.1016/0092-8674(86)90326-0

Lebrand, C., Dent, E. W., Strasser, G. A., Lanier, L. M., Krause, M., Svitkina, T. M., et al. (2004). Critical role of Ena/VASP proteins for filopodia formation in neurons and in function downstream of netrin-1. *Neuron* 42, 37–49. doi: 10.1016/s0896-6273(04)00108-4

Lee, S., and Kolodziej, P. A. (2002). Short Stop provides an essential link between F-actin and microtubules during axon extension. *Development* 129, 1195–1204. doi: 10.1242/dev.129.5.1195

Lee, S., Nahm, M., Lee, M., Kwon, M., Kim, E., Zadeh, A. D., et al. (2007). The F-actin-microtubule crosslinker Shot is a platform for Krasavietz-mediated translational regulation of midline axon repulsion. *Development* 134, 1767–1777. doi: 10.1242/dev.02842

Leeds, P., Kren, B. T., Boylan, J. M., Betz, N. A., Steer, C. J., Gruppuso, P. A., et al. (1997). Developmental regulation of CRD-BP, an RNA-binding protein that stabilizes c-myc mRNA *in vitro*. *Oncogene* 14, 1279–1286. doi: 10.1038/sj.onc.1201093

Lepelletier, L., Langlois, S. D., Kent, C. B., Welshhans, K., Morin, S., Bassell, G. J., et al. (2017). Sonic hedgehog guides axons via zipcode binding protein 1-mediated local translation. *J. Neurosci.* 37, 1685–1695. doi: 10.1523/JNEUROSCI.3016-16.2016

Letourneau, P. C. (2009). Actin in axons: stable scaffolds and dynamic filaments. *Results Probl. Cell Differ.* 48, 65–90. doi: 10.1007/400_2009_15

Leung, K.-M., Lu, B., Wong, H. H.-W., Lin, J. Q., Turner-Bridger, B., and Holt, C. E. (2018). Cue-polarized transport of β-actin mRNA Depends on 3'UTR and microtubules in live growth cones. *Front. Cell. Neurosci.* 12:300. doi: 10.3389/fncel.2018.00300

Leung, K.-M., van Horck, F. P. G., Lin, A. C., Allison, R., Standart, N., and Holt, C. E. (2006). Asymmetrical beta-actin mRNA translation in growth cones mediates attractive turning to netrin-1. *Nat. Neurosci.* 9, 1247–1256. doi: 10.1038/nn1775

Leung, L. C., Urbanèiè, V., Baudet, M.-L., Dwivedy, A., Bayley, T. G., Lee, A. C., et al. (2013). Coupling of NF-protocadherin signaling to axon guidance by cue-induced translation. *Nat. Neurosci.* 16, 166–173. doi: 10.1038/nn.3290

Levine, E. S., Dreyfus, C. F., Black, I. B., and Plummer, M. R. (1995). Brain-derived neurotrophic factor rapidly enhances synaptic transmission in hippocampal neurons via postsynaptic tyrosine kinase receptors. *Proc. Natl. Acad. Sci. U.S.A.* 92, 8074–8077. doi: 10.1073/pnas.92.17.8074

Li, W., Li, Y., and Gao, F.-B. (2005). Abelson, enabled, and p120 catenin exert distinct effects on dendritic morphogenesis in *Drosophila*. *Dev. Dyn.* 234, 512–522. doi: 10.1002/dvdy.20496

Li, W., Ma, L., Yang, G., and Gan, W.-B. (2017). REM sleep selectively prunes and maintains new synapses in development and learning. *Nat. Neurosci.* 20, 427–437. doi: 10.1038/nn.4479

Liao, L., Park, S. K., Xu, T., Vanderklish, P., and Yates, J. R. (2008). Quantitative proteomic analysis of primary neurons reveals diverse changes in synaptic protein content in fmr1 knockout mice. *Proc. Natl. Acad. Sci. U.S.A.* 105, 15281–15286. doi: 10.1073/pnas.0804678105

Lin, Y.-L., Lei, Y.-T., Hong, C.-J., and Hsueh, Y.-P. (2007). Syndecan-2 induces filopodia and dendritic spine formation via the neurofibromin-PKA-Ena/VASP pathway. *J. Cell Biol.* 177, 829–841. doi: 10.1083/jcb.200608121

Lu, R., Wang, H., Liang, Z., Ku, L., O'donnell, W. T., Li, W., et al. (2004). The fragile X protein controls microtubule-associated protein 1B translation and microtubule stability in brain neuron development. *Proc. Natl. Acad. Sci. U.S.A.* 101, 15201–15206. doi: 10.1073/pnas.0404995101

Lukinavièius, G., Reymond, L., D'Este, E., Masharina, A., Göttfert, F., Ta, H., et al. (2014). Fluorogenic probes for live-cell imaging of the cytoskeleton. *Nat. Methods* 11, 731–733. doi: 10.1038/nmeth.2972

Luo, L. (2002). Actin cytoskeleton regulation in neuronal morphogenesis and structural plasticity. *Annu. Rev. Cell Dev. Biol.* 18, 601–635. doi: 10.1146/annurev.cellbio.18.031802.150501

Manitt, C., Mimee, A., Eng, C., Pokinko, M., Stroh, T., Cooper, H. M., et al. (2011). The netrin receptor DCC is required in the pubertal organization of mesocortical dopamine circuitry. *J. Neurosci.* 31, 8381–8394. doi: 10.1523/JNEUROSCI.0606-11.2011

McConnell, R. E., Edward van Veen, J., Vidaki, M., Kwiatkowski, A. V., Meyer, A. S., and Gertler, F. B. (2016). A requirement for filopodia extension toward Slit during Robo-mediated axon repulsion. *J. Cell Biol.* 213, 261–274. doi: 10.1083/jcb.201509062

McKerracher, L., and Higuchi, H. (2006). Targeting Rho to stimulate repair after spinal cord injury. *J. Neurotrauma* 23, 309–317. doi: 10.1089/neu.2006.23.309

Medioni, C., Ramialison, M., Ephrussi, A., and Besse, F. (2014). Imp promotes axonal remodeling by regulating profilin mRNA during brain development. *Curr. Biol.* 24, 793–800. doi: 10.1016/j.cub.2014.02.038

Menzies, A. S., Aszodi, A., Williams, S. E., Pfeifer, A., Wehman, A. M., Goh, K. L., et al. (2004). Mena and vasodilator-stimulated phosphoprotein are required for multiple actin-dependent processes that shape the vertebrate nervous system. *J. Neurosci.* 24, 8029–8038. doi: 10.1523/JNEUROSCI.1057-04.2004

Merriam, E. B., Lumbard, D. C., Viesselmann, C., Ballweg, J., Stevenson, M., Pietila, L., et al. (2011). Dynamic microtubules promote synaptic NMDA receptor-dependent spine enlargement. *PLoS One* 6:e27688. doi: 10.1371/journal.pone.0027688

Merriam, E. B., Millette, M., Lumbard, D. C., Saengsawang, W., Fothergill, T., Hu, X., et al. (2013). Synaptic regulation of microtubule dynamics in dendritic spines by calcium, F-actin, and drebrin. *J. Neurosci.* 33, 16471–16482. doi: 10.1523/JNEUROSCI.0661-13.2013

Mili, S., Moissoglu, K., and Macara, I. G. (2008). Genome-Wide Screen Identifies Localized RNAs Anchored At Cell Protrusions Through Microtubules And APC. *Nature* 453, 115–119. doi: 10.1038/nature06888

Mimori-Kiyosue, Y., Shiina, N., and Tsukita, S. (2000). Adenomatous polyposis coli (APC) protein moves along microtubules and concentrates at their growing ends in epithelial cells. *J. Cell Biol.* 148, 505–518. doi: 10.1083/jcb.148.3.505

Mitchison, T., and Kirschner, M. (1984). Dynamic instability of microtubule growth. *Nature* 312, 237–242. doi: 10.1038/312237a0

Miyashiro, K. Y., Beckel-Mitchener, A., Purk, T. P., Becker, K. G., Barret, T., Liu, L., et al. (2003). RNA cargoes associating with FMRP reveal deficits in cellular functioning in Fmr1 null mice. *Neuron* 37, 417–431. doi: 10.1016/s0896-6273(03)00034-5

Mofatteh, M. (2020). mRNA localization and local translation in neurons. *AIMS Neurosci.* 7, 299–310. doi: 10.3934/Neuroscience.2020016

Mohajerani, M. H., Sivakumaran, S., Zacchi, P., Aguilera, P., and Cherubini, E. (2007). Correlated network activity enhances synaptic efficacy via BDNF and the ERK pathway at immature CA3 CA1 connections in the hippocampus. *Proc. Natl. Acad. Sci. U.S.A.* 104, 13176–13181. doi: 10.1073/pnas.0704533104

Morgan, I. G., and Austin, L. (1968). Synaptosomal protein synthesis in a cell-free system. *J. Neurochem.* 15, 41–51. doi: 10.1111/j.1471-4159.1968.tb06172.x

Murakoshi, H., Wang, H., and Yasuda, R. (2011). Local, persistent activation of Rho GTPases during plasticity of single dendritic spines. *Nature* 472, 100–104. doi: 10.1038/nature09823

Nakahata, Y., and Yasuda, R. (2018). Plasticity of spine structure: local signaling, translation and cytoskeletal reorganization. *Front. Synaptic Neurosci.* 10:29. doi: 10.3389/fnsyn.2018.00029

Napoli, I., Mercaldo, V., Boyl, P. P., Eleuteri, B., Zalfa, F., De Rubeis, S., et al. (2008). The fragile X syndrome protein represses activity-dependent translation through CYFIP1, a new 4E-BP. *Cell* 134, 1042–1054. doi: 10.1016/j.cell.2008.07.031

Näthke, I. S., Adams, C. L., Polakis, P., Sellin, J. H., and Nelson, W. J. (1996). The adenomatous polyposis coli tumor suppressor protein localizes to plasma membrane sites involved in active cell migration. *J. Cell Biol.* 134, 165–179. doi: 10.1083/jcb.134.1.165

Neves-Pereira, M., Müller, B., Massie, D., Williams, J. H. G., O'Brien, P. C. M., Hughes, A., et al. (2009). Deregulation of EIF4E: a novel mechanism for autism. *J. Med. Genet.* 46, 759–765. doi: 10.1136/jmg.2009.066852

Nicastro, G., Candel, A. M., Uhl, M., Oregioni, A., Hollingworth, D., Backofen, R., et al. (2017). Mechanism of β-actin mRNA Recognition by ZBP1. *Cell Rep.* 18, 1187–1199. doi: 10.1016/j.celrep.2016.12.091

Nielsen, J., Christiansen, J., Lykke-Andersen, J., Johnsen, A. H., Wewer, U. M., and Nielsen, F. C. (1999). A family of insulin-like growth factor II mRNA-binding proteins represses translation in late development. *Mol. Cell. Biol.* 19, 1262–1270. doi: 10.1128/MCB.19.2.1262

Nishino, J., Kim, S., Zhu, Y., Zhu, H., and Morrison, S. J. (2013). A network of heterochronic genes including Imp1 regulates temporal changes in stem cell properties. *eLife* 2:e00924. doi: 10.7554/eLife.00924

Nowicki, S. T., Tassone, F., Ono, M. Y., Ferranti, J., Croquette, M. F., Goodlin-Jones, B., et al. (2007). The Prader-Willi phenotype of fragile X syndrome. *J. Dev. Behav. Pediatr.* 28, 133–138. doi: 10.1097/01.DBP.0000267563.18952.c9

O'Roak, B. J., Vives, L., Fu, W., Egertson, J. D., Stanaway, I. B., Phelps, I. G., et al. (2012). Multiplex targeted sequencing identifies recurrently mutated genes in autism spectrum disorders. *Science* 338, 1619–1622. doi: 10.1126/science.1227764

Ostroff, L. E., Cain, C. K., Jindal, N., Dar, N., and Ledoux, J. E. (2012). Stability of presynaptic vesicle pools and changes in synapse morphology in the amygdala following fear learning in adult rats. *J. Comp. Neurol.* 520, 295–314. doi: 10.1002/cne.22691

Ostroff, L. E., Watson, D. J., Cao, G., Parker, P. H., Smith, H., and Harris, K. M. (2018). Shifting patterns of polyribosome accumulation at synapses over the course of hippocampal long-term potentiation. *Hippocampus* 28, 416–430. doi: 10.1002/hipo.22841

Parent, A. T., Barnes, N. Y., Taniguchi, Y., Thinakaran, G., and Sisodia, S. S. (2005). Presenilin attenuates receptor-mediated signaling and synaptic function. *J. Neurosci.* 25, 1540–1549. doi: 10.1523/JNEUROSCI.3850-04.2005

Patel, V. L., Mitra, S., Harris, R., Buxbaum, A. R., Lionnet, T., Brenowitz, M., et al. (2012). Spatial arrangement of an RNA zipcode identifies mRNAs under post-transcriptional control. *Genes Dev.* 26, 43–53. doi: 10.1101/gad.177428.111

Penzes, P., Cahill, M. E., Jones, K. A., VanLeeuwen, J.-E., and Woolfrey, K. M. (2011). Dendritic spine pathology in neuropsychiatric disorders. *Nat. Neurosci.* 14, 285–293. doi: 10.1038/nn.2741

Pinto-Costa, R., Sousa, S. C., Leite, S. C., Nogueira-Rodrigues, J., Ferreira da Silva, T., Machado, D., et al. (2020). Profilin 1 delivery tunes cytoskeletal dynamics toward CNS axon regeneration. *J. Clin. Invest.* 130, 2024–2040. doi: 10.1172/JCI125771

Piper, M., Anderson, R., Dwivedy, A., Weinl, C., van Horck, F., Leung, K. M., et al. (2006). Signaling mechanisms underlying Slit2-induced collapse of Xenopus retinal growth cones. *Neuron* 49, 215–228. doi: 10.1016/j.neuron.2005.12.008

Piper, M., Lee, A. C., van Horck, F. P. G., McNeilly, H., Lu, T. B., Harris, W. A., et al. (2015). Differential requirement of F-actin and microtubule cytoskeleton in cue-induced local protein synthesis in axonal growth cones. *Neural Dev.* 10:3. doi: 10.1186/s13064-015-0031-0

Powell, S. M., Zilz, N., Beazer-Barclay, Y., Bryan, T. M., Hamilton, S. R., Thibodeau, S. N., et al. (1992). APC mutations occur early during colorectal tumorigenesis. *Nature* 359, 235–237. doi: 10.1038/359235a0

Pradhan, J., Noakes, P. G., and Bellingham, M. C. (2019). The role of Altered BDNF/TrkB signaling in amyotrophic lateral sclerosis. *Front. Cell. Neurosci.* 13:368. doi: 10.3389/fncel.2019.00368

Preitner, N., Quan, J., Nowakowski, D. W., Hancock, M. L., Shi, J., Tcherkezian, J., et al. (2014). APC is an RNA-binding protein and its interactome provides a link to neural development and microtubule assembly. *Cell* 158, 368–382. doi: 10.1016/j.cell.2014.05.042

Purro, S. A., Ciani, L., Hoyos-Flight, M., Stamatakou, E., Siomou, E., and Salinas, P. C. (2008). Wnt regulates axon behavior through changes in microtubule growth directionality: a new role for adenomatous polyposis coli. *J. Neurosci.* 28, 8644–8654. doi: 10.1523/JNEUROSCI.2320-08.2008

Qian, W., Jin, N., Shi, J., Yin, X., Jin, X., Wang, S., et al. (2013). Dual-specificity tyrosine phosphorylation-regulated kinase 1A (Dyrk1A) enhances tau expression. *J. Alzheimers Dis.* 37, 529–538. doi: 10.3233/JAD-130824

Rangaraju, V., Lauterbach, M., and Schuman, E. M. (2019). Spatially stable mitochondrial compartments fuel local translation during plasticity. *Cell* 176, 73–84.e15. doi: 10.1016/j.cell.2018.12.013

Reyes, S., Fu, Y., Double, K. L., Cottam, V., Thompson, L. H., Kirik, D., et al. (2013). Trophic factors differentiate dopamine neurons vulnerable to Parkinson's disease. *Neurobiol. Aging* 34, 873–886. doi: 10.1016/j.neurobiolaging.2012.07.019

Romaniello, R., Tonelli, A., Arrigoni, F., Baschirotto, C., Triulzi, F., Bresolin, N., et al. (2012). A novel mutation in the β-tubulin gene TUBB2B associated with complex malformation of cortical development and deficits in axonal guidance. *Dev. Med. Child Neurol.* 54, 765–769. doi: 10.1111/j.1469-8749.2012.04316.x

Rubinfeld, B., Souza, B., Albert, I., Müller, O., Chamberlain, S. H., Masiarz, F. R., et al. (1993). Association of the APC gene product with beta-catenin. *Science* 262, 1731–1734. doi: 10.1126/science.8259518

Russell, S. A., and Bashaw, G. J. (2018). Axon guidance pathways and the control of gene expression. *Dev. Dyn.* 247, 571–580. doi: 10.1002/dvdy.24609

Sanchez, G., Dury, A. Y., Murray, L. M., Biondi, O., Tadesse, H., El Fatimy, R., et al. (2013). A novel function for the survival motoneuron protein as a translational regulator. *Hum. Mol. Genet.* 22, 668–684. doi: 10.1093/hmg/dds474

Santini, E., Huynh, T. N., Longo, F., Koo, S. Y., Mojica, E., D'Andrea, L., et al. (2017). Reducing eIF4E-eIF4G interactions restores the balance between protein synthesis and actin dynamics in fragile X syndrome model mice. *Sci. Signal.* 10:eaan0665. doi: 10.1126/scisignal.aan0665

Santini, E., Huynh, T. N., MacAskill, A. F., Carter, A. G., Pierre, P., Ruggero, D., et al. (2013). Exaggerated translation causes synaptic and behavioural aberrations associated with autism. *Nature* 493, 411–415. doi: 10.1038/nature11782

Sasaki, Y., Welshhans, K., Wen, Z., Yao, J., Xu, M., Goshima, Y., et al. (2010). Phosphorylation of zipcode binding protein 1 is required for brain-derived neurotrophic factor signaling of local beta-actin synthesis and growth cone turning. *J. Neurosci.* 30, 9349–9358. doi: 10.1523/JNEUROSCI.0499-10.2010

Saxton, R. A., and Sabatini, D. M. (2017). mTOR signaling in growth, metabolism, and disease. *Cell* 169, 361–371. doi: 10.1016/j.cell.2017.03.035

Scarnati, M. S., Kataria, R., Biswas, M., and Paradiso, K. G. (2018). Active presynaptic ribosomes in the mammalian brain, and altered transmitter release after protein synthesis inhibition. *eLife* 7:e36697. doi: 10.7554/eLife.36697

Schenck, A., Bardoni, B., Langmann, C., Harden, N., Mandel, J. L., and Giangrande, A. (2003). CYFIP/Sra-1 controls neuronal connectivity in *Drosophila* and links the Rac1 GTPase pathway to the fragile X protein. *Neuron* 38, 887–898. doi: 10.1016/s0896-6273(03)00354-4

Schenck, A., Bardoni, B., Moro, A., Bagni, C., and Mandel, J. L. (2001). A highly conserved protein family interacting with the fragile X mental retardation protein (FMRP) and displaying selective interactions with FMRP-related proteins FXR1P and FXR2P. *Proc. Natl. Acad. Sci. U.S.A.* 98, 8844–8849. doi: 10.1073/pnas.151231598

Schratt, G. M., Nigh, E. A., Chen, W. G., Hu, L., and Greenberg, M. E. (2004). BDNF regulates the translation of a select group of mRNAs by a mammalian target of rapamycin-phosphatidylinositol 3-kinase-dependent pathway during neuronal development. *J. Neurosci.* 24, 7366–7377. doi: 10.1523/JNEUROSCI.1739-04.2004

Segal, R. A., and Greenberg, M. E. (1996). Intracellular signaling pathways activated by neurotrophic factors. *Annu. Rev. Neurosci.* 19, 463–489. doi: 10.1146/annurev.ne.19.030196.002335

Shi, S.-H., Cheng, T., Jan, L. Y., and Jan, Y.-N. (2004). APC and GSK-3beta are involved in mPar3 targeting to the nascent axon and establishment of neuronal polarity. *Curr. Biol.* 14, 2025–2032. doi: 10.1016/j.cub.2004.11.009

Sieber, O. M., Heinimann, K., Gorman, P., Lamlum, H., Crabtree, M., Simpson, C. A., et al. (2002). Analysis of chromosomal instability in human colorectal adenomas with two mutational hits at APC. *Proc. Natl. Acad. Sci. U.S.A.* 99, 16910–16915. doi: 10.1073/pnas.012679099

Skruber, K., Warp, P. V., Shklyarov, R., Thomas, J. D., Swanson, M. S., Henty-Ridilla, J. L., et al. (2020). Arp2/3 and Mena/VASP require profilin 1 for actin network assembly at the leading edge. *Curr. Biol.* 30, 2651–2664.e5. doi: 10.1016/j.cub.2020.04.085

Soderling, S. H., Guire, E. S., Kaech, S., White, J., Zhang, F., Schutz, K., et al. (2007). A WAVE-1 and WRP signaling complex regulates spine density, synaptic plasticity, and memory. *J. Neurosci.* 27, 355–365. doi: 10.1523/JNEUROSCI.3209-06.2006

Song, M., Martinowich, K., and Lee, F. S. (2017). BDNF at the synapse: why location matters. *Mol. Psychiatry* 22, 1370–1375. doi: 10.1038/mp.2017.144

Sonnenberg, A., and Liem, R. K. H. (2007). Plakins in development and disease. *Exp. Cell Res.* 313, 2189–2203. doi: 10.1016/j.yexcr.2007.03.039

Spillane, M., Ketschek, A., Donnelly, C. J., Pacheco, A., Twiss, J. L., and Gallo, G. (2012). Nerve growth factor-induced formation of axonal filopodia and collateral branches involves the intra-axonal synthesis of regulators of the actin-nucleating Arp2/3 complex. *J. Neurosci.* 32, 17671–17689. doi: 10.1523/JNEUROSCI.1079-12.2012

Spillane, M., Ketschek, A., Merianda, T. T., Twiss, J. L., and Gallo, G. (2013). Mitochondria coordinate sites of axon branching through localized intra-axonal protein synthesis. *Cell Rep.* 5, 1564–1575. doi: 10.1016/j.celrep.2013.11.022

Stepanova, T., Slemmer, J., Hoogenraad, C. C., Lansbergen, G., Dortland, B., De Zeeuw, C. I., et al. (2003). Visualization of microtubule growth in cultured neurons via the use of EB3-GFP (end-binding protein 3-green fluorescent protein). *J. Neurosci.* 23, 2655–2664. doi: 10.1523/JNEUROSCI.23-07-02655.2003

Steward, O., and Levy, W. B. (1982). Preferential localization of polyribosomes under the base of dendritic spines in granule cells of the dentate gyrus. *J. Neurosci.* 2, 284–291. doi: 10.1523/JNEUROSCI.02-03-00284.1982

Steward, O., and Schuman, E. M. (2003). Compartmentalized synthesis and degradation of proteins in neurons. *Neuron* 40, 347–359. doi: 10.1016/s0896-6273(03)00635-4

Stone, M. C., Roegiers, F., and Rolls, M. M. (2008). Microtubules have opposite orientation in axons and dendrites of *Drosophila* neurons. *Mol. Biol. Cell* 19, 4122–4129. doi: 10.1091/mbc.e07-10-1079

Suter, D. M., and Forscher, P. (2000). Substrate-cytoskeletal coupling as a mechanism for the regulation of growth cone motility and guidance. *J. Neurobiol.* 44, 97–113.

Svitkina, T. M., Bulanova, E. A., Chaga, O. Y., Vignjevic, D. M., Kojima, S., Vasiliev, J. M., et al. (2003). Mechanism of filopodia initiation by reorganization of a dendritic network. *J. Cell Biol.* 160, 409–421. doi: 10.1083/jcb.200210174

Takenawa, T., and Suetsugu, S. (2007). The WASP-WAVE protein network: connecting the membrane to the cytoskeleton. *Nat. Rev. Mol. Cell Biol.* 8, 37–48. doi: 10.1038/nrm2069

Tam, G. W. C., van de Lagemaat, L. N., Redon, R., Strathdee, K. E., Croning, M. D. R., Malloy, M. P., et al. (2010). Confirmed rare copy number variants implicate novel genes in schizophrenia. *Biochem. Soc. Trans.* 38, 445–451. doi: 10.1042/BST0380445

Tanaka, E., and Sabry, J. (1995). Making the connection: cytoskeletal rearrangements during growth cone guidance. *Cell* 83, 171–176. doi: 10.1016/0092-8674(95)90158-2

Tcherkezian, J., Brittis, P. A., Thomas, F., Roux, P. P., and Flanagan, J. G. (2021). Transmembrane receptor DCC associates with protein synthesis machinery and regulates translation. *Cell* 184:2520. doi: 10.1016/j.cell.2021.04.018

Tejedor, F. J., and Hämmerle, B. (2011). MNB/DYRK1A as a multiple regulator of neuronal development. *FEBS J.* 278, 223–235. doi: 10.1111/j.1742-4658.2010.07954.x

Torres-Berrio, A., Hernandez, G., Nestler, E. J., and Flores, C. (2020). The Netrin-1/DCC guidance cue pathway as a molecular target in depression: translational evidence. *Biol. Psychiatry* 88, 611–624. doi: 10.1016/j.biopsych.2020.04.025

Tortosa, E., Galjart, N., Avila, J., and Sayas, C. L. (2013). MAP1B regulates microtubule dynamics by sequestering EB1/3 in the cytosol of developing neuronal cells. *EMBO J.* 32, 1293–1306. doi: 10.1038/emboj.2013.76

Trachtenberg, J. T., Chen, B. E., Knott, G. W., Feng, G., Sanes, J. R., Welker, E., et al. (2002). Long-term *in vivo* imaging of experience-dependent synaptic plasticity in adult cortex. *Nature* 420, 788–794. doi: 10.1038/nature01273

Tucker, P. K., Evans, I. R., and Wood, W. (2011). Ena drives invasive macrophage migration in *Drosophila* embryos. *Dis. Model. Mech.* 4, 126–134. doi: 10.1242/dmm.005694

Ueberham, U., and Thomas, A. (2013). "The role of SMAD proteins for development, differentiation and dedifferentiation of neurons," in *Trends in Cell Signaling Pathways in Neuronal Fate Decision*, ed. S. Wislet-Gendebien (Rijeka: IntechOpen), 75–111. doi: 10.5772/54532

Vale, R. D. (2003). The molecular motor toolbox for intracellular transport. *Cell* 112, 467–480. doi: 10.1016/s0092-8674(03)00111-9

van Bon, B. W. M., Coe, B. P., Bernier, R., Green, C., Gerdts, J., Witherspoon, K., et al. (2016). Disruptive de novo mutations of DYRK1A lead to a syndromic form of autism and ID. *Mol. Psychiatry* 21, 126–132. doi: 10.1038/mp.2015.5

van der Zwaag, B., Staal, W. G., Hochstenbach, R., Poot, M., Spierenburg, H. A., de Jonge, M. V., et al. (2010). A co-segregating microduplication of chromosome 15q11.2 pinpoints two risk genes for autism spectrum disorder. *Am. J. Med. Genet. B Neuropsychiatr. Genet.* 153B, 960–966. doi: 10.1002/ajmg.b.31055

Van Horck, F. P. G., and Holt, C. E. (2008). A cytoskeletal platform for local translation in axons. *Sci. Signal.* 1:e11. doi: 10.1126/stke.18pe11

Venticinque, L., Jamieson, K. V., and Meruelo, D. (2011). Interactions between laminin receptor and the cytoskeleton during translation and cell motility. *PLoS One* 6:e15895. doi: 10.1371/journal.pone.0015895

Verma, P., Chierzi, S., Codd, A. M., Campbell, D. S., Meyer, R. L., Holt, C. E., et al. (2005). Axonal protein synthesis and degradation are necessary for efficient growth cone regeneration. *J. Neurosci.* 25, 331–342. doi: 10.1523/JNEUROSCI.3073-04.2005

Vidaki, M., Drees, F., Saxena, T., Lanslots, E., Taliaferro, M. J., Tatarakis, A., et al. (2017). A requirement for Mena, an actin regulator, in local mRNA translation in developing neurons. *Neuron* 95, 608–622.e5. doi: 10.1016/j.neuron.2017.06.048

Vitriol, E. A., and Zheng, J. Q. (2012). Growth cone travel in space and time: the cellular ensemble of cytoskeleton, adhesion, and membrane. *Neuron* 73, 1068–1081. doi: 10.1016/j.neuron.2012.03.005

Voelzmann, A., Liew, Y.-T., Qu, Y., Hahn, I., Melero, C., Sánchez-Soriano, N., et al. (2017). Drosophila Short stop as a paradigm for the role and regulation of spectraplakins. *Semin. Cell Dev. Biol.* 69, 40–57. doi: 10.1016/j.semcdb.2017.05.019

von der Lippe, C., Rustad, C., Heimdal, K., and Rødningen, O. K. (2011). 15q11.2 microdeletion - seven new patients with delayed development and/or behavioural problems. *Eur. J. Med. Genet.* 54, 357–360. doi: 10.1016/j.ejmg.2010.12.008

Wahl, S., Barth, H., Ciossek, T., Aktories, K., and Mueller, B. K. (2000). Ephrin-A5 induces collapse of growth cones by activating Rho and Rho kinase. *J. Cell Biol.* 149, 263–270. doi: 10.1083/jcb.149.2.263

Walders-Harbeck, B., Khaitlina, S. Y., Hinssen, H., Jockusch, B. M., and Illenberger, S. (2002). The vasodilator-stimulated phosphoprotein promotes actin polymerisation through direct binding to monomeric actin. *FEBS Lett.* 529, 275–280. doi: 10.1016/s0014-5793(02)03356-2

Wang, C. S., Kavalali, E. T., and Monteggia, L. M. (2022). BDNF signaling in context: from synaptic regulation to psychiatric disorders. *Cell* 185, 62–76. doi: 10.1016/j.cell.2021.12.003

Watanabe, T., Wang, S., Noritake, J., Sato, K., Fukata, M., Takefuji, M., et al. (2004). Interaction with IQGAP1 links APC to Rac1, Cdc42, and actin filaments during cell polarization and migration. *Dev. Cell* 7, 871–883. doi: 10.1016/j.devcel.2004.10.017

Weidensdorfer, D., Stöhr, N., Baude, A., Lederer, M., Köhn, M., Schierhorn, A., et al. (2009). Control of c-myc mRNA stability by IGF2BP1-associated cytoplasmic RNPs. *RNA* 15, 104–115. doi: 10.1261/rna.1175909

Weil, T. T., Parton, R., Davis, I., and Gavis, E. R. (2008). Changes in bicoid mRNA anchoring highlight conserved mechanisms during the oocyte-to-embryo transition. *Curr. Biol.* 18, 1055–1061. doi: 10.1016/j.cub.2008.06.046

Welshhans, K., and Bassell, G. J. (2011). Netrin-1-induced local β-actin synthesis and growth cone guidance requires zipcode binding protein 1. *J. Neurosci.* 31, 9800–9813. doi: 10.1523/JNEUROSCI.0166-11.2011

Wen, Y., Eng, C. H., Schmoranzer, J., Cabrera-Poch, N., Morris, E. J. S., Chen, M., et al. (2004). EB1 and APC bind to mDia to stabilize microtubules downstream of Rho and promote cell migration. *Nat. Cell Biol.* 6, 820–830. doi: 10.1038/ncb1160

Westmark, C. J., and Malter, J. S. (2007). FMRP mediates mGluR5-dependent translation of amyloid precursor protein. *PLoS Biol.* 5:e52. doi: 10.1371/journal.pbio.0050052

Wiens, K. M., Lin, H., and Liao, D. (2005). Rac1 induces the clustering of AMPA receptors during spinogenesis. *J. Neurosci.* 25, 10627–10636. doi: 10.1523/JNEUROSCI.1947-05.2005

Winkelman, J. D., Bilancia, C. G., Peifer, M., and Kovar, D. R. (2014). Ena/VASP Enabled is a highly processive actin polymerase tailored to self-assemble parallel-bundled F-actin networks with Fascin. *Proc. Natl. Acad. Sci. U.S.A.* 111, 4121–4126. doi: 10.1073/pnas.1322093111

Xu, K., Zhong, G., and Zhuang, X. (2013). Actin, spectrin, and associated proteins form a periodic cytoskeletal structure in axons. *Science* 339, 452–456. doi: 10.1126/science.1232251

Yang, G., Pan, F., and Gan, W.-B. (2009). Stably maintained dendritic spines are associated with lifelong memories. *Nature* 462, 920–924. doi: 10.1038/nature08577

Yao, J., Sasaki, Y., Wen, Z., Bassell, G. J., and Zheng, J. Q. (2006). An essential role for beta-actin mRNA localization and translation in Ca2+-dependent growth cone guidance. *Nat. Neurosci.* 9, 1265–1273. doi: 10.1038/nn1773

Yasuda, K., Zhang, H., Loiselle, D., Haystead, T., Macara, I. G., and Mili, S. (2013). The RNA-binding protein Fus directs translation of localized mRNAs in APC-RNP granules. *J. Cell Biol.* 203, 737–746. doi: 10.1083/jcb.201306058

Yin, Y., Edelman, G. M., and Vanderklish, P. W. (2002). The brain-derived neurotrophic factor enhances synthesis of Arc in synaptoneurosomes. *Proc. Natl. Acad. Sci. U.S.A.* 99, 2368–2373. doi: 10.1073/pnas.042693699

Yisraeli, J. K. (2005). VICKZ proteins: a multi-talented family of regulatory RNA-binding proteins. *Biol. Cell* 97, 87–96. doi: 10.1042/BC20040151

Yuan, A., Rao, M. V., Veeranna, and Nixon, R. A. (2017). Neurofilaments and neurofilament proteins in health and disease. *Cold Spring Harb. Perspect. Biol* 9:a018309. doi: 10.1101/cshperspect.a018309

Yukawa, K., Tanaka, T., Bai, T., Ueyama, T., Owada-Makabe, K., Tsubota, Y., et al. (2005). Semaphorin 4A induces growth cone collapse of hippocampal neurons in a Rho/Rho-kinase-dependent manner. *Int. J. Mol. Med.* 16, 115–118.

Zalfa, F., Eleuteri, B., Dickson, K. S., Mercaldo, V., De Rubeis, S., di Penta, A., et al. (2007). A new function for the fragile X mental retardation protein in regulation of PSD-95 mRNA stability. *Nat. Neurosci.* 10, 578–587. doi: 10.1038/nn1893

Zalfa, F., Giorgi, M., Primerano, B., Moro, A., Di Penta, A., Reis, S., et al. (2003). The fragile X syndrome protein FMRP associates with BC1 RNA and regulates the translation of specific mRNAs at synapses. *Cell* 112, 317–327. doi: 10.1016/s0092-8674(03)00079-5

Zappulo, A., van den Bruck, D., Ciolli Mattioli, C., Franke, V., Imami, K., McShane, E., et al. (2017). RNA localization is a key determinant of neurite-enriched proteome. *Nat. Commun.* 8:583. doi: 10.1038/s41467-017-00690-6

Zeng, X., Tamai, K., Doble, B., Li, S., Huang, H., Habas, R., et al. (2005). A dual-kinase mechanism for Wnt co-receptor phosphorylation and activation. *Nature* 438, 873–877. doi: 10.1038/nature04185

Zhang, M., Wang, Q., and Huang, Y. (2007). Fragile X mental retardation protein FMRP and the RNA export factor NXF2 associate with and destabilize Nxf1 mRNA in neuronal cells. *Proc. Natl. Acad. Sci. U.S.A.* 104, 10057–10062. doi: 10.1073/pnas.0700169104

Zhang, Y. Q., Bailey, A. M., Matthies, H. J., Renden, R. B., Smith, M. A., Speese, S. D., et al. (2001). Drosophila fragile X-related gene regulates the MAP1B homolog Futsch to control synaptic structure and function. *Cell* 107, 591–603. doi: 10.1016/s0092-8674(01)00589-x

Zhao, Q., Li, T., Zhao, X., Huang, K., Wang, T., Li, Z., et al. (2013). Rare CNVs and tag SNPs at 15q11.2 are associated with schizophrenia in the Han Chinese population. *Schizophr. Bull.* 39, 712–719. doi: 10.1093/schbul/sbr197

Zimyanin, V. L., Belaya, K., Pecreaux, J., Gilchrist, M. J., Clark, A., Davis, I., et al. (2008). *In vivo* imaging of oskar mRNA transport reveals the mechanism of posterior localization. *Cell* 134, 843–853. doi: 10.1016/j.cell.2008.06.053

Zivraj, K. H., Tung, Y. C. L., Piper, M., Gumy, L., Fawcett, J. W., Yeo, G. S. H., et al. (2010). Subcellular profiling reveals distinct and developmentally regulated repertoire of growth cone mRNAs. *J. Neurosci.* 30, 15464–15478. doi: 10.1523/JNEUROSCI.1800-10.2010

Zou, W., Dong, X., Broederdorf, T. R., Shen, A., Kramer, D. A., Shi, R., et al. (2018). A dendritic guidance receptor complex brings together distinct actin regulators to drive efficient f-actin assembly and branching. *Dev. Cell* 45, 362–375.e3. doi: 10.1016/j.devcel.2018.04.008

frontiers | Frontiers in Molecular Neuroscience

TYPE Original Research
PUBLISHED 02 August 2022
DOI 10.3389/fnmol.2022.958568

OPEN ACCESS

EDITED BY
Francisco Garcia-Gonzalez,
Doñana Biological Station (CSIC), Spain

REVIEWED BY
Shiying Li,
Nantong University, China
André Luis Bombeiro,
Universidade de Lisboa, Portugal

*CORRESPONDENCE
Andrei V. Chernov
achernov@ucsd.edu

SPECIALTY SECTION
This article was submitted to Pain Mechanisms and Modulators, a section of the journal Frontiers in Molecular Neuroscience

RECEIVED 31 May 2022
ACCEPTED 04 July 2022
PUBLISHED 02 August 2022

CITATION
Chernov AV and Shubayev VI (2022) Sexually dimorphic transcriptional programs of early-phase response in regenerating peripheral nerves. *Front. Mol. Neurosci.* 15:958568. doi: 10.3389/fnmol.2022.958568

Sexually dimorphic transcriptional programs of early-phase response in regenerating peripheral nerves

Andrei V. Chernov[1,2]* and Veronica I. Shubayev[1,2]

[1]Department of Anesthesiology, University of California, San Diego, San Diego, CA, United States, [2]VA San Diego Healthcare System, San Diego, CA, United States

The convergence of transcriptional and epigenetic changes in the peripheral nervous system (PNS) reshapes the spatiotemporal gene expression landscape in response to nerve transection. The control of these molecular programs exhibits sexually dimorphic characteristics that remain not sufficiently characterized. In the present study, we recorded genome-wide and sex-dependent early-phase transcriptional changes in regenerating (proximal) sciatic nerve 24 h after axotomy. Male nerves exhibited more extensive transcriptional changes with male-dominant upregulation of cytoskeletal binding and structural protein genes. Regulation of mRNAs encoding ion and ionotropic neurotransmitter channels displayed prominent sexual dimorphism consistent with sex-specific mRNA axonal transport in an early-phase regenerative response. Protein kinases and axonal transport genes showed sexually dimorphic regulation. Genes encoding components of synaptic vesicles were at high baseline expression in females and showed post-injury induction selectively in males. Predictive bioinformatic analyses established patterns of sexually dimorphic regulation of neurotrophic and immune genes, including activation of glial cell line-derived neurotrophic factor Gfra1 receptor and immune checkpoint cyclin D1 (Ccnd1) potentially linked to X-chromosome encoded tissue inhibitor of matrix metallo proteinases 1 (Timp1). Regulatory networks involving Olig1, Pou3f3/Oct6, Myrf, and Myt1l transcription factors were linked to sex-dependent reprogramming in regenerating nerves. Differential expression patterns of non-coding RNAs motivate a model of sexually dimorphic nerve regenerative responses to injury determined by epigenetic factors. Combined with our findings in the corresponding dorsal root ganglia (DRG), unique early-phase sex-specific molecular triggers could enrich the mechanistic understanding of peripheral neuropathies.

KEYWORDS

sexual dimorphism, peripheral nerve, axotomy, nerve regeneration, RNA-seq

Abbreviations: CNS, central nervous system; DEG, differentially expressed gene; DRG, dorsal root ganglia; FC, fold change; FDR, false discovery rate; GDNF, glial cell line-derived neurotrophic factor; IPA, Ingenuity Pathway Analysis; ncRNA, non-coding RNAs; PNS, peripheral nervous system; RNA-seq, RNA sequencing; SV, synaptic vesicle; TF, transcription factor; TLR, toll-like receptors.

Introduction

The peripheral nervous system (PNS) displays strong regenerative potential compared to the brain and spinal cord. Substantial knowledge of mechanisms involved in PNS injury has been acquired using rodent models of sciatic nerve axotomy originally described by Augustus Waller in 1850 (Fawcett and Keynes, 1990; Stoll et al., 2002). The success of sensory recovery after PNS injury depends on molecular remodeling ensuing within 24 h post-axotomy in the proximal nerve segment (Gordon et al., 2003; McDonald et al., 2006; Zochodne, 2012) coordinated with an extensive transcriptional response within neuronal somas in the dorsal root ganglia (DRG) (McDonald et al., 2006; Chernov and Shubayev, 2021). Upon an initial die-back toward DRG, the proximal axotomized axons form axonal sprouts that mature into growth cones enriched in the cytoskeletal framework that drives axons to reestablish functional connections with the end organ (Lundborg, 1987; Burnett and Zager, 2004; Radtke and Vogt, 2009). The transcriptional landscape of the damaged PNS is enriched by axonally trafficked coding and non-coding (nc) RNAs (Cavalli et al., 2005; Avraham et al., 2021).

Axonal regrowth in the damaged PNS depends on trophic, immune, metabolic, and structural support of Schwann cells (Jessen and Mirsky, 2016, 2021; Merrell and Stanger, 2016; Milichko and Dyachuk, 2020), forming immediate partnerships with axons (McDonald et al., 2006). Schwann cells undergo extensive phenotypic transformation within 24 h post-injury in preparation for mitosis and alignment into bands of Büngner (Jessen and Mirsky, 2016, 2021; Merrell and Stanger, 2016; Milichko and Dyachuk, 2020). Schwann cells produce and deposit into basal lamina a plethora of growth-permissive and -inhibitory extracellular matrix (ECM) proteins and proteoglycans to guide axonal growth, such as laminin and chondroitin sulfate proteoglycans (McDonald et al., 2006). These activities are partly controlled by ECM-degrading matrix metalloproteinase (MMP)/ADAM families that reciprocally coregulate the ECM network with cytokines, chemokines, trophic factors, and adhesion molecules (Chattopadhyay and Shubayev, 2009; Liu et al., 2010, 2015; Kim et al., 2012; Chernov and Shubayev, 2021).

Sex is emerging as a key biological variable in models of PNS injury, as certain neuropathic states exhibit sex-specific prevalence, incidence, mechanisms, and clinical presentation (Unruh, 1996; Greenspan et al., 2007; Fillingim et al., 2009; Mogil, 2012; Sorge and Totsch, 2017; Boerner et al., 2018). Sexual dimorphism in the transcriptional landscape of adult PNS and its response to injury has been shown by RNA-sequencing (RNA-seq) analyses (North et al., 2019; Ray et al., 2019; Stephens et al., 2019; Chernov et al., 2020; Paige et al., 2020; Ahlström et al., 2021). Sex-related differences in the axon elongation (Kovacic et al., 2004) could potentially be attributed to metabolic, immune, neuroendocrine, and sex chromosome-related genetic programs that have shown sex-specific regulation in the damaged PNS (North et al., 2019; Ray et al., 2019; Stephens et al., 2019; Chernov et al., 2020; Mecklenburg et al., 2020; Paige et al., 2020; Tavares-Ferreira et al., 2020; Ahlström et al., 2021). Unique to females, the chromosome-wide epigenetic inactivation of one of the two X chromosomes (Xi) regulates the normal and aberrant activity of X-linked immunity-related genes (Bianchi et al., 2012), including that in DRG at 24 h after sciatic nerve axotomy (Chernov and Shubayev, 2021). Whether the corresponding regenerating nerve segments exhibit sexual dimorphism in response to PNS axotomy remains unknown.

Using high-depth RNA-seq, the present study identified sex-specific early-phase transcriptional changes in protein-coding and ncRNAs in regenerating (proximal) nerves at 24 h after sciatic nerve axotomy in male and female mice. Applying predictive bioinformatics, we determined unique signaling events related to regenerative, trophic, metabolic, and sex chromosome-linked systems.

Results

To determine the sex specificity of an early-phase PNS regenerative transcriptional program, sciatic nerve axotomy or sham operation was conducted in female and male mice. At 24 h post-axotomy, regenerating (proximal segment) tissues (**Figure 1A**) were subjected to whole-genome transcriptomics analysis by high-depth RNA-seq (**Supplementary Figure 1**, n = 6 mice/group, 2 mice/sample (pooled), 3 sample/group). At 24 h after the sham operation, nerve tissues were assessed for transcriptomic signatures without injury. Transcriptomics of the respective DRG tissues in the same animal cohorts was reported earlier (Chernov and Shubayev, 2021).

Males exhibited more extensive transcriptional changes in regenerating sciatic nerve

A total of 25,788 genes were detected by RNA-seq in the proximal nerve stumps, including 2,553 differentially expressed genes (DEGs, **Supplementary Table 1**) that conformed to the significance criteria (adjusted p-values (P_{adj}) < 0.1) and the expression fold change (FC) filter ($\log_2 FC > 1$ or $\log_2 FC < -1$, **Figure 1A**). In summary, more unique, highly expressed up-regulated DEGs ($n = 232$) were identified in males relative to females as presented on MA and scatter plots (**Figures 1B,C**). In addition, 65 and 159 DEGs were downregulated in female and male nerves, respectively.

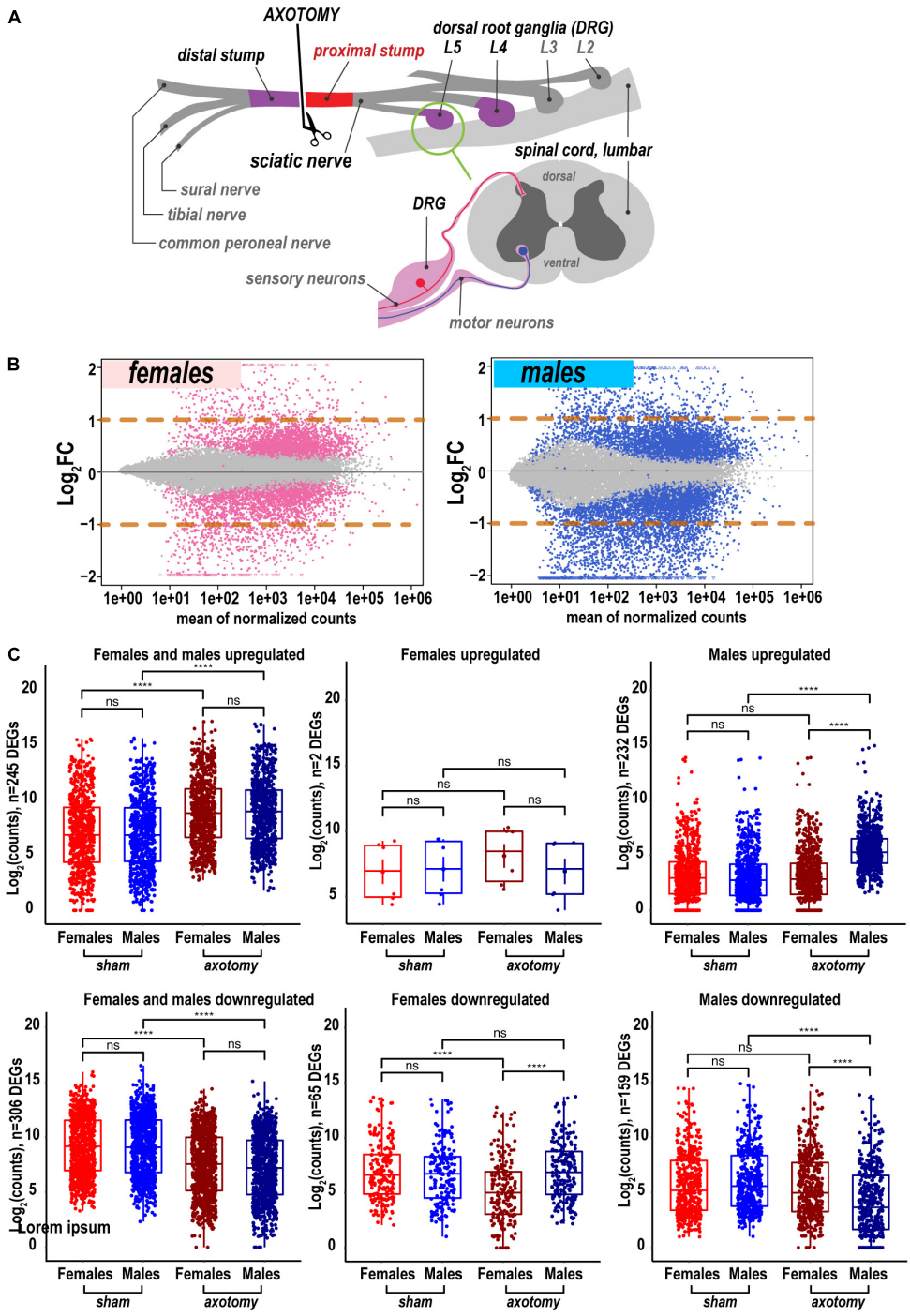

FIGURE 1
Global transcriptional changes in proximal nerve 24 h post-axotomy lead to a larger number of increased transcripts in males. **(A)** A schematic of the sciatic nerve axotomy followed by ipsilateral proximal stump tissue analysis. **(B)** MA plots display $\log_2$FC and mean counts normalized using *DESeq2* and adaptive t-prior *apeglm* method. The left and right panels show up- and downregulated genes in females (red dots) and males (blue dots), respectively. Dots indicate differentially expressed genes (DEGs) with $P_{adj} < 0.1$. Orange dashed lines show $\log_2$FC thresholds above 1 or below −1. **(C)** Scatter plots of significant up- and downregulated DEGs in females (light and dark red dots) and males (light and dark blue dots). Light and dark color intensity indicate DEGs in sham or axotomy samples (n = 6 mice/group, 2 mice/sample (pooled), 3 sample/group), respectively. DEGs ($P_{adj} < 0.1$) were filtered by $\log_2$FC either above 1 or below −1 (two-fold change or larger). Dots on the Y-axis correspond to the absolute gene expression measured as normalized mean counts following logarithm transformation of gene counts [$\log_2$(counts)] by the *normTransform* method in *DESeq2*. Specific expression data for DEGs is available in **Supplementary Table 1** and the GEO repository (accession numbers GSE182713 and GSE182709). Pairwise comparisons were made using the analysis of variance (ANOVA) with the Tukey *post hoc* test: ****, $p \leq 0.00005$; ns, not significant.

Sexually dimorphic gene regulation in injured nerves

Heatmaps (**Figure 2A**) and volcano plots (**Figure 2B**) present the identity of the most significant protein-coding DEGs in each sex. Principal component analysis (PCA) identified their contribution to variance in axotomized samples from males and females based on normalized count ranking. Sample-to-sample comparisons using PCA demonstrated that female and male samples aggregated as distinct clusters in the PC1/PC2 dimensions (**Figure 2C**).

The most significant DEGs that contributed to gene expression variance in females encoded a major acute-phase serum amyloid A-1 protein (*Saa1*), leucine-rich repeat-containing protein 15 (*Lrcc15*), neuronal pentraxin-2 (*Nptx2*), heterodimeric neurotropic cytokine receptor-like factor 1 (*Crlf1*), cardiotrophin-like cytokine factor 1 (*Clcf1*), and sonic hedgehog protein (*Shh*). In males, DEGs encoding the potassium channel subfamily T member 1 (*Kcnt1*), apoptosis-promoting dendrin (*Ddn*), inactive serine/threonine-protein kinase (*Plk5*), Toll-like receptor 9, and myelin-associated oligodendrocyte basic protein (*Mobp*) were the most significant drivers of variance. These and other DEGs identified by PCA (**Figures 2C,D**) could present potentially important sex-specific markers of early PNS injury response and nerve regeneration.

Gene ontology analysis identified sexual dimorphic genes relevant to peripheral nervous system (PNS) regeneration

Many sexually dimorphic and monomorphic DEGs were recognized as important components of cell signaling pathways in the nervous and immune systems. To gain further mechanistic insight into their role in nerve regeneration, gene ontology (GO) enrichment analysis was conducted. Molecular-level biochemical characteristics of DEGs were used to identify the most relevant GO clusters of molecular function (**Figures 3A,B**). GO clusters that included sexually dimorphic DEGs relevant to nerve injury response are illustrated in **Figure 3C** and detailed below.

Heterocyclic compound binding and ion binding proteins

Heterocyclic compound binding proteins interact with ATP, GTP, nucleobases, and their derivatives (cluster 1). Subunits of the ATP-driven Ca^{2+} ion pump (*Atp2b2, Atp2b3*), CaM kinase-like vesicle-associated protein (*Camkv*), ephrin type-A receptor 10 (*Epha10*), and N-acetylaspartylglutamate synthase A (*Rimkla*) were significantly upregulated in male nerves. In females, cyclin-dependent kinase 18 (*Cdk18*) and cGMP-dependent protein kinase 2 (*Prkg2*) were upregulated. Notably, most proteins that bind charged ions (cluster 2) were upregulated only in males, including the protein kinase C-binding protein Nell1, and Ca^{2+} sensors regulating vesicular release, the double C2-like domain-containing protein α (*Doc2a*), and Ca^{2+}-binding protein 7 (*Cabp7*), the hippocalcin-like protein 4 (*Hpcal4*), and β-synuclein (*Sncb*) involved in neuronal plasticity.

Carbohydrate derivative binding

Several carbohydrate-binding proteins (cluster 4) were downregulated in female nerves, including the protein kinase C (PKC)-binding protein (*Nell2*), inactive heparanase-2 (*Hpse2*), phospholipase A2 (*Pla2g5*), matrix-assembly related SPARC-related modular Ca^{2+}-binding protein (*Smoc2*), and a cysteine-rich secretory protein LCCL (*Crispld2*). In males, these proteins exhibited high levels of expression. In addition, genes encoding Nell1, neuronal adhesion neurocan core protein (*Ncan*), brevican core protein (*Bcan*), and β-amyloid precursor protein (*Aplp1*) were upregulated and expressed in males.

Cytoskeletal binding and structural proteins

Male nerves displayed higher up-regulation of the microtubule-associated neuronal migration protein doublecortin (*Dcx*), the actinin-interacting Cdk5 activator Cdk5r2, Gap junction β6 protein (*Gjb6*), GAR domain-containing protein (*BC024139*), the microtubule-stabilizing MAP6 domain-containing protein (*Map6d1*), cytoplasmic dynein intermediate (*Dync1i1*), and the microtubule-associated serine/threonine-protein kinase (*Mast1*) (cluster 8). Oppositely, mRNAs encoding kinesin-like motor enzymes Kif15/Kif22/Kif23, nucleolar and spindle associated protein (*Nusap1*), spindle/kinetochore-associated protein (*Ska1*), and a centromere-associated protein (*Cenpe*) were reduced in males. Microtubule-associated oxygen-regulated protein Rp1 and neuron navigator Nav3 demonstrated more robust upregulation in female nerves.

Genes encoding structural proteins demonstrated strong upregulation in both sexes (cluster cl24) of tubulin (*Tubb3, Tubb2b, Tuba8*, and *Tubb2a*), collagen (*Col28a1*, *Col2a1*, and *Col16a1*), and glial fibrillary acidic protein (*Gfap*) genes. In contrast, β-adducin (*Add2*), light and heavy chains of neurofilament (*Nefl* and *Nefh*, respectively), spectrin β chain (*Sptbn2*), and Laminin subunit α5 (*Lama5*) showed male-dominant upregulation.

Cytokine binding

Reduced expression of many cytokine receptors was observed in both sexes (cluster 9), including interleukin receptors (*Il31ra, Il5ra, Il12rb2*), chemokine receptors (*Ccrl2, Ccr5, Ccr2, Ccr9, Ccr1l1*, and *Ccr3*), and other receptors (*Tnfrsf14, Csf1r, Ackr1,* and *Ackr4*). Despite the decrease, the absolute expression levels of many cytokine receptor genes remained high. Only cytokine receptor-like factor 1 (*Crlf1*)

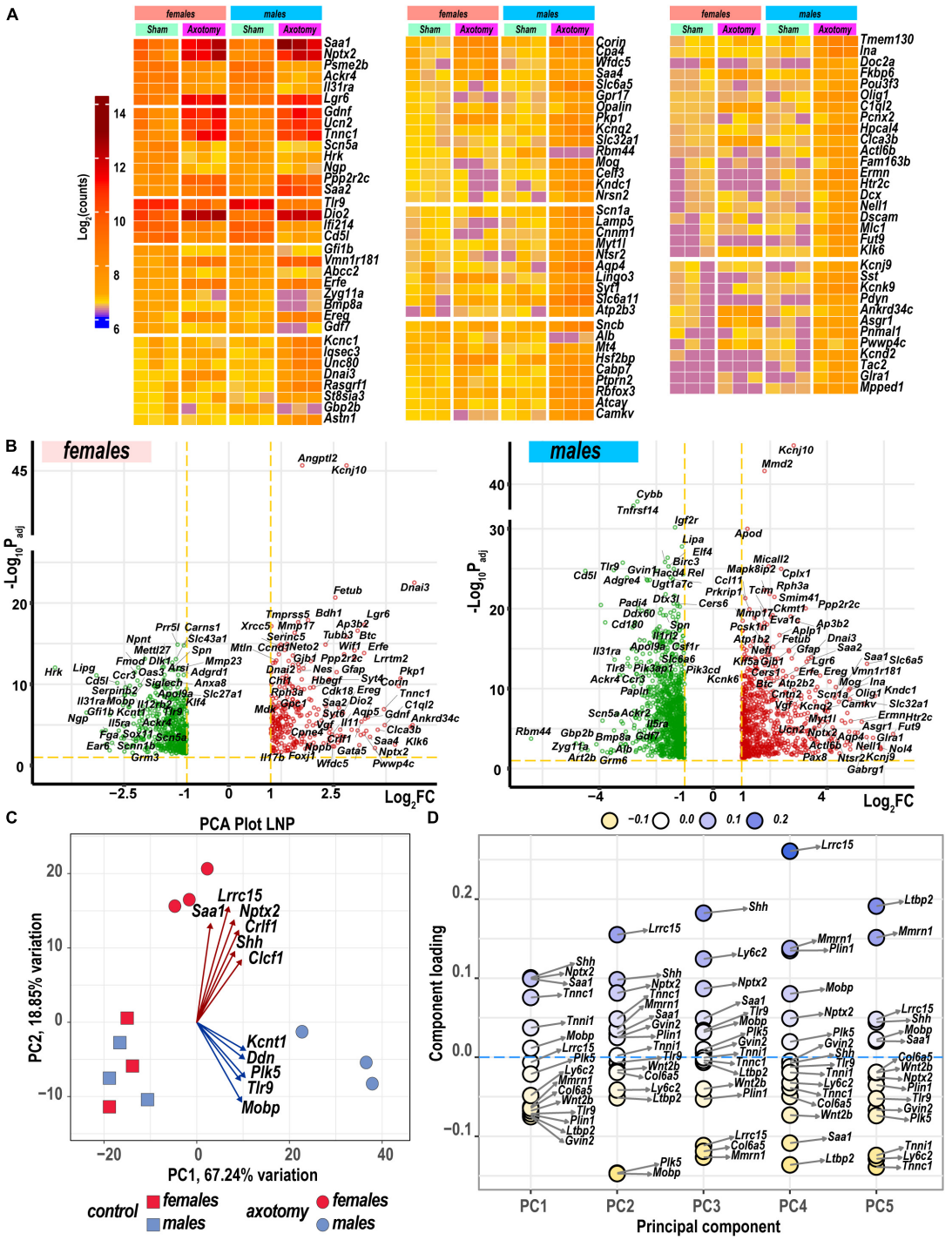

FIGURE 2
Nerve axotomy induced distinct sexually dimorphic regulation of differentially expressed genes (DEGs) in female and male mice. **(A)** Hierarchical clustering plot of 300 most significant upregulated DEGs ($log_2FC > 1$, $P_{adj} < 0.1$, $n = 6$ mice/group, 2 mice/sample (pooled), 3 sample/group). Heatmap colors correspond to mean log_2(counts)—Blue, yellow, and red – low, medium, and high expression, respectively. DEGs were sorted by log_2FC. **(B)** Significant DEGs in female (left panel) and male (right panel) mice. Volcano scatter plots show $-log_{10}P_{adj}$ and log_2FC. Red and green colors indicate up- and down-regulated DEGs, respectively. Thresholds ($log_2FC > 1$ or $log_2FC < -1$) and $-log_{10}P_{adj} < 0.1$ are indicated by yellow dashed lines. Selected DEG symbols are shown. **(C)** Principal component analysis of female (red) and male (blue) groups of sham (rectangles) and axotomy (circles) samples ($n = 3$ samples/group). Red and blue arrows indicate genes with the most influence on variance in females and males, respectively. **(D)** A principal component analysis (PCA) loading plot indicates genes influencing variance in the top five PCA projections (PC1 to PC5) within the top/bottom 5% of the loadings range. The dot color scale corresponds to component loading coefficients defined as the coordinates of the variables divided by the square root of the eigenvalue associated with the component.

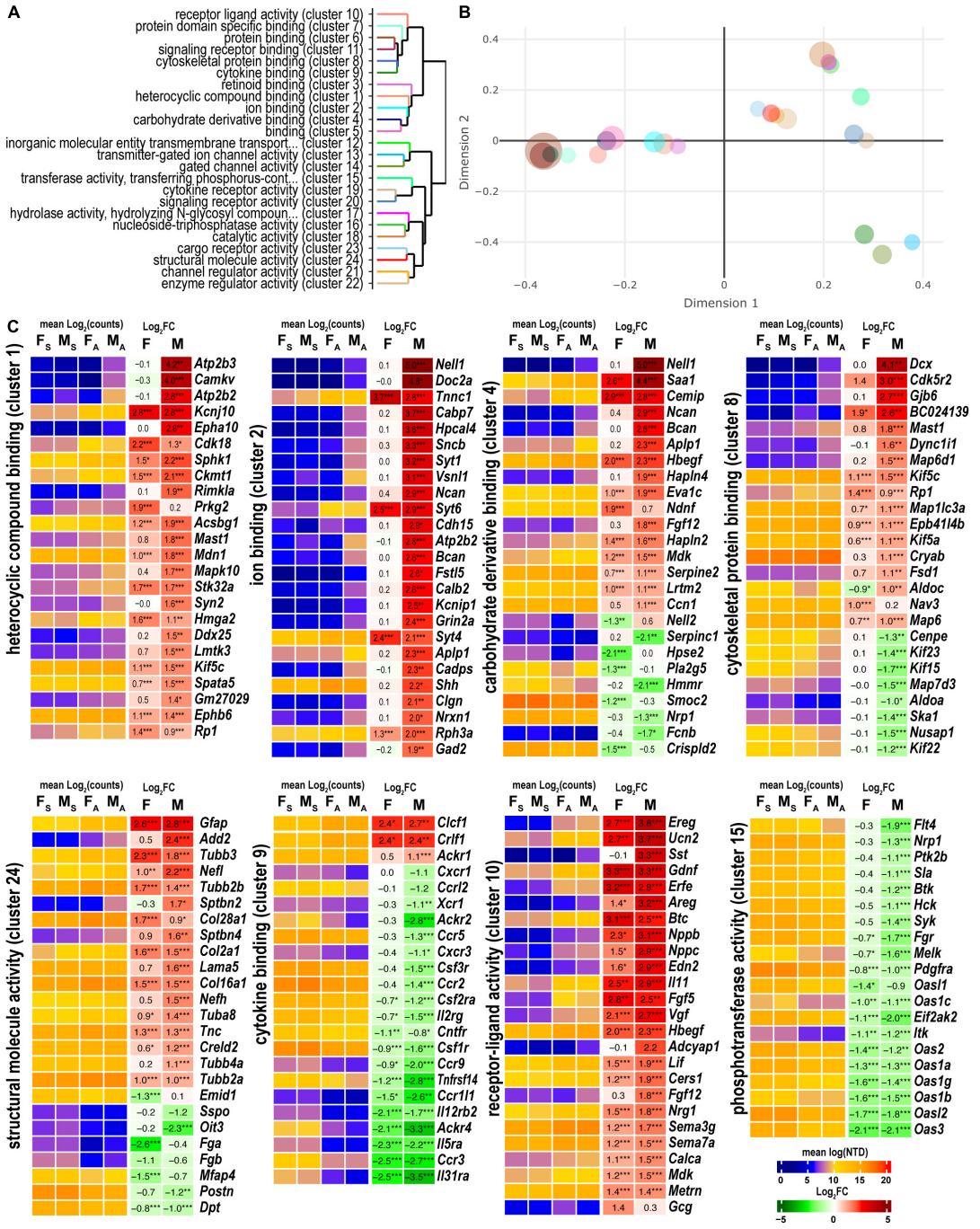

FIGURE 3
Axotomy influenced distinct molecular functions in each sex. **(A)** Clustering of significant gene ontology (GO) molecular functions based on best-match average (BMA) distances. **(B)** Wang distances of GO molecular function clusters projected on a two-dimensional scaling plot using the *ViSEAGO* R package. **(C)** Heatmaps of differentially expressed genes (DEGs) associated with eight GO molecular functions: heterocyclic compound binding (cluster 1), ion binding (cluster 2), carbohydrate derivative binding (cluster 4), cytoskeletal protein binding (cluster 8), cytokine binding (cluster 9), receptor-ligand activity (cluster 10), phosphotransferase activity (cluster 15), and structural molecule activity (cluster 24). Heatmaps display normalized mean $\log_2$(counts) in sample groups (F_S, female sham; M_S, male sham; F_A, female axotomy; M_A, male axotomy) and $\log_2$FC in female (F) and male (M); (n = 6 mice/group, 2 mice/sample (pooled), 3 sample/group) of respective DEGs. $\log_2$FC significance was determined in DESeq2 using Wald test: *, $p \leq 0.05$; **, $p \leq 0.005$; ***, $p \leq 0.0005$. DEGs were sorted by $\log_2$FC.

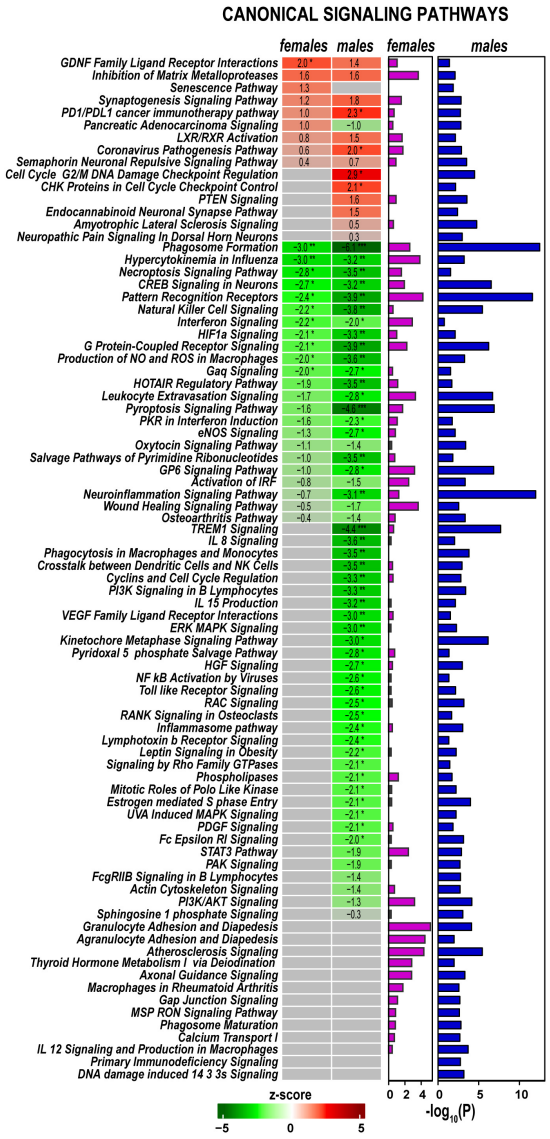

FIGURE 4
Canonical signaling pathways demonstrate distinct regulation patterns in females and males. Canonical pathways were predicted in Ingenuity Pathway Analysis (IPA) and ranked by z-scores. Positive (red) and negative (green) z-scores indicate pathway up-regulation or down-regulation, respectively, according to the color scale. Fisher's exact test *p*-values [$-\log_{10}$(P)] predicted for each canonical pathway are shown by purple (females) and blue (males) horizontal bars. Asterisks indicate significance *, z > 2.0 or z < −2; **, z > 3.0 or z < −3; ***, z > 4.0 or z < −4.

and corticotrophin-like cytokine factor 1 (*Clcf1*) demonstrated significant upregulation in both sexes.

Receptor ligand activity

Both males and females exhibited significant upregulation of ligand-encoding DEGs (cluster 10), including urocortin 2 (*Ucn2*), nerve growth factor inducible (*Vgf*), endothelin (*Edn2*), calcitonin (*Calca*), glial cell differentiation regulator meteorin (*Metrn*), leukemia inhibitory factor (*Lif*), glial-derived neurotrophic factor (*Gdnf*), epidermal growth factor β-cellulin (*Btc*), epidermal growth factor-like (*Egfl8*), and fibroblast growth factor (*Fgf5*). Male-specific upregulation of somatostatin (*Sst*), pituitary adenylate cyclase-activating polypeptide (*Adciap1*), cholecystokinin (*Cck*), neuropeptide galanin (*Gal*), ghrelin (*Ghrl*), and pro-opiomelanocortin (*Pomc*). Proglucagon (*Gcg*) and stanniocalcin-1 (*Stc1*) exhibited upregulation in females.

Phosphotransferase activity

Phosphotransferases (cluster 15), including non-receptor tyrosine kinases encoded by the *Btk, Hck, Syk,* and *Itk* genes, decreased in male nerves. In addition, both female and male nerves showed reduced expression of multiple members of the interferon-induced 2'-5'-oligoadenylate synthases members (*Oas3, Oasl2, Oas1b, Oas1g, Oas1a, Oas2, Oas1c,* and *Oasl1*).

Axotomy significantly reshaped cell signaling in regenerating nerves

Signaling pathways, upstream regulation, and interactive networks were predicted by Ingenuity Pathway Analysis (IPA) software using a highly stringent subset of DEGs ($P_{adj} < 0.001$ and $\log_2FC > 1$ or $\log_2FC < -1$). Significant canonical pathways were further ranked based on Fisher's exact test ($p < 0.05$). Positive or negative z-scores determined pathways' activation and deactivation.

Axotomy-induced significant changes in cellular signaling processes in both sexes (**Figure 4**), including pathways with female- or male-specificity. Accordingly, *GDNF Family Ligand Receptor Interactions*, *Inhibition of Matrix Metalloproteinases, Synaptogenesis Signaling Pathway, LXR/RXR Activation, PD1/PDL1 cancer immunotherapy pathway,* and *Coronavirus Pathogenesis Pathway* demonstrated activation in both sexes. *PTEN Signaling, CHK Proteins in Cell Cycle Checkpoint Control, Cell Cycle G2/M DNA Damage Checkpoint Regulation,* and *Endocannabinoid Neuronal Synapse* pathways were activated in males. In females, *Senescence Pathway* and *Pancreatic Adenocarcinoma Signaling* were activated. Many pathways exhibited downregulation in both sexes, including *Neuroinflammation Signaling, Pattern Recognition Receptors, Phagosome Formation, Pyroptosis Signaling, Leukocyte Extravasation Signaling, HOTAIR Regulatory Pathway, G Protein-Coupled Receptor Signaling,* and *Natural Killer Cell Signaling*. In addition, males specifically reduced *PI3K/AKT Signaling, Kinetochore Metaphase Signaling, IL-8 Signaling,* and *TREM1 Signaling* pathways. In both sexes, regenerating nerves displayed activation of *Macrophages in Rheumatoid Arthritis, Axonal Guidance, Thyroid Hormone Metabolism I via Deiodination, Atherosclerosis Signaling,*

and Agranulocyte/Granulocyte Adhesion and Diapedesis canonical pathways.

Upstream regulator molecules

Predictive analysis of upstream regulators was conducted in IPA to identify regulatory molecules, including transcription factors (TFs), any gene or small molecule that, with high probability, could affect the expression of their target DEGs. The activation or inhibition efficiency of each upstream regulator on target DEGs could be defined by positive or negative z-scores, respectively, as illustrated in **Figure 5** and summarized in **Supplementary Table 2**. Worth noting that upstream regulator z-scores do not directly reflect the expression of the regulator itself (Krämer et al., 2014), as different organs or tissues can contribute regulatory molecules. IPA identified many sexually dimorphic upstream regulators, including the brain-derived neurotrophic factor (Bdnf), a known stimulator of the nerve axon growth (Zhou and Shine, 2003). Bdnf was predicted to strongly affect gene expression in males but not females. Bdnf level was low in the proximal nerve stumps in both sexes. However, Bdnf mRNA was highly abundant in DRG and demonstrated a male-dominant increase post-axotomy (Chernov and Shubayev, 2021). Other male-specific upstream positive regulators included Sox2, Aire, Egr2, Cdkn1a, Map2k1/2, and other molecules. Ikzf3, Mek, Erk, and Akt1 were predicted as prospective positive regulators in females. Remarkably, IRFs, STATs, and cytokines were identified among significant negative regulators in both sexes.

Sexually dimorphic protein phosphorylation

Protein kinases and their regulatory molecules were identified as significant sexually dimorphic upstream regulators (**Figure 6A** and **Supplementary Table 2**). Male-specific upregulation of Kndc1 (also known as Very-KIND) may modulate Hras, Myc, Neu1, Ras, and Map2 (**Figure 6B**) during neuronal growth (Huang et al., 2007). Highly expressed Cdk5 was moderately activated by axotomy in male nerves. Cdk5 activator molecule that also controls cytoplasmic or nuclear localization of the Cdk5 complex demonstrated male-dominant upregulation. Co-upregulation of Cdk5-interacting and target molecules in males was significantly stronger than in females (**Figure 6C**). While female nerves upregulated fewer protein-coding DEGs than males, two female-specific interactive networks were determined using the STRING database (Szklarczyk et al., 2021). The first proposed network potentially conveys Gdnf signaling *via* the neuron-specific adaptor Shc3, the Gdnf receptor α1 (Gfra1), and neural cell adhesion proteins Chl1 and Cadm1 to regulate cell-cell adhesion and neuronal plasticity (**Figure 6D**). Another network is centered around the regulatory component of the Cyclin D1 (Ccnd1)-Cdk4 complex (**Figure 6E**). It is known to respond to Timp1 that activates cyclic AMP-induced regenerative program gene post-axotomy (Liu et al., 2015) partly *via* Cd63/Pi3k/Akt signaling (Rossi et al., 2015).

Cell signaling engages sexually dimorphic molecular programs

Regulatory signaling events reflect distinct molecular programs involved in regenerating nerves. Programs exhibiting sexually dimorphic regulation are as follows:

Neuronal survival and regeneration programs

GDNF Family Ligand Receptor Interactions pathway is modulated by the Gdnf and related ligands: neurturin (*Nrtn*), artemin (*Artn*), and persephin (*Pspn*). Notably, the *Gdnf* gene was highly upregulated in both sexes in the proximal stumps (**Figure 7A**) but not in DRG (Chernov and Shubayev, 2021). Neurturin was upregulated in males. Artemin was mildly expressed in distal stumps but significantly upregulated in male DRG. The ligand receptors encoded by Gfra1 and Gfra3 genes increased in both sexes.

Regeneration-associated genes (RAGs) were rapidly induced by axotomy in the corresponding DRG (Chernov and Shubayev, 2021). *Fos, Jun, Smad3, Creb1, Rac2, Klf6,* and *Atf3* mRNAs were detected in the nerves (**Figure 7B**). Cebpd, a bZip-containing CCAAT/enhancer-binding protein δ, increased in both sexes. The *Sox11* gene was 4-fold explicitly downregulated in females.

Extracellular matrix (ECM) homeostasis and regulation of proteolysis

Both male and female nerves upregulated matrix metalloproteinase (MMP) Mmp17 (MT4-MMP) expression (**Figure 7C**). Mmp24 moderately increased only in males. A group of MMP genes co-localized in the 9qA1 locus of the mouse chromosome 9, Mmp8, Mmp12, Mmp13, and Mmp27, synchronously decreased only in males. Mmp25 decreased in both sexes. Other MMP genes, including Mmp2, Mmp3, Mmp14, Mmp15, and Mmp19, demonstrated high expression levels in both sham and axotomy nerves irrespective of sex.

Many endogenous inhibitors of proteinases exhibited sexually dimorphic regulation of gene expression, including the WAP domain proteinase inhibitor (*Wfdc5*), the cysteine protease inhibitor (*Fetub*), and serine protease inhibitor Kazal-type 1 (*Spink1*). *Timp1* increased in both sexes, in agreement with our previous reports (Kim et al., 2012; Liu et al., 2015; Chernov and Shubayev, 2021). The glia-derived nexin (Serpine2) was upregulated, but other serine protease inhibitors of the serpin family were downregulated. Inter-α-trypsin

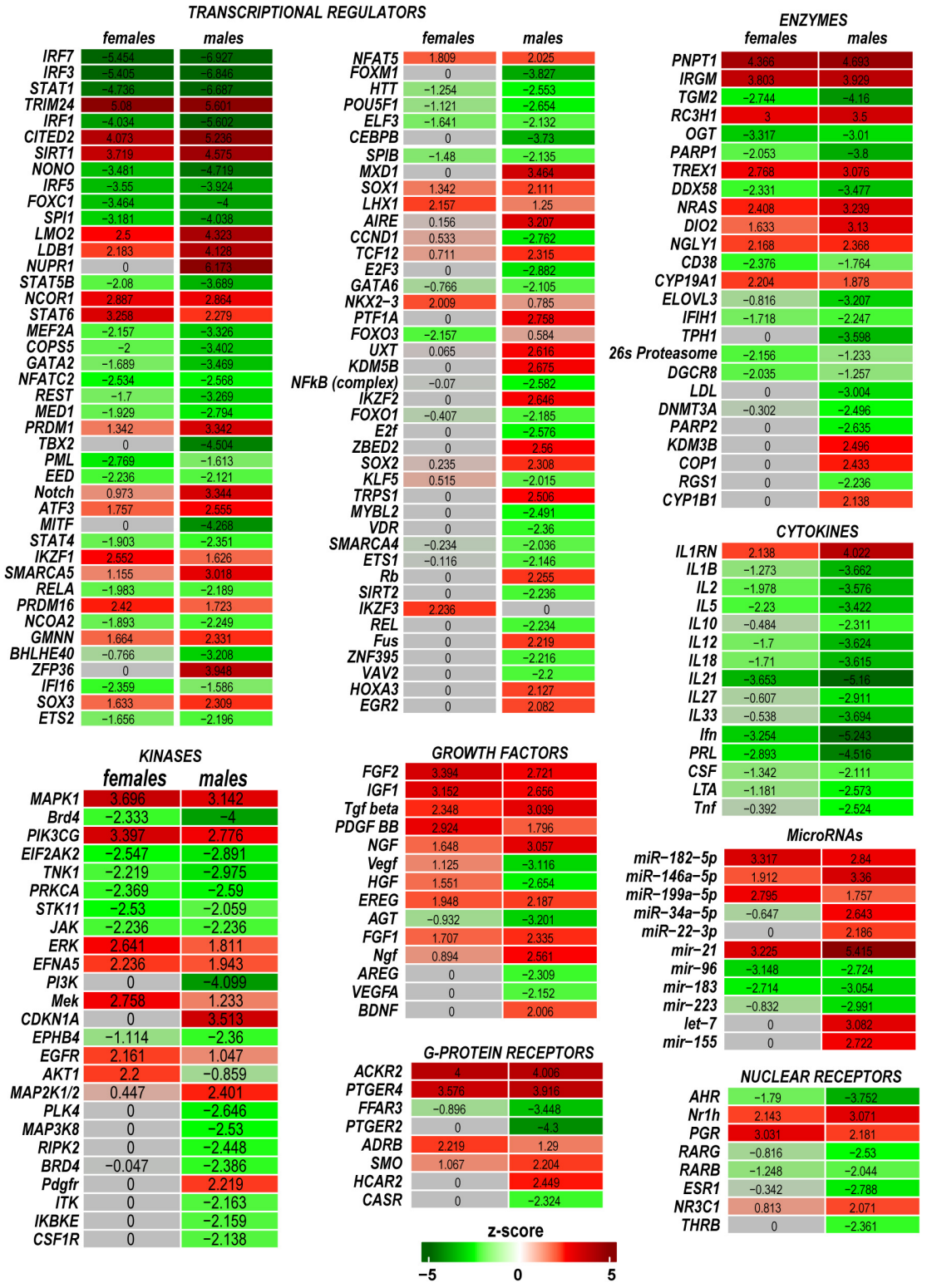

FIGURE 5
Upstream regulators of the post-injury response included transcriptional regulators, kinases, growth factors, G-protein receptors, enzymes, cytokines, microRNAs, and nuclear receptors. Positive (red) and negative (green) z-scores indicate regulator effects to upregulate or downregulate respective differentially expressed genes (DEGs). The color scale represents the z-score range.

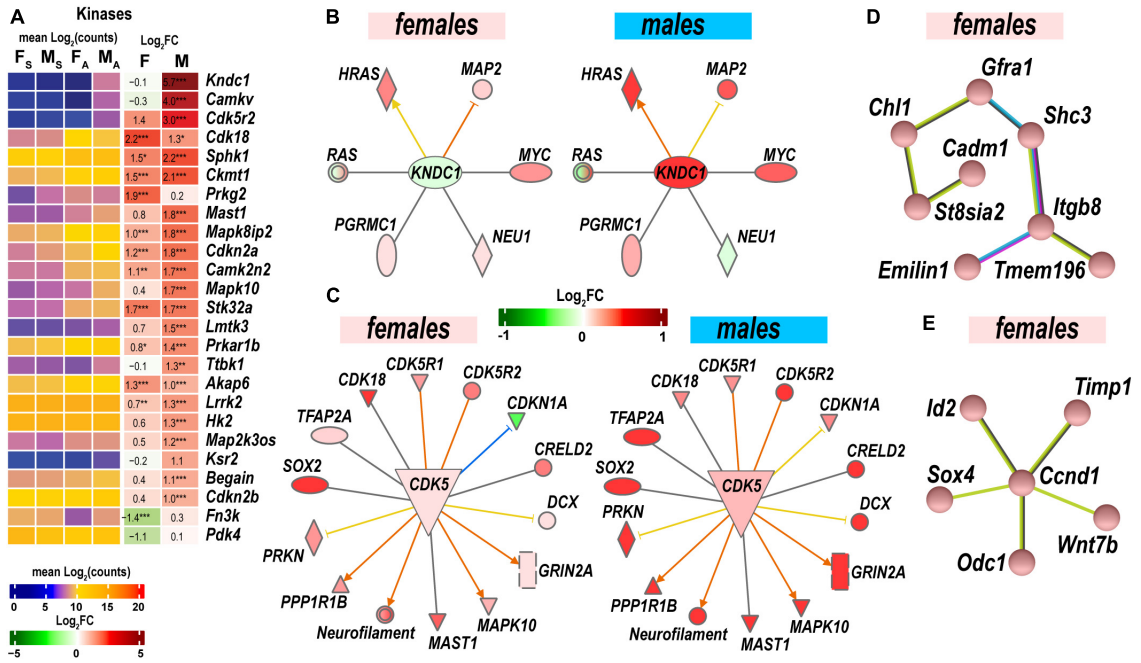

FIGURE 6

Protein phosphorylation was strongly activated to regulate cell-cell adhesion and neuronal plasticity. **(A)** Expression of differentially expressed genes (DEGs) with kinase activities. Heatmaps display normalized mean $\log_2$(counts) in sample groups (F_S, female sham; M_S, male sham; F_A, female axotomy; M_A, male axotomy) and $\log_2$FC in female (F) and male (M); (n = 6 mice/group, 2 mice/sample (pooled), 3 sample/group) of respective DEGs. Log_2FC significance was determine in DESeq2 using Wald test: *, $p \leq 0.05$; **, $p \leq 0.005$; ***, $p \leq 0.0005$. DEGs were sorted by $\log_2$FC. **(B)** RAS-Guanine nucleotide exchange factor KNDC1 links HRAS, MYC, NEU1, RAS, and MAP2. Male but not female nerves exhibit upregulation of key components. **(C)** Protein interaction networks regulated by CDK5 in females (left) and males (right). **(D)** Female-specific Gfra1/Cadm1 axis. **(E)** Proposed regulation by female-prevalent Ccnd1/Timp1 axis. The shape's colors on panels B and C correspond to up- (red) or down- (green) regulation of respective DEGs according to the Log_2FC scale. Protein interactive networks were predicted in IPA (panels **B** and **C**) and the STRING database (panels **D** and **E**).

inhibitor heavy chain H3 (Itih3) and serine proteinase inhibitor Serpinb1b demonstrated male-specific upregulation.

Regulation of synaptogenesis signaling

Synaptogenesis Signaling Pathway was distinctly regulated in both sexes. Genes encoding components of synaptic vesicles (SV) showed greater activation in males (Figure 7D). Consequently, the male-dominant increase of the pre-synaptic-like activity and vesicular transport can be mediated by synuclein subunits α, β, and γ, Rab3A oncogene, and vesicle-associated membrane protein (*Vamp2*). It is important to note that SV-related genes show high levels of expression in sham and axotomized female nerves; therefore, male-prevalent gene activation could level up pre-synaptic activity to match the activity in females.

Axonal transport

Axonal transport is essential for neuronal survival and function restoration after damage. Many kinesins involved in anterograde axonal transport decreased in males (Figure 7E), except Kif5 family members increased in males. Retrograde transport-related axonemal dynein/dynactin encoding genes showed remarkable sexually dimorphic regulation. Most notably, dynein intermediate chain mRNAs Dnai2 and Dnai3 highly increased in both sexes. Dynein heavy chain mRNA Dnah12/17 decreased in males.

Myelin sheath

Male nerves upregulated myelinogenesis- and neuron morphogenesis-related DEGs (according to GO term GO:0043209), including ermin (*Ermn*), α-internexin (*Ina*), myelin oligodendrocyte glycoprotein (*Mog*), opalin (*Opalin*), contactin 2 (*Cntn2*) (Figure 7F). The expression of these DEGs in females remained low. Other myelin sheath-related molecules were represented in both sexes and exhibited further upregulation in males. Notably, myelin-associated oligodendrocyte basic protein (*Mobp*) demonstrated significant sexually dimorphic regulation by upregulating in males and downregulating in females.

Regulation of neuroreceptors, transporters, and ion channels

Male, but not female, nerves demonstrated increased levels of transmitter-gated ion channel mRNAs (Figure 8A)

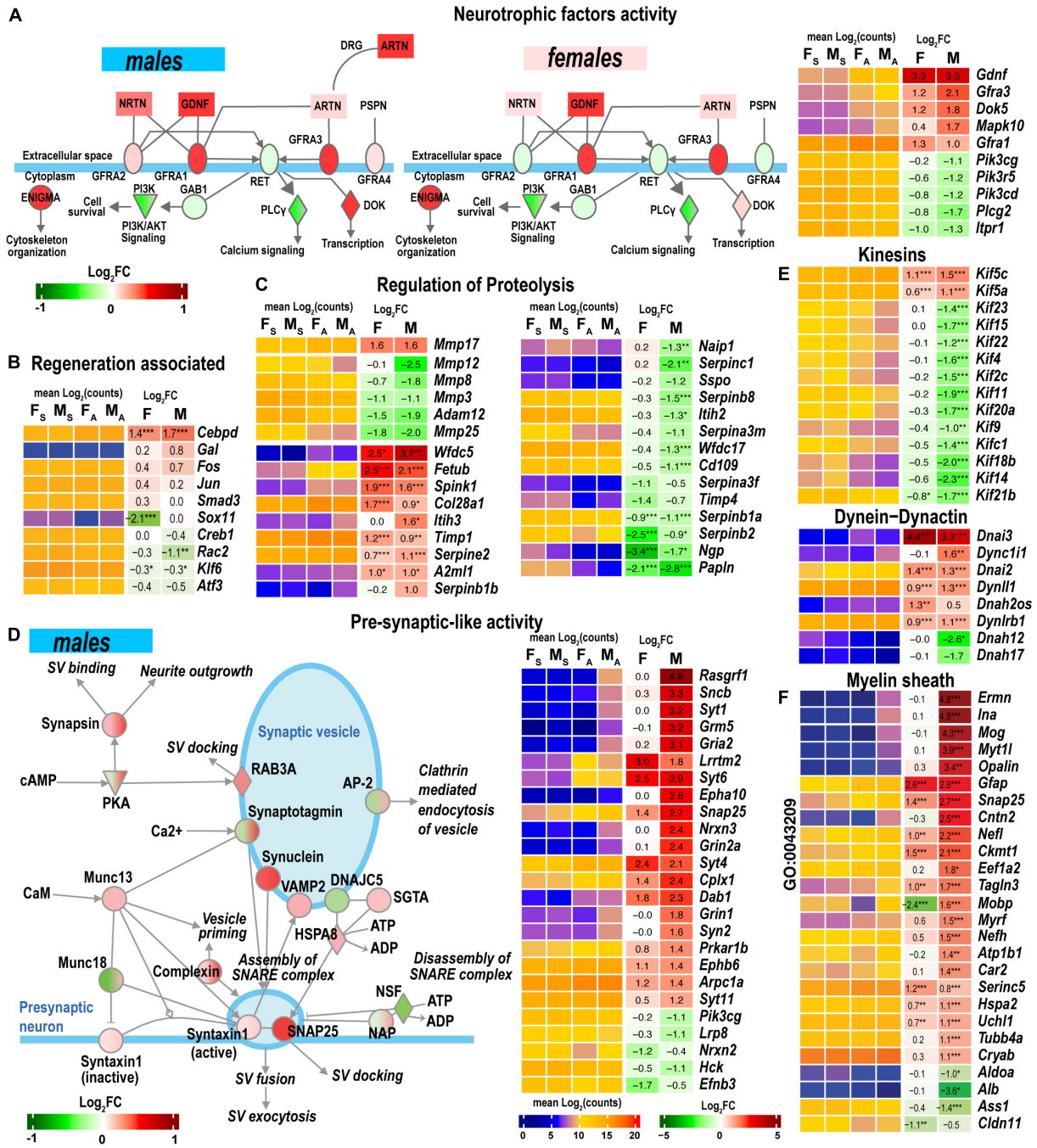

FIGURE 7

Nerve regeneration-related signaling and pre-synaptic-like activity exhibited sexually dimorphic activation. **(A)** glial cell line-derived neurotrophic factor (GDNF) family of ligands can drive the cytoskeleton organization, Pi3k/Akt signaling, Ca^{2+}-signaling, and regulate downstream gene transcription. The diagram partially corresponds to the *GDNF Family Ligand Receptor Interactions Pathway* predicted by Ingenuity Pathway Analysis (IPA). Colors correspond to up- (red) or down- (green) regulation of respective differentially expressed genes (DEGs) according to the Log_2FC scale. Protein interactive networks were predicted in IPA. **(B)** Regeneration-associated DEGs. **(C)** Regulation of extracellular proteolysis-related DEGs. **(D)** Pre-synaptic-like activity in male nerves. The diagram partially corresponds to the *Synaptogenesis Signaling Pathway* predicted by IPA. Colors correspond to up- (red) or down- (green) regulation of respective DEGs according to the Log_2FC scale. **(E)** Kinesins, dynein-dynactin DEGs. F, Myelin sheath-related DEGs. Heatmaps on panels **A–C, E**, and **F** display normalized mean log_2(counts) in sample groups (F_S, female sham; M_S, male sham; F_A, female axotomy; M_A, male axotomy) and log_2FC in female (F) and male (M); (n = 6 mice/group, 2 mice/sample (pooled), 3 sample/group) of respective DEGs. Log_2FC significance was determined in DESeq2 using Wald test: *, $p \leq 0.05$; **, $p \leq 0.005$; ***, $p \leq 0.0005$. DEGs were sorted by log_2FC.

encoding ionotropic γ-aminobutyric acid (GABA) receptors (*Gabra1, Gabra5, gabrg2, Gabrb1, Gabrb2, Gabrb3,* and *Gabrg1*), members of ionotropic glutamate receptor N-methyl-D-aspartic acid (NMDA) receptor subunits (*Grin1, Grin2a,* and *Grin3a*), α-amino-3-hydroxy-5-methyl-4-isoxazole propionic acid (AMPA) receptor subunits Gria1 and Gria2, kainic acid receptor subunit Grik1. Notably, mRNAs encoding 5-hydroxytryptamine 2C (serotonin) receptors Htr2c and Htr3a also increased. Male nerves exhibited increased potassium, calcium, and sodium voltage-gated ion channel-related mRNAs. Remarkably, levels of these mRNAs diminished in the respective DRGs measured in the same animal cohorts (Chernov and Shubayev, 2021), suggesting the involvement of sex-specific axonal mRNA transport in the redistribution of injury-related mRNAs during early-phase response. Female nerves showed no change in ion-channel mRNA levels, except for *Cacna1g, Scb5a, Kcnt1,* and *Kcnq5, demonstrating* a reduction.

Immune regulation

Cytokines Il11 and Il17b were upregulated in both sexes, while Il6 and Il19 were predominantly activated in males (**Figure 8B**). Genes related to adaptive (GO:0002250) and innate (GO:0045087) immunity showed a system-wide male-specific decrease. Many immunity-related canonical pathways were significantly downregulated after axotomy in both sexes' proximal nerve segments, including *Neuroinflammation Signaling Pathway, Activation of IRF, Leukocyte Extravasation, Signaling, Interferon Signaling, Pattern Recognition Receptors,* and *Phagosome Formation* pathways (**Figure 4**). The following immunity-related pathways demonstrated male-specific negative regulation: *Inflammasome Pathway, Toll-like Receptor Signaling, IL-15 Production, PI3K Signaling in B Lymphocytes, Phagocytosis in Macrophages* and *Monocytes, and IL-8 Signaling.*

Transcription regulators

Male nerves significantly upregulated neuronal differentiation and reprogramming-related TFs, the myelin transcription factor 1-like protein (Myt1l), and POU domain-containing Pou3f3 (**Figure 8C**). Upregulation of oligodendrocyte transcription factors 1/2 (*Olig1/2*), neurogenesis-related TFs (*Zic1, Pou3f1/Oct6, Esrrb, Myrf,* and *Prrxl1*), and nuclear protein Nupr1 were male-specific. Also, males upregulated Fox-family TFs (*Foxf2, Foxj1, Foxd3,* and *Foxc2*), Hox-family TFs (*Hoxb5, Hoxb2, Hoxb8,* and *Hoxb3os*), and Sox-family TF genes (*Sox2* and *Sox10*), and the RNA-binding proteins ZFP36 known to restrain T cell activation and antiviral immunity (Moore et al., 2018). Sox2 and Sox4 TFs increased in females, but Sox11 decreased after axotomy. mRNA level of Gata5 was higher in females than in males. We concluded that post-axotomy regulation of TFs is characterized by sexually dimorphic patterns to potentially execute distinct regenerative programs in the PNS of females and males.

Cation transporting ATPases

Males but not females upregulated plasma membrane Ca^{2+}-transporting ATPase subunits Atp2b2 and Atp2b3 (**Figure 8D**). mRNAs of Na^{+}/K^{+}-transporting ATPase subunits Atp1b1 and Atp1b2 were abundant in both sexes and exhibited further increase in males.

Non-coding RNAs

Levels of *Mir124-1hg* and *Mir124-hg2* RNAs, the precursors of the ubiquitous neuronal microRNA Mir-124, were higher in males than in females (**Figure 9A**). In addition, small nucleolar RNAs (snoRNAs) encoded by *Snhg9, Snhg6,* and *Snora57* host genes showed male-dominant expression. The erythroid differentiation regulator 1 ncRNA encoded by the X-linked Erdr1 gene was upregulated in males but downregulated in females. U1 spliceosome RNA (U1) and ribonuclease P RNA component H1 (Rpph1) were upregulated in females.

Antisense lncRNAs (asRNA) can potentially target co-localized PNS injury-related genes *via* cis-acting mechanisms. In females, genes encoding the axonemal dynein (*Dnah2*), tetraspanin 32 (*Tspan32*), pseudopodium-enriched atypical kinase 1 (*Peak1*), SAP30 binding protein (*Sap30bp*), and H3.3 histone (*H3f3a*) could be targeted by the respective asRNA (**Figure 9B**). In males, asRNAs could target genes encoding deiodinase (*Dios3*), MAP2 kinase (*Map2k3*), RAB26 oncogene (*Rab26*), homeobox B2/B3 (*Hoxb2, Hoxb3*), dynamin 3 (*Dnm3*), the transcriptional repressor CCCTC-binding factor (*Ctcf*), *de novo* DNA methyltransferase 3a (*Dnmt3a*), and insulin-like growth factor 1 (*Igf1*).

Sex chromosomes

As reported in the DRGs of the same animal cohort (Chernov and Shubayev, 2021), genomic localization of DEGs on a sex-chromosome could potentially determine sexually dimorphic expression. In the proximal nerve stumps, most X-linked DEGs exhibited male-specific regulation (**Figure 9C**). However, several female X-linked DEGs, including *Magix, Tmem255a, Tmem28, Map7d2, Timp1, Erdr1, 2010204K13Rik, Gjb1, Pcsk1n, Bex2,* and *Pwwp4c*, were elevated in both sexes. Male-specific Y-linked transcript Gm47283 was upregulated post-axotomy in males.

Discussion

We obtained novel evidence of sexually monomorphic and dimorphic regulation of the early-phase transcriptional programs in regenerating segments of injured peripheral nerves (**Figure 10**). The concerted accumulation of mRNAs that encode actin, microtubules, neurofilaments, cytoskeletal regulators,

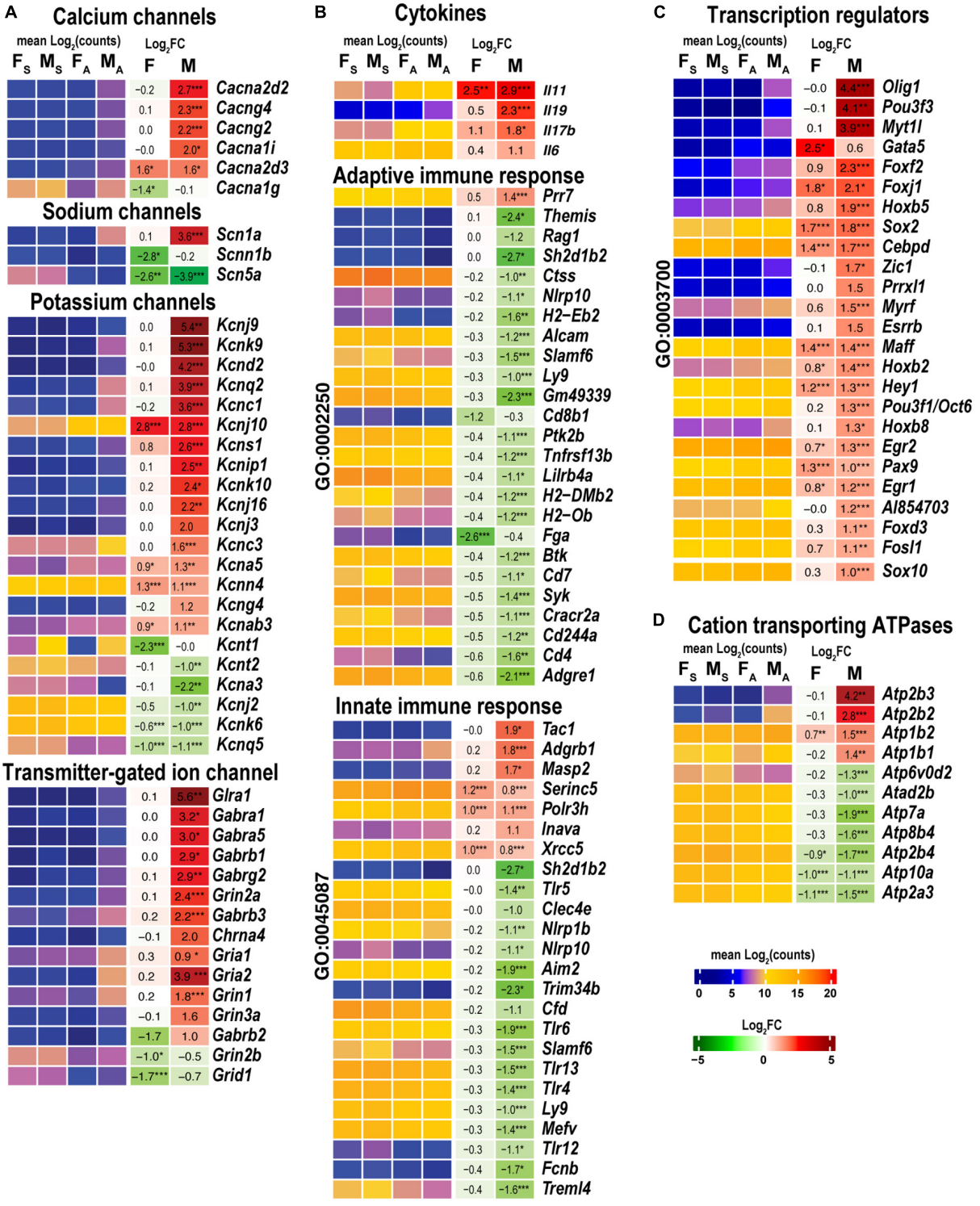

FIGURE 8
Males exhibited stronger activation of ion channels, transcriptional regulators, cation transporting ATPases, and select cytokines. Innate and adaptive immunity exhibited a male-specific decrease. **(A)** Ion channel genes. **(B)** Cytokines, adaptive (Go term GO:0002250), and innate (GO term GO:0045087) immunity-related DEGs. **(C)** DNA-binding transcriptional regulators (GO term GO:0003700). **(D)** Cation transporting ATPases. Heatmaps display normalized mean log_2(counts) in sample groups (F_S, female sham; M_S, male sham; F_A, female axotomy; M_A, male axotomy) and log_2FC in female (F) and male (M); (n = 6 mice/group, 2 mice/sample (pooled), 3 sample/group) of respective DEGs. Heatmap colors correspond to the respective scales. Log_2FC significance was determined in DESeq2 using Wald test: *, $p \leq 0.05$; **, $p \leq 0.005$; ***, $p \leq 0.0005$. DEGs were sorted by log_2FC.

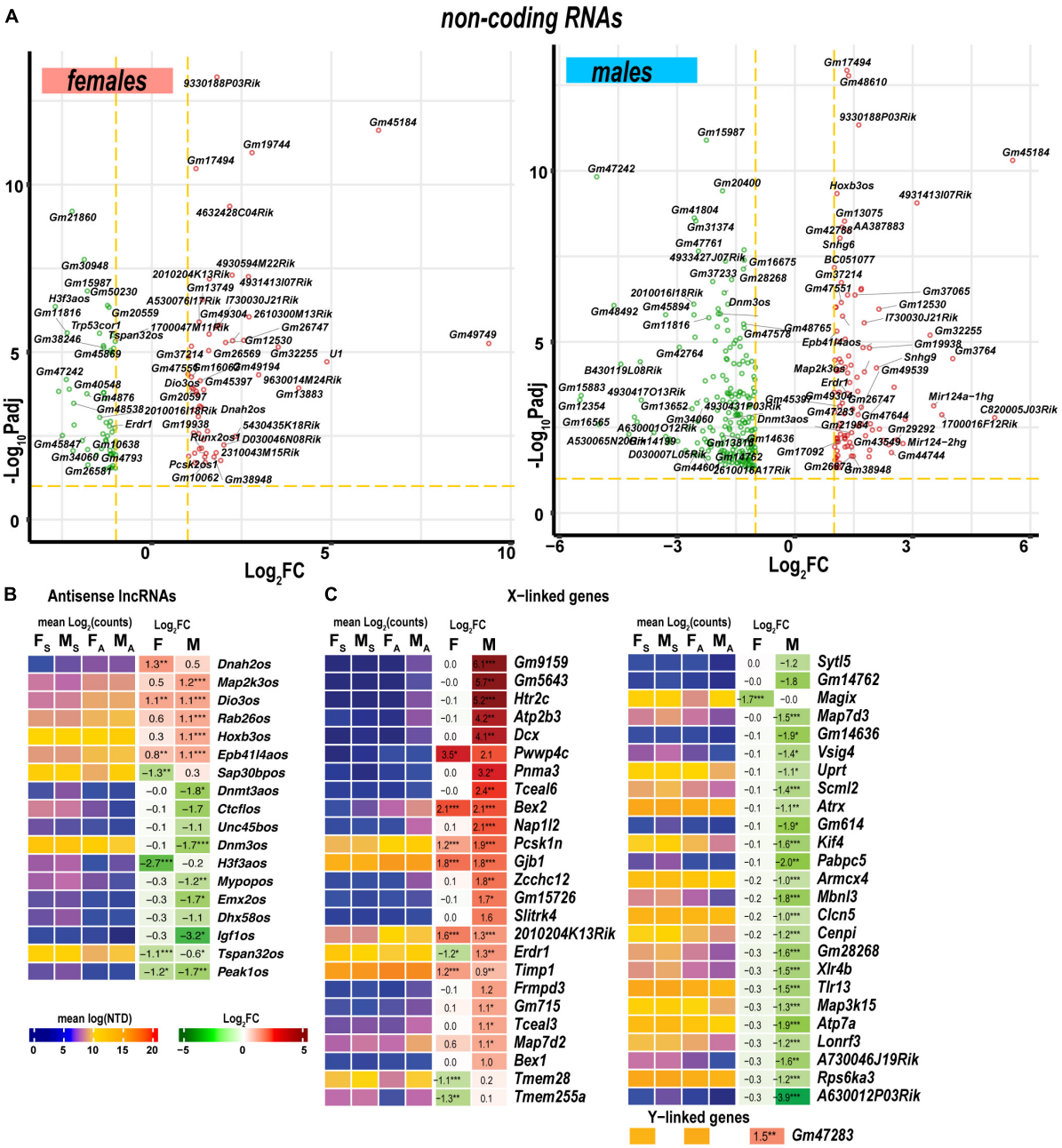

FIGURE 9
Regulated ncRNA and sex chromosome-linked differentially expressed genes (DEGs) exhibited profound sexual dimorphism. **(A)** Significant ncRNA DEGs in female (left panel) and male (right panel) mice. Volcano scatter plots show $-\log_{10}P_{adj}$ and $\log_2$FC. Red and green colors indicate up-and downregulated ncRNAs, respectively. Thresholds ($\log_2$FC > 1 or $\log_2$FC < −1) and $-\log_{10}P_{adj}$ < 0.1 are shown by yellow dotted lines. Selected DEGs are labeled by gene symbols. **(B)** Regulated antisense lncRNA DEGs. **(C)** Regulated sex chromosome-linked DEGs. Heatmaps display normalized mean $\log_2$(counts) in sample groups (F_S, female sham; M_S, male sham; F_A, female axotomy; M_A, male axotomy) and $\log_2$FC in female (F) and male (M); (n = 6 mice/group, 2 mice/sample (pooled), 3 sample/group) of respective DEGs. Heatmap colors correspond to the respective scales. $\log_2$FC significance was determined in DESeq2 using Wald test: *, $p \leq 0.05$; **, $p \leq 0.005$; ***, $p \leq 0.0005$. DEGs were sorted by $\log_2$FC.

and cytoskeleton-binding proteins was observed in proximal nerve stumps of both sexes, confirming extensive cytoskeletal remodeling aimed at rebuilding the growth cone (Lundborg, 1987; Burnett and Zager, 2004; Radtke and Vogt, 2009).

Schwann cell reprogramming

After nerve injury, Schwann cells assume a pro-regenerative function (Jessen and Mirsky, 2016, 2021;

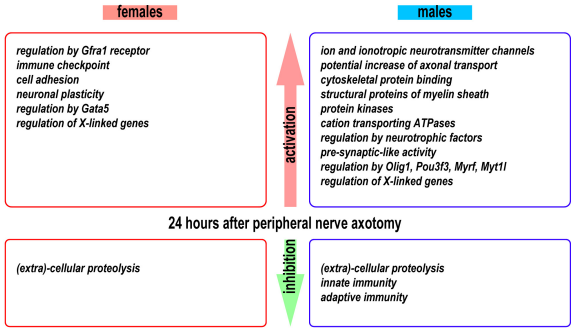

FIGURE 10
A summary of activated and inhibited transcriptional programs detected in the proximal nerve stumps 24 h post-axotomy in female and male mice.

Merrell and Stanger, 2016; Milichko and Dyachuk, 2020), exhibiting an exceptional phenotypic plasticity (Jessen and Arthur-Farraj, 2019; Stierli et al., 2019; Nocera and Jacob, 2020) that supports their de-differentiation, proliferation, and re-differentiation into myelinating and non-myelinating phenotype to facilitate repair of the respective axons. Schwann cell reprogramming is controlled by a set of TFs (Balakrishnan et al., 2021), including Myt1l, Pou3f1/Oct6, Myrf, Olig1/2, Jun, Sox-, Hox-, and Fox-family members TFs upregulated at 24 h post-axotomy predominantly in males. Transcripts of TF genes, such as *Fos, Smad3, Creb1, Rac2, Klf6,* and *Atf3*, that function as RAGs (reviewed in [Van Kesteren et al., 2011; Ma and Willis, 2015)] in the corresponding DRGs after PNS injury (Chernov and Shubayev, 2021) were detected in proximal nerve segments. In addition to transcriptional activity in cells of the PNS, this accumulation may reflect an anterograde transport from DRG in coordinated axonal regeneration processes post-axotomy. Single-cell RNA-seq and spatial transcriptomics analysis could provide crucial information on the identity of cell lineages activating these sexually dimorphic TFs.

The GDNF family of ligands (GDNF, neurturin, artemin, and persephin), known survival factors for neurons, bind to GFRA receptors, trigger the phosphorylation of RET tyrosine kinase receptor (Durbec et al., 1996) that is known to regulate Pi3k/Akt and Plcγ/Ip3r dependent Ca^{2+} signaling during neurogenesis (Fukuda et al., 2002; Lundgren et al., 2012) and, sometimes, hyperalgesia (Bogen et al., 2008). Furthermore, GDNF/Gfra1 could interact with neural cell adhesion molecules such as NCAM to induce an axonal expansion (Nielsen et al., 2009). GDNF family of ligands can act in a synergetic manner with other growth factors, including transforming growth factor-β (Tgf-β) and sonic hedgehog (Shh) [reviewed in Jessen and Mirsky (2021)]. GDNF signaling can stimulate the migration of neuronal precursors and Schwann cells (Iwase et al., 2005) to the injury site in both sexes.

Extracellular proteolysis

The outcome of nerve regeneration after sciatic nerve injury is partly dependent on the integrity of ECM-rich Schwann cell basal lamina and endoneurial tubes (Fawcett and Keynes, 1990). Proteolytic cleavage mediated by ECM proteinases and their endogenous inhibitors is indispensable for morphological remodeling of regenerating axons (Rivera et al., 2010; Fujioka et al., 2012; Bajor and Kaczmarek, 2013), after sciatic nerve injury (Liu et al., 2010). In addition, MMPs control the activity of critical growth factors, their ligands, and receptors in peripheral nerve, including IGF and neuregulin/ErbB (Chattopadhyay and Shubayev, 2009). Mmp17 was upregulated in both sexes and can convey inflammatory responses due to the TNFα-converting activity (English et al., 2000).

Intriguingly, a group of MMPs co-localized on the mouse chromosome 9 (Mmp3, Mmp8, Mmp12, Mmp13, and Mmp27) have decreased in both sexes. Because MMPs in the orthologous human chromosome 11q22.3 region could carry different histone modification marks (Chernov et al., 2010), epigenetic control of this set of metzincins may be involved. Consistent with our previous report, MMPs, and many disintegrin ADAM/ADAM-TS families of the ECM-remodeling metzincins demonstrate regulated expression in injured nerves (Chernov et al., 2015).

Notably, protease expression levels were high in intact and axotomized nerves. Processes of post-translational protease activation and binding to intrinsic proteinase inhibitors control potentially cytotoxic proteolytic activities. Aberrant cleavage of mediators of nociceptive signaling during neurogenesis potentially causes neuropathic pain (Remacle et al., 2015). Previously we identified Timps as key genes in the normal and damaged nerves (Kim et al., 2012; Nishihara et al., 2015) and post-axotomy DRG (Liu et al., 2015; Chernov and Shubayev, 2021). Timp1 binds and inhibits all MMPs, except Mmp14; Timp2 inhibits Mmp14 (Brew and Nagase, 2010). In the proximal nerve, Timp1 demonstrated strong

upregulation in both sexes. Other upregulated endogenous inhibitors of proteinases Wfdc5, Fetuin B, Spink1, Itih3, and Serpineb1b could serve a not well-understood role in nerve damage response.

Sex-specific control of axonal trafficking

An intact connection to DRG allows for dynamic axonal transport of protein and mRNA content between neuronal soma and the proximal segment of the axotomized nerve (Cavalli et al., 2005). The anterogradely transported mRNAs from DRG are directly used for the local protein synthesis at the site of the injury (Sahoo et al., 2018) and complemented by the transcriptional repertoire of the resident non-neuronal cells in the damaged nerve (e.g., Schwann cells, macrophages) that establish a microenvironment generally permissive for axon regeneration (Avraham et al., 2021).

Kinesins facilitate anterograde axonal transport of neurotransmitter receptors, mitochondria [reviewed in (Fan and Lai, 2021)], and also mRNAs [reviewed in (Kanai et al., 2004; Turner-Bridger et al., 2020)]. Remarkably, most kinesin mRNAs were depleted in proximal nerve segments at 24 h post-axotomy, except for members of the conventional kinesin-1 family Kif5a/b/c increased in males.

Retrograde transport of transcription factors from the site of nerve injury to DRG has been shown to facilitate the neuronal survival (Cox et al., 2008) and axon regeneration (Ito and Enomoto, 2016). In the corresponding DRGs of the same animal cohort, at 24 h post-axotomy, we observed male-specific reduction of mRNAs encoding calcium, sodium, and potassium ion channels as well as ionotropic AMPA, NMDA, and GABA receptors (Chernov and Shubayev, 2021) that correlated to their increase in proximal segments in the present study and presumably, anterograde axonal transport. We conclude that axonal transport of mRNAs contributes to sex-specific protein synthesis and downstream signaling programs both in DRG neurons and regenerating axons at the early stages of response to sensory nerve damage.

Sex chromosome encoded genes

Sex chromosome-encoded genes were activated in regenerating sciatic nerves. Several X-linked genes were differentially regulated in male and female nerves. Among X-linked genes induced in nerves of both sexes were *Timp1,* known to promote regeneration (Kim et al., 2012; Liu et al., 2015; Nishihara et al., 2015), and *Map7d2,* involved in kinesin-mediated cargo transport into the axon (Pan et al., 2019). It is worth noting that genes associated with the female-specific epigenetic X-chromosome inactivation (Xi) process were differentially expressed in DRGs within 24 h after post-axotomy in the same animal cohort (Chernov and Shubayev, 2021).

Conclusion

The noted remodeling represents baseline sexual dimorphism in uninjured peripheral nerves and an immediate regenerative response to nerve injury. The functional significance of the reported sexual dimorphism remains to be determined. It is conceivable that, at least partially, sex differences were equalized over the time-course of nerve injury. Single-cell RNA-seq and spatial transcriptomics analysis could provide crucial information on the identity of cell lineages activating these sexually dimorphic coding and non-coding RNAs.

Materials and methods

Reagents

Detailed descriptions of reagents and resources are included in **Supplementary Table 3**.

Animals

Female and male C57BL6/J mice (6–8 weeks old, Jackson Labs, n = 24) were housed in a temperature-controlled room (22°C) on a 12 h light/dark cycle with *ad libitum* access to food and water. The mice were randomly assigned to axotomy and sham groups by sex (n = 6/group). Under isoflurane anesthesia, the left sciatic nerve was exposed at the mid-thigh level, followed by a complete transection using sterile microsurgery scissors. In the sham group, anatomically equivalent nerves were subjected to exposure without transection. The muscle was sutured, and the skin stapled. At 24 h after surgery, proximal segments of the sciatic nerve, corresponding to previously investigated lumbar (L)4 and L5 DRG tissues (Chernov and Shubayev, 2021), were collected for RNA isolation. All animal procedures were performed according to the Policy on Humane Care and Use of Laboratory Animals and the protocol approved by the Institutional Animal Care and Use Committee at the VA San Diego Healthcare System.

Samples

All surgical and tissue harvesting instruments were sterilized and repeatedly treated with RNase Away reagent followed by RNase-free water rinse. Tissues were immediately submerged in 500 μl RNAlater Stabilization Solution to preserve RNA

integrity, placed at 4°C overnight, then transferred for storage at −20°C. All sample groups were processed in parallel to minimize batch effects. Proximal stumps of sciatic nerve tissues were pooled from 2 mice per group for RNA purification.

RNA purification

Nerve tissues were transferred in Trizol solution (Invitrogen) and disrupted by mechanical homogenization. Total RNAs were purified using RNeasy RNA purification reagents. RNA concentrations and quality were determined using Nanodrop absorbance ratios at 260/280 nm and 260/230 nm. RNA integrity indices were determined using the Agilent Bioanalyzer Nano RNA chip. 500 ng of total RNA samples (n = 6 mice/group, 2 mice/sample (pooled), 3 sample/group) with RIN ≥ 7.0 were used for RNA-seq.

RNA sequencing (RNA-seq)

mRNA libraries were generated following the TruSeq Stranded mRNA library preparation protocol (Illumina). In brief, the Poly-A enriched mRNAs were purified using poly-T oligo coupled magnetic beads, followed by mRNA fragmentation, first and second strands synthesis, cleaning on AMPure XP magnetic beads, and 3'-adenylation. Ligation of TruSeq dual-index adapters was used for barcoding. The quality of RNA-seq libraries was validated using qPCR. Libraries were sized on Agilent Bioanalyzer DNA high sensitivity chip and normalized. RNA-seq was performed using the paired-end 100 cycle program on the NovaSeq 6000 system at the Genomics High Throughput Facility (University of California Irvine). Base calls were recorded and converted to FASTQ files containing sequencing reads and the corresponding quality scores using Illumina software. Sequencing was conducted until we acquired at least 50 million paired-end reads per sample.

RNA sequencing (RNA-seq) data analysis

FASTQ files were uploaded to the Amazon S3 server and processed using Elastic Compute Cloud (EC2) [Amazon Web Services (AWS)] running Ubuntu Server 20.04 LTS (64-bit ARM). Data analysis steps are summarized in **Supplementary Figure 1** and **Supplementary Table 3**. FASTQ files were filtered to remove low-quality bases, TruSeq dual-index adapter sequences, and unpaired reads using *Trimmomatic* (Bolger et al., 2014). Transcript-level quantification and mapping were performed using Salmon (Patro et al., 2017) and the Gencode M29 mouse genome. Mapping coverage was estimated in *MultiQC* (Ewels et al., 2016). Transcript- to gene-level quantifications were done using *Tximeta* (Love et al., 2020). Gene count matrices were processed in the DESeq2 (Love et al., 2014). Log_2FC values were calculated using the Wald test and adjusted using the adaptive t-prior *apeglm* method (Love et al., 2014). Significant DEGs were identified by P_{adj} values below a false discovery rate (FDR) cutoff ($P_{adj} < 0.1$) (**Supplementary Table 1**). $P_{adj} < 0.1$ were used in downstream analyses unless otherwise noted. Batch effects were controlled using the *removeBatchEffect* tool (Ritchie et al., 2015) and *RUVseq* (Risso et al., 2014) functions. DEGs were visualized using *ggVennDiagramm*, *PCAtools*, *ComplexHeatmap*, and *EnhancedVolcano* R packages.

Signaling pathway analysis

Prediction and biological interpretation of the regulated signaling pathways and upstream regulators in female and male animals was made in IPA using the default parameters (Krämer et al., 2014). Significance criteria of $P_{adj} < 0.1$, $log_2FC > 1$ or $log_2FC < -1$ were applied. Regulation directionality was estimated in IPA based on z-scores. Gene ontology terms were determined using *Geneontology*[1] and the *STRING* database using the default parameters.

Data availability statement

The datasets presented in this study can be found in the Gene Expression Omnibus (GEO) public repository (accession numbers: GSE182713 and GSE182709).

Ethics statement

The animal study was reviewed and approved by Institutional Animal Care and Use Committee at the VA San Diego Healthcare System.

Author contributions

AC: conceptualization, methodology, software, formal analysis, investigation, data curation, writing – original draft, review and editing, and visualization. VS: conceptualization, resources, project administration, funding acquisition, and

1 http://geneontology.org

writing – original draft, review and editing. All authors contributed to the article and approved the submitted version.

Funding

The research was supported by the National Institutes of Health (NIH) RO1 DE022757 (to VS), and the Department of Veterans Affairs Merit Review Award 5I01BX000638 (to VS). The content is solely the authors' responsibility and does not necessarily represent the official views of the funding agencies.

Acknowledgments

The authors thank Jennifer Dolkas and Mila Angert for their expert technical assistance.

Conflict of interest

The authors declare that the research was conducted in the absence of any commercial or financial relationships that could be construed as a potential conflict of interest.

Publisher's note

Supplementary material

The Supplementary Material for this article can be found online at: https://www.frontiersin.org/articles/10.3389/fnmol.2022.958568/full#supplementary-material

SUPPLEMENTARY FIGURE 1
RNA-seq analysis workflow.

SUPPLEMENTARY TABLE 1
DEGs in murine female and male post-axotomy (24 h) proximal nerve stumps.

SUPPLEMENTARY TABLE 2
Predicted upstream regulators.

SUPPLEMENTARY TABLE 3
Key resources description.

References

Ahlström, F. H. G., Mätlik, K., Viisanen, H., Blomqvist, K. J., Liu, X., Lilius, T. O., et al. (2021). Spared nerve injury causes sexually dimorphic mechanical allodynia and differential gene expression in spinal cords and dorsal root ganglia in rats. *Mol. Neurobiol.* 58, 5396–5419. doi: 10.1007/s12035-021-02447-1

Avraham, O., Feng, R., Ewan, E. E., Rustenhoven, J., Zhao, G., and Cavalli, V. (2021). Profiling sensory neuron microenvironment after peripheral and central axon injury reveals key pathways for neural repair. *Elife* 10:e68457. doi: 10.7554/eLife.68457

Bajor, M., and Kaczmarek, L. (2013). Proteolytic remodeling of the synaptic cell adhesion molecules (CAMs) by metzincins in synaptic plasticity. *Neurochem. Res.* 38, 1113–1121. doi: 10.1007/s11064-012-0919-6

Balakrishnan, A., Belfiore, L., Chu, T.-H., Fleming, T., Midha, R., Biernaskie, J., et al. (2021). Insights into the role and potential of schwann cells for peripheral nerve repair from studies of development and injury. *Front. Mol. Neurosci.* 13:608442. doi: 10.3389/fnmol.2020.608442

Bianchi, I., Lleo, A., Gershwin, M. E., and Invernizzi, P. (2012). The X chromosome and immune associated genes. *J. Autoimmun.* 38, J187–J192. doi: 10.1016/j.jaut.2011.11.012

Boerner, K. E., Chambers, C. T., Gahagan, J., Keogh, E., Fillingim, R. B., and Mogil, J. S. (2018). Conceptual complexity of gender and its relevance to pain. *Pain* 159, 2137–2141. doi: 10.1097/j.pain.0000000000001275

Bogen, O., Joseph, E. K., Chen, X., and Levine, J. D. (2008). GDNF hyperalgesia is mediated by PLCgamma, MAPK/ERK, PI3K, CDK5 and Src family kinase signaling and dependent on the IB4-binding protein versican. *Eur. J. Neurosci.* 28, 12–19. doi: 10.1111/j.1460-9568.2008.06308.x

Bolger, A. M., Lohse, M., and Usadel, B. (2014). Trimmomatic: a flexible trimmer for Illumina sequence data. *Bioinformatics* 30, 2114–2120. doi: 10.1093/bioinformatics/btu170

Brew, K., and Nagase, H. (2010). The tissue inhibitors of metalloproteinases (TIMPs): an ancient family with structural and functional diversity. *Biochim. Biophys. Acta* 1803, 55–71. doi: 10.1016/j.bbamcr.2010.01.003

Burnett, M. G., and Zager, E. L. (2004). Pathophysiology of peripheral nerve injury: a brief review. *Neurosurg. Focus* 16:E1. doi: 10.3171/foc.2004.16.5.2

Cavalli, V., Kujala, P., Klumperman, J., and Goldstein, L. S. (2005). Sunday driver links axonal transport to damage signaling. *J. Cell Biol.* 168, 775–787. doi: 10.1083/jcb.200410136

Chattopadhyay, S., and Shubayev, V. I. (2009). MMP-9 controls Schwann cell proliferation and phenotypic remodeling via IGF-1 and ErbB receptor-mediated activation of MEK/ERK pathway. *Glia* 57, 1316–1325. doi: 10.1002/glia.20851

Chernov, A. V., Baranovskaya, S., Golubkov, V. S., Wakeman, D. R., Snyder, E. Y., Williams, R., et al. (2010). Microarray-based transcriptional and epigenetic profiling of matrix metalloproteinases, collagens, and related genes in cancer. *J. Biol. Chem.* 285, 19647–19659. doi: 10.1074/jbc.M109.088153

Chernov, A. V., Dolkas, J., Hoang, K., Angert, M., Srikrishna, G., Vogl, T., et al. (2015). The calcium-binding proteins S100A8 and S100A9 initiate the early inflammatory program in injured peripheral nerves. *J. Biol. Chem.* 290, 11771–11784. doi: 10.1074/jbc.M114.622316

Chernov, A. V., Hullugundi, S. K., Eddinger, K. A., Dolkas, J., Remacle, A. G., Angert, M., et al. (2020). A myelin basic protein fragment induces sexually dimorphic transcriptome signatures of neuropathic pain in mice. *J. Biol. Chem.* 295, 10807–10821. doi: 10.1074/jbc.RA120.013696

Chernov, A. V., and Shubayev, V. I. (2021). Sexual dimorphism of early transcriptional reprogramming in dorsal root ganglia after peripheral nerve injury. *Front. Mol. Neurosci.* 14:779024. doi: 10.3389/fnmol.2021.779024

Cox, L. J., Hengst, U., Gurskaya, N. G., Lukyanov, K. A., and Jaffrey, S. R. (2008). Intra-axonal translation and retrograde trafficking of CREB promotes neuronal survival. *Nat. Cell Biol.* 10, 149–159. doi: 10.1038/ncb1677

Durbec, P., Marcos-Gutierrez, C. V., Kilkenny, C., Grigoriou, M., Wartiowaara, K., Suvanto, P., et al. (1996). GDNF signalling through the Ret receptor tyrosine kinase. *Nature* 381, 789–793. doi: 10.1038/381789a0

English, W. R., Puente, X. S., Freije, J. M., Knauper, V., Amour, A., Merryweather, A., et al. (2000). Membrane type 4 matrix metalloproteinase

(MMP17) has tumor necrosis factor-alpha convertase activity but does not activate pro-MMP2. *J. Biol. Chem.* 275, 14046–14055. doi: 10.1074/jbc.275.19.14046

Ewels, P., Magnusson, M., Lundin, S., and Käller, M. (2016). MultiQC: summarize analysis results for multiple tools and samples in a single report. *Bioinformatics* 32, 3047–3048. doi: 10.1093/bioinformatics/btw354

Fan, R., and Lai, K. O. (2021). Understanding how kinesin motor proteins regulate postsynaptic function in neuron. *Febs J.* 289, 2128–2144. doi: 10.1111/febs.16285

Fawcett, J. W., and Keynes, R. J. (1990). Peripheral nerve regeneration. *Annu. Rev. Neurosci.* 13, 43–60.

Fillingim, R. B., King, C. D., Ribeiro-Dasilva, M. C., Rahim-Williams, B., and Riley, J. L. III (2009). Sex, gender, and pain: a review of recent clinical and experimental findings. *J. Pain* 10, 447–485. doi: 10.1016/j.jpain.2008.12.001

Fujioka, H., Dairyo, Y., Yasunaga, K.-I., and Emoto, K. (2012). Neural functions of matrix metalloproteinases: plasticity, neurogenesis, and disease. *Biochem. Res. Int.* 2012:789083. doi: 10.1155/2012/789083

Fukuda, T., Kiuchi, K., and Takahashi, M. (2002). Novel mechanism of regulation of rac activity and lamellipodia formation by RET Tyrosine Kinase. *J. Biol. Chem.* 277, 19114–19121. doi: 10.1074/jbc.M200643200

Gordon, T., Sulaiman, O., and Boyd, J. G. (2003). Experimental strategies to promote functional recovery after peripheral nerve injuries. *J. Peripher. Nerv. Syst.* 8, 236–250.

Greenspan, J. D., Craft, R. M., LeResche, L., Arendt-Nielsen, L., Berkley, K. J., Fillingim, R. B., et al. (2007). Studying sex and gender differences in pain and analgesia: a consensus report. *Pain* 132, S26–S45. doi: 10.1016/j.pain.2007.10.014

Huang, J., Furuya, A., and Furuichi, T. (2007). Very-KIND, a KIND domain containing RasGEF, controls dendrite growth by linking Ras small GTPases and MAP2. *J. Cell Biol.* 179, 539–552. doi: 10.1083/jcb.200702036

Ito, K., and Enomoto, H. (2016). Retrograde transport of neurotrophic factor signaling: implications in neuronal development and pathogenesis. *J. Biochem.* 160, 77–85. doi: 10.1093/jb/mvw037

Iwase, T., Jung, C. G., Bae, H., Zhang, M., and Soliven, B. (2005). Glial cell line-derived neurotrophic factor-induced signaling in Schwann cells. *J. Neurochem.* 94, 1488–1499. doi: 10.1111/j.1471-4159.2005.03290.x

Jessen, K. R., and Arthur-Farraj, P. (2019). Repair Schwann cell update: adaptive reprogramming, EMT, and stemness in regenerating nerves. *Glia* 67, 421–437. doi: 10.1002/glia.23532

Jessen, K. R., and Mirsky, R. (2016). The repair Schwann cell and its function in regenerating nerves. *J. Physiol.* 594, 3521–3531. doi: 10.1113/jp270874

Jessen, K. R., and Mirsky, R. (2021). The role of c-Jun and autocrine signaling loops in the control of repair schwann cells and regeneration. *Front. Cell Neurosci.* 15:820216. doi: 10.3389/fncel.2021.820216

Kanai, Y., Dohmae, N., and Hirokawa, N. (2004). Kinesin transports RNA: isolation and characterization of an RNA-transporting granule. *Neuron* 43, 513–525. doi: 10.1016/j.neuron.2004.07.022

Kim, Y., Remacle, A. G., Chernov, A. V., Liu, H., Shubayev, I., Lai, C., et al. (2012). The MMP-9/TIMP-1 axis controls the status of differentiation and function of myelin-forming Schwann cells in nerve regeneration. *PLoS One* 7:e33664. doi: 10.1371/journal.pone.0033664

Kovacic, U., Zele, T., Osredkar, J., Sketelj, J., and Bajrović, F. F. (2004). Sex-related differences in the regeneration of sensory axons and recovery of nociception after peripheral nerve crush in the rat. *Exp. Neurol.* 189, 94–104. doi: 10.1016/j.expneurol.2004.05.015

Krämer, A., Green, J., Pollard, J. Jr., and Tugendreich, S. (2014). Causal analysis approaches in Ingenuity Pathway Analysis. *Bioinformatics* 30, 523–530. doi: 10.1093/bioinformatics/btt703

Liu, H., Angert, M., Nishihara, T., Shubayev, I., Dolkas, J., and Shubayev, V. I. (2015). Spinal glia division contributes to conditioning lesion–induced axon regeneration into the injured spinal cord. *J. Neuropathol. Exp. Neurol.* 74, 500–511. doi: 10.1097/nen.0000000000000192

Liu, H., Kim, Y., Chattopadhyay, S., Shubayev, I., Dolkas, J., and Shubayev, V. I. (2010). Matrix metalloproteinase inhibition enhances the rate of nerve regeneration in vivo by promoting dedifferentiation and mitosis of supporting schwann cells. *J. Neuropathol. Exp. Neurol.* 69, 386–395. doi: 10.1097/NEN.0b013e3181d68d12

Love, M. I., Huber, W., and Anders, S. (2014). Moderated estimation of fold change and dispersion for RNA-seq data with DESeq2. *Genome. Biol.* 15:550. doi: 10.1186/s13059-014-0550-8

Love, M. I., Soneson, C., Hickey, P. F., Johnson, L. K., Pierce, N. T., Shepherd, L., et al. (2020). Tximeta: reference sequence checksums for provenance identification in RNA-seq. *PLoS Comput. Biol.* 16:e1007664. doi: 10.1371/journal.pcbi.1007664

Lundborg, G. (1987). Nerve regeneration and repair. a review. *Acta Orthop. Scand* 58, 145–169. doi: 10.3109/17453678709146461

Lundgren, T. K., Nakahata, K., Fritz, N., Rebellato, P., Zhang, S., and Uhlén, P. (2012). RET PLCγ phosphotyrosine binding domain regulates Ca2+ signaling and neocortical neuronal migration. *PLoS One* 7:e31258. doi: 10.1371/journal.pone.0031258

Ma, T. C., and Willis, D. E. (2015). What makes a RAG regeneration associated? *Front. Mol. Neurosci.* 8:43. doi: 10.3389/fnmol.2015.00043

McDonald, D., Cheng, C., Chen, Y., and Zochodne, D. (2006). Early events of peripheral nerve regeneration. *Neuron Glia Biol.* 2, 139–147.

Mecklenburg, J., Zou, Y., Wangzhou, A., Garcia, D., Lai, Z., Tumanov, A. V., et al. (2020). Transcriptomic sex differences in sensory neuronal populations of mice. *Sci. Rep.* 10:15278. doi: 10.1038/s41598-020-72285-z

Merrell, A. J., and Stanger, B. Z. (2016). Adult cell plasticity in vivo: de-differentiation and transdifferentiation are back in style. *Nat. Rev. Mol. Cell Biol.* 17, 413–425. doi: 10.1038/nrm.2016.24

Milichko, V., and Dyachuk, V. (2020). Novel glial cell functions: extensive potency, stem cell-like properties, and participation in regeneration and transdifferentiation. *Front. Cell Dev. Biol.* 8:809. doi: 10.3389/fcell.2020.00809

Mogil, J. S. (2012). Sex differences in pain and pain inhibition: multiple explanations of a controversial phenomenon. *Nat. Rev. Neurosci.* 13, 859–866. doi: 10.1038/nrn3360

Moore, M. J., Blachere, N. E., Fak, J. J., Park, C. Y., Sawicka, K., Parveen, S., et al. (2018). ZFP36 RNA-binding proteins restrain T cell activation and anti-viral immunity. *ELife* 7:e33057. doi: 10.7554/eLife.33057

Nielsen, J., Gotfryd, K., Li, S., Kulahin, N., Soroka, V., Rasmussen, K. K., et al. (2009). Role of glial cell line-derived neurotrophic factor (GDNF)-neural cell adhesion molecule (NCAM) interactions in induction of neurite outgrowth and identification of a binding site for NCAM in the heel region of GDNF. *J. Neurosci.* 29, 11360–11376. doi: 10.1523/JNEUROSCI.3239-09.2009

Nishihara, T., Remacle, A. G., Angert, M., Shubayev, I., Shiryaev, S. A., Liu, H., et al. (2015). Matrix metalloproteinase-14 both sheds cell surface neuronal glial antigen 2 (NG2) proteoglycan on macrophages and governs the response to peripheral nerve injury. *J. Biol. Chem.* 290, 3693–3707. doi: 10.1074/jbc.M114.603431

Nocera, G., and Jacob, C. (2020). Mechanisms of Schwann cell plasticity involved in peripheral nerve repair after injury. *Cell Mol. Life Sci.* 77, 3977–3989. doi: 10.1007/s00018-020-03516-9

North, R. Y., Li, Y., Ray, P., Rhines, L. D., Tatsui, C. E., Rao, G., et al. (2019). Electrophysiological and transcriptomic correlates of neuropathic pain in human dorsal root ganglion neurons. *Brain* 142, 1215–1226. doi: 10.1093/brain/awz063

Paige, C., Barba-Escobedo, P. A., Mecklenburg, J., Patil, M., Goffin, V., Grattan, D. R., et al. (2020). Neuroendocrine mechanisms governing sex differences in hyperalgesic priming involve prolactin receptor sensory neuron signaling. *J. Neurosci.* 40, 7080–7090. doi: 10.1523/jneurosci.1499-20.2020

Pan, X., Cao, Y., Stucchi, R., Hooikaas, P. J., Portegies, S., Will, L., et al. (2019). MAP7D2 localizes to the proximal axon and locally promotes kinesin-1-mediated cargo transport into the axon. *Cell Rep.* 26, 1988–1999.e6. doi: 10.1016/j.celrep.2019.01.084

Patro, R., Duggal, G., Love, M. I., Irizarry, R. A., and Kingsford, C. (2017). Salmon provides fast and bias-aware quantification of transcript expression. *Nat. Methods* 14, 417–419. doi: 10.1038/nmeth.4197

Radtke, C., and Vogt, P. M. (2009). Peripheral nerve regeneration: a current perspective. *Eplasty* 9:e47.

Ray, P. R., Khan, J., Wangzhou, A., Tavares-Ferreira, D., Akopian, A. N., Dussor, G., et al. (2019). Transcriptome analysis of the human tibial nerve identifies sexually dimorphic expression of genes involved in pain, inflammation, and neuro-immunity. *Front. Mol. Neurosci.* 12:37. doi: 10.3389/fnmol.2019.00037

Remacle, A. G., Kumar, S., Motamedchaboki, K., Cieplak, P., Hullugundi, S., Dolkas, J., et al. (2015). Matrix Metalloproteinase (MMP) Proteolysis of the extracellular loop of voltage-gated sodium channels and potential alterations in pain signaling. *J. Biol. Chem.* 290, 22939–22944. doi: 10.1074/jbc.C115.671107

Risso, D., Ngai, J., Speed, T. P., and Dudoit, S. (2014). Normalization of RNA-seq data using factor analysis of control genes or samples. *Nat. Biotechnol.* 32, 896–902. doi: 10.1038/nbt.2931

Ritchie, M. E., Phipson, B., Wu, D., Hu, Y., Law, C. W., Shi, W., et al. (2015). limma powers differential expression analyses for RNA-sequencing and microarray studies. *Nucleic Acids Res.* 43:e47. doi: 10.1093/nar/gkv007

Rivera, S., Khrestchatisky, M., Kaczmarek, L., Rosenberg, G. A., and Jaworski, D. M. (2010). Metzincin proteases and their inhibitors: foes or friends in nervous system physiology? *J. Neurosci.* 30, 15337–15357. doi: 10.1523/JNEUROSCI.3467-10.2010

Rossi, L., Forte, D., Migliardi, G., Salvestrini, V., Buzzi, M., Ricciardi, M. R., et al. (2015). The tissue inhibitor of metalloproteinases 1 increases the clonogenic efficiency of human hematopoietic progenitor cells through CD63/PI3K/Akt signaling. *Exp. Hematol.* 43, 974.e–985.e. doi: 10.1016/j.exphem.2015.07.003

Sahoo, P. K., Smith, D. S., Perrone-Bizzozero, N., and Twiss, J. L. (2018). Axonal mRNA transport and translation at a glance. *J. Cell Sci.* 131:jcs196808. doi: 10.1242/jcs.196808

Sorge, R. E., and Totsch, S. K. (2017). Sex Differences in Pain. *J. Neurosci. Res.* 95, 1271–1281. doi: 10.1002/jnr.23841

Stephens, K. E., Zhou, W., Ji, Z., Chen, Z., He, S., Ji, H., et al. (2019). Sex differences in gene regulation in the dorsal root ganglion after nerve injury. *BMC Genom.* 20:147. doi: 10.1186/s12864-019-5512-9

Stierli, S., Imperatore, V., and Lloyd, A. C. (2019). Schwann cell plasticity-roles in tissue homeostasis, regeneration, and disease. *Glia* 67, 2203–2215. doi: 10.1002/glia.23643

Stoll, G., Jander, S., and Myers, R. R. (2002). Degeneration and regeneration of the peripheral nervous system: from Augustus Waller's observations to neuroinflammation. *J. Peripher. Nerv. Syst.* 7, 13–27. doi: 10.1046/j.1529-8027.2002.02002.x

Szklarczyk, D., Gable, A. L., Nastou, K. C., Lyon, D., Kirsch, R., Pyysalo, S., et al. (2021). The STRING database in 2021: customizable protein-protein networks, and functional characterization of user-uploaded gene/measurement sets. *Nucleic Acids Res.* 49, D605–D612. doi: 10.1093/nar/gkaa1074

Tavares-Ferreira, D., Ray, P. R., Sankaranarayanan, I., Mejia, G. L., Wangzhou, A., Shiers, S., et al. (2020). Sex differences in nociceptor translatomes contribute to divergent prostaglandin signaling in male and female mice. *BioRxiv* [Preprint]. 2020.2007.2031.231753. doi: 10.1101/2020.07.31.231753

Turner-Bridger, B., Caterino, C., and Cioni, J. M. (2020). Molecular mechanisms behind mRNA localization in axons. *Open Biol.* 10:200177. doi: 10.1098/rsob.200177

Unruh, A. M. (1996). Gender variations in clinical pain experience. *Pain* 65, 123–167.

Van Kesteren, R., Mason, M., MacGillavry, H., Smit, A., and Verhaagen, J. (2011). A gene network perspective on axonal regeneration. *Front. Mol. Neurosci.* 4:46. doi: 10.3389/fnmol.2011.00046

Zhou, L., and Shine, H. D. (2003). Neurotrophic factors expressed in both cortex and spinal cord induce axonal plasticity after spinal cord injury. *J. Neurosci. Res.* 74, 221–226. doi: 10.1002/jnr.10718

Zochodne, D. W. (2012). The challenges and beauty of peripheral nerve regrowth. *J. Peripheral. Nervous Syst.* 17, 1–18. doi: 10.1111/j.1529-8027.2012.00378.x

frontiers | Frontiers in Molecular Neuroscience

TYPE Original Research
PUBLISHED 05 September 2022
DOI 10.3389/fnmol.2022.954928

OPEN ACCESS

EDITED BY
Detlev Boison,
Rutgers, The State University of New Jersey, United States

REVIEWED BY
Philip Wing-Lok Ho,
The University of Hong Kong, Hong Kong SAR, China
Alix Warburton,
National Institutes of Health (NIH), United States

*CORRESPONDENCE
John P. Quinn
jquinn@liverpool.ac.uk

†PRESENT ADDRESS
Jack N. G. Marshall,
Section of Infections of the Nervous System, National Institute of Neurological Disorders and Stroke, National Institutes of Health, Bethesda, MD, United States

‡These authors share first authorship

SPECIALTY SECTION
This article was submitted to Brain Disease Mechanisms, a section of the journal Frontiers in Molecular Neuroscience

RECEIVED 27 May 2022
ACCEPTED 22 July 2022
PUBLISHED 05 September 2022

CITATION
Marshall JNG, Fröhlich A, Li L, Pfaff AL, Middlehurst B, Spargo TP, Iacoangeli A, Lang B, Al-Chalabi A, Koks S, Bubb VJ and Quinn JP (2022) A polymorphic transcriptional regulatory domain in the amyotrophic lateral sclerosis risk gene *CFAP410* correlates with differential isoform expression. *Front. Mol. Neurosci.* 15:954928. doi: 10.3389/fnmol.2022.954928

A polymorphic transcriptional regulatory domain in the amyotrophic lateral sclerosis risk gene *CFAP410* correlates with differential isoform expression

Jack N. G. Marshall[1†‡], Alexander Fröhlich[1‡], Li Li[1,2], Abigail L. Pfaff[3,4], Ben Middlehurst[1], Thomas P. Spargo[5,6,7], Alfredo Iacoangeli[5,6,7], Bing Lang[2], Ammar Al-Chalabi[6,8], Sulev Koks[3,4], Vivien J. Bubb[1] and John P. Quinn[1*]

[1]Department of Pharmacology and Therapeutics, Institute of Systems, Molecular and Integrative Biology, University of Liverpool, Liverpool, United Kingdom, [2]Department of Psychiatry, National Clinical Research Centre for Mental Disorders, The Second Xiangya Hospital, Central South University, Changsha, China, [3]Centre for Molecular Medicine and Innovative Therapeutics, Murdoch University, Perth, WA, Australia, [4]Perron Institute for Neurological and Translational Science, Perth, WA, Australia, [5]Department of Biostatistics and Health Informatics, Institute of Psychiatry, Psychology and Neuroscience, King's College London, London, United Kingdom, [6]Department of Basic and Clinical Neuroscience, Maurice Wohl Clinical Neuroscience Institute, Institute of Psychiatry, Psychology and Neuroscience, King's College London, London, United Kingdom, [7]NIHR Biomedical Research Centre, South London and Maudsley NHS Foundation Trust, King's College London, London, United Kingdom, [8]Department of Neurology, King's College Hospital, London, United Kingdom

We describe the characterisation of a variable number tandem repeat (VNTR) domain within intron 1 of the amyotrophic lateral sclerosis (ALS) risk gene *CFAP410* (*Cilia and flagella associated protein 410*) (previously known as *C21orf2*), providing insight into how this domain could support differential gene expression and thus be a modulator of ALS progression or risk. We demonstrated the VNTR was functional in a reporter gene assay in the HEK293 cell line, exhibiting both the properties of an activator domain and a transcriptional start site, and that the differential expression was directed by distinct repeat number in the VNTR. These properties embedded in the VNTR demonstrated the potential for this VNTR to modulate *CFAP410* expression. We extrapolated these findings *in silico* by utilisation of tagging SNPs for the two most common VNTR alleles to establish a correlation with endogenous gene expression. Consistent with *in vitro* data, *CFAP410* isoform expression was found to be variable in the brain. Furthermore, although the number of matched controls was low, there was evidence for one specific isoform being correlated with lower expression in those with ALS. To address if the genotype of the VNTR was associated with ALS risk, we characterised the variation of the *CFAP410* VNTR in ALS cases and matched controls by PCR analysis of the VNTR length, defining eight alleles of the VNTR. No significant difference was observed between cases and controls, we noted, however, the cohort was unlikely to contain sufficient power to enable any firm conclusion to be drawn from this analysis. This data demonstrated that the VNTR domain has

the potential to modulate *CFAP410* expression as a regulatory element that could play a role in its tissue-specific and stimulus-inducible regulation that could impact the mechanism by which *CFAP410* is involved in ALS.

KEYWORDS

***CFAP410*, ALS, VNTR, gene expression, transcriptional regulation**

Introduction

Amyotrophic lateral sclerosis (ALS) is a fatal neurodegenerative disease primarily of the motor system, characterised by upper and lower motor neuron death, muscle atrophy and paralysis (Hardiman et al., 2017). ALS heritability has previously been estimated to be as high as 61%, indicating a significant genetic contribution to the variation in ALS risk and susceptibility (Al-Chalabi et al., 2010; Hardiman et al., 2017), and now there are over 40 genes associated with the disease, of varying effect sizes (Wroe et al., 2009; Abel et al., 2012; Shatunov and Al-Chalabi, 2021). Occasionally, patients can harbour multiple mutations, highlighting that ALS is a complex disease (van Blitterswijk et al., 2012a,b; Al-Chalabi and Visscher, 2014; Cady et al., 2015; Bury et al., 2016; Zou et al., 2017; Nguyen et al., 2018; Goldstein et al., 2019; Yilmaz et al., 2022). There is also evidence that ALS pathogenesis is a multistep process, with both genetic and environmental risk factors working in concert *via* gene–environment interaction (Al-Chalabi et al., 2014; Chio et al., 2018; Vucic et al., 2019; Garton et al., 2021). While genome-wide association studies have helped to uncover regions associated with ALS, it has been shown that single nucleotide polymorphisms (SNPs) only account for a small fraction of ALS heritability (van Rheenen et al., 2016). Furthermore, it has been shown that structural variants could be a key source of this missing heritability (Theunissen et al., 2020), with the hexameric repeat expansion in the first intron of the *C9orf72* gene the most commonly reported mutation in European ALS patients (Zou et al., 2017). Since the discovery of the *C9orf72* repeat expansion, there have been numerous studies investigating tandem repeat DNA and structural variation in ALS (DeJesus-Hernandez et al., 2011; Renton et al., 2011; Blauw et al., 2012; Lattante et al., 2018; Tazelaar et al., 2019, 2020; Course et al., 2020; Al Khleifat et al., 2022).

Abbreviations: ALS, Amyotrophic lateral sclerosis; ENCODE, The Encyclopaedia of DNA Elements; CFAP410, Cilia and flagella associated protein 410; MAF, Minor allele frequency; MND, Motor neuron disease; NNC, Non-neurological controls; NYGC ALS, New York Genome Centre Consortium Target ALS; SNP, Single nucleotide polymorphism; UCSC, University of California, Santa Cruz; VNTR, Variable number tandem repeat.

Tandem repeats are DNA sequence motifs that are recurrent and found contiguously in a region of the genome. Such tandem repeats constitute ∼3% of the human genome (Bakhtiari et al., 2018; Hannan, 2018). They are often found to be polymorphic in the general population and are thus termed variable number tandem repeats (VNTRs); furthermore, specific alleles can be risk factors for diseases, which are often neurological in nature (Lam et al., 2018; Roeck et al., 2018; Pacheco et al., 2019). Non-coding VNTRs can be functional in a number of ways: they can act as transcription factor binding sites (Hsieh et al., 2007; Ali et al., 2010; Zukic et al., 2010), drive gene expression on the basis of repeat number (Warburton et al., 2015), work in concert with other genetic variants to induce combinatorial regulation (Warburton et al., 2016), regulate splicing (Roeck et al., 2018) and modulate gene expression and CpG methylation levels at the genome-wide level (Gymrek et al., 2016; Quilez et al., 2016). Thus, VNTRs are key transcriptional regulatory domains within the human genome, with repeat copy numbers driving differential gene expression profiles, altering affinity for transcription factors at gene promoters and modifying the secondary structure of DNA, all of which would modify gene expression both in a tissue specific and stimulus inducible manner (Marshall, 2021).

To date, five genes linked to ALS have been identified to contain tandem repeat domains (*C9orf72*, *ATXN1*, *ATXN2*, *NIPA1* and *WDR7*) demonstrating that VNTRs are a strong candidate for genetic risk for this disease (Sproviero et al., 2017; Iacoangeli et al., 2019; Tazelaar et al., 2019, 2020; Course et al., 2020). More recent global analysis to prioritise causal genes within ALS-risk loci has utilised not only rare pathogenic variants but also analysis of short tandem repeat domains of six bases or less (van Rheenen et al., 2021). This study highlighted the association of SNP rs75087725 within *Cilia and flagella-associated protein 410* (*CFAP410*) as a missense variant associated with ALS but found no evidence for other variants including short-tandem repeat expansions within this locus associated with ALS. However, the bioinformatic pipelines used would not be able to accurately address larger VNTRs. Our analysis of transcriptional regulation of the *CFAP410* gene highlighted six tandem repeats at this locus, five of which were not variable in repeat copy number. However, there was a VNTR in intron 1 of *CFAP410* with a complex repeat domain of 22 bp or 35 bp extending to 500–600+bp in length (Marshall, 2021)

(Figure 1, Supplementary Figure 2B). We therefore tested the hypothesis that the *CFAP410* VNTR within intron 1 of the most 5' transcriptional start site is a transcriptional regulatory domain and that tandem repeat variation could be associated with both differential gene expression of *CFAP410* and risk for ALS.

Materials and methods

ALS cohort used for PCR genotyping of *CFAP410* VNTR

Genomic DNA purified from the blood of ALS cases and controls was obtained from the UK Motor Neuron Disease (MND) Collection DNA and Cell Bank, which was used for PCR-based genotyping of the *CFAP410* VNTR. A total of 500 ALS samples were provided, 456 from people fulfilling the El Escorial criteria, 21 with progressive muscular atrophy, 12 with ALS restricted to progressive bulbar palsy and 11 with primary lateral sclerosis. A total of 333 people with ALS were male and 167 were female, with an age range of 24–91 years old and a disease age of onset range of 23–88 years old. A panel of 499 controls was also obtained: 188 were male and 311 were female with an age range of 27–84 years old. The genotyping analysis was performed using this gender ratio because this was the total cohort size available to us in this database. We therefore did not generate a gender risk bias on the VNTR.

Identification of the *CFAP410* VNTR

Tandem repeats in the *CFAP410* locus were identified on UCSC HG19 (https://genome.ucsc.edu/) using the Simple Tandem Repeats track from Tandem Repeat Finder (https://tandem.bu.edu/trf/trf.submit.options.html) (Benson, 1999). A total of six distinct tandem repeats were identified over this locus; we focused on the repeat within intron 1, which is the only one we found to be variable in repeat number.

Genotyping the *CFAP410* VNTR

The VNTR was amplified by PCR, forward 5′ AACCCCAGACAACAGACCC 3′ and reverse 5′ CTGACGCGGAAGATGGTTC 3′ primers were designed to amplify the full-length VNTR sequence (584bp). Amplification reactions used KOD Hot Start DNA polymerase (Merck) with 1× hot start buffer and the recommended protocol. The products were analysed on 2% agarose gels stained with ethidium bromide. Association analysis was performed comparing allele frequencies between controls and ALS cases using the software programme CLUMP with 100,000 simulations (Sham and Curtis, 1995).

Cell culture

The human embryonic kidney cell line, HEK293 (ATCC® CRL-1573™), was cultured in the Dulbecco's Modified Eagle's Media (DMEM) (Gibco) containing 4.5 g/L D-glucose and 200 mM L-glutamine (Gibco), supplemented with 10% foetal bovine serum (Gibco), penicillin/streptomycin (100 U/ml, 100 mg/ml; Sigma) and 1% (v/v) 100 mM sodium pyruvate (Sigma). Cells were incubated at 37°C in 5% CO_2.

Generation of *CFAP410* VNTR reporter gene constructs

The *CFAP410* VNTR was amplified from genomic DNA by PCR using the KOD Hot Start DNA polymerase following the recommended protocol. The VNTR was subcloned into the intermediate Zero Blunt PCR Vector (Invitrogen). This intermediate plasmid was then digested with restriction enzymes and the VNTR insert was cloned within the multiple cloning site of the reporter gene vectors either pGL3-promoter (pGL3P) or pGL3-basic (pGL3B) (Promega) in both orientations (forward and reverse) [restriction digests, vector maps and sequencing available at Marshall (2021)]. In pGL3P the VNTR was located upstream of the SV40 minimal promoter to address action as an activator, and cloned in pGL3B to address putative function as an inherent transcriptional start site.

Cell transfection and dual luciferase assay

HEK293 cells were seeded at approximately 100,000 cells per well in 24-well-plates. After 48 h of incubation, cells were co-transfected with 1 μg reporter gene plasmid (firefly luciferase) containing the VNTR sequences and 20 ng pRL control vector for normalisation (Renilla luciferase; Novagen) using TurboFect™ transfection reagent (ThermoScientific/Fermentas), according to the manufacturer's protocol. TurboFect™ was removed after 4 h of incubation and replaced with fresh media. Luciferase activity of reporter constructs was measured 48 h post-transfection using a dual luciferase reporter assay system (Promega) according to the manufacturer's instructions.

Generation of *CFAP410* VNTR tagging SNPs

Samples from the UK MND Collections DNA bank had previously been analysed as part of Project MinE (van der Spek et al., 2019), and therefore, SNP genotype data were available for individuals that were part of this study. The genotypes of SNPs located within 500 kb of the *CFAP410* gene were extracted from

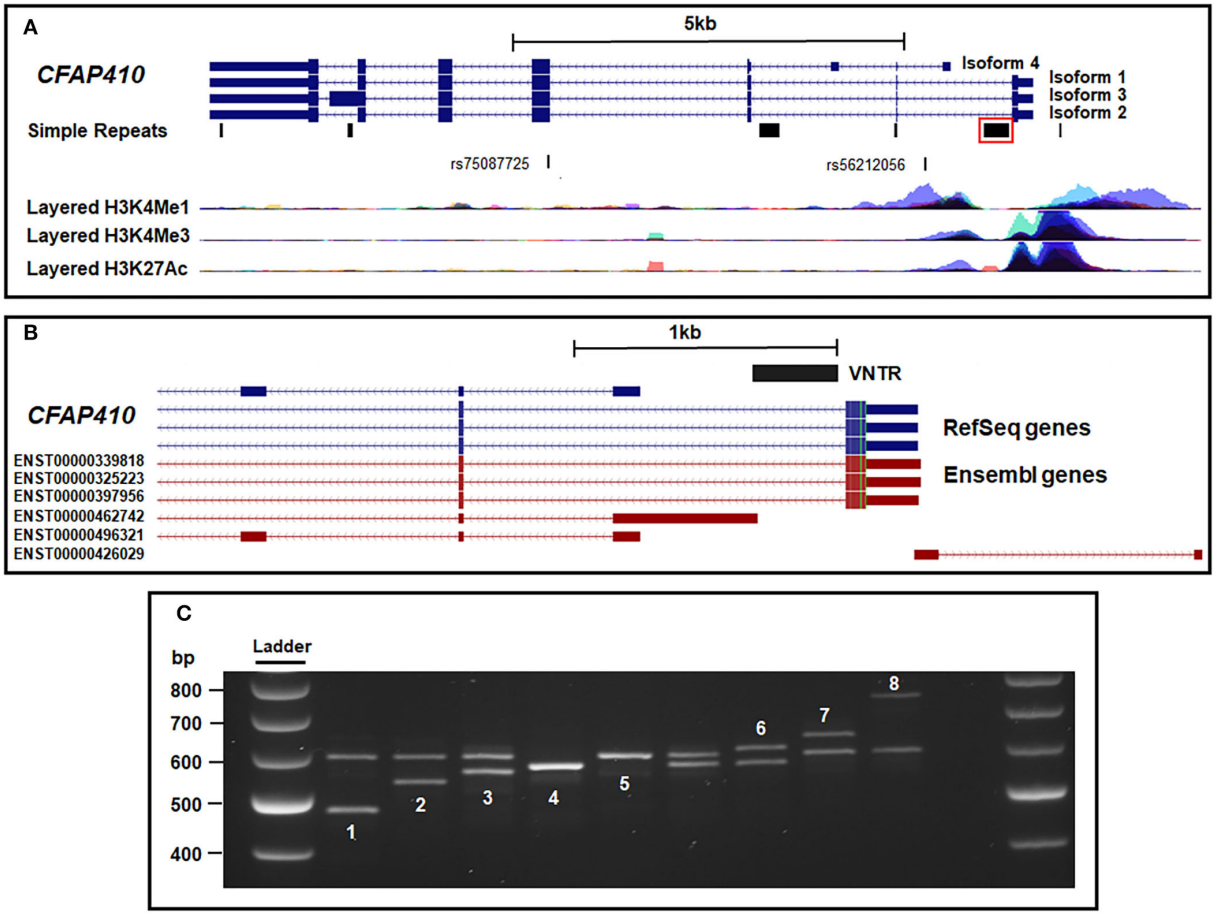

FIGURE 1
Location of multiple transcripts at the *CFAP410* gene locus relative to the intron 1 VNTR. **(A)** The four main isoforms of CFAP410 overlaid with the Simple Tandem Repeats track and histone marks from the ENCODE database. The ALS GWAS SNP (rs75087725) and identified tagging SNP (rs56212056) are also shown. The VNTR identified in this study is boxed in red. **(B)** *CFAP410* VNTR location overlaid with RefSeq genes from NCBI and predicted transcripts from Ensembl database. **(C)** PCR amplification and gel electrophoresis of the VNTR within the *CFAP410* locus. This region was confirmed to be polymorphic and eight alleles were identified (numbered 1–8 to reflect increasing length). Variant 7 was found only in a single ALS case. All samples were run at 100 V on 2% agarose for 3.5 h. All samples shown are from the cohort of ALS cases and controls that are genotyped in Table 1.

232 individuals who were either homozygous or heterozygous for the two commonest alleles (4 and 5) of the VNTR. Analysis was performed using plink (v1.07) (Purcell et al., 2007) to identify SNPs in linkage disequilibrium (r^2 >0.7) with alleles 4 and 5 of the VNTR.

Analysis of *CFAP410* isoform expression using NYGC ALS dataset

RNA-seq data from the Target ALS cohort obtained from the New York Genome Centre Consortium were analysed (https://www.targetals.org/research/resources-for-scientists/). Data were available from different tissues of 211 people, including 178 with ALS, 5 with other neurological diseases (frontotemporal dementia, Alzheimer's disease and multiple system atrophy), 2 with other motor neuron diseases (spinal bulbar muscular atrophy and polio) and 26 non-neurological controls (NNC). RNA-seq data from the following tissues (total 1,170) were included: cerebellum (161), frontal cortex (169), medial motor cortex (148), lateral motor cortex (147), unspecified motor cortex (9), occipital cortex (81), temporal cortex (10), sensory cortex (2), lumbar spinal cord (147), cervical spinal cord (161), thoracic spinal cord (76), iPS cell line (4), motor neuron cell line (4), choroid plexus (35), medulla (1) and liver (15) (Supplementary Table 1). Isoform quantification of RNA-seq data was performed using the Salmon tool (https://salmon.readthedocs.io). Salmon-generated quant files were imported into R using the *tximport* function from the *tximport* package of R (Soneson et al., 2015). Counts were extracted with

TABLE 1 Allele and genotype frequencies of *CFAP410* VNTR in MNDA cohort.

(A)

Cohort / Allele	ALS cohort		Control cohort		Total	% Difference (ALS–Control)	*p*-value (Fisher's exact test)
	Count	%	Count	%			
1	2	0.20	5	0.51	7	−0.30	0.67
2	3	0.31	2	0.20	5	0.10	0.50
3	10	1.02	11	1.12	21	−0.10	1.00
4	224	22.86	220	22.31	444	0.54	0.93
5	730	74.49	737	74.75	1,467	−0.26	0.75
6	5	0.51	6	0.61	11	−0.10	1.00
7	1	0.10	0	0	1	0.10	0.50
8	5	0.51	5	0.51	10	0.00	0.50
Total	980	100.00	986	100.00	1,966	0.00	N/A

(B)

Cohort / Genotype	ALS cohort		Control cohort		Total	% Difference (ALS - Control)	*p*-value (Fisher's exact test)
	Count	%	Count	%			
1.4	1	0.20	1	0.20	2	0.00	1.00
1.5	0	0.00	4	0.81	4	−0.81	0.22
2.2	1	0.20	0	0.00	1	0.20	1.00
2.4	1	0.20	0	0.00	1	0.20	0.50
2.5	0	0.00	2	0.41	2	−0.41	0.50
3.4	1	0.20	1	0.20	2	0.00	1.00
3.5	9	1.84	10	2.03	19	−0.19	0.71
4.4	28	5.71	27	5.48	55	0.24	0.57
4.5	161	32.86	159	32.25	320	0.61	0.59
4.6	3	0.61	3	0.61	6	0.00	0.50
4.8	1	0.20	2	0.41	3	−0.20	1.00
5.5	277	56.53	278	56.39	555	0.14	0.76
5.6	2	0.41	3	0.61	5	−0.20	0.61
5.7	1	0.20	0	0.00	1	0.20	0.50
1.8	1	0.20	0	0.00	1	0.20	1.00
5.8	3	0.61	3	0.61	6	0.00	1.00
Total	490	100.00	493	100.00	983	0.00	N/A

(A) The distribution of the eight identified alleles of the CFAP410 VNTR in an ALS cohort (n = 490) and matched controls (n = 493) was analysed. Alleles 2 and 7 were the least frequent, allele 7 being the rarest found only once in an ALS patient. There was no significant difference in allele frequency between the ALS cohort and matched controls (Fisher's exact test). **(B)** The distribution of the 12 identified genotypes of the CFAP410 VNTR in an ALS cohort and matched controls. There is no significant difference in genotype frequency between the ALS cohort and matched controls (Fisher's exact test).

the *DESeqDataSetFromTximport* function and raw counts were normalised using the median-of-ratios method, implemented in the *DESeq2* package (Love et al., 2014). The *DESeq2* package in R was also used to detect statistically significant differences in the *CFAP410* isoform expression profiles between different subject groups (ALS vs. NNC). The *ggplot2* package in R containing the *geom_boxplot* function was used to visualise the data specifying the *stat_summary* function to *mean*. The unpaired Wilcoxon test was used to compare two independent groups of samples and to demonstrate statistical significance (*p*-values and effect size can be found in Supplementary Figure 2A, and a histogram plot for the distribution of data for *CFAP410* ENST00000462742 is shown in Supplementary Figure 5).

Tagging SNP analysis identified that genotypes (*AA*, *GA* and *GG*) of rs56212056 are correlated with the two commonest alleles 4 (*A*) and 5 (*G*). The association of the three different SNP alleles with differential *CFAP410* isoform expression was analysed. The unpaired Wilcoxon test was used to compare two

independent groups of samples and to demonstrate statistical significance between different cases and controls and tagging SNP genotype, respectively (p-values and effect size can be found in Supplementary Figure 2B). LD analysis of the *CFAP410* locus including the analysis of 31 SNPs from 243 individuals within Project MinE shows no evidence for significant LD with any of the tested SNPs across the region other than the associations made for alleles 4 and 5 of the *CFAP410* VNTR (Supplementary Figure 3).

Results

Characterisation of isoform expression at the *CFAP410* locus

The *CFAP410* gene contains an SNP (rs75087725) that is associated with ALS risk ($p = 3.08 \times 10^{-10}$) (van Rheenen et al., 2016). Analysis of the *CFAP410* gene using the tandem repeat track on UCSC (https://genome.ucsc.edu/) led to the identification of six distinct tandem repeat domains at this locus. We focus in this communication on the VNTR in intron 1 (Figure 1A), which was the only one that was variable in repeat number. We noted its location relative to the transcriptional start sites and its primary sequence had high GC content (84%) and sequences related to those found in the *C9orf72* VNTR (Supplementary Figure 1 and Figure 1B). It is difficult for global analysis such as ChIPseq to correctly assign ENCODE data over VNTRs themselves; however, when the VNTR was overlaid with ENCODE data, it was found to be adjacent to the markers H3K4Me1 (a marker of regulatory domains associated with enhancers), H3K4Me3 (a marker of regulatory domains associated with promoters) and H3K12Ac (a marker of active regulatory domains associated with active enhancer elements) (Supplementary Figure 1). On RefSeq analysis, this VNTR was found within intron 1 of isoforms 1–3 of *CFAP410* and it could be a component of a promoter region for isoforms that initiate 3' of the VNTR. Extending RefSeq analysis to include Ensembl transcript data increased the number of isoforms identified at this locus (shown in red in Figure 1A). Specifically, this identified a predicted transcript initiating immediately 5' of the VNTR, Ensembl transcript (ENST00000462742), and an anti-sense transcript relative to *CFAP410,* which was annotated as a long non-coding RNA on Ensembl (ENST00000426029).

Expression of isoforms in CNS

Transcriptomic data from the Target ALS cohort was utilised to assess the expression of *CFAP410* isoforms in the CNS. Isoform expression analysis showed that five *CFAP410* isoforms are expressed in the CNS (Figure 5A). The anti-sense transcript (ENST00000426029) relative to *CFAP410* showed no expression in this RNA-seq dataset (Figure 5A). We next analysed the differential expression of *CFAP410* isoforms in case and control subjects (Figure 2). The isoform ENST00000462742 showed significantly reduced expression in cases compared to controls (Figure 2D). This isoform was annotated as a non-coding retained intron transcript. The other two predominantly expressed isoforms (ENST00000339818 and ENST00000325223) demonstrated a similar pattern of expression to ENST00000462742; however, these associations did not reach statistical significance (Figures 2A,B). The remaining *CFAP410* isoforms (ENST00000397956 and ENST00000496321) showed very low expression levels, therefore the data for these isoforms did not give us sufficient power to identify evidence for differential expression between case and control subjects (Figures 2C,E).

The intron 1 VNTR has a minimum of eight distinct alleles

PCR amplification and gel electrophoresis of the VNTR within the *CFAP410* locus was performed in a subset of the cohort from the UK MND Collection DNA Bank ($n = 983$). This region was confirmed to be polymorphic and eight alleles were identified (numbered 1–8 to reflect increasing length) (Figure 1C). The sequence of allele 5 of the VNTR (Supplementary Figure 1B) was found to be comprised of two distinct repeat lengths, 35 and 22bp long, respectively. Furthermore, four alleles were sequenced (Supplementary Figure 1B) and were found to contain the same two repeat lengths in varying patterns. From PCR of this limited number of genomes, the most common alleles were those termed 4 and 5, which contained 9 and 10 repeats, respectively (Supplementary Figure 1B).

The *CFAP410* VNTR has both the properties of an activator domain and a transcription start site

To determine the potential ability of the *CFAP410* VNTR to regulate transcription, *in vitro* reporter gene assays were used. The most common alleles (alleles 4 and 5) were cloned in both orientations of the VNTR into the pGL3-P vector upstream of the SV40 minimal promoter and luciferase activity was compared to the activity of the pGL3-P vector alone. Both alleles demonstrated transcriptional regulatory properties (Figure 3). Alleles 4 and 5 in the endogenous orientation demonstrated a 2.64- and 1.71-fold increase in expression of luciferase over pGL3p alone, respectively, with both being statistically significant (Allele 5, 1.71 ± 0.13, T-test, $p = 1.08 \times 10^{-6}$ and Allele 4, 2.64 ± 0.18, T-test, $p = 3.54 \times 10^{-6}$). Furthermore,

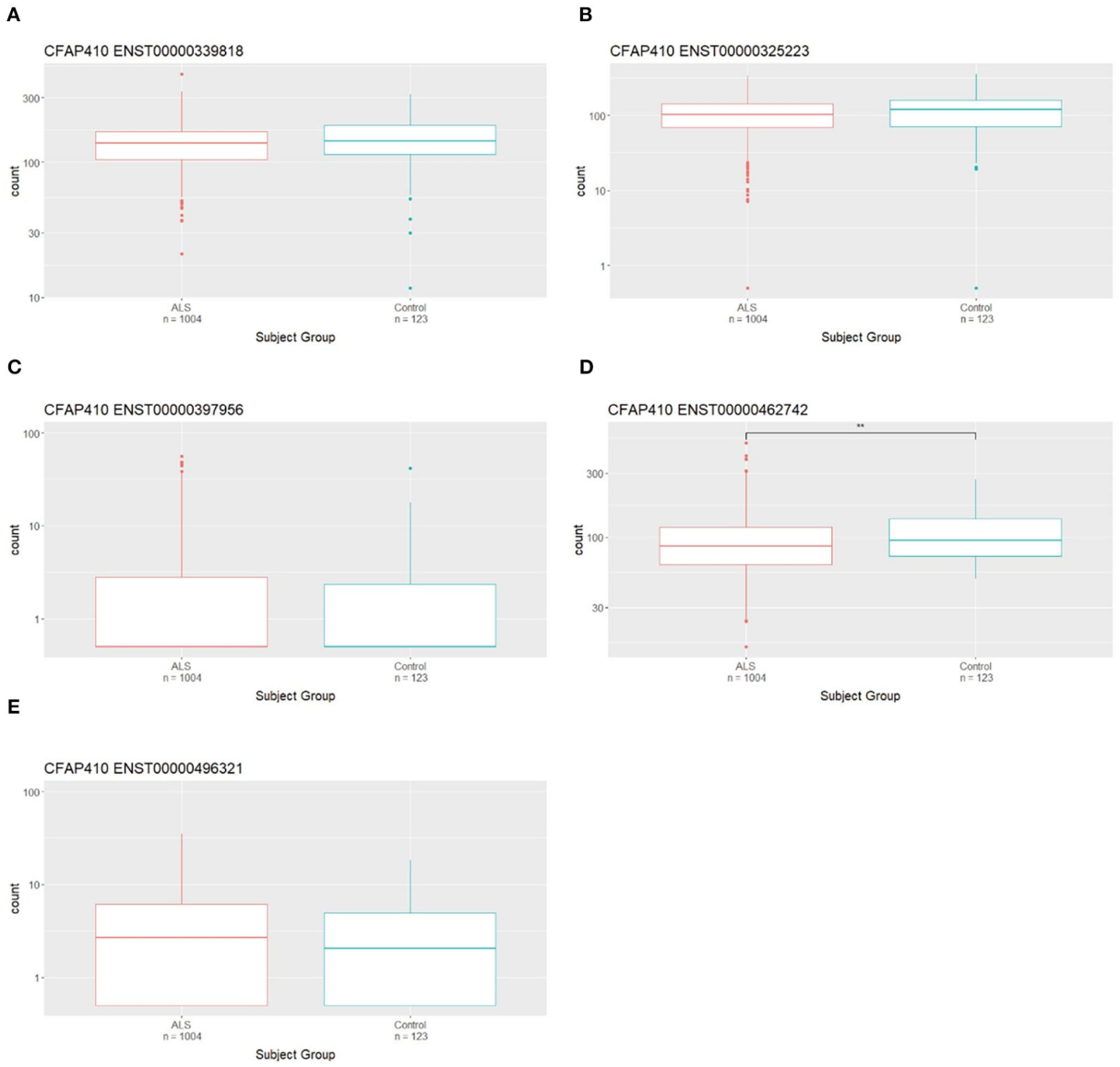

FIGURE 2
Differential expression of *CFAP410* in Case and Controls in the CNS using the NYG transcriptomic data. Expression analysis of *CFAP410* isoforms in ALS and control subjects. RNAseq data from the NYGC ALS cohort were used to compare expression of *CFAP410* isoforms ENST00000339818 **(A)**, ENST00000325223 **(B)**, ENST00000397956 **(C)**, ENST00000462742 **(D)** and ENST00000496321 **(E)**. Wilcoxon test was applied to demonstrate statistical significance indicated as asterisks. $^{**}P \leq 0.01$.

there was a significant difference in luciferase activity when cloned in this direction between alleles 4 and 5 (T-test, $p = 4.39 \times 10^{-7}$), with allele 4 showing a larger enhancement of reporter gene activity. In the reverse orientation, allele 5 alone demonstrated a mild decrease in expression compared to empty pGL3P (0.82 ± 0.03, T-test, $p = 1.49 \times 10^{-7}$), but no change from empty pGL3P was observed for allele 4 in the reverse orientation (1.04 ± 0.06, T-test, $p = 3.70 \times 10^{-1}$).

The location of the VNTR upstream of the Ensembl transcripts ENST00000462742 and ENS00000496321 (equivalent position to the RefSeq short isoform) and the anti-sense transcript (ENST00000426029) (Figures 1A,B) suggested that it could elicit promoter activity. This might be especially true for ENST00000462742, which is directly adjacent to the VNTR, as it has been known for some time that GC-rich sequences can act to initiate transcription in those promoters that lack a TATA box (Kageyama et al., 1989). The VNTR primary sequence demonstrated high GC content (84%), which was consistent with such a model. To address this hypothesis, alleles 4 and 5 of the VNTR were cloned in both orientations

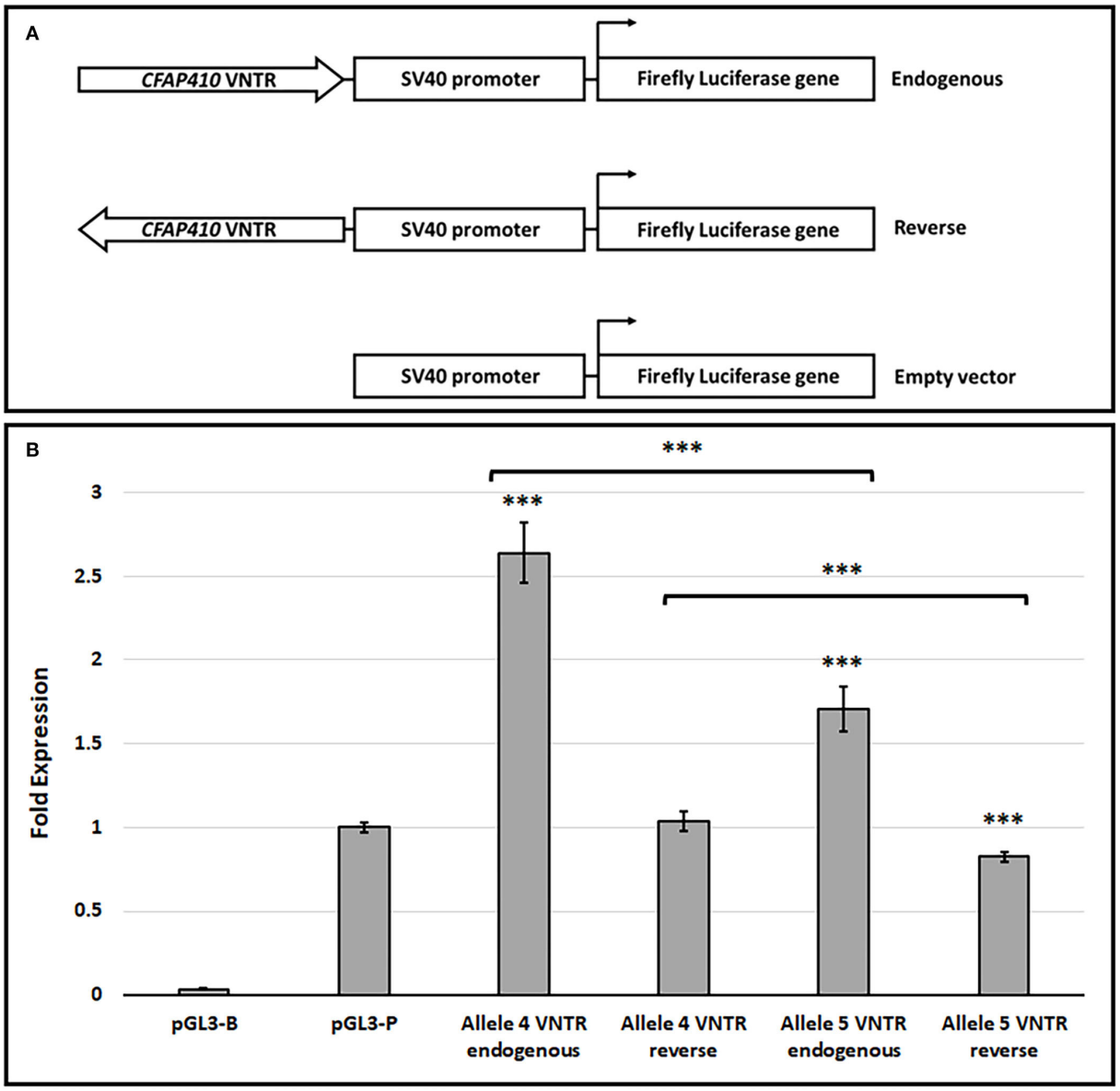

FIGURE 3
The *CFAP410* VNTR shows functional properties in the pGL3-P vector in the HEK293 cell line. **(A)** Schematic for VNTR containing constructs and pGL3 vectors (Promega) used in the luciferase assay. **(B)** The fold activity of alleles 4 and 5 of the *CFAP410* VNTR in the endogenous (forward) orientation within the pGL3P vector, normalised to the internal control Renilla luciferase (Biological replicate $n = 3$, technical replicate per assay $n = 4$). The promoter-less vector (pGL3-B) was included as a negative control. T-test was used to compare VNTR-containing constructs to SV40 unmodified vector (pGL3-P) and to compare all VNTR containing constructs against each other. ***$P = <0.001$.

into pGL3-B (Promega) containing a firefly luciferase reporter without a promoter, which is a well-characterised model to test if a region of DNA can act as a transcriptional start site in reporter gene studies. The unmodified pGL3-P vector (Figure 4) was included in this assay as it contains the minimal SV40 early promoter and therefore serves as a positive control for the level of expression directed by a well-characterised promoter in this cell line model. Both orientations of the VNTR demonstrated promoter activity which would require these domains to act as a transcriptional start site to allow expression of the luciferase reporter. This was especially true in the reverse orientation; VNTR orientations are given as endogenous and reverse to reflect that found in relation to the *CFAP410* gene. VNTR allele 4 in the endogenous orientation led to a 17.02-fold increase in luciferase expression (17.02 ± 0.67, *T*-test, $p = 1.81 \times 10^{-13}$), while the reverse orientation induced a 100.60-fold increase in reporter gene activity (100.60 ± 1.83, *T*-test, $p = 2.38 \times 10^{-17}$) (Figure 4). Similarly, a 20.37-fold increase in luciferase

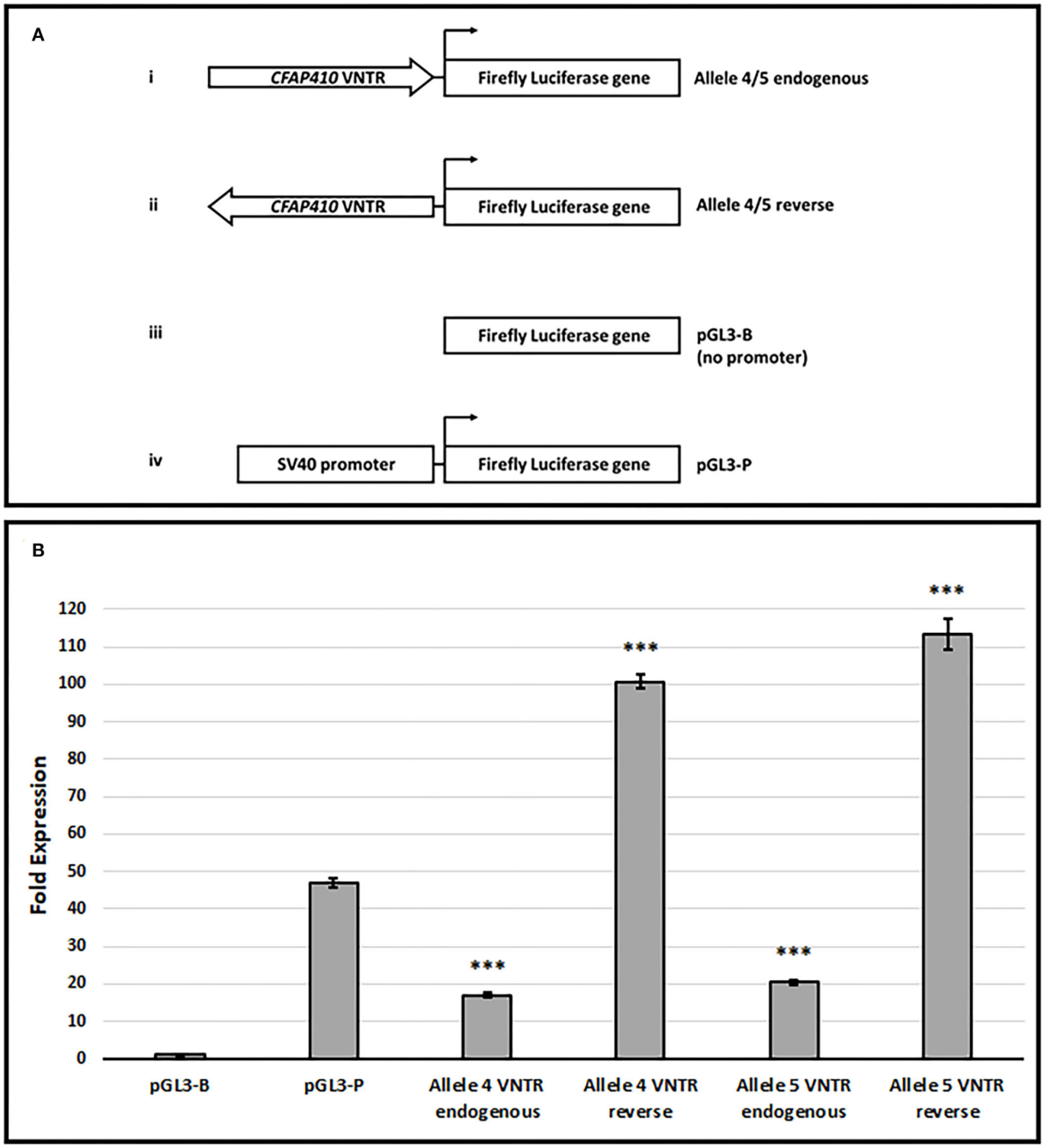

FIGURE 4
The *CFAP410* VNTR shows promoter activity in the pGL3-B vector in HEK293. **(A)** Schematic for VNTR containing constructs and pGL3 vectors (Promega) used in luciferase assay. **(B)** The fold activity of the *CFAP410* VNTR in the endogenous and reverse orientation within the pGL3-B vector normalised to the internal control Renilla luciferase (Biological replicate $n = 3$, technical replicate per assay $n = 4$). The pGL3-P vector was included as a positive control as this contains an SV40 promoter. *T*-test was used to compare VNTR containing constructs to each other (allele 4 vs. allele 5) and promoterless vector alone (pGL3-B). *T*-test was also used to compare VNTR containing constructs to the SV40 promoter vector (pGL3-P). ***$P = <0.001$.

expression was observed in the allele 5 endogenous construct (20.37±0.72, T-test, $p = 4.88 \times 10^{-14}$), while a 113.25-fold increase in luciferase activity in the allele 5 reverse orientation VNTR construct was observed (113.25 ± 4.16, *T*-test, $p = 5.27 \times 10^{-14}$). For comparison, the pGL3-P vector demonstrated a 46.98-fold increase in luciferase expression when compared

to empty pGL3-B (46.98±1.28, *T*-test, $p = 1.09 \times 10^{-15}$). Thus, overall, a moderate but statistically significant increase in luciferase activity was observed in both endogenous orientation VNTR constructs when compared to empty pGL3-B, but this was significantly less than the SV40 minimal promoter activity seen with pGL3-P (*T*-test, $p = 1.09 \times 10^{-15}$). However, in the reverse orientation, a statistically significant increase compared to pGL3-P was observed: a 2.1- and a 2.4-fold increase in luciferase expression by alleles 4 and 5, respectively. Overall, both alleles of the VNTR induced a significant increase in reporter gene expression compared to empty pGL3-B, but allele 5 drove the largest effect in this model. This data suggests the possibility that the VNTR has promoter activity to initiate and direct expression at the *CFAP410* locus.

VNTR variation is associated with *CFAP410* gene expression *in silico*

We identified SNP rs56212056 to be in moderate linkage disequilibrium ($r^2 = 0.75$, D' = 0.949) with the two most common alleles (termed alleles 4 and 5) of the VNTR. It was not possible to identify tagging SNPs for the rarer VNTR alleles in this study given their frequency in the population and the size of our cohort. The A allele of the SNP was found to be correlated with allele 4 of the VNTR and the G allele with allele 5. We used the Target ALS brain expression data to correlate these variants with *CFAP410* isoform expression. The association of three different SNP genotypes (*AA*, *GA* and *GG*) based on the correlation with allele 4 (*A*) or allele 5 (*G*) was analysed (Figure 5). We observed differential levels of isoform expression correlated with distinct G or A genotypes. Three *CFAP410* isoforms (ENST00000339818, ENST00000325223 and ENST00000462742) showed significantly reduced expression with *GG* genotype compared to both *GA* and *AA* genotype (Figures 5B–E). This was in contrast with the levels of expression of the isoform ENST00000496321 where the opposite pattern was observed (Figure 5E). Isoform ENST00000397956 correlated with significantly reduced expression in subjects with two copies of allele 5 (*GG* genotype) compared to subjects with the *GA* genotype only indicating one allele 4 and one allele 5 are present (Figure 5D). The data indicate that distinct VNTRs are able to support differential gene expression in the brain.

Genotyping the VNTR

To assess if specific VNTRs in this region were associated with ALS, the *CFAP410* VNTR was genotyped in a cohort of cases and controls (Table 1). The VNTR was amplified by PCR from blood-derived genomic DNA from patients ($n = 490$) and controls ($n = 493$) and a total of eight alleles of the *CFAP410* VNTR were identified and numbered according to increasing length. Allele 5 (reference genome variant, 584 bp) was the most common allele and was present in 74.49% of cases and 74.75% of controls; no significant difference in frequency was found between the two populations (Fisher's exact test, $p = 0.75$). The next most common variant was allele 4, which was identified in 22.86% of cases and 22.31% of controls: no significant difference in allele frequency was observed between the two groups (Fisher's exact test, $p = 0.93$). The other six alleles were infrequent in the population, with no statistically significant differences being observed (Table 1). There was also no significant difference in the allele frequencies of the eight alleles of the *CFAP410* VNTR when comparing controls and cases using CLUMP software (T_1, $p = 0.91$ and T_4, $p = 0.94$).

To determine the repeat composition and length of the VNTR alleles, the two alleles found most commonly in this cohort (alleles 4 and 5) and two of the rare variants (alleles 2 and 8) were cloned and sequence validated. All alleles were found to be a composite of various numbers of both a 22 bp and 35 bp repeat unit (Supplementary Figures 1A,B). The primary sequence of the VNTR demonstrated variation in the actual sequence of both the 22 or 35 bp repeat unit and the repeating structure indicated a more complex evolution of variation than simply separating into two blocks. It may be of interest to note that the most 5' repeat element had only 34 bp.

Discussion

We have demonstrated that the VNTR in intron 1 of the *CFAP410* gene was functional as a transcriptional regulator *in vitro*. It served as a transcriptional regulatory domain in reporter gene constructs in the HEK293 cell line and directed differential gene expression on the basis of repeat number as both an activator domain and transcriptional start site/promoter. These data were extended to *in silico* analysis in which tagging SNP analysis for the two most common alleles of this VNTR was associated with differential gene expression of *CFAP410* in the brain. This VNTR was found to be highly variable in the general population, with at least eight distinct variants, but there was no significant association of specific genotype with ALS risk. Nevertheless, our data indicated the regulatory properties of this VNTR could support differential regulation of *CFAP410* based on the copy number of the repeat. The ability of the VNTR to direct such expression could be one parameter that works in conjunction with other mechanisms at this locus that could lead to the progression or severity of ALS to specific challenges in the CNS.

It has been established that VNTRs can be both biomarkers for disease risk and also functional regulatory domains affecting both transcription and post-transcriptional mechanisms as reviewed recently (Marshall et al., 2021). These latter transcriptional properties can be exhibited together for the same VNTR as in the case of the monoamine oxidase A (*MAOA*) gene (Manca et al., 2018) and a VNTR in the mir137 gene (Warburton

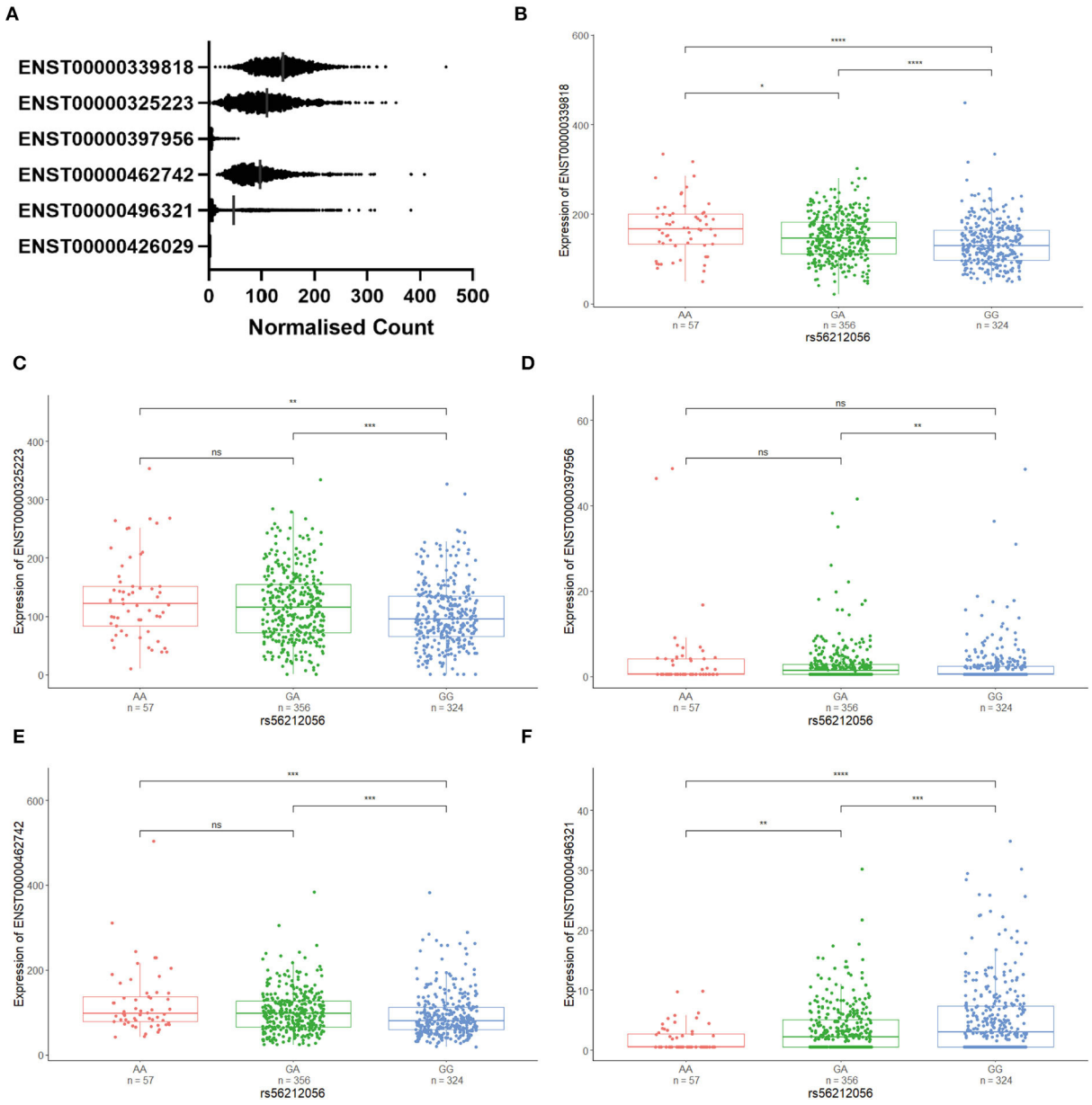

FIGURE 5
The expression of *CFAP410* isoforms is associated with tagging the SNP rs56212056 genotype. **(A)** CFAP410 isoform expression using RNAseq data from the NYGC Target ALS cohort. **(B–F)** Association of three different SNP genotypes (AA, GA, and GG) with an expression of isoforms ENST00000339818, ENST00000325223, ENST00000397956Q24, ENST00000462742, and ENST00000496321 was analysed based on the correlation with allele 4 (A) or allele 5 (G) using transcriptomic data from the NYGC ALS cohort. Wilcoxon test was applied to demonstrate statistical significance indicated as asterisks. *P = <0.05, **P = <0.01, ***P = <0.001, ****P = <0.0001, ns > 0.05.

et al., 2016). Indeed, we have previously demonstrated that a human-specific intron 2 VNTR within the serotonin transporter gene can direct both tissue-specific and differential levels of reporter gene expression in a mouse transgenic model (MacKenzie and Quinn, 1999). We hypothesise that similar mechanisms may operate on the *CFAP410* VNTR, which could lead to distinct levels of expression from different alleles in response to the same cellular challenge. Specifically, we theorise that the association of the two most common alleles with differential *CFAP410* expression can be extrapolated to such properties being embedded in the other minor VNTR alleles.

The genomic location of the *CFAP410* gene is a complex region with multiple isoforms that can be either coding or non-coding in nature, indeed one of the isoforms ENST00000462742

has the hallmarks of a retained intron (Monteuuis et al., 2019) (Figure 1). Interestingly, this isoform was significantly downregulated in the cases relative to the controls. Notably, retained introns have higher GC content compared to introns that are not and this is true for the large GC-rich VNTR found in this intron of *CFAP410*, similarly the difference in the size of the VNTR and thus relative GC content could affect the efficiency of retention. This is consistent with a model in which the presence of RNA structures induced by the GC-rich microsatellite expansions has an inhibitory effect on splicing (Sznajder et al., 2018). New techniques and improved sequencing protocols have demonstrated as much as 95% of the genome can be transcribed, hence alternative splicing and intron retention are emerging areas of importance for gene regulation and disease progression (Monteuuis et al., 2019). In addition to the aforementioned *CFAP410* isoforms, there is also a non-coding RNA that is antisense to the *CFAP410* gene (Figure 1); however, we could find no evidence for measurable levels of this antisense message in the CNS transcriptomic data.

Genotyping the *CFAP410* VNTR led to the discovery of eight alleles in the cases and controls used for this study ($n = 983$) (Figure 1C). The frequencies of all alleles and genotypes were not found to be significantly different between cases and controls (Table 1); however, our limited cohort size would likely to be insufficient to identify rare variants associated with ALS. ALS is a complex disease and given the small sample size we were unable to address many of the different metrics, which contribute to this disease, including disease severity, the onset of disease, disease pathology, age, ethnicity, and known ALS genetic mutations in these patients: the VNTR in question could be important in any one of these metrics. However, we do pose a potential mechanism as to how such variants could contribute to disease risk and show that tandem repeat numbers can drive differential gene expression. Furthermore, the original *CFAP410* ALS association was from a rare variant (van Rheenen et al., 2016), so such rare VNTR variants discovered here could be part of a yet unidentified polygenic risk score.

Unfortunately, expansion of the cohort size is both time- and resource consuming due to the requirement for PCR analysis of all samples. However, the properties of the VNTR to modulate gene expression *in vitro* and correlation with differential *CFAP410* expression *in silico* allowed us to hypothesise that this domain could regulate the expression of this locus in response to the same challenge, which could result in distinct levels of protein expression that could modulate risk and progression of ALS. The primary sequence of the *CFAP410* VNTR also contains consensus sequence binding sites for proteins predicted to bind the *C9ORF72* intronic VNTR (Supplementary Figure 4), potentially inferring contribution to the same signalling pathways. Similarly, modulation of the levels of *CFAP410* could have a significant effect on the function of other ALS risk genes, such as functional interactions with *NEK1* (Fang et al., 2015; Watanabe et al., 2020). These studies demonstrate the increased fusion of genetic risk with an environmental challenge to modulate ALS risk and progression.

Data availability statement

The original contributions presented in the study are included in the article/Supplementary material, further inquiries can be directed to the corresponding author.

Ethics statement

The studies involving human participants were reviewed and approved by Trent Research Ethics Committee in February 2003 ref MREC/02/4/107 and in July 2009, ref 09/HO405/32. Please see https://www.ncbi.nlm.nih.gov/pmc/articles/PMC4501191/ for more details. The patients/participants provided their written informed consent to participate in this study.

Author contributions

JM, AF, VB, and JQ: study idea and design. JM, AF, LL, BM, TS, AP, SK, VB, and JQ: data analysis and interpretation. JM: manuscript drafting. All authors reviewed and approved the final manuscript.

Funding

JM was funded by a Medical Research Council Doctoral Training Studentship [Grant Number MR/N013840/1]. AF is a recipient of a Andrzej Wlodarski Memorial Research Ph.D. scholarship. Motor Neurone Disease Association (Grant Number: 41/523) supports the work of VB and JQ. AF, VB, and JQ by the Andrzej Wlodarski Memorial Research. BM, VB, and JQ are supported by the Darby Rimmer MND Foundation. LL was supported by the Chinese Scholarship Council 201806370099. SK and AP were supported by MSWA and Perron Institute. AA-C is an NIHR Senior Investigator (NIHR202421), also supported by an EU Joint Programme—Neurodegenerative Disease Research (JPND) project grant through the following funding organisations under the aegis of JPND–www.jpnd.eu [United Kingdom, Medical Research Council (MR/L501529/1; MR/R024804/1) and Economic and Social Research Council (ES/L008238/1)] and through the Motor Neurone Disease Association, My Name'5 Doddie Foundation and Alan Davidson Foundation. This study represents an independent research part funded by the National Institute for Health Research (NIHR) Biomedical Research Centre at South London and Maudsley NHS Foundation Trust and King's

College London. This work was supported by resources provided by the Pawsey Supercomputing Centre with funding from the Australian Government and the Government of Western Australia.

Acknowledgments

Samples used in this research were obtained from the UK MND DNA Bank for ALS Research, funded by the MND Association and the Wellcome Trust. We would like to thank people with ALS and their families for their participation in this project. We acknowledge the Target ALS Human Postmortem Tissue Core, New York Genome Centre for Genomics of Neurodegenerative Disease, Amyotrophic Lateral Sclerosis Association and TOW Foundation for RNA-seq data of human ALS patients.

Conflict of interest

The authors declare that the research was conducted in the absence of any commercial or financial relationships that could be construed as a potential conflict of interest.

Publisher's note

Supplementary material

The Supplementary Material for this article can be found online at: https://www.frontiersin.org/articles/10.3389/fnmol.2022.954928/full#supplementary-material

SUPPLEMENTARY FIGURE 1
(A) *CFAP410* VNTR repeat unit breakdown. Number of 22 bp and 35 bp repeat units per allele of the *CFAP410* VNTR (confirmed through Sanger sequencing). **(B)** *CFAP410* VNTR alleles primary sequence and repeat order. Variants 2, 4, 5 and 8 of the *CFAP410* VNTR aligned and split into respective 22 bp and 35 bp repeat units. Allele 2 = 262 bp, allele 4 = 297 bp, allele 5 = 319 bp, allele 8 = 468 bp. Boxes indicate exemplars of the 35p and 22 bp repeat unit. All repeats have been aligned by eye and are therefore arbitrary.

SUPPLEMENTARY FIGURE 2
(A) P-values and effect size of analysis of *CFAP410* isoform expression using NYGC ALS dataset. **(B)** P-values and effect size of tagging SNP analysis of *CFAP410* VNTR.

SUPPLEMENTARY FIGURE 3
LD plot over *CFAP410* locus. LD plot over a 45kb region using 31 SNPs from 243 individuals from the Project MinE encompassing the *CFAP410* gene. Two blocks of LD are located 5′ and 3′ of the *CFAP410* gene. The * indicates rs56212056 which is the SNP in moderate LD with allele 4 and 5 of the VNTR located in *CFAP410*. There is minimal LD between rs56212056 and the other SNPs located in the region. Intensity of each square represents the r^2 between the two SNPs; darker the colour the larger the r^2.

SUPPLEMENTARY FIGURE 4
Alignment of *CFAP410* and *C9ORF72* intronic VNTRs. Both VNTR sequences are polymorphic and contained within intron 1 of the most 5′ start site. The hexamer sequence within *C9orf72* from the UCSC browser **(A)** contains the sequence CCCCGG and GCCCCG identified in red and green respectively which are also found in the CFAP410 sequence **(B)**.

SUPPLEMENTARY FIGURE 5
Histogram plot of the distribution of data in the Target ALS cohort for the *CFAP410* ENST00000462742 transcript.

SUPPLEMENTARY TABLE 1
Available tissues from the NYGC Target ALS cohort stratified by controls and ALS subjects.

References

Abel, O., Powell, J. F., Andersen, P. M., and Al-Chalabi, A. (2012). ALSoD: a user-friendly online bioinformatics tool for amyotrophic lateral sclerosis genetics. *Hum. Mutat.* 33, 1345–1351. doi: 10.1002/humu.22157

Al Khleifat, A., Iacoangeli, A., van Vugt, J., Bowles, H., Moisse, M., Zwamborn, R. A. J., et al. (2022). Structural variation analysis of 6,500 whole genome sequences in amyotrophic lateral sclerosis. *NPJ. Genom. Med.* 7, 8. doi: 10.1038/s41525-021-00267-9

Al-Chalabi, A., Calvo, A., Chio, A., Colville, S., Ellis, C. M., Hardiman, O., et al. (2014). Analysis of amyotrophic lateral sclerosis as a multistep process: a population-based modelling study. *Lancet Neurol.* 13, 1108–1113. doi: 10.1016/S1474-4422(14)70219-4

Al-Chalabi, A., Fang, F., Hanby, M. F., Leigh, P. N., Shaw, C. E., Ye, W., et al. (2010). An estimate of amyotrophic lateral sclerosis heritability using twin data. *J. Neurol. Neurosurg. Psychiatry* 81, 1324–1326. doi: 10.1136/jnnp.2010.207464

Al-Chalabi, A., and Visscher, P. M. (2014). Common genetic variants and the heritability of ALS. *Nat. Rev. Neurol.* 10, 549–550. doi: 10.1038/nrneurol.2014.166

Ali, F. R., Vasiliou, S. A., Haddley, K., Paredes, U. M., Roberts, J. C., Miyajima, F., et al. (2010). Combinatorial interaction between two human serotonin transporter gene variable number tandem repeats and their regulation by CTCF. *J. Neurochem.* 112, 296–306. doi: 10.1111/j.1471-4159.2009.06453.x

Bakhtiari, M., Shleizer-Burko, S., Gymrek, M., Bansal, V., and Bafna, V. (2018). Targeted genotyping of variable number tandem repeats with adVNTR. *Genome Res.* 28, 1709–1719. doi: 10.1101/gr.235119.118

Benson, G. (1999). Tandem repeats finder: a program to analyze DNA sequences. *Nucleic Acids Res.* 27, 573–580. doi: 10.1093/nar/27.2.573

Blauw, H. M., van Rheenen, W., Koppers, M., Van Damme, P., Waibel, S., Lemmens, R., et al. (2012). NIPA1 polyalanine repeat expansions are associated with amyotrophic lateral sclerosis. *Hum. Mol. Genet.* 21, 2497–2502. doi: 10.1093/hmg/dds064

Bury, J. J., Highley, J. R., Cooper-Knock, J., Goodall, E. F., Higginbottom, A., McDermott, C. J., et al. (2016). Oligogenic inheritance of optineurin (OPTN) and C9ORF72 mutations in ALS highlights localisation of OPTN in the TDP-43-negative inclusions of C9ORF72-ALS. *Neuropathology* 36, 125–134. doi: 10.1111/neup.12240

Cady, J., Allred, P., Bali, T., Pestronk, A., Goate, A., Miller, T. M., et al. (2015). Amyotrophic lateral sclerosis onset is influenced by the burden of rare

variants in known amyotrophic lateral sclerosis genes. *Ann. Neurol.* 77, 100–113. doi: 10.1002/ana.24306

Chio, A., Mazzini, L., D'Alfonso, S., Corrado, L., Canosa, A., Moglia, C., et al. (2018). The multistep hypothesis of ALS revisited: The role of genetic mutations. *Neurology* 91, e635–e642. doi: 10.1212/WNL.0000000000005996

Course, M. M., Gudsnuk, K., Smukowski, S. N., Winston, K., Desai, D., Ross, J. P., et al. (2020). Evolution of a human-specific tandem repeat associated with ALS. *Am. J. Hum. Genet.* 107, 445–460. doi: 10.1016/j.ajhg.2020.07.004

DeJesus-Hernandez, M., Mackenzie, I. R., Boeve, B. F., Boxer, A. L., Baker, M., Rutherford, N. J., et al. (2011). Expanded GGGGCC hexanucleotide repeat in non-coding region of C9ORF72 causes chromosome 9p-linked frontotemporal dementia and amyotrophic lateral sclerosis. *Neuron* 72, 245–256. doi: 10.1016/j.neuron.2011.09.011

Fang, X., Lin, H., Wang, X., Zuo, Q., Qin, J., and Zhang, P. (2015). The NEK1 interactor, C21ORF2, is required for efficient DNA damage repair. *Acta Biochim Biophys Sin.* 47, 834–841. doi: 10.1093/abbs/gmv076

Garton, F. C., Trabjerg, B. B., Wray, N. R., and Agerbo, E. (2021). Cardiovascular disease, psychiatric diagnosis and sex differences in the multistep hypothesis of amyotrophic lateral sclerosis. *Eur. J. Neurol.* 28, 421–429. doi: 10.1111/ene.14554

Goldstein, O., Kedmi, M., Gana-Weisz, M., Twito, S., Nefussy, B., Vainer, B., et al. (2019). Rare homozygosity in amyotrophic lateral sclerosis suggests the contribution of recessive variants to disease genetics. *J. Neurol. Sci.* 402, 62–68. doi: 10.1016/j.jns.2019.05.006

Gymrek, M., Willems, T., Guilmatre, A., Zeng, H., Markus, B., Georgiev, S., et al. (2016). Abundant contribution of short tandem repeats to gene expression variation in humans. *Nat. Genet.* 48, 22–29. doi: 10.1038/ng.3461

Hannan, A. J. (2018). Tandem repeats and repeatomes: Delving deeper into the 'dark matter' of genomes. *EBioMedicine.* 31, 3–4. doi: 10.1016/j.ebiom.2018.04.004

Hardiman, O., Al-Chalabi, A., Chio, A., Corr, E. M., Logroscino, G., Robberecht, W., et al. (2017a). Amyotrophic lateral sclerosis. *Nat. Rev. Dis. Primers* 3, 1–19. doi: 10.1038/nrdp.2017.71

Hsieh, T. Y., Shiu, T. Y., Huang, S. M., Lin, H. H., Lee, T. C., Chen, P. J., et al. (2007). Molecular pathogenesis of Gilbert's syndrome: decreased TATA-binding protein binding affinity of UGT1A1 gene promoter. *Pharmacogenet. Genomics* 17, 229–236. doi: 10.1097/FPC.0b013e328012d0da

Iacoangeli, A., Al Khleifat, A., Jones, A. R., Sproviero, W., Shatunov, A., Opie-Martin, S., et al. (2019). C9orf72 intermediate expansions of 24-30 repeats are associated with ALS. *Acta. Neuropathol. Commun.* 7, 115. doi: 10.1186/s40478-019-0724-4

Kageyama, R., Merlino, G. T., and Pastan, I. (1989). Nuclear factor ETF specifically stimulates transcription from promoters without a TATA box. *J. Biol. Chem.* 264, 15508–15514. doi: 10.1016/S0021-9258(19)84859-7

Lam, D., Ancelin, M.-L., Ritchie, K., Freak-Poli, R., Saffery, R., and Ryan, J. (2018). Genotype-dependent associations between serotonin transporter gene (SLC6A4) DNA methylation and late-life depression. *BMC Psychiatry* 18, 1–10. doi: 10.1186/s12888-018-1850-4

Lattante, S., Pomponi, M., Conte, A., Marangi, G., Bisogni, G., Patanella, A., et al. (2018). ATXN1 intermediate-length polyglutamine expansions are associated with amyotrophic lateral sclerosis. *Neurobiol. Aging.* 64, 157.e151–157.e155. doi: 10.1016/j.neurobiolaging.2017.11.011

Love, M. I., Huber, W., and Anders, S. (2014). Moderated estimation of fold change and dispersion for RNA-seq data with DESeq2. *Genome Biol.* 15, 1–21. doi: 10.1186/s13059-014-0550-8

MacKenzie, A., and Quinn, J. (1999). A serotonin transporter gene intron 2 polymorphic region, correlated with affective disorders, has allele-dependent differential enhancer-like properties in the mouse embryo. *Proc. Natl. Acad. Sci. USA.* 96, 15251–15255. doi: 10.1073/pnas.96.26.15251

Manca, M., Pessoa, V., Lopez, A. I., Harrison, P. T., Miyajima, F., Sharp, H., et al. (2018). The regulation of monoamine oxidase a gene expression by distinct variable number tandem repeats. *J. Mol. Neurosci.* 64, 459–470. doi: 10.1007/s12031-018-1044-z

Marshall, J. (2021). The role of non-coding tandem repeat DNA and non-LTR retrotransposons in Amyotrophic Lateral Sclerosis risk loci (Ph. D. thesis). University of Liverpool, England, United Kingdom. Available online at: https://livrepository.liverpool.ac.uk/3116866/1/200883864_March2021.pdf

Marshall, J. N., Lopez, A. I., Pfaff, A. L., Koks, S., Quinn, J. P., and Bubb, V. J. (2021). Variable number tandem repeats – their emerging role in sickness and health. *Exp. Biol. Med.* 246, 1368–1376. doi: 10.1177/15353702211003511

Monteuuis, G., Wong, J. J. L., Bailey, C. G., and Schmitz, U, Rasko, J. E. J. (2019). The changing paradigm of intron retention: regulation, ramifications and recipes. *Nucleic Acids Res.* 47, 11497–11513. doi: 10.1093/nar/gkz1068

Nguyen, H. P., Van Mossevelde, S., Dillen, L., De Bleecker, J. L., Moisse, M., Van Damme, P., et al. (2018). NEK1 genetic variability in a Belgian cohort of ALS and ALS-FTD patients. *Neurobiol Aging* 61 255.e251–255.e257. doi: 10.1016/j.neurobiolaging.2017.08.021

Pacheco, A., Berger, R., Freedman, R., and Law, A. J. (2019). A VNTR regulates miR-137 expression through novel alternative splicing and contributes to risk for schizophrenia. *Sci. Rep.* 9, 11793. doi: 10.1038/s41598-019-48141-0

Purcell, S., Neale, B., Todd-Brown, K., Thomas, L., Ferreira, M. A., Bender, D., et al. (2007). PLINK: a tool set for whole-genome association and population-based linkage analyses. *Am. J. Hum. Genet.* 81, 559–575. doi: 10.1086/519795

Quilez, J., Guilmatre, A., Garg, P., Highnam, G., Gymrek, M., Erlich, Y., et al. (2016). Polymorphic tandem repeats within gene promoters act as modifiers of gene expression and DNA methylation in humans. *Nucleic Acids Res.* 44, 3750–3762. doi: 10.1093/nar/gkw219

Renton, A. E., Majounie, E., Waite, A., Simón-Sánchez, J., Rollinson, S., Gibbs, J. R., et al. (2011). A hexanucleotide repeat expansion in C9ORF72 is the cause of chromosome 9p21-linked ALS-FTD. *Neuron* 72, 257–268. doi: 10.1016/j.neuron.2011.09.010

Roeck, A. D., Duchateau, L., Dongen, J. V., Cacace, R., Bjerke, M., Bossche, T. V., et al. (2018). An intronic VNTR affects splicing of ABCA7 and increases risk of Alzheimer's disease. *Acta Neuropathol.* 135, 827–837. doi: 10.1007/s00401-018-1841-z

Sham, P. C., and Curtis, D. (1995). Monte Carlo tests for associations between disease and alleles at highly polymorphic loci. *Ann. Hum. Genet.* 59, 97–105. doi: 10.1111/j.1469-1809.1995.tb01608.x

Shatunov, A., and Al-Chalabi, A. (2021). The genetic architecture of ALS. *Neurobiol. Dis.* 147, 105156. doi: 10.1016/j.nbd.2020.105156

Soneson, C., Love, M. I., and Robinson, M. D. (2015). Differential analyses for RNA-seq: transcript-level estimates improve gene-level inferences. *F1000Res* 4, 1521. doi: 10.12688/f1000research.7563.1

Sproviero, W., Shatunov, A., Stahl, D., Shoai, M., van Rheenen, W., Jones, A. R., et al. (2017). ATXN2 trinucleotide repeat length correlates with risk of ALS. *Neurobiol Aging* 51, 178.e1–178.e9. doi: 10.1016/j.neurobiolaging.2016.11.010

Sznajder, L. J., Thomas, J. D., Carrell, E. M., Reid, T., McFarland, K. N., Cleary, J. D., et al. (2018). Intron retention induced by microsatellite expansions as a disease biomarker. *Proc. Natl. Acad. Sci. USA.* 115, 4234–4239. doi: 10.1073/pnas.1716617115

Tazelaar, G. H. P., Boeynaems, S., De Decker, M., van Vugt, J., Kool, L., Goedee, H. S., et al. (2020). ATXN1 repeat expansions confer risk for amyotrophic lateral sclerosis and contribute to TDP-43 mislocalization. *Brain Commun.* 2, fcaa064. doi: 10.1093/braincomms/fcaa064

Tazelaar, G. H. P., Dekker, A. M., van Vugt, J., van der Spek, R. A., Westeneng, H. J., Kool, L., et al. (2019). Association of NIPA1 repeat expansions with amyotrophic lateral sclerosis in a large international cohort. *Neurobiol Aging* 74, 234.e239–234.e215. doi: 10.1016/j.neurobiolaging.2018.09.012

Theunissen, F., Flynn, L. L., Anderton, R.S., Mastaglia, F., Pytte, J., Jiang, L., et al. (2020). Structural variants may be a source of missing heritability in sALS. *Front. Neurosci.* 14, 47. doi: 10.3389/fnins.2020.00047

van Blitterswijk, M., van Es, M. A., Hennekam, E. A., Dooijes, D., van Rheenen, W., Medic, J., et al. (2012a). Evidence for an oligogenic basis of amyotrophic lateral sclerosis. *Hum. Mol. Genet.* 21, 3776–3784. doi: 10.1093/hmg/dds199

van Blitterswijk, M., van Es, M. A., Koppers, M., van Rheenen, W., Medic, J., Schelhaas, H. J., et al. (2012b). VAPB and C9orf72 mutations in 1 familial amyotrophic lateral sclerosis patient. *Neurobiol Aging* 33, 2950.e2951–2954. doi: 10.1016/j.neurobiolaging.2012.07.004

van der Spek, R. A. A., van Rheenen, W., Pulit, S. L., Kenna, K. P., van den Berg, L. H., Veldink, J. H., et al. (2019). The project MinE databrowser: bringing large-scale whole-genome sequencing in ALS to researchers and the public. *Amyotroph. Lateral Scler. Frontotemporal Degener.* 20, 432–440. doi: 10.1080/21678421.2019.1606244

van Rheenen, W., Shatunov, A., Dekker, A. M., McLaughlin, R. L., Diekstra, F. P., Pulit, S. L., et al. (2016). Genome-wide association analyses identify new risk variants and the genetic architecture of amyotrophic lateral sclerosis. *Nat. Genet.* 48, 1043–1048. doi: 10.1038/ng.3622

van Rheenen, W., van der Spek, R. A. A., Bakker, M. K., van Vugt, J. J. F. A., Hop, P. J., Zwamborn, R. A. J., et al. (2021). Common and rare variant association analyses in amyotrophic lateral sclerosis identify 15 risk loci with distinct genetic architectures and neuron-specific biology. *Nat. Genet.* 53, 1636–1648. doi: 10.1038/s41588-021-00973-1

Vucic, S., Westeneng, H. J., Al-Chalabi, A., Van Den Berg, L. H., Talman, P., and Kiernan, M. C. (2019). Amyotrophic lateral sclerosis as a multi-step process: an Australia population study. *Amyotroph. Lateral Scler. Frontotemporal Degener.* 20, 532–537. doi: 10.1080/21678421.2018.1556697

Warburton, A., Breen, G., Bubb, V. J., and Quinn, J. P. (2016). A GWAS SNP for Schizophrenia is linked to the internal mir137 promoter and supports differential allele-specific expression. *Schizophr. Bull.* 42, 1003–1008. doi: 10.1093/schbul/sbv144

Warburton, A., Breen, G., Rujescu, D., Bubb, V. J., and Quinn, J. P. (2015). Characterization of a REST-regulated internal promoter in the schizophrenia genome-wide associated gene MIR137. *Schizophr. Bull.* 41, 698–707. doi: 10.1093/schbul/sbu117

Watanabe, Y., Nakagawa, T., Akiyama, T., Nakagawa, M., Suzuki, N., Warita, H., et al. (2020). An amyotrophic lateral sclerosis-associated mutant of C21ORF2 is stabilized by NEK1-mediated hyperphosphorylation and the inability to bind FBXO3. *iScience* 23, 101491. doi: 10.1016/j.isci.2020.101491

Wroe, R., Butler, A. W.-L., Andersen, P. M., Powell, J. F., and Al-Chalabi, A. (2009). ALSOD: the amyotrophic lateral sclerosis online database. *Amyotrophic Lateral Sclerosis* 9, 249–250. doi: 10.1080/17482960802146106

Yilmaz, R., Weishaupt, K., Valkadinov, I., Knehr, A., Brenner, D., and Weishaupt, J.H. (2022). Quadruple genetic variants in a sporadic ALS patient. *Mol. Genet. Genomic Med*. 10, e1953. doi: 10.1002/mgg3.1953

Zou, Z.-Y., Zhou, Z.-R., Che, C.-H., Liu, C.-Y., He, R.-L., and Huang, H.-P. (2017). Genetic epidemiology of amyotrophic lateral sclerosis: a systematic review and meta-analysis. *J. Neurol. Neurosurg. Psychiatry*. 88, 540–549. doi: 10.1136/jnnp-2016-315018

Zukic, B., Radmilovic, M., Stojiljkovic, M., Tosic, N., Pourfarzad, F., Dokmanovic, L., et al. (2010). Functional analysis of the role of the TPMT gene promoter VNTR polymorphism in TPMT gene transcription. *Pharmacogenomics* 11, 547–557. doi: 10.2217/pgs.10.7

frontiers | Frontiers in Cellular Neuroscience

TYPE Review
PUBLISHED 29 September 2022
DOI 10.3389/fncel.2022.1013450

OPEN ACCESS

EDITED BY
Anwen Shao,
Zhejiang University, China

REVIEWED BY
Xiao Lin,
First Affiliated Hospital of Wenzhou Medical University, China
Wei Yu,
Zhejiang University, China

*CORRESPONDENCE
Li Zhang
zhangli2007js@126.com

SPECIALTY SECTION
This article was submitted to Cellular Neuropathology, a section of the journal Frontiers in Cellular Neuroscience

RECEIVED 08 August 2022
ACCEPTED 09 September 2022
PUBLISHED 29 September 2022

CITATION
Tian M, Mao L and Zhang L (2022) Crosstalk among N6-methyladenosine modification and RNAs in central nervous system injuries.
Front. Cell. Neurosci. 16:1013450.
doi: 10.3389/fncel.2022.1013450

Crosstalk among N6-methyladenosine modification and RNAs in central nervous system injuries

Mi Tian[1], Lei Mao[2] and Li Zhang[2]*

[1]Department of Anesthesiology, Affiliated Zhongda Hospital of Southeast University, Nanjing, Jiangsu, China, [2]Department of Neurosurgery, Jinling Hospital, School of Medicine, Nanjing University, Nanjing, Jiangsu, China

Central nervous system (CNS) injuries, including traumatic brain injury (TBI), intracerebral hemorrhage (ICH) and ischemic stroke, are the most common cause of death and disability around the world. As the most common modification on ribonucleic acids (RNAs), N6-methyladenosine (m6A) modification has recently attracted great attentions due to its functions in determining the fate of RNAs through changes in splicing, translation, degradation and stability. A large number of studies have suggested that m6A modification played an important role in brain development and involved in many neurological disorders, particularly in CNS injuries. It has been proposed that m6A modification could improve neurological impairment, inhibit apoptosis, suppress inflammation, reduce pyroptosis and attenuate ferroptosis in CNS injuries *via* different molecules including phosphatase and tensin homolog (PTEN), NLR family pyrin domain containing 3 (NLRP3), B-cell lymphoma 2 (Bcl-2), glutathione peroxidase 4 (GPX4), and long non-coding RNA (lncRNA). Therefore, m6A modification showed great promise as potential targets in CNS injuries. In this article, we present a review highlighting the role of m6A modification in CNS injuries. Hence, on the basis of these properties and effects, m6A modification may be developed as therapeutic agents for CNS injury patients.

KEYWORDS

central nervous system injuries, m6A modification, neurological impairment, apoptosis, inflammation, downstream molecules

Introduction

Central nervous system (CNS) injuries and their potential long-term consequences are of major concern for public health. High rates of morbidity and mortality making them a global health challenge (Hornby et al., 2020). CNS is highly sensitive to external mechanical damage, such as traumatic brain injury (TBI), spinal cord injury (SCI), subarachnoid hemorrhage (SAH), and stroke, presenting a limited capacity for regeneration due to its inability to restore either damaged neurons or synaptic network (Zhang and Wang, 2019). Although some of the pathological processes of CNS injuries such as blood brain barrier (BBB) disruption, inflammation and oxidative stress have been elucidated, the detailed mechanisms driving these processes are poorly understood (Devanney et al., 2020). Despite the progress has been made in the prevention and treatment of CNS injuries in the past, patients suffering from CNS injuries usually end up with poor prognosis (Liddelow and Barres, 2017). Therefore, it is urgently needed to find optimal therapies and improve patients' long-term neurological functioning after CNS injuries.

N6-methyladenosine (m6A) was firstly reported in 1974 (Reichel et al., 2019). It is evolutionarily conserved, ranging from yeasts, plants, insects to mammals (Malovic et al., 2021). M6A modification is one of the most common epigenetic modifications for eukaryotic ribonucleic acids (RNAs), not only in messenger RNAs (mRNAs) but also in a variety of non-coding RNAs (ncRNAs) such as long non-coding RNAs (lncRNAs) and circular RNAs (circRNAs) (Zhou L. et al., 2022). The modification process of m6A is regulated by methyltransferases (writers), demethylases (erasers), and RNA binding proteins (RBPs; readers) (Jang et al., 2022). Specifically, the sixth nitrogen atom on the RNA molecule is methylated by the catalysis of methyltransferase, the methylation site is then identified by RBPs and participates in the pathophysiological processes *via* mediating RNA splicing, transcription, translation and decay (Chen D. et al., 2022; Jang et al., 2022). However, the methylation sites can be demethylated under the effect of demethylase, indicating a dynamic and reversible process (Luo et al., 2022). Recently, the regulation role of m6A modification in CNS has gradually been explained. M6A is enriched in RNAs of neurogenesis, cell cycle and neuron differentiation (Chokkalla et al., 2020; Pan et al., 2021). The dysregulation of writer, eraser, and reader proteins of m6A modification is associated with the occurrence and conversion of neurological diseases including CNS injuries (Wang et al., 2021; Zhai et al., 2022).

In the present study, we provide an overview of m6A modification in CNS injuries and the associated molecular mechanisms. This review describes (1) Abnormal expression of m6A modification proteins in CNS injuries; (2) Detecting methods of m6A modification; (3) Function of m6A modification in CNS injuries; (4) Downstream molecules of m6A modification in CNS; (5) Crosstalk between m6A modification and RNAs in CNS injuries, and (6) Possible research directions of m6A modification in CNS injuries.

Abnormal expression of N6-methyladenosine modification proteins in central nervous system injuries: Writers, erasers and readers

The m6A modification-related proteins can act as writers or erasers to add or remove m6A, respectively, that means, these proteins determine whether m6A is methylated or demethylated. While, RBPs called readers recognize m6A sites to interact with RNA (Zhang F. et al., 2022). At present, it has been found that there was abnormal expression of m6A modification regulatory factors in CNS injuries, which may explain their pathological mechanisms (**Figure 1**).

Writers

Writers, also known as methyltransferase complexes (MTCs), are a class of functional proteins that promote the methylation modification of adenine base sites (Cai et al., 2022). The core proteins of m6A methyltransferase include methyltransferase-like protein 3 (METTL3), METTL14, Wilms tumor 1-associated protein (WTAP), Vir-like m6A methyltransferase-associated (VIRMA) and zinc finger CCCH-type containing 13 (ZC3H13) (Yang X. et al., 2022). METTL3 is the critical component protein in m6A MTCs. METTL3 has its own catalytic ability, which can bind with methyl alone to catalyze the formation of m6A, and promote protein translation in the cytoplasm (Wang and Zhou, 2022). Although METTL14 has no catalytic function and cannot promote the formation of m6A independently, it can form a heterodimer with METTL3 and recognizing the m6A specific sequence (Zhang and Liu, 2022). Therefore, these MTCs are not independent in organisms, they can form complexes to co-perform catalytic functions. WTAP owns the functions of stabilizing heterodimers, locating nuclear spots, facilitating RNA degradation and regulating cell differentiation. WTAP can promote m6A modification by guiding METTL3-14 heterodimer localization to nuclear spots (Akcaoz and Akgul, 2022). VIRMA, also known as KIAA1429, regulates m6A mRNA level by recruiting methyltransferase METTL3/METTL14/WTAP complex through its N-terminal (Sommerkamp et al., 2022). Under the recruitment of VIRMA, METTL3, and METTL14 form a heterodimer. Then WTAP stabilizes the heterodimer and forms the m6A MTC in the nucleus. The m6A MTC promotes the transfer of methyl from

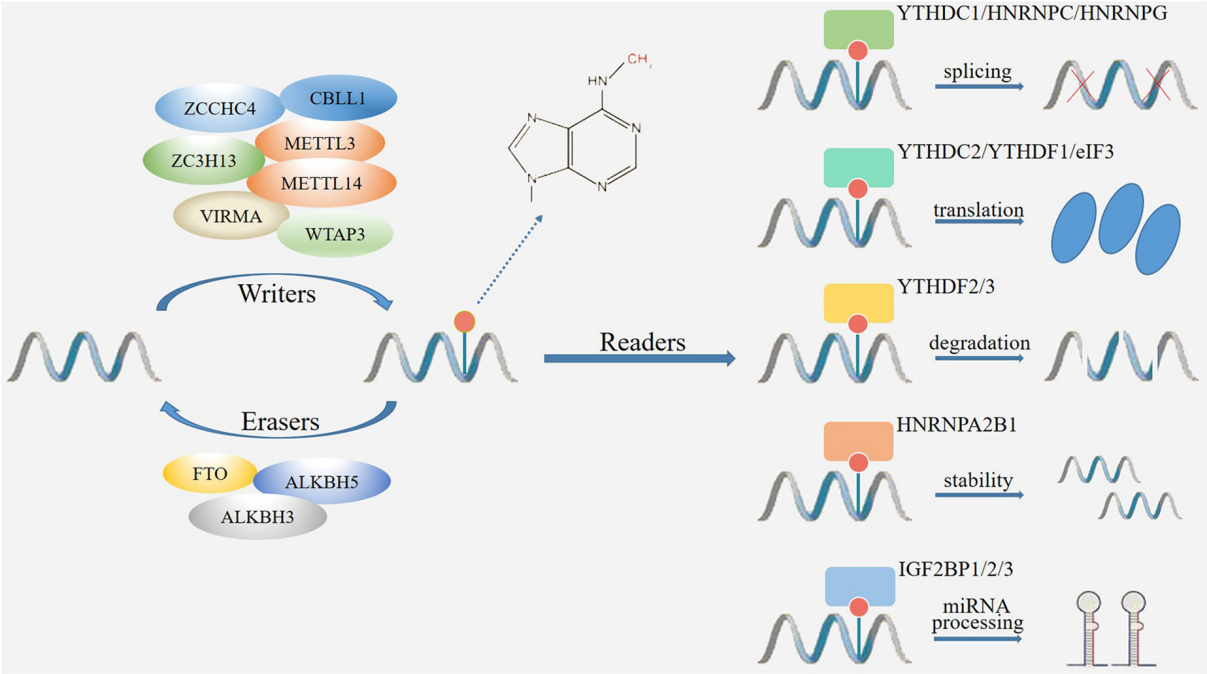

FIGURE 1
The mechanism of m6A modification. M6A modification is catalyzed by methyltransferase and demethylase acting as writers (METTL3, METTL14, WTAP3, VIRMA, ZC3H13, ZCCHC4, CBLL1) and erasers (FTO, ALKBH3, ALKBH5) to add and remove m6A. The m6A binding proteins (readers) include YTH and IGF2BP family proteins, which determine the fate of RNAs through changes in splicing, translation, degradation, stability, and miRNA processing.

the donor substrate S-adenosylmethionine, and combines with the nitrogen-containing base at the sixth position of adenylate to form m6A (Cayir, 2022). ZC3H13 can combine with WTAP to promote MTC deposition in nuclear and enhance m6A modification (Song et al., 2022). Recently, some novel methyltransferases have been recognized. For example, METTL5 has been shown to catalyze m6A installation by forming a METTL5-TRMT112 heterodimeric complex to increase metabolic stability, suggesting a novel RNA-binding pattern different from the METTL3-14 heterodimer (Oerum et al., 2021).

It has been indicated that CNS injuries could change the expression of writers. For example, in a mouse TBI model, genome-wide profiling of m6A-tagged transcripts was conducted by m6A-modified RNA immunoprecipitation sequencing (m6A-RIP-seq) and RNA sequencing (RNA-seq). The results showed that METTL3 was downregulated after TBI. In addition, 922 m6A peaks were differentially expressed as determined by m6A-RIP-seq, with 370 upregulated and 552 downregulated (Wang et al., 2019). Furthermore, in a rat TBI model, Yu et al. conducted a genome-wide profiling of mRNA m6A methylation in rat cortex *via* methylated RIP sequencing (MeRIP-Seq). They found that after TBI, the expressions of METTL14 were significantly down-regulated in rat cerebral cortex (Yu et al., 2020).

Erasers

Erasers, also known as demethylase complexes, demethylate m6A modification *via* demethylases such as fat mass and obesity associated protein (FTO) and α-ketoglutarate-dependent dioxygenase alk B homolog 5 (ALKBH5), thereby maintaining the dynamic and reversible of m6A modification (Li Y. et al., 2022). FTO is the first discovered demethylase that belongs to the ALKB family. It is an oxygenase dependent on Fe^{2+} and 2-oxoglutarate, which can catalyze the demethylation of nucleotides (Li L. et al., 2022). ALKBH5 is found after FTO, it is Fe^{2+} and α- Ketoglutarate (α-Kg) dependent non-heme oxygenase (Imanishi, 2022). Although both FTO and ALKBH5 are demethylases, they are differentially distribution in mammalian organs and have different substrate preferences. Firstly, FTO is enriched in brain, especially in neurons, and plays an important regulatory role in CNS. While ALKBH5 is highly expressed in testes and is essential for spermatogenesis. Secondly, although FTO and ALKBH5 are both demethylases of m6A, the main substrate of FTO is N6-hydroxymethyladenosine (hm6A) and N6-formyladenosine (fm6A) but the main substrate of ALKBH5 is original adenylate. Thirdly, FTO-mediated demethylation process is gradually completed. M6A is firstly converted to hm6A, then transformed to fm6A, and finally reduced to original adenylate. However, ALKBH5 can

directly reduce m6A to original adenylate (Kumari et al., 2022; Song et al., 2022). The difference between FTO and ALKBH5 in the metabolic mechanism of m6A results in different biological functions (Chen J. et al., 2022). Recently, ALKBH3 has been suggested to be a novel demethylase protein which mediates the demethylation of m6A, m1A and 3-methylcytidine (m3C) on tRNA (Liu et al., 2021).

The expression of erasers in CNS injuries has also been analyzed. In a rat stroke model, the protein levels of demethylases FTO and ALKBH5 were changed, both FTO and ALKBH5 co-regulated m6A demethylation, which played a crucial role in cerebral ischemia/reperfusion (I/R) injury (Xu K. et al., 2020).

Readers

Readers, also named as m6A methylation RBPs, can bind to specific m6A methylation sites of RNAs and determine the fates of m6A-methylated RNAs (Zhou H. et al., 2022). By recruiting specific methylation RBPs on RNAs, m6A interacts with its substrate to regulate different molecular effects, including RNA processing, mRNA enucleation, translation and shearing (Zhou W. et al., 2022). Currently, there are three RBPs that have been widely studied, including YT521-B homology (YTH) domain family proteins, insulin-like growth factor 2 mRNA-binding proteins (IGF2BPs) and heterogeneous nuclear ribonucleoproteins (HNRNP) family proteins (Liu C. et al., 2022). The YTH domain family proteins are important m6A methylation RBPs, which can bind to m6A and affect the outcome of m6A-methylated RNAs (Yan et al., 2022). YTH proteins mainly includes YTHDFs and YTHDCs subtypes. YTHDFs subtypes locate in the cytoplasm, among them YTHDF1 promotes mRNA translation, YTHDF2 induces RNA degradation and YTHDF assists YTHDF1/2 to exhibit functions (Liao J. et al., 2022). YTHDCs subtypes locate in the nucleus, among them YTHDC1 affects RNA splicing, enucleation and gene silencing, YTHDC2 suppresses RNA stability and promotes RNA translation (Han et al., 2021). In contrast to the YTH family proteins, IGF2BP proteins, including IGF2BP1/2/3, modulate gene expression output by increasing the stability and translation efficiency of m6A-modified RNAs (Ramesh-Kumar and Guil, 2022). HNRNP family proteins, such as HNRNPC, are located in the nucleus. HNRNPC can recognize and bind to m6A-modified regions in RNAs, thus affecting the abundance and alternative splicing of target RNAs (Huang et al., 2021).

The expression of readers was also changed after CNS injuries. In a rat cerebral ischemia model, YTHDC1 was up-regulated in the early phase of ischemic stroke. Knockdown of YTHDC1 exacerbated ischemic brain injury and overexpression of YTHDC1 protected rats against brain injury (Zhang Z. et al., 2020).

Detecting methods of N6-methyladenosine modification

In the past decades, due to the limitation in technical means, the detection of m6A and the identification of m6A at the single-base level had been progressing slowly (Shulman and Stern-Ginossar, 2020; Wang Y. N. et al., 2020). In recent years, with the continuous exploration and research on m6A, a number of methods have been developed to detect m6A modification, which further promoted m6A research.

Current methods for m6A detection are based on RNA chemistry or immunoprecipitation to assess an overall transcriptome-wide m6A level and high-throughput sequencing to evaluate the precise location of m6A sites. Dot blot technology (Nagarajan et al., 2019), chemical proteomics approach (Arguello et al., 2017) and high-performance liquid chromatography-mass spectrometry (HPLC-MS) method (Zhang Y. et al., 2020) are common approaches to observe overall m6A changes in transcriptome-wide level. However, they do achieve the quantitation or semi-quantitation, but fail to precisely locate the m6A sites (Zhang Y. et al., 2020). To date, methylated RNA immunoprecipitation (MeRIP)-seq (Meyer et al., 2012) and m6A-seq (Dominissini et al., 2012) are the most used approaches for the detection of m6A sites. These new methods are based on the high specificity of antibodies against m6A, and its combination with high-throughput sequencing makes it possible to describe the specific map of m6A modification in the mammalian transcriptome. The first step is to fragment the RNA, followed by the use of immuno-magnetic beads with m6A antibody to enrich the m6A-methylated RNA fragments and the purification of the enriched RNA fragments to construct a high-throughput sequencing library by performing on-machine sequencing. In addition, a common transcriptome library needs to be constructed separately as a control. Finally, the two sequencing libraries are put together for bioinformatics analyses, and the region with a higher degree of m6A methylation is obtained, which is also called m6A peak (Dominissini et al., 2012; Meyer et al., 2012). However, the approaches can only detect m6A peaks but not acquire the precise position of m6A residues.

To overcome the shortcoming, a novel method called m6A-specific ultraviolet crosslinking immunoprecipitation sequencing technology (miCLIP) was developed to achieve m6A sequencing at single-base resolution (Linder et al., 2015). MiCLIP is the combination of ultraviolet radiation-induced crosslinking coupled with immunoprecipitation sequencing (CLIP-seq) and MeRIP-seq. CLIP-seq can reveal interactions between RNA and RNA-binding proteins at the genome-wide level (Stojkovic et al., 2021). Therefore, this combination can provide m6A information beyond the conserved RRACH

sequence, which compensates for the deficiency of MeRIP-seq (Linder et al., 2015; Wang Y. et al., 2020). In addition, several other approaches such as m6A level and isoform-characterization sequencing (m6A-LAIC-seq) (Molinie et al., 2016), site-specific cleavage and radioactive labeling followed by ligation-assisted extraction and thin-layer chromatography (SCARLET) (Liu et al., 2013) and MAZTER-seq (Garcia-Campos et al., 2019) were newly developed to achieve more precise location even at single-nucleotide resolution.

Functions of N6-methyladenosine modification in central nervous system injuries

Regulation of m6A modification was firstly reported to exhibit neuroprotection on CNS injuries in Wang et al. (2019). Subsequently, a growing number of studies have demonstrated that modulation of m6A modification could provide neuroprotective effects in CNS injuries. The neuroprotection of m6A modification was reportedly attributed to its effects on improvement of neurological impairment, inhibition of inflammation, suppression of apoptosis, reduction of pyroptosis and regulation of ferroptosis (**Table 1**).

Neurological impairment

Neurological impairment covers a wide range of illnesses and injuries. Depending on the severity and type of impairment, people can be more or less affected (Kitzmuller et al., 2019). Neurological impairment may occur in CNS injuries, which is characterized by problems in sensory-motor, cognitive and psychological functions, thereby affecting the quality and meaningfulness of life (Benedictus et al., 2010; Hilton et al., 2018). Neurological impairment is a main determinant of functional disability, people suffering from neurological impairment may be unable to use both arms and legs sufficiently, leaving them highly dependent on others (Odgaard et al., 2017).

The effects of m6A modification on neurological impairment after CNS injuries have been studied. In a rat TBI model, a genome-wide profiling of mRNA m6A methylation in rat cortex was conducted *via* MeRIP-Seq. The analysis of both m6A peaks and mRNA expression revealed that there were 175 mRNAs significantly altered methylation and expression after TBI. Of these mRNAs, the expression of FTO was significantly down-regulated. Moreover, FTO inhibitor FB23-2 increased the modified neurological severity score (mNSS) score of rats after TBI, suggesting that inhibition of FTO exacerbated damage to neurological function caused by TBI (Yu et al., 2020). Furthermore, in a rat ischemic stroke model, overexpression of m6A reader YTHDC1 alleviated brain neurological deficits as measured by NSS through promoting phosphatase and tensin homolog (PTEN) mRNA degradation to increase protein kinase B (AKT) phosphorylation (Zhang Z. et al., 2020).

The precise mechanisms underlying how m6A modification regulated neurological impairment were unclear. It has been revealed that neurological impairment involved selective neuronal loss in the hippocampus and cortex (Wang Z. et al., 2014). Therefore, m6A modification may improve neurological impairment by intervene with these pathological processes.

Inflammation

Inflammation is one of the major determinants of secondary brain damage after CNS injuries (Shang et al., 2019). In normal conditions, inflammation is a vital physiological immune response against noxious stimuli (such as injury or infection) and defends the host against pathogenic threats (Yang and Zhou, 2019). However, in respond to CNS injuries, excessive inflammation may provoke substantial detrimental effects (Shi et al., 2019).

Numerous studies have proposed that m6A modification exerted a central effect in CNS injuries-induced inflammation. Wang B. et al. (2022) demonstrated that in a sepsis brain injury (SBI) model, lipopolysaccharide (LPS) increased the levels of tumor necrosis factor-α (TNF-α), interleukin-1β (IL-1β), IL-6 and decreased the levels of IL-10 in 1321N1 cells, indicating that LPS treatment induced inflammation in SBI. Treatment of emodin suppressed inflammation as evidenced by decreased levels of TNF-α, IL-1β, IL-6, and increased levels of IL-10 in LPS-treated 1321N1 cells. Moreover, emodin up-regulated m6A levels by activation of METTL3, knockdown of METTL3 reversed the effects of emodin on inflammation in SBI. These data demonstrated that emodin inhibited the inflammation of LPS-treated 1321N1 cells by regulation of METTL3 (Wang B. et al., 2022).

The underlying mechanisms of m6A modification-mediated inflammation are immensely complicated. Studies have indicated that the NF-κB signaling pathway might be the key target. It has been shown that METTL14 played a vital role in macrophage inflammation in atherosclerosis *via* the NF-κB/IL-6 signaling pathway (Zheng et al., 2022). Furthermore, METTL3 participated in sympathetic neural remodeling post-myocardial infarction (MI) *via* the NF-κB pathway and reactive oxygen species (ROS) production. Knockdown of METTL3 inhibited the activation of NF-κB pathway by suppressing the binding of METTL3 to tumor necrosis factor receptor-associated factor 6 (TRAF6), reducing the m6 A level of TRAF6 mRNA and TRAF6 expression, thus inhibiting ROS production and inflammatory responses. These data suggested that METTL3 played an important role in ROS production and inflammatory responses by regulating the TRAF6/NF-κB axis (Qi et al., 2022). Thus, m6A modification may also regulate

TABLE 1 Functions of m6A modification in CNS injuries.

Mechanisms	Factors	Associated molecules
Improve neurological impairment	Reduce neuronal loss in cortex and hippocampus	/
Suppress apoptosis	Reduce chromosomal DNA fragmentation and formation of apoptotic bodies	Bcl-2, caspase-3
Inhibit inflammation	Decrease inflammatory factors and attenuate inflammatory response	NF-κB, TNF-α, IL-1β, *IL-10*
Reduce pyroptosis	Inhibit the formation of inflammasomes	NLRP3, GSDMD-N, caspase-1
Attenuate ferroptosis	Suppress iron-mediated lipid free radical formation and accumulation	GPX4, GSH

CNS, central nervous system; DNA, deoxyribonucleic acid; Bcl-2, B-cell lymphoma-2; NF-κB, nuclear factor kappa-light-chain-enhancer of activated B cells; TNF-α, tumor necrosis factor-α; IL-1β, interleukin-1β; IL-10, interleukin-10; NLRP3, NLR family pyrin domain containing 3; GSDMD-N, N-terminal fragment of gasdermin D; GPX4, glutathione peroxidase 4; GSH: glutathione.

inflammation *via* NF-κB in CNS injuries, further studies are needed to confirm it.

Apoptosis

Apoptosis is a very tightly programmed cell death (PCD) occurring regularly to eliminate unnecessary and unwanted cells as well as to maintain a homeostatic balance between cell survival and cell death (Quillinan et al., 2016). Apoptosis is critical to animals especially long-lived mammals that must integrate multiple physiological and pathological death signals (Rodriguez et al., 2021). It has been shown that insufficient apoptosis can trigger cancer or autoimmunity, while excessive activation of apoptosis could contribute to abnormal cell death (Wang X. X. et al., 2020).

The functions of m6A modification in apoptosis have been explored. The results obtained by Xu S. et al. (2020) demonstrated that in an *in vitro* ischemic stroke model, oxygen and glucose deprivation/reoxygenation (OGD/R) treatment in SH-SY5Y cells induced apoptosis as evidenced by cleavage of caspase-3-poly (ADP-ribose) polymerase (PARP) and increase of Annexin V-positive staining. Additional experimental results showed that OGD/R induced mitochondrial depolarization and caused accumulation of JC-1 green monomers fluorescence. In addition, MeRIP-quantitative real-time polymerase chain reaction (qPCR) results showed that OGD/R induced METTL3-dependent lncRNA D63785 m6A methylation, knockdown of METTL3 caused accumulation of lncRNA D63785, thus suppressing neuronal cell death and apoptosis (Xu S. et al., 2020). In another study conducted by Xu K. et al. (2020) they found that the RNA m6A levels increased consecutive to the decrease of FTO expression in rats after middle cerebral artery occlusion (MCAO) and in primary neurons after OGD/R. Interestingly, the expression of demethylase ALKBH5 was increased significantly. Overexpression of FTO reduced cleaved caspase-3 levels and inhibited apoptosis, but knockdown of ALKBH5 enhanced cleaved caspase-3 levels and promoted apoptosis. The opposite expression of FTO and ALKBH5 might be that the increased ALKBH5 expression served to compensate for stress responses in the neuronal ischemia/hypoxia. Knockdown of ALKBH5 aggravated neuronal apoptosis, indicating that the compensatory rise of ALKBH5 was likely neuroprotective. The mechanism of how ALKBH5 and FTO co-regulated apoptosis was that the demethylation of ALKBH5 and FTO selectively demethylated the B-cell lymphoma 2 (Bcl-2) transcript, prevented Bcl-2 transcript degradation and induced Bcl-2 protein expression (Xu K. et al., 2020). In addition, Zhang Z. et al. (2020) found that after ischemic stroke, knockdown of YTHDC1 reduced the expression of anti-apoptotic protein Bcl-2 and increased the expression of cleaved caspase-3. Overexpression of YTHDC1 reversed these effects, confirming the protective effect of YTHDC1 on ischemic stroke-induced neuronal apoptosis. Mechanistically, YTHDC1 promoted PTEN mRNA degradation to increase AKT phosphorylation, thus up-regulating the expression of Bcl-2, down-regulating the expression of cleaved caspase-3 and facilitating neuronal survival after ischemic stroke (Zhang Z. et al., 2020).

Researches so far have studied the role of m6A modification on apoptosis in general. However, apoptosis can be divided into two pathways: the mitochondria-dependent pathway (the intrinsic pathway) and the death receptor-dependent pathway (the extrinsic pathway) (Radak et al., 2017). Although the function of m6A modification on mitochondria-dependent pathway has been well documented in CNS injuries, whether the death receptor-dependent pathway is associated with the effects of m6A modification in CNS injuries-induced apoptosis remains unclear and further studies are needed to clarify it.

Pyroptosis

Pyroptosis is a type of inflammatory PCD that triggered by inflammasomes (Lu et al., 2022). In the process of pyroptosis, inflammasomes activate caspase-1 or caspase-11/4/5, which

then cleaves gasdermin D (GSDMD) and separates its N-terminal pore-forming domain (PFD). The oligomers of PFD bind to the cell membrane and form macropores on the membrane, resulting in cell swelling and membrane rupture (Al Mamun et al., 2022). Increasing evidence indicates that pyroptosis is involved in many diseases, including CNS injuries (Mi et al., 2022; Wu et al., 2022).

Since pyroptosis aggravates CNS injuries-caused secondary injury, m6A modification may attenuate brain damage by suppressing pyroptosis. Consistent with this hypothesis, Wang B. et al. (2022) proposed that that in an LPS-induced SBI model, emodin treatment decreased the protein levels of syndecan-1 (SDC-1), NLRP3, caspase-1 and the N-terminal fragment of GSDMD (GSDMD-N) in 1321N1 cells, suggesting that emodin could inhibit pyroptosis. While Nigericin, a NLRP3 activator, reversed the effects of emodin on pyroptosis. Furthermore, emodin promoted m6A levels in NLRP3 by METTL3. METTL3 knockdown reversed the effects of emodin on the mRNA expression and stability of NLRP3, showing that emodin suppressed pyroptosis in SBI by inactivating METTL3-mediated NLRP3 expression (Wang B. et al., 2022). In addition, Diao et al. (2020) found that in cerebral ischemia/reperfusion (I/R) injury, hypothermia down-regulated the expression of pyroptosis-related proteins such as NLRP3, ASC, cleaved caspase-1 and GSDMD p30 in primary hippocampal neurons. Besides, the m6A methylated level of PTEN mRNA was elevated in respond to H/R, whereas this level remained stable after treatment of hypothermia. Up-regulation of the PTEN m6A methylated level alleviated the inhibitory effects of hypothermia on pyroptosis, suggesting that hypothermia protected neurons against H/R-induced pyroptosis *via* m6A-mediated activation of PTEN (Diao et al., 2020).

Ferroptosis

Ferroptosis is a non-apoptotic form of cell death that depends on iron-mediated lipid free radical formation and accumulation (Peng et al., 2023). It is characterized by increased lipid peroxidation (LPO) leading to cell death through disturbing membrane integrity (Fuhrmann and Brune, 2022). Ferroptosis can be inhibited by glutathione peroxidase 4 (GPX4) and glutathione (GSH), which are key regulators for protecting cells from LPO (Wang M. P. et al., 2022). Change of mitochondrial morphology is a characteristic of ferroptosis, which comprises mitochondrion condensation or swelling, increased membrane density, decreased crista, and ruptured outer membrane (Yang L. et al., 2022).

Ferroptosis contributes to tissue damage in the case of brain injury and inhibition of ferroptosis can provide neuroprotection. Ferroptosis can also be regulated by m6A modification in CNS injuries. Zhang L. et al. (2022) indicated that in intracerebral hemorrhage (ICH) models, silencing of METTL3 relieved Fe^{2+}, ROS, LPO, malondialdehyde (MDA) levels, and enhanced GSH levels in oxygen and glucose deprivation/hemin (OGD/H)-treated brain microvascular endothelial cells (BMVECs) and ICH mice, suggesting that METTL3 knockdown inhibited the ferroptosis development in ICH. Furthermore, silencing of METTL3 decreased the m6A levels of GPX4 and increased the mRNA levels of GPX4. GPX4 knockdown neutralized the role of METTL3 on inhibiting ferroptosis in OGD/H-treated BMVECs, demonstrating that METTL3 silencing effectively suppressed ferroptosis by regulating m6A and mRNA levels of GPX4 (Zhang L. et al., 2022).

Downstream molecules of N6-methyladenosine modification in central nervous system injuries

The specific mechanisms mediating the functions of m6A modification in CNS injuries have yet to be explained, recent studies have demonstrated that the regulatory factors of m6A modification can target some downstream molecules to play a role in CNS injuries (**Figure 2** and **Table 2**).

Phosphatase and tensin homolog

Phosphatase and tensin homolog is encoded by the p ten gene mapped to chromosome 10q23 (Walker et al., 2013). PTEN is a dual-function protein tyrosine phosphatase that dephosphorylates both proteins and lipids. It is also well known for its ability to regulate cell growth and proliferation (Li M. X. et al., 2022). PTEN is thought to exert its effects *via* negative regulation of phosphoinositide 3-kinase (PI3K). Deletion of PTEN firstly activates class I PI3K, then phosphorylates phosphatidylinositol 4,5-biphosphate (PIP2) to phosphatidylinositol 3,4,5-triphosphate (PIP3) and recruits signaling proteins, including AKT and downstream mammalian target of rapamycin (mTOR) activation (Khan et al., 2021; Alcaraz et al., 2022).

Phosphatase and tensin homolog is highly expressed in adult neurons (Gutilla and Steward, 2016). Under pathological conditions such as CNS injuries, PTEN is important for neuronal proliferation, growth and axon regeneration (Fang et al., 2022; Nieuwenhuis and Eva, 2022). M6A modification can also target PTEN to provide neuroprotection. It has been shown that inhibition of m6A-mediated activation of PTEN could protect neurons against neuronal H/R-induced pyroptosis (Diao et al., 2020). Moreover, YTHDC1, a m6A reader, promoted PTEN mRNA degradation to increase AKT phosphorylation, thus facilitating neuronal survival in ischemic stroke (Zhang Z. et al., 2020).

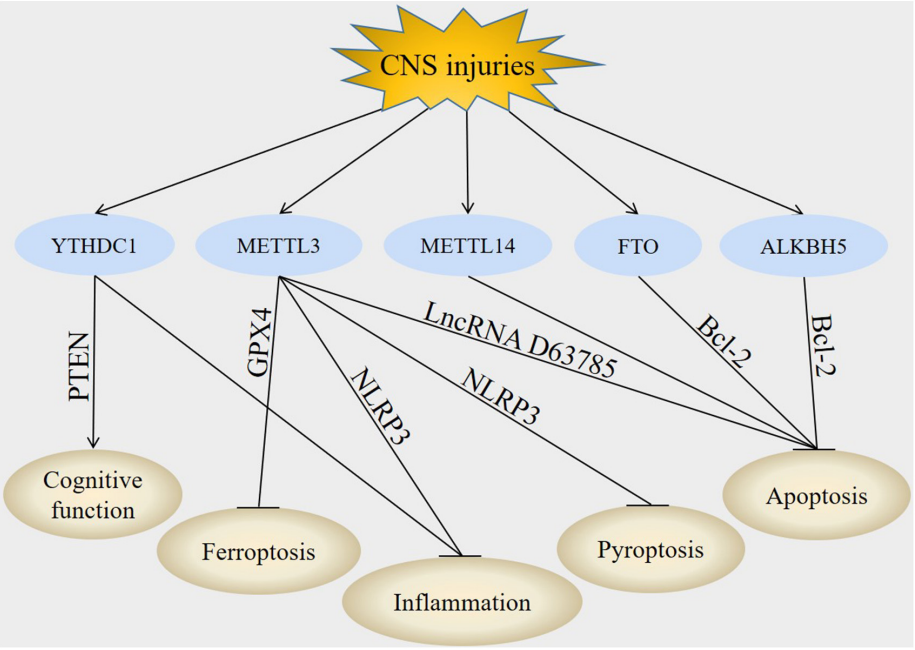

FIGURE 2
Downstream molecules of m6A modification in CNS injuries. In CNS injuries, regulation of YTHDC1, METTL3, METTL14, FTO, and ALKBH5 led to the modulation of PTEN, GPX4, NLRP3, lncRNA D63785, and Bcl-2. These downstream molecules subsequently improved cognitive function, inhibited inflammation, suppressed apoptosis, decreased pyroptosis and attenuate ferroptosis post-CNS injuries.

TABLE 2 The functions and molecular targets of m6A proteins in CNS injuries.

M6A proteins	Models	Animals and/or cells	Beneficial functions of m6A modification	Molecular targets	References
METTL3	ICH SBI Ischemic stroke TBI	Mice, BMVECs Astrocytoma 1321N1 cells SH-SY5Y cells and neurons Mice	Decrease ferroptosis and apoptosis Suppress inflammation and pyroptosis Inhibit cell death and apoptosis Regulate cellular metabolic process	GPX4 NLRP3 LncRNA D63785 /	Wang et al., 2019; Xu S. et al., 2020; Wang B. et al., 2022; Zhang L. et al., 2022
METTL14	TBI	Rats	Reduce apoptosis	/	Yu et al., 2020
FTO	I/R injury TBI	Rats, neurons Mice	Attenuate neuronal damage and apoptosis Repair neurological damage	Bcl-2 /	Xu K. et al., 2020; Yu et al., 2020
ALKBH5	I/R injury	Rats, neurons	Suppress neuronal damage and apoptosis	Bcl-2	Xu K. et al., 2020
YTHDC1	Ischemic stroke	Rats, neurons	Alleviate neurological deficits, increase neuronal survival	PTEN, AKT	Zhang Z. et al., 2020

CNS, central nervous system; ICH, intracerebral hemorrhage; BMVECs, brain microvascular endothelial cells; GPX4, glutathione peroxidase 4; SBI, sepsis brain injury; NLRP3, NLR family pyrin domain containing 3; LncRNA, long non-coding RNA; TBI, traumatic brain injury; I/R, ischemia/reperfusion; Bcl-2, B-cell lymphoma 2; PTEN, phosphatase and tensin homolog; AKT, protein kinase B.

NLR family pyrin domain containing 3

NLR family pyrin domain containing 3 inflammasome is an intracellular protein complex that has emerged as a key mediator of inflammation in many pathologies (Wang M. et al., 2022). NLRP3 inflammasome includes NLRP3, ASC and protease caspase-1. NLRP3 interacts with ASC after activation and then recruits protease caspase-1 by recognizing pathogen-related molecular patterns (PAMPs) or host-derived danger signal molecules (DAMPs) to promote shear activation. Activated

caspase-1 cleaves the precursor IL-1β and IL-18 into mature IL-1β and IL-18, and triggers a series of subsequent inflammatory response (Coll et al., 2022; Wang L. et al., 2022).

The NLRP3 inflammasome is an important defensive component in respond to stress, and its role in CNS injuries has also attracted much attention (Kalra et al., 2022). It has been suggested that inactivation of METTL3-mediated NLRP3 expression could suppress SBI-induced inflammation and pyroptosis in 1321N1 cells (Wang B. et al., 2022).

B-cell lymphoma 2

B-cell lymphoma 2 is an anti-apoptotic protein encoded by the Bcl-2 gene in the human genome specified as an oncogene, it plays an important role in the mitochondria-mediated intrinsic apoptosis pathway (Flores-Romero et al., 2022; Parrondo et al., 2022). Bcl-2 can bind to the pro-apoptotic proteins BAX/BAK, inhibit their recruitment, thereby blocking the release of cytochrome c and activation of caspases that stimulate apoptosis (Sekar et al., 2022; Xu and Ye, 2022). Abnormal expression of Bcl-2 proteins is a common finding in CNS injuries (Nhu et al., 2021). After brain injury, Bcl-2 promotes cell survival and regulates mitochondrial dynamics like fusion and fission. Thus, activation of Bcl-2 can exert a targeted therapeutic effect and inhibit apoptosis (Wang X. X. et al., 2020).

Bcl-2 could also be regulated by m6A modification in CNS injuries. In a cerebral ischemia-reperfusion injury model, demethylation of ALKBH5 and FTO selectively demethylated Bcl-2 transcript, prevented Bcl-2 transcript degradation and enhanced Bcl-2 protein expression, resulting in decreased apoptosis (Xu K. et al., 2020).

Glutathione peroxidase 4

Glutathione peroxidase 4, initially called phospholipid hydroperoxide glutathione peroxidase (PHGPX), was first purified in 1982 (Weaver and Skouta, 2022). GPX4 is the main endogenous antioxidant against lipid peroxidation, it also regulates ROS chain reaction caused by iron accumulation (Zhao et al., 2022). GPX4 can reduce complex hydrogen peroxide such as phospholipid hydrogen peroxide and cholesterol hydrogen peroxide to their respective peroxidation products, thus blocking the chain reaction of LPO and suppressing ferroptosis (Wang Y. et al., 2022). The functional activity of GPX4 depends on the biosynthesis of tripeptide GSH, depletion of GSH causes GPX4 inactivation and increases intracellular LPO (Li D. et al., 2022). Recently, a number of GPX4-targeted therapeutic regimens have been proposed for the treatment of CNS injuries (Huang et al., 2022; Peeples and Genaro-Mattos, 2022; Yuan et al., 2022).

The effects of m6A modification on GPX4 have been reported. It has been shown that knockdown of METTL3 inhibited ferroptosis, decreased the m6A levels of GPX4 and increased the mRNA levels of GPX4 in OGD/H-treated BMVECs and ICH mice. GPX4 knockdown reversed the role of METTL3 on relieving Fe^{2+}, ROS, LPO and MDA levels in OGD/H-treated BMVECs and ICH mice, implying that METTL3 silencing suppressed ferroptosis by regulating m6A and mRNA levels of GPX4 in ICH (Zhang L. et al., 2022).

Long non-coding RNA D63785

Long non-coding RNA refer to the transcripts of non-coding RNAs that are >200 nucleotides in length, they include five different subtypes: sense lncRNA, antisense lncRNA, bidirectional lncRNA, intergenic lncRNA and intronic lncRNA (Cao et al., 2022). LncRNAs were primarily considered as simply transcriptional by-products, recent research have found that they regulate various physiological and pathophysiological processes, such as immunity, cell differentiation and proliferation (Zhang and Wang, 2019). LncRNAs regulate gene expression at the epigenetic, transcriptional, post-transcriptional and chromatin remodeling levels *via* interacting with the 3′ untranslated region (UTR) of mRNA (Chen et al., 2021). LncRNAs also interact with other biomolecules including deoxyribonucleic acids (DNAs), RNAs and proteins through several mechanisms, including acting as inhibitory sponges for miRNAs, participating in chromatin remodeling and affecting protein stability (Wang J. et al., 2022).

The crosstalk between m6A modification and lncRNA has been explained in ischemic stroke. In SH-SY5Y cells and primary murine neurons, OGD/R induced cell death and apoptosis through activation of METTL3-dependent lncRNA D63785 m6A methylation (Xu S. et al., 2020).

Crosstalk between N6-methyladenosine modification and RNAs in central nervous system injuries

Although the relationships between m6A modification and RNAs has been found in CNS injuries, the detailed mechanisms of how m6A modification regulated RNAs were not explained in CNS injuries. However, in other models, accumulating evidences have identified that m6A modification had regulatory effects on RNAs, including their splicing, processing, translation and degradation.

N6-methyladenosine modification modulates the splicing and maturation of RNAs

Nascent transcripts synthesized from DNA must undergo splicing before transformation into mature transcripts with biological functions and m6A modification regulates gene expression by interfering with this process. It has been shown that HNRNPC, HNRNPG, and HNRNPA2B1 were associated with mRNA structure switching, thus regulating gene expression (Liu et al., 2015). M6A modification could affect the binding between HNRNPC and RNA, therefore regulating the alternative splicing and processing of target RNA, resulting in RNA maturation (Liu et al., 2015). Moreover, FTO has been found in the nucleoplasm in a speckle-like manner and partially co-localized with splicing or splicing-associated speckle factors (Jia et al., 2011). FTO-regulated m6A modification was enriched in exon regions on both sides of the 5′ and 3′ splicing sites. These regions overlapped spatially with the enhancer-binding region of the serine- and arginine-rich splicing factor (SRSF), which modulated mRNA splicing (Zhao et al., 2014). It has been suggested that depletion of FTO enhanced the m6A level and promoted the affinity of SRSF2 binding with RNA, thereby increasing the number of target exons and inducing RNA maturation (Zhu et al., 2021). Furthermore, the m6A reader YTHDC1 could recruit the splicing factor SRSF3 to promote exon inclusion but antagonize SRSF10 mRNA binding, which facilitated exon skipping (Xiao et al., 2016). In addition, transactivation responsive RNA-binding protein 2 (TARBP2) recruited the MTCs to deposit m6A marks on transcripts, leading to intron retention *via* the splicing factor SRSF1 (Fish et al., 2019). Besides, METTL3 and YTHDC1 could modulate the maturation of circRNA ZNF609, both METTL3 and YTHDC1 displayed specific m6A signatures that controlled the accumulation of circRNA ZNF609 (Di Timoteo et al., 2020). These results strongly confirmed the essential role of m6A RNA modification in RNA splicing and maturation.

N6-methyladenosine modification regulates the translation of RNAs

The mechanism by which m6A modification improves the translation efficiency is mainly dependent on the binding of reader proteins to protein factors that are required in the translation process, the presence of m6A in exons and surrounding stop codon regions may have an impact on protein production (Liu R. et al., 2022). It has been indicated that ablation of METTL3 enhanced translation efficiency in mouse embryonic stem cells (mESCs) and embryoid bodies (EBs), demonstrating that m6A played a translational regulatory role (Geula et al., 2015). Besides, Lin et al. (2019) found that during the epithelial-mesenchymal transition, YTHDF1 mediates the coding sequence (CDS) m6A-enhanced translation elongation of Snail mRNA *via* interactions with the translation elongation factor eEF2. Moreover, Liu et al. (2020) showed that the eukaryotic translation initiation factor 3 subunit C (EIF3C) was a direct target of YTHDF1. By binding to m6A-modified EIF3C mRNA, YTHDF1 enhanced the translation of EIF3C in an m6A-dependent manner and promoted overall translation output. Furthermore, Jin et al. (2019) found that METTL3, YTHDF1/3 and eIF3b directly promoted the translation of YAP mRNA through interaction with the translation initiation process. In addition, Yang et al. (2017) identified that m6A residues were abundant in circRNAs and could drive efficient initiation of protein translation from circRNAs. The m6A-induced translation of circRNAs could be increased by METTL3/14 and decreased by FTO (Yang et al., 2017). Besides, Di Timoteo et al. (2020) discovered that circRNA ZNF609 translation was modulated through recognition by YTHDF3 and eIF4G2.

N6-methyladenosine modification controls the stability and degradation of RNAs

The stability and degradation of RNAs are critical for the response of living organisms to changeable environments and m6A-containing transcripts can mediate RNA stability and degradation *via* different molecular mechanisms. Wang Y. et al. (2014) indicated that knockdown of METTL3/14 increased the stability of target mRNAs and prevented mRNA degradation in mouse embryonic stem cells, suggesting that mRNA instability was associated with m6A RNA modification. Moreover, Cai et al. (2021) reported that IGF2BP1 increased the stability of YES1 mRNA and prevented its degradation. Furthermore, Wang X. et al. (2014) showed that YTHDF2 selectively recognized an m6A site according to the carboxyl-terminal domain, and the amino-terminal domain was responsible for translocating the YTHDF2-mRNA complex to a cellular RNA decay site to regulate mRNA degradation. In addition, Wu et al. (2021) suggested that METTL3-mediated m6A modification stabilized the expression of circRNA CUX1, which conferred radio-resistance in hypopharyngeal squamous cell carcinoma. Collectively, these data revealed the role of m6A RNA modification in RNAs stability and degradation.

Possible research directions of N6-methyladenosine modification in central nervous system injuries

Central nervous system injuries, caused by cerebrovascular pathologies or mechanical contusions, comprise a diverse group of pathological processes, including autophagy, oxidative

stress, inflammation and apoptosis (Nakamura et al., 2020). Although the functions of m6A modification on CNS injuries-induced neurological impairment, inflammation, apoptosis, pyroptosis and ferroptosis have been widely described, its roles in autophagy, oxidative stress, axonal and synaptic regeneration have not been illustrated.

Autophagy

Autophagy is a highly conserved intracellular clearance mechanism that functions to maintain cellular homeostasis by engulfing cellular targets, including damaged organelles, unfolded proteins and pathogens (Liao M. F. et al., 2022). When autophagy is activated, the damaged organelles are enclosed by an isolation membrane to form autophagosome (Zhang et al., 2021a). Autophagosome then fuses with lysosome to form autolysosome and the damaged organelles are degraded by lysosomal enzymes (Zhang and Wang, 2018a).

The functions of m6A modification in autophagy have also been well established. It has been shown that Unc-51-like kinase 1 (ULK1) expression was regulated in an FTO-m6A-dependent and YTHDF2-mediated manner in gastric cancer. Knockdown of FTO reversed cisplatin resistance of gastric cancer cells both *in vitro* and *in vivo*, which was attributed to the inhibition of ULK1-mediated autophagy (Zhang Y. et al., 2022). Furthermore, in diabetic skin models, knockdown of endogenous YTHDC1 resulted in a blockade of autophagic flux and delayed wound healing by droving SQSTM1 mRNA degradation in the nucleus (Liang et al., 2022). Therefore, m6A modification may also intervene autophagy in CNS injuries. However, further studies are needed to verify it.

Oxidative stress

Oxidative stress, defined as imbalance between the biological systems leading to the generation of oxidant (free) radicals and the systems responsible for the removal of free radicals, is harmful to cells due to the excessive generation of oxidant compounds such as ROS and reactive nitrogen species (RNS) (Zhang and Wang, 2018b). Excessive generation of ROS and RNS due to depletion of the antioxidant system or excitotoxicity leads to the oxidation of biological molecules such as lipids, proteins and DNA, resulting in oxidative damage in cells, tissues and organs (Khatri et al., 2018).

There were also researches suggesting that m6A modification could regulate oxidative stress. Ding et al. (2022) showed that in bovine granulosa cells, FTO and YTHDF2 regulated MAX network transcriptional repressor (MNT) expression through m6A modification. FTO overexpression alleviated cadmium (Cd)-induced oxidative stress as proven by increased expression of nuclear factor erythroid 2-related factor-2 (Nrf2), superoxide dismutase (SOD), catalase (CAT) and NAD(P)H: quinone oxidoreductase 1 (NQO1), and reduced expression of MDA. However, this process could be reversed using si-MNT. Moreover, Zhuang et al. (2019) found that in clear cell renal cell carcinoma (ccRCC), FTO induced oxidative stress and increased reactive oxygen (ROS) levels by reducing m6A methylation of peroxisome proliferator-activated receptor gamma coactivator-1 α (PGC1α) and increasing PGC1α mRNA translation efficiency. Therefore, the role of m6A modification in CNS injuries induced-oxidative stress needed to be further studied.

Axonal and synaptic regeneration

Central nervous system injuries lead to a rapid loss of neurons and axons which accounts for the loss of nerve connections during the acute phase and subsequently induces various degrees of plasticity during the spontaneous recovery phase (Cramer, 2018). It has been shown that stroke-mediated injury could induce axon sprouting, dendritic branching and synaptogenesis for remapping of neural circuits (Carmichael et al., 2017). The speed of axonal and synaptic regeneration is affected by axonal transportation and neurotrophic growth factors, which are secreted by Schwann cells (SCs). In respond to CNS injuries, SCs are activated and involved in the entire process of injury and regeneration. The proliferating SCs form Bungner bands, which guide the growth of newly sprouting axons (Chu et al., 2022).

After nerve injury, m6A modification may have the function of regulating axonal regeneration and synaptic regeneration. Zhang et al. (2021b) performed MeRIP-seq to reveal the m6A methylation landscape in peripheral nervous injury (PNI). They found that 4,014 m6A peaks were significantly altered after PNI. Moreover, GO analysis and KEGG pathway analysis showed that these genes were mainly involved in axon regeneration (Zhang et al., 2021b). Furthermore, Wang X. L. et al. (2022) reported that in a mouse neuropathic pain (NP) model, downregulation of FTO in the anterior cingulate cortex (ACC) could promote angiogenesis, axon growth and neural plasticity as proven by up-regulation of matrix metalloproteinase-9 (MMP-9), decreased levels of precursor brain-derived neurotrophic factor (proBDNF) and increased levels of mature brain-derived neurotrophic factor (mBDNF). The current researches have focused m6A modification on the peripheral nerve injury, which had certain reference for the application of m6A modification in the CNS injuries.

Concluding remarks

N6-methyladenosine modification plays essential roles in CNS injuries and participates in a number of cellular and

molecular processes of CNS injuries. In this review, we summarize the abnormal expression of m6A modification proteins, the function of m6A modification and the crosstalk between m6A modification and RNAs in CNS injuries. These observations make m6A modification to be attractive therapeutic targets for patients suffering from CNS injuries. Moreover, microarray, proteomic and metabolomic analyses of the downstream moleculars of m6A modification may offer new avenues for restoring normal neuronal network and blocking the vital nodes promoting brain damage. Continued discoveries in this field will bring novel insights on m6A modification involved in biological functions and disease progression. Ultimately, m6A modification may hold promise for clinical challenges.

Author contributions

LZ conceived the whole work design, finished the figures and tables, and played a vital role in manuscript submissions. MT finished the original manuscript. LM revised the manuscript. All authors contributed to the article and approved the submitted version.

Funding

This work was supported by Grants from the Jiangsu Postdoctoral Research Funding Program (No. 2021K367C) and the Discipline upgrading plan of Southeast University (No. 4060692202/017) from MT.

Conflict of interest

The authors declare that the research was conducted in the absence of any commercial or financial relationships that could be construed as a potential conflict of interest.

Publisher's note

References

Akcaoz, A., and Akgul, B. (2022). Epitranscriptomics changes the play: m(6)A RNA modifications in apoptosis. *Adv. Exp. Med. Biol.* doi: 10.1007/5584_2022_721 [Epub ahead of print].

Al Mamun, A., Suchi, S. A., Aziz, M. A., Zaeem, M., Munir, F., Wu, Y., et al. (2022). Pyroptosis in acute pancreatitis and its therapeutic regulation. *Apoptosis.* 27, 465–481. doi: 10.1007/s10495-022-01729-w

Alcaraz, L. P., Prellwitz, L., Alves, G., Souza-Fabjan, J. M. G., and Dias, A. J. B. (2022). Role of phosphoinositide 3-kinase/ protein kinase B/ phosphatase and tensin homologue (PI3K/AKT/PTEN) pathway inhibitors during in vitro maturation of mammalian oocytes on in vitro embryo production: A systematic review. *Theriogenology* 189, 42–52. doi: 10.1016/j.theriogenology.2022.06.009

Arguello, A. E., DeLiberto, A. N., and Kleiner, R. E. (2017). RNA chemical proteomics reveals the N(6)-methyladenosine (m(6)A)-regulated protein-RNA interactome. *J. Am. Chem. Soc.* 139, 17249–17252. doi: 10.1021/jacs.7b09213

Benedictus, M. R., Spikman, J. M., and van der Naalt, J. (2010). Cognitive and behavioral impairment in traumatic brain injury related to outcome and return to work. *Arch. Phys. Med. Rehabil.* 91, 1436–1441. doi: 10.1016/j.apmr.2010.06.019

Cai, X., Chen, Y., Man, D., Yang, B., Feng, X., Zhang, D., et al. (2021). RBM15 promotes hepatocellular carcinoma progression by regulating N6-methyladenosine modification of YES1 mRNA in an IGF2BP1-dependent manner. *Cell Death Discov.* 7:315. doi: 10.1038/s41420-021-00703-w

Cai, X., Liang, C., Zhang, M., Xu, Y., Weng, Y., Li, X., et al. (2022). N6-methyladenosine modification and metabolic reprogramming of digestive system malignancies. *Cancer Lett.* 544:215815. doi: 10.1016/j.canlet.2022.215815

Cao, Y., Liu, J., Lu, Q., Huang, K., Yang, B., Reilly, J., et al. (2022). An update on the functional roles of long noncoding RNAs in ischemic injury (Review). *Int. J. Mol. Med.* 50:91. doi: 10.3892/ijmm.2022.5147

Carmichael, S. T., Kathirvelu, B., Schweppe, C. A., and Nie, E. H. (2017). Molecular, cellular and functional events in axonal sprouting after stroke. *Exp. Neurol.* 287(Pt 3), 384–394. doi: 10.1016/j.expneurol.2016.02.007

Cayir, A. (2022). RNA modifications as emerging therapeutic targets. *Wiley Interdiscipl. Rev.* 13:e1702. doi: 10.1002/wrna.1702

Chen, D., Cheung, H., Lau, H. C., Yu, J., and Wong, C. C. (2022). N(6)-methyladenosine RNA-binding protein YTHDF1 in gastrointestinal cancers: Function, molecular mechanism and clinical implication. *Cancers* 14:3489. doi: 10.3390/cancers14143489

Chen, J., Fang, Y., Xu, Y., and Sun, H. (2022). Role of m6A modification in female infertility and reproductive system diseases. *Int. J. Biol. Sci.* 18, 3592–3604. doi: 10.7150/ijbs.69771

Chen, M., Lai, X., Wang, X., Ying, J., Zhang, L., Zhou, B., et al. (2021). Long non-coding RNAs and circular RNAs: Insights into microglia and astrocyte mediated neurological diseases. *Front. Mol. Neurosci.* 14:745066. doi: 10.3389/fnmol.2021.745066

Chokkalla, A. K., Mehta, S. L., and Vemuganti, R. (2020). Epitranscriptomic regulation by m(6)A RNA methylation in brain development and diseases. *J. Cereb. Blood Flow Metab.* 40, 2331–2349. doi: 10.1177/0271678X20960033

Chu, X. L., Song, X. Z., Li, Q., Li, Y. R., He, F., Gu, X. S., et al. (2022). Basic mechanisms of peripheral nerve injury and treatment via electrical stimulation. *Neural Regen. Res.* 17, 2185–2193. doi: 10.4103/1673-5374.335823

Coll, R. C., Schroder, K., and Pelegrin, P. (2022). NLRP3 and pyroptosis blockers for treating inflammatory diseases. *Trends Pharmacol. Sci.* 43, 653–668. doi: 10.1016/j.tips.2022.04.003

Cramer, S. C. (2018). Treatments to promote neural repair after stroke. *J. Stroke* 20, 57–70. doi: 10.5853/jos.2017.02796

Devanney, N. A., Stewart, A. N., and Gensel, J. C. (2020). Microglia and macrophage metabolism in CNS injury and disease: The role of immunometabolism in neurodegeneration and neurotrauma. *Exp. Neurol.* 329:113310. doi: 10.1016/j.expneurol.2020.113310

Di Timoteo, G., Dattilo, D., Centron-Broco, A., Colantoni, A., Guarnacci, M., Rossi, F., et al. (2020). Modulation of circRNA metabolism by m(6)A modification. *Cell Rep.* 31:107641. doi: 10.1016/j.celrep.2020.107641

Diao, M. Y., Zhu, Y., Yang, J., Xi, S. S., Wen, X., Gu, Q., et al. (2020). Hypothermia protects neurons against ischemia/reperfusion-induced pyroptosis via m6A-mediated activation of PTEN and the PI3K/Akt/GSK-3beta signaling pathway. *Brain Res. Bull.* 159, 25–31. doi: 10.1016/j.brainresbull.2020.03.011

Ding, H., Li, Z., Li, X., Yang, X., Zhao, J., Guo, J., et al. (2022). FTO Alleviates CdCl2-induced apoptosis and oxidative stress via the AKT/Nrf2

pathway in bovine granulosa cells. *Int. J. Mol. Sci.* 23:4948. doi: 10.3390/ijms23094948

Dominissini, D., Moshitch-Moshkovitz, S., Schwartz, S., Salmon-Divon, M., Ungar, L., Osenberg, S., et al. (2012). Topology of the human and mouse m6A RNA methylomes revealed by m6A-seq. *Nature* 485, 201–206. doi: 10.1038/nature11112

Fang, Y., Cui, H., Liu, F., Su, S., Wang, T., Yuan, B., et al. (2022). Astrocytic PTEN regulates neuropathic pain by facilitating HMGCR-dependent cholesterol biosynthesis. *Pain*. doi: 10.1097/j.pain.0000000000002682 [Epub ahead of print].

Fish, L., Navickas, A., Culbertson, B., Xu, Y., Nguyen, H. C. B., Zhang, S., et al. (2019). Nuclear TARBP2 drives oncogenic dysregulation of RNA splicing and decay. *Mol. Cell* 75, 967–981.e9. doi: 10.1016/j.molcel.2019.06.001

Flores-Romero, H., Hohorst, L., John, M., Albert, M. C., King, L. E., Beckmann, L., et al. (2022). BCL-2-family protein tBID can act as a BAX-like effector of apoptosis. *EMBO J.* 41:e108690. doi: 10.15252/embj.2021108690

Fuhrmann, D. C., and Brune, B. (2022). A graphical journey through iron metabolism, microRNAs, and hypoxia in ferroptosis. *Redox Biol.* 54:102365. doi: 10.1016/j.redox.2022.102365

Garcia-Campos, M. A., Edelheit, S., Toth, U., Safra, M., Shachar, R., Viukov, S., et al. (2019). Deciphering the "m(6)A Code" via Antibody-Independent quantitative profiling. *Cell* 178, 731–747.e16. doi: 10.1016/j.cell.2019.06.013

Geula, S., Moshitch-Moshkovitz, S., Dominissini, D., Mansour, A. A., Kol, N., Salmon-Divon, M., et al. (2015). Stem cells. m6A mRNA methylation facilitates resolution of naive pluripotency toward differentiation. *Science* 347, 1002–1006. doi: 10.1126/science.1261417

Gutilla, E. A., and Steward, O. (2016). Selective neuronal PTEN deletion: Can we take the brakes off of growth without losing control? *Neural Regen. Res.* 11, 1201–1203. doi: 10.4103/1673-5374.189160

Han, B., Wei, S., Li, F., Zhang, J., Li, Z., and Gao, X. (2021). Decoding m(6)A mRNA methylation by reader proteins in cancer. *Cancer Lett.* 518, 256–265. doi: 10.1016/j.canlet.2021.07.047

Hilton, G., Unsworth, C., and Murphy, G. (2018). The experience of attempting to return to work following spinal cord injury: A systematic review of the qualitative literature. *Disabil. Rehabil.* 40, 1745–1753. doi: 10.1080/09638288.2017.1312566

Hornby, T. G., Reisman, D. S., Ward, I. G., Scheets, P. L., Miller, A., Haddad, D., et al. (2020). Clinical practice guideline to improve locomotor function following chronic stroke, incomplete spinal cord injury, and brain injury. *J. Neurol. Phys. Ther.* 44, 49–100. doi: 10.1097/NPT.0000000000000303

Huang, J., Shao, Y., and Gu, W. (2021). Function and clinical significance of N6-methyladenosine in digestive system tumours. *Exp. Hematol. Oncol.* 10:40. doi: 10.1186/s40164-021-00234-1

Huang, Y., Wu, H., Hu, Y., Zhou, C., Wu, J., Wu, Y., et al. (2022). Puerarin attenuates oxidative stress and ferroptosis via AMPK/PGC1alpha/Nrf2 pathway after subarachnoid hemorrhage in rats. *Antioxidants* 11:1259. doi: 10.3390/antiox11071259

Imanishi, M. (2022). Mechanisms and strategies for determining m(6) A RNA modification sites by natural and engineered m(6) A effector proteins. *Chem. Asian J.* 17:e202200367. doi: 10.1002/asia.202200367

Jang, K. H., Heras, C. R., and Lee, G. (2022). m(6)A in the signal transduction network. *Mol. Cells* 45, 435–443. doi: 10.14348/molcells.2022.0017

Jia, G., Fu, Y., Zhao, X., Dai, Q., Zheng, G., Yang, Y., et al. (2011). N6-methyladenosine in nuclear RNA is a major substrate of the obesity-associated FTO. *Nat. Chem. Biol.* 7, 885–887. doi: 10.1038/nchembio.687

Jin, D., Guo, J., Wu, Y., Du, J., Yang, L., Wang, X., et al. (2019). m(6)A mRNA methylation initiated by METTL3 directly promotes YAP translation and increases YAP activity by regulating the MALAT1-miR-1914-3p-YAP axis to induce NSCLC drug resistance and metastasis. *J. Hematol. Oncol.* 12:135. doi: 10.1186/s13045-019-0830-6

Kalra, S., Malik, R., Singh, G., Bhatia, S., Al-Harrasi, A., Mohan, S., et al. (2022). Pathogenesis and management of traumatic brain injury (TBI): Role of neuroinflammation and anti-inflammatory drugs. *Inflammopharmacology* 30, 1153–1166. doi: 10.1007/s10787-022-01017-8

Khan, H., Singh, A., Thapa, K., Garg, N., Grewal, A. K., and Singh, T. G. (2021). Therapeutic modulation of the phosphatidylinositol 3-kinases (PI3K) pathway in cerebral ischemic injury. *Brain Res.* 1761:147399. doi: 10.1016/j.brainres.2021.147399

Khatri, N., Thakur, M., Pareek, V., Kumar, S., Sharma, S., and Datusalia, A. K. (2018). Oxidative stress: Major threat in traumatic brain injury. *CNS Neurol. Disord. Drug Targets* 17, 689–695. doi: 10.2174/1871527317666180627120501

Kitzmuller, G., Mangset, M., Evju, A. S., Angel, S., Aadal, L., Martinsen, R., et al. (2019). Finding the way forward: The lived experience of people with stroke after participation in a complex psychosocial intervention. *Qual. Health Res.* 29, 1711–1724. doi: 10.1177/1049732319833366

Kumari, R., Ranjan, P., Suleiman, Z. G., Goswami, S. K., Li, J., Prasad, R., et al. (2022). mRNA modifications in cardiovascular biology and disease: With a focus on m6A modification. *Cardiovasc. Res.* 118, 1680–1692. doi: 10.1093/cvr/cvab160

Li, D., Pi, W., Sun, Z., Liu, X., and Jiang, J. (2022). Ferroptosis and its role in cardiomyopathy. *Biomed. Pharmacother.* 153:113279. doi: 10.1016/j.biopha.2022.113279

Li, L., Xu, N., Liu, J., Chen, Z., Liu, X., and Wang, J. (2022). m6A methylation in cardiovascular diseases: From mechanisms to therapeutic potential. *Front. Genet.* 13:908976. doi: 10.3389/fgene.2022.908976

Li, M. X., Weng, J. W., Ho, E. S., Chow, S. F., and Tsang, C. K. (2022). Brain delivering RNA-based therapeutic strategies by targeting mTOR pathway for axon regeneration after central nervous system injury. *Neural Regen. Res.* 17, 2157–2165. doi: 10.4103/1673-5374.335830

Li, Y., Su, R., Deng, X., Chen, Y., and Chen, J. (2022). FTO in cancer: Functions, molecular mechanisms, and therapeutic implications. *Trends Cancer* 8, 598–614. doi: 10.1016/j.trecan.2022.02.010

Liang, D., Lin, W. J., Ren, M., Qiu, J., Yang, C., Wang, X., et al. (2022). m(6)A reader YTHDC1 modulates autophagy by targeting SQSTM1 in diabetic skin. *Autophagy* 18, 1318–1337. doi: 10.1080/15548627.2021.1974175

Liao, J., Wei, Y., Liang, J., Wen, J., Chen, X., Zhang, B., et al. (2022). Insight into the structure, physiological function, and role in cancer of m6A readers-YTH domain-containing proteins. *Cell Death Discov.* 8:137. doi: 10.1038/s41420-022-00947-0

Liao, M. F., Lu, K. T., Hsu, J. L., Lee, C. H., Cheng, M. Y., and Ro, L. S. (2022). The role of autophagy and apoptosis in neuropathic pain formation. *Int. J. Mol. Sci.* 23:2685. doi: 10.3390/ijms23052685

Liddelow, S. A., and Barres, B. A. (2017). Reactive astrocytes: Production, function, and therapeutic potential. *Immunity* 46, 957–967. doi: 10.1016/j.immuni.2017.06.006

Lin, X., Chai, G., Wu, Y., Li, J., Chen, F., Liu, J., et al. (2019). RNA m(6)A methylation regulates the epithelial mesenchymal transition of cancer cells and translation of snail. *Nat. Commun.* 10:2065. doi: 10.1038/s41467-019-09865-9

Linder, B., Grozhik, A. V., Olarerin-George, A. O., Meydan, C., Mason, C. E., and Jaffrey, S. R. (2015). Single-nucleotide-resolution mapping of m6A and m6Am throughout the transcriptome. *Nat. Methods* 12, 767–772. doi: 10.1038/nmeth.3453

Liu, C., Gu, L., Deng, W., Meng, Q., Li, N., Dai, G., et al. (2022). N6-methyladenosine RNA methylation in cardiovascular diseases. *Front. Cardiovasc. Med.* 9:887838. doi: 10.3389/fcvm.2022.887838

Liu, C., Yang, S., Zhang, Y., Wang, C., Du, D., Wang, X., et al. (2021). Emerging roles of N6-methyladenosine demethylases and its interaction with environmental toxicants in digestive system cancers. *Cancer Manag. Res.* 13, 7101–7114. doi: 10.2147/CMAR.S328188

Liu, N., Dai, Q., Zheng, G., He, C., Parisien, M., and Pan, T. (2015). N(6)-methyladenosine-dependent RNA structural switches regulate RNA-protein interactions. *Nature* 518, 560–564. doi: 10.1038/nature14234

Liu, N., Parisien, M., Dai, Q., Zheng, G., He, C., and Pan, T. (2013). Probing N6-methyladenosine RNA modification status at single nucleotide resolution in mRNA and long noncoding RNA. *RNA* 19, 1848–1856. doi: 10.1261/rna.041178.113

Liu, R., Jia, Y., Kong, G., and He, A. (2022). Novel insights into roles of N6-methyladenosine reader YTHDF2 in cancer progression. *J. Cancer Res. Clin. Oncol.* 148, 2215–2230. doi: 10.1007/s00432-022-04134-7

Liu, T., Wei, Q., Jin, J., Luo, Q., Liu, Y., Yang, Y., et al. (2020). The m6A reader YTHDF1 promotes ovarian cancer progression via augmenting EIF3C translation. *Nucleic Acids Res.* 48, 3816–3831. doi: 10.1093/nar/gkaa048

Lu, L., Zhang, Y., Tan, X., Merkher, Y., Leonov, S., Zhu, L., et al. (2022). Emerging mechanisms of pyroptosis and its therapeutic strategy in cancer. *Cell Death Discov.* 8:338. doi: 10.1038/s41420-022-01101-6

Luo, L., Zhen, Y., Peng, D., Wei, C., Zhang, X., Liu, X., et al. (2022). The role of N6-methyladenosine-modified non-coding RNAs in the pathological process of human cancer. *Cell Death Discov.* 8:325. doi: 10.1038/s41420-022-01113-2

Malovic, E., Ealy, A., Kanthasamy, A., and Kanthasamy, A. G. (2021). Emerging roles of N6-methyladenosine (m6A) epitranscriptomics in toxicology. *Toxicol. Sci.* 181, 13–22. doi: 10.1093/toxsci/kfab021

Meyer, K. D., Saletore, Y., Zumbo, P., Elemento, O., Mason, C. E., and Jaffrey, S. R. (2012). Comprehensive analysis of mRNA methylation reveals enrichment in 3' UTRs and near stop codons. *Cell* 149, 1635–1646. doi: 10.1016/j.cell.2012.05.003

Mi, L., Min, X., Chai, Y., Zhang, J., and Chen, X. (2022). NLRP1 inflammasomes: A potential target for the treatment of several types of brain injury. *Front. Immunol.* 13:863774. doi: 10.3389/fimmu.2022.863774

Molinie, B., Wang, J., Lim, K. S., Hillebrand, R., Lu, Z. X., Van Wittenberghe, N., et al. (2016). m(6)A-LAIC-seq reveals the census and complexity of the m(6)A epitranscriptome. *Nat. Methods* 13, 692–698. doi: 10.1038/nmeth.3898

Nagarajan, A., Janostiak, R., and Wajapeyee, N. (2019). Dot blot analysis for measuring global N(6)-methyladenosine modification of RNA. *Methods Mol. Biol.* 1870, 263–271. doi: 10.1007/978-1-4939-8808-2_20

Nakamura, Y., Park, J. H., and Hayakawa, K. (2020). Therapeutic use of extracellular mitochondria in CNS injury and disease. *Exp. Neurol.* 324:113114. doi: 10.1016/j.expneurol.2019.113114

Nhu, N. T., Li, Q., Liu, Y., Xu, J., Xiao, S. Y., and Lee, S. D. (2021). Effects of Mdivi-1 on neural mitochondrial dysfunction and mitochondria-mediated apoptosis in ischemia-reperfusion injury after stroke: A systematic review of preclinical studies. *Front. Mol. Neurosci.* 14:778569. doi: 10.3389/fnmol.2021.778569

Nieuwenhuis, B., and Eva, R. (2022). Promoting axon regeneration in the central nervous system by increasing PI3-kinase signaling. *Neural Regen. Res.* 17, 1172–1182. doi: 10.4103/1673-5374.327324

Odgaard, L., Johnsen, S. P., Pedersen, A. R., and Nielsen, J. F. (2017). Return to work after severe traumatic brain injury: A nationwide follow-up study. *J. Head Trauma Rehabil.* 32, E57–E64. doi: 10.1097/HTR.0000000000000239

Oerum, S., Meynier, V., Catala, M., and Tisne, C. (2021). A comprehensive review of m6A/m6Am RNA methyltransferase structures. *Nucleic Acids Res.* 49, 7239–7255. doi: 10.1093/nar/gkab378

Pan, T., Wu, F., Li, L., Wu, S., Zhou, F., Zhang, P., et al. (2021). The role m(6)A RNA methylation is CNS development and glioma pathogenesis. *Mol. Brain* 14:119. doi: 10.1186/s13041-021-00831-5

Parrondo, R. D., Paulus, A., and Ailawadhi, S. (2022). Updates in the use of BCL-2-family small molecule inhibitors for the treatment of relapsed/refractory multiple myeloma. *Cancers* 14:3330. doi: 10.3390/cancers14143330

Peeples, E. S., and Genaro-Mattos, T. C. (2022). Ferroptosis: A promising therapeutic target for neonatal hypoxic-ischemic brain injury. *Int. J. Mol. Sci.* 23:7420. doi: 10.3390/ijms23137420

Peng, H., Zhang, X., Yang, P., Zhao, J., Zhang, W., Feng, N., et al. (2023). Defect self-assembly of metal-organic framework triggers ferroptosis to overcome resistance. *Bioact. Mater.* 19, 1–11. doi: 10.1016/j.bioactmat.2021.12.018

Qi, L., Wang, Y., Hu, H., Li, P., Hu, H., Li, Y., et al. (2022). m(6)A methyltransferase METTL3 participated in sympathetic neural remodeling post-MI via the TRAF6/NF-kappaB pathway and ROS production. *J. Mol. Cell. Cardiol.* 170, 87–99. doi: 10.1016/j.yjmcc.2022.06.004

Quillinan, N., Herson, P. S., and Traystman, R. J. (2016). Neuropathophysiology of brain injury. *Anesthesiol. Clin.* 34, 453–464. doi: 10.1016/j.anclin.2016.04.011

Radak, D., Katsiki, N., Resanovic, I., Jovanovic, A., Sudar-Milovanovic, E., Zafirovic, S., et al. (2017). Apoptosis and acute brain ischemia in ischemic stroke. *Curr. Vasc. Pharmacol.* 15, 115–122. doi: 10.2174/1570161115666161104095522

Ramesh-Kumar, D., and Guil, S. (2022). The IGF2BP family of RNA binding proteins links epitranscriptomics to cancer. *Semin. Cancer Biol.* doi: 10.1016/j.semcancer.2022.05.009 [Epub ahead of print].

Reichel, M., Koster, T., and Staiger, D. (2019). Marking RNA: m6A writers, readers, and functions in *Arabidopsis*. *J. Mol. Cell Biol.* 11, 899–910. doi: 10.1093/jmcb/mjz085

Rodriguez, J., Li, T., Xu, Y., Sun, Y., and Zhu, C. (2021). Role of apoptosis-inducing factor in perinatal hypoxic-ischemic brain injury. *Neural Regen. Res.* 16, 205–213. doi: 10.4103/1673-5374.290875

Sekar, G., Ojoawo, A., and Moldoveanu, T. (2022). Protein-protein and protein-lipid interactions of pore-forming BCL-2 family proteins in apoptosis initiation. *Biochem. Soc. Trans.* 50, 1091–1103. doi: 10.1042/BST20220323

Shang, P., Zhang, Y., Ma, D., Hao, Y., Wang, X., Xin, M., et al. (2019). Inflammation resolution and specialized pro-resolving lipid mediators in CNS diseases. *Exp. Opin. Ther. Targets* 23, 967–986. doi: 10.1080/14728222.2019.1691525

Shi, K., Tian, D. C., Li, Z. G., Ducruet, A. F., Lawton, M. T., and Shi, F. D. (2019). Global brain inflammation in stroke. *Lancet Neurol.* 18, 1058–1066. doi: 10.1016/S1474-4422(19)30078-X

Shulman, Z., and Stern-Ginossar, N. (2020). The RNA modification N(6)-methyladenosine as a novel regulator of the immune system. *Nat. Immunol.* 21, 501–512. doi: 10.1038/s41590-020-0650-4

Sommerkamp, P., Brown, J. A., Haltalli, M. L. R., Mercier, F. E., Vu, L. P., and Kranc, K. R. (2022). m(6)A RNA modifications: Key regulators of normal and malignant hematopoiesis. *Exp. Hematol.* 111, 25–31. doi: 10.1016/j.exphem.2022.04.006

Song, N., Cui, K., Zhang, K., Yang, J., Liu, J., Miao, Z., et al. (2022). The role of m6A RNA methylation in cancer: Implication for nature products anti-cancer research. *Front. Pharmacol.* 13:933332. doi: 10.3389/fphar.2022.933332

Stojkovic, V., Weinberg, D. E., and Fujimori, D. G. (2021). miCLIP-MaPseq identifies substrates of radical SAM RNA-methylating enzyme using mechanistic cross-linking and mismatch profiling. *Methods Mol. Biol.* 2298, 105–122. doi: 10.1007/978-1-0716-1374-0_7

Walker, C. L., Liu, N. K., and Xu, X. M. (2013). PTEN/PI3K and MAPK signaling in protection and pathology following CNS injuries. *Front. Biol.* 8, 421–433. doi: 10.1007/s11515-013-1255-1

Wang, B., Liu, Y., Jiang, R., Liu, Z., Gao, H., Chen, F., et al. (2022). Emodin relieves the inflammation and pyroptosis of lipopolysaccharide-treated 1321N1 cells by regulating methyltransferase-like 3 -mediated NLR family pyrin domain containing 3 expression. *Bioengineered* 13, 6740–6749. doi: 10.1080/21655979.2022.2045836

Wang, J., Zhao, J., Hu, P., Gao, L., Tian, S., and He, Z. (2022). Long non-coding RNA HOTAIR in central nervous system disorders: New insights in pathogenesis, diagnosis, and therapeutic potential. *Front. Mol. Neurosci.* 15:949095. doi: 10.3389/fnmol.2022.949095

Wang, L., Ren, W., Wu, Q., Liu, T., Wei, Y., Ding, J., et al. (2022). NLRP3 inflammasome activation: A therapeutic target for cerebral ischemia-reperfusion injury. *Front. Mol. Neurosci.* 15:847440. doi: 10.3389/fnmol.2022.847440

Wang, M. P., Joshua, B., Jin, N. Y., Du, S. W., and Li, C. (2022). Ferroptosis in viral infection: The unexplored possibility. *Acta Pharmacol. Sin.* 43, 1905–1915. doi: 10.1038/s41401-021-00814-1

Wang, M., Lin, X., Yang, X., and Yang, Y. (2022). Research progress on related mechanisms of uric acid activating NLRP3 inflammasome in chronic kidney disease. *Renal Fail.* 44, 615–624. doi: 10.1080/0886022X.2022.2036620

Wang, Q., Liang, Y., Luo, X., Liu, Y., Zhang, X., and Gao, L. (2021). N6-methyladenosine RNA modification: A promising regulator in central nervous system injury. *Exp. Neurol.* 345:113829. doi: 10.1016/j.expneurol.2021.113829

Wang, X. L., Wei, X., Yuan, J. J., Mao, Y. Y., Wang, Z. Y., Xing, N., et al. (2022). Downregulation of fat mass and obesity-related protein in the anterior cingulate cortex participates in anxiety- and depression-like behaviors induced by neuropathic pain. *Front. Cell. Neurosci.* 16:884296. doi: 10.3389/fncel.2022.884296

Wang, X. X., Zhang, B., Xia, R., and Jia, Q. Y. (2020). Inflammation, apoptosis and autophagy as critical players in vascular dementia. *Eur. Rev. Med. Pharmacol. Sci.* 24, 9601–9614. doi: 10.26355/eurrev_202009_23048

Wang, X., Lu, Z., Gomez, A., Hon, G. C., Yue, Y., Han, D., et al. (2014). N6-methyladenosine-dependent regulation of messenger RNA stability. *Nature* 505, 117–120. doi: 10.1038/nature12730

Wang, Y. N., Yu, C. Y., and Jin, H. Z. (2020). RNA N(6)-methyladenosine modifications and the immune response. *J. Immunol. Res.* 2020:6327614. doi: 10.1155/2020/6327614

Wang, Y., and Zhou, X. (2022). N(6)-methyladenosine and its implications in viruses. *Genomics Proteomics Bioinf.* doi: 10.1016/j.gpb.2022.04.009 [Epub ahead of print].

Wang, Y., Li, Y., Toth, J. I., Petroski, M. D., Zhang, Z., and Zhao, J. C. (2014). N6-methyladenosine modification destabilizes developmental regulators in embryonic stem cells. *Nat. Cell Biol.* 16, 191–198. doi: 10.1038/ncb2902

Wang, Y., Mao, J., Wang, X., Lin, Y., Hou, G., Zhu, J., et al. (2019). Genome-wide screening of altered m6A-tagged transcript profiles in the hippocampus after traumatic brain injury in mice. *Epigenomics* 11, 805–819. doi: 10.2217/epi-2019-0002

Wang, Y., Tang, B., Zhu, J., Yu, J., Hui, J., Xia, S., et al. (2022). Emerging mechanisms and targeted therapy of ferroptosis in neurological diseases and neuro-oncology. *Int. J. Biol. Sci.* 18, 4260–4274. doi: 10.7150/ijbs.72251

Wang, Y., Zhang, Y., Du, Y., Zhou, M., Hu, Y., and Zhang, S. (2020). Emerging roles of N6-methyladenosine (m(6)A) modification in breast cancer. *Cell Biosci.* 10:136. doi: 10.1186/s13578-020-00502-3

Wang, Z., Ji, C., Wu, L., Qiu, J., Li, Q., Shao, Z., et al. (2014). Tert-butylhydroquinone alleviates early brain injury and cognitive dysfunction after experimental subarachnoid hemorrhage: Role of Keap1/Nrf2/ARE pathway. *PLoS One* 9:e97685. doi: 10.1371/journal.pone.0097685

Weaver, K., and Skouta, R. (2022). The selenoprotein glutathione peroxidase 4: From molecular mechanisms to novel therapeutic opportunities. *Biomedicines* 10:891. doi: 10.3390/biomedicines10040891

Wu, P., Fang, X., Liu, Y., Tang, Y., Wang, W., Li, X., et al. (2021). N6-methyladenosine modification of circCUX1 confers radioresistance of

hypopharyngeal squamous cell carcinoma through caspase1 pathway. *Cell Death Dis.* 12:298. doi: 10.1038/s41419-021-03558-2

Wu, Y., Liu, Y., Zhou, C., Wu, Y., Sun, J., Gao, X., et al. (2022). Biological effects and mechanisms of caspases in early brain injury after subarachnoid hemorrhage. *Oxid. Med. Cell. Longev.* 2022:3345637. doi: 10.1155/2022/3345637

Xiao, W., Adhikari, S., Dahal, U., Chen, Y. S., Hao, Y. J., Sun, B. F., et al. (2016). Nuclear m(6)A reader YTHDC1 regulates mRNA splicing. *Mol. Cell* 61, 507–519. doi: 10.1016/j.molcel.2016.01.012

Xu, K., Mo, Y., Li, D., Yu, Q., Wang, L., Lin, F., et al. (2020). N(6)-methyladenosine demethylases Alkbh5/Fto regulate cerebral ischemia-reperfusion injury. *Ther. Adv. Chron. Dis.* 11:2040622320916024. doi: 10.1177/2040622320916024

Xu, S., Li, Y., Chen, J. P., Li, D. Z., Jiang, Q., Wu, T., et al. (2020). Oxygen glucose deprivation/re-oxygenation-induced neuronal cell death is associated with Lnc-D63785 m6A methylation and miR-422a accumulation. *Cell Death Dis.* 11:816. doi: 10.1038/s41419-020-03021-8

Xu, Y., and Ye, H. (2022). Progress in understanding the mechanisms of resistance to BCL-2 inhibitors. *Exp. Hematol. Oncol.* 11:31. doi: 10.1186/s40164-022-00283-0

Yan, H., Zhang, L., Cui, X., Zheng, S., and Li, R. (2022). Roles and mechanisms of the m(6)A reader YTHDC1 in biological processes and diseases. *Cell Death Discov.* 8:237. doi: 10.1038/s41420-022-01040-2

Yang, L., Cao, L. M., Zhang, X. J., and Chu, B. (2022). Targeting ferroptosis as a vulnerability in pulmonary diseases. *Cell Death Dis.* 13:649. doi: 10.1038/s41419-022-05070-7

Yang, Q. Q., and Zhou, J. W. (2019). Neuroinflammation in the central nervous system: Symphony of glial cells. *Glia* 67, 1017–1035. doi: 10.1002/glia.23571

Yang, X., Patil, S., Joshi, S., Jamla, M., and Kumar, V. (2022). Exploring epitranscriptomics for crop improvement and environmental stress tolerance. *Plant Physiol. Biochem.* 183, 56–71. doi: 10.1016/j.plaphy.2022.04.031

Yang, Y., Fan, X., Mao, M., Song, X., Wu, P., Zhang, Y., et al. (2017). Extensive translation of circular RNAs driven by N(6)-methyladenosine. *Cell Res.* 27, 626–641. doi: 10.1038/cr.2017.31

Yu, J., Zhang, Y., Ma, H., Zeng, R., Liu, R., Wang, P., et al. (2020). Epitranscriptomic profiling of N6-methyladenosine-related RNA methylation in rat cerebral cortex following traumatic brain injury. *Mol. Brain* 13:11. doi: 10.1186/s13041-020-0554-0

Yuan, B., Zhao, X. D., Shen, J. D., Chen, S. J., Huang, H. Y., Zhou, X. M., et al. (2022). Activation of SIRT1 alleviates ferroptosis in the early brain injury after subarachnoid hemorrhage. *Oxid. Med. Cell. Longev.* 2022:9069825. doi: 10.1155/2022/9069825

Zhai, G., Xiao, L., Jiang, C., Yue, S., Zhang, M., Zheng, J., et al. (2022). Regulatory role of N6-methyladenosine (m6A) modification in osteoarthritis. *Front. Cell Dev. Biol.* 10:946219. doi: 10.3389/fcell.2022.946219

Zhang, C., and Liu, N. (2022). N6-methyladenosine (m6A) modification in gynecological malignancies. *J. Cell. Physiol.* 237, 3465–3479. doi: 10.1002/jcp.30828

Zhang, F., Liu, H., Duan, M., Wang, G., Zhang, Z., Wang, Y., et al. (2022). Crosstalk among m(6)A RNA methylation, hypoxia and metabolic reprogramming in TME: From immunosuppressive microenvironment to clinical application. *J. Hematol. Oncol.* 15:84. doi: 10.1186/s13045-022-01304-5

Zhang, L., and Wang, H. (2018a). Autophagy in traumatic brain injury: A new target for therapeutic intervention. *Front. Mol. Neurosci.* 11:190. doi: 10.3389/fnmol.2018.00190

Zhang, L., and Wang, H. (2018b). Targeting the NF-E2-related factor 2 pathway: A novel strategy for traumatic brain injury. *Mol. Neurobiol.* 55, 1773–1785. doi: 10.1007/s12035-017-0456-z

Zhang, L., and Wang, H. (2019). Long non-coding RNA in CNS injuries: A new target for therapeutic intervention. *Mol. Ther. Nucleic Acids* 17, 754–766. doi: 10.1016/j.omtn.2019.07.013

Zhang, L., Dai, L., and Li, D. (2021a). Mitophagy in neurological disorders. *J. Neuroinflamm.* 18:297. doi: 10.1186/s12974-021-02334-5

Zhang, L., Hao, D., Ma, P., Ma, B., Qin, J., Tian, G., et al. (2021b). Epitranscriptomic analysis of m6A methylome after peripheral nerve injury. *Front. Genet.* 12:686000. doi: 10.3389/fgene.2021.686000

Zhang, L., Wang, X., Che, W., Yi, Y., Zhou, S., and Feng, Y. (2022). Methyltransferase-like 3 silenced inhibited the ferroptosis development via regulating the glutathione peroxidase 4 levels in the intracerebral hemorrhage progression. *Bioengineered* 13, 14215–14226. doi: 10.1080/21655979.2022.2084494

Zhang, Y., Gao, L. X., Wang, W., Zhang, T., Dong, F. Y., and Ding, W. P. (2022). M(6) A demethylase fat mass and obesity-associated protein regulates cisplatin resistance of gastric cancer by modulating autophagy activation through ULK1. *Cancer Sci.* 113, 3085–3096. doi: 10.1111/cas.15469

Zhang, Y., Geng, X., Li, Q., Xu, J., Tan, Y., Xiao, M., et al. (2020). m6A modification in RNA: Biogenesis, functions and roles in gliomas. *J. Exp. Clin. Cancer Res.* 39:192. doi: 10.1186/s13046-020-01706-8

Zhang, Z., Wang, Q., Zhao, X., Shao, L., Liu, G., Zheng, X., et al. (2020). YTHDC1 mitigates ischemic stroke by promoting Akt phosphorylation through destabilizing PTEN mRNA. *Cell Death Dis.* 11:977. doi: 10.1038/s41419-020-03186-2

Zhao, Q., Liu, F., Zhou, B., Liu, H., Wang, X., and Li, S. (2022). Ferroptosis: A novel therapeutic direction of spinal cord injury. *Comput. Math. Methods Med.* 2022:7906218. doi: 10.1155/2022/7906218

Zhao, X., Yang, Y., Sun, B. F., Shi, Y., Yang, X., Xiao, W., et al. (2014). FTO-dependent demethylation of N6-methyladenosine regulates mRNA splicing and is required for adipogenesis. *Cell Res.* 24, 1403–1419. doi: 10.1038/cr.2014.151

Zheng, Y., Li, Y., Ran, X., Wang, D., Zheng, X., Zhang, M., et al. (2022). Mettl14 mediates the inflammatory response of macrophages in atherosclerosis through the NF-kappaB/IL-6 signaling pathway. *Cell. Mol. Life Sci.* 79:311. doi: 10.1007/s00018-022-04331-0

Zhou, H., Mao, L., Xu, H., Wang, S., and Tian, J. (2022). The functional roles of m(6)A modification in T lymphocyte responses and autoimmune diseases. *Cytokine Growth Factor Rev.* 65, 51–60. doi: 10.1016/j.cytogfr.2022.04.004

Zhou, L., Gao, G., Tang, R., Wang, W., Wang, Y., Tian, S., et al. (2022). m(6)A-mediated regulation of crop development and stress responses. *Plant Biotechnol. J.* 20, 1447–1455. doi: 10.1111/pbi.13792

Zhou, W., Wang, X., Chang, J., Cheng, C., and Miao, C. (2022). The molecular structure and biological functions of RNA methylation, with special emphasis on the roles of RNA methylation in autoimmune diseases. *Crit. Rev. Clin. Lab. Sci.* 59, 203–218. doi: 10.1080/10408363.2021.2002256

Zhu, B., Chen, H. X., Li, S., Tan, J. H., Xie, Y., Zou, M. X., et al. (2021). Comprehensive analysis of N6-methyladenosine (m(6)A) modification during the degeneration of lumbar intervertebral disc in mice. *J. Orthopaed. Transl.* 31, 126–138. doi: 10.1016/j.jot.2021.10.008

Zhuang, C., Zhuang, C., Luo, X., Huang, X., Yao, L., Li, J., et al. (2019). N6-methyladenosine demethylase FTO suppresses clear cell renal cell carcinoma through a novel FTO-PGC-1alpha signalling axis. *J. Cell. Mol. Med.* 23, 2163–2173. doi: 10.1111/jcmm.14128

frontiers | Frontiers in Molecular Neuroscience

TYPE Original Research
PUBLISHED 02 November 2022
DOI 10.3389/fnmol.2022.1033224

OPEN ACCESS

EDITED BY
Enrico Tongiorgi,
University of Trieste,
Italy

REVIEWED BY
Marc Forrest,
Northwestern University,
United States
Brady J. Maher,
Lieber Institute for Brain Development,
United States
Germana Meroni,
University of Trieste,
Italy

*CORRESPONDENCE
Tõnis Timmusk
tonis.timmusk@taltech.ee

†These authors have contributed equally to this work and share first authorship

SPECIALTY SECTION
This article was submitted to Neuroplasticity and Development, a section of the Frontiers in Molecular Neuroscience

RECEIVED 31 August 2022
ACCEPTED 05 October 2022
PUBLISHED 02 November 2022

CITATION
Sirp A, Shubina A, Tuvikene J, Tamberg L, Kiir CS, Kranich L and Timmusk T (2022) Expression of alternative transcription factor 4 mRNAs and protein isoforms in the developing and adult rodent and human tissues.
Front. Mol. Neurosci. 15:1033224.
doi: 10.3389/fnmol.2022.1033224

Expression of alternative transcription factor 4 mRNAs and protein isoforms in the developing and adult rodent and human tissues

Alex Sirp[1†], Anastassia Shubina[1†], Jürgen Tuvikene[1,2], Laura Tamberg[1], Carl Sander Kiir[1], Laura Kranich[1] and Tõnis Timmusk[1,2*]

[1]Department of Chemistry and Biotechnology, Tallinn University of Technology, Tallinn, Estonia, [2]Protobios LLC, Tallinn, Estonia

Transcription factor 4 (TCF4) belongs to the class I basic helix–loop–helix family of transcription factors (also known as E-proteins) and is vital for the development of the nervous system. Aberrations in the *TCF4* gene are associated with several neurocognitive disorders such as schizophrenia, intellectual disability, post-traumatic stress disorder, depression, and Pitt-Hopkins Syndrome, a rare but severe autism spectrum disorder. Expression of the human *TCF4* gene can produce at least 18 N-terminally distinct protein isoforms, which activate transcription with different activities and thus may vary in their function during development. We used long-read RNA-sequencing and western blot analysis combined with the analysis of publicly available short-read RNA-sequencing data to describe both the mRNA and protein expression of the many distinct TCF4 isoforms in rodent and human neural and nonneural tissues. We show that TCF4 mRNA and protein expression is much higher in the rodent brain compared to nonneural tissues. TCF4 protein expression is highest in the rodent cerebral cortex and hippocampus, where expression peaks around birth, and in the rodent cerebellum, where expression peaks about a week after birth. In human, highest *TCF4* expression levels were seen in the developing brain, although some nonneural tissues displayed comparable expression levels to adult brain. In addition, we show for the first time that out of the many possible TCF4 isoforms, the main TCF4 isoforms expressed in the rodent and human brain and other tissues are TCF4-B, -C, -D, -A, and-I. Taken together, our isoform specific analysis of TCF4 expression in different tissues could be used for the generation of gene therapy applications for patients with TCF4-associated diseases.

KEYWORDS

transcription factor TCF4, basic helix–loop–helix transcription factor, western blot analysis, neurodevelopment, long-read RNA sequencing, brain tissue, peripheral tissue

Introduction

Transcription factor 4 (TCF4) is a member of the class I basic helix–loop–helix transcription factor family (also known as E-proteins) and is the main E-protein expressed in the adult mouse brain (Massari and Murre, 2000; Fischer et al., 2014). TCF4 regulates numerous genes involved in neurodevelopment (Forrest et al., 2018) and has been shown to mediate its function by forming either homo-or heterodimers with proneural interaction partners such as achaete-scute homolog 1 (ASCL1; Persson et al., 2000) and neurogenic differentiation factor 2 (NEUROD2; Brzózka et al., 2010) as well as negative regulators known as inhibitor of DNA binding (ID) proteins (Chiaramello et al., 1995; Einarson and Chao, 1995). The expression of TCF4 interaction partners is strictly regulated, allowing TCF4 to possibly exert different functions during the development of the nervous system (Quednow et al., 2011).

Changes in the *TCF4* gene are linked to the development of many severe neurocognitive disorders such as schizophrenia (Stefansson et al., 2009; Ripke et al., 2014; Doostparast Torshizi et al., 2019), intellectual disability (Kharbanda et al., 2016), post-traumatic stress disorder (Gelernter et al., 2019), and depression (Wray et al., 2018). In addition, *de novo* mutations in one of the *TCF4* alleles cause Pitt-Hopkins syndrome (Brockschmidt et al., 2007; Zweier et al., 2007)—an autism spectrum disorder described by severe cognitive impairment, breathing abnormalities, motor delay, and distinctive facial features (Zollino et al., 2019). Interestingly, in addition to deletions and translocations, just a single nucleotide mutation in the basic helix–loop–helix encoding domain can completely impair the normal functionality of the TCF4 protein (Amiel et al., 2007; Zweier et al., 2007; Sepp et al., 2012; Sirp et al., 2021). *Tcf4* heterozygous mutant mice exhibit memory deficits, impaired motor control, and social isolation (Kennedy et al., 2016; Thaxton et al., 2018). Similar results have been noted in *Drosophila melanogaster*, where downregulation of Daughterless, the orthologue of TCF4, impairs memory and learning (Tamberg et al., 2020). Overexpression of *Tcf4* in mouse brain causes impairments in cognition and sensorimotor gating (Brzózka et al., 2010), and increased long term depression at synapses (Badowska et al., 2020). Homozygous *Tcf4* knockout mice have low viability and usually die around birth (Zhuang et al., 1996).

Expression of *Tcf4* was first described during late embryonic and early postnatal development in different mouse brain regions using northern blot analysis and *in situ* hybridization (Soosaar et al., 1994; Pscherer et al., 1996; Ravanpay and Olson, 2008). More recent studies have used quantitative droplet digital PCR and reverse-transcription quantitative PCR to show that in the cerebral cortex *TCF4* mRNA expression peaks around birth and declines rapidly in the following 2 weeks (Li et al., 2019; Phan et al., 2020). Expression of TCF4 protein in the developing and adult mouse brain has been described in detail by Jung et al. (2018) using immunostaining with antibodies specific for longer TCF4 protein isoforms. During embryonic development of the brain, expression levels of long TCF4 isoforms are high in the areas which will develop into the cortex and the hippocampus. More specifically, long TCF4 isoforms are largely expressed in the germinal regions that will give rise to GABAergic and glutamatergic neurons of the cortex (Jung et al., 2018). In the brain of adult mice, TCF4 expression of long TCF4 isoforms is high in the cortex, hippocampus, and cerebellum (Jung et al., 2018). Similar results have been obtained by Kim and colleagues who used TCF4-GFP mice to characterize total TCF4 expression (Kim et al., 2020).

In human, TCF4 is expressed broadly, with the expression of different TCF4 isoforms varying between tissues (de Pontual et al., 2009; Sepp et al., 2011). Further analysis of human RNA sequencing (RNA-seq) data has revealed that the mRNA expression dynamics of *TCF4* in human and mouse appear to be conserved in the cerebral cortex—*TCF4* mRNA is highly expressed during fetal stages of development and reaches the maximum before birth, rapidly declines around birth until entering a relatively stable expression level from the early postnatal period to adulthood (Ma et al., 2018). As *TCF4* remains stably expressed in adult humans and rodents alike (de Pontual et al., 2009; Jung et al., 2018; Ma et al., 2018; Li et al., 2019) its expression is probably important for the normal functioning of the organism (Sarkar et al., 2021).

To date, none of the previous studies of *TCF4* mRNA (Ma et al., 2018; Li et al., 2019; Phan et al., 2020) and protein (Jung et al., 2018; Kim et al., 2020) expression have described expression of the variety of TCF4 isoforms. Expression of the mouse and human *TCF4* gene results in many different transcripts encoding N-terminally distinct protein isoforms which vary in their intracellular localization, transactivation capability (Sepp et al., 2011, 2017; Nurm et al., 2021) and possibly mediate their function depending on dosage (Ravanpay and Olson, 2008). Here, we investigated the complex expression dynamics of different TCF4 mRNAs and protein isoforms in the developing and adult rodent and human tissues. Our results can be used to estimate which TCF4 isoforms and at which proportions should be introduced into different tissues during development to generate gene therapy applications of the TCF4-associated diseases.

Abbreviations: TCF4, Transcription factor 4; RNA-seq, RNA sequencing; RT, Room temperature; RT-qPCR, Reverse transcription quantitative PCR; gRNA, Guide RNA; P, Postnatal; E, Embryonic; CTX, Cerebral cortex; HC, Hippocampi; CB, Cerebellum; OB, Olfactory bulb; HTH, Hypothalamus; MB, Midbrain; TH, Thalamus; STRT, Striatum.

Materials and methods

Direct TCF4 RNA sequencing

Total RNA was extracted from a mixture of cerebral cortices from three P3 BALB/c mice using the RNeasy lipid tissue mini kit

(Qiagen). Genomic DNA was digested on-column using RNase-Free DNase Set (Qiagen). Concentration of the purified RNA was determined with BioSpec-nano spectrophotometer (Shimadzu).

Before RNA-seq library preparation, 20 µg of P3 BALB/c cortical RNA was enriched for *Tcf4* transcripts in wash/binding buffer (0.5 M NaCl, 20 mM Tris–HCl pH 7.5, and 1 mM EDTA) with 8 µM each of three 5′ biotinylated oligonucleotides (Microsynth AG)—two oligonucleotides were complementary to the 3` untranslated region of *Tcf4*, and one was complementary to the bHLH region of *Tcf4* (Supplementary Table S1). As there are no known *Tcf4* transcripts that lack the bHLH region or exon 21, we expect that our *Tcf4* mRNA enrichment strategy is unbiased and enriches all possible TCF4 transcripts (Sepp et al., 2011; Nurm et al., 2021). First the mixture was incubated at 70°C for 2 min and then cooled to room temperature in about 30 min in a heating block. When the heating block reached 60°C, 100 units of RiboLock RNase Inhibitor (Thermo Fisher Scientific) was added to the mixture.

Next, Pierce streptavidin magnetic beads (Thermo Fisher Scientific) were prepared for the binding reaction. For that, 40 µl of magnetic beads was washed in 800 µl wash/binding buffer and then suspended in 30 µl of wash/binding buffer. The magnetic beads were then added to the previously annealed oligonucleotide-RNA mixture for the binding reaction. The bead-oligonucleotide-RNA mixture was incubated at RT for 90 min with occasional agitation by hand. After 90 min, the flow-through sample was collected and after that the beads were washed twice with 100 µl of wash/bind buffer followed by three washes with 100 µl of ice-cold low salt buffer (0.15 M NaCl, 20 mM Tris–HCl pH 7.5, and 1 mM EDTA). For elution, the magnetic beads were incubated at 70°C for 5 min in 25 µl of nuclease free water (Qiagen) twice, with the total volume of eluted RNA being 50 µl. In total, two *Tcf4* RNA enrichments were done—the first *Tcf4* enriched RNA sample was sequenced twice and the second once.

RNA sequencing library was prepared separately for each of the three sequencing experiments according to the Sequence-specific direct RNA sequencing protocol SQK-RNA002 (Oxford Nanopore Technologies). The RNAClean XP beads (Agencourt) were substituted with the Mag-Bind total pure NGS magnetic beads (Omega Bio-tek). Sequencing was done three times with the MinION sequencer, FLO-MIN106 flow-cell (new flow cells were used for each experiment), and SQK-RNA002 kit using MinKNOW software (version 3.6.5; Oxford Nanopore Technologies).

Base-calling of the direct RNA sequencing data was performed using Guppy Basecalling Software (version 4.0.11 + f1071ceb, Oxford Nanopore Technologies) with high-accuracy basecalling algorithm. Failed reads were discarded and the passed reads were mapped to mouse GRCm38.p6 genome (obtained from Gencode) using Minimap2 (version 2.17-r941) with the following settings: -ax splice-uf -k14. The generated sam files were converted to bam format using Samtools (version 1.9), the alignments of all three replicates were combined and only reads mapping to the *Tcf4* gene locus were kept. The resulting merged and filtered bam file was then converted to bed12 file format using bedtools (version 2.28.0) for easier visualization. All reads mapping to the *Tcf4* locus in bed12 format can be found in Data Sheet 1. Raw sequencing reads mapping to the *Tcf4* locus can be found in Data Sheet 2. The final data was visualized in Integrated Genomics Viewer and the transcripts encoding *Tcf4* isoforms were manually quantified. Aberrant transcripts were excluded from the analysis.

Guide RNA design and cloning

The University of California Santa Cruz Genome Browser Gateway[1] was used to define the genomic region of mouse exon 3 and exon 10a protein coding regions for guide RNA (gRNA) design. The genomic region for mouse exon 3 and exon 10a was chr18:69,347,299–69,347,369 and chr18:69,593,516–69,593,584, respectively, according to mouse GRCm38/mm10 (Dec. 2011) assembly. In total, three gRNAs were designed for exon 3 and two for exon 10a using Benchling Inc.[2] CRISPR guide design software.

To insert the gRNA targeting region-containing oligonucleotides effectively into the PX459 (Addgene #62988) expression vector, nucleotides were added to the 5` ends of gRNAs that were complementary to the sticky ends produced after restriction of the PX459 plasmid with the BbsI restriction enzyme (Thermo Scientific). In addition, a guanine nucleotide was added to the 5′ end of each forward oligonucleotide sequence of gRNA as it has been found to increase targeting efficiency.[3] The designed sequences are included in Supplementary Table S2. The oligonucleotides were ordered from Microsynth AG.

Cell culture and transfection

Mouse Neuro2a and human SH-SY5Y cells were grown in DMEM (Dulbecco's modified Eagle's medium, Thermo Scientific) medium, supplemented with 10% fetal bovine serum (Pan Biotech), 100 U/ml penicillin, and 0.1 mg/ml streptomycin (Thermo Scientific).

For transfection, cells were plated on a 12-well plate (Greiner) in 800 µl medium per well 24–48 h before transfection. At the time of the transfection, the cells were at 50–70% confluency. Neuro2a cells were transfected with 500 ng of the pEGFP plasmid and 500 ng of the PX459 plasmid expressing the respective gRNA, Cas9, and Puromycin resistance gene using Lipofectamine 2000 (Invitrogen). In each experiment, DNA to transfection reagent ratio was 1:2. For preparation of protein lysates, the cells were lysed in in 1x Laemmli buffer [0.062 M Tris–HCl pH 6.8, 2% SDS, 5% 2-mercaptoethanol (Roth), 10% glycerol, and 0.01% bromophenol blue].

1 https://genome.ucsc.edu
2 https://benchling.com
3 http://www.addgene.org/crispr/zhang/

Reverse transcription PCR

Total RNA was extracted from Neuro2a cells using the RNeasy mini kit (Qiagen). Genomic DNA was digested on-column using RNase-Free DNase Set (Qiagen). Concentrations of the purified RNAs were determined with BioSpec-nano spectrophotometer (Shimadzu). cDNA was synthesized from Neuro2a total RNA using Superscript IV Reverse Transcriptase (Invitrogen) according to the manufacturer's instructions. Primers used for reverse transcription PCR are listed in Supplementary Table S3.

Animal husbandry

The protocols involving animals were approved by the ethics committee of animal experiments at Ministry of Agriculture of Estonia (Permit Number: 45). All experiments were performed in accordance with the relevant guidelines and regulations. WISTAR rats (RccHan:WI, Envigo) and C57BL/6 and BALB/c mouse strains (Envigo) were used in this study. Animals were maintained in conventional polycarbonate or H-TEMP polysulfone cages (2–4 animals per cage) with *ad libitum* access to clean water and food pellets (ssniff Spezialdiäten) under a 12-h light/dark cycle in humidity and temperature-controlled room (temperature 22 ± 1°C and humidity 50 ± 10%).

To establish timed pregnancy for studying embryonic (E) development, the female mouse estrous cycle was monitored by visual observations of the vaginal opening of each female mouse based on the criteria described by Champlin et al. (1973). Mice in the proestrus or estrous phase of the cycle were selected for mating. Animals were bred in the evening and vaginal post-coitum protein plug was checked in the next morning no more than 12 h later. The morning that a plug was found was designated as E0.5 gestational stage. The day of the animal birth was designated as postnatal (P) 0 stage.

Tissue isolation and protein extraction

Mice and rats were euthanized by carbon dioxide inhalation and decapitated with a guillotine. Dissection of tissue samples was done in ice-cold 1x phosphate-buffered saline solution. Each sample contained tissues pooled together from three different animals for biological diversity and sufficient protein extraction at early developmental stages. The mouse and rat cerebral cortex, hippocampus, cerebellum, olfactory bulb, hypothalamus, and pons including medulla, midbrain, and thalamus were collected. Striatum was collected only for the BALB/c mouse strain. Tissue collection for mouse and rat brain regions occurred at P0, 3, 5, 7, 10, 14, 21, 60, and P0, 3, 5, 10, 14, 30, 60, respectively. In addition to postnatal days, collection of total mouse brain samples occurred at E13, 15, and 18. Mouse and rat peripheral tissues, skin, lung, kidney, heart, diaphragm, muscle, bladder, stomach, pancreas, thymus, spleen, liver, and blood, were collected at developmental stages P0, 14, and 60. After collection, tissue samples were stored at −80°C until further processing.

Tissues were homogenized on ice with tissue grinder PELLET PESTLE® Cordless Motor (Kimble-Chase, DWK Life Sciences) in ice-cold Radioimmunoprecipitation assay buffer [RIPA, 50 mM Tris pH 8.0, 150 mM NaCl, 1% NP-40, 0.5% Na-deoxycholate, 0.5% sodium dodecyl sulfate (SDS), and 1x Roche Protease Inhibitor Cocktail Complete]. Lysates were sonicated for 15 s with Torbeo Ultrasonic probe sonicator (36810-series, Cole Parmer), and insoluble material was removed by centrifugation at 4°C for 20 min at 16,000 *g*. Protein concentration was measured with Pierce BCA Protein Assay Kit (Thermo Scientific).

Protein lysates from human post-mortem cerebral cortex and hippocampus were prepared like rodent lysates. All protocols using human tissue samples were approved by Tallinn Committee for Medical Studies, National Institute for Health Development (Permit Number 402). All experiments were performed in accordance with relevant guidelines and regulations.

In vitro protein translation

TCF4-A$^+$, -A$^-$, -B$^+$, B$^-$, -C$^-$, -D$^-$ and TCF4-I$^-$isoforms were translated *in vitro* using pcDNA3 plasmids encoding the respective TCF4 isoforms (Sepp et al., 2011) with TnT Quick Coupled Transcription/Translation System (Promega). Equal volumes of *in vitro* translated TCF4 protein mixtures were used for western blot analysis.

Western blot analysis

For western blot analysis, protein lysates in RIPA were diluted to the same concentration in 1x Laemmli buffer. 55 µg of each sample was electrophoretically separated by SDS-polyacrylamide gel electrophoresis in 8% gel and transferred to polyvinylidene difluoride membrane (Millipore) in Towbin buffer (25 mM Tris, 192 mM glycine, 20% methanol, 0.1% SDS, and pH 8.3) using wet transfer. Membranes were blocked with 5% skimmed milk (Sigma-Aldrich) in 1x Tris Buffered Saline with 0.1% Tween-20 (TBST, Sigma Aldrich) before incubating with primary [mouse monoclonal anti-ITF-2 (TCF4); C-8, 1:1,000 dilution, Santa Cruz] and secondary (goat polyclonal anti-mouse IgG HRP-conjugated antibody 1:5,000 dilution, Thermo Scientific) antibody in 2.5% skimmed milk-TBST solution overnight at 4°C and 1 h at room temperature, respectively. Specificity of the anti-ITF-2 (TCF4; C-8, Santa Cruz) antibody has been previously validated using tissue lysates from *Tcf4* knockout mice (Nurm et al., 2021). For peripheral tissues, mouse IgG kappa binding protein conjugated to HRP was used as a secondary antibody (1:5,000 dilution, Santa Cruz). Chemiluminescence signal detection with SuperSignal West Femto or Atto Chemiluminescence Substrate (Thermo Scientific). The chemiluminescence signal was visualized with ImageQuant LAS 4000 bioimager (GE Healthcare) and densitometric quantification was performed with ImageQuant TL

8.2 image analysis software (GE Healthcare). Membrane staining with Coomassie solution (0.1% Coomassie Brilliant Blue R-250, 25% ethanol, and 7% acetic acid) was used as a loading control and for total protein normalization.

Analysis of publicly available RNA-seq datasets

Raw RNA-seq datasets of human, mouse, and rat were obtained from EMBL-EBI European Nucleotide Archive database using www.sra-explorer.info (Keane et al., 2011; ENCODE Project Consortium, 2012; Schmitt et al., 2014; Yu et al., 2014; Vied et al., 2016; Li et al., 2017; Söllner et al., 2017; Cardoso-Moreira et al., 2019; Luo et al., 2020; Shafik et al., 2021; see Supplementary Table S4 for accession numbers and sample information). Adapter and quality trimming were done using BBDuk (part of BBMap version 38.90) with the following parameters: ktrim = r k = 23 mink = 11 hdist = 1 tbo qtrim = lr trimq = 10 maq = 10 minlen = 25. Mouse reads were mapped to mm10 (primary assembly and annotation obtained from GENCODE, release M25, GRCm38), rat reads were mapped to rn6 (primary assembly and annotation obtained from Ensembl, release 104, RGSC 6.0/Rnor_6.0), and human reads were mapped to hg19 (primary assembly and annotation obtained from GENCODE, release 37, GRCh37) using STAR aligner (version 2.7.4a) with default parameters. To increase sensitivity for unannotated splice junctions, splice junctions obtained from the first pass were combined per dataset and filtered as follows: junctions on mitochondrial DNA and non-canonical intron motifs were removed; only junctions detected in at least 10% of samples (rounded up to the nearest integer) in the whole dataset were kept. Filtered junctions were added to the second pass mapping using STAR. Intron spanning reads were quantified using FeatureCounts (version 2.0.1). The following parameters were used for paired-end data: -p –B –C –J; and single-end data: -J. To count reads from *TCF4* extended exons (exons 4c and 7bII), reads crossing a 1 bp region 2 bp 5′ from the internal exon 4 and 7, respectively, were quantified using FeatureCounts and a custom-made saf file. Splice junctions in the *TCF4* locus were manually curated and annotated to TCF4 isoforms according to Sepp et al. (2011).

A custom R script[4] was used to quantify the expression of different *TCF4* transcripts from analyzed RNA-seq datasets. Briefly, RNA-seq reads crossing the indicated *TCF4* splice-junctions were normalized using all splice-junction crossing reads in the respective sample. Then, the data were summarized by the Exon column (Supplementary Tables S5–S7). To acquire total *TCF4* mRNA levels, the mean value of exon-junctions from 10–11 to 19–20 was taken for the analysis. Aggregated mouse and rat data was meta-analyzed in tandem with human data to study *TCF4* expression during development. The expression of *TCF4* transcripts encoding specific isoforms was assessed by quantifying the number of reads crossing the exon-junctions specific for the TCF4 isoforms. Data were summarized in each tissue and age group by the Isoform column. Values for each isoform were then divided with the sum of all annotated isoforms to show isoform composition in percentages. The results were visualized using ggplot2 (version 3.3.5) in R (version 4.1.2). The *TCF4* exon-junction data used for the analysis of *TCF4* transcripts in mouse, rat, and human datasets can be found in Supplementary Tables S5–S7, respectively.

Data mining and visualization was also performed on human GTEx portal exon-exon junction dataset (dbGaP Accession phs000424.v8.p2) and human developmental transcriptome data from BrainSpan (RNA-Seq Gencode v10 summarized to genes). The human GTEx data used for the analyses described in this manuscript were obtained from the GTEx Portal[5] on 12/01/2021 and the human BrainSpan data was obtained from the BrainSpan Atlas of the Developing Human Brain[6] on 12/01/2021. For information about rodent and human developmental stages and the number of individual data points per developmental stage, see Supplementary Tables S8–S12.

Results

Five N-terminally distinct TCF4 protein isoforms are expressed in the developing mouse cerebral cortex

The use of numerous alternative 5′ exons results in the expression of many transcripts from the *Tcf4* gene, resulting in a variety of TCF4 protein isoforms with different expression patterns between tissue types (Sepp et al., 2011; Nurm et al., 2021). We have previously described transcripts from the mouse *Tcf4* gene based on available mRNA and expressed sequence tag data from various tissues (Nurm et al., 2021) but characterizing all the isoform encoding transcripts using short-read sequencing is complicated. Here, we did long-read direct RNA-sequencing (RNA-seq) on the Oxford Nanopore Technologies platform from postnatal day 3 (P3) mouse cerebral cortex. Direct RNA-seq eliminates the bias which may result from complementary DNA synthesis used in conventional RNA-seq methods. Briefly, we extracted total RNA from the P3 mouse cerebral cortex which was then enriched for *Tcf4* transcripts using a combination of oligonucleotides complementary to the 3′ untranslated region and the basic helix–loop–helix region of *Tcf4* (Figure 1A; Supplementary Table S1). The Oxford Nanopore Technologies platform begins sequencing from the 3′ end of RNA meaning that early sequencing termination can result in reads which do not reach the 5′ exons of *Tcf4* transcripts. Analysis of our results

4 https://github.com/CSKiir/Sirp_et_al_2022

5 https://gtexportal.org

6 http://brainspan.org

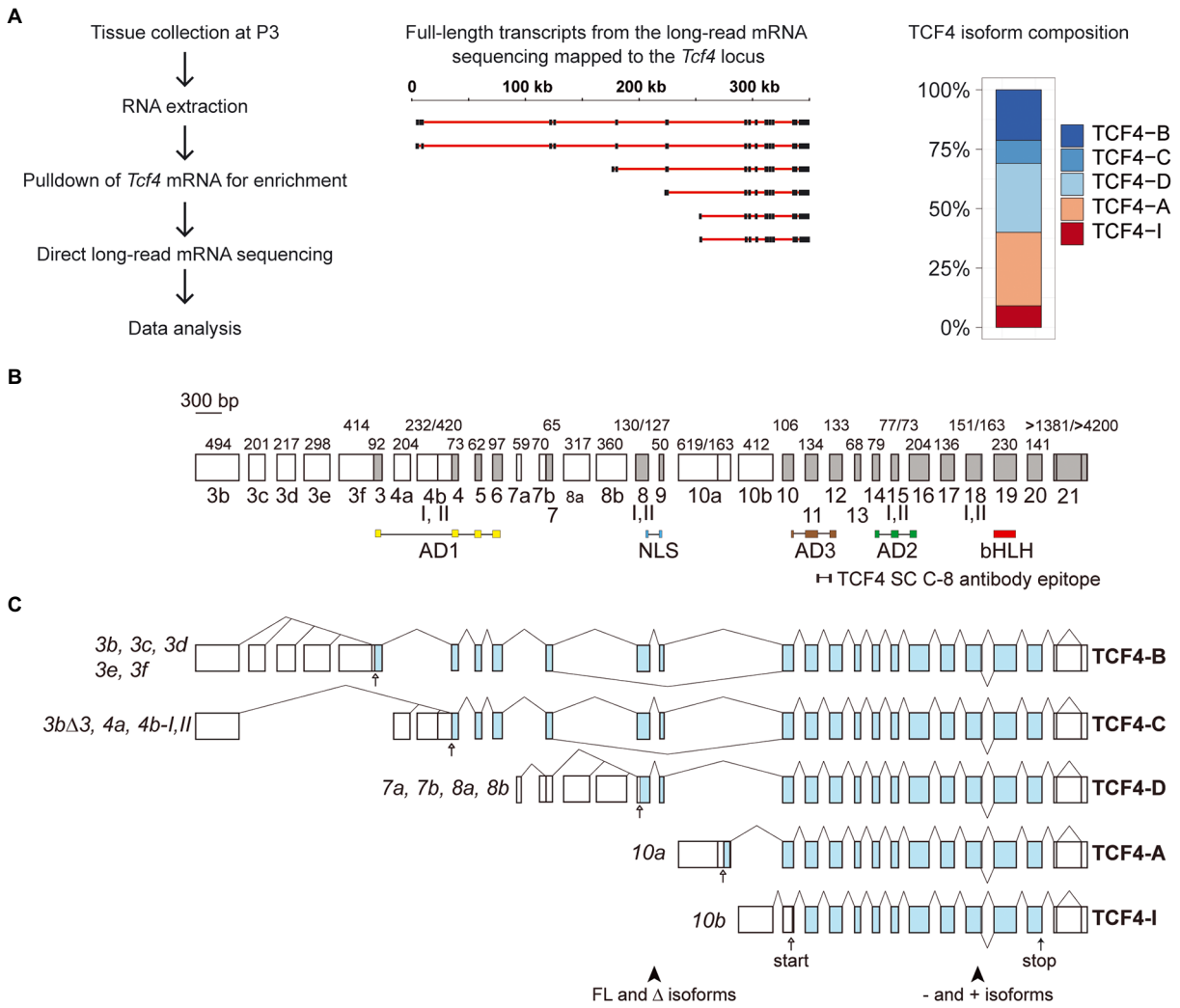

FIGURE 1
Tcf4 mRNA isoforms expressed in the developing mouse cerebral cortex encode five N-terminally distinct protein isoforms. **(A)** Schema of experimental design for direct RNA-sequencing. The cerebral cortices of postnatal day 3 (P3) mice were collected, followed by RNA extraction and *Tcf4* mRNA enrichment before direct long-read mRNA sequencing. A selection of *Tcf4* transcripts mapped to the mouse *Tcf4* locus is shown for reference. Black boxes represent exons and red lines show introns. Scale bar in kilobases is shown on top. *Tcf4* transcripts encoding the different TCF4 isoforms (TCF4-B, -C, -D, -A, and-I) were quantified and the distribution is shown on the right. Each isoform is represented with different color as shown in the legend on the right. **(B)** Mouse *Tcf4* genomic organization with exons drawn in scale. Exons are named according to the human *TCF4* gene (Sepp et al., 2011). 5′ exons are shown as white boxes while internal and 3′ exons are shown as gray boxes. Exon names are shown below boxes. Numbers above the exons designate the size of the exon in base pairs. Roman numerals below exons show alternative splice sites. Regions encoding different domains are marked below the gene structure (AD1, NLS, AD3, AD2, and bHLH) as well as the epitope for the TCF4 antibody C-8 (Santa Cruz, SC) used in the present study. **(C)** Schematic structure of *Tcf4* transcripts expressed in the developing mouse cerebral cortex. Untranslated regions are shown as white boxes and translated regions as blue boxes. Each transcript is named (shown on the left) according to the 5′ exon and with the number of the splice site where indicated. The names of the protein isoforms encoded by the transcripts are shown on the right. Positions of alternative splice region that generates full-length (FL), Δ, – and+isoforms are shown at the bottom. The position of the first in-frame start codon is shown with an arrow for each transcript and the common stop codon with an arrow at the bottom. AD, activation domain; NLS, nuclear localization signal; bHLH, basic helix–loop–helix; FL, full-length; and Δ, lack of exons 8–9.

showed that most of the 1,336 RNAs which mapped to the mouse *Tcf4* gene were short and mapped only to the last exon of *Tcf4* gene. However, we obtained 163 *Tcf4* transcripts that reached from the 3′untranslated region to the 5′ terminal exons and were thus considered full-length based on previous knowledge about the rodent *Tcf4* gene structure (Nurm et al., 2021). We then quantified the potential TCF4 protein isoforms encoded by these transcripts (Figure 1A). The results showed that in the mouse P3 cerebral cortex ~20% of mRNAs transcribed from *Tcf4* gene encode isoform TCF4-B; 10% encode isoform TCF4-C; 30% encode isoform TCF4-D; 30% encode isoform TCF4-A and 10% encode isoform TCF4-I (Figure 1A). The presence of plus (containing the RSRS amino acid sequence) and minus (without the RSRS amino acid sequence; Corneliussen et al., 1991; Nurm et al., 2021) TCF4

isoforms encoded by *Tcf4* mRNAs was roughly equal. Overall, our data show that the expression of mouse *Tcf4* gene leads to numerous transcripts due to the presence of 32 exons out of which 13 are alternative 5′ exons and 18 are internal exons and one is a terminal 3′ exon (Figures 1B,C). Using long-read sequencing, we discovered two novel 5′ exons (exon 3e and 3f) that are included in *Tcf4* transcripts encoding TCF4-B isoform (Figures 1B,C).

We then described the expression pattern of TCF4 protein isoforms in SDS-PAGE/western blot analysis. For that, we used *in vitro* translated TCF4-B, -C, -D, -A, and-I plus or minus TCF4 isoforms. This allowed us to compare different combinations of *in vitro* translated TCF4 isoforms in western blot to the TCF4 protein pattern in the mouse cerebral cortex. In good agreement with our RNA-seq experiment, the combination of *in vitro* translated proteins TCF4-B, -C, -D, -A, and -I resembled the protein pattern of TCF4 in the cerebral cortex (Figure 2A). The variability in *in vitro* translated TCF4 isoform levels in western blot (Figure 2A) could arise from differential translation rate of the respective TCF4 isoform encoding plasmids. Next, we determined the apparent molecular weight and location of endogenously expressed TCF4 isoforms—TCF4-B and TCF4-A in SDS-PAGE/western blot analysis. To this end, we constructed a CRISPR-Cas9 system to inhibit the expression of these TCF4 isoforms in Neuro2a cell line by generating frameshift mutations in the unique exons encoding these isoforms (exons 3 and 10a, respectively). We could not specifically silence the expression of TCF4-D since its translation start site is in internal exon 8—a frameshift mutation in exon 8 would cause the silencing of not only TCF4-D, but also TCF4-B and-C isoforms. We used Neuro2a cells, which show high endogenous expression of TCF4 as confirmed by RT-PCR and western blot analysis (Figure 2B; Supplementary Figure S1). By expressing the generated CRISPR-Cas9 system in Neuro2a cells, we were able to inhibit the expression of TCF4-B and-A and thus confirm the location of these protein isoforms in western blot analysis (Figure 2B). Furthermore, western blot analysis showed that expression pattern of TCF4 isoforms was similar in Neuro2a cells and P3 mouse cerebral cortex (Figure 2B).

Taken together, the main N-terminally distinct TCF4 isoforms expressed in the early postnatal mouse cerebral cortex are TCF4-B, -C, -D, -A, and -I. We classified the detected TCF4 signals into three groups based on their molecular weight: long isoforms (TCF4-B and-C), medium isoforms (TCF4-D), and short isoforms (TCF4-A and-I; Figure 2C).

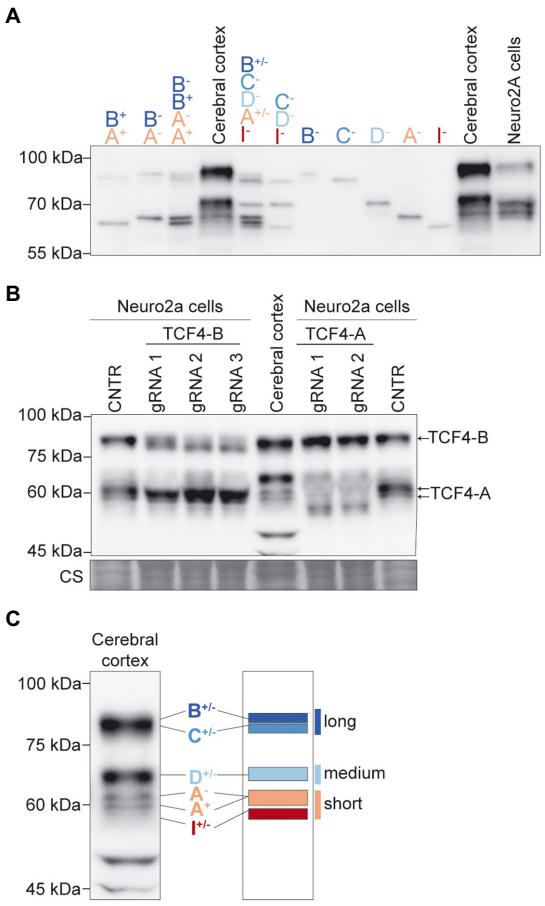

FIGURE 2
TCF4 protein isoforms expressed in the mouse cerebral cortex can be grouped into long, medium, and short isoforms based on apparent molecular weight in SDS-PAGE. **(A)** Western blot analysis of different combinations of *in vitro* translated TCF4 isoforms (shown on the top) to identify the mobility of TCF4 isoforms in the lysates from the mouse cerebral cortex and Neuro2a cells in SDS-PAGE. **(B)** Western blot analysis of Neuro2a cells transfected with CRISPR-Cas9 silencing system. Two exon 10a-specific gRNAs were used to silence TCF4-A and three exon 3-specific gRNAs were used to silence TCF4-B. Cells overexpressing CRISPR-Cas9 vector without the exon-specific gRNA targeting sequence was used as control (CNTR). Mouse cerebral cortex tissue lysate was used to compare TCF4 isoform expression pattern to the pattern in Neuro2a cells. Locations of TCF4-A and TCF4-B isoforms are depicted on the right. Coomassie staining (CS) was used a loading control and is shown at the bottom. **(C)** Schematic layout of the locations of TCF4 isoforms in the protein lysate of the mouse cerebral cortex in western blot. TCF4 isoforms were grouped into three—long, medium and short isoforms. The locations of TCF4 isoform groups are color coded and shown on the right. In each panel, molecular weight is shown on the left in kilodaltons.

Expression of TCF4 protein in the mouse brain is highest around birth

Next, we studied the changes in TCF4 protein expression in the mouse brain throughout pre-and postnatal development. For that, we made mouse whole brain lysates from two strains (BALB/C and C57BL/6) at 11 different developmental stages ranging from E13.5 to P60, and performed western blot analysis (Figures 3A,B). Both mouse strains exhibited expression of long, medium, and short TCF4 isoforms, with the highest expression of total TCF4 detected at late prenatal and early postnatal development. After peaking, TCF4 expression gradually declined

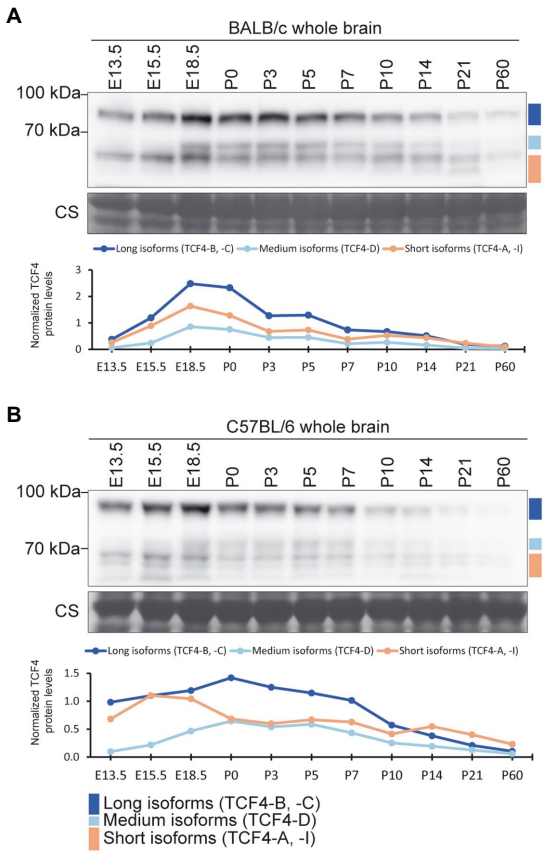

FIGURE 3
Protein expression of TCF4 in the mouse brain peaks around birth. **(A,B)** Western blot analysis of TCF4 protein expression through the pre-and postnatal development in the BALB/c **(A)** and C57BL/6 **(B)** mouse whole brain. Tissue lysates from the whole brain were made at different embryonic (E) and postnatal (P) days. The locations of TCF4 isoform groups are color coded and shown on the right. In each panel, molecular weight is shown on the left in kilodaltons. Under each western plot panel, a line graph depicting the quantification of long, medium, and short TCF4 protein isoforms during development is shown. TCF4 protein levels were normalized to the total TCF4 signal of the P10 cerebral cortex of the respective mouse strain.

during postnatal development of the brain (Figures 3A,B). While long and short TCF4 isoforms were detected at all stages, the medium-sized TCF4 isoforms became more apparent at later fetal stages and were almost undetectable before stage E18.5 (Figures 3A,B).

To better compare TCF4 total levels and isoform expression patterns between the two mouse strains, brain samples of the two strains from early postnatal development (P0–10) were analyzed in the same western blot experiment (Supplementary Figure S2). Our results revealed that the two mouse strains showed no major differences in TCF4 expression levels or expression patterns (Supplementary Figure S2). Altogether, these results indicated that TCF4 is expressed at both pre-and postnatal stages of the mouse brain development, with long and short TCF4 isoforms presented at all stages.

Expression of TCF4 is highest in the cerebral cortex, hippocampus, cerebellum, and olfactory bulb in the rodent brain

Next, we analyzed mRNA and protein expression of TCF4 in various rodent brain regions. First, we conducted a meta-analysis of available short-read RNA-seq data (Keane et al., 2011; ENCODE Project Consortium, 2012; Schmitt et al., 2014; Yu et al., 2014; Vied et al., 2016; Li et al., 2017; Söllner et al., 2017; Cardoso-Moreira et al., 2019; Luo et al., 2020; Shafik et al., 2021) to quantify the expression of total *Tcf4* mRNA and different *Tcf4* transcripts encoding distinct protein isoforms in rodents. Where possible, *Tcf4* expression dynamics was studied during different stages of pre-and postnatal development.

In the mouse brain, *Tcf4* mRNA expression was highest in the cerebral cortex, followed by the cerebellum, midbrain and hypothalamus (Figure 4A; Supplementary Figure S3A). A decrease in *Tcf4* mRNA expression after birth was seen for all the studied brain regions except for the cerebellum, which displayed relatively stable *Tcf4* mRNA levels during postnatal development. The majority of expressed *Tcf4* transcripts encoded isoforms TCF4-B, -C, -D, -A, and -I, with transcripts encoding TCF4-A showing the highest overall expression (Figure 4A; Supplementary Figure S4A) in the mouse brain. The cerebral cortex was the only brain region that displayed a notable change in the expression pattern of transcripts encoding different TCF4 isoforms—during development the expression of TCF4-A decreased and the expression of TCF4-D increased (Figure 4A).

We then sought to describe TCF4 expression at the protein level in mouse brain regions. For this, we dissected the cerebral cortex, hippocampus, cerebellum, striatum, pons, olfactory bulb, hypothalamus, thalamus, and midbrain at eight postnatal stages (P0, 3, 5, 7, 10, 14, 21, and 60) from BALB/C (Figure 4) and C57BL/6 (Supplementary Figure S5) mice, prepared protein lysates and analyzed TCF4 levels by western blot. First, we compared TCF4 protein expression across distinct brain regions at two postnatal stages, P0 and P10 by western blot analysis (Figures 4B,C; Supplementary Figures S5A,B). We observed high TCF4 expression levels in the cerebral cortex and hippocampus at P0, and in the cerebellum at P10 (Figures 4B,C; Supplementary Figures S5A,B). The long and short TCF4 protein isoforms were present in all studied brain regions (Figures 4B,C; Supplementary Figures S5A,B). The medium isoforms had more restricted patterns being detected at high levels in the cerebral cortex and hippocampus, at low levels in the cerebellum, olfactory bulb, and pons, and were below the detection limits in other brain regions (Figures 4B,C).

Next, we focused on the developmental dynamics of TCF4 protein expression in all the dissected mouse brain regions during postnatal development (P0-60; Figure 4D; Supplementary Figure S5C). To better compare TCF4 signals between individual brain regions across development, we used tissue lysate from the P10 cerebral cortex in each experiment as

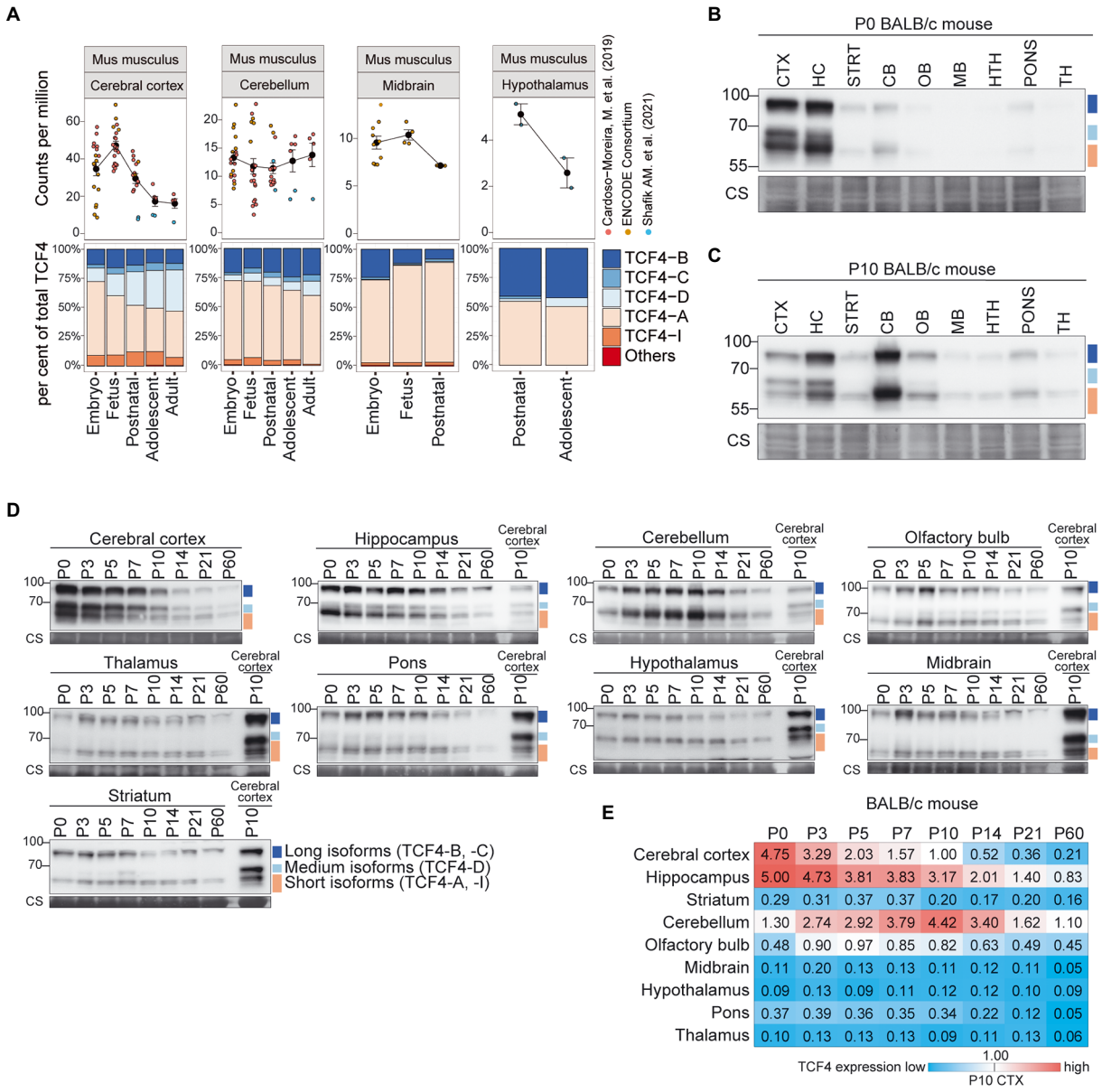

	P0	P3	P5	P7	P10	P14	P21	P60
Cerebral cortex	4.75	3.29	2.03	1.57	1.00	0.52	0.36	0.21
Hippocampus	5.00	4.73	3.81	3.83	3.17	2.01	1.40	0.83
Striatum	0.29	0.31	0.37	0.37	0.20	0.17	0.20	0.16
Cerebellum	1.30	2.74	2.92	3.79	4.42	3.40	1.62	1.10
Olfactory bulb	0.48	0.90	0.97	0.85	0.82	0.63	0.49	0.45
Midbrain	0.11	0.20	0.13	0.13	0.11	0.12	0.11	0.05
Hypothalamus	0.09	0.13	0.09	0.11	0.12	0.12	0.10	0.09
Pons	0.37	0.39	0.36	0.35	0.34	0.22	0.12	0.05
Thalamus	0.10	0.13	0.13	0.13	0.09	0.11	0.13	0.06

FIGURE 4
Expression of TCF4 is high in the mouse cerebral cortex, hippocampus and cerebellum. **(A)** Three independent datasets from Cardoso-Moreira et al. (2019), ENCODE Consortium (ENCODE Project Consortium, 2012; Luo et al., 2020), and Shafik et al. (2021) were combined for meta-analysis of *Tcf4* mRNA expression in mouse cerebral cortex, cerebellum, midbrain, and hypothalamus throughout development. mRNA expression of total *Tcf4* is visualized as a line chart (upper panel) where the solid line connects the mean of *Tcf4* expression for each developmental stage and error bars represent standard error of the mean (SEM). The distribution of isoform-specific transcripts is shown as bars (lower panel). Each isoform is represented with different color, as shown in the legend on the right. (**B–D**) Western blot analysis of TCF4 protein expression in different brain areas of BALB/c mouse at P0 **(B)**, P10 **(C)**, and throughout postnatal development **(D)**. The examined brain areas are shown on the top of each panel together with the day of postnatal development. P10 cerebral cortex was used for normalization **(D)**. Coomassie membrane staining (CS) shown at the bottom of each western blot was used as a loading control. The locations of TCF4 isoform groups are color coded and shown on the right. In each panel, molecular weight is shown on the left in kilodaltons. **(E)** TCF4 signals from western blot analysis of different brain areas of BALB/c mouse were quantified and normalized using Coomassie staining. The normalized signal from P10 cerebral cortex was set as 1, and the quantification results are visualized as a heatmap. Color scale gradient represents the relative TCF4 expression level, where blue and red color represents the lowest and the highest total TCF4 protein level, respectively. The studied brain regions are shown on the left and developmental stages on top. CTX, cerebral cortex; HC, hippocampus; CB, cerebellum; STRT, striatum; OB, olfactory bulb; MB, midbrain; HTH, hypothalamus; TH, thalamus; P, postnatal day; and CS, Coomassie staining.

a calibrator and quantified the results (Figure 4E; Supplementary Figure S5F). In agreement with our direct comparisons (Figures 4B,C; Supplementary Figures S5A,B), the highest levels of TCF4 expression were observed in the cerebral cortex, hippocampus, and cerebellum, with all the other studied brain regions showing either moderate (olfactory bulb) or low (striatum, midbrain, hypothalamus, pons, and thalamus) TCF4 expression (Figure 4E; Supplementary Figure S5F). While in the

cerebral cortex and hippocampus TCF4 expression peaked just after birth (Figure 4E; Supplementary Figure S5F), cerebellum displayed a slightly delayed increase in TCF4 expression, peaking around a week after birth (Figure 4E; Supplementary Figure S5F). Notably, cerebellum and hippocampus retained a higher expression of TCF4 for a longer period compared to the cerebral cortex (Figure 4E; Supplementary Figure S5F).

To extend our observations for the mouse, we next characterized TCF4 expression in the brain of another important model organism, the rat (Figure 5). *Tcf4* mRNA expression was highest in the rat cortex, hippocampus, and cerebellum (Figure 5A; Supplementary Figure S3B). At P0 and P10, the highest TCF4 protein expression levels were seen in the cerebral cortex, hippocampus, and cerebellum (Figures 5B,C). The

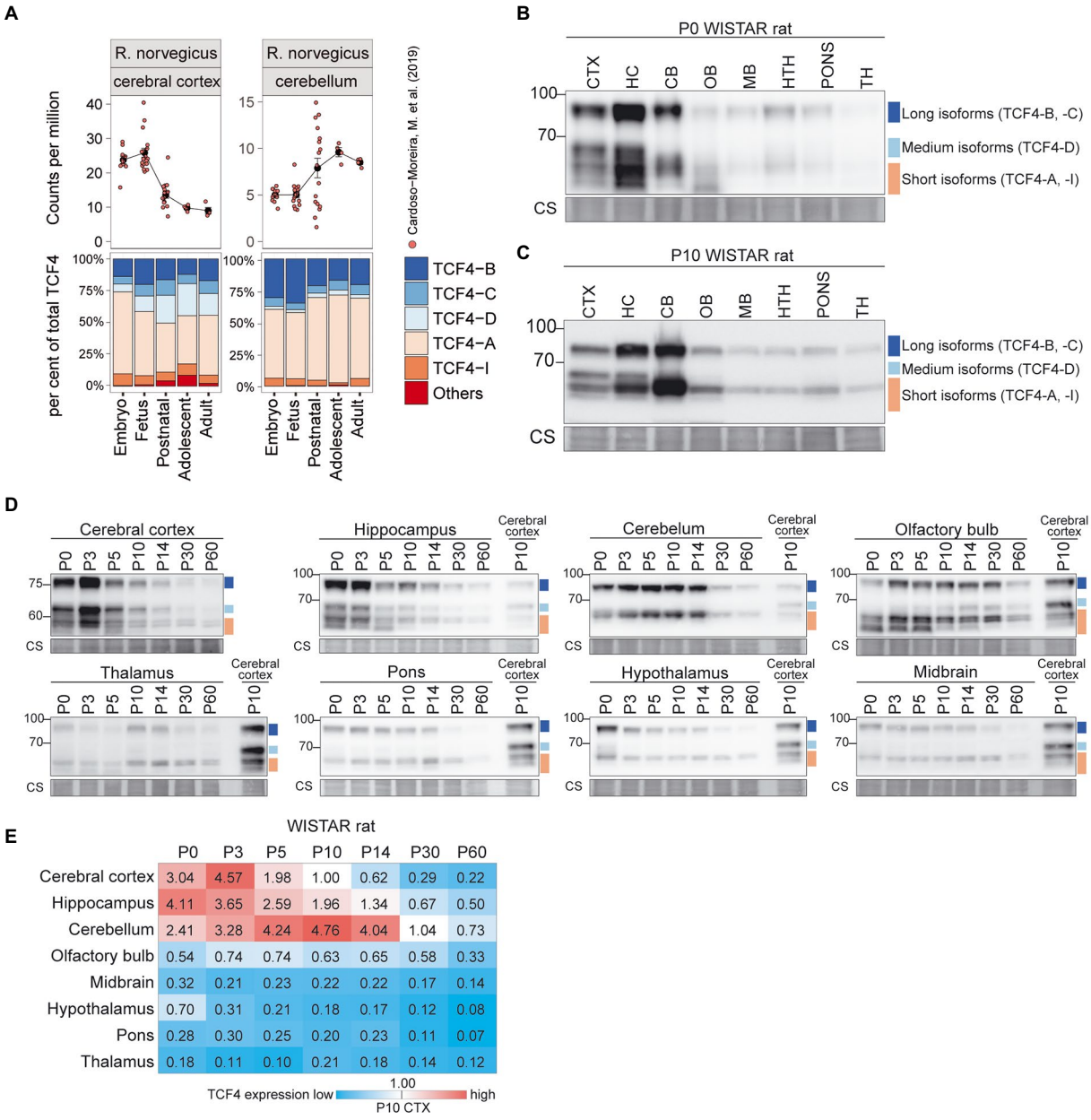

FIGURE 5
Expression of TCF4 is high in the rat cerebral cortex, hippocampus, and cerebellum. **(A)** Dataset from Cardoso-Moreira et al. (2019) was analyzed for TCF4 expression in rat cerebral cortex and cerebellum throughout development. Total *Tcf4* mRNA expression and the TCF4 isoform distribution was analyzed and visualized similarly to mouse. For more information see legend of Figure 4A. **(B–D)** Western blot analyses of TCF4 protein expression in different brain areas of WISTAR rat at P0 **(B)**, P10 **(C)**, and throughout postnatal development **(D)**. For more details see legend of Figures 4B–D. **(E)** TCF4 signals from western blot analysis of different brain areas of WISTAR rat were quantified, normalized using Coomassie staining, and visualized as a heatmap. For more details see legend of Figure 4E. CTX, cerebral cortex; HC, hippocampus; CB, cerebellum; OB, olfactory bulb; MB, midbrain; HTH, hypothalamus; TH, thalamus; P, postnatal day; and CS, Coomassie staining.

expression dynamics of TCF4 protein isoforms across postnatal development were similar to mouse (Figures 5D,E). Notably, in P0-5 rat cerebral cortex, hippocampus, and olfactory bulb an isoform migrating faster than the TCF4-A isoforms was seen, potentially corresponding to TCF4-I (Figures 5B–D).

Taken together, our data showed that TCF4 expression pattern and dynamics were similar in the mouse and rat brain—the highest TCF4 protein expression was seen in the cerebral cortex and hippocampus around birth, and in the cerebellum 1–2 weeks after birth. TCF4 expression in other brain regions was relatively low. In addition to the differences in overall expression of TCF4, our data revealed that the composition of TCF4 isoforms expressed varies across brain regions in mouse and rat.

Expression of TCF4 is lower in rodent nonneural organs compared to the brain

We then focused on mouse nonneural organs and performed a meta-analysis of available short-read RNA-seq data (Keane et al., 2011; ENCODE Project Consortium, 2012; Schmitt et al., 2014; Yu et al., 2014; Vied et al., 2016; Li et al., 2017; Söllner et al., 2017; Cardoso-Moreira et al., 2019; Luo et al., 2020; Shafik et al., 2021). We analyzed *Tcf4* mRNA expression in the lung, kidney, thymus, spleen, liver, heart, and stomach (Figure 6A; Supplementary Figures S3A, S4A). These tissues displayed comparable *Tcf4* mRNA expression levels except for the liver, where almost no *Tcf4* mRNA expression was seen after birth (Figure 6A; Supplementary Figure S3A). Of the transcripts encoding different TCF4 protein isoforms in nonneural organs, the ones encoding TCF4-A were most prominently expressed, followed by TCF4-B-encoding transcripts (Figure 6A; Supplementary Figure S4A).

Next, we prepared protein lysates from BALB/c (Figure 6) and C57BL/6 (Supplementary Figure S5) mouse heart, diaphragm, muscle, skin, lung, kidney, bladder, stomach, pancreas, thymus, spleen, liver, and blood cells at P0, 14, and 60 for western blot analysis (Figures 6B,C, Supplementary Figure S5). In nonneural tissues, the composition of TCF4 protein isoforms was similar to the one in the brain—both long and short TCF4 protein isoforms were always present, whereas medium-sized TCF4 isoforms were not observed in any of the nonneural tissues (Figures 6B,C; Supplementary Figure S5D,E). Among the studied nonneural tissues, the highest levels of TCF4 protein were seen in the skin at P0 (Figure 6D; Supplementary Figure S5G). Very low TCF4 protein levels were detected in the pancreas, spleen, kidney and liver, and TCF4 protein expression was not seen in the blood cells (Figure 6D; Supplementary Figure S5G).

We also investigated TCF4 expression in rat nonneural tissues (Figure 7; Supplementary Figures S3B, S4B). Rat *Tcf4* mRNA expression was comparable in all the nonneural tissues except for the liver, where *Tcf4* expression was very low (Figure 7A; Supplementary Figure S3B). Different from mouse, transcripts encoding TCF4-A did not account for the majority of rat *Tcf4* transcripts expressed in nonneural tissues, as also high expression of transcripts encoding TCF4-B and TCF4-C were present (Figure 7A; Supplementary Figure S4B).

Western blot analysis of rat nonneural tissues showed that different from mouse, TCF4 protein expression levels were more uniform between tissues (Figures 7B–D). In rat, TCF4 protein expression was highest in the thymus and was not observed in the pancreas (Figures 7B–D). The expression pattern of TCF4 isoforms in rat nonneural tissues was similar to mouse, i.e., mainly long and short TCF4 isoforms being present (Figures 7B,C).

Overall, the expression of TCF4 in the rodent nonneural tissues was much lower compared to the expression levels observed in the early postnatal development of the central nervous system. In addition, medium-sized TCF4 protein isoforms were almost non-existent in rodent nonneural tissues.

Expression of TCF4 in human tissues is highest around birth

Next, we analyzed available short-read RNA-seq data to describe *TCF4* total and isoform-specific mRNA expression in humans. We first analyzed the dataset published by Cardoso-Moreira and colleagues, which contained RNA-seq data from the human brain, heart, kidney, liver, and testis (Cardoso-Moreira et al., 2019). Of the noted tissues, the highest TCF4 mRNA expression was detected in the brain (Figure 8A). Human nonneural tissues showed detectable but lower *TCF4* mRNA levels compared to the brain, especially in the earlier stages of development (Figure 8A). Very low *TCF4* mRNA expression was noted for the liver (Figure 8A). In contrast to other tissues where *TCF4* mRNA levels were relatively stable throughout development, *TCF4* mRNA expression in the forebrain and kidney peaked during prenatal development (Figure 8A). We then used developmental transcriptome data from the BrainSpan project[7] to describe the changes in total *TCF4* mRNA expression in different brain regions during human development (Supplementary Figure S6). Results were similar in all brain regions—*TCF4* mRNA expression peaked during embryonic development and decreased after birth (Supplementary Figure S6).

Next, we conducted a similar analysis for adult human RNA-seq data from the Genotype-Tissue Expression (GTEx) project.[8] A selection of adult human tissues is shown in Figure 8B and all the studied tissues can be found in Supplementary Figure S7. When comparing different adult human tissues, the highest *TCF4* mRNA expression levels were seen in the adult human brain and adipose tissues (Figure 8B; Supplementary Figure S7). Almost no *TCF4* mRNA was detected in the human pancreas, liver, and whole blood (Figure 8B; Supplementary Figure S7).

7 http://brainspan.org
8 https://gtexportal.org

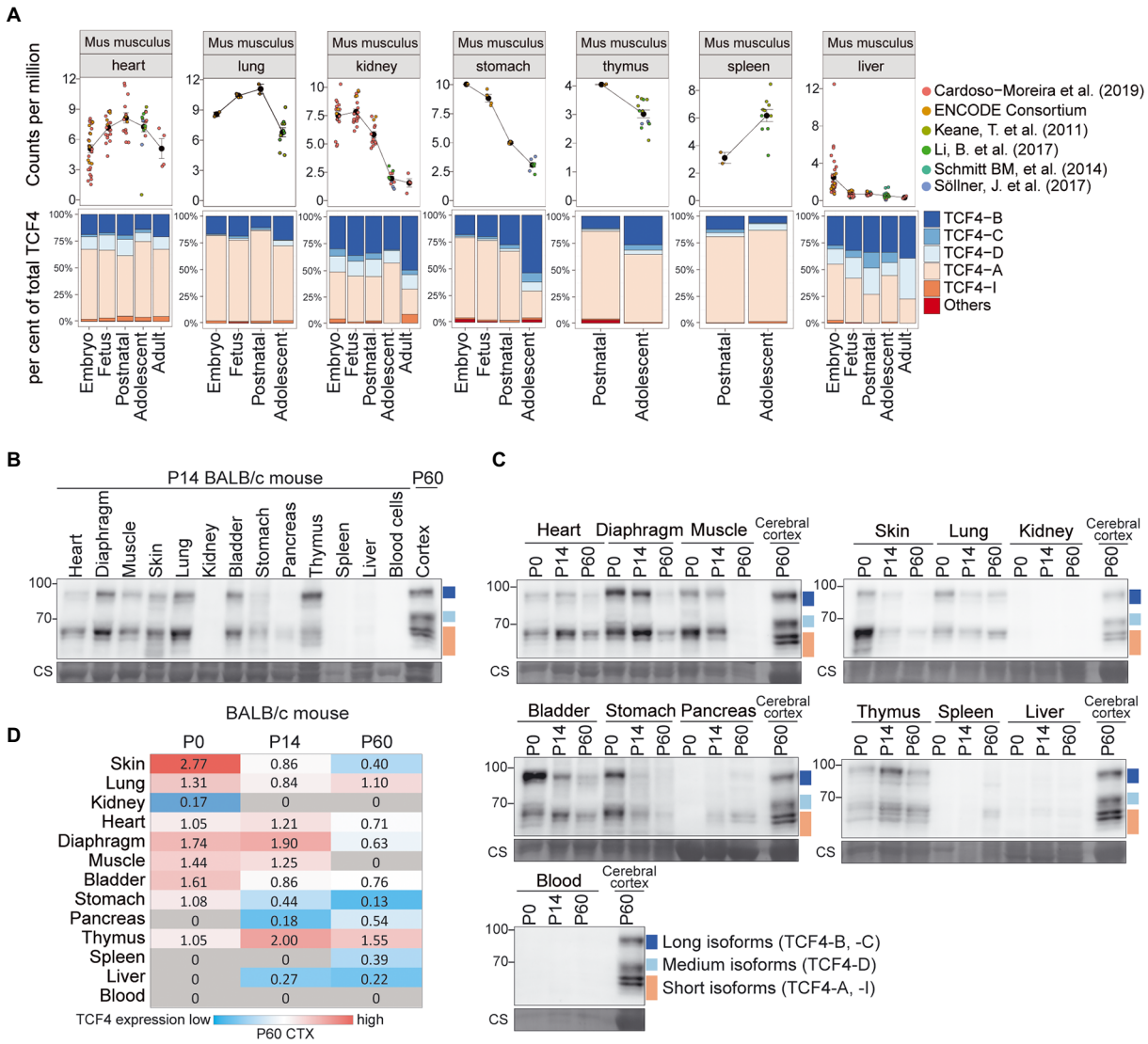

FIGURE 6
Expression of TCF4 in mouse nonneural tissues. **(A)** Six independent datasets shown on the right were combined for meta-analysis *of Tcf4* expression in mouse heart, lung, kidney, stomach, thymus, spleen, and liver throughout development. Total *Tcf4* levels and the distribution of isoform-specific transcripts is visualized. For more information see legend of Figure 4A. **(B,C)** Western blot analysis of TCF4 protein expression in different nonneural tissues of BALB/c mouse at P14 **(B)**, and throughout postnatal development **(C)**. TCF4 signal from the P60 cerebral cortex was used in each experiment for normalization. Coomassie membrane staining (CS) shown at the bottom of each western blot was used as a loading control. The locations of TCF4 isoform groups are color coded and shown on the right. In each panel, molecular weight is shown on the left in kilodaltons. **(D)** TCF4 signals from western blot analysis of different peripheral tissues of BALB/c mouse were quantified and normalized using Coomassie staining. The signal was then normalized to the signal of the P60 cerebral cortex, and the quantification result is visualized as a heatmap. Color scale gradient represents the relative TCF4 expression level, where blue and red color represents the lowest and the highest total TCF4 protein level, respectively. Gray boxes indicate no detectable TCF4 expression. The studied nonneural tissues are shown on the left and developmental stages on top. P, postnatal day; CS, Coomassie staining.

For both Cardoso-Moreira et al. and GTEx datasets, transcripts encoding TCF4-A made up around 50% of the total TCF4 mRNA levels in all the studied tissues, with the only exception being the testis (Figures 8A,B; Supplementary Figure S7). In the human testis, mRNA transcripts encoding TCF4-J accounted for the majority of total *TCF4* levels beginning from adolescence, which coincides with the start of spermatogenesis (Figure 8A; Supplementary Figure S6). The other major isoform-specific transcripts expressed in human tissues were TCF4-B, -C, and-D (Figures 8A,B; Supplementary Figure S6).

Next, we aimed to investigate TCF4 isoform composition in the adult human cerebral cortex and hippocampus. For this, we prepared protein lysates from these brain regions and human neuroblastoma cell line SH-SY5Y used for isoforms' mobility comparison. Western blot analysis revealed that TCF4 protein

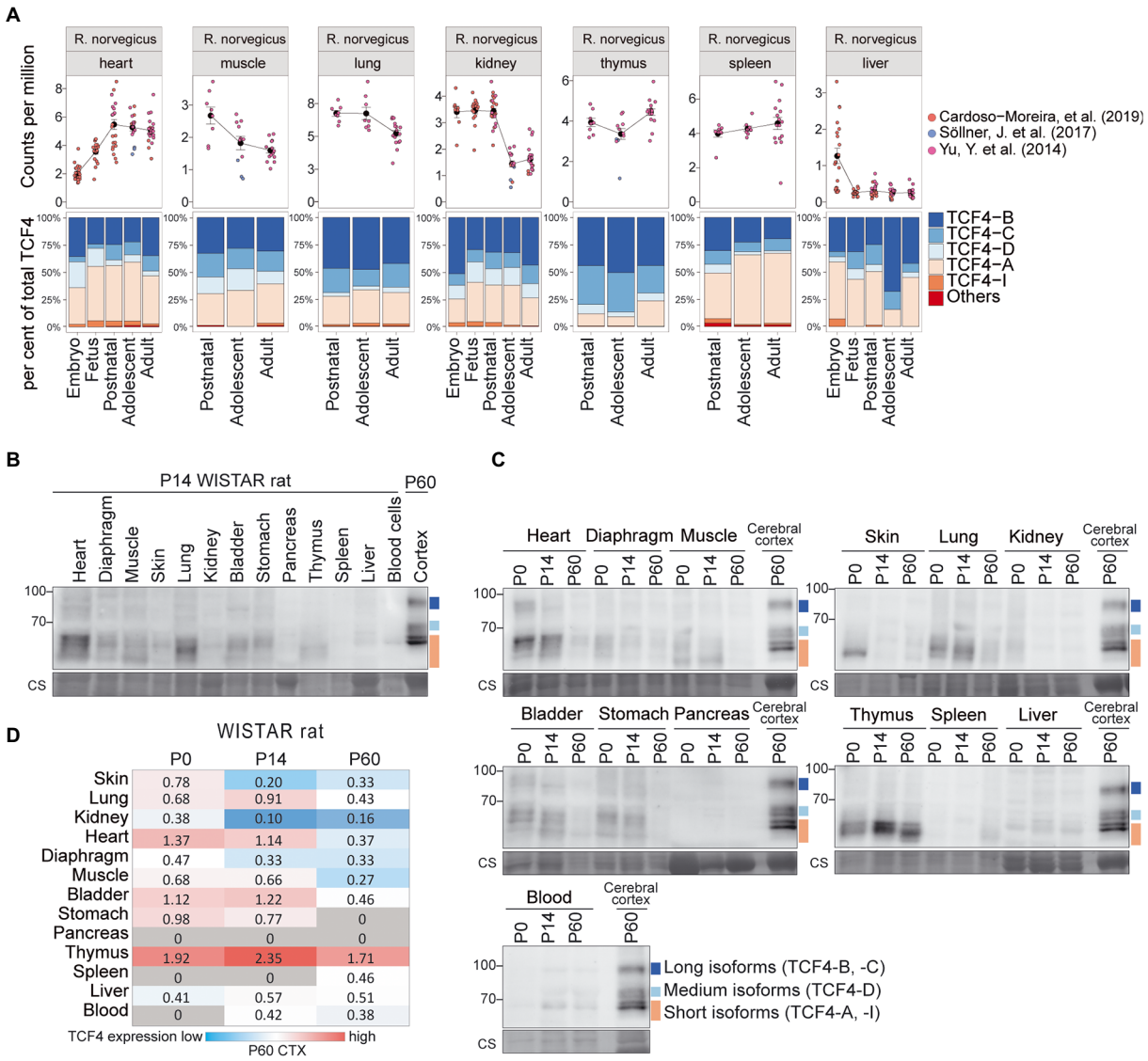

FIGURE 7
Expression of TCF4 in rat nonneural tissues. **(A)** Three independent datasets shown on the right were combined for meta-analysis of *Tcf4* expression in rat heart, muscle, lung, kidney, thymus, spleen, and liver throughout development. Total *Tcf4* levels and the distribution of isoform-specific transcripts is visualized. For more information see Figure 4A. (**B,C**) Western blot analyses of TCF4 protein expression in different peripheral tissues of WISTAR rat at P14 **(B)**, and throughout postnatal development **(C)**. For more details see legend of Figures 6B,C. **(D)** TCF4 signals from western blot analysis of different nonneural tissues of WISTAR rat were quantified, normalized using Coomassie staining, and visualized as a heatmap. For more details see legend of Figure 6D. P, postnatal day; CTX, cerebral cortex.

signal was detectable in both adult human brain and SH-SY5Y cell line (Figure 9). We also detected a possible non-specific signal located between the long and medium TCF4 isoforms in both SH-SY5Y and human brain lysates (Figure 9) since this signal was not detected using other TCF4 antibodies (data not shown) validated by us before (Nurm et al., 2021). Different to SH-SY5Y cell line, we detected all three TCF4 isoform groups in the adult human brain, however expression level of longer TCF4 isoforms was higher compared to the medium and short isoforms (Figure 9; Supplementary Figure S8). This result was on the contrary with protein isoform patterns seen in the rodent brain and the results from our human RNA-seq data analysis, which could result from protein stability, post-mortem artifacts or signal masking by other similar-sized proteins. Nevertheless, the presence of long, medium and short TCF4 isoforms in adult human brain matched with TCF4 isoform pattern in rodents, however the species-and tissue-specific temporal expression dynamics of different TCF4 isoforms during the development cannot be emphasized more.

Altogether, our results show that *TCF4* mRNA is expressed at high levels in the human brain during development and the expression is retained in the adulthood. In most tissues transcripts

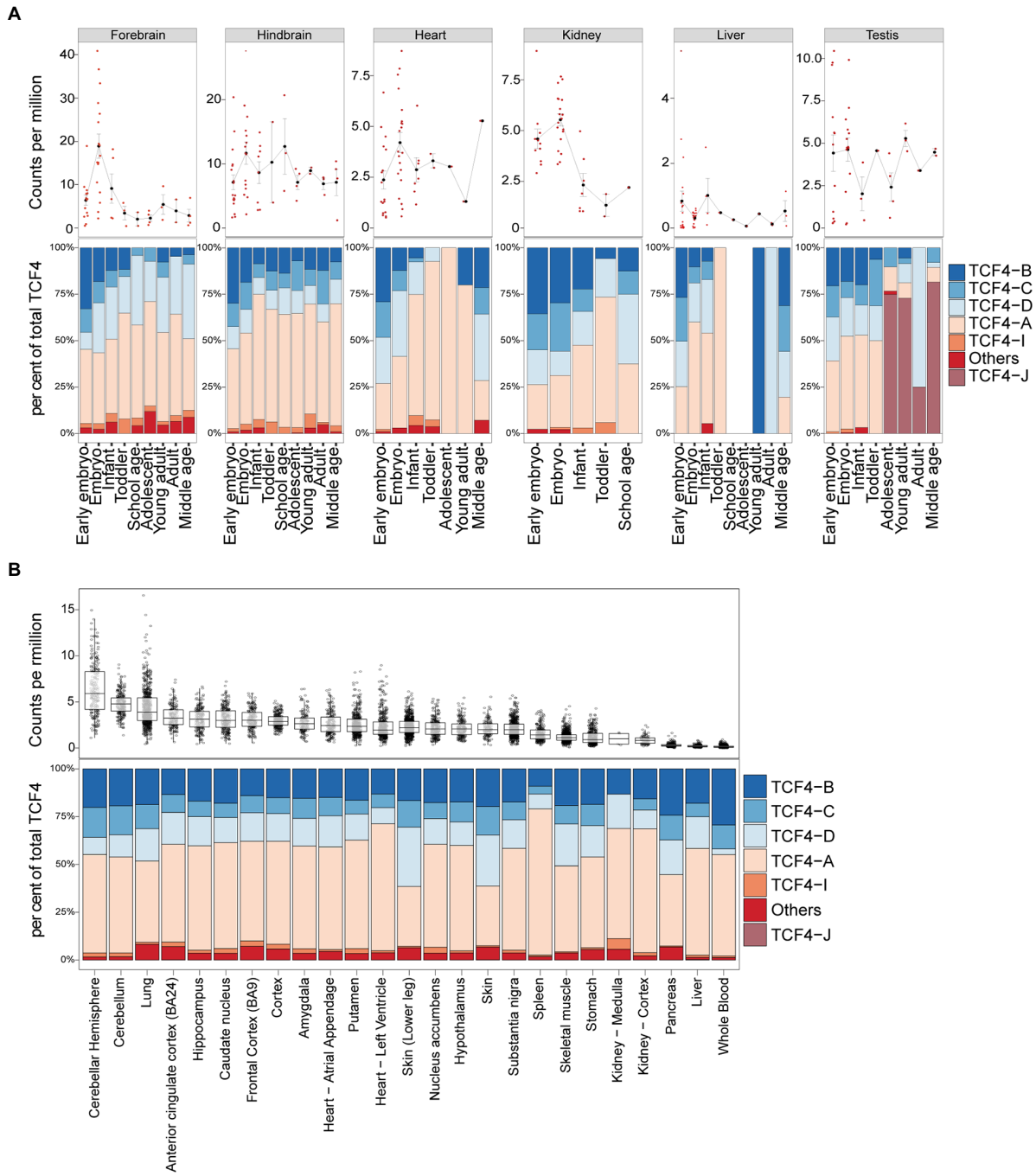

FIGURE 8
TCF4 transcripts encoding TCF4-A account for the majority of total *TCF4* expression in the human brain and nonneural tissues. Data from Cardoso-Moreira et al. **(A)** (Cardoso-Moreira et al., 2019) and the Genotype-Tissue Expression (GTEx) project **(B)** was analyzed for *TCF4* expression in the brain and nonneural tissues in humans through development **(A)** or in adults **(B)**. mRNA expression of total *TCF4* is visualized either as a line chart **(A)** or box plot **(B)**, and the distribution of isoform-specific transcripts is shown as bars **(A,B)**. **(A)** Average values are presented as dots and error bars represent SEM. **(B)** The hinges show 25 and 75% quartiles, the horizontal line shows the median value, the upper whisker extends from the hinge to the largest value no further than 1.5 of the inter-quartile range from the hinge, the lower whisker extends from the hinge to the smallest value at most 1.5 * inter-quartile range of the hinge. Each isoform is represented with different color, as shown in the legend on the right. Individual data points are presented as small dots.

encoding for TCF4-A were the most prominent ones, while in the testis TCF4-J encoding transcripts were mostly expressed. In adult human brain, long, medium and short TCF4 protein isoforms are expressed.

Discussion

Transcription factor TCF4 has been extensively studied due to its linkage with neurocognitive disorders such as intellectual

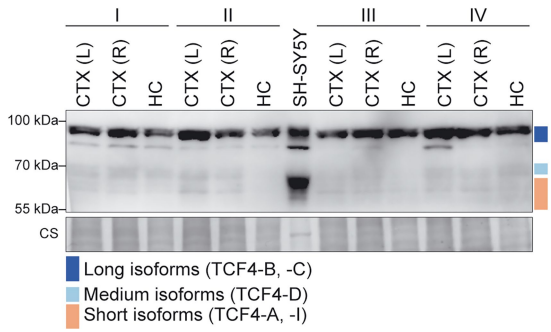

FIGURE 9
Expression of TCF4 protein isoforms in adult human cerebral cortex and hippocampus. Western blot analysis of TCF4 protein expression in the adult human cerebral cortex left (L) and right (R) hemisphere, hippocampus, and SH-SY5Y cell line. Samples from four individuals aged 62 (I), 65 (II), 67 (III), and 70 (IV) yearswere used. Coomassie staining (CS) shown at the bottom was used as loading control. The locations of TCF4 isoform groups are color coded and shown on the right. In each panel, molecular weight is shown on the left in kilodaltons. CS, coomassie staining.

disability, schizophrenia and Pitt-Hopkins syndrome (Stefansson et al., 2009; Kharbanda et al., 2016; Zollino et al., 2019). Knowledge of TCF4 expression across tissues and development would lay the foundation to understanding how these diseases develop and may help with the generation of gene therapy applications for the many TCF4 associated diseases. Transcripts from the mouse and human *TCF4* gene have been previously described in our lab using mRNA and expressed sequence tag data from public databases (Sepp et al., 2011; Nurm et al., 2021). Short read RNA-seq data can also be used to describe *Tcf4* transcripts. However, due to the structure of the *Tcf4* gene, it can be complicated to describe expression of transcripts encoding different isoforms based only on short read RNA-seq data as splicing features or 5′ exons can be difficult to detect. Our direct long-read RNA-seq analysis of *Tcf4* transcripts in the rodent brain revealed that transcription from the *Tcf4* gene results in transcripts encoding 5 N-terminally distinct TCF4 protein isoforms in the rodent brain – TCF4-B, -C, -D, -A, and-I. This result falls in line with previous observations by Nurm et al. (2021).

Expression of total *Tcf4* mRNA during development has been extensively studied mainly in the mouse cerebral cortex at the total mRNA level, with the highest expression reported around birth (E16-P6; Li et al., 2019; Phan et al., 2020). This is in accordance with our RNA-seq meta-analysis and applies for both mouse and rat. In addition, we show that the expression dynamics of *Tcf4* in the rodent brain and nonneural tissues are similar—highest *Tcf4* expression can be detected around birth, followed by a decline during postnatal development. However, studying only total *Tcf4* mRNA levels provides only partial information about *Tcf4* expression as transcription from the *Tcf4* gene results in numerous transcripts, and encoded protein isoforms have different functional protein domains and transactivation capability (Sepp et al., 2011, 2017; Nurm et al., 2021). We have previously developed a method which quantifies the expression of different *Tcf4* protein isoform-encoding transcripts using short read RNA-seq data (Sirp et al., 2020). Here, we applied the same approach to describe the expression of different TCF4 isoforms throughout development using previously published RNA-seq data. When leaving aside the great increase in the expression of TCF4-J in the adolescent human testis (transcripts encoding TCF4-J are not present in rodents), no drastic change concerning switching from the expression of one TCF4 isoform to the other was detected during the rodent and human development. This suggests that the same TCF4 isoforms that are necessary during development may also be vital for the TCF4-mediated normal functioning of the adult organism.

The necessity of so many different TCF4 isoforms remains unknown. In humans, mutations in the 5′ region of *TCF4* gene, which affect only the longer isoforms, lead to mild–moderate intellectual disability (Kharbanda et al., 2016). As the resulting disease is not as severe as the Pitt-Hopkins syndrome, it may mean that a slight decrease in overall TCF4 expression causes the phenotype. However, it is also possible that the longer TCF4 isoforms have specific functions which cannot be compensated by other TCF4 isoforms, and mutations affecting only a subset of TCF4 isoforms result in less severe effects than seen for mutations affecting all the isoforms. Recently, it has been shown that postnatal normalization of TCF4 expression to wild type levels can rescue the phenotype of TCF4 heterozygous knockout mice (Kim et al., 2022). In addition, studies of Daughterless, the orthologue of TCF4 in the fruit fly, have shown that it is possible to partially rescue the severe embryonic neuronal phenotype of Daughterless null mutation by overexpressing either human TCF4-A or TCF4-B (Tamberg et al., 2015). The generation of TCF4 isoform-specific mutant mice would help to identify whether TCF4 isoforms have distinct or similar functions. Such a model could be used to determine whether it is possible to rescue the negative phenotype resulting from a knock-out of a single TCF4 isoform by increasing the level of an another TCF4 isoform. However, generating such a model comes with many challenges. To begin with, it can be complicated to silence all the TCF4 isoforms individually by causing just frameshift mutations as only some isoforms (e.g., TCF4-B and-A) have their translation start sites located in independent 5′ exons. In addition, mutating one *TCF4* transcript can result in the upregulation of another *TCF4* transcript – an effect that we saw when silencing TCF4-A in Neuro2a cells that resulted in an increase in TCF4-I levels. We have also previously shown that Fuchs' Endothelial Dystrophy-related endogenous downregulation of transcripts encoding longer TCF4 isoforms results in the upregulation of shorter isoforms (Sirp et al., 2020).

To fully characterize TCF4 expression, it is important to consider all TCF4 protein isoforms. Previously, a large study on the expression of TCF4 protein during neurodevelopment has been performed by Matthias Jung and colleagues using immunohistochemical analysis with an antibody specific only for the long TCF4 protein isoforms (Jung et al., 2018). Another study

by Kim and colleagues used TCF4-GFP reporter mice to characterize total TCF4 expression in the mouse brain (Kim et al., 2020). A major limitation of these methods is that they cannot be used to describe the expression of different TCF4 protein isoforms. Overall, our results of total TCF4 protein expression levels during postnatal development of different mouse brain areas agree with the previously reported data. However, by using a TCF4 antibody specific for all the TCF4 isoforms in western blot analysis, we were able to distinguish TCF4 protein expression in three different groups – long (TCF4-B, TCF4-C), medium (TCF4-D) and short TCF4 isoforms (TCF4-A, TCF4-I). Isoform-specific silencing of TCF4 and *in vitro* translated TCF4 protein isoforms confirmed the locations of TCF4 isoforms in western blot. However, it should be noted that a similar pattern of TCF4 isoforms in western blot analysis between different tissues may not necessarily indicate the presence of exactly the same TCF4 isoforms. We acknowledge that *in vitro* and *in vivo* translated proteins can migrate differently in western blot analysis due to the differences in post-translational modifications of the proteins in various cell types.

The expression dynamics of TCF4 during the development varied in different brain regions. In contrast to the cerebral cortex where TCF4 expression levels decline after birth, in the cerebellum, hippocampus and olfactory bulb we saw a more prolonged high TCF4 protein expression. In the cerebellum TCF4 protein expression peaks about a week later than in any of the other brain regions. While the majority of the neurogenesis in the central nervous system happens during prenatal development, the granule cell precursors of the cerebellum and olfactory bulb, and the dentate gyrus of the hippocampus proliferate and differentiate after birth (Chen et al., 2017), where TCF4 was shown to be highly expressed (Jung et al., 2018; Kim et al., 2020), and regulate the maturation of the cerebellar granule cells (Kim et al., 2020). We propose that high TCF4 expression is necessary for the maturation of distinct brain regions, whereas fully developed brain areas display low and stable TCF4 expression necessary for normal function of the adult nervous system.

Expression of long and short TCF4 protein isoforms was seen in all brain regions and nonneural tissues where TCF4 was detectable. However, in rodents the medium TCF4 isoforms (TCF4-D) were only observed in the brain, specifically in the cerebral cortex, hippocampus, and olfactory bulb. Interestingly, in the whole rodent brain the expression of medium isoforms became apparent only in later stages of embryonic development. The only well-known functional protein domain located in the N-terminal region of longer TCF4 isoforms is activation domain 1. While the long TCF4 isoforms (TCF4-B and-C) contain this domain, TCF4-D lacks it. In addition, different from short TCF4 isoforms (TCF4-A and-I), TCF4-D contains a nuclear localisation signal. It remains to be studied what the function of TCF4-D in the development of the nervous system is and why this TCF4 isoform is missing in the cerebellum where TCF4 is otherwise highly expressed.

Based on the results of the present study we propose that a mixture consisting of TCF4-B, -C, -D, -A, and-I encoding constructs could be used in gene therapy approaches for Pitt-Hopkins syndrome. However, it should be noted that TCF4 expression levels vary between brain regions and cell types during development (Jung et al., 2018; Kim et al., 2020), suggesting that the dosage of TCF4 isoforms needs to be highly regulated. The direct administration of a cocktail of TCF4 isoforms may allow easier control of each isoform compared to other gene therapy approaches such as activation of endogenous promoters and enhancers. As a next step of this study, a similar TCF4 protein expression analysis should be done for human brain regions with a focus on the hippocampus and cerebral cortex, as studies of structural brain anomalies in PTHS-patients and *Tcf4*-heterozygous mice have shown hypoplasia of these brain regions (Marangi and Zollino, 2015). In addition, the expression of TCF4 different transcripts and the protein isoforms they encode should be studied at the single cell level to better understand how the many TCF4 isoforms are regulated between cell types.

Data availability statement

The datasets analyzed and presented in this study can be found in online repositories and in the Supplementary material. The names of the repository/repositories and accession number(s) can be found in the article.

Ethics statement

The studies involving human participants were reviewed and approved by Tallinn Committee for Medical Studies, National Institute for Health Development (Permit Number 402). The patients/participants provided their written informed consent to participate in this study. The animal study was reviewed and approved by Ministry of Agriculture of Estonia (Permit Number: 45).

Author contributions

ASi and JT designed research, performed research, analyzed data, and wrote the paper. ASh, LT, and CK performed research, analyzed data, and wrote the paper. LK performed research. TT designed research, wrote the paper, and acquired funding. All authors contributed to the article and approved the submitted version.

Funding

This study was supported by Estonian Research Council (grant PRG805), European Union through the European Regional Development Fund (project no. 2014-2020.4.01.15-0012) and H2020-MSCA-RISE-2016 (EU734791), and Pitt Hopkins Research Foundation (grant no. 21). The funding sources were not

involved in study design, analysis and interpretation of data, writing of the report and in the decision to submit the article for publication.

Acknowledgments

We thank Epp Väli for technical assistance, Enn Jõeste for the dissection of human tissue samples and Mari Sepp for critical reading of the manuscript. We would like to acknowledge the ENCODE Consortium and the ENCODE production laboratories for generating the datasets used in this study. We thank the "TUT Institutional Development Program for 2016–2022" Graduate School in Clinical Medicine, which received funding from the European Regional Development Fund under program ASTRA 2014-2020.4.01.16-0032 in Estonia.

Conflict of interest

JT and TT were employed by Protobios LLC.

The remaining authors declare that the research was conducted in the absence of any commercial or financial relationships that could be construed as a potential conflict of interest.

Publisher's note

All claims expressed in this article are solely those of the authors and do not necessarily represent those of their affiliated organizations, or those of the publisher, the editors and the reviewers. Any product that may be evaluated in this article, or claim that may be made by its manufacturer, is not guaranteed or endorsed by the publisher.

Supplementary material

The Supplementary material for this article can be found online at: https://www.frontiersin.org/articles/10.3389/fnmol.2022.1033224/full#supplementary-material

References

Amiel, J., Rio, M., de Pontual, L., Redon, R., Malan, V., Boddaert, N., et al. (2007). Mutations in TCF4, encoding a class I basic helix-loop-helix transcription factor, are responsible for Pitt-Hopkins syndrome, a severe epileptic encephalopathy associated with autonomic dysfunction. *Am. J. Hum. Genet.* 80, 988–993. doi: 10.1086/515582

Badowska, D. M., Brzózka, M. M., Kannaiyan, N., Thomas, C., Dibaj, P., Chowdhury, A., et al. (2020). Modulation of cognition and neuronal plasticity in gain-and loss-of-function mouse models of the schizophrenia risk gene Tcf4. *Transl. Psychiatry* 10:343. doi: 10.1038/s41398-020-01026-7

Brockschmidt, A., Todt, U., Ryu, S., Hoischen, A., Landwehr, C., Birnbaum, S., et al. (2007). Severe mental retardation with breathing abnormalities (Pitt–Hopkins syndrome) is caused by haploinsufficiency of the neuronal bHLH transcription factor TCF4. *Hum. Mol. Genet.* 16, 1488–1494. doi: 10.1093/hmg/ddm099

Brzózka, M. M., Radyushkin, K., Wichert, S. P., Ehrenreich, H., and Rossner, M. J. (2010). Cognitive and sensorimotor gating impairments in transgenic mice overexpressing the schizophrenia susceptibility gene Tcf4 in the brain. *Biol. Psychiatry* 68, 33–40. doi: 10.1016/j.biopsych.2010.03.015

Cardoso-Moreira, M., Halbert, J., Valloton, D., Velten, B., Chen, C., Shao, Y., et al. (2019). Gene expression across mammalian organ development. *Nature* 571, 505–509. doi: 10.1038/s41586-019-1338-5

Champlin, A. K., Dorr, D. L., and Gates, A. H. (1973). Determining the stage of the estrous cycle in the mouse by the appearance of the vagina. *Biol. Reprod.* 8, 491–494. doi: 10.1093/biolreprod/8.4.491

Chen, V. S., Morrison, J. P., Southwell, M. F., Foley, J. F., Bolon, B., and Elmore, S. A. (2017). Histology atlas of the developing prenatal and postnatal mouse central nervous system, with emphasis on prenatal days E7.5 to E18.5. *Toxicol. Pathol.* 45, 705–744. doi: 10.1177/0192623317728134

Chiaramello, A., Neuman, K., Palm, K., Metsis, M., and Neuman, T. (1995). Helix-loop-helix transcription factors mediate activation and repression of the p75LNGFR gene. *Mol. Cell. Biol.* 15, 6036–6044. doi: 10.1128/MCB.15.11.6036

Corneliussen, B., Thornell, A., Hallberg, B., and Grundström, T. (1991). Helix-loop-helix transcriptional activators bind to a sequence in glucocorticoid response elements of retrovirus enhancers. *J. Virol.* 65, 6084–6093. doi: 10.1128/jvi.65.11.6084-6093.1991

de Pontual, L., Mathieu, Y., Golzio, C., Rio, M., Malan, V., Boddaert, N., et al. (2009). Mutational, functional, and expression studies of the TCF4 gene in Pitt-Hopkins syndrome. *Hum. Mutat.* 30, 669–676. doi: 10.1002/humu.20935

Doostparast Torshizi, A., Armoskus, C., Zhang, H., Forrest, M. P., Zhang, S., Souaiaia, T., et al. (2019). Deconvolution of transcriptional networks identifies TCF4 as a master regulator in schizophrenia. *Sci. Adv.* 5:eaau4139. doi: 10.1126/sciadv.aau4139

Einarson, M. B., and Chao, M. V. (1995). Regulation of Id1 and its association with basic helix-loop-helix proteins during nerve growth factor-induced differentiation of PC12 cells. *Mol. Cell. Biol.* 15, 4175–4183. doi: 10.1128/MCB.15.8.4175

ENCODE Project Consortium (2012). An integrated encyclopedia of DNA elements in the human genome. *Nature* 489, 57–74. doi: 10.1038/nature11247

Fischer, B., Azim, K., Hurtado-Chong, A., Ramelli, S., Fernández, M., and Raineteau, O. (2014). E-proteins orchestrate the progression of neural stem cell differentiation in the postnatal forebrain. *Neural Dev.* 9:23. doi: 10.1186/1749-8104-9-23

Forrest, M. P., Hill, M. J., Kavanagh, D. H., Tansey, K. E., Waite, A. J., and Blake, D. J. (2018). The psychiatric risk gene transcription factor 4 (TCF4) regulates neurodevelopmental pathways associated with schizophrenia, autism, and intellectual disability. *Schizophr. Bull.* 44, 1100–1110. doi: 10.1093/schbul/sbx164

Gelernter, J., Sun, N., Polimanti, R., Pietrzak, R., Levey, D. F., Bryois, J., et al. (2019). Genome-wide association study of posttraumatic stress disorder (PTSD) re-experiencing symptoms in >165,000 US veterans. *Nat. Neurosci.* 22, 1394–1401. doi: 10.1038/s41593-019-0447-7

Jung, M., Häberle, B. M., Tschaikowsky, T., Wittmann, M.-T., Balta, E.-A., Stadler, V.-C., et al. (2018). Analysis of the expression pattern of the schizophrenia-risk and intellectual disability gene TCF4 in the developing and adult brain suggests a role in development and plasticity of cortical and hippocampal neurons. *Mol. Autism.* 9:20. doi: 10.1186/s13229-018-0200-1

Keane, T. M., Goodstadt, L., Danecek, P., White, M. A., Wong, K., Yalcin, B., et al. (2011). Mouse genomic variation and its effect on phenotypes and gene regulation. *Nature* 477, 289–294. doi: 10.1038/nature10413

Kennedy, A. J., Rahn, E. J., Paulukaitis, B. S., Savell, K. E., Kordasiewicz, H. B., Wang, J., et al. (2016). Tcf4 regulates synaptic plasticity, DNA methylation, and memory function. *Cell Rep.* 16, 2666–2685. doi: 10.1016/j.celrep.2016.08.004

Kharbanda, M., Kannike, K., Lampe, A., Berg, J., Timmusk, T., and Sepp, M. (2016). Partial deletion of TCF4 in three generation family with non-syndromic intellectual disability, without features of Pitt-Hopkins syndrome. *Eur. J. Med. Genet.* 59, 310–314. doi: 10.1016/j.ejmg.2016.04.003

Kim, H., Berens, N. C., Ochandarena, N. E., and Philpot, B. D. (2020). Region and cell type distribution of TCF4 in the postnatal mouse brain. *Front. Neuroanat.* 14:42. doi: 10.3389/fnana.2020.00042

Kim, H., Gao, E. B., Draper, A., Berens, N. C., Vihma, H., Zhang, X., et al. (2022). Rescue of behavioral and electrophysiological phenotypes in a Pitt-Hopkins syndrome mouse model by genetic restoration of Tcf4 expression. *elife* 11:e72290. doi: 10.7554/eLife.72290

Li, B., Qing, T., Zhu, J., Wen, Z., Yu, Y., Fukumura, R., et al. (2017). A comprehensive mouse Transcriptomic BodyMap across 17 tissues by RNA-seq. *Sci. Rep.* 7:4200. doi: 10.1038/s41598-017-04520-z

Li, H., Zhu, Y., Morozov, Y. M., Chen, X., Page, S. C., Rannals, M. D., et al. (2019). Disruption of TCF4 regulatory networks leads to abnormal cortical development and mental disabilities. *Mol. Psychiatry* 24, 1235–1246. doi: 10.1038/s41380-019-0353-0

Luo, Y., Hitz, B. C., Gabdank, I., Hilton, J. A., Kagda, M. S., Lam, B., et al. (2020). New developments on the encyclopedia of DNA elements (ENCODE) data portal. *Nucleic Acids Res.* 48, D882–D889. doi: 10.1093/nar/gkz1062

Ma, C., Gu, C., Huo, Y., Li, X., and Luo, X.-J. (2018). The integrated landscape of causal genes and pathways in schizophrenia. *Transl. Psychiatry* 8:67. doi: 10.1038/s41398-018-0114-x

Marangi, G., and Zollino, M. (2015). Pitt–Hopkins syndrome and differential diagnosis: a molecular and clinical challenge. *J. Pediatr. Genet.* 4, 168–176. doi: 10.1055/s-0035-1564570

Massari, M. E., and Murre, C. (2000). Helix-loop-helix proteins: regulators of transcription in eucaryotic organisms. *Mol. Cell. Biol.* 20, 429–440. doi: 10.1128/MCB.20.2.429-440.2000

Nurm, K., Sepp, M., Castany-Pladevall, C., Creus-Muncunill, J., Tuvikene, J., Sirp, A., et al. (2021). Isoform-specific reduction of the basic helix-loop-helix transcription factor TCF4 levels in Huntington's disease. *eNeuro* 8:ENEURO.0197-21.2021. doi: 10.1523/ENEURO.0197-21.2021

Persson, P., Jögi, A., Grynfeld, A., Påhlman, S., and Axelson, H. (2000). HASH-1 and E2-2 are expressed in human neuroblastoma cells and form a functional complex. *Biochem. Biophys. Res. Commun.* 274, 22–31. doi: 10.1006/bbrc.2000.3090

Phan, B. N., Bohlen, J. F., Davis, B. A., Ye, Z., Chen, H.-Y., Mayfield, B., et al. (2020). A myelin-related transcriptomic profile is shared by Pitt-Hopkins syndrome models and human autism spectrum disorder. *Nat. Neurosci.* 23, 375–385. doi: 10.1038/s41593-019-0578-x

Pscherer, A., Dörflinger, U., Kirfel, J., Gawlas, K., Rüschoff, J., Buettner, R., et al. (1996). The helix-loop-helix transcription factor SEF-2 regulates the activity of a novel initiator element in the promoter of the human somatostatin receptor II gene. *EMBO J.* 15, 6680–6690. doi: 10.1002/j.1460-2075.1996.tb01058.x

Quednow, B. B., Ettinger, U., Mössner, R., Rujescu, D., Giegling, I., Collier, D. A., et al. (2011). The schizophrenia risk allele C of the TCF4 rs9960767 polymorphism disrupts sensorimotor gating in schizophrenia Spectrum and healthy volunteers. *J. Neurosci.* 31, 6684–6691. doi: 10.1523/JNEUROSCI.0526-11.2011

Ravanpay, A. C., and Olson, J. M. (2008). E protein dosage influences brain development more than family member identity. *J. Neurosci. Res.* 86, 1472–1481. doi: 10.1002/jnr.21615

Ripke, S., Neale, B. M., Corvin, A., Walters, J. T., Farh, K.-H., Holmans, P. A., et al. (2014). Biological insights from 108 schizophrenia-associated genetic loci. *Nature* 511, 421–427. doi: 10.1038/nature13595

Sarkar, D., Shariq, M., Dwivedi, D., Krishnan, N., Naumann, R., Bhalla, U. S., et al. (2021). Adult brain neurons require continual expression of the schizophrenia-risk gene Tcf4 for structural and functional integrity. *Transl. Psychiatry* 11, 494–411. doi: 10.1038/s41398-021-01618-x

Schmitt, B. M., Rudolph, K. L. M., Karagianni, P., Fonseca, N. A., White, R. J., Talianidis, I., et al. (2014). High-resolution mapping of transcriptional dynamics across tissue development reveals a stable mRNA-tRNA interface. *Genome Res.* 24, 1797–1807. doi: 10.1101/gr.176784.114

Sepp, M., Kannike, K., Eesmaa, A., Urb, M., and Timmusk, T. (2011). Functional diversity of human basic helix-loop-helix transcription factor TCF4 isoforms generated by alternative 5′ exon usage and splicing. *PLoS One* 6:e22138. doi: 10.1371/journal.pone.0022138

Sepp, M., Pruunsild, P., and Timmusk, T. (2012). Pitt–Hopkins syndrome-associated mutations in TCF4 lead to variable impairment of the transcription factor function ranging from hypomorphic to dominant-negative effects. *Hum. Mol. Genet.* 21, 2873–2888. doi: 10.1093/hmg/dds112

Sepp, M., Vihma, H., Nurm, K., Urb, M., Page, S. C., Roots, K., et al. (2017). The intellectual disability and schizophrenia associated transcription factor TCF4 is regulated by neuronal activity and protein kinase a. *J. Neurosci.* 37, 10516–10527. doi: 10.1523/JNEUROSCI.1151-17.2017

Shafik, A. M., Zhang, F., Guo, Z., Dai, Q., Pajdzik, K., Li, Y., et al. (2021). N6-methyladenosine dynamics in neurodevelopment and aging, and its potential role in Alzheimer's disease. *Genome Biol.* 22:17. doi: 10.1186/s13059-020-02249-z

Sirp, A., Leite, K., Tuvikene, J., Nurm, K., Sepp, M., and Timmusk, T. (2020). The Fuchs corneal dystrophy-associated CTG repeat expansion in the TCF4 gene affects transcription from its alternative promoters. *Sci. Rep.* 10:18424. doi: 10.1038/s41598-020-75437-3

Sirp, A., Roots, K., Nurm, K., Tuvikene, J., Sepp, M., and Timmusk, T. (2021). Functional consequences of TCF4 missense substitutions associated with Pitt-Hopkins syndrome, mild intellectual disability, and schizophrenia. *J. Biol. Chem.* 297:101381. doi: 10.1016/j.jbc.2021.101381

Söllner, J. F., Leparc, G., Hildebrandt, T., Klein, H., Thomas, L., Stupka, E., et al. (2017). An RNA-Seq atlas of gene expression in mouse and rat normal tissues. *Sci. Data* 4:170185. doi: 10.1038/sdata.2017.185

Soosaar, A., Chiaramello, A., Zuber, M. X., and Neuman, T. (1994). Expression of basic-helix-loop-helix transcription factor ME2 during brain development and in the regions of neuronal plasticity in the adult brain. *Mol. Brain Res.* 25, 176–180. doi: 10.1016/0169-328X(94)90297-6

Stefansson, H., Ophoff, R. A., Steinberg, S., Andreassen, O. A., Cichon, S., Rujescu, D., et al. (2009). Common variants conferring risk of schizophrenia. *Nature* 460, 744–747. doi: 10.1038/nature08186

Tamberg, L., Jaago, M., Säälik, K., Sirp, A., Tuvikene, J., Shubina, A., et al. (2020). Daughterless, the drosophila orthologue of TCF4, is required for associative learning and maintenance of the synaptic proteome. *Dis. Model. Mech.* 13:dmm042747. doi: 10.1242/dmm.042747

Tamberg, L., Sepp, M., Timmusk, T., and Palgi, M. (2015). Introducing Pitt-Hopkins syndrome-associated mutations of TCF4 to drosophila daughterless. *Biol. Open* 4, 1762–1771. doi: 10.1242/bio.014696

Thaxton, C., Kloth, A. D., Clark, E. P., Moy, S. S., Chitwood, R. A., and Philpot, B. D. (2018). Common pathophysiology in multiple mouse models of Pitt-Hopkins syndrome. *J. Neurosci.* 38, 918–936. doi: 10.1523/JNEUROSCI.1305-17.2017

Vied, C., Ray, S., Badger, C.-D., Bundy, J. L., Arbeitman, M. N., and Nowakowski, R. S. (2016). Transcriptomic analysis of the hippocampus from six inbred strains of mice suggests a basis for sex-specific susceptibility and severity of neurological disorders. *J. Comp. Neurol.* 524, 2696–2710. doi: 10.1002/cne.23989

Wray, N. R., Ripke, S., Mattheisen, M., Trzaskowski, M., Byrne, E. M., Abdellaoui, A., et al. (2018). Genome-wide association analyses identify 44 risk variants and refine the genetic architecture of major depression. *Nat. Genet.* 50, 668–681. doi: 10.1038/s41588-018-0090-3

Yu, Y., Fuscoe, J. C., Zhao, C., Guo, C., Jia, M., Qing, T., et al. (2014). A rat RNA-Seq transcriptomic BodyMap across 11 organs and 4 developmental stages. *Nat. Commun.* 5:3230. doi: 10.1038/ncomms4230

Zhuang, Y., Cheng, P., and Weintraub, H. (1996). B-lymphocyte development is regulated by the combined dosage of three basic helix-loop-helix genes, E2A, E2-2, and HEB. *Mol. Cell. Biol.* 16, 2898–2905. doi: 10.1128/MCB.16.6.2898

Zollino, M., Zweier, C., Van Balkom, I. D., Sweetser, D. A., Alaimo, J., Bijlsma, E. K., et al. (2019). Diagnosis and management in Pitt-Hopkins syndrome: first international consensus statement. *Clin. Genet.* 95, 462–478. doi: 10.1111/cge.13506

Zweier, C., Peippo, M. M., Hoyer, J., Sousa, S., Bottani, A., Clayton-Smith, J., et al. (2007). Haploinsufficiency of TCF4 causes Syndromal mental retardation with intermittent hyperventilation (Pitt-Hopkins syndrome). *Am. J. Hum. Genet.* 80, 994–1001. doi: 10.1086/515583

frontiers | Frontiers in Molecular Neuroscience

TYPE Review
PUBLISHED 16 November 2022
DOI 10.3389/fnmol.2022.1002018

OPEN ACCESS

EDITED BY
Guilherme Lucas,
University of São Paulo, Brazil

REVIEWED BY
Hitoshi Uchida,
Niigata University, Japan
Tingjun Chen,
Mayo Clinic, United States
Yongxi Song,
The First Affiliated Hospital of China Medical University, China

*CORRESPONDENCE
Jingjing Jiang
jjj_sj@163.com

SPECIALTY SECTION
This article was submitted to Pain Mechanisms and Modulators, a section of the journal Frontiers in Molecular Neuroscience

RECEIVED 24 July 2022
ACCEPTED 28 October 2022
PUBLISHED 16 November 2022

CITATION
Zhang K, Li P, Jia Y, Liu M and Jiang J (2022) Non-coding RNA and n6-methyladenosine modification play crucial roles in neuropathic pain.
Front. Mol. Neurosci. 15:1002018.
doi: 10.3389/fnmol.2022.1002018

Non-coding RNA and n6-methyladenosine modification play crucial roles in neuropathic pain

Kexin Zhang, Pei Li, Yuanyuan Jia, Ming Liu and Jingjing Jiang*

Department of Anesthesiology, Shengjing Hospital of China Medical University, Shenyang, China

After peripheral nerve injury, pain signals are transmitted from primary sensory neurons in the dorsal root ganglion (DRG) to the central nervous system. Epigenetic modification affects neuropathic pain through alterations in the gene expression in pain-related areas and glial cell activation. Recent studies have shown that non-coding RNA and n6-methyladenosine (m6A) methylation modification play pivotal regulatory roles in the occurrence and maintenance of neuropathic pain. Dysregulation of the RNA m6A level *via* dynamic changes in methyltransferase and demethylase after central or peripheral nerve injury commonly regulates pain-associated genes, contributing to the induction and maintenance of neuropathic pain. The dynamic process has significant implications for the development and maintenance of neuropathic pain. However, the underlying mechanisms by which non-coding RNA and m6A RNA modification regulate neuropathic pain are not well-characterized. This article elucidates the multiple mechanisms of non-coding RNA and m6A methylation in the context of neuropathic pain, and summarizes its potential functions as well as recent advances.

KEYWORDS

n6-methyladenosine (m6A), non-coding RNAs (ncRNAs), neuropathic pain, glial cell, neuroinflammation

Introduction

Neuropathic pain is a pain disorder caused by a lesion or disease of the somatosensory nervous system, which can be composed of peripheral neuropathic pain and central neuropathic pain (Scholz et al., 2019). The main symptoms of neuropathic pain are allodynia (a painful response to a normally non-painful stimulus) and hyperalgesia (an increased pain from a stimulus that normally provokes pain), which substantially reduce the quality of life of patients, such as through the development of sleep disorders, anxiety, and depression (Baron, 2009). Clinical management strategy for neuropathic pain remains one of the major challenges because painful symptoms are heterogenous and multidimensional (Bouhassira, 2019). Commonly used treatments for

neuropathic pain such as antidepressants, anticonvulsants, and analgesics have moderate efficacy and increase the risk of central nervous system side effects. Investigating the molecular mechanisms of neuropathic pain and identifying its specific treatments will be the main directions for future research.

Following peripheral nerve injury, the pain signaling is subsequently transmitted to the central nervous system including the dorsal horn of the spinal cord and pain-related brain regions connected to the nociceptors at the end of the primary sensory neurons in the DRG, resulting in central sensitization (Carlton et al., 2009). There are diverse reciprocal interactions between sensory neurons and glial cells which form a unit linking glial cell activation and spinal sensitization in the context of neuropathic pain. Glial cell activation is linked to neuropathic pain induction and maintenance, playing a crucial role in the transmission of pain signals (Yu et al., 2020; Donnelly et al., 2020). Epigenetic regulation at the gene level has increasingly attracted attention with the expansion of research on neuropathic pain. Epigenetic modifications such as non-coding RNAs (ncRNAs), histone covalent modifications, DNA methylation, and RNA methylation by n6-methyladenosine (m6A) regulate the expression of genes related to axon growth and glial cell activation after peripheral nerve injury (Zhang L. et al., 2021; Liu et al., 2022). Recent studies have unraveled the role of ncRNAs as potential regulators between nerve injury, inflammation, and neuropathic pain (Sommer et al., 2018).

n6-methyladenosine modification is the most prevalent internal modification of eukaryotic mRNAs and occurs primarily with adenine in mRNAs (Meyer et al., 2012). Mediated by methyltransferase, demethylase and m6A-binding protein, m6A regulates mammalian cell proliferation and differentiation *via* mRNA splicing, translation, and stability (Mauer et al., 2017; Zaccara et al., 2019). m6A methylation of mRNA is a gene level modification similar to DNA methylation, that contributes to heritable alterations in gene expression without changing the gene sequence (Zhao et al., 2020). m6A modification exists not only in mRNAs, but also in almost all types of ncRNAs (Zhao et al., 2021). However, the differing roles of m6A on ncRNAs in mammalian cells are less clear. Herein, we aim to investigate the epigenetic mechanism by which ncRNAs and m6A methylation influence nerve injury-induced neuropathic pain.

Non-coding RNAs and neuropathic pain

Classification and features of non-coding RNAs

Non-coding RNAs are small RNA molecules that typically do not encode detectable protein. Compared with coding RNAs, ncRNAs functions are more complex. Nearly 70% of the genome is translated to ncRNAs. There are many types of ncRNAs. In this review, we focus on three types of ncRNAs: miRNA (microRNA), lncRNA (long non-coding RNA), and circRNA (circular RNA).

The processing of primary miRNAs with hairpin-like structure into mature miRNAs entails splicing by RNase III proteins, Drosha and Dicer (Lee et al., 2003). The length of endogenous lncRNAs exceeds 200 nucleotides, lncRNAs may bind target genes more specifically and selectively due to their length. LncRNAs can also be categorized into five types with respect to their complimentary protein-coding gene, which can be orientated in a sense and/or antisense direction: (1) sense, (2) antisense, (3) bidirectional, (4) intronic and (5) intergenic (Qi and Du, 2013). CircRNA is the circular non-coding RNA formed by covalent binding of 3′ arm and 5′ arm after reverse splicing. Several studies have demonstrated the involvement of lncRNAs and circRNAs in the regulatory mechanisms involved in the development of neuropathic pain. lncRNAs and circRNAs which have multiple complementary binding sites of miRNAs participate in the development of neuropathic pain principally through acting as competing endogenous RNAs (ceRNAs). ceRNAs sponge their target miRNAs to decrease the expression of target gene of miRNAs (Salmena et al., 2011).

Non-coding RNAs regulate the expression of pain-associated genes in neuropathic pain

Dysregulation of pain-associated genes is related to epigenetic modification of injured neurons. Moreover, investigations of pain-associated genes by ncRNAs provide insights into the mechanisms underlying neuropathic pain (**Table 1**).

miRNAs are estimated to regulate more than 30% of genes *in vivo* and participate in the development and maintenance of neuropathic pain. Some miRNAs affect neuropathic pain by modulating gene expression and inducing activation of glial cells. Overexpression of miR-34c was shown to reduce the secretion of NLRP3, ASC, caspase-1, IL-1β, and IL-18 in the spinal cord. miR-34c greatly ameliorates neuropathic pain by inhibiting NLRP3-mediated neuroinflammation and cell apoptosis (Xu et al., 2019). Downregulation of miR-34c-5p was found to relieve neuropathic pain through SIRT1/STAT3 (signal transducer and activator of transcription 3) signaling pathway (Mo et al., 2020). Ablation of miR-23a in partial sciatic nerve ligation (pSNL) mice was shown to directly inhibit the expression of CXCR4 on microglia and regulate TXNIP/NLRP3 expression leading to neuropathic pain (Pan et al., 2018). miR-26a-5p is significantly decreased in chronic constrictive injury (CCI) model and in turn downregulates mitogen-activated protein kinase (MAPK) 6, which exacerbates neuropathic pain (Zhang et al., 2018). miR-146a-5p in DRG and SDH was shown to inhibit IRAK1 and TRAF6 through TLRs and IL-1 receptor

TABLE 1 Non-coding RNAs in different pain models regulate pain-related genes.

Pain model	Dysregulated miRNAs	Regulation	Target	Site	References
pSNL	miR-23a	Downregulation	TXNIP/NLRP3 axis	Spinal glial cell	Pan et al., 2018
CCI	miR-26a-5p	Downregulation	MAPK6	Spinal cord	Zhang et al., 2018
CCI	miR-146a-5p	Upregulation	IRAK1/TRAF6 signaling	DRG, SDH	Wang Z. et al., 2018
CCI	miR-34c	Downregulation	NLRP3	Spinal cord	Xu et al., 2019
SNI	miR-30c-5p	Upregulation	BAMBI	Spinal cord, DRG, CSF, plasma	Tramullas et al., 2018
CCI	miR-381	Downregulation	HMGB1/CXCR4	Spinal cord	Zhan et al., 2018
SNL	miR-124-3p	Downregulation	Egr1	DRG, SDH	Jiang et al., 2021
CCI	miR-34c-5p	Upregulation	SIRT1/STAT3	DRG	Mo et al., 2020
CCI	LncRNA XIST	Upregulation	miR-150/ZEB1 axis	Spinal cord	Yan et al., 2018
CCI	LncRNA XIST	Upregulation	miR-137/TNFAIP1axis	Spinal cord	Zhao et al., 2018
CCI	LncRNA XIST	Upregulation	miR-544/STAT3 axis	Spinal cord	Jin et al., 2018
CCI	LncRNA NEAT1	Upregulation	miR-381/HMGB1 axis	Spinal cord	Xia et al., 2018
CCI	LncRNA CRNDE	Upregulation	miR-136/IL6R axis	Spinal cord	Zhang D. et al., 2019
SNL	LncRNA SNHG1	Upregulation	CDK4	Spinal cord	Zhang J. Y. et al., 2020
SNL	Kcna2 antisense RNA	Upregulation	Zinc finger protein 1/Kcna2	DRG	Zhao et al., 2013
SNL	circAnks1a	Upregulation	miR-324-3p/VEGFB	SDH	Zhang S. B. et al., 2019
CCI	Circ_0005075	Upregulation	miR-151a-3p/NOTCH2 axis	Spinal cord	Zhang Y. et al., 2021
CCI	circRNA zRANB1	Upregulation	miR-24-3p/LPAR3	Spinal cord	Wei et al., 2020

(TIR) pathway, and finally relieve CCI-induced neuropathic pain (Wang Z. et al., 2018). After sciatic nerve injury (SNI), miR-30c-5p was up-regulated in the spinal cord, DRG, cerebrospinal fluid (CSF), and plasma, while miR-30c-5p was causally involved in neuropathic pain. Analysis indicated that the expression of miR-30c-5p in plasma and CSF may help predict neuropathic pain (Tramullas et al., 2018). Aberrant overexpression of mir-26a-5p suppresses neuropathic pain and neuroinflammation *via* target gene MAPK6 (Zhang et al., 2018). miR-381 in CCI rats showed a negative correlation with high mobility group box 1 (HMGB1) and CXCR4 to regulate neuropathic pain (Zhan et al., 2018). SNL-induced downregulation of miR-124-3p in DRG and dorsal horn is related to up-regulation of Egr1, and affects neuropathic pain (Jiang et al., 2021).

There is a large body of evidence suggesting a crucial role of lncRNAs in the pathophysiology of neuropathic pain (Li T. et al., 2019). Following peripheral nerve injury, dysregulated lncRNAs in the injured neurons were shown to modulate neuropathic pain by regulating the expression of pain-related genes (Jia et al., 2020). lncRNA XIST affects neuropathic pain by sponging target miRNAs to influence pain-related genes. XIST affects the expression of TNFAIP1 gene and may further promote neuropathic pain by specifically sponging miR-137 (Zhao et al., 2018). XIST sponges miR-544 to activate STAT3 (Jin et al., 2018), and XIST modulates the expression of ZEB1 through targeting miR-150 (Yan et al., 2018). XIST is a novel pronociceptive lncRNA in the context of neuropathic pain. In addition to the role of lncRNA NEAT1 in cancer, silencing of NEAT1 can also inhibit neuropathic pain and neuroinflammation. NEAT1 targets miR-381 to affect HMGB1, and induces post-CCI neuropathic pain (Xia et al., 2018). Overexpression of CRNDE, which act as a sponge for miR-136, was found to enhance neuropathic pain and neuroinflammation (Zhang D. et al., 2019). lncRNA SNHG1 blocked SNL-induced neuropathic pain because of the CDK4 level which can regulate inflammatory factors (Zhang J. Y. et al., 2020). After SNL, there is an activation of myeloid zinc finger protein 1 which is a transcription factor that can target the Kcna2 antisense RNA promoter region. The upregulation of Kcna2 antisense RNA, a conserved lncRNA, in injured DRG ultimately suppresses neuropathic pain symptoms (Zhao et al., 2013). This study revealed that endogenous Kcna2 antisense RNA may act as a therapeutic target for neuropathic pain.

In addition, an accumulating body of evidence has shed new light on the relationship of circRNA in DRG and spinal dorsal horn with neuropathic pain. Circ_0005075 contributes to CCI-induced neuropathic pain through sponging miR-151a-3p which regulates Notch2 expression (Zhang Y. et al., 2021). In the cytoplasm, circAnks1a serves as a ceRNA binding miR-324-3p to regulate VEGFB expression. Upregulation of VEGFB increases the excitability of dorsal horn neurons and aggravates neuropathic pain (Zhang S. B. et al., 2019). In CCI rats, LPAR3 expression level was significantly altered by circRNA zRANB1 which is an upstream regulator of miR-24-3p (Wei et al., 2020).

Non-coding RNAs regulate neuropathic pain *via* glial cell activation

Recently, several studies have demonstrated the molecular mechanism by which miRNAs contribute to neuroinflammation, glial cell migration, and apoptosis. After

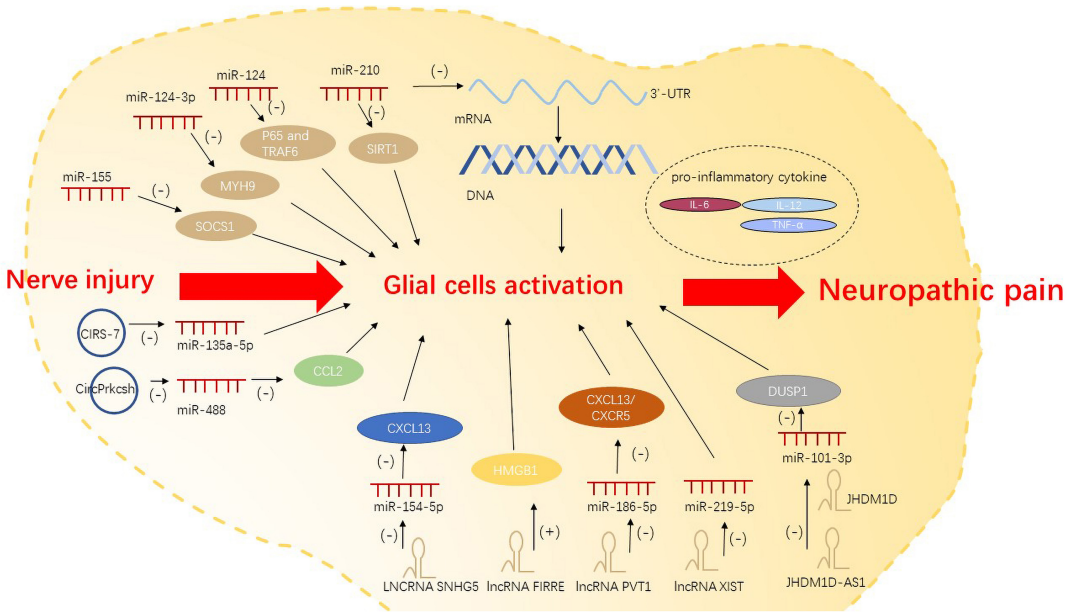

FIGURE 1
Non-coding RNAs regulate neuropathic pain *via* glial cell activation.

peripheral nerve injury, miRNAs bind to specific transcription factors or 3′-UTR of target mRNA to dampen mRNA translation and degradation; this alters the cell phenotype and the activation state of glial cells. miRNAs such as miR-124-3p (Jiang et al., 2020) and miR-210 (Li B. et al., 2020) can respectively promote and inhibit the activation of glial cells. miR-155 activates microglia by regulating inflammation-related gene SOCS1 and inflammatory cytokines (Tan et al., 2015). miR-124 was found to control the activation of microglia by inhibiting p65- and TRAF6-dependent TLR signaling (Qiu et al., 2015). Intrathecal injection of miR-124 was shown to alleviate M1/M2 type markers of microglia after nerve injury, which is a potential tool for the treatment of neuropathic pain (Willemen et al., 2012).

lncRNAs can act on microglia and astrocytes to trigger neuropathic pain (Liu et al., 2020). Significant upregulation of lncRNA SNHG5 in SNL model promotes the activation of microglia and astrocytes and exacerbates neuropathic pain by targeting miR-154-5p/CXCL13 (Chen M. et al., 2020). In CCI, lncRNA FIRRE was upregulated in the spinal cord. It contributes to neuropathic pain in mice by increasing HMGB1expression in microglia (Wen et al., 2021). LncRNA PVT1 is believed to target miR-186-5p/CXCL13/CXCR5 axis, and is responsible for neuropathic pain caused by overactivation of astrocytes (Zhang P. et al., 2021). Sponging of miR-219-5p by lncRNA XIST inhibited the viability of microglia cells, thereby affecting neuropathic pain (Zhong et al., 2021). In recent studies, antisense lncRNAs were also found to affect neuropathic pain. After total brachial plexus root avulsion (tBPRA), the downregulation of lncRNA JHDM1D antisense 1 (JHDM1D-AS1) may act as a ceRNA negatively regulating miR-101-3p. JHDM1D-AS1 can suppress microglial inflammation to influence neuropathic pain *via* miR-101-3p (Liu et al., 2020).

circRNAs can also act as ceRNAs to inhibit miRNA expression, and then regulate the pro-inflammatory genes and the activation of glial cells. Studies have identified a variety of regulatory pathways by which circRNAs regulate the activation and polarization of microglia (Li M. et al., 2021; Jiang et al., 2022). In a study, the expression of CIRS-7 in spinal dorsal horn showed a positive correlation with the occurrence of CCI-induced neuropathic pain. Binding of CIRS-7 with miR-135a-5p was shown to enhance the activation of microglia by promoting the pro-inflammatory cytokines IL-6, IL-12, and TNF-α (Cai et al., 2020). Lastly, spinal cord injury(SCI)-induced inflammatory response was shown to be inhibited by CircPrkcsh through the miR-488/CCL2 axis in astrocytes (Chen et al., 2022; **Figure 1**).

n6-methyladenosine methylation and neuropathic pain

Structure and molecular function of n6-methyladenosine

n6-methyladenosine "writers"-methyltransferases

Methyltransferases, also known as m6A "writers" increase the expression of m6A. This family of enzymes consists of

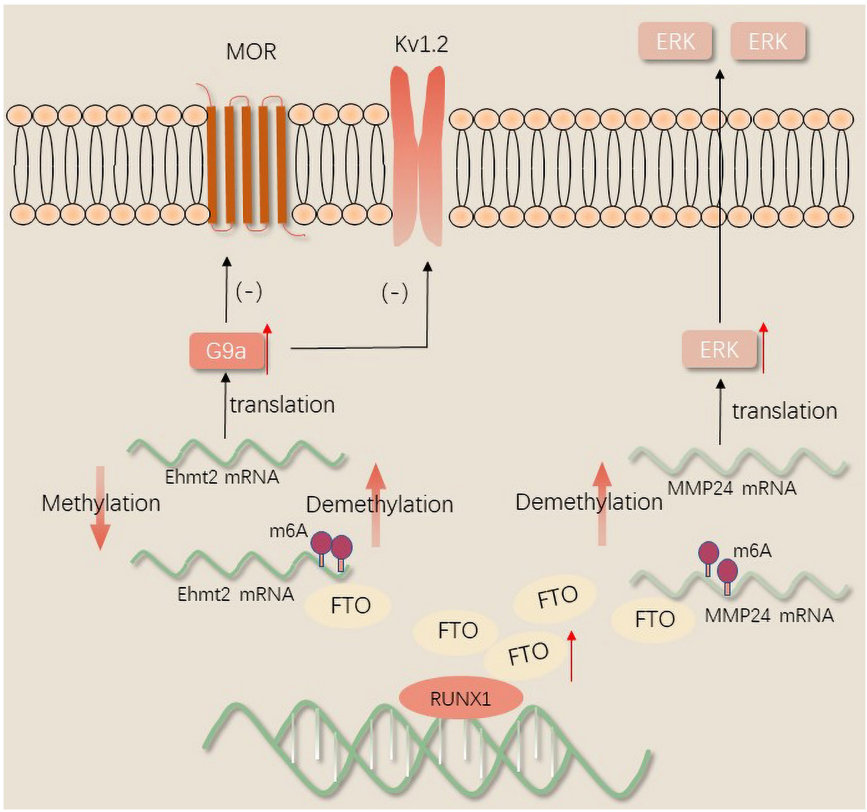

FIGURE 2
The mechanism of FTO regulates neuropathic pain.

METTL3, METTL14, and Wilms' tumor 1-associating protein (WTAP) (Bokar et al., 1997). Methyltransferases form a methyltransferase complex and function in conjunction with each other. The enzymes can be identified by diverse M6A "readers" through YTH domain proteins, indicating the effects of m6a are dynamic and reversible. The activity of the methyltransferase complex is also affected by miRNAs (Chen et al., 2015).

n6-methyladenosine "erasers"- demethylases

Currently, there are two known m6A-specific demethylases, FTO, and ALKBH5. FTO, a fat-mass and obesity-associated protein, participates in RNA m6A modification. FTO belongs to the ALKB dioxygenase family and is dependent on α-Ketoglutarate (α-ketoglutaric acid, α-Kg) and divalent iron ions located in both the nucleus and cytoplasm. m6A can be restored to adenosine under the enzymatic action of the m6A RNA demethylase FTO or ALKBH5 in mammals, indicating that m6A modification is dynamically reversible (Jia et al., 2011). The substantial increase of FTO identified in injured DRG tissue after peripheral nerve injury suggests that FTO may be a key target of neuropathic pain in future research (Li Y. et al., 2020).

n6-methyladenosine "readers"- n6-methyladenosine -binding proteins

n6-methyladenosine "readers" refers to a large class of reading proteins, such as YTH domain family proteins (m6A-binding protein YTH domain family) and insulin like growth factor 2 mRNA binding proteins (IGF2BP family proteins). These readers can recognize methylated mRNAs and directly or indirectly combine with them to promote m6A methylation together with methyltransferase. YTH domain family proteins may affect the pathological process of neuropathic pain by regulating RNA metabolism in terms of transcription, translation, splicing, transportation, and degradation.

n6-methyladenosine methylation regulates the expression of pain-associated genes in neuropathic pain

The imbalance of methylase and demethylase can modify m6A level, which regulates the transcription of pain-associated genes and the release of inflammatory mediators after nerve injury, finally affecting neuropathic pain.

METTL3 regulates the expression of pain-associated genes

n6-methyladenosine deletion caused by cerebellar conditional knockdown of METTL3 reduces the half-lives of the mRNAs of development- and apoptosis-related genes and triggers abnormal splicing of the mRNAs of synapse-associated genes, resulting in abnormal cell differentiation and apoptosis (Wang C. X. et al., 2018). Many studies have indicated the involvement of apoptosis in nerve damage and the process of development of neuropathic pain (Zhou et al., 2019; Chen X. J. et al., 2020).

It is well established that specific suppressors of the spinal cord such as METTL3 and YTHDF2 have a positive correlation with the upregulation of TET1 which is a DNA demethylase (Albik and Tao, 2021). TET1 overexpression relieves neuropathic pain *via* affecting the μ-Opioid receptor (MOR) and Kv1.2 expression to modulate pain-associated genes (Wu et al., 2019). Data available in the literature indicate that the downregulation of METTL3 has a specific positive correlation with the downregulation of m6A modification of TET1 mRNA in the spinal cord, subsequently resulting in the reduction of YTHDF2 binding to TET1 mRNA in the complete Freund adjuvant (CFA) model. CFA reduced both YTHDF2 and its target binding site in TET1 mRNA (Pan et al., 2021b), and the increased expression of TET1 mRNA contributes to neuropathic pain. YTHDF2 reduces the demethylation of the brain-derived neurotrophic factor (BDNF) gene by repressing TET1 expression, and the inhibited expression subsequently reduces pain (Hsieh et al., 2016).

FTO regulates the expression of pain-associated genes

FTO in the injured DRG may contribute to neuropathic pain by stabilizing the differential expression of G9a, a histone methyltransferase encoded by EHMT2 mRNA that can remarkably inhibit transcription (Laumet et al., 2015). Transcription activator Runx1 was reported to increase the expression of FTO in the DRG in a model of SNL. After peripheral nerve injury, Runx1 may be responsible for the loss of the m6A site in the EHMT2 mRNA encoding G9a through binding to FTO gene promoter and increasing the FTO gene expression in the injured DRG. The upregulation of the G9a protein in the DRG induces and maintains neuropathic pain by reducing the amount of MOR in the injured DRG (Li Y. et al., 2020). A recent study revealed that the gene silencing of potassium channels and the downregulation of Kv1.2 promote peripheral nerve injury-induced neuropathic pain through selective knockdown of G9a in the DRG (Zheng et al., 2021). Nerve injury results in a loss of MOR expression in DRG and spinal cord neurons. Therefore, opioids exhibit a lower analgesic effect on neuropathic pain. Recently, it was found that FTO was correlated with MMP24 expression in spinal cord neurons. FTO binding to MMP24 mRNA following SNL diminishes the m6A enrichment in MMP24 mRNA, subsequently accelerates the translation of MMP24 to activate extracellular signal-regulated protein kinases(ERKs), and ultimately resulting in neuropathic pain (Ma et al., 2021; **Figure 2**).

n6-methyladenosine regulates neuropathic pain *via* glial cell activation

Glial cells mainly consist of oligodendrocytes, astrocytes and microglia. The activation mechanism of glial cells provides some insights into the mechanism of neuropathic pain (Navia-Pelaez et al., 2021). Microglia activation-induced neuroinflammation is a major component of neuropathic pain. The upregulation and activation of the P2 × 4 receptor and protein kinase p38 MAPKs in microglia can provoke neuropathic pain after peripheral nerve injury (Williams et al., 2019; Mai et al., 2020). This provides evidence that injured primary afferent neurons release neurotransmitters and activate microglia; for example, colony stimulating factor 1 (CSF1) from the injured DRG binds to the CSF1 receptor (CSF1R) on the microglia to activate and proliferate (Guan et al., 2016). Conditional deletion of cholesterol transporters ABCA1 and ABCG1 in microglia occurs in response to neuroinflammation and neuropathic pain (Navia-Pelaez et al., 2021). Overexpression of the m6A methyltransferase METTL3 increases the levels of the pro-inflammatory cytokines, and promotes the lipopolysaccharide (LPS) induced microglial inflammatory response by activating the TRAF6-NF-κB pathway (Wen et al., 2022). Conditional knockdown of YTHDC1 increases the markers and mediators of pro-inflammatory phenotype (M1) microglia by elevating the phosphorylation of STAT3 (Zhou et al., 2021). The rapid aggregation and activation of spinal glial cells that trigger neuroinflammation suggest that the bidirectional interactions of spinal glial cells affect the development of neuropathic pain (Yu et al., 2020).

There are differences in the role of astrocytes and microglia in neuropathic pain (Chen et al., 2018) as well as differences in their activation processes and duration. Microglia are activated immediately after the nervous system injured. Microglia activation precedes astrocyte activation, and astrocytes play a persistent role thereafter (Ji et al., 2013). Evidence suggests that astrocyte-mediated neuroinflammation shows efficacy in the maintenance of neuropathic pain. Astrocytes proliferate and show morphological and functional changes after nerve injury. Astrocytes present several changes such as activation, releasing inflammatory mediators and leading to neuroinflammation and neuropathic pain (Li Z. et al., 2019). The expression of METTL3 in astrocytes was increased in mouse SCI model (Xing et al., 2021). IL-33 levels in oligodendrocytes in the dorsal spinal cord were found to be elevated after SCI, and intrathecal injection of IL-33 enhanced pain hypersensitivity after painful injury through TNF-α and IL-1β (Zarpelon et al., 2016). The role of

oligodendrocytes in neuropathic pain regulation is mediated by interaction with microglia and astrocytes. Glial cells can also form a positive feedback loop through intercellular interaction to develop and maintain neuropathic pain. The mediators secreted by glial cells, such as cytokines and chemokines, lead to mechanical and thermal hyperalgesia. For instance, the chemokine CX3CL1 regulates neuropathic pain through neuron-microglia interactions, CCL2 and CXCL1 regulates neuropathic pain through astrocyte-neuron interactions in the spinal cord, and CXCL13 promotes neuropathic pain through neuron-astrocyte interactions (Zhang et al., 2017).

n6-methyladenosine regulates neuropathic pain *via* non-coding RNAs

m6A methylation not only regulates target mRNAs, but also ncRNAs to participate in diverse biological processes. The crosstalk of m6A and ncRNAs is pervasive and inspiring, extending the scope of epigenetics. m6A methylation has been shown to regulate miRNA maturation and further affect neuropathic pain in *in vitro* (Alarcón et al., 2015). METTL3 is sufficient to methylate massive pri-miRNAs to reinforce miRNA maturation. In spared nerve injury state, ablation of METTL3 was associated with m6A on primiR-150. The underlying mechanism involved cooperation of METTL3 with YTHDF2 accelerating miR-150 maturation. The maturation of primiR-150 was inhibited by DGCR8, and primiR-150 further impaired the target protein BDNF to promote neuropathic pain (Zhang et al., 2022). DGCR8 which is a microprocessor complex subunit initiates miRNA synthesis and maturation (Quick-Cleveland et al., 2014). Silencing of METTL3 can inhibit the maturation of miR-7212-5p (Mi et al., 2020). In the CFA-induced neuropathic pain condition, overexpression of METTL3 in the spinal cord, which increases the levels of m6A, influences nociceptive sensitization by primiR-365-3p, which is recognized by DGCR8 (Zhang C. et al., 2020). Additionally, METTL14-mediated m6A modification can regulate the maturation of primiR-126 (Ma et al., 2017).

n6-methyladenosine modulates the expression and stability of lncRNAs. METTL3-mediated m6A modification increased the expression level of lncRNA MALAT1. At the same time, METTL3/YTHDF3 complex increased the stability of lncRNA MALAT1 (Jin et al., 2019). MALAT1 can also disturb the development and occurrence of neuropathic pain through the miR-206/ZEB2 axis (Chen et al., 2019). YTHDC1 has been illustrated to preferentially bind m6A sites in diverse ncRNAs, such as XIST, NEAT1 and MALAT1, but its function has only been probed in the case of XIST (Patil et al., 2016). m6A-driven translation is highly abundant in circRNAs. Mechanistically, m6A initiates the protein synthesis of circRNA by recruiting YTHDF3 and initiation factors eIF4G2 (Yang et al., 2017). circ_0008542 can bind to miR-185-5p by its own m6A methylation modification mediated by ALKBH5 or METTL3 (Wang W. et al., 2021). miR-185-5p attenuates CCI-induced neuropathic pain and neuroinflammation by co-targeting MyD88 and CXCR4 (Huang et al., 2022). METTL3 was found to stabilize circux1 through m6A methylation modification. Circux1 sponges caspase1 mRNA and inhibits caspase1-mediated neuroinflammation and neuropathic pain (Wu et al., 2021; **Figure 3**).

Discussion

Neuropathic pain can adversely impair the quality of life of patients. Exploration of the complex pathogenetic mechanism of neuropathic pain is inherently challenging. The transcriptional and translational changes in DRG, spinal dorsal horn, and other pain-related areas (including cortex and dorsal hippocampus) after peripheral nerve injury are believed to be involved in the causation of neuropathic pain (Wang N. et al., 2021; Wei et al., 2021). An increasing number of studies have suggested that ncRNAs can affect neuropathic pain by regulating transcription factors after peripheral nerve injury. miRNAs regulate gene expression by directly binding to the 3'-UTR of the target mRNA, resulting in translational repression or degradation of the mRNA. miR-122-5p directly inhibits PDK4 expression suppressing the progression of neuropathic pain (Wan et al., 2021). In addition, miRNAs regulate transcription *via* regulating the binding of DNA and protein. Loss of miR-30a-3p was found to modify the level of BDNF and acetylated histone H3 and H4 in CCI rats. Moreover, miR-30a-3p was shown to target E-cadherin transcriptional activator (EP300), which modulated BDNF through enhancing acetylated histone H3 and H4 on the promoter (Tan et al., 2020). Histone methylation-mediated miR-32-5p down-regulation regulated trigeminal neuropathic pain by targeting Cav3.2 channels (Qi et al., 2022). LncRNAs, as regulators, modulate the interactions between transcription factors and target genes. Downregulation of DRG-specifically enriched lncRNA (DS-lncRNA) promotes Ehmt2 transcription in injured DRG and likely contributes to neuropathic pain. This indicated that DS-lncRNA downregulation increases the binding of RALY to RNA polymerase II and the Ehmt2 gene promoter (Pan et al., 2021a). Both lncRNAs and circRNAs can regulate glial activation and expression of the pro-inflammatory genes by sponging pain-related miRNAs. As a ceRNA, it induces glial cells to release inflammatory factors, to further regulate neuropathic pain. Besides as miRNA sponges, lncRNAs and circRNAs can interact with many different RNA-binding proteins (RBP) to play several roles in biological processes such as neuropathic pain (Zhang Z. et al., 2021).

In addition to DNA methylation and histone modification, studies have also highlighted the role of m6A methylation in neuropathic pain. m6A modification was shown to regulate the

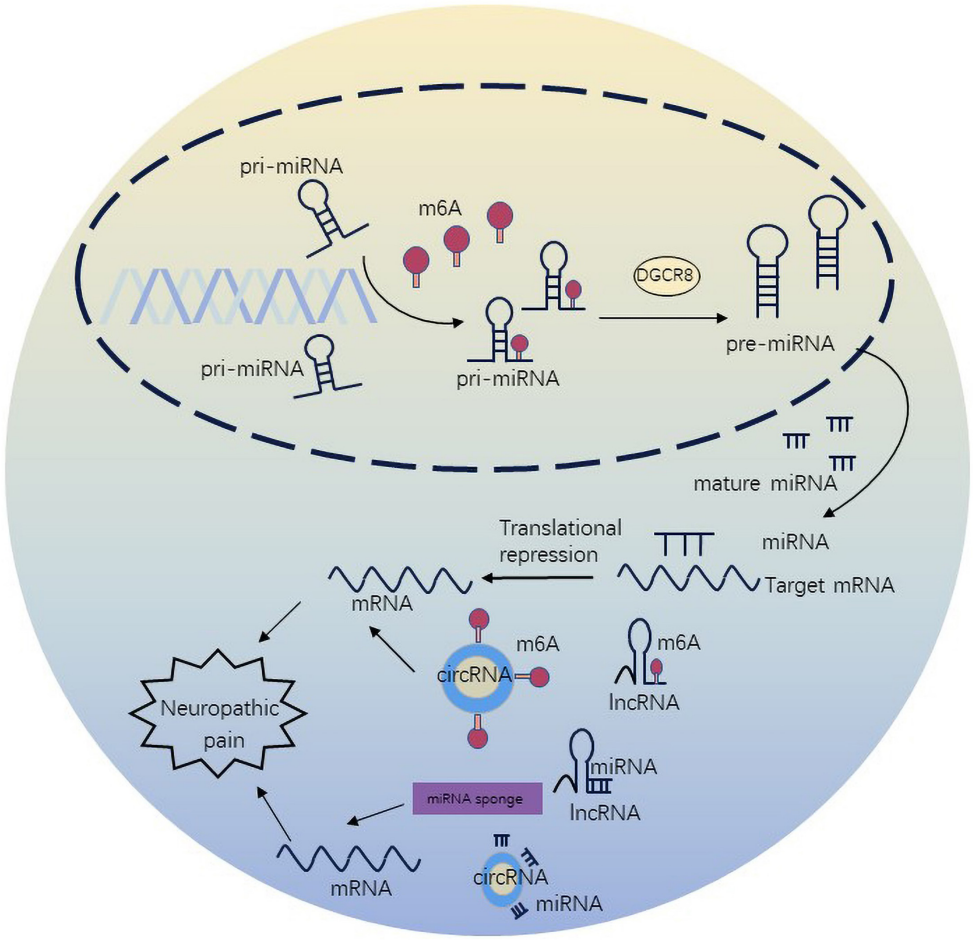

FIGURE 3
n6-methyladenosine methylation regulate non-coding RNAs to affect neuropathic pain.

activation of glial cells at the epigenetic level. KEGG analysis showed that the main pathways of mRNA methylation in the activated microglia were the pathways regulating the immune system processes (RAS, HIF-1, TNF, mTOR, Notch, ErbB, FoxO, JAK-STAT, and MAPK signals) and signal transduction pathways (chemokines, RAS, NOD/TLR, B cell/T cell receptors, IL-17) (Li Q. et al., 2021). These data can help inform further studies of the detailed mechanisms by which m6A methylation affects neuropathic pain through glial cell activation. The recognition of the role of m6A methylation modification has changed the traditional research ideas and has become one of the contemporary research hotspots.

There is a bidirectional network between m6A methylation and ncRNAs. m6A level affects the gene expression by affecting the m6A methylation of ncRNAs. For example, ablation of METTL3 was found to negatively affect the maturation of primiR-7212-5p, and then alter the expression of miR-7212-5p (Mi et al., 2020). METTL3-mediated m6A induces upregulation of lncRNA LINC00958 by binding to miR-3619-5p (Zuo et al., 2020). Moreover, ncRNAs can also regulate m6A methylation level. miRNA can regulate the binding of METTL3 to the target site of miRNA (Chen et al., 2015). We surprisingly found that overexpression of miR-124a and miR-155 results in neuropathic pain *via* repressing the expression of target gene SIRT1 to promote differentiation of T cells toward anti-inflammatory phenotype (Heyn et al., 2016). Conversely, YTHDC1 deficiency decreased the stability of SIRT1 mRNA, resulting in microglia polarization and inflammatory response (Zhou et al., 2021). ncRNAs and m6A methylation modification act on the same target gene, but cause different effects. The underlying mechanisms of this phenomenon also need further exploration.

Recent years have witnessed rapid advances in high-throughput RNA sequencing (RNA-seq) and bioinformatics algorithms. Recent studies have shown decreased expression of miR-183 in CCI rat models, which was involved in the progression of neuropathic pain. In addition, increased miR-183 expression was shown to negatively regulates its

downstream target MAP3K4, which leads to the downregulation of inflammatory cytokines correlated with neuropathic pain. This suggests that miR-183 is a potential biomarker and therapeutic target for neuropathic pain (Huang and Wang, 2020). Linc00311 and lncRNA-AK141205 were upregulated in bCCI rats. *In vitro* and *in vivo* experiments also indicated that they activated the STAT3 signaling in spinal microglia. Silencing of linc00311 and lncRNA-AK141205 may be a promising treatment for neuropathic pain (Pang et al., 2020). Significant downregulation of METTL3 and m6A methylation was found both in spared nerve injury-induced neuropathic pain rats and Shingles-induced neuropathic pain patients. Serum METTL3 could may serve as an unfavorable prognostic marker in patients with neuropathic pain. It may also be helpful for dynamic monitoring of diseases after treatment of neuropathic pain (Zhang et al., 2022). Detection of dysregulated m6A levels may provide a promising method for the diagnosis, prediction, and assessment of neuropathic pain in future. Overall, more in-depth understanding of ncRNAs and m6A modification biogenesis, and their effects might aid the potential application of diagnostic biomarkers.

Overcoming drug resistance through regulation of pain-related genes may provide an alternative strategy. Achieving *in vivo* delivery of ncRNAs, like other biomolecules, is a major challenge. Currently, the most direct way to inhibit miRNAs is to use antisense oligonucleotides, also named miRNA blockers, that are complementary to the mature miRNAs. However, the exogenous RNA fragment is unstable before entering the cell and is highly susceptible to degradation by nucleases. The use of viruses (e.g., retroviruses, lentiviruses, adenoviruses, adeno-associated viruses) as gene vectors is an efficient method for transfection, but also has many problems, such as oncogenicity, immunogenicity, poor cellular targeting, and localization, limited gene loading capacity, difficulty in vector preparation, and environmental risks. Nowadays, the most commonly researched non-viral vectors are polymers, lipids, peptides, inorganic particles, and hybrid systems (Zu and Gao, 2021). However, non-viral carriers have limitations with respect to the ability to penetrate nuclear membranes, transfection efficiency, and protein expression after transfection. Therefore, development of specific, stable, efficient and safe non-viral vectors is a key imperative. Recently, Pfizer-BioNTech used the BNT162b2 COVID-19 vaccine successfully using mRNA-based lipid nanoparticles which showed 95% effectiveness in preventing COVID-19 (Polack et al., 2020). With the development of material science, especially nanobiotechnology, the delivery of nanoparticles containing tissue-specific miRNA antagomir can target neuron-glial cell communication.

The epigenetic mechanism of ncRNAs and m6A modifications in neuropathic pain needs to be further investigated. This would help to achieve the goal of personalized medical treatment, and provide a theoretical basis for the optimization of clinical therapy and the exploration of new therapies.

Author contributions

KZ made the substantial contributions to the manuscript text. PL and YJ prepared the **Figures 1–3**. JJ and ML provided the editing and writing assistant. All authors reviewed the manuscript and approved the submitted version.

Funding

This work was supported by Natural Science Foundation of Liaoning Province (2022-YGJC-37) and 345 Talent Project of Shengjing Hospital.

Conflict of interest

The authors declare that the research was conducted in the absence of any commercial or financial relationships that could be construed as a potential conflict of interest.

The reviewer YS declared a shared parent affiliation with the authors to the handling editor at the time of review.

Publisher's note

References

Alarcón, C. R., Lee, H., Goodarzi, H., Halberg, N., and Tavazoie, S. F. (2015). N6-methyladenosine marks primary micrornas for processing. *Nature* 519, 482–485.

Albik, S., and Tao, Y. X. (2021). Emerging role of RNA m6A modification in chronic pain. *Pain* 162, 1897–1898. doi: 10.1097/j.pain.0000000000002219

Baron, R. (2009). Neuropathic pain: A clinical perspective. *Handb. Exp. Pharmacol.* 194, 3–30.

Bokar, J. A., Shambaugh, M. E., Polayes, D., Matera, A. G., and Rottman, F. M. (1997). Purification and cdna cloning of the AdoMet-binding subunit of the human mRNA (N6-adenosine)-methyltransferase. *RNA* 3, 1233–1247.

Bouhassira, D. (2019). Neuropathic pain: Definition, assessment and epidemiology. *Rev. Neurol. (Paris)* 175, 16–25.

Cai, W., Zhang, Y., and Su, Z. (2020). cirs-7 targeting miR-135a-5p promotes neuropathic pain in Cci rats via inflammation and autophagy. *Gene* 736:144386. doi: 10.1016/j.gene.2020.144386

Carlton, S. M., Du, J., Tan, H. Y., Nesic, O., Hargett, G. L., Bopp, A. C., et al. (2009). Peripheral and central sensitization in remote spinal cord regions contribute to central neuropathic pain after spinal cord injury. *Pain* 147, 265–276.

Chen, G., Luo, X., Qadri, M. Y., Berta, T., and Ji, R. R. (2018). Sex-dependent glial signaling in pathological pain: Distinct roles of spinal microglia and astrocytes. *Neurosci. Bull.* 34, 98–108. doi: 10.1007/s12264-017-0145-y

Chen, J. N., Zhang, Y. N., Tian, L. G., Zhang, Y., Li, X. Y., and Ning, B. (2022). Down-regulating circular RNA PRKCSH suppresses the inflammatory response after spinal cord injury. *Neural Regen. Res.* 17, 144–151. doi: 10.4103/1673-5374.314114

Chen, M., Yang, Y., Zhang, W., Li, X., Wu, J., Zou, X., et al. (2020). Long noncoding RNA Snhg5 knockdown alleviates neuropathic pain by targeting the miR-154-5p/Cxcl13 axis. *Neurochem. Res.* 45, 1566–1575. doi: 10.1007/s11064-020-03021-2

Chen, X. J., Wang, L., and Song, X. Y. (2020). Mitoquinone alleviates vincristine-induced neuropathic pain through inhibiting oxidative stress and apoptosis via the improvement of mitochondrial dysfunction. *Biomed Pharmacother.* 125:110003. doi: 10.1016/j.biopha.2020.110003

Chen, T., Hao, Y. J., Zhang, Y., Li, M. M., Wang, M., Han, W., et al. (2015). m(6)A RNA methylation is regulated by micrornas and promotes reprogramming to pluripotency. *Cell Stem Cell* 16, 289–301. doi: 10.1016/j.stem.2015.01.016

Chen, Z. L., Liu, J. Y., Wang, F., and Jing, X. (2019). Suppression of Malat1 ameliorates chronic constriction injury-induced neuropathic pain in rats via modulating miR-206 and Zeb2. *J. Cell. Physiol.* 234, 15647–15653. doi: 10.1002/jcp.28213

Donnelly, C. R., Andriessen, A. S., Chen, G., Wang, K., Jiang, C., Maixner, W., et al. (2020). Central nervous system targets: Glial cell mechanisms in chronic pain. *Neurotherapeutics* 17, 846–860.

Guan, Z., Kuhn, J. A., Wang, X., Colquitt, B., Solorzano, C., Vaman, S., et al. (2016). Injured sensory neuron-derived CSF1 induces microglial proliferation and DAP12-dependent pain. *Nat. Neurosci.* 19, 94–101. doi: 10.1038/nn.4189

Heyn, J., Luchting, B., Hinske, L. C., Hübner, M., Azad, S. C., and Kreth, S. (2016). miR-124a and miR-155 enhance differentiation of regulatory T cells in patients with neuropathic pain. *J. Neuroinflammation* 13:248.

Hsieh, M. C., Lai, C. Y., Ho, Y. C., Wang, H. H., Cheng, J. K., Chau, Y. P., et al. (2016). Tet1-dependent epigenetic modification of BDNF expression in dorsal horn neurons mediates neuropathic pain in rats. *Sci. Rep.* 6:37411. doi: 10.1038/srep37411

Huang, A., Ji, L., Huang, Y., Yu, Q., and Li, Y. (2022). miR-185-5p alleviates CCI-induced neuropathic pain by repressing NLRP3 inflammasome through dual targeting MyD88 and CXCR4. *Int. Immunopharmacol.* 104:108508. doi: 10.1016/j.intimp.2021.108508

Huang, L., and Wang, L. (2020). Upregulation of miR-183 represses neuropathic pain through inhibiton of MAP3K4 in CCI rat models. *J. Cell. Physiol.* 235, 3815–3822. doi: 10.1002/jcp.29276

Ji, R. R., Berta, T., and Nedergaard, M. (2013). Glia and pain: Is chronic pain a gliopathy? *Pain* 154(Suppl. 1), S10–S28.

Jia, G., Fu, Y., Zhao, X., Dai, Q., Zheng, G., Yang, Y., et al. (2011). N6-methyladenosine in nuclear RNA is a major substrate of the obesity-associated Fto. *Nat. Chem. Biol.* 7, 885–887. doi: 10.1038/nchembio.687

Jia, Y., Zhang, M., Li, P., Tang, W., Liu, Y., Hu, Y., et al. (2020). Bioinformatics analysis of long non-coding RNAs involved in nerve regeneration following sciatic nerve injury. *Mol. Pain* 16:1744806920971918.

Jiang, D., Gong, F., Ge, X., Lv, C., Huang, C., Feng, S., et al. (2020). Neuron-derived exosomes-transmitted miR-124-3p protect traumatically injured spinal cord by suppressing the activation of neurotoxic microglia and astrocytes. *J. Nanobiotechnol.* 18:105. doi: 10.1186/s12951-020-00665-8

Jiang, F., Liu, X., Cui, X., Hu, J., Wang, L., Xue, F., et al. (2022). Circ_0000518 promotes macrophage/microglia M1 polarization via the Fus/Camkkβ/AMPK pathway to aggravate multiple sclerosis. *Neuroscience* 490, 131–143. doi: 10.1016/j.neuroscience.2021.12.012

Jiang, M., Zhang, X., Wang, X., Xu, F., Zhang, J., Li, L., et al. (2021). MicroRNA-124-3p attenuates the development of nerve injury-induced neuropathic pain by targeting early growth response 1 in the dorsal root ganglia and spinal dorsal horn. *J. Neurochem.* 158, 928–942. doi: 10.1111/jnc.15433

Jin, D., Guo, J., Wu, Y., Du, J., Yang, L., Wang, X., et al. (2019). m(6)A mRNA methylation initiated by Mettl3 directly promotes yap translation and increases yap activity by regulating the Malat1-miR-1914-3p-Yap axis to induce Nsclc drug resistance and metastasis. *J. Hematol. Oncol.* 12:135.

Jin, H., Du, X. J., Zhao, Y., and Xia, D. L. (2018). Xist/miR-544 axis induces neuropathic pain by activating Stat3 in a rat model. *J. Cell. Physiol.* 233, 5847–5855. doi: 10.1002/jcp.26376

Laumet, G., Garriga, J., Chen, S. R., Zhang, Y., Li, D. P., Smith, T. M., et al. (2015). G9a is essential for epigenetic silencing of K(+) channel genes in acute-to-chronic pain transition. *Nat. Neurosci.* 18, 1746–1755. doi: 10.1038/nn.4165

Lee, Y., Ahn, C., Han, J., Choi, H., Kim, J., Yim, J., et al. (2003). The nuclear RNAse Iii Drosha initiates microRNA processing. *Nature* 425, 415–419.

Li, B., Dasgupta, C., Huang, L., Meng, X., and Zhang, L. (2020). MiRNA-210 induces microglial activation and regulates microglia-mediated neuroinflammation in neonatal hypoxic-ischemic encephalopathy. *Cell. Mol. Immunol.* 17, 976–991. doi: 10.1038/s41423-019-0257-6

Li, Y., Guo, X., Sun, L., Xiao, J., Su, S., Du, S., et al. (2020). N(6)-methyladenosine demethylase Fto contributes to neuropathic pain by stabilizing G9a expression in primary sensory neurons. *Adv. Sci. (Weinh)* 7:1902402. doi: 10.1002/advs.201902402

Li, M., Hu, J., Peng, Y., Li, J., and Ren, R. (2021). Circptk2-miR-181c-5p-Hmgb1: A new regulatory pathway for microglia activation and hippocampal neuronal apoptosis induced by sepsis. *Mol. Med.* 27:45. doi: 10.1186/s10020-021-00305-3

Li, Q., Wen, S., Ye, W., Zhao, S., and Liu, X. (2021). The potential roles of m(6)A modification in regulating the inflammatory response in microglia. *J. Neuroinflamm.* 18:149. doi: 10.1186/s12974-021-02205-z

Li, Z., Li, X., Chen, X., Li, S., Ho, I. H. T., Liu, X., et al. (2019). Emerging roles of long non-coding RNAs in neuropathic pain. *Cell Prolif.* 52:e12528.

Li, T., Chen, X., Zhang, C., Zhang, Y., and Yao, W. (2019). An update on reactive astrocytes in chronic pain. *J. Neuroinflamm.* 16:140. doi: 10.1186/s12974-019-1524-2

Liu, L. P., Zhang, J., Pu, B., Li, W. Q., and Wang, Y. S. (2020). Upregulation of Jhdm1D-As1 alleviates neuroinflammation and neuronal injury via targeting miR-101-3p-Dusp1 in spinal cord after brachial plexus injury. *Int. Immunopharmacol.* 89;106962. doi: 10.1016/j.intimp.2020.106962

Liu, M., Li, P., Jia, Y., Cui, Q., Zhang, K., and Jiang, J. (2022). Role of non-coding RNAs in axon regeneration after peripheral nerve injury. *Int. J. Biol. Sci.* 18, 3435–3446.

Ma, J. Z., Yang, F., Zhou, C. C., Liu, F., Yuan, J. H., Wang, F., et al. (2017). METTL14 suppresses the metastatic potential of hepatocellular carcinoma by modulating N(6) -methyladenosine-dependent primary MicroRNA processing. *Hepatology* 65, 529–543. doi: 10.1002/hep.28885

Ma, L., Huang, Y., Zhang, F., Gao, D. S., Sun, N., Ren, J., et al. (2021). MMP24 contributes to neuropathic pain in an FTO-dependent manner in the spinal cord neurons. *Front. Pharmacol.* 12:673831. doi: 10.3389/fphar.2021.673831

Mai, L., Zhu, X., Huang, F., He, H., and Fan, W. (2020). p38 mitogen-activated protein kinase and pain. *Life Sci.* 256:117885.

Mauer, J., Luo, X., Blanjoie, A., Jiao, X., Grozhik, A. V., Patil, D. P., et al. (2017). Reversible methylation of m(6)A(m) in the 5' cap controls mRNA stability. *Nature* 541, 371–375. doi: 10.1038/nature21022

Meyer, K. D., Saletore, Y., Zumbo, P., Elemento, O., Mason, C. E., and Jaffrey, S. R. (2012). Comprehensive analysis of mRNA methylation reveals enrichment in 3'. Utrs and near stop codons. *Cell* 149, 1635–1646. doi: 10.1016/j.cell.2012.05.003

Mi, B., Xiong, Y., Yan, C., Chen, L., Xue, H., Panayi, A. C., et al. (2020). Methyltransferase-like 3-mediated N6-methyladenosine modification of miR-7212-5p drives osteoblast differentiation and fracture healing. *J. Cell. Mol. Med.* 24, 6385–6396. doi: 10.1111/jcmm.15284

Mo, Y., Liu, B., Qiu, S., Wang, X., Zhong, L., Han, X., et al. (2020). Down-regulation of microRNA-34c-5p alleviates neuropathic pain via the Sirt1/Stat3 signaling pathway in rat models of chronic constriction injury of sciatic nerve. *J. Neurochem.* 154, 301–315. doi: 10.1111/jnc.14998

Navia-Pelaez, J. M., Choi, S. H., Dos Santos Aggum Capettini, L., Xia, Y., Gonen, A., Agatisa-Boyle, C., et al. (2021). Normalization of cholesterol metabolism in spinal microglia alleviates neuropathic pain. *J. Exp. Med.* 218:e20202059. doi: 10.1084/jem.20202059

Pan, Z., Zhang, Q., Liu, X., Zhou, H., Jin, T., Hao, L. Y., et al. (2021b). Methyltransferase-like 3 contributes to inflammatory pain by targeting

Tet1 in Ythdf2-dependent manner. *Pain* 162, 1960–1976. doi: 10.1097/j.pain.0000000000002218

Pan, Z., Du, S., Wang, K., Guo, X., Mao, Q., Feng, X., et al. (2021a). Downregulation of a dorsal root ganglion-specifically enriched long noncoding RNA is required for neuropathic pain by negatively regulating raly-triggered EHMT2 expression. *Adv. Sci.* 8:e2004515. doi: 10.1002/advs.202004515

Pan, Z., Shan, Q., Gu, P., Wang, X. M., Tai, L. W., Sun, M., et al. (2018). miRNA-23a/Cxcr4 regulates neuropathic pain via directly targeting Txnip/Nlrp3 inflammasome axis. *J. Neuroinflamm.* 15:29. doi: 10.1186/s12974-018-1073-0

Pang, H., Ren, Y., Li, H., Chen, C., and Zheng, X. (2020). LncRNAs linc00311 and Ak141205 are identified as new regulators in Stat3-mediated neuropathic pain in bcci rats. *Eur. J. Pharmacol.* 868:172880. doi: 10.1016/j.ejphar.2019.172880

Patil, D. P., Chen, C. K., Pickering, B. F., Chow, A., Jackson, C., Guttman, M., et al. (2016). m(6)A RNA methylation promotes Xist-mediated transcriptional repression. *Nature* 537, 369–373. doi: 10.1038/nature19342

Polack, F. P., Thomas, S. J., Kitchin, N., Absalon, J., Gurtman, A., Lockhart, S., et al. (2020). Safety and efficacy of the Bnt162b2 mRNA Covid-19 vaccine. *N. Engl. J. Med.* 383, 2603–2615.

Qi, P., and Du, X. (2013). The long non-coding RNAs, a new cancer diagnostic and therapeutic gold mine. *Mod. Pathol.* 26, 155–165. doi: 10.1038/modpathol.2012.160

Qi, R., Cao, J., Sun, Y., Li, Y., Huang, Z., Jiang, D., et al. (2022). Histone methylation-mediated microRNA-32-5p down-regulation in sensory neurons regulates pain behaviors via targeting Cav3.2 channels. *Proc. Natl. Acad. Sci. U.S.A.* 119:e2117209119. doi: 10.1073/pnas.2117209119

Qiu, S., Feng, Y., Lesage, G., Zhang, Y., Stuart, C., He, L., et al. (2015). Chronic morphine-induced microRNA-124 promotes microglial immunosuppression by modulating P65 and Traf6. *J. Immunol.* 194, 1021–1030. doi: 10.4049/jimmunol.1400106

Quick-Cleveland, J., Jacob, J. P., Weitz, S. H., Shoffner, G., Senturia, R., and Guo, F. (2014). The DGCR8 RNA-binding heme domain recognizes primary micrornas by clamping the hairpin. *Cell Rep.* 7, 1994–2005. doi: 10.1016/j.celrep.2014.05.013

Salmena, L., Poliseno, L., Tay, Y., Kats, L., and Pandolfi, P. P. (2011). A ceRNA hypothesis: The rosetta stone of a hidden RNA language? *Cell* 146, 353–358.

Scholz, J., Finnerup, N. B., Attal, N., Aziz, Q., Baron, R., Bennett, M. I., et al. (2019). The IASP classification of chronic pain for ICD-11: Chronic neuropathic pain. *Pain* 160, 53–59.

Sommer, C., Leinders, M., and Üçeyler, N. (2018). Inflammation in the pathophysiology of neuropathic pain. *Pain* 159, 595–602.

Tan, M., Shen, L., and Hou, Y. (2020). Epigenetic modification of BDNF mediates neuropathic pain via miR-30a-3p/Ep300 axis in CCI rats. *Biosci. Rep.* 40:BSR20194442. doi: 10.1042/BSR20194442

Tan, Y., Yang, J., Xiang, K., Tan, Q., and Guo, Q. (2015). Suppression of microRNA-155 attenuates neuropathic pain by regulating SOCS1 signalling pathway. *Neurochem. Res.* 40, 550–560. doi: 10.1007/s11064-014-1500-2

Tramullas, M., FrancéS, R., De La Fuente, R., Velategui, S., CarceléN, M., GarcíA, R., et al. (2018). MicroRNA-30c-5p modulates neuropathic pain in rodents. *Sci. Transl. Med.* 10:eaao6299. doi: 10.1126/scitranslmed.aao6299

Wan, L., Su, Z., Li, F., Gao, P., and Zhang, X. (2021). MiR-122-5p suppresses neuropathic pain development by targeting Pdk4. *Neurochem. Res.* 46, 957–963. doi: 10.1007/s11064-020-03213-w

Wang, Z., Liu, F., Wei, M., Qiu, Y., Ma, C., Shen, L., et al. (2018). Chronic constriction injury-induced microRNA-146a-5p alleviates neuropathic pain through suppression of IRAK1/TRAF6 signaling pathway. *J. Neuroinflamm.* 15:179. doi: 10.1186/s12974-018-1215-4

Wang, C. X., Cui, G. S., Liu, X., Xu, K., Wang, M., Zhang, X. X., et al. (2018). METTL3-mediated m6A modification is required for cerebellar development. *PLoS Biol.* 16:e2004880. doi: 10.1371/jouRNAl.pbio.2004880

Wang, W., Qiao, S. C., Wu, X. B., Sun, B., Yang, J. G., Li, X., et al. (2021). Circ_0008542 in osteoblast exosomes promotes osteoclast-induced bone resorption through m6A methylation. *Cell Death Dis.* 12:628. doi: 10.1038/s41419-021-03915-1

Wang, N., Zhang, Y. H., Wang, J. Y., and Luo, F. (2021). current understanding of the involvement of the insular cortex in neuropathic pain: A narrative review. *Int. J. Mol. Sci.* 22:2648. doi: 10.3390/ijms22052648

Wei, M., Li, L., Zhang, Y., Zhang, M., and Su, Z. (2020). Downregulated circular RNA zRANB1 mediates Wnt5a/β-Catenin signaling to promote neuropathic pain via miR-24-3p/LPAR3 axis in CCI rat models. *Gene* 761:145038. doi: 10.1016/j.gene.2020.145038

Wei, X., Centeno, M. V., Ren, W., Borruto, A. M., Procissi, D., Xu, T., et al. (2021). Activation of the dorsal, but not the ventral, hippocampus relieves neuropathic pain in rodents. *Pain* 162, 2865–2880.

Wen, L., Sun, W., Xia, D., Wang, Y., Li, J., and Yang, S. (2022). The m6A methyltransferase METTL3 promotes LPS-induced microglia inflammation through TRAF6/Nf-κB pathway. *Neuroreport* 33, 243–251. doi: 10.1097/WNR.0000000000001550

Wen, Y., Fan, X., Bu, H., Ma, L., Kong, C., Huang, C., et al. (2021). Downregulation of lncRNA FIRRE relieved the neuropathic pain of female mice by suppressing HMGB1 expression. *Mol. Cell. Biochem.* 476, 841–852. doi: 10.1007/s11010-020-03949-7

Willemen, H. L., Huo, X. J., Mao-Ying, Q. L., Zijlstra, J., Heijnen, C. J., and Kavelaars, A. (2012). MicroRNA-124 as a novel treatment for persistent hyperalgesia. *J. Neuroinflamm.* 9:143. doi: 10.1186/1742-2094-9-143

Williams, W. A., Linley, J. E., Jones, C. A., Shibata, Y., Snijder, A., Button, J., et al. (2019). Antibodies binding the head domain of P2X4 inhibit channel function and reverse neuropathic pain. *Pain* 160, 1989–2003. doi: 10.1097/j.pain.0000000000001587

Wu, P., Fang, X., Liu, Y., Tang, Y., Wang, W., Li, X., et al. (2021). N6-methyladenosine modification of circCUX1 confers radioresistance of hypopharyngeal squamous cell carcinoma through caspase1 pathway. *Cell Death Dis.* 12:298. doi: 10.1038/s41419-021-03558-2

Wu, Q., Wei, G., Ji, F., Jia, S., Wu, S., Guo, X., et al. (2019). TET1 overexpression mitigates neuropathic pain through rescuing the expression of μ-opioid receptor and Kv1.2 in the primary sensory neurons. *Neurotherapeutics* 16, 491–504. doi: 10.1007/s13311-018-00689-x

Xia, L. X., Ke, C., and Lu, J. M. (2018). NEAT1 contributes to neuropathic pain development through targeting miR-381/HMGB1 axis in CCI rat models. *J. Cell. Physiol.* 233, 7103–7111. doi: 10.1002/jcp.26526

Xing, L., Cai, Y., Yang, T., Yu, W., Gao, M., Chai, R., et al. (2021). Epitranscriptomic m6A regulation following spinal cord injury. *J. Neurosci. Res.* 99, 843–857. doi: 10.1002/jnr.24763

Xu, L., Wang, Q., Jiang, W., Yu, S., and Zhang, S. (2019). MiR-34c ameliorates neuropathic pain by targeting NLRP3 in a mouse model of chronic constriction injury. *Neuroscience* 399, 125–134. doi: 10.1016/j.neuroscience.2018.12.030

Yan, X. T., Lu, J. M., Wang, Y., Cheng, X. L., He, X. H., Zheng, W. Z., et al. (2018). XIST accelerates neuropathic pain progression through regulation of miR-150 and ZEB1 in CCI rat models. *J. Cell. Physiol.* 233, 6098–6106. doi: 10.1002/jcp.26453

Yang, Y., Fan, X., Mao, M., Song, X., Wu, P., Zhang, Y., et al. (2017). Extensive translation of circular RNAs driven by N(6)-methyladenosine. *Cell Res.* 27, 626–641. doi: 10.1038/cr.2017.31

Yu, X., Liu, H., Hamel, K. A., Morvan, M. G., Yu, S., Leff, J., et al. (2020). Dorsal root ganglion macrophages contribute to both the initiation and persistence of neuropathic pain. *Nat. Commun.* 11:264.

Zaccara, S., Ries, R. J., and Jaffrey, S. R. (2019). Reading, writing and erasing mRNA methylation. *Nat. Rev. Mol. Cell Biol.* 20, 608–624.

Zarpelon, A. C., Rodrigues, F. C., Lopes, A. H., Souza, G. R., Carvalho, T. T., Pinto, L. G., et al. (2016). Spinal cord oligodendrocyte-derived alarmin Il-33 mediates neuropathic pain. *FASEB J.* 30, 54–65. doi: 10.1096/fj.14-267146

Zhan, L. Y., Lei, S. Q., Zhang, B. H., Li, W. L., Wang, H. X., Zhao, B., et al. (2018). Overexpression of miR-381 relieves neuropathic pain development via targeting HMGB1 and CXCR4. *Biomed. Pharmacother.* 107, 818–823. doi: 10.1016/j.biopha.2018.08.053

Zhang, J. Y., Lv, D. B., Su, Y. N., Wang, X. L., Sheng, W. C., Yang, G., et al. (2020). LncRNA SNHG1 attenuates neuropathic pain following spinal cord injury by regulating CDK4 level. *Eur. Rev. Med. Pharmacol. Sci.* 24, 12034–12040. doi: 10.26355/eurrev_202012_23992

Zhang, C., Wang, Y., Peng, Y., Xu, H., and Zhou, X. (2020). Mettl3 regulates inflammatory pain by modulating m(6)A-dependent pri-miR-365-3p processing. *FASEB J.* 34, 122–132. doi: 10.1096/fj.201901555R

Zhang, S. B., Lin, S. Y., Liu, M., Liu, C. C., Ding, H. H., Sun, Y., et al. (2019). CircAnks1a in the spinal cord regulates hypersensitivity in a rodent model of neuropathic pain. *Nat. Commun.* 10:4119. doi: 10.1038/s41467-019-12049-0

Zhang, D., Mou, J. Y., Wang, F., Liu, J., and Hu, X. (2019). CRNDE enhances neuropathic pain via modulating miR-136/Il6R axis in CCI rat models. *J. Cell. Physiol.* 234, 22234–22241. doi: 10.1002/jcp.28790

Zhang, L., Hao, D., Ma, P., Ma, B., Qin, J., Tian, G., et al. (2021). Epitranscriptomic analysis of m6A methylome after peripheral nerve injury. *Front. Genet.* 12:686000. doi: 10.3389/fgene.2021.686000

Zhang, Y., Gao, T., Li, X., Wen, C. C., Yan, X. T., Peng, C., et al. (2021). Circ_0005075 targeting miR-151a-3p promotes neuropathic pain in CCI rats via inducing NOTCH2 expression. *Gene* 767:145079. doi: 10.1016/j.gene.2020.145079

Zhang, Z., Sun, X., Zhao, G., Ma, Y., and Zeng, G. (2021). LncRNA embryonic stem cells expressed 1 (Lncenc1) is identified as a novel regulator in neuropathic

pain by interacting with EZH2 and downregulating the expression of Bai1 in mouse microglia. *Exp. Cell Res.* 399:112435. doi: 10.1016/j.yexcr.2020.112435

Zhang, P., Sun, H., and Ji, Z. (2021). Downregulating lncRNA PVT1 relieves astrocyte overactivation induced neuropathic pain through targeting miR-186-5p/CXCL13/CXCR5 Axis. *Neurochem. Res.* 46, 1457–1469. doi: 10.1007/s11064-021-03287-0

Zhang, L., Zhao, X., Wang, J., Jin, Y., Gong, M., Ye, Y., et al. (2022). Mettl3 suppresses neuropathic pain via modulating N6-methyladenosine-dependent primary miR-150 processing. *Cell Death Discov.* 8:80. doi: 10.1038/s41420-022-00880-2

Zhang, Y., Su, Z., Liu, H. L., Li, L., Wei, M., Ge, D. J., et al. (2018). Effects of miR-26a-5p on neuropathic pain development by targeting MAPK6 in in CCI rat models. *Biomed. Pharmacother.* 107, 644–649. doi: 10.1016/j.biopha.2018.08.005

Zhang, Z. J., Jiang, B. C., and Gao, Y. J. (2017). Chemokines in neuron-glial cell interaction and pathogenesis of neuropathic pain. *Cell. Mol. Life Sci.* 74, 3275–3291. doi: 10.1007/s00018-017-2513-1

Zhao, W., Qi, X., Liu, L., Ma, S., Liu, J., and Wu, J. (2020). Epigenetic regulation of m(6)A modifications in human cancer. *Mol. Ther. Nucleic Acids* 19, 405–412.

Zhao, X., Tang, Z., Zhang, H., Atianjoh, F. E., Zhao, J. Y., Liang, L., et al. (2013). A long noncoding RNA contributes to neuropathic pain by silencing Kcna2 in primary afferent neurons. *Nat. Neurosci.* 16, 1024–1031. doi: 10.1038/nn.3438

Zhao, Y., Chen, Y., Jin, M., and Wang, J. (2021). The crosstalk between m(6)A RNA methylation and other epigenetic regulators: A novel perspective in epigenetic remodeling. *Theranostics* 11, 4549–4566. doi: 10.7150/thno.54967

Zhao, Y., Li, S., Xia, N., Shi, Y., and Zhao, C. M. (2018). Effects of XIST/miR-137 axis on neuropathic pain by targeting TNFAIP1 in a rat model. *J. Cell. Physiol.* 233, 4307–4316. doi: 10.1002/jcp.26254

Zheng, B. X., Guo, X., Albik, S., Eloy, J., and Tao, Y. X. (2021). Effect of pharmacological inhibition of fat-mass and obesity-associated protein on nerve trauma-induced pain hypersensitivities. *Neurotherapeutics* 18, 1995–2007. doi: 10.1007/s13311-021-01053-2

Zhong, X., Bao, Y., Wu, Q., Xi, X., Zhu, W., Chen, S., et al. (2021). Long noncoding RNA Xist knockdown relieves the injury of microglia cells after spinal cord injury by sponging miR-219-5p. *Open Med. (Wars)* 16, 1090–1100. doi: 10.1515/med-2021-0292

Zhou, D., Zhang, S., Hu, L., Gu, Y. F., Cai, Y., Wu, D., et al. (2019). Inhibition of apoptosis signal-regulating kinase by paeoniflorin attenuates neuroinflammation and ameliorates neuropathic pain. *J. Neuroinflamm.* 16:83. doi: 10.1186/s12974-019-1476-6

Zhou, H., Xu, Z., Liao, X., Tang, S., Li, N., and Hou, S. (2021). Low expression of YTH domain-containing 1 promotes microglial M1 polarization by reducing the stability of sirtuin 1 mRNA. *Front. Cell. Neurosci.* 15:774305. doi: 10.3389/fncel.2021.774305

Zu, H., and Gao, D. (2021). Non-viral vectors in gene therapy: Recent development. challenges, and prospects. *AAPS J.* 23:78.

Zuo, X., Chen, Z., Gao, W., Zhang, Y., Wang, J., Wang, J., et al. (2020). M6A-mediated upregulation of Linc00958 increases lipogenesis and acts as a nanotherapeutic target in hepatocellular carcinoma. *J. Hematol. Oncol.* 13:5. doi: 10.1186/s13045-019-0839-x

frontiers | Frontiers in Molecular Neuroscience

TYPE Original Research
PUBLISHED 16 November 2022
DOI 10.3389/fnmol.2022.1014751

OPEN ACCESS

EDITED BY
Verena Kohler,
University of Graz, Austria

REVIEWED BY
Gizem Donmez,
Adnan Menderes University, Turkey
Simona Ceccarelli,
Sapienza University of Rome, Italy

*CORRESPONDENCE
Creed Stary
cstary@stanford.edu

SPECIALTY SECTION
This article was submitted to Neuroplasticity and Development, a section of the journal Frontiers in Molecular Neuroscience

RECEIVED 08 August 2022
ACCEPTED 25 October 2022
PUBLISHED 16 November 2022

CITATION
Griffiths B, Xu L, Sun X, Greer M, Murray I and Stary C (2022) Inhibition of microRNA-200c preserves astrocyte sirtuin-1 and mitofusin-2, and protects against hippocampal neurodegeneration following global cerebral ischemia in mice. *Front. Mol. Neurosci.* 15:1014751. doi: 10.3389/fnmol.2022.1014751

Inhibition of microRNA-200c preserves astrocyte sirtuin-1 and mitofusin-2, and protects against hippocampal neurodegeneration following global cerebral ischemia in mice

Brian Griffiths[1], Lijun Xu[1], Xiaoyun Sun[1], Majesty Greer[2], Isabella Murray[1] and Creed Stary[1]*

[1]Department of Anesthesiology, Perioperative and Pain Medicine, Stanford University School of Medicine, Stanford, CA, United States, [2]Howard University College of Medicine, Washington, DC, United States

Memory impairment remains a leading disability in survivors of global cerebral ischemia, occurring secondary to delayed neurodegeneration of hippocampal cornu ammonis-1 (CA1) neurons. MicroRNA-200c (miR-200c) is induced following ischemic stress and we have previously demonstrated that pre-treatment with anti-miR-200c is protective against embolic stroke in mice. In the present study we assessed the role of miR-200c on CA1 neurodegeneration, sirtuin-1 (SIRT1), and mitochondrial dynamic protein expression in a mouse model of transient global cerebral ischemia and *in vitro* in primary mouse astrocyte cultures after simulated ischemia. Mice were subjected to 10 min bilateral common carotid artery occlusion plus hypotension with 5% isoflurane. After 2 h recovery mice were treated with intravenous injection of either anti-miR-200c or mismatch control. Memory function was assessed by Barnes maze at post-injury days 3 and 7. Mice were sacrificed at post-injury day 7 for assessment of brain cell-type specific expression of miR-200c, SIRT1, and the mitochondrial fusion proteins mitofusin-2 (MFN2) and OPA1 *via* complexed fluorescent *in situ* hybridization and fluorescent immunohistochemistry. Global cerebral ischemia induced significant loss of CA1 neurons, impaired memory performance and decreased expression of CA1 SIRT1, MFN2, and OPA1. Post-injury treatment with anti-miR-200c significantly improved survival, prevented CA1 neuronal loss, improved post-injury performance in Barnes maze, and was associated with increased post-injury expression of CA1 SIRT1 and MFN2 in astrocytes. *In vitro*, primary mouse astrocyte cultures pre-treated with miR-200c inhibitor prior to oxygen/glucose deprivation preserved expression of SIRT1 and MFN2, and decreased reactive oxygen species generation, whereas pre-treatment with miR-200c mimic had opposite effects that could be reversed by co-treatment

with SIRT1 activator. These results suggest that miR-200c regulates astrocyte mitochondrial homeostasis *via* targeting SIRT1, and that CA1 astrocyte mitochondria and SIRT1 represent potential post-injury therapeutic targets to preserve cognitive function in survivors of global cerebral ischemia.

KEYWORDS

glia, stroke, mitochondrial dynamics, SIRT1, MFN2

Introduction

The hippocampal cornu ammonis-1 (CA1) subregion is central to learning and memory but is selectively vulnerable to ischemic injury. The clinical impact of select CA1 vulnerability to even transient decreases in cerebral blood flow is most commonly represented in survivors of cardiac arrest: while resuscitation rates approach 30% for the over 500,000 cases of adult cardiac arrest in the US per year, over 90% of survivors suffer cognitive impairment (Benjamin et al., 2019) secondary to delayed neuronal loss in CA1. Despite promising pre-clinical trials focused on the delayed nature of CA1 death, no post-injury pharmaceutical interventions are available, and the only effective intervention to prevent CA1 neuronal loss remains application of whole-body hypothermia. To date, the molecular and cellular mechanisms regulating delayed CA1 neuronal loss remain a knowledge gap. We and others have provided increasing evidence supporting a role for microRNAs (miRs) in the brain's acute and extended response to cerebral ischemia (Ouyang et al., 2013a; Stary and Giffard, 2015; Li and Stary, 2016). MiRs are a well-characterized class of noncoding RNAs that regulate the translation of transcribed genes that can act in a regional and cell-type specific manner.

Astrocytes are the most numerous cell type in the mammalian brain, and support neurons during development, under normal physiologic conditions and after injury (Verkhratsky and Nedergaard, 2018). Astrocytes regulate synaptic glutamate levels, secrete neurotrophic factors, maintain ionic balance, and stabilize neuronal energy balance, all underscored by properly functioning astrocytic mitochondria (Pfrieger, 2009; Heneka et al., 2010). Neurons sustain a high rate of oxidative metabolism while astrocytes preferentially utilize glycolytic pathways, although both cell types contain equivalent numbers of mitochondria (Belanger et al., 2011). Astrocytes also serve to mitigate the downstream effects of pro-inflammatory cytokines on generation of reactive oxygen species (ROS) and secrete soluble factors to indirectly modulate resident neuronal mitochondrial function. Mitochondria are central to normal physiologic brain function and in repair of the injured brain by maintaining phosphorylation potential (ATP) to support energy requirements for a host of biological processes. Mitochondria are well-known targets of ischemic injury and prior work using has demonstrated efficacy in neuroprotection against stroke when astrocyte mitochondria are protected (Xu et al., 2010). A detailed determination of the mechanisms that regulate cell-type specific mitochondrial dysfunction in neurons and astrocytes has been a central barrier impeding novel stroke therapies. Mitochondrial homeostasis is maintained by an interdependent balance between mitochondrial dynamics (fission and fusion), ROS and metabolic energy state (Dorn and Kitsis, 2015; Zhou et al., 2021). Mitochondria maintain a steady state of continuous fusion/fission maintaining the normal physiological function (Dorn and Kitsis, 2015). An imbalance in mitochondrial dynamics can affect energy metabolism and post-stroke neuronal function by regulating the function of mitochondria. Prior work identifies hippocampal subregional and cell-type-dependent states of mitochondrial impairment, underscoring a previously unexploited therapeutic niche. All hippocampal mitochondria are disrupted 2 h after transient global cerebral ischemia but astrocytes exhibit rapid restoration by 24 h (Kumar et al., 2016). Conversely CA1 neuronal mitochondrial function remains selectively disrupted for an extended period of days (Shiino et al., 1998; Kumar et al., 2016) in contrast to neurons in the nearby ischemia-resistant dentate gyrus (DG). The molecular mechanisms regulating this hippocampal subregional- and cell-type specific mitochondrial response are entirely unknown.

MicroRNA-200c (miR-200c) is known to target the mitochondrial regulatory protein sirtuin-1 (SIRT1), which plays a central role in maintaining mitochondrial bioenergetics, fission/fusion balance, and ROS production. We have recently reported that miR-200c selectively increases in astrocytes relative to neurons after cerebral ischemia (Arvola et al., 2021) and demonstrated that miR-200c inhibition protected neurons from experimental stroke (Stary et al., 2015), however, whether miR-200c plays a role in delayed CA1 neuronal cell death after global cerebral ischemia is unknown. Therefore, in the present study we assessed whether post-injury treatment with anti-miR-200c reduced CA1 neurodegeneration in a mouse model of global cerebral ischemia. In parallel we assessed the role of miR-200c in cell-type specific post-injury changes in CA1 SIRT1 and mitochondrial fusion proteins *in vivo* and in primary mouse astrocyte cell cultures.

Materials and methods

In vivo global cerebral ischemia

All experimental protocols using animals were performed according to protocols approved by the Stanford University Animal Care and Use Committee and in accordance with the National Institutes of Health *Guide for the Care and Use of Laboratory Animals*. Global cerebral ischemia was induced in 8–10 week-old male C57BL/6J mice (Charles River Laboratories, Wilmington, VA, USA) *via* bilateral carotid artery occlusion (two-vessel occlusion, 2VO) + isoflurane (Onken et al., 2012; Kristian and Hu, 2013; Owens et al., 2015). Briefly, after anesthesia induction with 2.5% isoflurane and surgical incisions were complete, hypotension (mean arterial pressure, <40 mmHg) was induced with 5% isoflurane during continuous femoral arterial blood pressure monitoring (TA100 transducer, Moor Instruments, Wilmington, DE, USA). After 2 min of 5% isoflurane the common carotid arteries were clamped bilaterally. After 6 mins of simultaneous 5% isoflurane and bilateral common carotid artery clamping the isoflurane was reduced to 2.5%. Rectal temperature (37 ± 0.5°C) was controlled by a homeothermic blanket (Harvard Apparatus, Cambridge, MA, USA). Respiratory rate, heart rate, and pulse oximetry were monitored with a small animal oximeter (STARR Life Sciences, Oakmount, PA, USA). Cerebral perfusion pressure was continuously monitored *via* laser doppler (Model VMS-LDF1, Moor Instruments). After 10 min clamps were removed and isoflurane was decreased to 1% maintenance until closure of surgical incisions. Core body temperature was maintained during recovery at 37°C with a heating pad post-surgery to eliminate any neuroprotective effects of hypothermia. Mice were then randomized by coin flip and 2 h after global cerebral ischemia mice were re-anesthetized with 2% isoflurane and either anti-miR-200c inhibitor (Anti-miR™ miRNA Inhibitor, #AM17000, ThermoFisher Scientific, Waltham, MA, USA) or mismatch control (MM-control, ThermoFisher Scientific) in sterile saline (100 μl) was administered into the internal jugular vein as previously described (Xu et al., 2015).

Barnes maze

Memory testing in mice was performed as we have previously reported (Griffiths et al., 2019b). Mice were placed in the center of a circle platform with 20 equally spaced holes and visual clues; one of the holes was connected to a safe chamber (SD Instruments, San Diego, CA, USA). Aversive noise (85 dB) in conjunction with bright light (200 W) was shed on the platform to encourage the mouse to find the safe target. All mice were trained for 4 consecutive days with 3 min per trial, 4 trials per day. Their reference memory was tested on day 3 (short-term retention) and day 7 (long-term retention). Each mouse had only one trial on each of these two test days. The latency to find the target box during each trial was recorded and analyzed in real time by TopScan™ software (CleverSyS, Reston, VA, USA).

In vivo histological assessment

Animals were sacrificed at 7 days after injury by isoflurane overdose, and brains immediately perfused with transcardial ice-cold saline, then fixed with 4% phosphate-buffered paraformaldehyde (PFA) for stereological analysis. Coronal vibratome sections (50 μm) were used for combined immunohistochemical (IHC) analysis and fluorescent *in situ* hybridization (FISH) for miR-200c using miRCURY LNA miR Detection Probes (ThermoFisher Scientific) as we have previously done (Arvola et al., 2019). All fixed sections were stained for miR-200c, the astrocyte marker glial fibrillary acidic protein (GFAP, #ab90601, Abcam, Boston, MA, USA, 1:500 dilution), the mature neuronal marker NeuN (#ab104224, Abcam, 1:500 dilution), SIRT1 (# ab189494, Abcam, 1:500 dilution) and the mitochondrial fusion markers MFN2 (# bs2988R, BiossUSA, Woburn, MA, USA, 1:500 dilution) and OPA1 (#ab42364, Abcam, 1:500 dilution). The CA1 and DG regions were identified anatomically with DAPI and demarcated according to Newton et al. (2005) and as we have previously done (Stary et al., 2016; Griffiths et al., 2019a,b). Images were acquired by an observer blinded to conditions using an upright Zeiss Axio-Imager M2 fluorescent microscope equipped with Apotome 2.0 for optical sectioning, and Zeiss EC-Plan Neofluar 20×, Zeiss Plan Apochromat 40×, and Zeiss LC-Plan Neofluar 63× objectives. Qualitative protein expression with GFAP+ co-localized was performed using the "masking" function in ImageJ v1.49b software (NIH, Bethesda, MD, USA). In brief, Z-stack images were first independently analyzed in the GFAP channel, and then masked to generate GFAP+ regions of interest (ROIs). Next, GFAP+ ROIs were superimposed on the channel of interest, and then fluorescence intensities were measured and collated, for all sections. All imaging for a given protein were collected using a fixed excitation intensity, exposure time, and gain, to minimize variability. No post-imaging processing was performed. An observer blinded to conditions quantified from maximum projection Z-stack images the cell-type specific relative intensity of miR-200c fluorescence and the relative fluorescent intensity of NeuN, mitofusin-2 (MFN2), OPA1, and SIRT1 proteins using StereoInvestigator™ (MicroBrightField, Williston, VT, USA) software and ImageJ v1.49b software (NIH, Bethesda, MD, USA) as we have previously done (Arvola et al., 2019, 2021; Griffiths et al., 2019a).

Primary brain cell cultures

Primary astrocyte cultures were prepared from postnatal (days 1–3) Swiss Webster mice (Charles River Laboratories,

Wilmington, MA, USA) as described previously (Li et al., 2021). Isolated astrocytes were seeded on 24-well plates in plating medium consisting of Eagle's Minimal Essential Medium (Gibco, Grand Island, NY, USA) supplemented with 10% fetal bovine serum and 10% equine serum (HyClone, Logan, UT, USA), 21 mM (final concentration) glucose, and 10 ng/ml epidermal growth factor. Cultures were maintained at 37°C in a 5% CO_2 incubator. Primary astrocyte cultures were transfected with 50 nmol negative control (*mir*Vana® #4464061, ThermoFisher Scientific), miR-200c mimic (*mir*Vana® #4464066, ThermoFisher Scientific), or inhibitor (*mir*Vana® #4464084, ThermoFisher Scientific) using Lipofectamine 2000 (Invitrogen) according to the manufacturer's protocol on day *in vitro* (DIV) 16. In some experiments cultures were co-treated with the SIRT1 activator YK 3-237 (10 μM, Tocris #5667). In parallel experiments astrocytes were selectively cultured from CA1 and DG as previously described (Stary et al., 2016). Briefly, the left and right hippocampi were identified morphologically and by anatomical location, and dissected free in their entirety, while maintaining the anatomical orientation. The dorsal region of the hippocampus containing primarily CA1 was dissected free of the remainder of the hippocampus. The ventral hippocampus (containing DG) was further dissected with removal of the CA3 region. CA1 and DG hippocampal regions from individual animals were pooled, treated with 0.05% trypsin/EDTA (Life Technologies, Carlsbad, CA, USA), and plated in Dulbecco's modified Eagle medium (Gibco, Grand Island, NY, USA) with 10% equine serum (ES, HyClone), 10% fetal bovine serum (FBS, HyClone) and 10 ng/ml epidermal growth factor (Sigma Chemicals, St Louis, MO, USA). In some experiments primary neuronal cultures were utilized, prepared as previously described (Newton et al., 2005) from embryonic (E16-E18) mouse cortices. Briefly, the dissected cortices were dissociated with 0.05% trypsin/EDTA for 15 min at 37°C, triturated, then plated in medium containing 5% FBS and 5% ES (HyClone). A relatively pure neuronal culture was obtained by adding cytosine arabinoside (3 mol/L, Sigma) 24 h after plating to curb glial proliferation. For all experiments 3–4 independent cultures were tested as replicates within each experiment.

In vitro injury and fluorescent imaging

In vitro ischemia was induced by oxygen-glucose deprivation (OGD) as previously described (Ouyang et al., 2011). Briefly, 24 h following transfection primary astrocyte cultures were washed three times with glucose-free culture medium equilibrated with 100% N_2 in an anoxia chamber maintained at <350 ppm (<0.02%) O_2 (COY Laboratory Product Inc.). After 3 h OGD the medium was reoxygenated and glucose was added at 5.5 mM. For oxidative stress assays, glucose deprivation alone was selected as an ischemia-like stress for astrocyte cultures, as it reliably induces an extended period of mitochondrial dysfunction with increased ROS production prior to cell death, as we have employed previously (Stary et al., 2016). Cells were maintained at 37°C and 5% CO_2 in an atmospherically controlled chamber (Ibidi GmbH, Martinsried, Germany) for imaging of live-cell ROS generation after 30 min incubation with 5 μM CellROX™ Green (ThermoFisher Scientific, Waltham, MA, USA). Automated fluorescent image capture was performed at 200× using a Lumascope™ 720 (Etaluma, Carlsbad, CA, USA) as we have previously performed (Xia et al., 2018). For each well five replicate images were obtained and averaged. Mean intensity of fluorescence was quantified by an observer blinded to conditions ImageJ v1.49b software (NIH). Unbiased changes in fluorescence were normalized to MM-control transfection treatment. For assessment of astrocyte SIRT1 and MFN2, fluorescence immunocytochemistry was performed on astrocyte cell cultures in 24-well plates as described previously (Ouyang et al., 2013b). Cultures were fixed in 4% paraformaldehyde for 30 min at room temperature. Nonspecific binding was blocked with 5% normal goat serum and 0.3% Triton X-100 in PBS for 1 h. Cells were incubated with mouse monoclonal primary antibody to SIRT1 (# ab189494, Abcam, 1:100 dilution) or MFN2 (# bs2988R, BiossUSA, 1:100 dilution) overnight at 4°C. Cells were then washed and incubated with Alexa Fluor 488 nm-conjugated secondary antibody (1:500; Invitrogen, Grand Island, NY, USA) for 1 h. Cells were counterstained with the nuclear dye DAPI (4′,6′-diamidino-2-phenylindole, 0.5 μg/ml; Sigma-Aldrich, St Louis, MO, USA) and automated fluorescent image capture was performed at 200× using a Lumascope™ 720 (Etaluma, Carlsbad, CA, USA). For each well nine replicate images were obtained and averaged. Unbiased mean intensity of fluorescence was quantified by an observer blinded to treatment groups using ImageJ v1.49b software (NIH) and normalized to cell count (DAPI). Differences in fluorescence intensity between treatment groups were compared by normalizing to miR-200c mimic wash treatment for each condition.

Reverse transcription quantitative polymerase chain reaction

Total RNA was isolated with TRIzol® (ThermoFisher Scientific, Waltham, MA, USA) from CA1 tissue 24 h after injury and from astrocyte culture 3 h after wash control or OGD injury. Reverse transcription was performed as previously described (Stary et al., 2015) using the TaqMan MicroRNA Reverse Transcription Kit (Applied Biosystems, Foster City, CA, USA). Predesigned primer/probes for PCR were obtained from ThermoFisher Scientific for mmu-miR-200c–3p (#4426961) and

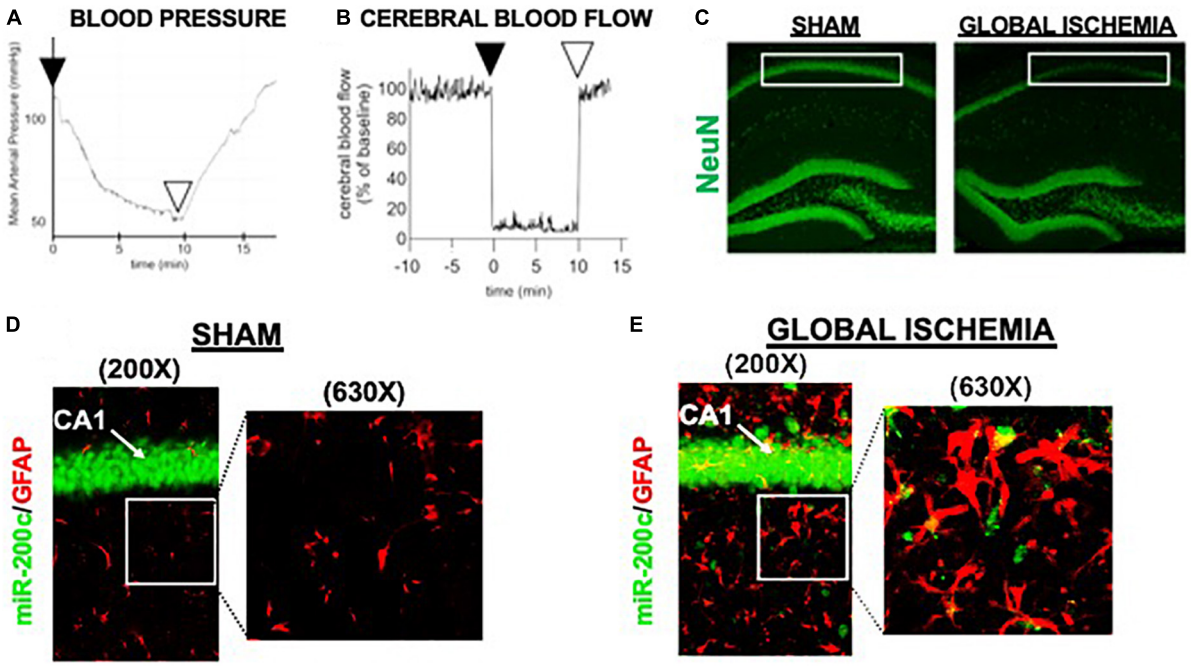

FIGURE 1
Mouse global cerebral ischemia model. Invasive blood pressure monitoring **(A)** and laser doppler cerebral blood flow measurement **(B)** during bilateral carotid artery occlusion (2 vessel, 2VO) plus 5% isoflurane-induced hypotension. **(C)** Representative image of fluorescent immunohistochemical (IHC) labeling for neurons (NeuN, green) in mouse hippocampus 7 days after global cerebral ischemia. Note post-injury reductions in NeuN+ cells in cornu ammonis-1 (CA1) sub-region (boxed). **(D,E)** Representative images of CA1 labeled for the astrocyte marker glial fibrillary acidic protein (GFAP, red) complexed with fluorescent *in situ* hybridization for miR-200c (green) expression. Note augmented miR-200c expression in astrocytes 7 days after global cerebral ischemia **(E)**.

U6 small nuclear RNA (U6, #01973). PCR reactions were conducted as previously described (Stary et al., 2015) using the TaqMan® Assay Kit (Applied Biosystems). Measurements for miR-200c were normalized to U6 (ΔCt) and comparisons were calculated as the inverse log of the ΔΔCT from controls (Livak and Schmittgen, 2001).

Immunoblots

Total protein from primary astrocyte cultures was isolated as previously described (Stary et al., 2017). Briefly, cultures were first washed with cold 0.1% phosphate buffered saline, then total cellular protein was quantified by Pierce BCA protein assay kit [ThermoFisher Scientific (Stary et al., 2017)]. Equal amounts of protein were loaded and separated on 10–12.5% polyacrylamide gels, then transferred to Immobilon polyvinylidene fluoride membranes (EMD Millipore Corp). Membranes were blocked with 5% skimmed dry milk and incubated overnight with primary antibody against SIRT1 (Abcam, #ab110304), MFN2 (Abcam, #ab124773), β-actin (LI-COR Bioscience #926–42,210) and/or β-tubulin (Abcam, #ab6046). Membranes were then washed and incubated with secondary antibodies (LI-COR Bioscience) for 1 h followed by washing again and visualizing by using the LICOR Odyssey infrared imaging system. Densitometric analysis of bands was performed *via* Image Studio Lite (LI-COR Biosciences), and the intensity of all proteins was normalized to β-actin or β-tubulin as a control.

Statistical analyses

Numbers of animals are indicated in figure legends. Data reported are means ± SE. Statistical difference was determined using *t*-test for comparison of two groups or ANOVA followed by Bonferroni correction for experiments with $N > 2$ groups using Sigmaplot (Systat Software, San Jose, CA, USA). $p < 0.05$ was considered significant.

Results

Anti-microRNA-200c treatment improves physiologic outcomes after global cerebral ischemia

A period of 10 min of 2VO and 5% isoflurane reliably resulted in hypotension (**Figure 1A**), cerebral hypoperfusion

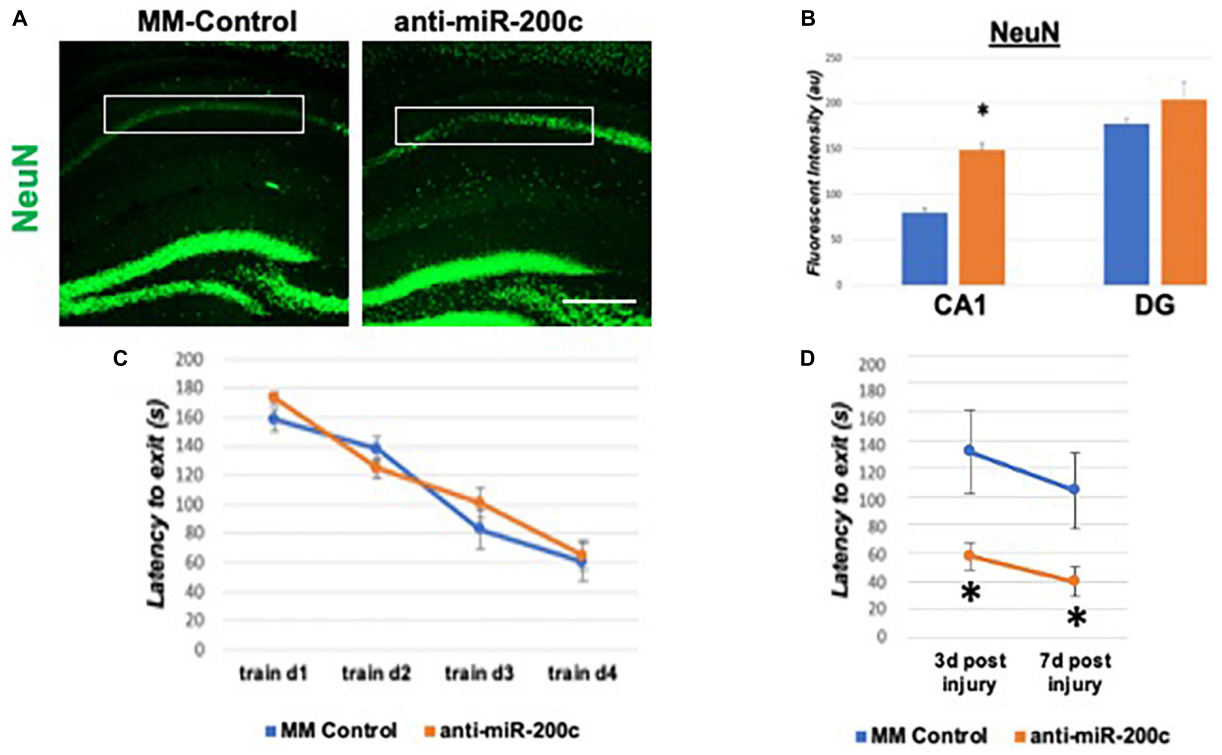

FIGURE 2
Effect of 2 h post-injury intravenous anti-miR-200c or MM-control treatment on sirtuin-1 (SIRT1) expression 7 days after global cerebral ischemia in mice. **(A)** Representative images of fluorescent IHC labeling for neurons (NeuN, green) in mouse hippocampus 7 days after global cerebral ischemia with and without post-injury anti-miR-200c treatment. **(B)** Quantification of post-injury CA1 NeuN fluorescence with and without IV anti-miR-200c post-treatment. **(C)** Escape latency during pre-injury Barnes maze training. **(D)** Escape latency at post-injury days 3 and 7 in mice with and without IV anti-miR-200c post-treatment. (N = 5–8 animals per treatment group, mean ± SEM, *$p < 0.05$). Scale bar, 1 mm.

(Figure 1B) and in loss of CA1 neurons (Figure 1C). This injury paradigm also resulted in a significant ($p < 0.05$) increase by 9.8 ± 4.5-fold in miR-200c expression in CA1, with visual evidence of post-injury augmentation of miR-200c expression in CA1 astrocytes *via* histological assessment (Figures 1D,E). Post-injury treatment with intravenous anti-miR-200c 2 h after global cerebral ischemia resulted in a significant ($p < 0.05$) reduction in post-injury CA1 miR-200c expression by 36.4 ± 22% relative to animals treated with mismatch control sequence (MM-control), reduced post-injury weight loss by time-of-sacrifice (10.7 ± 2 versus 19.2 ± 6%) and improved overall survival (100 versus 72.5%). Anti-miR-200c treatment also significantly ($p < 0.05$) reduced loss of CA1 neurons at post-injury day 7 (Figures 2A,B). Conversely no differences were observed between treatments in the adjacent ischemia-resistant DG. Pre-injury Barnes maze training demonstrated progressive adaptive decreases in escape latency (Figure 2C). While global cerebral ischemia increased escape latency, post-injury IV treatment with anti-miR-200c significantly ($p < 0.05$) decreased escape latency at both post-injury days 3 and 7 (Figure 2D).

Anti-microRNA-200c treatment increases global hippocampal mitochondrial dynamic protein expression after injury in a cell-type specific manner

Next, we assessed hippocampal sub-regional expression of the mitochondrial fission proteins MFN2 and OPA1 in the CA1 and DG. Relative to DG, MFN2 expression significantly ($p < 0.05$) decreased in CA1 after global cerebral ischemia in mice treated with post-injury MM-control (Figures 3A,B). In contrast, mice treated with post-injury anti-miR-200c demonstrated significantly ($p < 0.05$) preserved CA1 MFN2 expression (Figures 3A,B). In parallel relative to DG, OPA1 expression significantly ($p < 0.05$) decreased in CA1 after global cerebral ischemia in mice treated with post-injury MM-control (Figures 3A,C), while mice treated with anti-miR-200c demonstrated significantly ($p < 0.05$) preserved CA1 OPA1 expression (Figures 3A,C). Cell-type specific analysis revealed that post-injury astrocyte-specific expression of MFN2 was

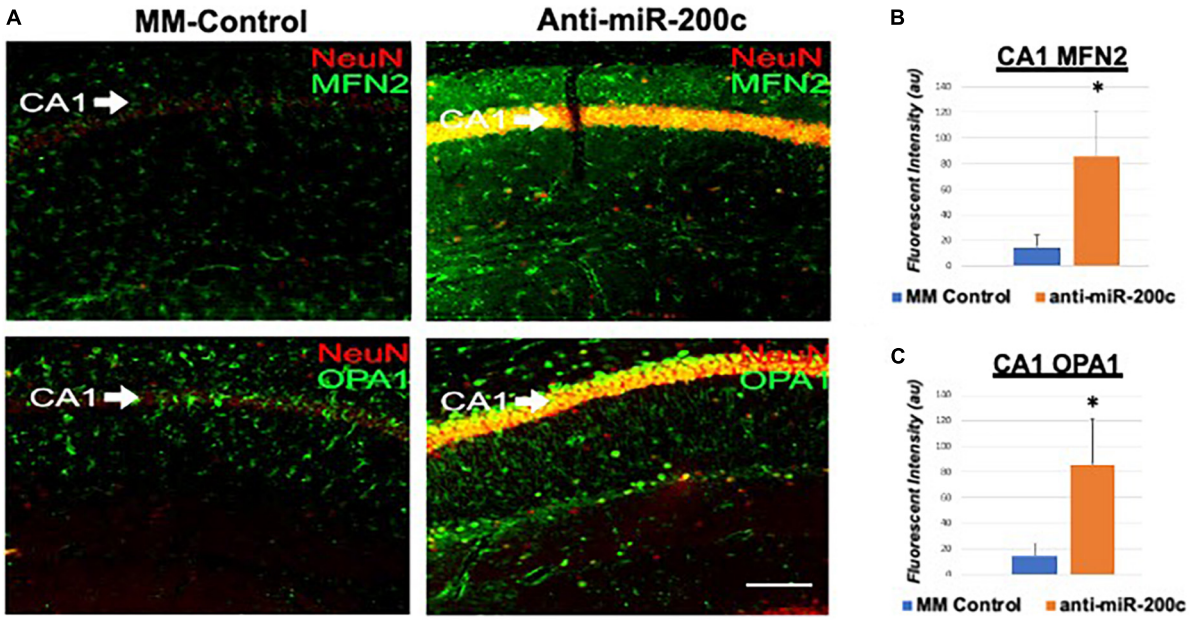

FIGURE 3
Mitofusin-2 (MFN2) and OPA1 expression in CA1 after global cerebral ischemia in mice. **(A)** Representative images of fluorescent IHC labeling of hippocampal NeuN (red) and MFN2 or OPA1 expression (green) 7 days after global cerebral ischemia with and without IV anti-miR-200c post-treatment. Quantification of MFN2 **(B)** and OPA1 **(C)** in all cells within CA1. $N = 5–8$ animals per treatment group, mean ± SEM, $^*p < 0.05$. Scale bar, 25 μm.

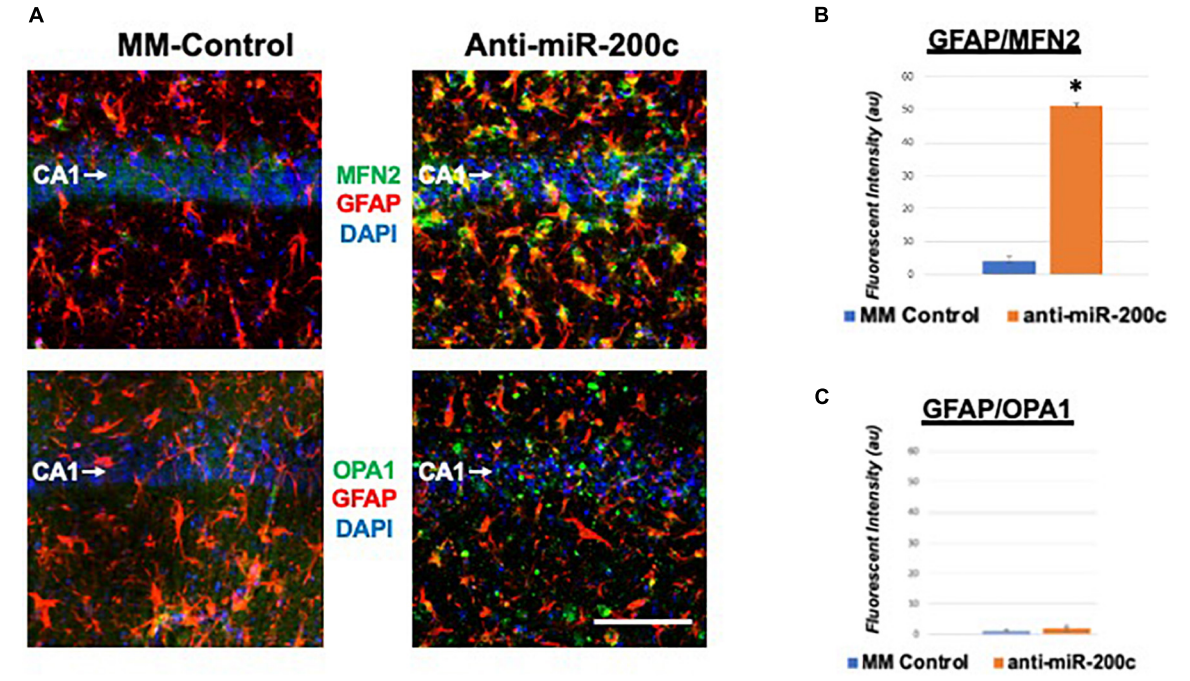

FIGURE 4
Astrocyte-specific CA1 MFN2 and OPA1 expression after global cerebral ischemia in mice. **(A)** Representative images of fluorescent IHC labeling of hippocampal GFAP (red) and MFN2 or OPA1 expression (green) 7 days after global cerebral ischemia with and without IV anti-miR-200c post-treatment. Quantification of co-labeled GFAP/mitofusin-2 (MFN2, **B**) and GFAP/OPA1 fluorescence **(C)** in CA1. $N = 5–8$ animals per treatment group, mean ± SEM, $^*p < 0.05$. Scale bar, 25 μm.

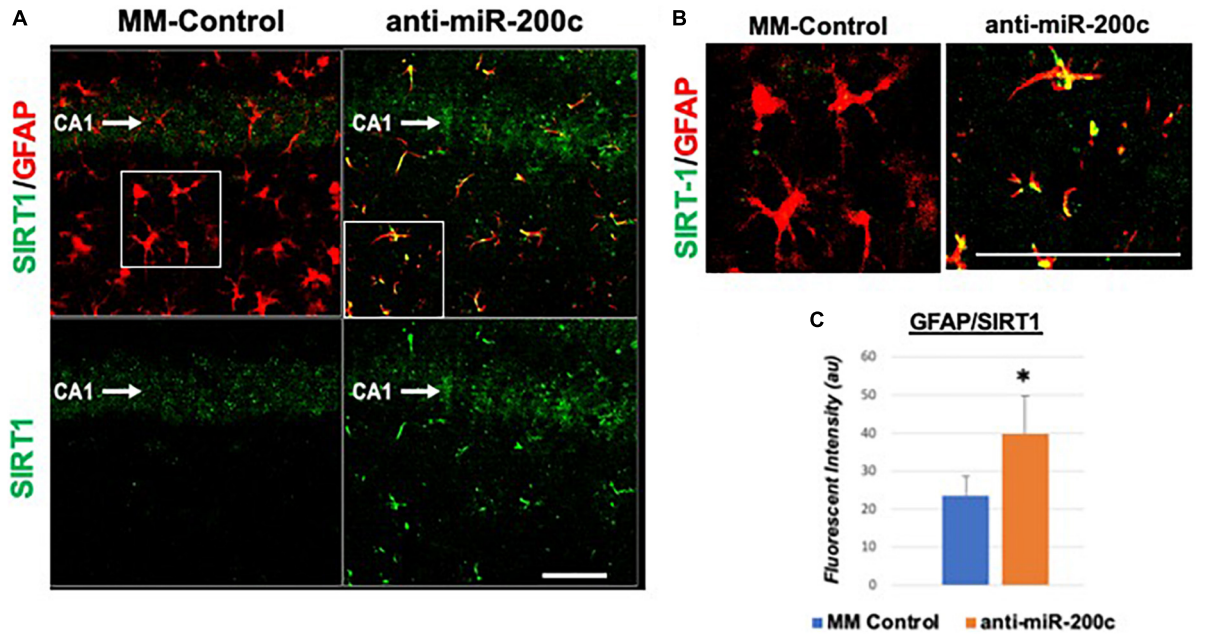

FIGURE 5
Astrocyte-specific CA1 SIRT1 expression after global cerebral ischemia in mice. Low power (200×, **A**) and high power (600×, **B**) representative images of fluorescent IHC labeling of hippocampal GFAP (red) and SIRT1 expression (green) 7 days after global cerebral ischemia with and without IV anti-miR-200c post-treatment. Quantification of co-labeled GFAP/SIRT1 **(C)** in CA1. *N* = 5–8 animals per treatment group, mean ± SEM, **p* < 0.05. Scale bar, 25 μm.

significantly ($p < 0.05$) higher in mice treated with anti-miR-200c relative to MM-control treated mice (Figures 4A,B). Conversely no differences were observed in astrocyte-specific OPA1 expression between treatment groups, suggesting the global CA1 decrease in OPA1 occurred in alternative cell types (Figures 4A,C). Cell-type specific analysis of SIRT1 expression revealed significantly ($p < 0.05$) augmented post-injury expression isolated to CA1 astrocytes (Figures 5A–C).

MicroRNA-200c modulates astrocyte oxidative stress *via* sirtuin-1

In vivo we assessed miR-200c expression after 3 h OGD injury in primary hippocampal astrocyte cultures from CA1 and DG (Figure 6A), and in primary cortical astrocyte and primary cortical neuron cell cultures (Figure 6B). We observed a significant ($p < 0.05$) increase in miR-200c expression in both CA1 and primary cortical astrocyte cultures, but not in DG astrocyte or neuronal cultures (Figures 6A,B). To assess the role of miR-200c in oxidative stress, primary astrocyte cultures were pre-treated with either miR-200c mimic, mimic + 5 the SIRT1 activator YK 3-237 inhibitor 24 h prior to 24 h of glucose deprivation. Transfection by mimic significantly ($p < 0.05$) increased (157 ± 22%) and inhibitor decreased (18 ± 4%) miR-200c expression. Relative to MM-control sequence, miR-200c mimic significantly ($p < 0.05$) exacerbated ROS generation, an effect that was significantly attenuated by co-treatment with SIRT1 activator, while treatment with miR-200c inhibitor provided a comparable significant antioxidant effect (Figures 6C,D).

MicroRNA-200c modulates astrocyte mitofusin-2 expression *via* sirtuin-1

Primary astrocyte cultures were assessed for post-injury expression of SIRT1 and MFN2 with miR-200c mimic or inhibitor pre-treatment. Relative to miR-200c mimic, treatment with miR-200c inhibitor significantly increased SIRT1 expression in the absence of injury (Figures 7A,B). Twenty-four hours after 3 h OGD, SIRT1 expression was significantly ($p < 0.05$) decreased in both treatment groups relative to wash control, however, post-injury SIRT1 expression was significantly ($p < 0.05$) higher in miR-200c inhibitor-treated cells versus post-injury miR-200c mimic-treated cells (Figures 7A,B). In parallel OGD induced a significant ($p < 0.05$) reduction in MFN2 post-injury expression in primary cortical astrocyte cultures 24 h after 3 h OGD (Figures 8A,B). Similar to SIRT1, miR-200c inhibitor resulted in significantly preserved post-injury MFN2 expression

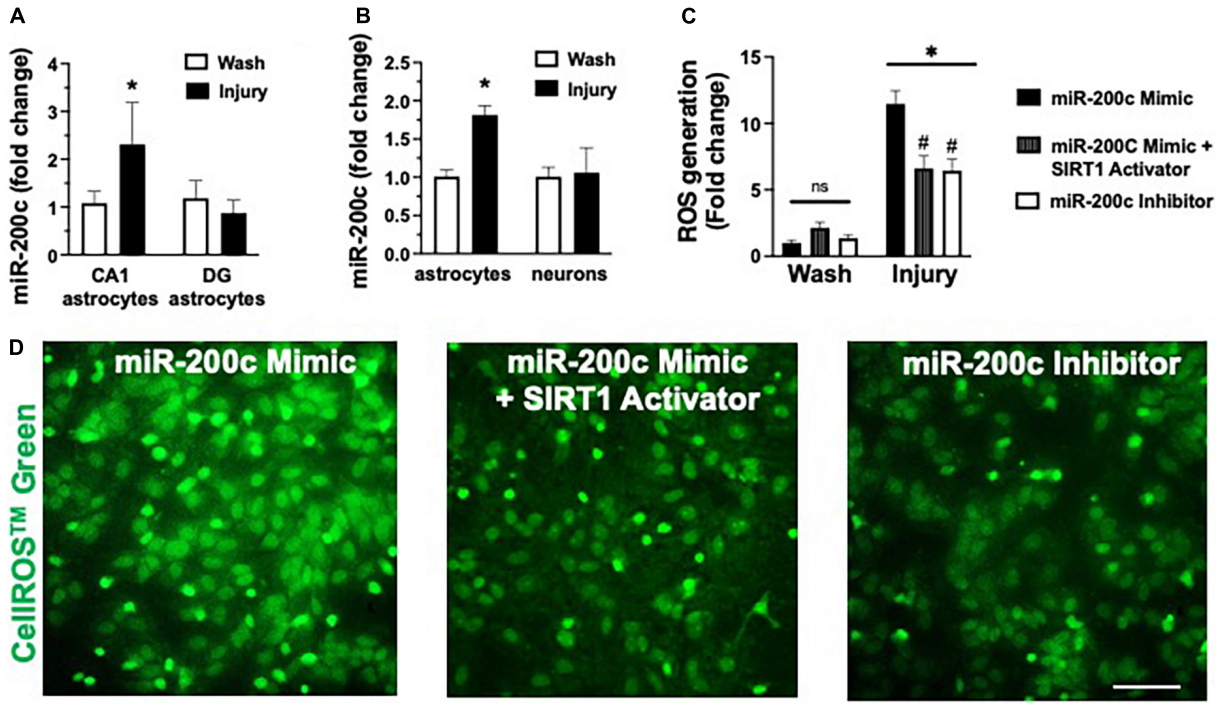

FIGURE 6
Post-injury miR-200c expression and SIRT1 activation and reactive oxygen species (ROS) production in astrocyte cultures. **(A)** Quantification of miR-200c expression after 3 h combined oxygen glucose deprivation (OGD) injury in primary hippocampal CA1 and DG astrocyte cultures. **(B)** Quantification of miR-200c expression after 3 h OGD in primary cortical astrocyte and neuronal cultures. **(C)** Quantification of ROS production in primary astrocytes pre-treated with MM-control, miR-200c mimic, miR-200c mimic + SIRT1 activator YK 3-237, or miR-200c inhibitor 24 h after 3 h OGD injury. **(D)** Representative live-cell images of astrocyte ROS production *via* CellROS^{TM} Green fluorescence. $N = 3$ independent cultures, mean ± SEM, $^{*}p < 0.05$ versus within treatment wash control and $^{\#}p < 0.05$ versus mimic injury. Scale bar, 25 μ m.

in miR-200c inhibitor-treated cells, and in cells co-treated with miR-200c mimic and SIRT1 activator, relative to cells pre-treated with miR-200c mimic alone (**Figures 8A,B**).

Discussion

Hippocampal CA1 circuits are central for memory formation (De Jong et al., 1999; Liu et al., 2005; Farkas et al., 2006; Bartsch et al., 2011; Lana et al., 2020). Clinical case studies of memory impairment in survivors of cardiac arrest have demonstrated that select loss of hippocampal CA1 neurons is the reason for their cognitive impairment (Zola-Morgan et al., 1986; Petito et al., 1987; Ng et al., 1989). This phenomenon has been repeatedly recapitulated in experimental rodent models of global cerebral ischemia (Kadar et al., 1998; Kristian and Hu, 2013), allowing for a stable platform for testing of therapeutic interventions to prevent CA1 neuronal loss and preserve CA1-dependent behavior. Cardiac arrest and resuscitation represent the largest clinical etiology of clinical transient global cerebral ischemia, with treatment options currently limited to mild hypothermia in survivors who have sustained severe neurological deficits. In the present study we observed neuroprotection in delayed CA1 neuronal cell death and reduced impairment in memory tasks with post-injury intravenous anti-miR-200c treatment after experimental global cerebral ischemia, demonstrating clinical efficacy for neuroprotection with a novel pharmaceutical approach within a clinically relevant 2 h post-injury treatment window.

MicroRNAs are central regulators of mitochondrial function, redox state, and apoptotic pathways (Ouyang et al., 2013a; Stary and Giffard, 2015). MiR-200c is highly enriched in the brain and is strongly induced by oxidative stress (Magenta et al., 2011; Stary et al., 2015; Arvola et al., 2021), augmenting ROS production in a positive feedback loop to dysregulate mitochondrial function (Carlomosti et al., 2017). We have previously demonstrated that pre-treatment with anti-miR-200c was protective in experimental stroke (Stary et al., 2015). Our observations in the present study indicate that post-injury anti-miR-200c therapy coincided with robust CA1 expression of MFN2. Metabolic energy state is closely associated with the balance between mitochondrial fusion and fission (Zhou et al., 2021), and mitochondria maintain a steady state of continuous fusion/fission maintaining the

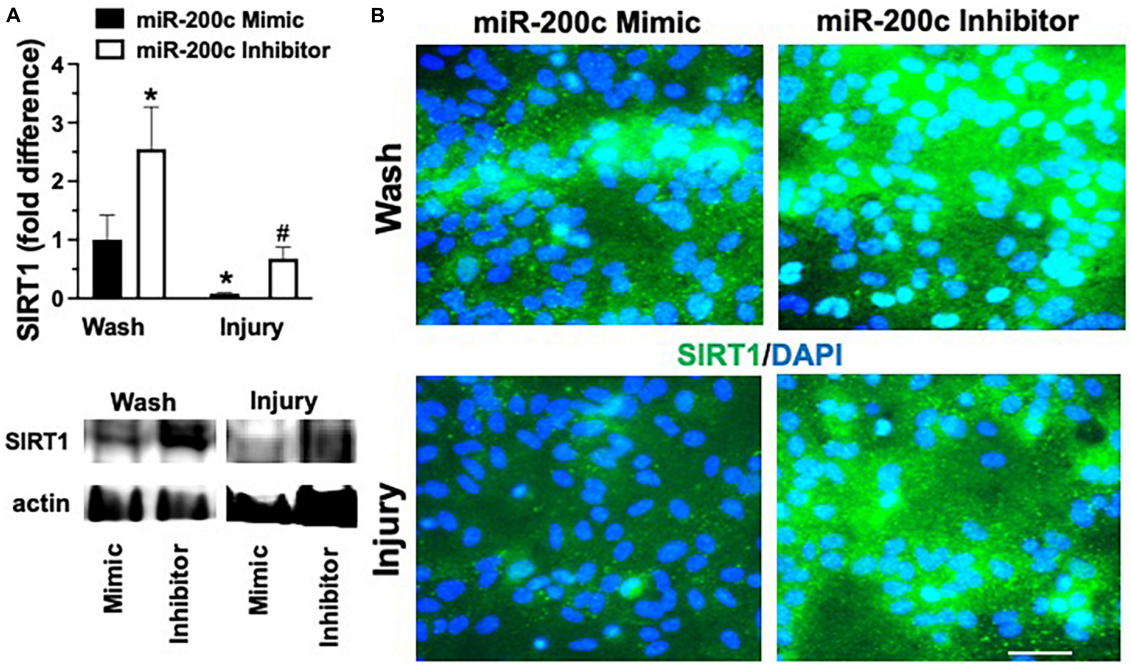

FIGURE 7
Effect of miR-200c on pre- and post-injury astrocyte SIRT1 in astrocyte cultures. Quantification **(A)** and representative images **(B)** of SIRT1 fluorescence 24 h after 3 h combined oxygen glucose deprivation injury in primary cortical astrocyte cultures with miR-200c mimic or miR-200c inhibitor pre-treatment. $N = 3$ independent cultures, mean ± SEM, $^{*}p < 0.05$ versus mimic wash control and $^{\#}p < 0.05$ versus wash within treatment. Scale bar, 15 μm.

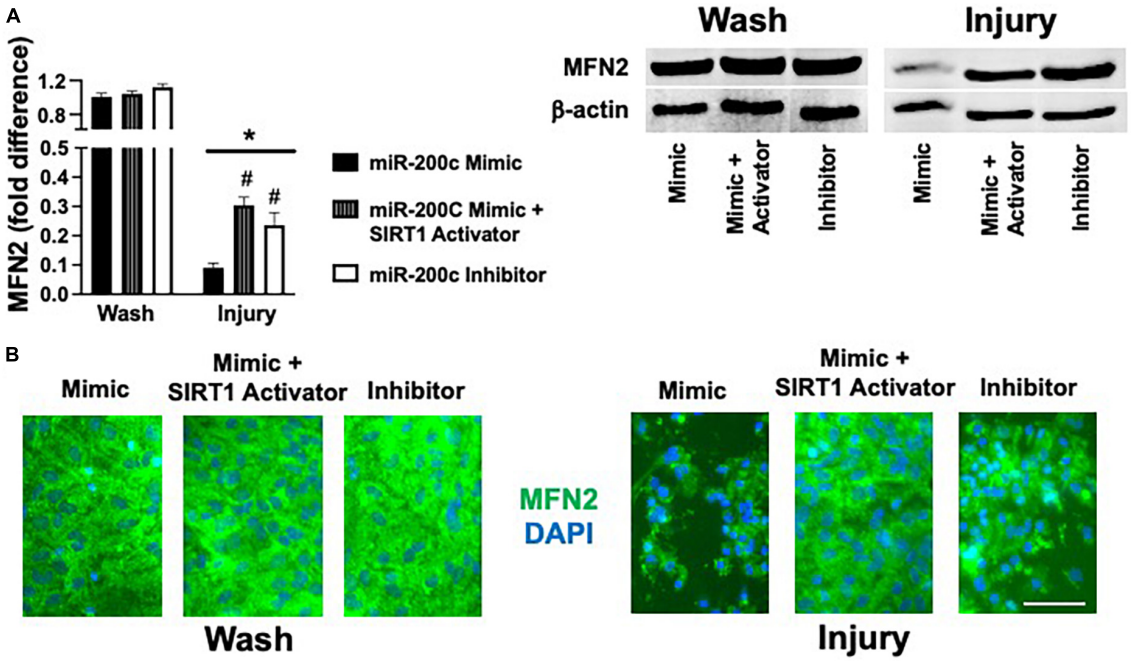

FIGURE 8
Effect of miR-200c and SIRT1 activation on pre- and post-injury astrocyte MFN2 expression in astrocyte cultures. Quantification **(A)** and representative images **(B)** of MFN2 fluorescence 24 h after 3 h combined oxygen glucose deprivation injury in primary cortical astrocyte cultures with miR-200c mimic, miR-200c mimic + SIRT1 activator YK 3-237, or miR-200c inhibitor pre-treatment. $N = 3$ independent cultures, mean ± SEM, $^{*}p < 0.05$ versus within treatment wash control and $^{\#}p < 0.05$ versus mimic injury. Scale bar, 15 μm.

normal physiological function of cells (Dorn and Kitsis, 2015). Imbalance in mitochondrial dynamics can affect energy metabolism and post-stroke neuronal function by regulating the number, morphology, and function of mitochondria. Ischemia disrupts the dynamic balance of fusion and fission in part by inhibiting expression of fusion proteins MFN2 and OPA1 and recent studies in experimental stroke suggests that inhibition of mitochondrial fission and promotion of fusion is protective (Zhou et al., 2021).

Our observations from the present study indicate that augmented expression of CA1 MFN2 was localized to CA1 astrocytes, and *in vitro*, an early (3 h) increase in miR-200c in response to simulated ischemia was limited to CA1 and cortical astrocyte cultures. As specialized glia, astrocytes represent the most plentiful cell type in the mammalian brain, serving many housekeeping functions (Verkhratsky and Nedergaard, 2018) and indispensable for neurotransmitter homeostasis and maintenance and maturation of synapses (Pfrieger, 2009; Heneka et al., 2010). Neurons and astrocytes are functionally tightly coupled in the brain. Neurons consume 75–80% of total brain energy (Hyder et al., 2013) to support restoration of neuronal membrane potentials, for neurotransmitter synthesis, vesicle packaging, axoplasmic transport, and neurotransmitter release (Attwell and Laughlin, 2001; Rangaraju et al., 2014; Pathak et al., 2015). In astrocytes, energy stores are localized mainly as glycogen to buffer transient energy requirements from neurons (Kong et al., 2002) that do not store energy. Normal brain activity depends on metabolic plasticity of astrocytes and requires not only glucose supply from blood but also glycogen stored in astrocytes that can last beyond when glucose is depleted (Brown and Ransom, 2007). In response to inflammation or oxidative stress, astrocytes also upregulate glycolysis-producing ATP and lactate, which support energy metabolism to neurons (Volobouéva et al., 2008). Prior work has reported that selective dysfunction of hippocampal CA1 astrocytes occurs at early reperfusion times, long before CA1 neurons die (Ouyang et al., 2007) and that increased generation of ROS and mitochondrial dysfunction in CA1 astrocytes contribute to delayed death of CA1 neurons (Ouyang et al., 2007). Astrocytes in CA1 show early mitochondrial impairment and increased vulnerability to ischemia even when isolated in primary culture, compared to similarly isolated DG astrocytes. The results from the present study suggest that augmented CA1 astrocyte MFN2 may play a role in mitigating post-injury astrocyte mitochondrial destabilization, thereby leading to secondary CA1 neuronal protection.

Activation of SIRT1 has also been shown to be a promising therapeutic target for protective strategies for stroke (Zhu et al., 2010; Miao et al., 2016; Zhang et al., 2018). Oxidative stress induces regulatory changes in several SIRT1-associated genes, including those involved in metabolism, apoptosis, ion transport, cell motility, and G-protein signaling (Oberdoerffer et al., 2008). SIRT1 maintains bioenergetic balance by activating (PCG1-α) (Nogueiras et al., 2012), a transcriptional co-activator of respiratory genes and a regulator of mitochondrial biogenesis (Nemoto et al., 2005), and activates the transcription factor p53 which decreases ROS (Tan et al., 1999; Hussain et al., 2004; Sablina et al., 2005). SIRT1 can also exert *intercellular* control of mitochondrial function *via* glial cell line-derived neurotropic factor (GDNF) expression (Corpas et al., 2017), which functions to remotely maintain neuronal mitochondrial function (Mitroshina et al., 2019), and *via* p53, which is transported in extracellular exosomes (Pavlakis et al., 2020). SIRT1 is targeted by miR-200c: in brain microvascular endothelial cells miR-200c inhibition provided protection against *in vitro* ischemia *via* SIRT1 (Wang et al., 2019). In the present study SIRT1 activation was sufficient to mitigate the augmentation of ROS production with miR-200c mimic with ischemic injury in astrocytes, supporting a mechanistic role for miR-200c/SIRT1 in the present conditions. Prior studies have demonstrated SIRT1 preserves mitochondria after ischemia by selectively interacting with MFN2 (Biel et al., 2016). Our observations in the present study indicate that SIRT1 levels were augmented in CA1 astrocytes in mice and in primary astrocyte cultures with anti-miR-200c treatment, consistent with our observations identifying augmented MFN2 expression in astrocytes with post-injury anti-miR-200c treatment. Similar to oxidative stress, activation of SIRT1 in astrocytes was sufficient to reverse decreases in MFN2 after ischemic injury associated with miR-200c mimic, supporting a role for SIRT1 in mediating miR-200c regulation of astrocyte mitochondrial dynamics. Future studies should extend the mechanistic intercellular miR-200c/SIRT1/MFN2 signaling to the context of intercellular signaling between astrocytes and neurons, and as well extend preclinical testing of anti-miR-200c and SIRT1 activation as a post-injury therapy to include the biological variables of sex and age.

Data availability statement

The raw data supporting the conclusions of this article will be made available by the authors, without undue reservation.

Ethics statement

The animal study was reviewed and approved by the Stanford University Animal Care and Use Committee and in

accordance with the National Institutes of Health Guide for the Care and Use of Laboratory Animals.

Author contributions

BG and CS conceived the project and assembled and edited the manuscript. LX and XS performed experiments. BG, MG, and IM performed image and data analysis. All authors contributed to the article and approved the submitted version.

Funding

This study was supported by NIH Grant #NS119462 to CS.

Conflict of interest

The authors declare that the research was conducted in the absence of any commercial or financial relationships that could be construed as a potential conflict of interest.

Publisher's note

All claims expressed in this article are solely those of the authors and do not necessarily represent those of their affiliated organizations, or those of the publisher, the editors and the reviewers. Any product that may be evaluated in this article, or claim that may be made by its manufacturer, is not guaranteed or endorsed by the publisher.

References

Arvola, O., Griffiths, B., Rao, A., Xu, L., Pastroudis, I. A., and Stary, C. M. (2021). Expression of miR-200c corresponds with increased reactive oxygen species and hypoxia markers after transient focal ischemia in mice. *Neurochem. Int.* 149:105146. doi: 10.1016/j.neuint.2021.105146

Arvola, O., Kaidonis, G., Xu, L., Griffiths, B., and Stary, C. M. (2019). Hippocampal sub-regional differences in the microRNA response to forebrain ischemia. *Mol. Cell Neurosci.* 98, 164–178. doi: 10.1016/j.mcn.2019.05.003

Attwell, D., and Laughlin, S. B. (2001). An energy budget for signaling in the grey matter of the brain. *J. Cereb. Blood Flow Metab.* 21, 1133–1145. doi: 10.1097/00004647-200110000-00001

Bartsch, T., Dohring, J., Rohr, A., Jansen, O., and Deuschl, G. (2011). CA1 neurons in the human hippocampus are critical for autobiographical memory, mental time travel, and autonoetic consciousness. *Proc. Natl. Acad. Sci.U.S.A.* 108, 17562–17567. doi: 10.1073/pnas.1110266108

Belanger, M., Allaman, I., and Magistretti, P. J. (2011). Brain energy metabolism: Focus on astrocyte-neuron metabolic cooperation. *Cell Metab.* 14, 724–738. doi: 10.1016/j.cmet.2011.08.016

Benjamin, E. J., Muntner, P., Alonso, A., Bittencourt, M. S., Callaway, C. W., Carson, A. P., et al. (2019). Heart disease and stroke statistics-2019 Update: A report from the american heart association. *Circulation* 139, e56–e528. doi: 10.1161/CIR.0000000000000659

Biel, T. G., Lee, S., Flores-Toro, J. A., Dean, J. W., Go, K. L., Lee, M. H., et al. (2016). Sirtuin 1 suppresses mitochondrial dysfunction of ischemic mouse livers in a mitofusin 2-dependent manner. *Cell Death Differ.* 23, 279–290. doi: 10.1038/cdd.2015.96

Brown, A. M., and Ransom, B. R. (2007). Astrocyte glycogen and brain energy metabolism. *Glia* 55, 1263–1271. doi: 10.1002/glia.20557

Carlomosti, F., D'Agostino, M., Beji, S., Torcinaro, A., Rizzi, R., Zaccagnini, G., et al. (2017). Oxidative Stress-Induced miR-200c Disrupts the Regulatory Loop Among SIRT1, FOXO1, and eNOS. *Antioxid. Redox Signal.* 27, 328–344. doi: 10.1089/ars.2016.6643

Corpas, R., Revilla, S., Ursulet, S., Castro-Freire, M., Kaliman, P., Petegnief, V., et al. (2017). SIRT1 overexpression in mouse hippocampus induces cognitive enhancement through proteostatic and neurotrophic mechanisms. *Mol. Neurobiol.* 54, 5604–5619. doi: 10.1007/s12035-016-0087-9

De Jong, G. I., Farkas, E., Stienstra, C. M., Plass, J. R., Keijser, J. N., de la Torre, J. C., et al. (1999). Cerebral hypoperfusion yields capillary damage in the hippocampal CA1 area that correlates with spatial memory impairment. *Neuroscience* 91, 203–210. doi: 10.1016/s0306-4522(98)00659-9

Dorn, G. W. II, and Kitsis, R. N. (2015). The mitochondrial dynamism-mitophagy-cell death interactome: Multiple roles performed by members of a mitochondrial molecular ensemble. *Circ. Res.* 116, 167–182. doi: 10.1161/CIRCRESAHA.116.303554

Farkas, E., Institoris, A., Domoki, F., Mihaly, A., and Bari, F. (2006). The effect of pre- and posttreatment with diazoxide on the early phase of chronic cerebral hypoperfusion in the rat. *Brain Res.* 1087, 168–174. doi: 10.1016/j.brainres.2006.02.134

Griffiths, B. B., Ouyang, Y. B., Xu, L., Sun, X., Giffard, R. G., and Stary, C. M. (2019a). Postinjury inhibition of miR-181a promotes restoration of hippocampal CA1 neurons after transient forebrain ischemia in rats. *eNeuro* 6. doi: 10.1523/ENEURO.0002-19.2019

Griffiths, B. B., Sahbaie, P., Rao, A., Arvola, O., Xu, L., Liang, D., et al. (2019b). Pre-treatment with microRNA-181a antagomir prevents loss of parvalbumin expression and preserves novel object recognition following mild traumatic brain injury. *Neuromolecular Med.* 21, 170–181. doi: 10.1007/s12017-019-08532-y

Heneka, M. T., Rodriguez, J. J., and Verkhratsky, A. (2010). Neuroglia in neurodegeneration. *Brain Res. Rev.* 63, 189–211. doi: 10.1016/j.brainresrev.2009.11.004

Hussain, S. P., Amstad, P., He, P., Robles, A., Lupold, S., Kaneko, I., et al. (2004). p53-induced up-regulation of MnSOD and GPx but not catalase increases oxidative stress and apoptosis. *Cancer Res.* 64, 2350–2356. doi: 10.1158/0008-5472.can-2287-2

Hyder, F., Rothman, D. L., and Bennett, M. R. (2013). Cortical energy demands of signaling and nonsignaling components in brain are conserved across mammalian species and activity levels. *Proc. Natl. Acad. Sci. U.S.A.* 110, 3549–3554. doi: 10.1073/pnas.1214912110

Kadar, T., Dachir, S., Shukitt-Hale, B., and Levy, A. (1998). Sub-regional hippocampal vulnerability in various animal models leading to cognitive dysfunction. *J. Neural. Transm (Vienna)* 105, 987–1004. doi: 10.1007/s007020050107

Kong, J., Shepel, P. N., Holden, C. P., Mackiewicz, M., Pack, A. I., and Geiger, J. D. (2002). Brain glycogen decreases with increased periods of wakefulness: Implications for homeostatic drive to sleep. *J. Neurosci.* 22, 5581–5587. doi: 10.1523/JNEUROSCI.22-13-05581.2002

Kristian, T., and Hu, B. (2013). Guidelines for using mouse global cerebral ischemia models. *Transl. Stroke Res.* 4, 343–350. doi: 10.1007/s12975-012-0236-z

Kumar, R., Bukowski, M. J., Wider, J. M., Reynolds, C. A., Calo, L., Lepore, B., et al. (2016). Mitochondrial dynamics following global cerebral ischemia. *Mol. Cell Neurosci.* 76, 68–75. doi: 10.1016/j.mcn.2016.08.010

Lana, D., Ugolini, F., and Giovannini, M. G. (2020). An overview on the differential interplay among neurons-astrocytes-microglia in CA1 and CA3 hippocampus in hypoxia/ischemia. *Front. Cell Neurosci.* 14:585833. doi: 10.3389/fncel.2020.585833

Li, L., and Stary, C. (2016). Targeting glial mitochondrial function for protection from cerebral ischemia: Relevance, mechanisms, and the role of MicroRNAs. *Oxid. Med. Cell Longev.* 2016:6032306. doi: 10.1155/2016/6032306

Li, L., Volobouevа, L., Griffiths, B. B., Xu, L., Giffard, R. G., and Stary, C. M. (2021). MicroRNA-338 inhibition protects against focal cerebral ischemia and preserves mitochondrial function in vitro in astrocytes and neurons via COX4I1. *Mitochondrion* 59, 105–112. doi: 10.1016/j.mito.2021.04.013

Liu, H. X., Zhang, J. J., Zheng, P., and Zhang, Y. (2005). Altered expression of MAP-2, GAP-43, and synaptophysin in the hippocampus of rats with chronic cerebral hypoperfusion correlates with cognitive impairment. *Brain Res. Mol. Brain Res.* 139, 169–177. doi: 10.1016/j.molbrainres.2005.05.014

Livak, K. J., and Schmittgen, T. D. (2001). Analysis of relative gene expression data using real-time quantitative PCR and the 2(-Delta Delta C(T)) Method. *Methods* 25, 402–408.

Magenta, A., Cencioni, C., Fasanaro, P., Zaccagnini, G., Greco, S., Sarra-Ferraris, G., et al. (2011). miR-200c is upregulated by oxidative stress and induces endothelial cell apoptosis and senescence via ZEB1 inhibition. *Cell Death Differ.* 18, 1628–1639. doi: 10.1038/cdd.2011.42

Miao, Y., Zhao, S., Gao, Y., Wang, R., Wu, Q., Wu, H., et al. (2016). Curcumin pretreatment attenuates inflammation and mitochondrial dysfunction in experimental stroke: The possible role of Sirt1 signaling. *Brain Res. Bull.* 121, 9–15. doi: 10.1016/j.brainresbull.2015.11.019

Mitroshina, E. C., Mishchenko, T. A., Shirokova, O. M., Astrakhanova, T. A., Loginova, M. M., Epifanova, E. A., et al. (2019). Intracellular neuroprotective mechanisms in neuron-glial networks mediated by glial cell line-derived neurotrophic factor. *Oxid. Med. Cell Longev.* 2019:1036907. doi: 10.1155/2019/1036907

Nemoto, S., Fergusson, M. M., and Finkel, T. (2005). SIRT1 functionally interacts with the metabolic regulator and transcriptional coactivator PGC-1{alpha}. *J. Biol. Chem.* 280, 16456–16460. doi: 10.1074/jbc.M501485200

Newton, I. G., Forbes, M. E., Legault, C., Johnson, J. E., Brunso-Bechtold, J. K., and Riddle, D. R. (2005). Caloric restriction does not reverse aging-related changes in hippocampal BDNF. *Neurobiol. Aging* 26, 683–688. doi: 10.1016/j.neurobiolaging.2004.06.005

Ng, T., Graham, D. I., Adams, J. H., and Ford, I. (1989). Changes in the hippocampus and the cerebellum resulting from hypoxic insults: Frequency and distribution. *Acta Neuropathol.* 78, 438–443. doi: 10.1007/BF00688181

Nogueiras, R., Habegger, K. M., Chaudhary, N., Finan, B., Banks, A. S., Dietrich, M. O., et al. (2012). Sirtuin 1 and sirtuin 3: Physiological modulators of metabolism. *Physiol. Rev.* 92, 1479–1514. doi: 10.1152/physrev.00022.2011

Oberdoerffer, P., Michan, S., McVay, M., Mostoslavsky, R., Vann, J., Park, S. K., et al. (2008). SIRT1 redistribution on chromatin promotes genomic stability but alters gene expression during aging. *Cell* 135, 907–918. doi: 10.1016/j.cell.2008.10.025

Onken, M., Berger, S., and Kristian, T. (2012). Simple model of forebrain ischemia in mouse. *J. Neurosci.* 204, 254–261. doi: 10.1016/j.jneumeth.2011.11.022

Ouyang, Y., Stary, C., Yang, G., and Giffard, R. (2013a). microRNAs: Innovative targets for cerebral ischemia and stroke. *Curr. Drug Targets* 14, 90–101.

Ouyang, Y., Volobouevа, L., Xu, L., and Giffard, R. (2007). Selective dysfunction of hippocampal CA1 astrocytes contributes to delayed neuronal damage after transient forebrain ischemia. *J. Neurosci.* 27, 4253–4260. doi: 10.1523/JNEUROSCI.0211-07.2007

Ouyang, Y., Xu, L., Emery, J., Lee, A., and Giffard, R. (2011). Overexpressing GRP78 influences Ca2+ handling and function of mitochondria in astrocytes after ischemia-like stress. *Mitochondrion* 11, 279–286. doi: 10.1016/j.mito.2010.10.007

Ouyang, Y., Xu, L., Lu, Y., Sun, X., Yue, S., Xiong, X., et al. (2013b). Astrocyte-enriched miR-29a targets PUMA and reduces neuronal vulnerability to forebrain ischemia. *Glia* 61, 1784–1794. doi: 10.1002/glia.22556

Owens, K., Park, J. H., Gourley, S., Jones, H., and Kristian, T. (2015). Mitochondrial dynamics: Cell-type and hippocampal region specific changes following global cerebral ischemia. *J. Bioenerg. Biomembr.* 47, 13–31. doi: 10.1007/s10863-014-9575-7

Pathak, D., Shields, L. Y., Mendelsohn, B. A., Haddad, D., Lin, W., Gerencser, A. A., et al. (2015). The role of mitochondrially derived ATP in synaptic vesicle recycling. *J. Biol. Chem.* 290, 22325–22336. doi: 10.1074/jbc.M115.656405

Pavlakis, E., Neumann, M., and Stiewe, T. (2020). Extracellular Vesicles: Messengers of p53 in tumor-stroma communication and cancer metastasis. *Int. J. Mol. Sci.* 21:9648. doi: 10.3390/ijms21249648

Petito, C. K., Feldmann, E., Pulsinelli, W. A., and Plum, F. (1987). Delayed hippocampal damage in humans following cardiorespiratory arrest. *Neurology* 37, 1281–1286. doi: 10.1212/wnl.37.8.1281

Pfrieger, F. W. (2009). Roles of glial cells in synapse development. *Cell Mol. Life Sci.* 66, 2037–2047. doi: 10.1007/s00018-009-0005-7

Rangaraju, V., Calloway, N., and Ryan, T. A. (2014). Activity-driven local ATP synthesis is required for synaptic function. *Cell* 156, 825–835. doi: 10.1016/j.cell.2013.12.042

Sablina, A. A., Budanov, A. V., Ilyinskaya, G. V., Agapova, L. S., Kravchenko, J. E., and Chumakov, P. M. (2005). The antioxidant function of the p53 tumor suppressor. *Nat. Med.* 11, 1306–1313. doi: 10.1038/nm1320

Shiino, A., Matsuda, M., Handa, J., and Chance, B. (1998). Poor recovery of mitochondrial redox state in CA1 after transient forebrain ischemia in gerbils. *Stroke* 29, 2421–2424;discussion5. doi: 10.1161/01.str.29.11.2421

Stary, C. M., Xu, L., Li, L., Sun, X., Ouyang, Y. B., Xiong, X., et al. (2017). Inhibition of miR-181a protects female mice from transient focal cerebral ischemia by targeting astrocyte estrogen receptor-alpha. *Mol. Cell Neurosci.* 82, 118–125. doi: 10.1016/j.mcn.2017.05.004

Stary, C., and Giffard, R. (2015). Advances in astrocyte-targeted approaches for stroke therapy: An emerging role for mitochondria and microRNAS. *Neurochem. Res.* 40, 301–307. doi: 10.1007/s11064-014-1373-4

Stary, C., Sun, X., Ouyang, Y., Li, L., and Giffard, R. (2016). miR-29a Differentially Regulates Cell Survival in Astrocytes from Cornu Ammonis-1 and Dentate Gyrus by Targeting VDAC1. *Mitochondrion* 30, 248–254. doi: 10.1016/j.mito.2016.08.013

Stary, C., Xu, L., Sun, X., Ouyang, Y., White, R., Leong, J., et al. (2015). MicroRNA-200c contributes to injury from transient focal cerebral ischemia by targeting Reelin. *Stroke* 46, 551–556. doi: 10.1161/STROKEAHA.114.007041

Tan, M., Li, S., Swaroop, M., Guan, K., Oberley, L. W., and Sun, Y. (1999). Transcriptional activation of the human glutathione peroxidase promoter by p53. *J. Biol. Chem.* 274, 12061–12066. doi: 10.1074/jbc.274.17.12061

Verkhratsky, A., and Nedergaard, M. (2018). Physiology of Astroglia. *Physiol. Rev.* 98, 239–389. doi: 10.1152/physrev.00042.2016

Volobouevа, L., Duan, M., Ouyang, Y., Emery, J., Stoy, C., and Giffard, R. (2008). Overexpression of mitochondrial Hsp70/Hsp75 protects astrocytes against ischemic injury in vitro. *J. Cereb. Blood Flow Metab.* 28, 1009–1016. doi: 10.1038/sj.jcbfm.9600600

Wang, S., Han, X., Mao, Z., Xin, Y., Maharjan, S., and Zhang, B. (2019). MALAT1 lncRNA induces autophagy and protects brain microvascular endothelial cells against oxygen-glucose deprivation by binding to miR-200c-3p and upregulating SIRT1 expression. *Neuroscience* 397, 116–126. doi: 10.1016/j.neuroscience.2018.11.024

Xia, Y., Sun, X., Luo, Y., and Stary, C. M. (2018). Ferroptosis contributes to isoflurane neurotoxicity. *Front. Mol. Neurosci.* 11:486. doi: 10.3389/fnmol.2018.00486

Xu, L. J., Ouyang, Y. B., Xiong, X., Stary, C. M., and Giffard, R. G. (2015). Post-stroke treatment with miR-181 antagomir reduces injury and improves long-term behavioral recovery in mice after focal cerebral ischemia. *Exp. Neurol.* 264, 1–7. doi: 10.1016/j.expneurol.2014.11.007

Xu, L., Emery, J., Ouyang, Y., Volobouevа, L., and Giffard, R. (2010). Astrocyte targeted overexpression of Hsp72 or SOD2 reduces neuronal vulnerability to forebrain ischemia. *Glia* 58, 1042–1049. doi: 10.1002/glia.20985

Zhang, J. F., Zhang, Y. L., and Wu, Y. C. (2018). The Role of Sirt1 in Ischemic Stroke: Pathogenesis and Therapeutic Strategies. *Front. Neurosci.* 12:833. doi: 10.3389/fnins.2018.00833

Zhou, X., Chen, H., Wang, L., Lenahan, C., Lian, L., Ou, Y., et al. (2021). Mitochondrial dynamics: A potential therapeutic target for ischemic stroke. *Front. Aging Neurosci.* 13:721428. doi: 10.3389/fnagi.2021.721428

Zhu, H. R., Wang, Z. Y., Zhu, X. L., Wu, X. X., Li, E. G., and Xu, Y. (2010). Icariin protects against brain injury by enhancing SIRT1-dependent PGC-1alpha expression in experimental stroke. *Neuropharmacology* 59, 70–76. doi: 10.1016/j.neuropharm.2010.03.017

Zola-Morgan, S., Squire, L. R., and Amaral, D. G. (1986). Human amnesia and the medial temporal region: Enduring memory impairment following a bilateral lesion limited to field CA1 of the hippocampus. *J. Neurosci.* 6, 2950–2967.

frontiers | Frontiers in Molecular Neuroscience

TYPE Original Research
PUBLISHED 01 December 2022
DOI 10.3389/fnmol.2022.1048634

OPEN ACCESS

EDITED BY
Stefan Liebau,
University of Tübingen,
Germany

REVIEWED BY
Ana Isabel Arroba,
Fundación para la gestión de la investigación Biomédica de Cádiz, Spain
Susanne Mohr,
Michigan State University,
United States
David Arthur Simpson,
Queen's University Belfast, United Kingdom

*CORRESPONDENCE
Mingzhe Cao
caomzh7@mail.sysu.edu.cn
Guoguo Yi
yigg@mail.sysu.edu.cn
Min Fu
min_fu1212@163.com

†These authors have contributed equally to this work

SPECIALTY SECTION
This article was submitted to Molecular Signalling and Pathways, a section of the journal Frontiers in Molecular Neuroscience

RECEIVED 19 September 2022
ACCEPTED 10 November 2022
PUBLISHED 01 December 2022

CITATION
Wang Y, Yang X, Li Q, Zhang Y, Chen L, Hong L, Xie Z, Yang S, Deng X, Cao M, Yi G and Fu M (2022) Single-cell RNA sequencing reveals the Müller subtypes and inner blood–retinal barrier regulatory network in early diabetic retinopathy. *Front. Mol. Neurosci.* 15:1048634. doi: 10.3389/fnmol.2022.1048634

Single-cell RNA sequencing reveals the Müller subtypes and inner blood–retinal barrier regulatory network in early diabetic retinopathy

Yan Wang[1†], Xiongyi Yang[2†], Qiumo Li[2†], Yuxi Zhang[2†], Lin Chen[3†], Libing Hong[2], Zhuohang Xie[2], Siyu Yang[4], Xiaoqing Deng[2], Mingzhe Cao[4*], Guoguo Yi[5*] and Min Fu[6*]

[1]Department of Ophthalmology, South China Hospital of Shenzhen University, Shenzhen, China, [2]The Second Clinical School, Southern Medical University, Guangzhou, Guangdong, China, [3]Department of Anesthesiology, Shenzhen Hospital, Southern Medical University, Shenzhen, Guangdong, China, [4]Department of Ophthalmology, The Seventh Affiliated Hospital, Sun Yat-Sen University, Shenzhen, China, [5]Department of Ophthalmology, The Sixth Affiliated Hospital, Sun Yat-Sen University, Guangzhou, Guangdong, China, [6]Department of Ophthalmology, Zhujiang Hospital, Southern Medical University, Guangzhou, Guangdong, China

As the basic pathological changes of diabetic retinopathy (DR), the destruction of the blood-retina barrier (BRB) and vascular leakage have attracted extensive attention. Without timely intervention, BRB damage will eventually lead to serious visual impairment. However, due to the delicate structure and complex function of the BRB, the mechanism underlying damage to the BRB in DR has not been fully clarified. Here, we used single-cell RNA sequencing (RNA-seq) technology to analyze 35,910 cells from the retina of healthy and streptozotocin (STZ)-induced diabetic rats, focusing on the degeneration of the main cells constituting the rat BRB in DR and the new definition of two subpopulations of Müller cells at the cell level, *Ctxn3*$^{+}$Müller and *Ctxn3*$^{-}$Müller cells. We analyzed the characteristics and significant differences between the two groups of Müller cells and emphasized the importance of the *Ctxn3*$^{+}$Müller subgroup in diseases. In endothelial cells, we found possible mechanisms of self-protection and adhesion and recruitment to pericytes. In addition, we constructed a communication network between endothelial cells, pericytes, and Müller subsets and clarified the complex regulatory relationship between cells. In summary, we constructed an atlas of the iBRB in the early stage of DR and elucidate the degeneration of its constituent cells and Müller cells and the regulatory relationship between them, providing a series of potential targets for the early treatment of DR.

KEYWORDS

single-cell RNA sequencing, blood–retinal barrier, Müller cell, diabetic retinopathy, communication network

Introduction

Due to the continuous increase in the global prevalence of diabetes, diabetic retinopathy (DR) is still the main cause of vision loss in many developed countries (Antonetti et al., 2021). Among 246 million patients with diabetes, approximately one-third have signs of diabetic retinopathy (Teo et al., 2021). The pathogenesis of DR is very complex and has not yet been fully elucidated, and its basic pathological changes are the destruction of the blood-retina barrier (BRB) and the formation of retinal neovascularization (Klaassen et al., 2013).

The BRB is composed of the inner BRB (iBRB) and the outer BRB (oBRB), which regulate the movement of liquids and molecules between the ocular vascular bed and retinal tissue and prevent macromolecules and other potentially harmful substances from penetrating the retina (Guymer et al., 2004). The iBRB is established by the tight junction between endothelial cells (Fresta et al., 2020), which is located on the basal layer covered by Müller cells, while pericytes are wrapped in the basal layer and in close contact with endothelial cells. Therefore, damage to the iBRB is considered to be one of the main causes of retinal vascular diseases and has also attracted increasing research and attention. Previous studies have shown that retinal Müller cells play a key role in maintaining the structure and characteristics of the iBRB by relying on their own structural characteristics and strong secretion (Abbott et al., 2006). Pericytes not only provide mechanical support but also form a barrier between microvessels and tissue spaces with endothelial cells, interact with endothelial cells through physical contact and paracrine signals, and regulate the permeability of the BRB barrier, retinal blood flow, and stress response, which are important factors to maintain the stability of the internal environment (Fresta et al., 2020). Most of the current studies focus on the middle and late stages of DR, but more and more evidence supports that the inflammatory response of the retina in the early stage precedes microvascular disease. In the mouse model, the increase of inflammatory mediators such as MIP-1, IL-1, and IL-3 precedes the formation of new blood vessels, and is considered to be the cause of retinal nerve cell death in early diabetes. Studies on some DR animal models have confirmed that inhibiting or knocking out proinflammatory molecules can inhibit diabetes-induced retinal vascular and neurodegenerative diseases. Due to the large number of cells involved in the inflammatory response and the complex regulatory mechanism between cells, the mechanism of iBRB injury in the early stage of DR is not completely clear, and its exploration is still a major challenge.

To solve the above problems, researchers have used single-cell RNA sequencing (scRNA-seq) technology. We used five rat retinal samples (2 normal SD rats, 1 DR sample at 2 weeks, 4 weeks, and 8 weeks each), constructed a single-cell map of a total of 35,910 transcripts, and explored the cellular mechanism of iBRB injury in the early stage of DR. Single-cell sequencing can better reveal the structure of the iBRB and the interaction between iBRB cells through high-resolution detection of each cell in the retina.

We explored the characteristics of pericytes, endothelial cells and two Müller cell subtypes, and constructed a regulatory network among them in the early stage of DR. Our research once again emphasizes the important role of the iBRB and provides a new target for protecting the iBRB and inhibiting the further development of DR, which has far-reaching clinical significance and social value.

Results

An atlas of cell types in the inner blood–retinal barrier

To simulate early DR, we used streptozotocin (STZ) to induce type 2 diabetes in rats. We stripped the retinas of 5 rats (2 normal rats and 3 treated with STZ for 2, 4, and 8 weeks) and isolated and diluted these samples for single-cell transcriptome sequencing (Figure 1A). After quality control, 35,910 high-quality cells were retained: 11,073 cells from normal samples and 24,837 cells from diabetic rats (Supplementary Figure S1A). We performed unbiased clustering on cells with similar gene expression profiles and found 34 clusters. A red blood cell type defined as having a very small number of cells was removed, so we finally obtained 33 cell subtypes. We used uniform manifold approximation and projection (UMAP) dimensional reduction to visualize all cell subtypes. According to a previously reported list of genes expressed in retinal cell types (Supplementary Table S1), we divided 33 clusters into 10 cell types, including a blood-derived macrophage type and a retinal resident cell type. Resident cells included neuronal cells (rod cells, cone cells, horizontal cells, amacrine cells, and bipolar cells), glial cells (Müller cells and microglia cells), endothelial cells, and pericytes (Figure 1B; Supplementary Figures S1B–D).

Based on CellChat analysis, we found that endothelial cells, pericytes, and Müller cells have more complex connections and communication modes than other cells (Figure 1C). These cells are involved in the composition and regulation of the blood–retinal barrier. In addition, we counted the differentially expressed genes (DEGs) of various retinal cells in normal rats and diabetic rats and found that the main cells that make up the iBRB—Müller cells, endothelial cells, and pericytes—changed significantly in the early stage of DR (Figure 1D). Gene Ontology (GO) enrichment analysis showed that all three cell types were related to the formation and proliferation of blood vessels, hypoxia, and cell adhesion, pericytes were also related to vasoconstriction, and Müller cells were also related to the formation and development of neurons (Figure 1E). Therefore, we next focused on the cellular and molecular mechanisms involved in the iBRB microvascular regulatory network, and we also newly defined the marker gene of these cells (Supplementary Table S2).

10.3389/fnmol.2022.1048634

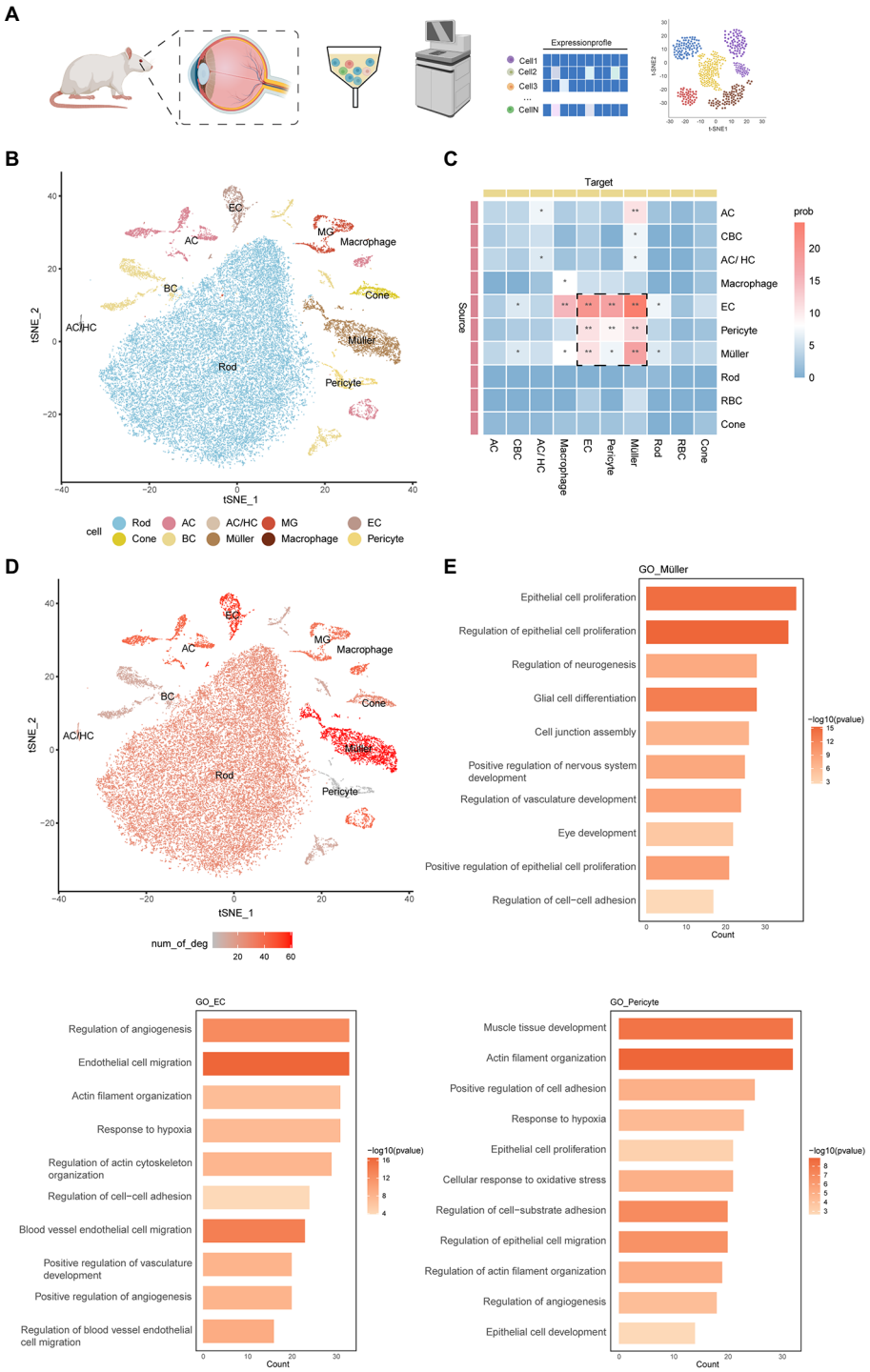

FIGURE 1
An atlas of cell types in the inner blood–retinal barrier. **(A)** Experimental design overview. Cell suspensions were collected from the experimental group (2weeks, 4weeks, 8weeks) and the control group and subjected to 10x library preparation and sequencing, followed by downstream analyses. **(B)** tSNE plot showing different cell types. Cells assigned to the same cluster are similarly colored. AC, amacrine cell; HC, horizontal cell; EC, endothelial cell; MG, microglial cell; BC, bipolar cell. **(C)** The heatmap shows the communication relationships between cells. The source is the sender of the signal, the target is the receiver, and more asterisks indicate stronger communication. Strong communication is shown in red, and weak communication is shown in blue. Prob represents the strength of intercellular communication. **(D)** The feature plot shows the number of DEGs in different cells under DR and normal conditions. The three cells with the largest numbers were pericytes, Müller cells, and endothelial cells. **(E)** The histogram shows the GO enrichment results of pericytes, Müller cells, and endothelial cells, with length representing count and color representing -log10 (*p*-value).

The characteristics of the two subtypes of Müller cells

Müller glial cells are the most important glial cells in the rat retina. They can provide energy and a variety of neurotrophic factors for nerve cells, participate in the transport of neurotransmitters and ions, and play an important role in maintaining the morphological structure of the BRB, protecting the integrity of neurons, and maintaining the homeostasis of the retinal environment. In the early stage of DR, Müller cell injury can lead to the destruction of retinal homeostasis. According to the previous markers (*Apoe*, *Glul*, and *Clu*), we identified two groups of Müller cells and named the two groups of cells *Ctxn3*$^{+}$Müller and *Ctxn3*$^{-}$Müller (Figures 2A,B), according to the expression of the *Ctxn3* gene. We use immunofluorescence experiment to explore the existence of two subpopulations, but more experiments need to be further implemented due to the ambiguity of the results (Figure 2C; Supplementary Figure S2A).

By analyzing the differentially expressed genes of the two groups of Müller cells (Figure 2D), we identified γ-aminobutyric acid (GABA) transporters, as well as the ability to remove excess glutamate through glutamate transporters on the cell membrane and intracellular glutamine synthetase to avoid cytotoxicity caused by glutamate accumulation(Coughlin et al., 2017). The ingested GABA is then acted on by GABA aminotransferase on mitochondria, and *Ctxn3*$^{-}$Müller cells showed lower levels of this transporter than *Ctxn3*$^{+}$Müller cells. We also found that both types of Müller cells express glutathione transferases (GSTs) and aquaporins (AQP4). GSTs protect retinal neurons from oxidative damage. AQP4 is involved in the drainage process of the neuroretina and avoids retinal tissue edema. Interestingly, glutathione transferase and AQP4 are more highly expressed in *Ctxn3*$^{+}$Müller cells. In addition, the overexpression of matrix metalloproteinase (MMP-14) and inhibitor of DNA binding/differentiation (ID) were observed in *Ctxn3*$^{+}$Müller cells. The former participates in the degradation of collagen in the extracellular matrix, which has an important protective effect on the fibrosis of retinal tissue after ischemia and hypoxia. Moreover, MMP-14 and Id proteins were related to neocapillaries. In terms of inflammation, *Ctxn3*$^{+}$Müller cells specifically overexpressed the vascular adhesion molecule VCAM1, which may suggest its possible role in the pathogenesis of diabetic microangiopathy. Furthermore, Müller cells can release inflammatory factors such as interleukin 33 (Il33), suggesting that *Ctxn3*$^{+}$Müller cells can participate in the inflammatory response in the retina. Interestingly, however, many genes related to photosensitivity, such as *Pde6b* and *Cngb1*, were observed to be highly expressed in some *Ctxn3*$^{-}$Müller cells. Combined with previous studies, Müller cells may exist as a special type of optical fiber while researchers have found that Müller cells also have an inseparable relationship with photoreceptor differentiation. However, our data cannot avoid the possibility of photoreceptor containment and whether *Ctxn3*$^{-}$Müller cells have these effects here is our further research content (Reichenbach and Bringmann, 2013).

To further explore the role of *Ctxn3*$^{+}$Müller cells in disease, we conducted SCENIC analysis (Figure 2E). Two types of transcription factors are mainly upregulated in *Ctxn3*$^{+}$Müller cells: (1) AP-1 family members, such as Jun, Fos, and Jund; and (2) SOX family members, such as Sox2 and Sox9. We showed the expression of target genes downstream of important transcription factors with UMAP plots (Figures 2F,G; Supplementary Figure S2B). Through the network diagram, we found that the AP-1 family can regulate the changes in Id protein (Figure 2H). Id1-4 have been observed to be upregulated in *Ctxn3*$^{+}$Müller cells. Id1 and Id3 were closely related to angiogenesis in previous studies and are loops in the amplification loop of vascular endothelial growth factor (Vegf) and transforming growth factor Tgf-β (Song et al., 2011; Georgiadou et al., 2014; Young et al., 2015). Similarly, elevated levels of *Egr1*, a gene downstream of Fos and Jun, have been shown to mediate retinal vascular dysfunction in diabetic rats (Ao et al., 2019). The above findings suggest that *Ctxn3*$^{+}$Müller cells actively participate in the occurrence and development of the disease. Sox proteins are a class of transcription factors found in animals. These molecules belong to the DNA binding proteins of the high mobility group (HMG) superfamily. We observed that Sox2 and Sox9 jointly regulate many genes related to Müller cell structure and function, such as retinol-binding protein 1 (*Rlbp1*), receptor *Gpr37*, and integrated membrane protein. Many studies have shown that Notch signaling is an important regulator of developmental and postdevelopmental processes. *Notch2* and the Notch downstream genes *Hes1* and *Sox9*, which are abundant in mature retina, are important factors for retinal Müller cells to maintain structural stability and development and survival (Muto et al., 2009; Bhatia et al., 2011; Zhu et al., 2013; Bachleda et al., 2016). Notably, Sox2 can also regulate the release of Il33, which further proves that *Ctxn3*$^{+}$Müller is involved in retinal inflammation. In conclusion, we believe that *Ctxn3*$^{+}$Müller cells, as an important component of Müller cells in the iBRB regulatory network, play a major role by expressing angiogenic factors and coordinating angiogenesis-related transcription factors. We found potential targets that may regulate and affect the participation of *Ctxn3*$^{+}$Müller cells in destruction of vascular function, angiogenesis, and the inflammatory response. We also explored important factors that maintain the stability of cell structure and function, providing new ideas for the treatment of diseases.

Characteristics and interrelationship of endothelial cells and pericytes

Cluster 8 was defined as the endothelial cell population because of the high expression of claudin-5 (*Cldn5*) and occludin (*Ocln*). Claudin-5 is the main structural determinant of the paracellular endothelial barrier, which can promote the closure of tight junctions, thereby reducing vascular permeability and enhancing endothelial barrier function. Occludin is also a transmembrane component of tight junctions between the endothelium, which can regulate the permeability of the BRB. Platelet-derived growth factor

10.3389/fnmol.2022.1048634

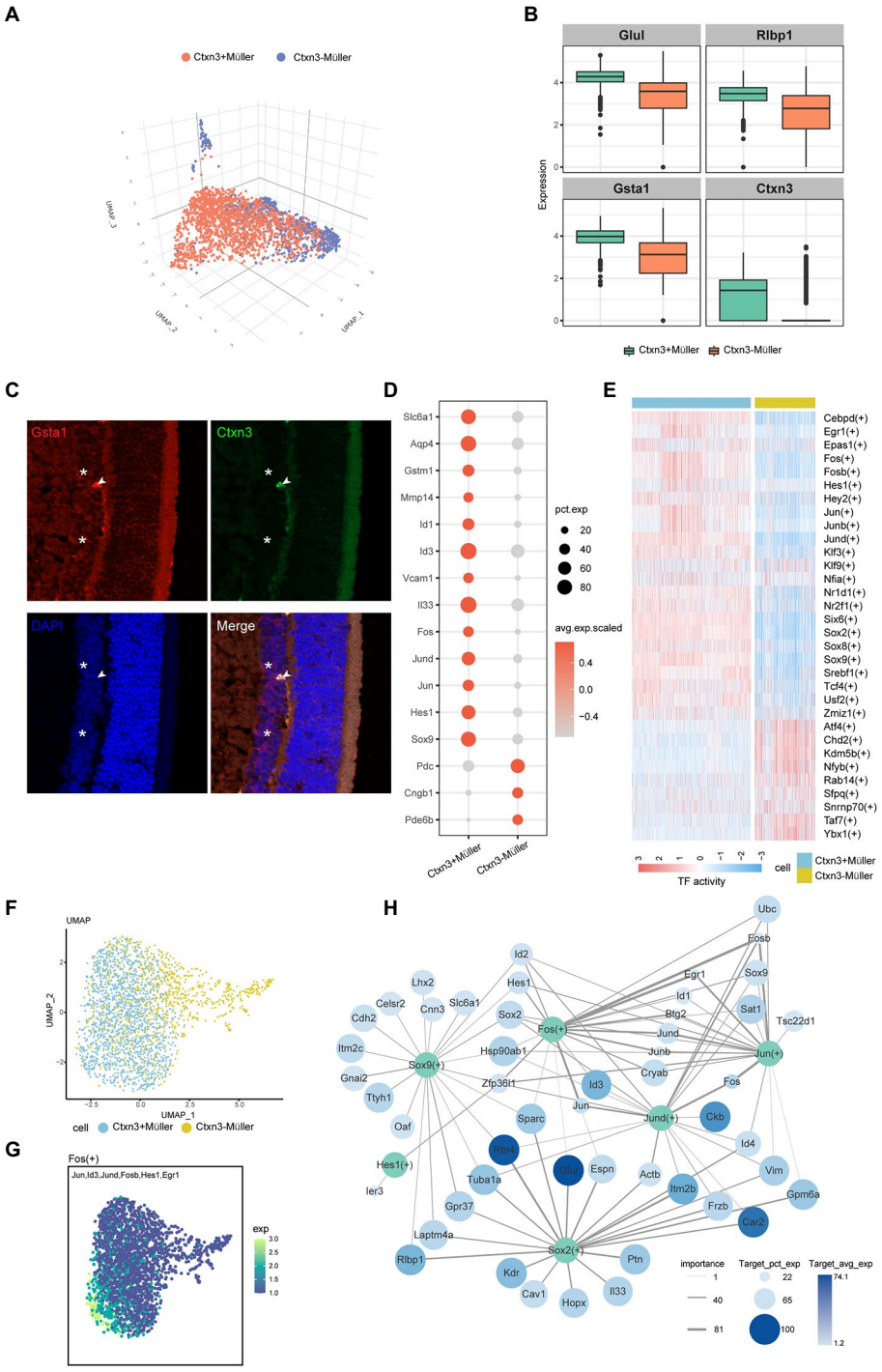

FIGURE 2
The characteristics of the two subtypes of Müller cells. **(A)** Three-dimensional UMAP plot of *Ctxn3*$^{+}$Müller and *Ctxn3*$^{-}$Müller cells. The different colors correspond to different cell types. **(B)** Box diagram showing the expression of the marker genes, which distinguishes the two groups of Müller cells. **(C)** Immunofluorescence labeling for *Gsta1* (red) and *Ctxn3* (green) and DAPI nuclear staining (blue) in the rat retina. *Ctxn3*$^{+}$Müller are indicated by arrowheads, and *Ctxn3*$^{-}$Müller are indicated by asterisk (40×, scale bar 20μm). **(D)** The bubble plot shows the expression of important cytokines in *Ctxn3*$^{+}$Müller and *Ctxn3*$^{-}$Müller cells. The bubble size represents pct.exp., and the color represents avg.exp.scaled. **(E)** Heatmap showing the activity of important TFs in *Ctxn3*$^{+}$Müller and *Ctxn3*$^{-}$Müller cells according to AUCell. **(F)** UMAP plot showing two subclusters of Müller cells. **(G)** UMAP showing the expression of target genes of Fos. The color from dark to light represents increased expression. **(H)** The network diagram shows the important TFs in *Ctxn3*$^{+}$Müller cells and their downstream target gene associations. TFs are shown in green, and the color of the target gene represents Target_avg_exp; the size of the circle represents Target_pct_exp, and the line thickness represents importance. TF with avg. exp.>6 among the top 10 avg. exp. * pct.exp. values was selected as the research object. We selected the top 20 genes by the Target_avg_exp*importance value among the target genes with importance >5 for each TF.

receptor beta (pdgfrβ), which plays essential roles in the development of vascular mural cells, including pericytes and vascular smooth muscle cells, was highly expressed in clusters 20 and 27. Therefore, we defined these two cell groups as pericytes, named Pericyte_A and Pericyte_B, respectively (Figure 3A).

By analyzing the characteristics of vascular endothelial cells, we found a series of important factors that may be new targets for future disease treatment (Figure 3B; Supplementary Figure S3A). In addition to the characteristic markers of endothelial cells and Vegf receptors, we observed that in DR, the expression of the mitogen-activated protein kinase ERK and its downstream AP-1 family, NF-κB, and other factors in endothelial cells was high. NF-κB further promoted the expression of *Gadd45g*, which is related to cell growth and the apoptosis-related genes *Ctsd* and *Pmaip1*, and regulated the survival of endothelial cells. In addition, endothelial cells highly express the Wnt receptor Fzd4 and the transcription factor lymphoid enhancer Lef1. The typical Wnt/β-catenin signaling pathway has been reported to be one of the key systems that coordinates endothelial cell behavior and regulates angiogenesis(De, 2011), and Lef1 is mainly involved in this signaling pathway. Activation of the classical pathway further promotes the transcription of AP-1 family genes, such as *Jun,* downstream and regulates cell function. There are many factors that affect endothelial injury and promote angiogenesis. In addition to the important role of Vegf and angiotensin, more studies have shown that early growth factor 1 (*Egr1*) is the main mediator in response to Vegf stimulation (Mechtcheriakova et al., 1999). In our data, Vegf promotes an increase in *Egr1* content, which may affect the proliferation and differentiation of endothelial cells and promote angiogenesis and injury. Moreover, we found that von Willebrand factor (VWF) is highly expressed in endothelial cells and is an important factor that aggravates vascular endothelial cell damage and promotes the development of retinopathy (Lip et al., 2000). In addition, endothelial cells specifically overexpress connective tissue growth factor CTGF (*Ccn2*), which is related to the pathogenesis of microvascular complications in diabetes (Tikellis et al., 2004). More studies have shown that hyperglycemia increases the expression of CTGF in rat and human retinas, accompanied by an increase in Vegf (Hughes et al., 2007) and Tgf-β (Tikellis et al., 2004) expression, suggesting that CTGF may be an important target for the treatment of DR. In conclusion, through the analysis of specific factors in endothelial cells, we revealed its role in disease, providing new targets for slowing down the damage to the iBRB.

Interestingly, in the early stage, endothelial cells seem to have protective mechanisms to reduce their own damage. We found that the Notch pathway is significantly activated, and studies have shown that the Vegf and Notch signaling pathways are involved in the process of inducing and selecting tip cells. Inhibiting the Notch pathway can cause the proliferation of vascular endothelial cells and promote the formation of neovascular branches (Hellstrom et al., 2007). The increase in the content of the *Dll4* gene downstream of Vegf can inhibit the formation of new branches and neovascularization of blood vessels through the Notch pathway. Furthermore, endothelial cells increase the contents of bone morphogenetic protein receptor (Bmpr2) and nuclear factor erythrocyte-related factor 2 (Nfe2l2). The lack of the former is a factor leading to severe endothelial inflammation (Simic, 2013), while Nfe2l2 can induce the expression of the glutathione transferase GST gene (Suzuki and Yamamoto, 2015), which can protect cells from damage by active substances. Therefore, we suspect that endothelial cells may play a role in self-protection in the early stage of disease through the above mechanisms. In addition, the tyrosine kinase receptor Tie2, which plays a central role in vascular stability, is mainly located on vascular endothelial cells, and it can be activated by angiopoietin 1 (Angpt1) secreted by Pericyte_A. Activated Tie2 can enhance the survival, adhesion, and integrity of endothelial cells to stabilize blood vessels (Campochiaro and Peters, 2016).

As one of the main cellular components of retinal microvessels, pericytes are closely related to endothelial cells. KEGG analysis showed that Pericyte_A and Pericyte_B showed enhanced vascular smooth muscle contraction, cGMP-PKG, cAMP, and other signaling pathways, which are closely related to the characteristics of pericytes such as regulation of the blood flow of local microvessels through contraction (Figure 3C). In addition, both groups of pericytes have increased tight junctions and other signaling pathways, which are closely related to the location and morphology of pericytes. Pericytes are in close contact with capillary endothelial cells, connecting and adhering to each other. Tight junctions formed by Jamb (Jam2)-Jamc (Jam3) and integrins highly expressed on the surface of pericytes play an important role in maintaining the iBRB and mediating the adhesion of endothelial cells and pericytes.

Next, we compared the two groups of pericytes (Figure 3D; Supplementary Figure S3B). Interestingly, we found that in addition to Pdgfa, Pericyte_ B also expressed Pgf and Ntf3. Pgf was found to negatively regulate endothelial cell barrier function through Vegfr1. Pgf and its receptor Vegfr1 may be new therapeutic targets for angiogenic diseases in human retinal endothelial cells in a high glucose environment. The neurotrophic factor Ntf3 can promote the development and survival of retinal neurons. In contrast, Pericyte_A secretes angiopoietin 2 (*Angpt2*). In ischemic diseases such as DR, the upregulation of Angpt2 inactivates Tie2, leading to vascular leakage, pericyte loss, and inflammation. The coexpression of Angpt2 and Vegfa will accelerate neovascularization in developing retina and ischemic retina models (Campochiaro and Peters, 2016). Both groups of cells express insulin-like growth factor (*Igf1*), and the overexpression of *Igf1* may lead to the accumulation of Vegf. These changes increase the permeability of blood vessels and are related to the loss of vascular tight junction integrity (Chantelau et al., 2008). In terms of receptor expression, both groups of pericytes express endothelin receptor (ETA), reflecting the contractile characteristics of pericytes themselves. In addition, Pericyte_A showed significantly upregulated Pdgfrb and advanced glycation end product-specific receptor (Ager), indicating that it may have

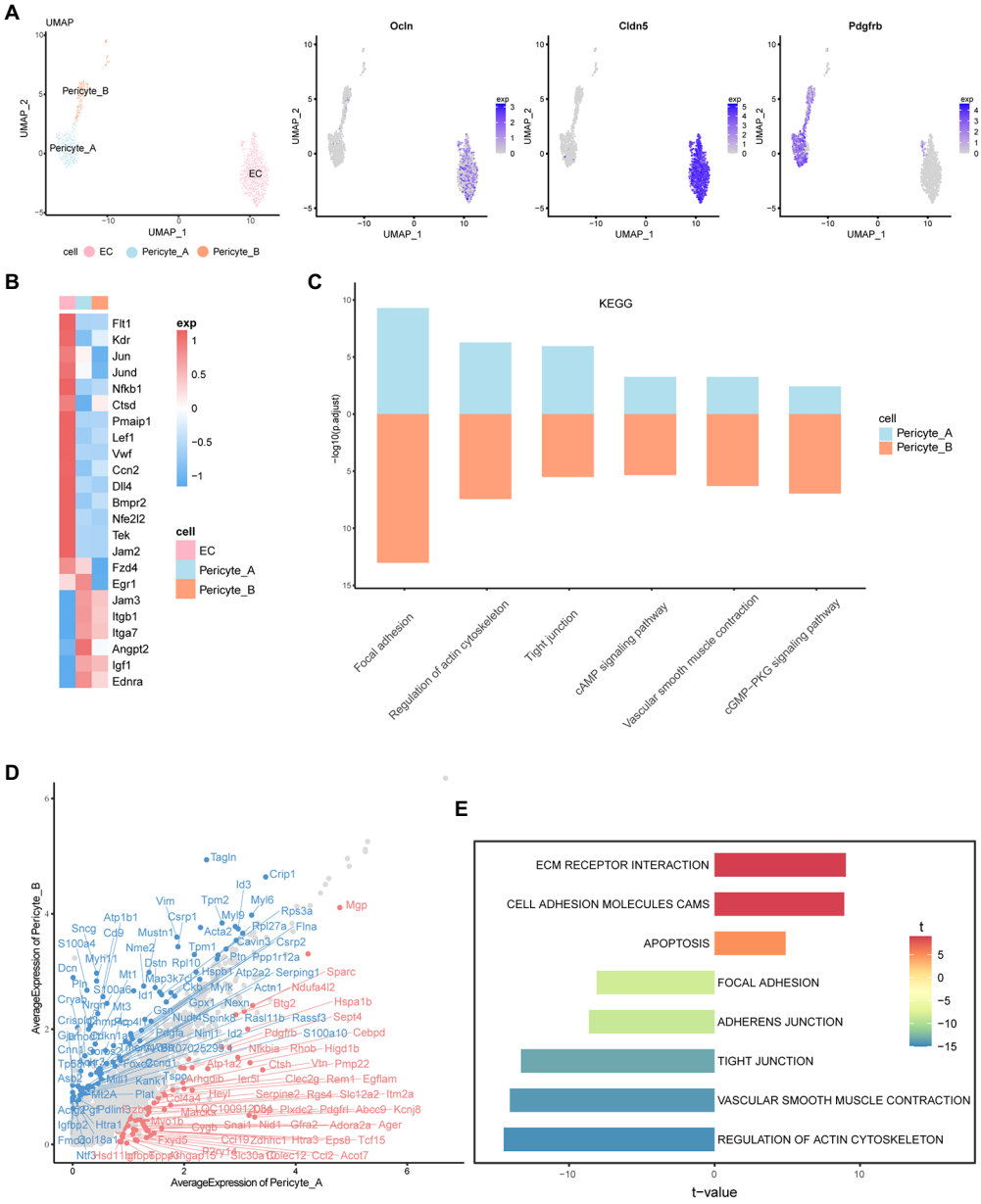

FIGURE 3
Characteristics and interrelationship of endothelial cells and pericytes. **(A)** UMAP diagram of EC, Pericyte_A, and Pericyte_B. The feature plot shows the expression of marker genes in each of the three cells. **(B)** The heatmap shows the expression of important cytokines in the three groups of cells. High expression is in red, and low expression is in blue. **(C)** The histogram shows the KEGG enrichment results of Pericyte_A and Pericyte_B, and the length represents -log10 (p.adjust). **(D)** The scatter plot shows the difference in gene expression between the two groups of cells. The red one is the upregulated gene of Pericyte_A relative to Pericyte_B. Genes with abs (avg_logFC)≥log2 (1.55) and p_val_adj ≤0.01 are labeled. **(E)** The two-way histogram shows the GSVA enrichment results of Pericyte_A compared with Pericyte_B, and both length and color represent the t value. T value is the statistical value of the t test, which is used to infer the size of *p* value.

a stronger ability to migrate to and recruit endothelial cells and may be more susceptible to the effects of high glucose(Zhang et al., 2020).

Gene set variation analysis (GSVA) showed that Pericyte_A had increased ECM receptor interactions and other pathways, while vascular smooth muscle contraction and actin cytoskeleton regulation and other pathways were significantly enriched in Pericyte_B (Figure 3E). Combined with the GSVA and the expression characteristics of factors and receptors secreted by the two groups of peripheral cells, we found that they play different roles in iBRB regulation: Pericyte_A seems to be more vulnerable to a hyperglycemic environment and may be more vulnerable to damage and loss, while Pericyte_B is more similar to vascular smooth muscle cells and has a stronger ability to mediate peripheral cell contraction and regulate retinal blood flow; it also secretes a variety of factors to regulate other cells in the iBRB.

Communication network between the Müller and iBRB

To reveal the mechanism underlying the damage to the iBRB in early DR, we deeply studied the complex communication among Müller cells, endothelial cells, and pericytes. Using CellChat analysis, we found that Müller plays a potential role in the regulation of iBRB through secreting factors (Figure 4A). We found that both groups of Müller cells can secrete VEGF, which can increase vascular permeability and promote the migration and proliferation of vascular endothelial cells and the formation of neovascularization. Vegfr1 (*Flt1*) and Vegfr2 (*Kdr*) receptors are simultaneously expressed on endothelial cells, and Vegf mainly exerts its effect by binding to Vegfr2. Notably, Müller cells themselves also express Vegfr. We speculate that Vegf produced by Müller cells can also act on themselves, but the effect is not clear. However, studies have shown that the Vegf/Vegfr2 signaling pathway is most likely to affect the biological synthesis, secretion, or degradation of brain-derived neurotrophic factor (BDNF) and glial cell-derived neurotrophic factor (GDNF) in Müller cells (Le et al., 2021), promote the survival of Müller cells and have neuroprotective effects. In addition, two groups of Müller cells may act on the receptor Igf2r on Pericyte_B by secreting insulin-like growth factor 2 (Igf2) to regulate its proliferation, differentiation, and survival (Figures 4B,C). Tgf-β is released by Müller cells. It can participate in endothelial cell proliferation, apoptosis, diffusion, and vascular endothelial formation, but its specific role in DR deserves further study.

In DR, abnormal metabolic and pathological conditions, such as oxidative stress and inflammation, can destroy the communication between pericytes and endothelial cells, resulting in the destruction of the BRB. Angiopoietin-like protein 4 (Angptl4) is secreted by endothelial cells and not only acts on Müller cells and pericytes but also affects itself (Figure 4D). Previous studies have confirmed that Angptl4 can regulate the integrity of EC-EC connections, promote an increase in vascular permeability and have a synergistic effect with Vegf (Sodhi et al., 2019). Endothelial cells have a certain regulatory effect on Müller cells and pericytes through Angptl4-Cdh11/Sdc4/Sdc2, but their specific function is worthy of further study (Figure 4E). In addition, we explored some potential methods of pericyte recruitment. Endothelial cells can secrete the protein product Gas6 encoded by growth arrest-specific gene 6, which is an important factor promoting angiogenesis. Gas6 has a selective high affinity for its receptor Axl. Endothelial cells may promote the recruitment and adhesion of pericytes by binding Gas6 to the receptor Axl on pericytes (Lei et al., 2016). Similarly, we found that Pdgfrβ, the receptor of Pdgfβ, was also expressed in the two groups of pericytes. When Pdgfβ secreted by endothelial cells binds to pericyte-specific receptors, it will have the same effect as Gas6. Pdgfβ secreted by endothelial cells binds to the specific receptor Pdgfr of two groups of pericytes, resulting in pericyte recruitment and adhesion to endothelial cells. Interestingly, endothelial cells and Pericyte_B also specifically secrete the chemokines Cxcl12 and Pdgfa, respectively, and act on the corresponding receptors of Pericyte_B and endothelial cells, and whether they have the above recruitment function needs further study.

Discussion

The iBRB is an important structure that ensures the homeostasis of the retina and plays an important role in the pathogenesis of various retinal diseases. It is important to further study and explore the related mechanisms of the steady state and destruction of the blood–retinal barrier to promote the treatment of diabetic retinopathy. Due to the heterogeneity of the retina and the loss of cell type specificity, high-resolution methods such as scRNA-seq with bulk RNA-Seq approaches have inestimable value for the study of the destruction mechanism of the iBRB in DR. Using scRNA-seq, we identified two different Müller cell subsets and constructed a communication network among endothelial cells, pericytes, and Müller cells in the iBRB.

Müller cells are important cells for maintaining the normal structure and function of the iBRB, especially in cell communication. We defined two new Müller cell subpopulations, *Ctxn3*$^{+}$ Müller and *Ctxn3*$^{-}$ Müller, according to the expression of the *Ctxn3* gene. However, our immunofluorescence experiment results are somewhat ambiguous, and since our results are based on the scRNA-seq, they may just reflect a series of Müller cell phenotypes, so more accurate experiments are needed to verify the correctness of clustering. Our work is consistent with the previous observation that Müller cells participate in the formation and regulation of nerves and blood vessels by secreting cytokines to maintain BRB integrity. Interestingly, there were significant functional differences between the two groups of Müller cells. Our analysis data showed that *Ctxn3*$^{+}$Müller cells specifically overexpressed many genes related to metabolic waste clearance of the BRB, such as aquaporin AQP4 and GABA transporter. However, *Ctxn3*$^{-}$ Müller cells showed upregulation of many genes related to photosensitivity, such as *Pde6b* and *Cngb1*. In addition, compared with *Ctxn3*$^{-}$ Müller cells, *Ctxn3*$^{+}$ Müller cells upregulated the regulation of differentiation inhibitors (Id1-4) and transcription factors Hes1 and Sox9, suggesting that they may have potential roles in promoting endothelial injury and angiogenesis. The above research shows that there is a special Müller cell subpopulation, *Ctxn3*$^{+}$ Müller, which may have important significance in maintaining iBRB and early retinal vascular leakage. It is urgent to reduce the damage of retinal Müller cells to iBRB and thus hinder the progress of DR. Therefore, further research is needed to determine the more specific mechanism of *Ctxn3*$^{+}$ Müller cells in the early stage of DR.

We also investigated the function of endothelial cells in the inner blood–retinal barrier in early DR. This study explored the protective mechanism of endothelial cells and proposed a series of potential early therapeutic targets for DR. The results showed that *Dll4*, *Bmpr2*, and *Nrf2* were highly expressed in endothelial

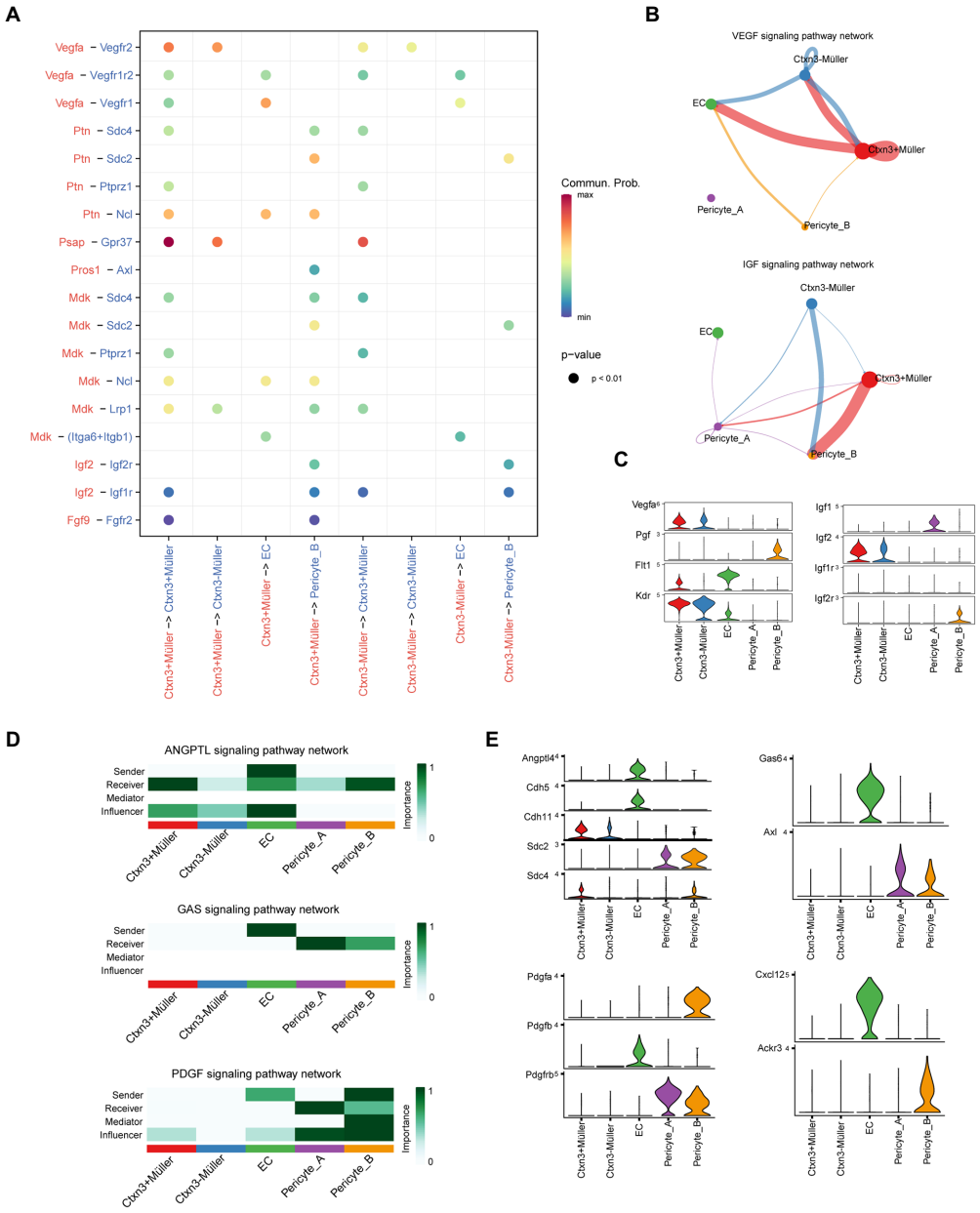

FIGURE 4
Communication network between Müller cells and the iBRB. **(A)** Comparison of the significant ligand–receptor pairs. The color indicates the value of communication probability, and the point size indicates the p-value. Ligands and signal senders are marked in red, while receptors and receivers of signals are marked in blue. **(B)** VEGF and IGF signaling pathway networks among Müller cells, ECs, and pericytes. The thickness of the line represents the strength of the communication signal. **(C)** Violin diagram shows the expression of genes of ligand–receptor pairs in the VEGF and IGF signaling pathway network. **(D)** The heatmap shows the sender, receiver, mediator, and influencer of each signaling pathway network. The color represents the strength of the communication signal. **(E)** Violin diagram showing the expression of genes of ligand–receptor pairs in the ANGPTL, GAS, PDGF, and CXCL signaling pathway networks.

cells. Inhibition of the Dll4-Notch1 pathway promotes excessive sprouts and endothelial proliferation in the retina (Zhu et al., 2022), and the high expression of *Bmpr2* is also conducive to regulating excessive angiogenesis. In an experimental model of *Bmpr2* knockout, vascular endothelial cell proliferation was observed (Theilmann et al., 2020). *Nrf2* can activate the expression of many antioxidant enzymes, and ROS produced by NADPH oxidase can also activate *Nrf2*. Its function in preventing atherosclerosis has been confirmed (Alonso-Pineiro et al., 2021). Since ROS are significantly increased in the early stage of DR, we speculate that *Nrf2* is also involved in endothelial self-protection during DR. Tie2, which plays an important role in vascular stability, is highly expressed in endothelial cells. Previous studies have shown that activated Tie2 increases endothelial cell

survival and cell connectivity integrity (Campochiaro and Peters, 2016), thereby stabilizing the vascular system.

After we studied the changes in various cells in DR, our CellChat analysis of the main cells of the iBRB identified the communication and connection modes between them through direct and indirect mechanisms, thus generating important insights into the regulatory mechanism of the iBRB. The cellular communication network is a weighted digraph consisting of significant ligand–receptor pairs between interacting cell groups, showing the number of ligand–receptor interactions detected between different cell groups. The same cell group can send or receive signals. CellChat uses network analysis to infer the strength of different cell groups as senders and receivers of signals during cell communication. Cell grouping is a prerequisite for using CellChat. Before cell communication analysis, cell clustering needs to be carried out carefully to capture cell groups with biological significance. CellChat can quantify the similarity between all significant signal pathways and group them according to the similarity of their cell communication networks. In particular, we observed that the Notch pathway plays an important role in their communication. Previous studies have shown that *Jag1* and *Dll4* are secondary to increased hyperglycemia, activate the normative and non-normative Notch1 pathways, and destroy the endothelial adhesion connection in the retina in diabetes (Miloudi et al., 2019), which is consistent with our findings. Moreover, inhibiting the proliferation of Müller cells by targeting Notch ligands inhibits the overexpression of ECM proteins (Fan et al., 2020) and prevents proliferative diabetes retinopathy and retinal fibrosis. These new findings suggest that the Notch pathway plays an important role in the destruction of the iBRB in the early stage of DR through intercellular communication. We found that in the communication network of the iBRB, Müller cells and endothelial cells are primarily responsible for secreting signal proteins, while pericytes receive secretory factors. Our data suggest that Müller cells regulate the survival of pericytes by secreting Igf2. Moreover, Vegf secreted by Müller cells not only regulates the proliferation of endothelial cells but also acts on Vegfr expressed by itself. Studies have shown that the Vegf/Vegfr2 signaling pathway promotes the survival of Müller cells and has neuroprotective effects (Xu et al., 2019). We found that endothelial cells connect with pericytes through Wnt5b-Fzd4 and affect cell migration and inflammation in angiogenesis through the ncWNT signaling pathway (Zhang et al., 2018; Carvalho et al., 2019), which may be an important target for DR treatment. These newly discovered intercellular communications are crucial to deciphering the regulatory mechanism of the iBRB in the early stage of DR.

In conclusion, we used scRNA-seq to investigate the role and connection of cells in the formation of the iBRB in the early stage of DR, emphasizing the importance of the new Müller subgroup *Ctxn3*$^{+}$ Müller in the mechanism of injury and disease. In addition, our study proposes a global view of new therapeutic targets and cell functions of DR, cell communication, and its relationship in early DR. These data provide new insights into the stability of the iBRB and the mechanism of early destruction in DR. However, our experiment does have the problem of fewer samples, and more experiments and data need to be used to study and prove these findings.

Materials and methods

Ethics statement

All animals were housed in a pathogen-free environment and had free access to food. The animal care and use agreement was approved by the Science and Technology Commission of Shanghai Municipality and complies with all applicable institutional and government regulations on the ethical use of animals.

Animals

The SD rats were fed with high sugar and high fat diet for 4 weeks, and were fasted but watered after 12 h, and administered 40 mg/kg streptozotocin (STZ, 10 g/l, Sigma company, United States) diluted with sterile fresh citrate buffer (0.1 mM, pH 4.3–4.5) to establish the diabetic rat model *via* one-time intraperitoneal injection. If the tail vein blood glucose was higher than 16.7 mmol/l on the third and seventh days after injection, the type 2 diabetes model was successful. If the standard was not met, repeat the injection once. Those who failed to meet the standard twice were excluded. At the same time, the control group used sodium citrate instead of STZ for intraperitoneal injection.

Tissue processing and cell purification

Animals believed to have diabetes were maintained on a high sugar diet, and tail vein blood samples were regularly collected and measured to assess blood glucose levels. The control group was fed with D12450B 10 kcal% feed, and the experimental group was fed with D12492 60 kcal% feed. The imported feed is produced by American Research Diets. The rats in the experimental group (2 weeks, 4 weeks, 8 weeks) and the control group were anesthetized by intraperitoneal injection and fixed in the supine position. First, the eyeball was removed, and then, the corneoscleral margin was cut. The eyeball was radially incised, the anterior segment and vitreous were removed, and the iris structure was slowly separated from the intact retina and placed in a protective solution.

The tissues were transported in sterile culture dishes with 10 ml of 1x Dulbecco's phosphate-buffered saline (DPBS; Thermo Fisher, Cat. No. 14190144) on ice. The residual tissue storage solution was removed, and the tissues were then minced on ice. We used 0.25% trypsin (dissociation enzyme; Thermo Fisher, Cat. No. 25200–072) and 10 μg/ml DNase I (Sigma, Cat. no. 11284932001) dissolved in PBS with 5% fetal bovine serum (FBS; Thermo Fisher, Cat. No. SV30087.02) to digest the tissues. The tissues were dissociated at 37°C with a shaking speed of 50 RPM

for approximately 40 min. We repeatedly collected the dissociated cells at intervals of 20 min to increase cell yield and viability. The cell suspensions were filtered using a 40 μm nylon cell strainer, and red blood cells were removed by 1X Red Blood Cell Lysis Solution (Thermo Fisher, Cat. No. 00–4,333-57). The dissociated cells were washed with 1x DPBS containing 2% FBS. The cells were stained with 0.4% Trypan Blue (Thermo Fisher, Cat. No. 14190144), and viability was assessed on a Countess® II Automated Cell Counter (Thermo Fisher).

Preparation and sequencing of the 10x library

Beads with unique molecular identifiers (UMIs) and cell barcodes were loaded close to saturation so that each cell was paired with a bead in gel beads-in-emulsion (GEMs). After exposure to cell lysis buffer, polyadenylated RNA molecules hybridized to the beads. The beads were retrieved into a single tube for reverse transcription. In cDNA synthesis, each cDNA molecule was tagged on the 5′ end (that is, the 3′ end of the messenger RNA transcript) with the UMI and a cell label indicating its cell of origin. Briefly, 10× beads were subjected to second-strand cDNA synthesis, adaptor ligation, and universal amplification. Sequencing libraries were prepared using randomly interrupted whole-transcriptome amplification products to enrich the 3′ ends of the transcripts linked with the cell barcodes and UMIs. All the remaining procedures, including library construction, were performed according to the standard manufacturer's protocol (CG000206 Rev. D). The sequencing libraries were quantified using a High Sensitivity DNA Chip (Agilent) on a Bioanalyzer 2,100 and with a Qubit High Sensitivity DNA Assay (Thermo Fisher Scientific). The libraries were sequenced on a NovaSeq6000 instrument (Illumina) in 2 × 150 bp mode.

scRNA-seq analysis

The Read10X() function in the Seurat package (3.2.2) was used to merge the data from all samples into R (4.0.2) and generate an aggregated Seurat object (Butler et al., 2018; Stuart et al., 2019). Low-quality cells (<350 genes/cell, >3,000 genes/cell, <3 cells/gene, >20% mitochondrial genes, and > 20% ribosomal genes) were excluded. Finally, 35,910 single cells were further studied: 11073 normal tissue-derived cells and 24,837 diabetes tissue-derived cells. For identification of cell clusters, the highly variable gene list was first analyzed by principal component analysis. Jackstraw analysis was used to identify important PCs, and the first 20 PCs were used in this process. We used the FindClusters() function to perform clustering (resolution 1.0). We used two data dimensionality reduction algorithms (2D UMAP and tSNE; Becht et al., 2018; Kobak and Berens, 2019) for visualization. For standardized gene expression data, we used the FndAllMarkers function to list the markers of each cell cluster. Compared with other cells, the expression of these marker genes was upregulated by at least 1.3 times. The main cell types were determined according to the markers described in the literature. A cluster identified as red blood cells (cluster 32, cell number 52) was removed, and 10 cell types were finally obtained.

Gene enrichment analysis

The FindMarkers function was used to identify DEGs between two clusters (adjusted p value <0.01 and fold change [FC] >1.3). The R package clusterProfiler (Yu et al., 2012) was used to perform GO (Gene Ontology C, 2015) and Kyoto Encyclopedia of Genes and Genomes (KEGG; Kanehisa et al., 2016) pathway enrichment for the DEGs.

Based on the gene set data for *Rattus norvegicus* in the msigdbr package (selections: C2 for category and CP: KEGG for subcategory; Liberzon et al., 2015), we performed GSVA to analyze the enriched gene sets between different cell subtypes. GSVA mainly converts the expression matrix of genes among different strains into the expression matrix of gene sets among samples to evaluate whether different pathways are enriched among different strains. Basic gene set enrichment uses genes in a predefined gene set to evaluate the distribution trend in the gene table sorted by phenotype correlation, so as to judge its contribution to phenotype. Subsequently, the limma package was used to determine the gene sets with significant differences (Ritchie et al., 2015). Differentially enriched signatures were defined as having FDR adjusted p values <0.05 and |mean score difference| values ≥0.1.

Cell–cell interaction analysis

To visualize and analyze intercellular communications from scRNA-seq data, we conducted CellChat analysis (Jin et al., 2021). We create a new CellChat object from our Seurat object. The cell types were added to the CellChat object as cell metadata. CellChat identified differentially overexpressed ligands and receptors for each cell group and associated each interaction with a probability value to quantify communications between the two cell groups mediated by these signaling genes. Significant interactions were identified on the basis of a statistical test that randomly permuted the group labels of cells and then recalculated the interaction probability.

Immunostaining

Rats were deeply anesthetized with ketamine and xylazine and then sacrificed by cervical dislocation. The eyes were immediately removed, the corneas were incised, and each eye was immersed in 2% paraformaldehyde (PFA) for 3 h at room temperature. After immersion and fixation, the eyes were washed with phosphate-buffered saline (PBS), and the lenses were carefully removed. The eyes were immersed in 10% sucrose for 30 min, 20% sucrose for

2 h, and 30% sucrose overnight at 4°C for cryoprotection before being embedded in Tissue-Tek optimal cutting temperature compound (OCT) and frozen on dry ice. Eighteen micron sections were cut on a cryostat. The sections were blocked for 1 h with 10% normal goat or donkey serum in PBS with 0.5% Triton X-100, incubated overnight at 4°C with primary antibodies, and then incubated with secondary antibodies.

SCENIC analysis

SCENIC is a computational method for simultaneous gene regulatory network reconstruction and cell-state identification from single-cell RNA-seq data (Aibar et al., 2017).[1] We first obtained the scores of different TFs in cell subtypes through R and then screened according to the criteria of avg.exp. ≥ 1, pct.exp. ≥ 20 and RelativeActivity ≥1 to obtain important TFs. We obtained the target gene information of TFs using pyscenic and screened them with the same criteria. The input matrix used for pyscenic was the normalized expression matrix output from Seurat.

According to the expression of TFs and target genes and their importance, we visualized the results using the Cytoscape tool (version 3.8.2; specific screening criteria are shown in the legend). The interactions of each TF and target were merged manually to analyze the overall interactions. We also visualized the target genes of several important TFs with a UMAP plot.

Data availability statement

The datasets presented in this study can be found in the National Center for Biotechnology Information Gene Expression Omnibus database under accession number GSE209872.

Ethics statement

The animal study was reviewed and approved by the Science and Technology Commission of Shanghai Municipality.

1 http://scenic.aertslab.org

Author contributions

YW designed the experiments. YZ performed the data analysis and constructed the datasets. XY drew the figures. SY collected the biopsies and performed the immunofluorescence experiments. XY, QL, and YZ wrote the manuscript. YW, MF, GY, and MC supervised this project. All authors reviewed and edited the manuscript, contributed to the article, and approved the submitted version.

Acknowledgments

We thank all members of this project for stimulating discussions during the preparation of this manuscript.

Conflict of interest

The authors declare that the research was conducted in the absence of any commercial or financial relationships that could be construed as a potential conflict of interest.

Publisher's note

Supplementary material

The Supplementary material for this article can be found online at: https://www.frontiersin.org/articles/10.3389/fnmol.2022.1048634/full#supplementary-material

References

Abbott, N. J., Ronnback, L., and Hansson, E. (2006). Astrocyte-endothelial interactions at the blood-brain barrier. *Nat. Rev. Neurosci.* 7, 41–53. doi: 10.1038/nrn1824

Aibar, S., Gonzalez-Blas, C. B., Moerman, T., Huynh-Thu, V. A., Imrichova, H., Hulselmans, G., et al. (2017). SCENIC: single-cell regulatory network inference and clustering. *Nat. Methods* 14, 1083–1086. doi: 10.1038/nmeth.4463

Alonso-Pineiro, J. A., Gonzalez-Rovira, A., Sanchez-Gomar, I., Moreno, J. A., and Duran-Ruiz, M. C. (2021). Nrf2 and Heme Oxygenase-1 involvement in atherosclerosis related oxidative stress. *Antioxidants (Basel).* 10, 1463. doi: 10.3390/antiox10091463

Antonetti, D. A., Silva, P. S., and Stitt, A. W. (2021). Current understanding of the molecular and cellular pathology of diabetic retinopathy. *Nat. Rev. Endocrinol.* 17, 195–206. doi: 10.1038/s41574-020-00451-4

Ao, H., Liu, B., Li, H., and Lu, L. (2019). Egr1 mediates retinal vascular dysfunction in diabetes mellitus via promoting p53 transcription. *J. Cell. Mol. Med.* 23, 3345–3356. doi: 10.1111/jcmm.14225

Bachleda, A. R., Pevny, L. H., and Weiss, E. R. (2016). Sox2-deficient Muller glia disrupt the structural and functional maturation of the mammalian retina. *Invest. Ophthalmol. Vis. Sci.* 57, 1488–1499. doi: 10.1167/iovs.15-17994

Becht, E., McInnes, L., Healy, J., Dutertre, C. A., Kwok, I. W. H., Ng, L. G., et al. (2018). Dimensionality reduction for visualizing single-cell data using UMAP. *Nat. Biotechnol.* 37, 38–44. doi: 10.1038/nbt.4314

Bhatia, B., Singhal, S., Tadman, D. N., Khaw, P. T., and Limb, G. A. (2011). SOX2 is required for adult human muller stem cell survival and maintenance

of progenicity in vitro. *Invest. Ophthalmol. Vis. Sci.* 52, 136–145. doi: 10.1167/iovs.10-5208

Butler, A., Hoffman, P., Smibert, P., Papalexi, E., and Satija, R. (2018). Integrating single-cell transcriptomic data across different conditions, technologies, and species. *Nat. Biotechnol.* 36, 411–420. doi: 10.1038/nbt.4096

Campochiaro, P. A., and Peters, K. G. (2016). Targeting Tie2 for treatment of diabetic retinopathy and diabetic macular edema. *Curr. Diab. Rep.* 16:126. doi: 10.1007/s11892-016-0816-5

Carvalho, J. R., Fortunato, I. C., Fonseca, C. G., Pezzarossa, A., Barbacena, P., Dominguez-Cejudo, M. A., et al. (2019). Non-canonical Wnt signaling regulates junctional mechanocoupling during angiogenic collective cell migration. elife. 8, e45853. doi: 10.7554/eLife.45853

Chantelau, E., Kimmerle, R., and Meyer-Schwickerath, R. (2008). Insulin, insulin analogues and diabetic retinopathy. *Arch. Physiol. Biochem.* 114, 54–62. doi: 10.1080/13813450801900553

Coughlin, B. A., Feenstra, D. J., and Mohr, S. (2017). Muller cells and diabetic retinopathy. *Vis. Res.* 139, 93–100. doi: 10.1016/j.visres.2017.03.013

De, A. (2011). Wnt/Ca2+ signaling pathway: a brief overview. *Acta Biochim. Biophys. Sin. Shanghai* 43, 745–756. doi: 10.1093/abbs/gmr079

Fan, J., Shen, W., Lee, S. R., Mathai, A. E., Zhang, R., Xu, G., et al. (2020). Targeting the notch and TGF-beta signaling pathways to prevent retinal fibrosis in vitro and in vivo. *Theranostics.* 10, 7956–7973. doi: 10.7150/thno.45192

Fresta, C. G., Fidilio, A., Caruso, G., Caraci, F., Giblin, F. J., Leggio, G. M., et al. (2020). A new human blood-retinal barrier model based on endothelial cells, Pericytes, and astrocytes. *Int. J. Mol. Sci.* 21:1636. doi: 10.3390/ijms21051636

Gene Ontology C (2015). Gene ontology consortium: going forward. *Nucleic Acids Res.* 43, D1049–D1056. doi: 10.1093/nar/gku1179

Georgiadou, D., Sergentanis, T. N., Sakellariou, S., Filippakis, G. M., Zagouri, F., Vlachodimitropoulos, D., et al. (2014). VEGF and id-1 in pancreatic adenocarcinoma: prognostic significance and impact on angiogenesis. *Eur. J. Surg. Oncol.* 40, 1331–1337. doi: 10.1016/j.ejso.2014.01.004

Guymer, R. H., Bird, A. C., and Hageman, G. S. (2004). Cytoarchitecture of choroidal capillary endothelial cells. *Invest. Ophthalmol. Vis. Sci.* 45, 1660–1666. doi: 10.1167/iovs.03-0913

Hellstrom, M., Phng, L. K., Hofmann, J. J., Wallgard, E., Coultas, L., Lindblom, P., et al. (2007). Dll4 signalling through Notch1 regulates formation of tip cells during angiogenesis. *Nature* 445, 776–780. doi: 10.1038/nature05571

Hughes, J. M., Kuiper, E. J., Klaassen, I., Canning, P., Stitt, A. W., Van Bezu, J., et al. (2007). Advanced glycation end products cause increased CCN family and extracellular matrix gene expression in the diabetic rodent retina. *Diabetologia* 50, 1089–1098. doi: 10.1007/s00125-007-0621-4

Jin, S., Guerrero-Juarez, C. F., Zhang, L., Chang, I., Ramos, R., Kuan, C. H., et al. (2021). Inference and analysis of cell-cell communication using cell chat. *Nat. Commun.* 12:1088. doi: 10.1038/s41467-021-21246-9

Kanehisa, M., Sato, Y., Kawashima, M., Furumichi, M., and Tanabe, M. (2016). KEGG as a reference resource for gene and protein annotation. *Nucleic Acids Res.* 44, D457–D462. doi: 10.1093/nar/gkv1070

Klaassen, I., Van Noorden, C. J., and Schlingemann, R. O. (2013). Molecular basis of the inner blood-retinal barrier and its breakdown in diabetic macular edema and other pathological conditions. *Prog. Retin. Eye Res.* 34, 19–48. doi: 10.1016/j.preteyeres.2013.02.001

Kobak, D., and Berens, P. (2019). The art of using t-SNE for single-cell transcriptomics. *Nat. Commun.* 10:5416. doi: 10.1038/s41467-019-13056-x

Le, Y. Z., Xu, B., Chucair-Elliott, A. J., Zhang, H., and Zhu, M. (2021). VEGF mediates retinal Muller cell viability and neuroprotection through BDNF in diabetes. *Biomol. Ther.* 11, 712. doi: 10.3390/biom11050712

Lei, X., Chen, M., Nie, Q., Hu, J., Zhuo, Z., Yiu, A., et al. (2016). In vitro and in vivo antiangiogenic activity of desacetylvinblastine monohydrazide through inhibition of VEGFR2 and Axl pathways. *Am. J. Cancer Res.* 6, 843–858.

Liberzon, A., Birger, C., Thorvaldsdottir, H., Ghandi, M., Mesirov, J. P., and Tamayo, P. (2015). The molecular signatures database (MSigDB) hallmark gene set collection. *Cell Syst.* 1, 417–425. doi: 10.1016/j.cels.2015.12.004

Lip, P. L., Belgore, F., Blann, A. D., Hope-Ross, M. W., Gibson, J. M., and Lip, G. Y. (2000). Plasma VEGF and soluble VEGF receptor FLT-1 in proliferative retinopathy: relationship to endothelial dysfunction and laser treatment. *Invest. Ophthalmol. Vis. Sci.* 41, 2115–2119. PMID: 10892852

Mechtcheriakova, D., Wlachos, A., Holzmuller, H., Binder, B. R., and Hofer, E. (1999). Vascular endothelial cell growth factor-induced tissue factor expression in endothelial cells is mediated by EGR-1. *Blood* 93, 3811–3823. doi: 10.1182/blood.V93.11.3811

Miloudi, K., Oubaha, M., Menard, C., Dejda, A., Guber, V., Cagnone, G., et al. (2019). NOTCH1 signaling induces pathological vascular permeability in diabetic retinopathy. *Proc. Natl. Acad. Sci. U. S. A.* 116, 4538–4547. doi: 10.1073/pnas.1814711116

Muto, A., Iida, A., Satoh, S., and Watanabe, S. (2009). The group E sox genes Sox8 and Sox9 are regulated by notch signaling and are required for Muller glial cell development in mouse retina. *Exp. Eye Res.* 89, 549–558. doi: 10.1016/j.exer.2009.05.006

Reichenbach, A., and Bringmann, A. (2013). New functions of Muller cells. *Glia* 61, 651–678. doi: 10.1002/glia.22477

Ritchie, M. E., Phipson, B., Wu, D., Hu, Y., Law, C. W., Shi, W., et al. (2015). Limma powers differential expression analyses for RNA-sequencing and microarray studies. *Nucleic Acids Res.* 43:e47. doi: 10.1093/nar/gkv007

Simic, T. (2013). Anti-inflammatory and anti-atherogenic role of BMP receptor II in atherosclerosis. *Futur. Cardiol.* 9, 619–622. doi: 10.2217/fca.13.61

Sodhi, A., Ma, T., Menon, D., Deshpande, M., Jee, K., Dinabandhu, A., et al. (2019). Angiopoietin-like 4 binds neuropilins and cooperates with VEGF to induce diabetic macular edema. *J. Clin. Invest.* 129, 4593–4608. doi: 10.1172/JCI120879

Song, X., Liu, S., Qu, X., Hu, Y., Zhang, X., Wang, T., et al. (2011). BMP2 and VEGF promote angiogenesis but retard terminal differentiation of osteoblasts in bone regeneration by up-regulating Id1. *Acta Biochim. Biophys. Sin. Shanghai* 43, 796–804. doi: 10.1093/abbs/gmr074

Stuart, T., Butler, A., Hoffman, P., Hafemeister, C., Papalexi, E., Mauck, W. M. 3rd, et al. (2019). Comprehensive integration of single-cell data. *Cells* 177, 1888–1902.e21. doi: 10.1016/j.cell.2019.05.031

Suzuki, T., and Yamamoto, M. (2015). Molecular basis of the Keap1-Nrf2 system. *Free Radic. Biol. Med.* 88, 93–100. doi: 10.1016/j.freeradbiomed.2015.06.006

Teo, Z. L., Tham, Y. C., Yu, M., Chee, M. L., Rim, T. H., Cheung, N., et al. (2021). Global prevalence of diabetic retinopathy and projection of burden through 2045: systematic review and meta-analysis. *Ophthalmology* 128, 1580–1591. doi: 10.1016/j.ophtha.2021.04.027

Theilmann, A. L., Hawke, L. G., Hilton, L. R., Whitford, M. K. M., Cole, D. V., Mackeil, J. L., et al. (2020). Endothelial BMPR2 loss drives a proliferative response to BMP (bone morphogenetic protein) 9 via prolonged canonical signaling. *Arterioscler. Thromb. Vasc. Biol.* 40, 2605–2618. doi: 10.1161/ATVBAHA.119.313357

Tikellis, C., Cooper, M. E., Twigg, S. M., Burns, W. C., and Tolcos, M. (2004). Connective tissue growth factor is up-regulated in the diabetic retina: amelioration by angiotensin-converting enzyme inhibition. *Endocrinology* 145, 860–866. doi: 10.1210/en.2003-0967

Xu, B., Zhang, H., Zhu, M., and Le, Y. Z. (2019). Critical role of trophic factors in protecting Muller glia: implications to neuroprotection in age-related macular degeneration, diabetic retinopathy, and anti-VEGF therapies. *Adv. Exp. Med. Biol.* 1185, 469–473. doi: 10.1007/978-3-030-27378-1_77

Young, V. J., Ahmad, S. F., Brown, J. K., Duncan, W. C., and Horne, A. W. (2015). Peritoneal VEGF-A expression is regulated by TGF-beta1 through an ID1 pathway in women with endometriosis. *Sci. Rep.* 5:16859. doi: 10.1038/srep16859

Yu, G., Wang, L. G., Han, Y., and He, Q. Y. (2012). Cluster profiler: an R package for comparing biological themes among gene clusters. *OMICS* 16, 284–287. doi: 10.1089/omi.2011.0118

Zhang, S. S., Hu, J. Q., Liu, X. H., Chen, L. X., Chen, H., Guo, X. H., et al. (2020). Role of Moesin phosphorylation in retinal Pericyte migration and detachment induced by advanced glycation Endproducts. *Front Endocrinol (Lausanne).* 11:603450. doi: 10.3389/fendo.2020.603450

Zhang, C., Lai, M. B., Pedler, M. G., Johnson, V., Adams, R. H., Petrash, J. M., et al. (2018). Endothelial cell-specific inactivation of TSPAN12 (Tetraspanin 12) reveals pathological consequences of barrier defects in an otherwise intact vasculature. *Arterioscler. Thromb. Vasc. Biol.* 38, 2691–2705. doi: 10.1161/ATVBAHA.118.311689

Zhu, M. Y., Gasperowicz, M., and Chow, R. L. (2013). The expression of NOTCH2, HES1 and SOX9 during mouse retinal development. *Gene Expr. Patterns* 13, 78–83. doi: 10.1016/j.gep.2012.12.001

Zhu, G., Lin, Y., Ge, T., Singh, S., Liu, H., Fan, L., et al. (2022). A novel peptide inhibitor of Dll4-Notch1 signalling and its pro-angiogenic functions. *Br. J. Pharmacol.* 179, 1716–1731. doi: 10.1111/bph.15743

frontiers | Frontiers in Cellular Neuroscience

TYPE Original Research
PUBLISHED 12 December 2022
DOI 10.3389/fncel.2022.1046050

OPEN ACCESS

EDITED BY
Shuxin Li,
Temple University, United States

REVIEWED BY
Saijilafu,
Medical College of Soochow University, China
Li Zhang,
Nanjing General Hospital of Nanjing Military Command, China

*CORRESPONDENCE
Ling-Chi Xu
xulingchi@ntu.edu.cn

†These authors have contributed equally to this work and share first authorship

SPECIALTY SECTION
This article was submitted to Cellular Neuropathology, a section of the journal Frontiers in Cellular Neuroscience

RECEIVED 23 September 2022
ACCEPTED 28 November 2022
PUBLISHED 12 December 2022

CITATION
Cao H-J, Huang L, Zheng M-R, Zhang T and Xu L-C (2022) Characterization of circular RNAs in dorsal root ganglia after central and peripheral axon injuries. *Front. Cell. Neurosci.* 16:1046050. doi: 10.3389/fncel.2022.1046050

Characterization of circular RNAs in dorsal root ganglia after central and peripheral axon injuries

Hong-Jun Cao[1†], Li Huang[1†], Meng-Ru Zheng[1], Tao Zhang[2] and Ling-Chi Xu[1*]

[1]Jiangsu Clinical Medicine Center of Tissue Engineering and Nerve Injury Repair, Co-Innovation Center of Neuroregeneration, Nantong University, Nantong, Jiangsu, China, [2]School of Medicine and Holistic Integrative Medicine, Nanjing University of Chinese Medicine, Nanjing, Jiangsu, China

In central nervous system, axons fail to regenerate after injury while in peripheral nervous system, axons retain certain regenerative ability. Dorsal root ganglion (DRG) neuron has an ascending central axon branch and a descending peripheral axon branch stemming from one single axon and serves as a suitable model for the comparison of growth competence following central and peripheral axon injuries. Molecular alterations underpin different injury responses of DRG branches have been investigated from many aspects, such as coding gene expression, chromatin accessibility, and histone acetylation. However, changes of circular RNAs are poorly characterized. In the present study, we comprehensively investigate circular RNA expressions in DRGs after rat central and peripheral axon injuries using sequencing analysis and identify a total of 33 differentially expressed circular RNAs after central branch injury as well as 55 differentially expressed circular RNAs after peripheral branch injury. Functional enrichment of host genes of differentially expressed circular RNAs demonstrate the participation of Hippo signaling pathway and Notch signaling pathway after both central and peripheral axon injuries. Circular RNA changes after central axon injury are also linked with apoptosis and cellular junction while changes after peripheral axon injury are associated with metabolism and PTEN-related pathways. Altogether, the present study offers a systematic evaluation of alterations of circular RNAs in rat DRGs following injuries to the central and peripheral axon branches and contributes to the deciphering of essential biological activities and mechanisms behind successful nerve regeneration.

KEYWORDS

circular RNAs, dorsal root ganglion, nerve regeneration, central axon injury, peripheral axon injury

Introduction

Axon injury elicits distal nerve degeneration, impairs neuronal functions, and causes motor incapacity, sensation loss, and neuropathic pain (Stoll and Muller, 1999; Hu, 2016). The recovery effects and consequences of axon injury largely rely on the special localizations of injured axons. In the mammalian central nervous system, injured axons fail to regenerate toward their original targets and thus permanent functional disability is commonly observed after central nerve injury (Mahar and Cavalli, 2018). On the contrast, in the peripheral nervous system, injured axons preserve certain regenerative abilities and functional recovery of injured peripheral nerves may be achieved, especially after mild peripheral nerve injury, such as nerve crush and nerve injury with short gaps (He and Jin, 2016).

Dorsal root ganglion (DRG) neurons are pseudounipolar neurons that have two separate axonal branches stemming from one single axon. The central branch extends into the central nervous system and is generally incapable of regeneration after axon injury while the peripheral branch projects to peripheral target and often obtains a remarkable growth capacity (Neumann and Woolf, 1999; Nascimento et al., 2018). Despite different local microenvironment of central and peripheral axon, such as surrounding oligodendrocytes, astrocytes, and microglial cells in central nerves versus Schwann cells in peripheral nerves, the intrinsic regenerative status of DRG neurons are distinct after injury to central and peripheral branches (Hoffman, 2010; Renthal et al., 2020). Injury to the two separate axon branches generates a useful model for the direct comparisons of molecular alterations in DRGs and offers valuable insights into failed central axon growth and successful peripheral axon growth.

Recently, the application of high-throughput RNA sequencing discriminates genetic changes in DRGs after central and peripheral axon injury and reveals the essential roles of reactive oxygen species in axon regeneration by comparing changes between non-regenerative central axon injury and regenerative peripheral axon injury (Hervera et al., 2018). ATAC and ChIP sequencing explore underlying epigenomic characteristics (Palmisano et al., 2019). Recent data further decipher distinct cellular changes in DRGs after central axon injury and peripheral axon injury using single cell sequencing (Avraham et al., 2021). However, the unique features of circular RNAs in DRGs following central and peripheral axon injuries are less understood.

Circular RNAs are endogenous non-coding RNAs with covalently closed loop structures formed by transcript back splicing (Zhang et al., 2014; Chen and Yang, 2015). Although the abundances of a large number of circular RNAs are lower than their counterpart linear RNAs, circular RNAs are generally stably expressed (Memczak et al., 2013; Zhang et al., 2019). Moreover, many circular RNAs exhibit distinctive tissue and development expression patterns and play important regulatory roles under various physiological and pathological conditions (Memczak et al., 2013). Here, we made a injury to DRG central axon branch as well as a injury to the peripheral axon branch, collected DRGs at 24 h after nerve injury, and investigated circular RNA signatures in response to central and peripheral axon injuries, aiming to decipher key elements for effective nerve regeneration from the aspect of regulatory RNAs.

Materials and methods

Animals

A total of 56 8-week-old male Sprague Dawley rats (∼200 g) were obtained from the Animal Center of Nantong University. Rats were randomly divided into central axon branch injury group, central axon branch sham surgery group, peripheral axon branch injury group, and peripheral axon branch sham surgery group, with 14 rats in each group.

Animal work was carried out in accordance with the guidelines of Nantong University Institutional Animal Care and Ethical approved by the Administration Committee of Experimental Animals, Nantong University, Jiangsu Province, China.

Surgery procedures

Central and peripheral axon injuries were performed according to a previous publication with modifications (Avraham et al., 2021). Briefly, for central axon branch injury, after anesthesia, a small midline skin incision was made at the L2-L3 vertebral level, dura mater was removed, and dorsal root was cut. For central axon branch sham surgery, dura mater was removed while dorsal root was not injured. Rats subjected to central axon branch injury or central axon branch sham surgery were designated as DR-Exp and DR-Sham, respectively. For peripheral axon branch injury, after anesthesia, a skin incision was made on the lateral aspect of the mid-thigh of rat hind limb and sciatic nerve was cut. For peripheral axon branch sham surgery, sciatic nerve was exposed but not injured. Rats subjected to peripheral axon branch injury or peripheral axon branch sham surgery were designated as SN-Exp and SN-Sham, respectively. Rat L4-L5 DRGs were collected at 24 h after surgery and stored at −80°C.

Sequencing analysis

Total RNAs was extracted from rat L4-L5 DRGs using TRIzol reagent kit (Invitrogen, Carlsbad, CA, USA) and subjected to RNA quality check using an Agilent Bioanalyzer (Agilent Technologies, Palo Alto, CA, USA). mRNA was enriched, fragmented into short fragments, and reverse transcripted to cDNA. cDNA fragments were ligated to Illumina

sequencing adapters and sequencing was performed using HiSeq^{TM} 4000 platform. RNA libraries were sequenced on the Illumina sequencing platform by Genedenovo Biotechnology Co., Ltd. (Guangzhou, China). Sequencing data were stored in Genome Sequence Archive database with accession number CRA006070.

For bioinformatic analysis, raw reads obtained from sequencing were filtered by fastp (version 0.18.0) to obtain high quality clean reads (Chen et al., 2018). Clean reads were mapped to the reference genome. Circular RNAs were identified using bioinformatic tools bowtie 2 and find_circ (Memczak et al., 2013). Identified circular RNAs were then filtered to obtain highly reliable data under following conditions: breakpoint equal to 1, anchor_overlap less than or equal to 2, edit less than or equal to 2, n_uniq greater than 2, best_qual_A greater than 35, or best_qual_B greater than 35, n_uniq greater than int (samples/2), and length less than 100 k. The abundances of circular RNAs were quantified using back-spliced reads per million mapped reads (RPM) according to the formula RPM = 10^6C/N, where C represented the back-spliced reads of target genes and N represented total back-spliced reads. RNA differential expression analysis was performed using edgeR by normalization and p-value calculation. Circular RNAs with $\log_2$ (fold change) > 1 or < -1 and p-value < 0.05 were screened and considered as differentially expressed. The functions of host genes of differentially expressed circular RNAs were discovered using kyoto encyclopedia of genes and genomes (KEGG) pathway enrichment analysis (Kanehisa and Goto, 2000), reactome enrichment analysis, and gene ontology (GO) term enrichment analysis (Croft et al., 2011; Fabregat et al., 2018). The significances of KEGG pathways, reactome pathways, or GO terms were calculated based on the numbers of all genes and candidate genes that with KEGG, reactome, or GO annotation as well as the numbers of all genes and candidate genes annotated to specific KEGG pathways, reactome pathways, or GO terms.

The competing endogenous RNA (ceRNA) network was constructed by assembling all co-expression competing circular RNAs, microRNAs, and mRNAs. Expression correlations between circular RNAs and microRNAs as well as microRNAs and mRNAs were analyzed using the Spearman Rank correlation coefficient (SCC) to screen negatively co-expressed circular RNA-microRNA pairs or microRNA-mRNA pairs. Expression correlations between circular RNAs and mRNAs were analyzed using Pearson correlation coefficient (PCC) to screen positively co-expressed circular RNA-mRNA pairs. The interactions between circular RNAs, microRNAs, and mRNAs in the ceRNA network were displayed using Cytoscape software (v3.6.0).

Real-time PCR

Total RNA extracted from rat L4-L5 DRG was reversely transcribed to cDNA using PrimeScript RT Reagent Kit (TaKaRa Biotechnology Co., Ltd., Dalian, China). The characterization of circular RNA was determined using the divergent primers annealing at the distal end. PCR product was subjected to agarose gel electrophoresis and Sanger sequencing (Genewiz, Inc., Suzhou, China). The relative abundance of novel_circ_000290, novel_circ_001817 and novel_circ_000991 was determined using the comparative $2^{-\Delta\Delta Ct}$ method with GAPDH as the reference gene. Primer sequences were as follows (5′−3′): novel_circ_000290-F TGACTCCCTCTCTGGTGACA, novel_circ_000290-R GCTTCCTCAACACCATCACC, novel_circ_001817-F AGGCTATTCGCTTAGGATTCCA, novel_circ_001817-R CCAGGTAGTTGTGTCCGATGTA, novel_circ_000991-F CATCCACGTCATGAGGAACAG, novel_circ_000991-R TACAAGACACTCGGTCTACCAA, GAPDH-F ACAGCAACAGGGTGGTGGAC, and GAPDH-R TTTGAGGGTGCAGCGAACTT.

Statistical analysis

Numerical data were expressed as mean with SEM. Comparisons between DR-Exp and DR-sham as well as SN-Exp and SN-sham were generated using unpaired t-test (GraphPad Prism 6.0 software, GraphPad Software, La Jolla, CA, USA). Significantly difference was set at a p-value < 0.05.

Results

Overview of circular RNA profiles in rat DRGs following central and peripheral axon injuries

Dorsal root ganglions of rats underwent central axon branch injury, peripheral axon branch injury, or corresponding sham surgery were collected at 24 h after surgery and subjected to sequencing to obtain a global view of circular RNAs in rat DRGs after central and peripheral axon injuries (**Figure 1A**). Sequencing clean reads were mapped to approximately 97% of total reads. More than 90% mapped reads were uniquely mapped, indicating high read quality for RNA sequencing (**Figure 1B**).

Bioinformatic analysis identified a total of 2,310 circular RNAs in rat DRGs. These circular RNAs showed similar sample expression distributions after central and peripheral axon injuries (**Figure 1C**). The localizations of circular RNAs were also comparable in difference groups. About 18% of circular RNAs were derived from intergenic regions, about 16% were derived from intronic regions, while the majority were derived from exonic regions (**Figure 1D**). Most circular RNAs were localized in nuclear genome instead of the mitochondrial genome. Among all chromosomes, chromosome 1 contained the largest numbers of circular RNAs (**Figure 1E**).

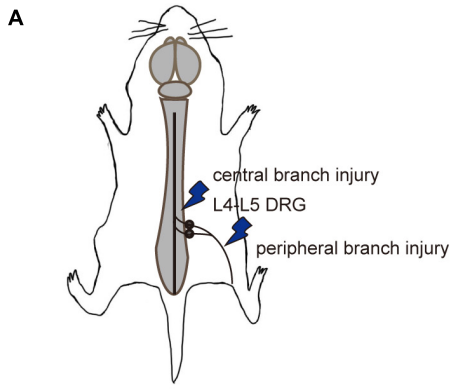

B

Sample	Total	Unique Mapped(%)	Multiple Mapped(%)	Total Mapped(%)
DR-Exp	64370696	58195941 (90.41%)	4246256 (6.60%)	62442197 (97.00%)
DR-Sham	81438480	73790674 (90.61%)	5262692 (6.46%)	79053366 (97.07%)
SN-Exp	88505424	80078114 (90.48%)	5858160 (6.62%)	85936274 (97.10%)
SN-Sham	80130636	72394606 (90.35%)	5229953 (6.53%)	77624559 (96.87%)

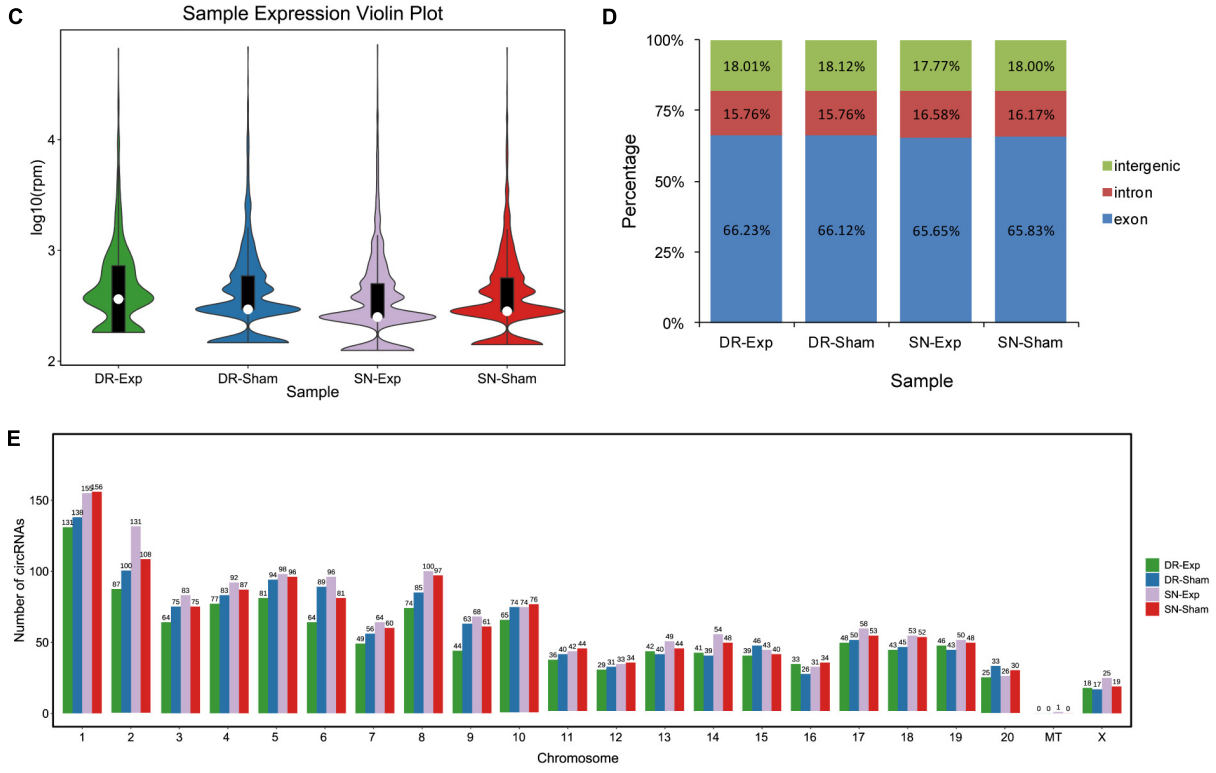

FIGURE 1
Characterization of circular RNAs in dorsal root ganglions (DRGs). **(A)** Schematic representation of nerve injury model. **(B)** The alignment of sequencing reads to the reference genome in rats underwent central injury, peripheral injury, or corresponding sham surgery. **(C)** The violin plot of the abundances of circular RNAs. **(D)** Genomic origins of circular RNAs. **(E)** Numbers of circular RNAs in each chromosome.

Identification of differentially expressed circular RNAs following central and peripheral axon injuries

The expression levels of circular RNAs after central and peripheral axon injuries were determined to screen differentially expressed circular RNAs. A total of 33 circular RNAs were found to be differentially expressed after central branch injury versus central branch sham surgery, with 9 circular RNAs up-regulated and 24 circular RNAs down-regulated (Figures 2A, B). A larger number of circular RNAs showed different expression levels after peripheral branch injury versus peripheral branch sham surgery, with 32 circular RNAs up-regulated and 23 circular RNAs down-regulated (Figures 2A, C). The expression patterns of these differentially expressed circular RNAs were displayed in heatmaps (Figures 2D, E) and circular RNAs with the most robust changes were presented (Figure 2F). The abundances of these up-regulated or down-regulated circular RNAs were further examined using real-time PCR to validate the accuracy of sequencing analysis. PCR results showed that, in keeping with sequencing data, peripheral axon injuries

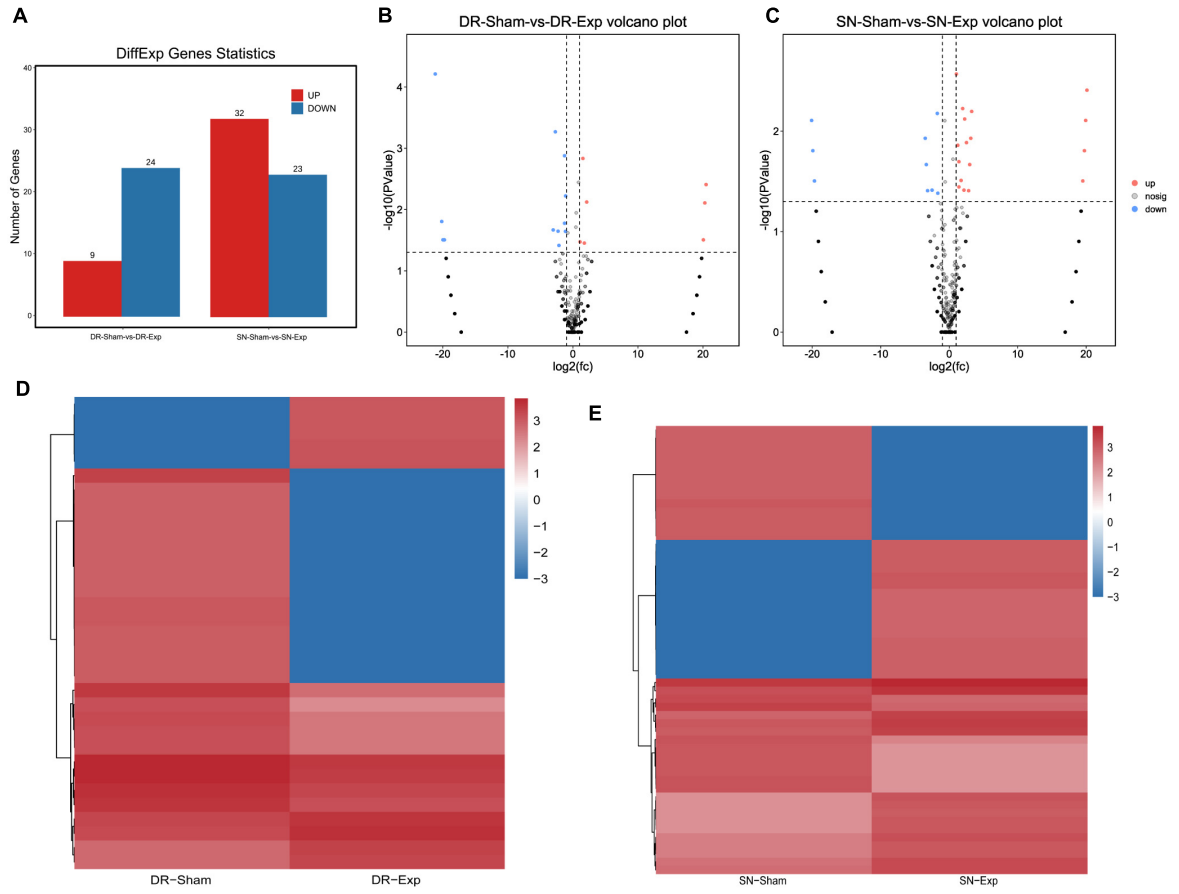

F

Up-regulated after DR	log2(fc)	PValue
novel_circ_000047	20.47	0.00
novel_circ_001159	20.28	0.01
novel_circ_000359	20.06	0.03
novel_circ_001612	20.06	0.03
novel_circ_002279	20.06	0.03
Down-regulated after DR	log2(fc)	PValue
novel_circ_001677	-21.16	0.00
novel_circ_000151	-20.16	0.02
novel_circ_000677	-20.16	0.02
novel_circ_000595	-19.97	0.03
novel_circ_001577	-19.97	0.03

Up-regulated after SN	log2(fc)	PValue
novel_circ_000804	20.10	0.00
novel_circ_001812	20.10	0.00
novel_circ_000020	19.93	0.01
novel_circ_002033	19.93	0.01
novel_circ_002099	19.93	0.01
Down-regulated after SN	log2(fc)	PValue
novel_circ_002307	-20.10	0.01
novel_circ_000290	-19.91	0.02
novel_circ_000447	-19.91	0.02
novel_circ_000633	-19.91	0.02
novel_circ_001413	-19.91	0.02

FIGURE 2
Changes of circular RNAs after rat central and peripheral axon injuries. **(A)** Numbers of differentially expressed circular RNAs after rat central and peripheral axon injuries. Red indicates up-regulated after nerve injury while blue indicates down-regulated after nerve injury. **(B,C)** The volcano plots of differentially expressed circular RNAs in DRGs after **(B)** central axon injury and **(C)** peripheral axon injury. **(D,E)** Heatmaps of differentially expressed circular RNAs in dorsal root ganglions (DRGs) after **(D)** central axon injury and **(E)** peripheral axon injury. Red indicates relatively high abundance and blue indicates relatively low abundance. **(F)** Top 5 up-regulated and top 5 down-regulated circular RNAs after rat central and peripheral axon injuries.

reduced novel_circ_000290 and novel_circ_001817 expression, and central axon injuries induced novel_circ_000290 expression (Figure 3).

Detailed information of all differentially expressed circular RNAs, including their chromosome localizations, genomic start/end sites, spliced lengths, annotation types (intergenic,

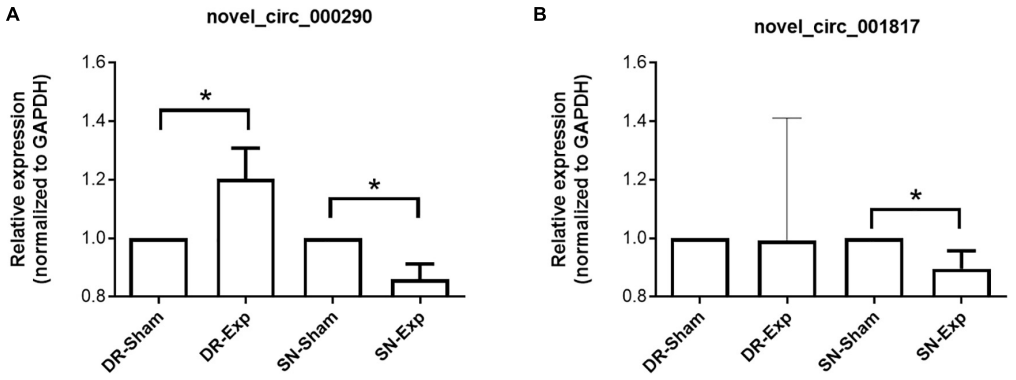

FIGURE 3
Validation of the expression of differentially expressed circular RNAs after rat central and peripheral axon injuries. Relative expression levels of novel_circ_000290 **(A)** and novel_circ_001817 **(B)** after rat central and peripheral axon injuries. Data are summarized from 3 experiments and presented as mean with SEM. *P-value < 0.05.

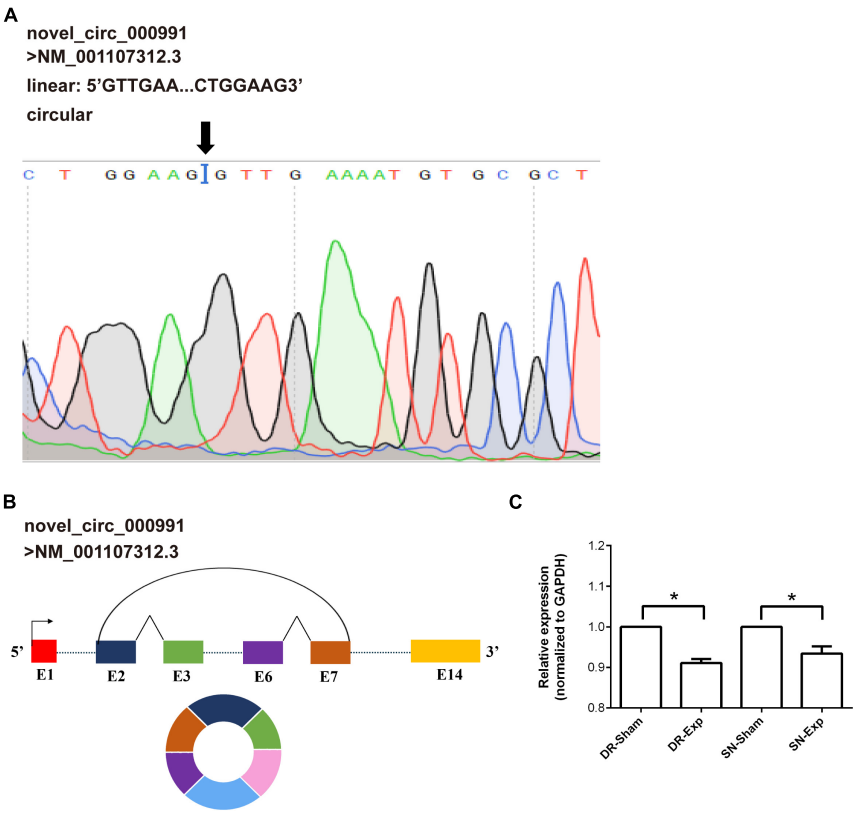

FIGURE 4
Validation of the characterization and expression of circular RNA novel_circ_000991. **(A)** Determination of novel_circ_000991 by Sanger sequencing. Black arrow indicates the site of back-splicing. **(B)** Schematic representation of the genomic locus of novel_circ_000991 in its host gene Mtmr7 (NM_001107312.3). **(C)** Relative expression levels of novel_circ_000991 after rat central and peripheral axon injuries. Data are summarized from 3 experiments and presented as mean with SEM. *P-value < 0.05.

intronic, and exonic), and host genes, was provided in Supplementary Tables 1, 2.

Among these differentially expressed circular RNAs, circular RNA novel_circ_000991 exhibited relative high abundances in all groups and thus was further examined for its characterization and expression. Consistent with RNA sequencing outcome, Sanger sequencing recognized Mtmr7 (NM_001107312.3) as the host gene of novel_circ_000991 (Figure 4A). The cyclization

site of novel_circ_000991 was demonstrated in a schematic diagram (Figure 4B). Moreover, the relative expression pattern of novel_circ_000991 was measured by RT-PCR. Sequencing data revealed a considerable reduction of the abundance of novel_circ_000991 after central axon branch injury and a decreasing trend (although not of statistical significance) after peripheral axon branch injury. RT-PCR results supported that central and peripheral axon injuries reduced novel_circ_000991 expression (Figure 4C).

Functional analysis for host genes of differentially expressed circular RNAs following central axon injury

To discover biological implications of differentially expressed circular RNAs in DRGs after central axon injury, host genes of these differentially expressed circular RNAs were annotated with KEGG database. Top enrich KEGG pathways were listed in Table 1 and displayed in a circular graph. A large number of development and regeneration-related pathways, such as Hippo signaling pathway (ko04391 and ko04392), Notch signaling pathway (ko04330), phosphatidylinositol signaling pathway (ko04070), and Neurotrophin signaling pathway (ko04722), were identified as significantly enriched KEGG pathways. Many cellular processes, including apoptosis (ko04214) and cellular junction-related pathways, i.e., adherens junction (ko04520) and gap junction (ko04540), were also found to be highly enriched (Figure 5A).

Reactome analysis further demonstrated the considerable participation of Hippo signaling (Signaling by Hippo, R-RNO-2028269) and apoptosis (Apoptosis cleavage of cellular proteins, R-RNO-111465; Apoptotic execution phase, R-RNO-75153; and Cleavage of p-STK3 (p-MST2) by caspase 3, R-RNO-2028697) in DRGs after central axon injury. The enrichment of reactome pathways WWTR1 (TAZ) binds to ZO-1 (TJP1) (R-RNO-2064417), phosphorylation of Cx43 by c-src (R-RNO-191636), c-src mediated regulation of Cx43 function and closure of gap junctions (R-RNO-191647), and regulation of gap junction activity (R-RNO-191654) implied changes of cellular junction. The identification of significantly involved reactome pathway Caspase-mediated cleavage of TJP1 (R-RNO-351913) further indicated the association of apoptosis and cellular junction regulation. Moreover, the recognition of reactome pathways IL6 binds IL6R-2 (R-RNO-1067640), IL6 binds IL6R (R-RNO-1067667), and IL6:IL6R-2 binds IL6ST-2 (R-RNO-1067676) illuminated the involvement of immune responses in central axon injury-mediated molecular features (Figure 5B).

Gene ontology term enrichment revealed the involvement of GO biological processes biological regulation, cellular process, regulation of biological process, GO cellular components cell, cell part, and GO molecular function binding (Figure 5C).

Functional analysis for host genes of differentially expressed circular RNAs following peripheral axon injury

Host genes of differentially expressed circular RNAs in DRGs after peripheral axon injury were subjected to functional enrichment as well. Similar as changes after central axon injury, Hippo signaling pathway and Notch signaling pathway were found to be enriched after peripheral axon injury. A metabolism-related pathway, Inositol phosphate metabolism (ko00562), was also discovered as a commonly involved KEGG pathway in host genes of differentially expressed circular RNAs after both central and peripheral axon injuries. Besides Inositol phosphate metabolism, many other metabolism-related pathways, i.e., Glycosphingolipid biosynthesis-ganglio series (ko00604), Mucin type O-glycan biosynthesis (ko00512), Fatty acid degradation (ko00071), and Fatty acid metabolism (ko01212) were also significantly changed in DRGs after peripheral axon injury (Table 2 and Figure 6A).

Reactome enrichment analysis showed the essential involvement of PTEN in peripheral axon injury-induced changes in DRGs as many significant reactome pathways were related to PTEN, including Regulation of PTEN gene transcription (R-RNO-8943724), SALL4 recruits NuRD to PTEN gene (R-RNO-8943780), and PTEN Regulation (R-RNO-6807070). Furthermore, TP53-related reactome pathways

TABLE 1 Top 20 enriched kyoto encyclopedia of genes and genomes (KEGG) pathways for host genes of differentially expressed circular RNAs after rat central axon injury.

No	ID	Description
1	ko04391	Hippo signaling pathway -fly
2	ko04392	Hippo signaling pathway–multiple species
3	ko04214	Apoptosis–fly
4	ko04330	Notch signaling pathway
5	ko05110	Vibrio cholerae infection
6	ko04961	Endocrine and other factor-regulated calcium reabsorption
7	ko04978	Mineral absorption
8	ko05120	Epithelial cell signaling in Helicobacter pylori infection
9	ko04520	Adherens junction
10	ko00562	Inositol phosphate metabolism
11	ko05412	Arrhythmogenic right ventricular cardiomyopathy (ARVC)
12	ko01521	EGFR tyrosine kinase inhibitor resistance
13	ko04061	Viral protein interaction with cytokine and cytokine receptor
14	ko04540	Gap junction
15	ko04260	Cardiac muscle contraction
16	ko05410	Hypertrophic cardiomyopathy (HCM)
17	ko04070	Phosphatidylinositol signaling system
18	ko04974	Protein digestion and absorption
19	ko05017	Spinocerebellar ataxia
20	ko04722	Neurotrophin signaling pathway

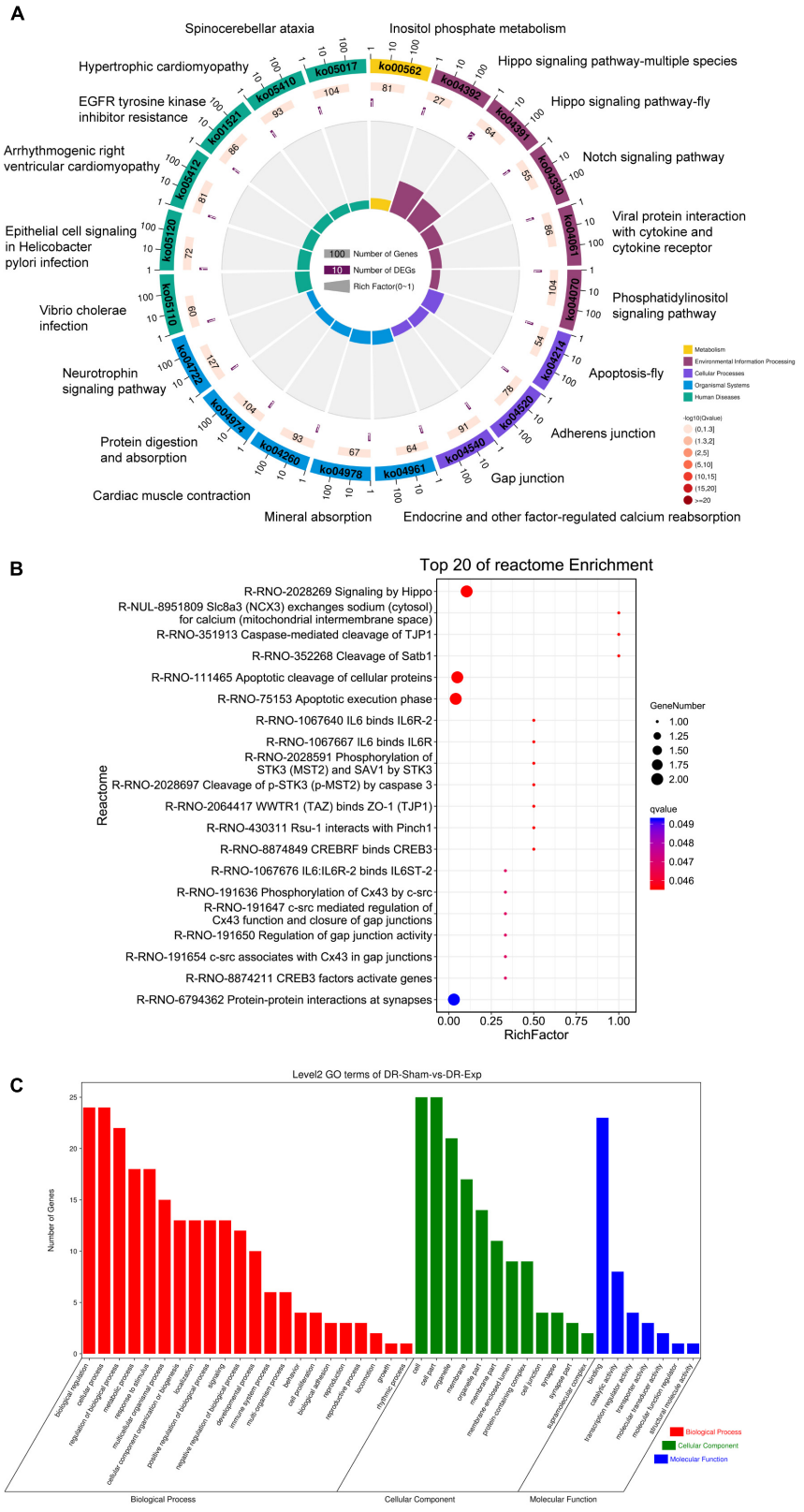

FIGURE 5
Annotation of host genes of differentially expressed circular RNAs after rat central axon injury. Enriched **(A)** KEGG pathways, **(B)** reactome pathways, and **(C)** GO terms.

TABLE 2 Top 20 enriched kyoto encyclopedia of genes and genomes (KEGG) pathways for host genes of differentially expressed circular RNAs after rat peripheral axon injury.

No	ID	Description
1	ko05017	Spinocerebellar ataxia
2	ko04919	Thyroid hormone signaling pathway
3	ko00604	Glycosphingolipid biosynthesis–ganglio series
4	ko04320	Dorso-ventral axis formation
5	ko05206	MicroRNAs in cancer
6	ko00512	Mucin type O-glycan biosynthesis
7	ko05202	Transcriptional misregulation in cancers
8	ko00071	Fatty acid degradation
9	ko00970	Aminoacyl-tRNA biosynthesis
10	ko04330	Notch signaling pathway
11	ko01212	Fatty acid metabolism
12	ko04391	Hippo signaling pathway -fly
13	ko04213	Longevity regulating pathway–multiple species
14	ko05014	Amyotrophic lateral sclerosis (ALS)
15	ko04137	Mitophagy–animal
16	ko05031	Amphetamine addiction
17	ko05016	Huntington disease
18	ko04015	Rap1 signaling pathway
19	ko00562	Inositol phosphate metabolism
20	ko04721	Synaptic vesicle cycle

MTA2-NuRD complex deacetylates TP53 (R-RNO-6805650) and Regulation of TP53 activity through acetylation (R-RNO-6804758) as well as ATF-associated pathway MSK1 activates ATF1 (R-RNO-6804758) were also identified as top enriched reactome pathways (**Figure 6B**).

Gene ontology analysis revealed cellular process as the most significantly enriched GO biological process, cell and cell part as the most significantly enriched GO cellular components, and binding as the most significantly enriched GO molecular function (**Figure 6C**).

Given the essential participation of PTEN-related pathways in peripheral axon injury-induced changes, circular RNAs sourced from genes involved in PTEN pathways are worthy of note. Novel_circ_002033, a circular RNA cyclizated from Gatad2b, was found to be up-regulated after peripheral axon branch injury versus sham surgery but not significantly altered after central axon branch injury. Therefore, besides the function of the host gene of novel_circ_002033, the regulatory roles of novel_circ_002033 was also explored by generating the ceRNA network of novel_circ_002033. Regulatory network showed that novel_circ_002033 might function as a microRNA sponge and regulate the target genes of miR-6331-z (i.e., Abcf1, Serpine1, Cxcl1, Zfp286a, Adcy3, Wdtc1, Slamf8, Acox1, Cd16412, Cacul1, Cd28, LOC100912604, Jak1, Furin, Myo6, Chd2, Crips3, Sbno2, RGD1304884, AABR07032097.1, Clec5a, Lair1, Vps9d1, Sesn2, and LOC103689964) and miR-129-x (i.e., Vash2, Aff4, Smpx, Frmd4b, Slc39a14, Casp3, Prickle2, Peg3, Spata2L, Phf23, Pik3r1, Ecel1, Ppfibp2, AABR07032097.1, Tcaf2, B3galt5, and Il18rap) (**Figure 7**).

Discussion

Dorsal root ganglion neurons are extensively used to investigate axon regeneration as the central and peripheral axon branches of DRG neurons have different axon regrowth abilities (Chen et al., 2016). Identifying different injury responses in DRGs after central and peripheral axon branches help to illuminate the molecular basis of successful axon regeneration and provides prospects for the treatment of central nerve injury.

Previously, our laboratory has investigated changes in DRGs at a series of time points, i.e., 0 h, 3 h, 9 h, 24 h, 4, and 7 days after rat sciatic nerve injury and found that many genes exhibited altered expression levels at 24 h post peripheral axon injury (Gong et al., 2016). To examine differences between peripheral and central axon injuries, herein, we performed rat central and peripheral axon injuries, collected DRGs at 24 h after nerve injury, and observed injury-induced changes in DRGs from the aspect of circular RNAs. The database of rat circular RNA is not as comprehensive as human circular RNAs, many identified circular RNAs in rat DRGs are thus labeled as novel circular RNAs. The genomic origins and localizations of these circular RNAs demonstrate that circular RNAs are chiefly derived from exonic regions and largely transcribed from rat chromosome 1, which is consistent with observations of circular RNAs in DRGs after sciatic nerve injury (Mao et al., 2019). Similar as the findings of the amounts of changed coding genes and accessible genes (Palmisano et al., 2019), the numbers of differentially expressed circular RNAs in DRGs are much larger after peripheral axon injury as compared with that in DRGs after central axon injury, indicating that sciatic nerve injury-induced changes may be more remarkable. Among these differentially expressed genes, only one circular RNA, that is novel_circ_000986, a circular RNA derived from linear Tshz2, is found to be up-regulated after both central and peripheral axon injuries, and only one circular RNA, that is novel_circ_000151, a circular RNA derived from linear Tesk2, is consistently down-regulated. The low-degree of genetic overlapping indicates that nerve injuries at central and peripheral axon branches induce diverse injury responses.

Functional analyses of host genes of circular RNAs provide important biological implications as circular RNAs regulate their host genes (Zhou et al., 2022). Hippo signaling pathway, a regeneration-promoting signaling pathway that orchestrates neural crest cell development and glial cell expansion (Serinagaoglu et al., 2015; Jeanette et al., 2021; Zhao et al., 2021) and Notch signaling pathway, a regeneration-inhibiting signaling pathway that prevents growth cone formation (El Bejjani and Hammarlund, 2012), are commonly involved after central and peripheral axon injuries. Besides

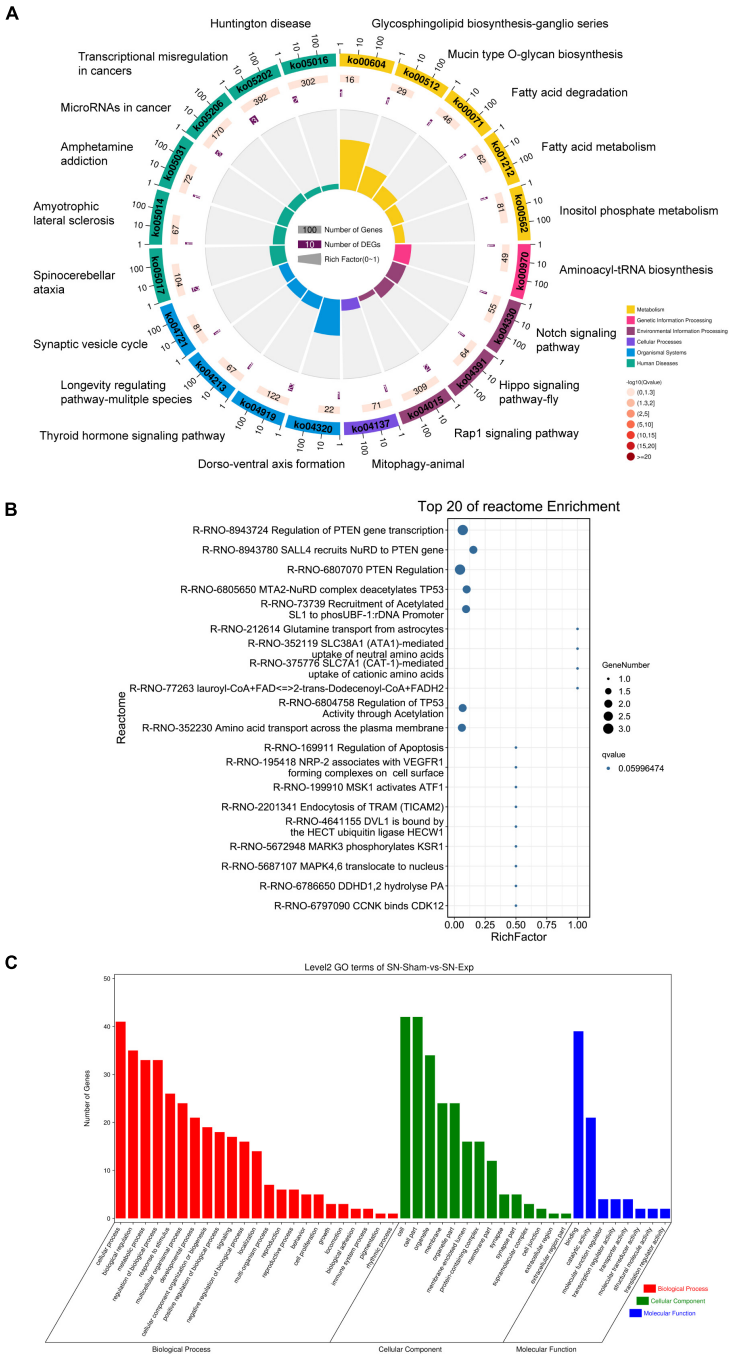

FIGURE 6
Annotation of host genes of differentially expressed circular RNAs after rat peripheral axon injury. Enriched **(A)** KEGG pathways, **(B)** reactome pathways, and **(C)** GO terms.

the recognization of concurrent changes, the identification of unique signaling pathways may also be very meaningful as it reflects different responses to central and peripheral injuries. KEGG and reactome pathway annotation show the enrichment of apoptosis and cellular junction after central axon injury instead of peripheral axon injury. Significant involvement of apoptosis after central axon injury is in agreement with experimental observations that spinal cord injury elicit severe neuron loss while sciatic nerve injury only lead to the death of 10–30% sensory neurons (Navarro et al., 2007; Park et al., 2008). Therefore, improving neuronal survival may be effective for the treatment of central nerve injury. Changes of

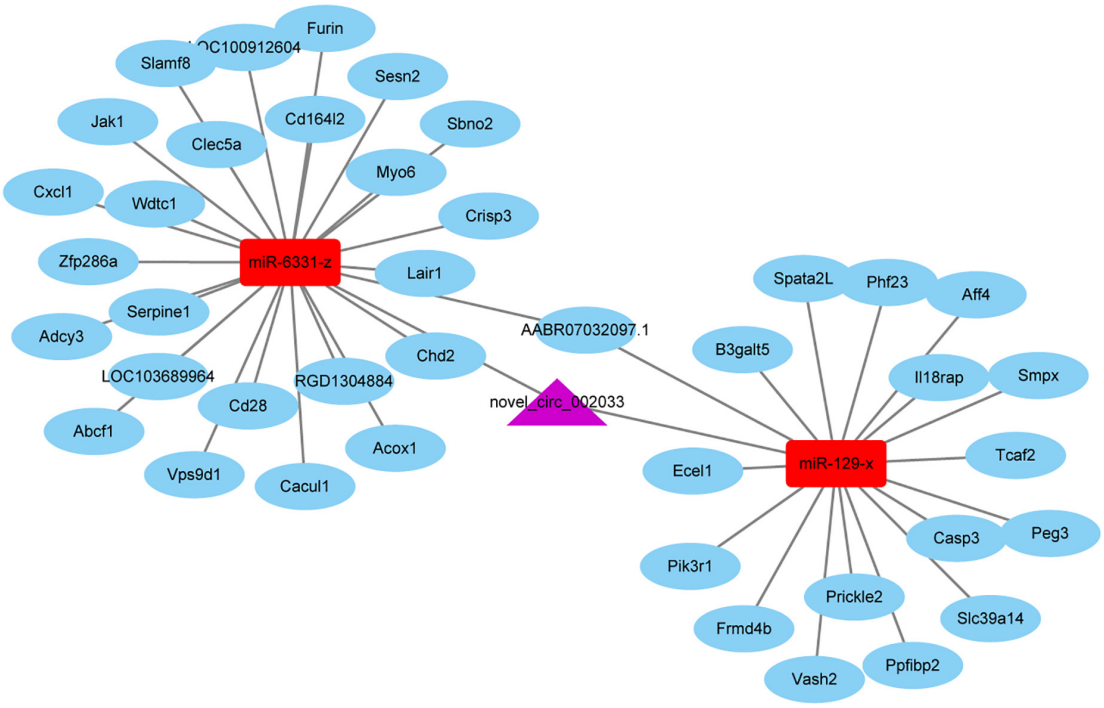

FIGURE 7
The competing endogenous RNA (ceRNA) network of novel_circ_002033. Purple indicates circular RNA novel_circ_002033, red indicates microRNAs miR-6331-z and miR-129-x, and blue indicates target genes.

blood-nerve-barrier have been recently detected in post-injury sensory neuron microenvironment by single cell sequencing (Avraham et al., 2021). Here, the significant involvements of adherens junction, gap junction, and more importantly, the mediation of tight junction protein 1 (TJP1, ZO-1) by caspase in central axon injury-induced alterations indicate that elevated apoptosis may contribute to cellular junction disruption and the remodeling of neuron microenvironment.

The most distinctive feature of host genes of differentially expressed circular RNAs after peripheral axon injury is the enrichment of PTEN-related pathways. PTEN/mTOR pathway has been long recognized as an essential regulator of nerve regeneration (Park et al., 2008; Abe et al., 2010; Christie et al., 2010; Liu et al., 2010). Endosomal NADPH oxidase 2, a DRG regenerative outgrowth contributing factor identified by comparing coding genes in DRGs after central and peripheral axon injuries, executes a promoting role in nerve regeneration *via* PTEN oxidation and inactivation (Hervera et al., 2018). Therefore, both analyses of coding genes and non-coding circular RNAs reveal the significance of PTEN signaling and indicate that inactivated PTEN may be a prerequisite for success axon regeneration.

Circular RNAs often function as ceRNA sponges, competitively bind to microRNAs, and increase the abundances of target genes of these microRNAs (Hansen et al., 2013; Li et al., 2018). By analyzing the targeting relationship and expression correlations of circular RNAs, microRNAs, and mRNAs, ceRNA networks were constructed and many circular RNAs that might be involved in ceRNA networks were screened, such as novel_circ_000013, novel_circ_000020, and novel_circ_000047. A full list of correlated circular RNAs, microRNAs, and mRNAs was provided in **Supplementary Table 3**. Among involved circular RNAs, novel_circ_002033 is cyclized from linear Gatad2b, a gene involved in PTEN signaling. Therefore, we investigated a novel_circ_002033-centered ceRNA network in detail. Notably, some downstream target genes in the ceRNA network have already been reported to be complicated in the nerve regeneration process. For instance, Acox1, a downstream target molecule of miR-6331-z, is required for axon regeneration and its mutation induces axonal loss and axon degeneration (Chung et al., 2020; Griffin and Ackerman, 2020; Shimizu et al., 2022). Ecel1, a target of miR-129-x, displays robust transcriptional responses to nerve injury and is considered as a potential therapeutic target for nerve regeneration (Kiryu-Seo et al., 2019). Therefore, other molecules in the constructed ceRNA network with currently unknown functions may also play important roles in nerve repair and regeneration and are worth further investigating.

Taken together, in the present study, we investigated novel circular RNA expression profiles of DRGs following nerve

injury and discovered unique responses of DRGs to central and peripheral projecting axon injuries. These identified genetic signatures in DRGs may benefit the understanding of molecular changes underlying failed central axon injury and success peripheral axon injury and contribute to the development of therapeutic strategies for central nerve regeneration.

Data availability statement

The datasets presented in this study can be found in online repositories. The names of the repository/repositories and accession number(s) can be found in the article/**Supplementary material**.

Ethics statement

The animal study was reviewed and approved by Nantong University Institutional Animal Care and Ethical approved by the Administration Committee of Experimental Animals, Nantong University, Jiangsu Province, China.

Author contributions

H-JC, LH, M-RZ, and TZ performed the experiment. L-CX designed the experiment. All authors wrote the manuscript.

Funding

This study was supported by Priority Academic Program Development of Jiangsu Higher Education Institutions (PAPD) and Nantong Applied Research Program (JC12022010).

Acknowledgments

We thank Guangzhou Genedenovo Biotechnology Co., Ltd., in assistance with sequencing and bioinformatics analysis.

Conflict of interest

The authors declare that the research was conducted in the absence of any commercial or financial relationships that could be construed as a potential conflict of interest.

Publisher's note

All claims expressed in this article are solely those of the authors and do not necessarily represent those of their affiliated organizations, or those of the publisher, the editors and the reviewers. Any product that may be evaluated in this article, or claim that may be made by its manufacturer, is not guaranteed or endorsed by the publisher.

Supplementary material

The Supplementary Material for this article can be found online at: https://www.frontiersin.org/articles/10.3389/fncel.2022.1046050/full#supplementary-material

SUPPLEMENTARY TABLE 1
List of differentially expressed circular RNAs after rat central axon injury.

SUPPLEMENTARY TABLE 2
List of differentially expressed circular RNAs after rat peripheral axon injury.

SUPPLEMENTARY TABLE 3
List of predicted correlations between circular RNAs, microRNAs, and mRNAs.

References

Abe, N., Borson, S. H., Gambello, M. J., Wang, F., and Cavalli, V. (2010). Mammalian target of rapamycin (mTOR) activation increases axonal growth capacity of injured peripheral nerves. *J. Biol. Chem.* 285, 28034–28043. doi: 10.1074/jbc.M110.125336

Avraham, O., Feng, R., Ewan, E. E., Rustenhoven, J., Zhao, G., and Cavalli, V. (2021). Profiling sensory neuron microenvironment after peripheral and central axon injury reveals key pathways for neural repair. *Elife* 10:e68457. doi: 10.7554/eLife.68457

Chen, L. L., and Yang, L. (2015). Regulation of circRNA biogenesis. *RNA Biol.* 12, 381–388. doi: 10.1080/15476286.2015.1020271

Chen, S., Zhou, Y., Chen, Y., and Gu, J. (2018). fastp: An ultra-fast all-in-one FASTQ preprocessor. *Bioinformatics* 34, i884–i890. doi: 10.1093/bioinformatics/bty560

Chen, W., Lu, N., Ding, Y., Wang, Y., Chan, L. T., Wang, X., et al. (2016). Rapamycin-resistant mTOR activity is required for sensory axon regeneration induced by a conditioning lesion. *eNeuro* 3, 1–17. doi: 10.1523/ENEURO.0358-16.2016

Christie, K. J., Webber, C. A., Martinez, J. A., Singh, B., and Zochodne, D. W. (2010). PTEN inhibition to facilitate intrinsic regenerative outgrowth of adult peripheral axons. *J. Neurosci.* 30, 9306–9315. doi: 10.1523/JNEUROSCI.6271-09.2010

Chung, H. L., Wangler, M. F., Marcogliese, P. C., Jo, J., Ravenscroft, T. A., Zuo, Z., et al. (2020). Loss- or Gain-of-function mutations in ACOX1 cause axonal loss via different mechanisms. *Neuron* 106, 589–606 e6. doi: 10.1016/j.neuron.2020.02.021

Croft, D., O'Kelly, G., Wu, G., Haw, R., Gillespie, M., Matthews, L., et al. (2011). Reactome: A database of reactions, pathways and biological processes. *Nucleic Acids Res.* 39, D691–D697. doi: 10.1093/nar/gkq1018

El Bejjani, R., and Hammarlund, M. (2012). Notch signaling inhibits axon regeneration. *Neuron* 73, 268–278. doi: 10.1016/j.neuron.2011.11.017

Fabregat, A., Jupe, S., Matthews, L., Sidiropoulos, K., Gillespie, M., Garapati, P., et al. (2018). The reactome pathway knowledgebase. *Nucleic Acids Res.* 46, D649–D655. doi: 10.1093/nar/gkx1132

Gong, L., Wu, J., Zhou, S., Wang, Y., Qin, J., Yu, B., et al. (2016). Global analysis of transcriptome in dorsal root ganglia following peripheral nerve injury in rats. *Biochem. Biophys. Res. Commun.* 478, 206–212. doi: 10.1016/j.bbrc.2016.07.067

Griffin, E. N., and Ackerman, S. L. (2020). Lipid metabolism and axon degeneration: An ACOX1 balancing act. *Neuron* 106, 551–553. doi: 10.1016/j.neuron.2020.04.030

Hansen, T. B., Jensen, T. I., Clausen, B. H., Bramsen, J. B., Finsen, B., Damgaard, C. K., et al. (2013). Natural RNA circles function as efficient microRNA sponges. *Nature* 495, 384–388. doi: 10.1038/nature11993

He, Z., and Jin, Y. (2016). Intrinsic control of axon regeneration. *Neuron* 90, 437–451. doi: 10.1016/j.neuron.2016.04.022

Hervera, A., De Virgiliis, F., Palmisano, I., Zhou, L., Tantardini, E., Kong, G., et al. (2018). Reactive oxygen species regulate axonal regeneration through the release of exosomal NADPH oxidase 2 complexes into injured axons. *Nat. Cell Biol.* 20, 307–319. doi: 10.1038/s41556-018-0039-x

Hoffman, P. N. (2010). A conditioning lesion induces changes in gene expression and axonal transport that enhance regeneration by increasing the intrinsic growth state of axons. *Exp. Neurol.* 223, 11–18. doi: 10.1016/j.expneurol.2009.09.006

Hu, Y. (2016). Axon injury induced endoplasmic reticulum stress and neurodegeneration. *Neural Regen. Res.* 11, 1557–1559. doi: 10.4103/1673-5374.193225

Jeanette, H., Marziali, L. N., Bhatia, U., Hellman, A., Herron, J., Kopec, A. M., et al. (2021). YAP and TAZ regulate Schwann cell proliferation and differentiation during peripheral nerve regeneration. *Glia* 69, 1061–1074. doi: 10.1002/glia.23949

Kanehisa, M., and Goto, S. (2000). KEGG: Kyoto encyclopedia of genes and genomes. *Nucleic Acids Res.* 28, 27–30. doi: 10.1093/nar/28.1.27

Kiryu-Seo, S., Nagata, K., Saido, T. C., and Kiyama, H. (2019). New insights of a neuronal peptidase DINE/ECEL1: Nerve development, nerve regeneration and neurogenic pathogenesis. *Neurochem. Res.* 44, 1279–1288. doi: 10.1007/s11064-018-2665-x

Li, X., Yang, L., and Chen, L. L. (2018). The biogenesis, functions, and challenges of circular RNAs. *Mol. Cell* 71, 428–442. doi: 10.1016/j.molcel.2018.06.034

Liu, K., Lu, Y., Lee, J. K., Samara, R., Willenberg, R., Sears-Kraxberger, I., et al. (2010). PTEN deletion enhances the regenerative ability of adult corticospinal neurons. *Nat. Neurosci.* 13, 1075–1081. doi: 10.1038/nn.2603

Mahar, M., and Cavalli, V. (2018). Intrinsic mechanisms of neuronal axon regeneration. *Nat. Rev. Neurosci.* 19, 323–337. doi: 10.1038/s41583-018-0001-8

Mao, S., Huang, T., Chen, Y., Shen, L., Zhou, S., Zhang, S., et al. (2019). Circ-Spidr enhances axon regeneration after peripheral nerve injury. *Cell Death Dis.* 10:787. doi: 10.1038/s41419-019-2027-x

Memczak, S., Jens, M., Elefsinioti, A., Torti, F., Krueger, J., Rybak, A., et al. (2013). Circular RNAs are a large class of animal RNAs with regulatory potency. *Nature* 495, 333–338. doi: 10.1038/nature11928

Nascimento, A. I., Mar, F. M., and Sousa, M. M. (2018). The intriguing nature of dorsal root ganglion neurons: Linking structure with polarity and function. *Prog. Neurobiol.* 168, 86–103. doi: 10.1016/j.pneurobio.2018.05.002

Navarro, X., Vivo, M., and Valero-Cabre, A. (2007). Neural plasticity after peripheral nerve injury and regeneration. *Prog. Neurobiol.* 82, 163–201. doi: 10.1016/j.pneurobio.2007.06.005

Neumann, S., and Woolf, C. J. (1999). Regeneration of dorsal column fibers into and beyond the lesion site following adult spinal cord injury. *Neuron* 23, 83–91. doi: 10.1016/S0896-6273(00)80755-2

Palmisano, I., Danzi, M. C., Hutson, T. H., Zhou, L., McLachlan, E., Serger, E., et al. (2019). Epigenomic signatures underpin the axonal regenerative ability of dorsal root ganglia sensory neurons. *Nat. Neurosci.* 22, 1913–1924. doi: 10.1038/s41593-019-0490-4

Park, K. K., Liu, K., Hu, Y., Smith, P. D., Wang, C., Cai, B., et al. (2008). Promoting axon regeneration in the adult CNS by modulation of the PTEN/mTOR pathway. *Science* 322, 963–966. doi: 10.1126/science.1161566

Renthal, W., Tochitsky, I., Yang, L., Cheng, Y. C., Li, E., Kawaguchi, R., et al. (2020). Transcriptional reprogramming of distinct peripheral sensory neuron subtypes after axonal injury. *Neuron* 108, 128–144 e9 doi: 10.1016/j.neuron.2020.07.026

Serinagaoglu, Y., Pare, J., Giovannini, M., and Cao, X. (2015). Nf2-Yap signaling controls the expansion of DRG progenitors and glia during DRG development. *Dev. Biol.* 398, 97–109. doi: 10.1016/j.ydbio.2014.11.017

Shimizu, T., Sugiura, K., Sakai, Y., Dar, A. R., Butcher, R. A., Matsumoto, K., et al. (2022). Chemical signaling regulates axon regeneration via the GPCR-gqalpha pathway in *Caenorhabditis elegans*. *J. Neurosci.* 42, 720–730. doi: 10.1523/JNEUROSCI.0929-21.2021

Stoll, G., and Muller, H. W. (1999). Nerve injury, axonal degeneration and neural regeneration: Basic insights. *Brain Pathol.* 9, 313–325. doi: 10.1111/j.1750-3639.1999.tb00229.x

Zhang, P., Chao, Z., Zhang, R., Ding, R., Wang, Y., Wu, W., et al. (2019). Circular RNA regulation of myogenesis. *Cells* 8:885. doi: 10.3390/cells8080885

Zhang, X. O., Wang, H. B., Zhang, Y., Lu, X., Chen, L. L., and Yang, L. (2014). Complementary sequence-mediated exon circularization. *Cell* 159, 134–147. doi: 10.1016/j.cell.2014.09.001

Zhao, X., Le, T. P., Erhardt, S., Findley, T. O., and Wang, J. (2021). Hippo-Yap pathway orchestrates neural crest ontogenesis. *Front. Cell Dev. Biol.* 9:706623. doi: 10.3389/fcell.2021.706623

Zhou, Z., Li, K., Liu, J., Zhang, H., Fan, Y., Chen, Y., et al. (2022). Expression profile analysis to identify circular RNA expression signatures in muscle development of Wu'an goat longissimus dorsi tissues. *Front. Vet. Sci.* 9:833946. doi: 10.3389/fvets.2022.833946

frontiers | Frontiers in Molecular Neuroscience

TYPE Original Research
PUBLISHED 20 December 2022
DOI 10.3389/fnmol.2022.953365

OPEN ACCESS

EDITED BY
Serena Carra,
University of Modena and Reggio Emilia, Italy

REVIEWED BY
Alessandro Rosa,
Sapienza University of Rome, Italy
Manuela Basso,
University of Trento, Italy

*CORRESPONDENCE
Masahiro Nogami
✉ masahiro.nogami@takeda.com
Masato Yano
✉ myano@med.niigata-u.ac.jp

†These authors have contributed equally to this work

SPECIALTY SECTION
This article was submitted to Brain Disease Mechanisms, a section of the Frontiers in Molecular Neuroscience

RECEIVED 27 May 2022
ACCEPTED 30 November 2022
PUBLISHED 20 December 2022

CITATION
Nogami M, Sano O, Adachi-Tominari K, Hayakawa-Yano Y, Furukawa T, Iwata H, Ogi K, Okano H and Yano M (2022) DNA damage stress-induced translocation of mutant FUS proteins into cytosolic granules and screening for translocation inhibitors. *Front. Mol. Neurosci.* 15:953365. doi: 10.3389/fnmol.2022.953365

DNA damage stress-induced translocation of mutant FUS proteins into cytosolic granules and screening for translocation inhibitors

Masahiro Nogami[1,2*†], Osamu Sano[1†], Keiko Adachi-Tominari[1], Yoshika Hayakawa-Yano[3,4], Takako Furukawa[4], Hidehisa Iwata[1], Kazuhiro Ogi[1,2], Hideyuki Okano[3] and Masato Yano[3,4*†]

[1]Innovative Biology Laboratories, Neuroscience Drug Discovery Unit, Research, Takeda Pharmaceutical Company Limited, Fujisawa, Japan, [2]Shonan Incubation Laboratories, Research, Takeda Pharmaceutical Company Limited, Fujisawa, Japan, [3]Department of Physiology, School of Medicine, Keio University, Tokyo, Japan, [4]Division of Neurobiology and Anatomy, Graduate School of Medical and Dental Sciences, Niigata University, Niigata, Japan

Fused in sarcoma/translated in liposarcoma (FUS) is an RNA-binding protein, and its mutations are associated with neurodegenerative diseases, including amyotrophic lateral sclerosis (ALS), through the DNA damage stress response, aberrant stress granule (SG) formation, etc. We previously reported that translocation of endogenous FUS into SGs was achieved by cotreatment with a DNA double-strand break inducer and an inhibitor of DNA-PK activity. In the present study, we investigated cytoplasmic SG formation using various fluorescent protein-tagged mutant FUS proteins in a human astrocytoma cell (U251) model. While the synergistic enhancement of the migration of fluorescent protein-tagged wild-type FUS to cytoplasmic SGs upon DNA damage induction was observed when DNA-PK activity was suppressed, the fluorescent protein-tagged FUS^{P525L} mutant showed cytoplasmic localization. It migrated to cytoplasmic SGs upon DNA damage induction alone, and DNA-PK inhibition also showed a synergistic effect. Furthermore, analysis of 12 sites of DNA-PK–regulated phosphorylation in the N-terminal LC region of FUS revealed that hyperphosphorylation of FUS mitigated the mislocalization of FUS into cytoplasmic SGs. By using this cell model, we performed screening of a compound library to identify compounds that inhibit the migration of FUS to cytoplasmic SGs but do not affect the localization of the SG marker molecule G3BP1 to cytoplasmic SGs. Finally, we successfully identified 23 compounds that inhibit FUS-containing SG formation without changing normal SG formation.

Highlights

1. Characterization of DNA-PK-dependent FUS stress granule localization.
2. A compound library was screened to identify compounds that inhibit the formation of FUS-containing stress granules.

KEYWORDS

FUS, stress granule, amyotrophic lateral scelerosis, compound library screening, RNA-binding protein

Introduction

Control of the integration and localization of macromolecular machines is essential for normal cellular function (Spannl et al., 2019). These functional assemblies of large molecules are now broadly categorized as organelles with lipid bilayer membranes and membraneless organelles (Gomes and Shorter, 2019). In particular, most membraneless organelles, which are called RNP granules, consist of nucleic acids, RNA, and RNA-binding proteins (RBPs). There are many types of RNP granules, and many RBPs have the intrinsic ability to promote the formation of large molecular assemblies through the process of liquid–liquid phase separation (LLPS; Mateju et al., 2017). Among these assemblies, stress granules (SGs), which are cytoplasmic granules formed under stress conditions, are a normal cellular defense against intracellular and environmental stresses and contain many cytoplasmic types of RBPs, translation control factors, etc., thereby repressing general mRNA translation during cellular stress (Maziuk et al., 2017; Markmiller et al., 2018; Wolozin and Ivanov, 2019). On the other hand, nuclear-localized RBPs do not necessarily localize to SGs during the cellular stress response but have been reported to migrate to SGs in response to various stimuli. Extensive studies have indicated that SGs are transient RNPs, but chronic stresses associated with aging lead to irreversible SG formation related to pathological protein aggregation (Gao et al., 2017; Wolozin and Ivanov, 2019). Posttranslational modification of RBPs is strongly involved in the RBP translocation and SG formation (Wolozin and Ivanov, 2019). Interestingly, a nucleus-enriched RBP, TDP-43, translocates to cytoplasmic SGs in response to some stimuli and has been identified as a core component of pathogenic protein aggregation, called "TDP-43 proteinopathy" in amyotrophic lateral sclerosis (ALS), Huntington's disease, Alzheimer's disease, and FTD (Arai et al., 2006; Hasegawa et al., 2008; Tada et al., 2012; Ling et al., 2013). In addition, FUS, TIA-1, hnRNPA2B1, and hnRNPA1, which are also nuclear RBPs, are closely related to pathological protein aggregation in ALS and FTD (Neumann et al., 2009; Kim et al., 2013; Ling et al., 2013; Mackenzie et al., 2017; Wolozin and Ivanov, 2019). These pathological aggregates of nuclear-enriched proteins are often observed in the cytoplasm. Therefore, the molecular mechanism underlying the cytoplasmic-nuclear shuttling activity of the causative RBPs has attracted attention as a cause of ALS pathology. The C-terminal region of FUS, called the noncanonical R/H/KX2-5PY NLS, has sufficient nuclear import activity. Mutations in this C-terminal region have been identified in many patients with familial FUS-ALS (Lee et al., 2006; Belzil et al., 2009; Chiò et al., 2009; Kwiatkowski et al., 2009; Vance et al., 2009). Furthermore, it has been reported that the NLS activity of FUS mutant proteins, which is involved in the cytoplasmic-nuclear localization of these proteins, correlates with a decrease in the age at disease onset (Dormann et al., 2010).

Other groups and we have been establishing an *in vitro* motor neuron model of ALS and analyzing its molecular mechanisms using iPS cell technologies (Higelin et al., 2016; Ichiyanagi et al., 2016; Fujimori et al., 2018; Matsuo et al., 2021). These disease models are extremely useful tools not only for analysis of the molecular mechanisms of disease but also as a biologically relevant tool for small molecule compound library screening of human diseases (Okano et al., 2020; Okano and Morimoto, 2022). In particular, we established a familial ALS disease model by establishing iPS cells from a family with a mutation in the *FUS* gene and isogenic iPS cells with the same mutation. In differentiated motor neurons, the FUS protein exhibits slight cytoplasmic leakage in FUS^{H517D}-mutated cells than in control cells, and arsenite treatment causes mislocalization of FUS^{H517D} into G3BP1-positive SGs. In contrast, wild-type FUS is not mislocalized (Ichiyanagi et al., 2016). Furthermore, in our iBRN analysis, a method that classifies the molecules with a substantial impact on transcriptomic data in FUS^{H517D} mutant cells, we identified *PRKDC*, *TIMELESS*, *miR125b*, etc. using cellular models of familial FUS-ALS (Nogami et al., 2021a). All three molecules contribute to a common pathway in the DNA damage response, and *PKRDC*, encoding DNA-dependent protein kinase (DNA-PK), has been reported to be involved in hyperphosphorylation of the FUS protein and to have a mitigating effect on LLPS of the FUS protein *in vitro* (Deng et al., 2014; Murray et al., 2017). Furthermore, we found that in addition to DNA damage induction, cotreatment with inhibitors of DNA-PK resulted in translocation of endogenous wild-type FUS into SGs (Nogami et al., 2021a). Similar studies have also indicated that mutations in the FUS NLS induce an abnormal poly-ADP-ribose polymerase (PARP)-dependent DNA damage response that is responsible for neurodegeneration and FUS mislocalization and aggregate formation (Naumann et al., 2018). Therefore, DNA damage response signaling due to the aberrant nucleocytoplasmic shuttling of the FUS protein is believed to be an upstream molecular target for ameliorating FUS-ALS pathology.

Here, we performed detailed experiments on FUS-containing cytoplasmic SG formation using various pathogenic FUS mutants and FUS with mutations in the DNA-PK–regulated

Abbreviations: FUS, Fused in sarcoma/translated in liposarcoma; SGs, Stress granules; ALS, Amyotrophic lateral sclerosis; RBP, RNA binding protein; LLPS, Liquid-liquid phase separation; CLM, Calicheamicin.

phosphorylation site further to explore the molecular mechanisms of FUS-positive SG formation. We observed a synergistic effect of the DNA damage inducer CLM and the DNA-PK inhibitor NU7441 on the translocation of FUS into SGs. We confirmed that this synergistic effect was dependent on the activity of DNA-PK. Furthermore, we screened for small compounds that specifically inhibited the formation of only FUS-positive SGs without affecting the formation of FUS-negative SGs and succeeded in identifying essential compounds, including signal transduction-inhibiting and chromatin-related molecules.

Materials and methods

Vector construction and plasmid preparation

Vector construction was performed by a service provider (GENEWIZ, South Plainfield, NJ). The synthesized Venus-human FUS^{WT}, Venus-human FUS^{H517D}, Venus-human FUS^{P525L}, and mCherry-human G3BP1 sequences were subcloned into the *Hin*dIII/*Not*I sites in the pcDNA3.1(+) vector (Invitrogen, Carlsbad, CA) to obtain the corresponding expression vectors with N-terminal fusion tags. In addition, the synthesized Venus-human $FUS^{WT\text{-}Ala}$ and Venus-human $FUS^{WT\text{-}Asp}$ sequences were subcloned into the *Bam*HI/*Xho*I sites in the pcDNA3.1(+) vector to obtain pcDNA3.1(+)-Venus-human $FUS^{WT\text{-}Ala}$ and pcDNA3.1(+)-Venus-human $FUS^{WT\text{-}Asp}$, respectively. To obtain expression vectors for Venus-$FUS^{P525L\text{-}Ala}$ and Venus-$FUS^{P525L\text{-}Asp}$, mutagenesis of pcDNA3.1(+)-Venus-human $FUS^{WT\text{-}Ala}$ and pcDNA3.1(+)-Venus-human $FUS^{WT\text{-}Asp}$ was performed to replace Pro with Lys at amino acid position 525 in the FUS protein.

Cell culture and transfection

The human astrocytoma cell line U251 MG (KO) was purchased from the JCRB Cell Bank (Tokyo, Japan). U251 MG (KO) cells were cultured in E-MEM containing L-glutamine, phenol red, sodium pyruvate, nonessential amino acids, and 1,500 mg/l sodium bicarbonate (Wako, Osaka, Japan; #055–08975) supplemented with 10% fetal bovine serum (Life Technologies; #10437085) and 100 U/ml penicillin–streptomycin (Life Technologies; #15140122) under 5% CO^2 at 37°C. To obtain cells stably overexpressing Venus-tagged FUS and mCherry-tagged G3BP1, the appropriate expression vectors were introduced into cells with Lipofectamine 3000 (Life Technologies) in Opti-MEM I (Thermo Fisher Scientific, Waltham, MA; #31985070) following the manufacturer's instructions. U251 MG (KO) cells positive for Venus and mCherry signals were selected with 100 μg/ml G418 (geneticin; Thermo Fisher Scientific). To induce DNA damage, cells were treated with 10–100 nM CLM (MedChem Express, Monmouth Junction, NJ; #HY19609) with or without 1–10 μM NU7441 (Wako; #143-09001), a high-potency selective DNA-PK inhibitor.

Western blotting

Western blotting was performed as described in the previous study with slight modification (Nogami et al., 2021b). U251 MG (KO) cells were collected into 1× SDS Blue loading buffer (NEB, Tokyo, Japan; #B7703S) and heated at 95°C for 5 min. Next, genomic DNA in the samples was sheared using a syringe needle (Terumo, Tokyo, Japan; #SS-05 M2913). Electrophoresis was performed with TGX AnyKD gels and 7.5% gels (Bio-Rad; #4569036), and proteins were transferred with a Transblot Turbo blotting system PVDF PAK MINI (Bio-Rad, Hercules, CA; #1794156). The protein-containing membranes were blocked with 5% nonfat dry milk (Cell Signaling Technology; #9999S) in Tris-buffered saline containing Tween 20 (TBST; Cell Signaling Technology; #9997S) for 30 min at room temperature. The membranes were then incubated with mouse monoclonal anti-phospho-histone H2A.X (Ser139; Millipore; #05–636), rabbit polyclonal anti-TDP-43 (Proteintech, Chicago, IL; #1078-2-AP), mouse monoclonal anti-FUS (Santa Cruz Biotechnology, Santa Cruz, CA; #SC-47711), and anti-β-actin (Novus Biologicals, Littleton, CO; #NB600-532) primary antibodies in blocking buffer overnight at 4°C. After three washes with TBST, the membranes were incubated with horseradish peroxidase-conjugated anti-mouse IgG (Cell Signaling Technology; #7076P2) or horseradish peroxidase-conjugated anti-rabbit IgG (Cell Signaling Technology; #7074P2) secondary antibodies in TBST for 30 min at room temperature. Luminescence signals on the membranes were detected by an image reader (LAS-4000 system; Fujifilm, Tokyo, Japan) with SignalFire ECL Reagent (Cell Signaling Technology; #6883S). The acquired images were processed with Multi Gauge version 3.1 software equipped with the LAS-4000 system and iBright CL1000 (Invitrogen).

Immunofluorescence microscopy

U251 MG (KO) cells were cultured in noncoated Cell Carrier 96-well plates. After washing with phosphate-buffered saline (PBS; Wako; #166–23,555), the cells were fixed with 4% paraformaldehyde/phosphate buffer solution (Wako; #163–20,145) for 15–30 min on ice and permeabilized by three incubations with 0.1% Triton X-100 in high-salt buffer (500 mM NaCl, 1 mM $NaH_2PO_4{\cdot}2H_2O$, 9 mM Na2HPO4, and 0.1% Tween 20) for 10 min at room temperature. The cells were then treated with 1% bovine serum albumin (Sigma; #A7030-100G) for 30 min at room temperature and incubated with mouse monoclonal anti-phospho-Histone H2A.X (Ser139; Millipore; #05–636), mouse monoclonal anti-FUS (Santa Cruz Biotechnology; #sc-47711; diluted 1:250), rabbit polyclonal anti-G3BP1 or mouse monoclonal anti-G3BP (Bethyl Laboratories, Montgomery, TX; #A302-033A;

diluted 1:250, BD Transduction #611127 diluted 1:500), rabbit polyclonal anti-TDP-43 (Proteintech; #1078-2-AP; diluted 1:250), anti-Flag-M2 (Sigma F3165 1:500), anti-QKI5 (Bethyl Laboratories; diluted 1:500), anti-GFP (Proteintech, #50430-2-AP 1:250 & Rockland #600–101-215 1:250) primary antibodies in low-salt buffer (0.05% Tween 20 in PBS) overnight at 4°C. After three 5-min washes with high-salt buffer at room temperature, the cells were incubated with Alexa Fluor 488 goat anti-rabbit IgG (H + L; Invitrogen; #A11034) and Alexa Fluor 594 goat anti-mouse IgG (H + L; Invitrogen; #A11032) secondary antibodies in a low-salt buffer for 30 min at room temperature. After three 5-min washes with high-salt buffer at room temperature, immunofluorescence signals were observed under a fluorescence microscope (Keyence, Osaka, Japan; BZ-X710 and BZ-X810) equipped with a 20× (Nikon, Tokyo, Japan; PlanApo l, NA = 0.75) or 40× (Nikon; PlanApo l, NA = 0.95) objective lens, and images were acquired with the equipped software (BZ-X Viewer and Analyzer).

Measurement of Venus-positive granule signal intensities

Images were acquired with an IN Cell Analyzer 6000 system (GE Healthcare Japan) using a 40× objective lens. The intensities of Venus fluorescence signals in cytosolic SGs or nuclear granules were calculated from the acquired images using IN Cell Developer Toolbox software (GE Healthcare Japan).

The precise method used for quantification was as follows.

Step 1: "Nucleus" segmentation using images of Hoechst staining. The "nuclear center" was predefined as a seed region in the nucleus with the objective segmentation module and postprocessing nodes, such as erosion and sieving. The "nucleus" was defined as the nuclear region corresponding to the "nuclear center" with the objective segmentation module. Postprocessing nodes, such as clump breaking with the "nuclear center," erosion, sieving, and border object removal, were used to separate spatially close nuclei and properly segment the diverse nuclear phenotypes.

Step 2: "Cell" segmentation using images from the Venus channel. The "cell" was defined as the cellular region with the objective segmentation module, with high sensitivity to detect weak signals. Postprocessing nodes, such as erosion, clump breaking using the "nucleus," sieving, and filling holes, were used to separate spatially close cells adequately.

Step 3: "Granule" segmentation. The Venus-FUS fluorescence images were used to detect textures, such as granules and vesicles, which were recognized by the vesicle segmentation module. The "cell" and "nucleus" were linked with the "granules" using a one-to-many target linking approach to quantify the density × area of "granules" in each cell.

Step 4: Measurement nodes. After individual cells were segmented, the total vesicle intensity and nuclear vesicle intensity per cell were calculated. The cytosolic vesicle intensity per cell was calculated using the following equation: "Cytosolic vesicle intensity per cell" = "total vesicle intensity per cell" – "nuclear vesicle intensity per cell."

Compound screening

The human astrocytoma cell line U251 MG (KO) was grown in DMEM (high glucose, GlutaMAX Supplement, containing pyruvate; Life Technologies, #10569–010) supplemented with 10% FBS (Corning, #35-076-CVR) and penicillin–streptomycin solution (Wako, #168–23,191) and maintained at 37°C in 5% CO_2. mCherry-G3BP1-and Venus-FUS^{P525L}-expressing U251 MG (KO) astrocytoma cells were seeded separately in a Cell Carrier-384 Ultra Plate (6057302) at 3000 cells/well and incubated in a CO_2 incubator at 37°C overnight. Approximately 8,000 compounds were tested at a single concentration (3 μM) on the 1st screen. For the 2nd screen, 303 compounds adjacent to the 61 hit compounds identified in the 1st screen were tested at four concentrations (10, 3, 0.3, and 0.03 μM). After the cells were treated with the compounds overnight, calicheamicin (CLM; 100 nM; MedChem Express, #HY-19609/CS-5320) and NU7441 (1 μM, Wako, #149–09003) were added simultaneously and incubated in a CO_2 incubator at 37°C for 3.5–5 h. Then, the cells were fixed with 4% PFA (containing Hoechst 33258 or Hoechst 33342) and washed with PBS. Images were acquired using an IN Cell Analyzer 6,000 (GE Healthcare Japan) with a 40x objective lens. Granular Venus fluorescence signals in the cytoplasm or nucleus were analyzed with the IN Cell Developer Toolbox (GE Healthcare Japan). The intensity of nuclear granules was quantitated as "intensity of all granules" - "intensity of nuclear granules."

Results

Subcellular localization of Venus-tagged FUS^{WT} and mutated FUS proteins in response to DNA damage stress

To investigate the change in the subcellular localization of mutated FUS proteins in response to DNA damage stress, we generated U251 MG (KO) cells that stably expressed FUS^{WT} (Venus-FUS^{WT}) and mutated FUS proteins tagged with Venus, an improved yellow fluorescent protein (Nagai et al., 2002), to observe the effects of DNA damage stress. As expected in our previous study (Nogami et al., 2021a), treatment with calicheamicin (CLM) induced shifts in the Venus-FUS^{WT} and Venus-FUS^{H517D} protein bands in addition to endogenous FUS at high molecular weights, indicating that hyperphosphorylation of these proteins in response to DNA damage stress. In contrast, the Venus-FUS^{P525L} protein was not phosphorylated well, and its nonphosphorylated form remained after CLM treatment (Figures 1A,B). These results indicated that the Venus-FUS^{P525L} protein had a lower ability about 30% to undergo phosphorylation by DNA-PK than the Venus-FUS^{WT} and Venus-FUS^{H517D} proteins

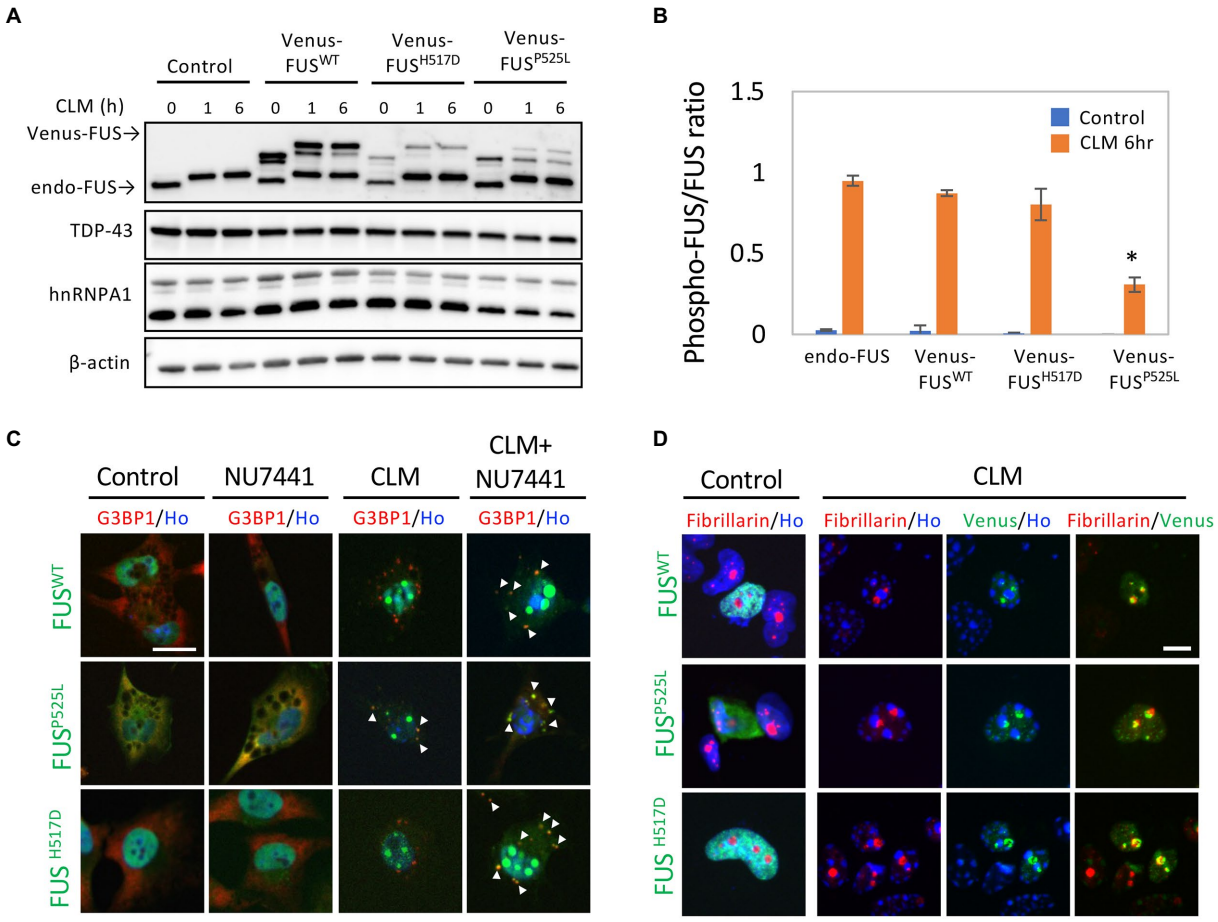

FIGURE 1
Subcellular localization of Venus-tagged FUS^{WT} (Venus-FUS^{WT}) and mutated FUS proteins in living cells. **(A)** U251 MG (KO) cells overexpressing Venus-FUS^{WT}, Venus-FUS$^{H517D.}$ and Venus-FUS^{P525L} were generated, and Western blotting with an anti-FUS antibody was performed to confirm the expression of Venus-tagged FUS. Cells were treated with 100nM calicheamicin (CLM) for 1 and 6h. An anti-"TDP-43/hnRNPA1/β-actin" antibodies were used as a control. **(B)** Quantification of ratio between phosphorylated FUS associated with band shift and normal molecular weight FUS band in endogenous and Venus-FUS^{WT}, Venus-FUS^{H517D} and Venus FUS^{P525L} at the normal and CLM 6h treatment with the Image J. The migration of Venus-FUS^{P525L} protein shows significantly lower compared to other FUS variants by CLM stimulation. Asterisk indicates significant change from three independent experiments (*t*-test $p<0.001$). **(C)** The subcellular distribution of Venus-FUS^{WT}, Venus-FUS$^{H517D.}$ and Venus-FUS^{P525L} (Green) co-stained with G3BP1 (Red), a marker for SGs and Hoechst (Blue), a marker for nuclei was observed in cells by fluorescence microscopy. Cells were treated with the DNA-PK inhibitor NU7441 (1μM) for 3h and were then treated with 100nM CLM or DMSO (control) for 6h in the presence of 1μM NU7441 or DMSO (control). Arrowheads indicate G3BP1 positive cytosolic SGs with Venus-FUS^{WT} or Venus-FUS mutant proteins. Scale bar: 20μm. **(D)** The Venus-FUS^{WT}, Venus-FUS^{H517D} and Venus-FUS^{P525L} protein were colocalized with the nucleolar marker fibrillarin in a CLM-dependent manner by CLM stimulation for 6h. Scale bar: 10μm.

(Figure 1B). We next investigated the subcellular localization of the Venus-FUS^{WT}, Venus-FUS^{H517D}, and Venus-FUS^{P525L} proteins by microscopy. In the absence of DNA damage stress, the Venus-FUS^{WT} and Venus-FUS^{H517D} proteins were mainly localized in the nucleus, while the Venus-FUS^{P525L} protein was distributed not only in the nucleus but also in the cytosol, similar to G3BP1 protein, known as a cytosolic RBP (Figure 1C). Upon CLM treatment, the Venus-FUS^{WT} and Venus-FUS^{H517D} proteins remained in the nucleus, while the Venus-FUS^{P525L} protein was translocated into cytosolic SGs, co-labeled with G3BP1 protein as a marker for cytosolic SGs (Figure 1C). After cotreatment with CLM and NU7441, an inhibitor of DNA-PK, which is known to be a kinase of FUS (Deng et al., 2014), the Venus-FUS^{WT}, Venus-FUS^{H517D} and Venus-FUS^{P525L} proteins were obviously translocated into cytosolic SGs (Figure 1C). Importantly, we confirmed that most of the cytoplasmic granules of Venus-FUS^{wt} and mutants are G3BP1-positive SGs under the cotreatment with CLM and NU7441 (Supplementary Figures 1A–C).

In a previous report, the topoisomerase I inhibitor camptothecin rapidly induced the translocation of FUS into the nucleolus (Martinez-Macias et al., 2019). We also observed the translocation of FUS into the nucleolus, which is a fibrillarin-positive nuclear structure, by a similar stimulus, i.e., the CLM-induced DNA damage response. Interestingly, this nucleolar localization was also observed in FUS^{WT}, FUS^{P525L} and FUS^{H517D}, suggesting the independence on FUS mutation (Figure 1D). To

better understand the translocation mode of FUS proteins and SG formation, we conducted live cell imaging of Venus-FUS^{WT}, Venus-FUS^{P525L}, and mCherry-tagged G3BP1 (mCherry-G3BP1) proteins. SG formation was monitored *via* the subcellular localization of mCherry-G3BP1. Within 3 h after CLM treatment, formation of mCherry-G3BP1-positive cytosolic SGs was observed, but Venus-FUS^{WT} remained in the nucleus, although nucleolar accumulation of FUS was observed (Figure 2A). At 6 h after CLM treatment, Venus-FUS^{WT} was translocated into cytosolic SGs, while the nucleolar accumulation of FUS was relatively weakened (Figures 2A,B). These results mirrored the localization of endogenous FUS and another fusion tag protein FLAG-FUS^{WT}, which was not translocated into cytosolic SGs within 3 h after treatment with CLM and NU7441 but was translocated at 6 h (Nogami et al., 2021a; Supplementary Figure 1B). On the other hand, Venus-FUS^{P525L} was partially translocated into cytosolic SGs at 3 h after cotreatment with CLM/NU7441 and fully translocated into cytosolic SGs at 6 h (Figure 2A). These observations suggest that G3BP1-positive SGs first form, and cytosolic nonphosphorylated FUS is then incorporated into G3BP1-positive cytosolic SGs during DNA damage stress under the impairment of DNA-PK activation by treatment with NU7441, indicating the unique feature of the FUS protein for FUS-SGs formation. In fact, we have obtained the consistent result that show the DNA-PK dependency by immunocytochemistry for endogenous FUS protein. On the other hands, another nuclear-enriched RBP, TDP-43 translocate to the cytoplasm and into SGs after stimulation with CLM alone, similar to G3BP1, while the localization of QKI5 does not change even under cotreatment with CLM/NU7441 for 6 h (Supplementary Figures 2A–C).

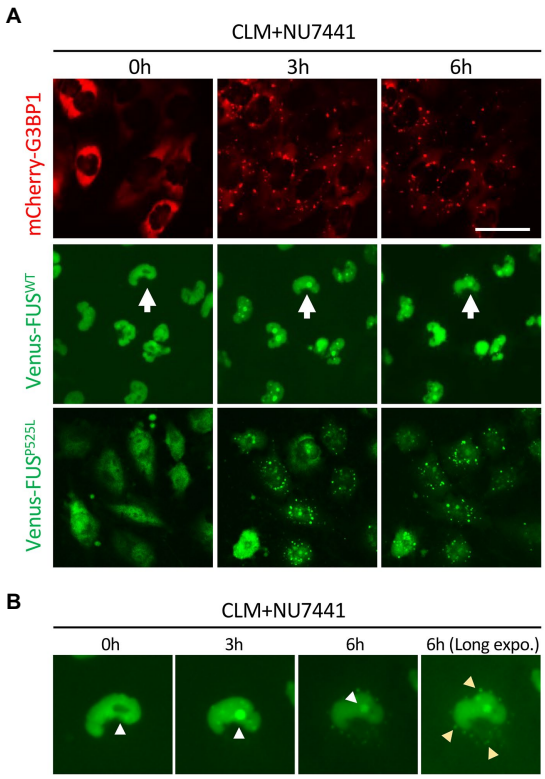

FIGURE 2
Live imaging of cells stably expressing mCherry-G3BP1, Venus-FUS^{WT} and Venus-FUS^{P525L}. **(A)** Cells were treated with 1μM NU7441 for 3h and were then treated with 100nM CLM for 0, 3, and 6h in the presence of 1μM NU7441. To visualize cytosolic SGs, U251 MG (KO) cells overexpressing mCherry-G3BP1 were generated and treated with 100nM CLM for 3 and 6h. Scale bar: 50μm. **(B)** The cells with white arrows in the images are shown at high magnification. The yellow arrowheads indicate SGs in the long-exposure image.

A role of Ser/Thr residues in the N-terminal region of FUS in the protective effect against mislocalization to cytosolic SGs

We observed that Venus-FUS^{P525L} is more likely to mistranslocate into cytoplasmic SGs with CLM treatment alone and is less efficiently phosphorylated by DNA-PK than are Venus-FUS^{WT} and Venus-FUS^{H517D} (Figures 1A–C). Considering that 12 Ser/Thr residues in the N-terminal region of FUS are phosphorylated by DNA-PK (Deng et al., 2014; Monahan et al., 2017), we hypothesized that the impaired phosphorylation of FUS^{P525L} is the cause of FUS^{P525L} mislocalization into cytoplasmic SGs. To elucidate the roles of the 12 phosphorylation sites in FUS, we replaced these 12 Ser/Thr residues with Ala and Asp residues to generate DNA-PK–non-phosphorylatable forms and DNA-PK phospho-mimic forms, respectively, in Venus-FUS^{WT} and Venus-FUS^{P525L} (Supplementary Figure 3A). The Venus-FUS$^{WT\text{-}Ala}$ and Venus-FUS$^{WT\text{-}Asp}$ protein bands on the SDS–PAGE gels were consistent with the nonphosphorylated and phosphorylated forms of the Venus-FUS proteins, respectively (Figure 3A). Importantly, we confirmed that the band shift associated with CLM stimulated phosphorylation in both endogenous and exogenous FUS were cancelled by DNA-PK inhibitor NU7441, reflecting the previous reports from phos-tag gel shift assay to prove that the band shift of FUS is well correlated to phosphorylation levels (Rhoads et al., 2018; Nogami et al., 2021a; Supplementary Figure 3B). We found that Venus-FUS$^{WT\text{-}Asp}$ was not localized into cytoplasmic SGs even after treatment with both CLM and NU7441. At the same time, Venus-FUS$^{WT\text{-}Ala}$ was recruited into cytoplasmic SGs by treatment with CLM alone, indicating the unique feature of DNA-PK dependent FUS-SGs formation and suggesting the possibility that DNA-PK activity protects against recruitment into cytoplasmic SGs (Figures 3B,C). However, we did not observe differences in nucleolar accumulation in the FUS mutants with the replacement of the 12 Ser/Thr residues (Figure 3B).

We next investigated the effects of the 12 Ser/Thr phosphorylation sites in Venus-FUS^{P525L}. Interestingly, FUS^{P525L} showed a synergistic increase in recruitment to cytoplasmic granules and the fluorescence intensity per cell from CLM stimulation alone to cotreatment with CLM and NU7441 (Figures 4A–C; Supplementary Table 1). We confirmed that FUS

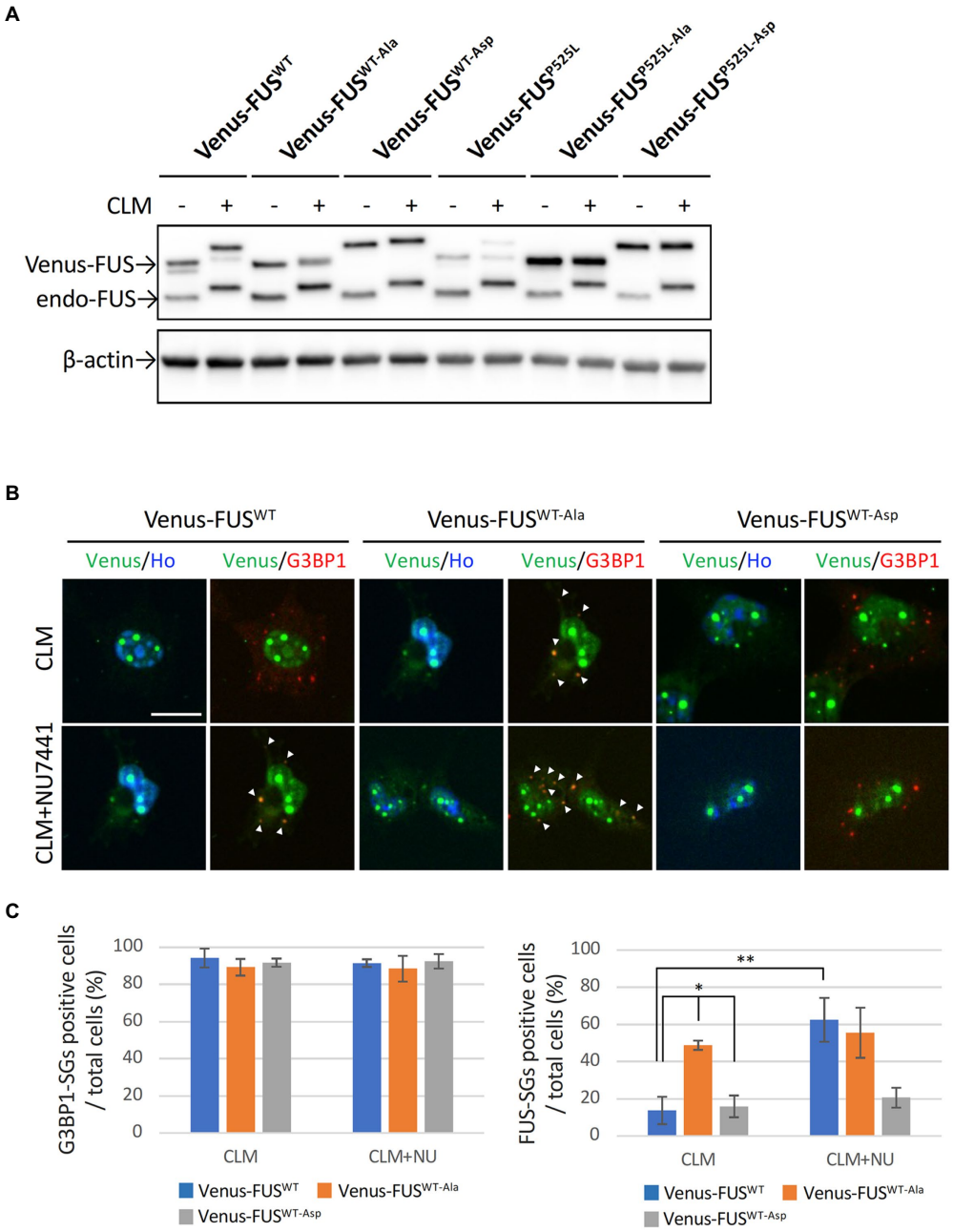

FIGURE 3
Effect of replacing 12S/TQ residues with AQ or DQ residues in the N-terminal region of wild-type and mutant FUS proteins. **(A)** U251 MG (KO) cells stably overexpressing Venus-FUS^{WT-Ala}, Venus-FUS^{WT-Asp}, Venus-FUS$^{P525L-Ala.}$ and Venus-FUS$^{P525L-Asp}$ were cloned, and Western blotting with an anti-FUS antibody was performed to confirm the expression of Venus-tagged FUS and endogenous FUS proteins in each cell line from three biological replicates. Cells were treated with 100nM CLM for 5h. An anti-β-actin antibody was used as a control. **(B)** The subcellular distribution of Venus-FUS^{WT}, Venus-FUS^{WT-Ala} and Venus-FUS^{WT-Asp} (Green) co-stained with G3BP1 (Red), a marker for SGs and Hoechst (Blue), a marker for nuclei was observed in cells by fluorescence microscopy. Cells were treated with 1μM NU7441 for 1h and were then treated with 100nM CLM for 5h in the presence of 1μM NU7441 or DMSO (control). Arrowheads indicate G3BP1 positive cytosolic SGs with Venus-FUS^{WT} or Venus-FUS^{WT-Ala} proteins. Scale bar: 20μm. **(C)** Quantitative data of the ratio of G3BP1-SGs-positive cells (Left) and FUS-positive SGs (Right) in total cells (at least 3 biological replicates; mean±SD; *p <0.001; Dunnett's test and **p <0.001 t-test).

cytoplasmic granule co-stained with G3BP1 positive SGs. On the other hand, unlike the other mutants, FUS$^{P525L-Ala}$ showed a marked increase in recruitment to cytoplasmic granules with CLM stimulation alone but did not show a synergistic increase in recruitment to SGs under cotreatment with CLM and NU7441. Although the Venus-FUS$^{P525L-Asp}$ mutation failed to inhibit recruitment to cytoplasmic SGs, unlike in cells expressing Venus-FUS^{WT-Asp} (Figures 3B–C), the synergistic increase in recruitment

to SGs by cotreatment with NU7441 was abolished (Figures 4A–C; Supplementary Table 1). Importantly, nucleolar accumulation of all FUS^{P525L} mutants was observed, but no synergistic increase by treatment with NU7441 was detected, indicating that nucleolar accumulation is not DNA-PK dependent (Figure 4A,D,E; Supplementary Table 1). These data suggest that DNA-PK plays a protective role against cytosolic mislocalization of FUS to SGs through phosphorylation of the FUS N-terminal domain during DNA damage stress.

Compound screening

We next performed a compound screen to identify compounds that can inhibit CLM-and NU7441-induced formation of FUS^{P525L}-positive SGs without changing the formation of G3BP1-positive SGs as the 1st screen using mCherry-G3BP1-and Venus-FUS^{P525L}-expressing U251 MG (KO) astrocytoma cell lines. In the 1st screening, the 7,658 compounds were evaluated at a single concentration (3 μM). To eliminate compounds that were toxic to cells, compounds leaving at least 70% more viable cells than observed in the control cell group were selected based on cell counts from images of nuclear Hoechst staining in both Venus-FUS^{P525L}-expressing and mCherry-G3BP1-expressing cells (Figure 5A). Next, cytoplasmic Venus-FUS puncta that appeared under CLM and NU7441 stimulation were quantified, and compounds for which the number of puncta was reduced by 40% or less compared to that in control cells were selected (116 compounds; Figure 5A). To identify compounds that reduced the number of FUS puncta without changing the number of SGs, we quantified cytoplasmic mCherry-G3BP1 puncta that appeared under CLM and NU7441 stimulation and selected compounds that reduced the number of puncta to 50% or more compared to that in control cells (61 compounds; Figure 5A). In the 2nd screen, to check the reproducibility of the 61 hit compounds from the 1st screening, 303 compounds, including the compounds adjacent to the 61 hits, were evaluated at 4 concentrations (10, 3, 0.3, and 0.03 μM). To exclude false-positives, the compounds showing concentration dependency with a low signal-to-noise ratio were selected from the compounds that reduced the FUS-positive SG count without reducing the G3BP1 SG count, as in the 1st screen. Finally, we obtained 23 compounds as hit compounds (Figure 5A). The representative compound F-17, showing a typical trend, was a commercially available compound—MI-2, also known to be a Menin-MLL interaction inhibitor (Figures 5B,C). Importantly, we confirmed that compound F17 did not affect cell viability at any concentration under the CLM and NU7441 stimulation (Supplementary Figures 4A,B). We next tested whether these compounds truly inhibit the localization of not only exogenous FUS^{P525L}-SGs but also endogenous FUS protein to SGs. First, we confirmed that endogenous FUS also localized in mCherry-G3BP1-positive stress granules upon cotreatment with CLM and NU7441 (Supplementary Figure 1C). We used three commercially available compounds—spautin-1 (F1), known to be an autophagy inhibitor *via* targeting two ubiquitin-specific peptidases (USP-10 and USP-13) (Liu et al., 2011), the Menin-MLL interaction inhibitor (Grembecka et al., 2012) MI-2 (F17), and MI-3 (F16)—and observed their effects on endogenous FUS localization into SGs. Pretreatment with any of the three compounds (3 μM) obviously inhibited the localization of endogenous FUS to SGs without altering the localization of G3BP1 or TDP-43 proteins to SGs, indicating the validity of our compound screen (Figures 5D,E). In addition, treatment with these three compounds did not alter the protein level of endogenous FUS itself (Supplementary Figure 5). Furthermore, we examined FUS into SGs inhibitory activity in the ALS-linked mutations of FUS using two compounds, F1 and F17, which is the same molecular target with F16 since mutant FUS proteins have been shown to localize SGs due to oxidative stress, such as arsenite unlike wild-type FUS proteins (Supplementary Figure 6A). However, no inhibitory activity of mutant FUS into SGs was observed, possibly due to the different molecular pathways do not DNA damage response (Supplementary Figure 6B,C). Finally, we added the list of hit compounds, including graphs showing the concentration dependence of the counts of FUS-and G3BP1-positive SGs and their IC50 (μM) of the number of FUS-positive SGs with compounds structure (Figure 6; Supplementary Table 2).

Discussion

We previously reported the localization of the FUS protein to cytoplasmic SGs by a combination of DNA damage induction and treatment with an inhibitor of DNA-PK (Nogami et al., 2021a). In the present study, we clarified the requirement for DNA-PK activity in the localization of FUS to cytoplasmic SGs in detail by using Venus-tagged FUS proteins carrying ALS-linked mutations and mutations in the sites of DNA-PK–regulated phosphorylation. Using this system, we also screened small molecule compounds that inhibited FUS localization but not G3BP1 to cytoplasmic SGs. As a result, we identified small molecule compounds with activities such as protein kinase inhibition and chromatin regulation. The effects of these compounds on the translocation of endogenous FUS protein were also validated (Figures 5, 6).

SGs are structural membraneless organelles that are thought to be one of the cellular defense components essential for maintaining cellular function. SGs contain mainly mRNAs and cytoplasmic RNA-binding proteins; for example, G3BP1 is a major marker protein (Gomes and Shorter, 2019). SGs can divide specific sub compartments, cores versus shells. G3BP1 exists in SGs cores and is a key protein of SGs formation. Upon stress, ALS-associated RBPs, such as FUS and TDP-43, may contribute towards formation of SGs shell component, which is sensitive to RNase treatment (Fang et al., 2019). Previous report have indicated that siFUS KD, but not siTDP-43, did not affect the SGs assembly (Aulas et al., 2012). In our cell system, the nuclear-enriched RBP FUS does not localize to SGs and affect SGs formation in response to arsenite stimulation, suggesting FUS does not play a role of SGs formation. On the other hand, the C-terminal mutants of FUS, such as FUS^{H517D}, FUS^{R521C}, and FUS^{P525L}, which harbor various mutations in FUS

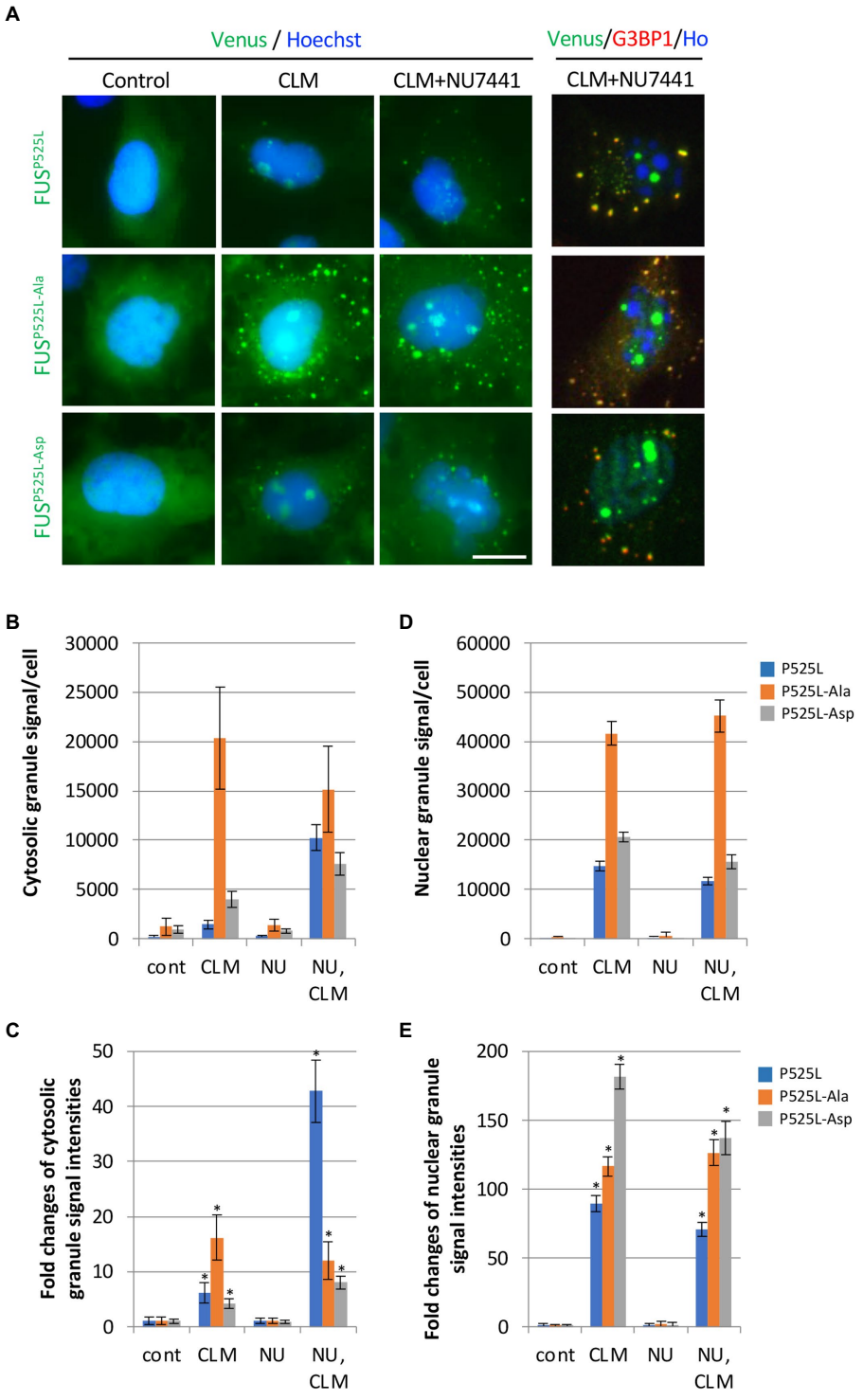

FIGURE 4
Synergistic effect of replacing 12S/TQ residues with AQ or DQ residues in the N-terminal region of FUS^{P525L} on SG formation during CLM/NU7441 stimulation. **(A)** The subcellular distribution of Venus-FUS^{P525L}, Venus-FUS$^{P525L\text{-}Ala}$, and Venus-FUS$^{P525L\text{-}Asp}$ proteins co-stained with G3BP1 (Red), a marker for SGs and Hoechst (Blue), a marker for nuclei was observed by fluorescence microscopy. Cells were pretreated with 1μM NU7441 and were then treated with 100nM CLM in the presence of 1μM NU7441 or DMSO (control) for 5h. Scale bar: 20μm. **(B,C)** Quantification of Venus fluorescence signals at cytosolic granules and fold changes of their signals to each control of Venus-FUS^{P525L}, Venus-FUS$^{P525L\text{-}Ala}$ and Venus-FUS$^{P525L\text{-}Asp}$ with the IN Cell Analyzer imaging system. The result of statistical analysis is shown in Supplementary Table 1. **(D,E)** Quantification of Venus fluorescence signals at nuclear granules and fold changes of their signals to each control of Venus-FUS^{P525L}, Venus-FUS$^{P525L\text{-}Ala}$ and Venus-FUS$^{P525L\text{-}Asp}$ with the IN Cell Analyzer imaging system. Asterisk indicates significant change relative to FUS derivates-SGs containing cells of DMSO control with CLM+NU7441 treatment (*t*-test p <0.001). The result of statistical analysis is also shown in Supplementary Table 1.

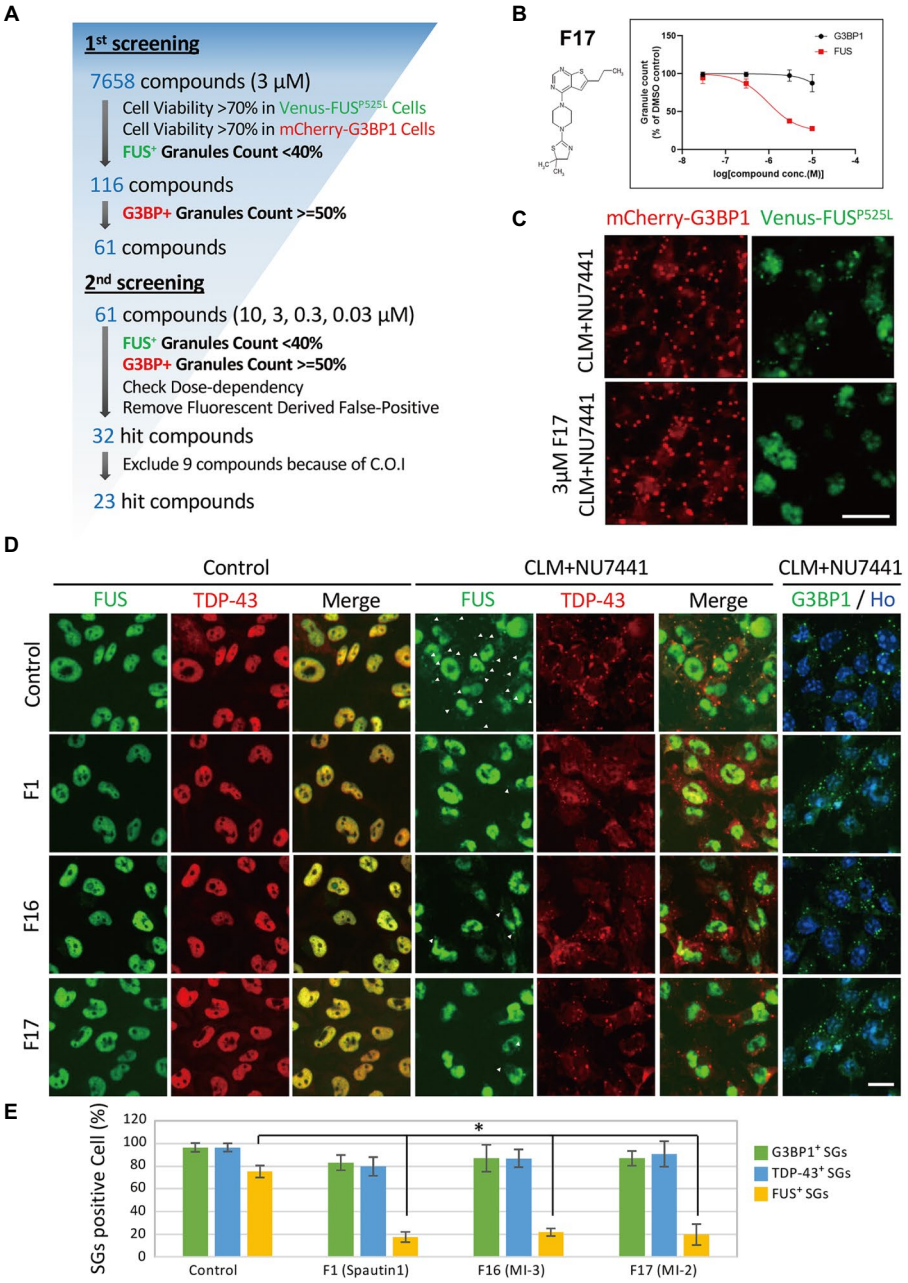

FIGURE 5
Compound screening for inhibition of FUS-containing SG formation. **(A)** Compound screening flowchart. See the methods section for details. **(B)** Dose-response curve of Compound F17 as one of the 23 hit compounds. T-3811487 (3μM), a representative hit compound, did not inhibit the formation of G3BP1-positive SGs (black line) but inhibited the localization of FUS^{P525L} (red line) to SGs. The vertical axis shows the inhibition rate (%) of granule formation. **(C)** Fluorescence image of cells treated with 3μM F17. The scale bars represent 20μm. **(D)** Validation of the effects of the hit compounds on endogenous FUS protein localization. U251MG (KO) cells were pretreated with 3μM F1, F16, and F17 and were then treated with 100nM CLM and 10μM NU7441 or with DMSO (control) for 6h. The images show immunocytochemistry for G3BP1-positive puncta G3BP1 (green) and Hoechst (blue), control for SGs, TDP-43 (red), and FUS (green). The arrowheads indicate FUS-positive SGs. The scale bars represent 20μm. **(E)** Relative population of the cells containing cytosolic stress granules were calculated to total cells. Values represent mean ±SD. Asterisk indicates significant change relative to FUS-SGs containing cells of DMSO control with CLM+NU7441 treatment (*t*-test $p<0.001$).

identified as ALS-linked mutations, show evident recruitment to SGs under stress conditions (Higelin et al., 2016; Ichiyanagi et al., 2016; Supplementary Figure 6A). This could be due to cytoplasmic leakage of the mutated FUS protein itself, caused by its weakened nuclear translocation signal. It has also been reported that the cytoplasmic localization of these three mutants correlates with the severity of neurodegeneration in ALS, suggesting a risk of cytoplasmic leakage (Dormann et al.,

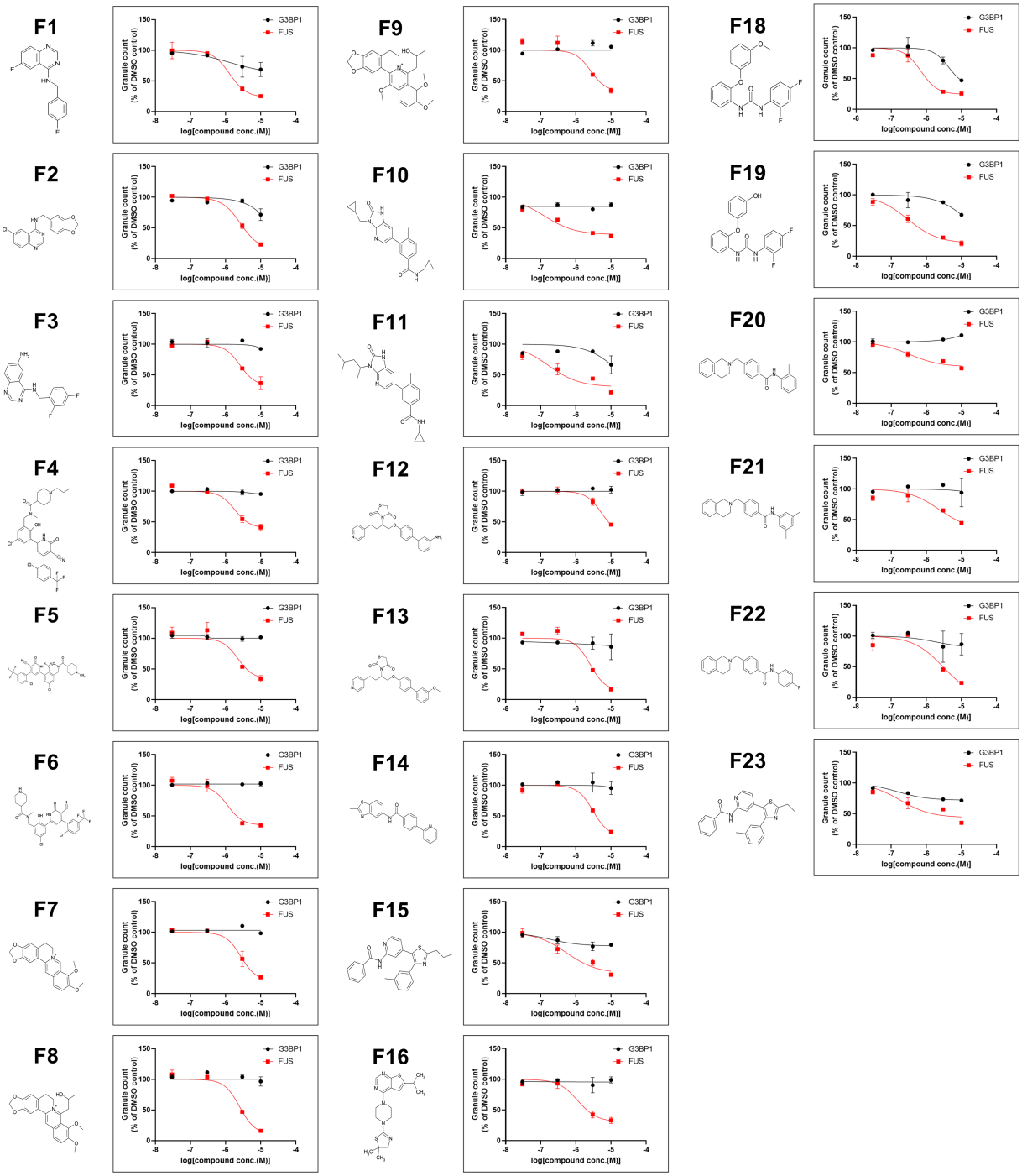

FIGURE 6
A list of 23 hit compounds that inhibit FUS-positive SG formation. Structures of the 23 hit compounds except for F17 are shown in Figure 5B and dose-response curves for reduced mislocalization of FUS^{P525L} at cytosolic SGs.

2010). Therefore, the localization of insoluble and aggregating molecules such as FUS in SGs is considered a risk factor for neurodegeneration, as opposed to SG formation as an intrinsic stress defense function. Modifying the FUS translocation to SG without inhibiting SGs assembly by small molecules might be useful like a previous study for TDP-43 protein (Fang et al., 2019). However, we could not deny the possibility of secondary effects by the compounds, including inhibition of unknown function of wild type FUS protein and nuclear-retained mutated FUS proteins in SGs. Other groups and we have reported that the endogenous FUS migrates to SGs in response to DNA damage stress mediated by topoisomerase I induction

or CLM stimulation (Rhoads et al., 2018; Martinez-Macias et al., 2019; Nogami et al., 2021a). In particular, we argue that the translocation of endogenous FUS to SGs is dependent on DNA-PK activity (Figure 3; Nogami et al., 2021a). Although ATM pathway, which is another down stream of DNA damage response, have not been considered in this study, we believe that DNA-PK activity plays important roles in FUS cellular dynamics as evidenced by the solubility of phospho-mimic mutant FUS protein (Supplementary Figure 7A). In contrast, the other nuclear-enriched RBPs, TDP-43 and QKI5 behaved differently under DNA damage stress conditions, showing no DNA-PK dependence (Supplementary Figure 2). While these three proteins show broadly similar nuclear subcellular localization under unstressed conditions, TDP-43 is concentrated in the nucleus at Gem, and nuclear speckles (Tsuiji et al., 2013), and QKI5 is localized at nuclear speckles and regulates pre-mRNA splicing in neural stem cells (Hayakawa-Yano et al., 2017). The difference in the mechanism of subcellular translocation of these three nuclear RBP families might be due to their distinct NLS types and protein modifications (Wu et al., 1999; Lee et al., 2006; Hofweber et al., 2018; François-Moutal et al., 2019). Given the above observations, the activation of DNA-PK and the control of the corresponding signaling pathway by the compounds found in this study might provide critical tools to mitigate FUS-specific condensation and aggregation, thereby ameliorating FUS-ALS pathology.

In this study, we found that the FUS protein rapidly localizes to the nucleolar cap before the formation of FUS-positive cytoplasmic granules. The localization of endogenous and Venus-tagged FUS to the nucleolus, specifically in response to topoisomerase I-induced DNA cleavage, has recently been reported (Martinez-Macias et al., 2019). Alternatively, it has been reported that transcription-arresting agents also induce FUS accumulation in pol-II DNA damage foci, and this accumulation could be involved in the prevention or repair of R-loop–associated DNA damage (Hill et al., 2016). Interestingly, our observations indicate that FUS does not localize to the nucleolus under steady-state conditions but rapidly changes its localization to the nucleolus upon induction of DNA damage by CLM (Figure 1D) and that when the localization of FUS to cytoplasmic SGs occurs, the localization of FUS to the nucleolus is decreased (Figure 2B). Our analysis did not clarify whether the FUS localized to cytoplasmic SGs originates from the nucleolar cap during CLM/NU7441 stimulation. On the other hand, we found that this localization of FUS to SGs was synergistically increased by cotreatment with CLM and NU7441; in contrast, the translocation of FUS to the nucleolus did not show a synergistic response, suggesting that the mechanism of nucleolar localization is independent of DNA-PK activity (Figures 4D,E). In the future, further analysis, including the various compounds that we identified in this study, will clarify the mechanisms involved in the translocation of FUS from the nucleolar cap and SG formation.

Among the 23 compounds, we found several compounds that act on p38 MAP kinase pathways in this study. Significantly, the general p38 MAP kinase inhibitor SB203580 also inhibited the localization of endogenous FUS to SGs (Supplementary Figure 7B). In addition, F17, listed as an example of a representative compound in Figure 5, was a Menin-MLL interaction inhibitor; this compound is also called MI-2 and is a commercial compound. Importantly, MI-3, which also showed a similar action, was also identified as a hit compound; therefore, this chromatin-regulating pathway is thought to be involved in the inhibition of FUS translocation. Both of these compounds, as expected, inhibited the formation of FUS-positive SGs under CLM/NU7441 cotreatment (Figures 5D,E). Although the present U251 cellular model is actually a limitation in this study, we would like to extend such effects to the 23 other compounds and validate them by using previous our iPS-derived motor neuron models in the future. Another significant compound is F7, berberine chloride, which is an alkaloid also known to be a ligand of DNA/RNA G-quadruplexes (Che et al., 2018; Dumas et al., 2021). Recently, the interaction between FUS/FUS-ALS mutations and G4-DNA/RNA was well characterized based on G4-RNA–dependent LLPS and liquid-to-solid transition *in vitro* (Ishiguro et al., 2021a,b). In both *in vitro* and *in vivo* systems, the roles of FUS, G4-RNA interactions, and G4-RNA ligands in SG and aggregate formation will be further studied in the future. These results suggest that it must be feasible to enrich target candidates in screens using our biologically annotated library and conventional chemical screens. However, we did not find a common biological pathway to which all hit compounds directly correlate, suggesting that each compound acts to mitigate the formation of FUS-SGs through different molecular pathways. Therefore, these hit compounds can be used as tools to elucidate the mechanisms of FUS localization to several intracellular membraneless organelles and FUS protein aggregation. Finally, we hope that these compounds will help to elucidate the FUS aggregation mechanism and the etiological mechanisms of ALS and neurodegeneration.

Data availability statement

The raw data supporting the conclusions of this article will be made available by the authors, without undue reservation.

Author contributions

MN, HO, and MY: conceptualization. MN, OS, KA-T, YH-Y, and TF: data curation. MN, OS, and MY: formal analysis. MY and HO: funding acquisition. KO, HI, MY, and HO: project administration. MN, OS, HI, and MY: resources. MY and HO: supervision. MN, KO, HO, and MY: validation. MN, OS, and MY: visualization. MY and MN: writing – original draft. MY, MN, YH-Y, and HO: writing – review and editing. All authors contributed to the article and approved the submitted version.

Funding

This work was supported by grants from the SIL Research Fund from Takeda Pharmaceutical Company, Ltd., Japan and a Grant-in-Aid for Scientific Research from the JSPS (grant number JP20H00485a) to MY and HO. This work is also supported by a Grant-in-Aid for Transformative Research Areas (A) from The MEXT (grant number JP22H05589) and a Grant-in-Aid for Scientific Research from the JSPS (grant number P19H03543), the Takeda Science Foundation, Japan, Takeda-COCKPI-T and the SERIKA Fund to MY the Takeda Science Foundation and the ALS Foundation (Japan ALS Association) to YH-Y.

Acknowledgments

We thank Hiroyuki Kato, Takahisa Ogasawara, Sho Ninomiya, Yukinobu Hayashi and Airi Hasegawa for technical assistance. We also thank Hajime Komano, Masato Yugami, and Tsuyoshi Matsuo for valuable discussions. We would like to express our deep appreciation to Masaaki Funata, Principal Scientist of Neuroscience DDU-iBL, for his help in searching for structurally related compounds from the 1st screening hit compounds in conducting this research. We would like to thank the Neuroscience Drug Discovery Unit (DDU)-Innovative Biology Laboratories (iBL) for their support. Finally, we would like to thank Yoshiyuki Tsujihata, Director, and Keiji Yamamoto, Senior director of Neuroscience DDU-iBL, for giving us the opportunity to conduct this research.

Conflict of interest

HO is a paid member of the Scientific Advisory Board of San Bio Co., Ltd., and K Pharma, Inc. MY is a scientific advisor of K Pharma, Inc.

MN, OS, KA-T, KO, and HI were employed by the company Takeda Pharmaceutical Company Limited.

The remaining authors declare that the research was conducted in the absence of any commercial or financial relationships that could be construed as a potential conflict of interest.

Publisher's note

All claims expressed in this article are solely those of the authors and do not necessarily represent those of their affiliated organizations, or those of the publisher, the editors and the reviewers. Any product that may be evaluated in this article, or claim that may be made by its manufacturer, is not guaranteed or endorsed by the publisher.

Supplementary material

The Supplementary material for this article can be found online at: https://www.frontiersin.org/articles/10.3389/fnmol.2022.953365/full#supplementary-material

References

Arai, T., Hasegawa, M., Akiyama, H., Ikeda, K., Nonaka, T., Mori, H., et al. (2006). TDP-43 is a component of ubiquitin-positive tau-negative inclusions in frontotemporal lobar degeneration and amyotrophic lateral sclerosis. *Biochem. Biophys. Res. Commun.* 351, 602–611. doi: 10.1016/j.bbrc.2006.10.093

Aulas, A., Stabile, S., and Vande Velde, C. (2012). Endogenous TDP-43, but not FUS, contributes to stress granule assembly via G3BP. *Mol. Neurodegener.* 7:54. doi: 10.1186/1750-1326-7-54

Belzil, V. V., Valdmanis, P. N., Dion, P. A., Daoud, H., Kabashi, E., Noreau, A., et al. (2009). Mutations in FUS cause FALS and SALS in French and French Canadian populations. *Neurology* 73, 1176–1179. doi: 10.1212/WNL.0b013e3181bbfeef

Che, T., Wang, Y. Q., Huang, Z. L., Tan, J. H., Huang, Z. S., and Chen, S. B. (2018). Natural alkaloids and heterocycles as G-Quadruplex ligands and potential anticancer agents. *Molecules* 23:493. doi: 10.3390/molecules23020493

Chiò, A., Restagno, G., Brunetti, M., Ossola, I., Calvo, A., Mora, G., et al. (2009). Two Italian kindreds with familial amyotrophic lateral sclerosis due to FUS mutation. *Neurobiol. Aging* 30, 1272–1275. doi: 10.1016/j.neurobiolaging.2009.05.001

Deng, Q., Holler, C. J., Taylor, G., Hudson, K. F., Watkins, W., Gearing, M., et al. (2014). FUS is phosphorylated by DNA-PK and accumulates in the cytoplasm after DNA damage. *J. Neurosci.* 34, 7802–7813. doi: 10.1523/JNEUROSCI.0172-14.2014

Dormann, D., Rodde, R., Edbauer, D., Bentmann, E., Fischer, I., Hruscha, A., et al. (2010). ALS-associated fused in sarcoma (FUS) mutations disrupt Transportin-mediated nuclear import. *EMBO J.* 29, 2841–2857. doi: 10.1038/emboj.2010.143

Dumas, L., Herviou, P., Dassi, E., Cammas, A., and Millevoi, S. (2021). G-Quadruplexes in RNA biology: recent advances and future directions. *Trends Biochem. Sci.* 46, 270–283. doi: 10.1016/j.tibs.2020.11.001

Fang, M. Y., Markmiller, S., Vu, A. Q., Javaherian, A., Dowdle, W. E., Jolivet, P., et al. (2019). Small-molecule modulation of TDP-43 recruitment to stress granules prevents persistent TDP-43 accumulation in ALS/FTD. *Neuron* 103, 802–819.e11. doi: 10.1016/j.neuron.2019.05.048

François-Moutal, L., Perez-Miller, S., Scott, D. D., Miranda, V. G., Mollasalehi, N., and Khanna, M. (2019). Structural insights into TDP-43 and effects of post-translational modifications. *Front. Mol. Neurosci.* 12:301. doi: 10.3389/fnmol.2019.00301

Fujimori, K., Ishikawa, M., Otomo, A., Atsuta, N., Nakamura, R., Akiyama, T., et al. (2018). Modeling sporadic ALS in iPSC-derived motor neurons identifies a potential therapeutic agent. *Nat. Med.* 24, 1579–1589. doi: 10.1038/s41591-018-0140-5

Gao, F. B., Almeida, S., and Lopez-Gonzalez, R. (2017). Dysregulated molecular pathways in amyotrophic lateral sclerosis-frontotemporal dementia spectrum disorder. *EMBO J.* 36, 2931–2950. doi: 10.15252/embj.201797568

Gomes, E., and Shorter, J. (2019). The molecular language of membraneless organelles. *J. Biol. Chem.* 294, 7115–7127. doi: 10.1074/jbc.TM118.001192

Grembecka, J., He, S., Shi, A., Purohit, T., Muntean, A. G., Sorenson, R. J., et al. (2012). Menin-MLL inhibitors reverse oncogenic activity of MLL fusion proteins in leukemia. *Nat. Chem. Biol.* 8, 277–284. doi: 10.1038/nchembio.773

Hasegawa, M., Arai, T., Nonaka, T., Kametani, F., Yoshida, M., Hashizume, Y., et al. (2008). Phosphorylated TDP-43 in frontotemporal lobar degeneration and amyotrophic lateral sclerosis. *Ann. Neurol.* 64, 60–70. doi: 10.1002/ana.21425

Hayakawa-Yano, Y., Suyama, S., Nogami, M., Yugami, M., Koya, I., Furukawa, T., et al. (2017). An RNA-binding protein, Qki5, regulates embryonic neural stem cells through pre-mRNA processing in cell adhesion signaling. *Genes Dev.* 31, 1910–1925. doi: 10.1101/gad.300822.117

Higelin, J., Demestre, M., Putz, S., Delling, J. P., Jacob, C., Lutz, A. K., et al. (2016). FUS mislocalization and vulnerability to DNA damage in ALS patients derived hiPSCs and aging motoneurons. *Front. Cell. Neurosci.* 10:290. doi: 10.3389/fncel.2016.00290

Hill, S. J., Mordes, D. A., Cameron, L. A., Neuberg, D. S., Landini, S., Eggan, K., et al. (2016). Two familial ALS proteins function in prevention/repair of transcription-associated DNA damage. *Proc. Natl. Acad. Sci. U. S. A.* 113, E7701–E7709. doi: 10.1073/pnas.1611673113

Hofweber, M., Hutten, S., Bourgeois, B., Spreitzer, E., Niedner-Boblenz, A., Schifferer, M., et al. (2018). Phase separation of FUS is suppressed by its nuclear import receptor and arginine methylation. *Cells* 173, 706–719.e13. doi: 10.1016/j.cell.2018.03.004

Ichiyanagi, N., Fujimori, K., Yano, M., Ishihara-Fujisaki, C., Sone, T., Akiyama, T., et al. (2016). Establishment of in vitro FUS-associated familial amyotrophic lateral sclerosis model using human induced pluripotent stem cells. *Stem Cell Rep.* 6, 496–510. doi: 10.1016/j.stemcr.2016.02.011

Ishiguro, A., Katayama, A., and Ishihama, A. (2021a). Different recognition modes of G-quadruplex RNA between two ALS/FTLD-linked proteins TDP-43 and FUS. *FEBS Lett.* 595, 310–323. doi: 10.1002/1873-3468.14013

Ishiguro, A., Lu, J., Ozawa, D., Nagai, Y., and Ishihama, A. (2021b). ALS-linked FUS mutations dysregulate G-quadruplex-dependent liquid-liquid phase separation and liquid-to-solid transition. *J. Biol. Chem.* 297:101284. doi: 10.1016/j.jbc.2021.101284

Kim, H. J., Kim, N. C., Wang, Y. D., Scarborough, E. A., Moore, J., Diaz, Z., et al. (2013). Mutations in prion-like domains in hnRNPA2B1 and hnRNPA1 cause multisystem proteinopathy and ALS. *Nature* 495, 467–473. doi: 10.1038/nature11922

Kwiatkowski, T. J. J., Bosco, D. A., Leclerc, A. L., Tamrazian, E., Vanderburg, C. R., Russ, C., et al. (2009). Mutations in the FUS/TLS gene on chromosome 16 cause familial amyotrophic lateral sclerosis. *Science* 323, 1205–1208. doi: 10.1126/science.1166066

Lee, B. J., Cansizoglu, A. E., Süel, K. E., Louis, T. H., Zhang, Z., and Chook, Y. M. (2006). Rules for nuclear localization sequence recognition by karyopherin beta 2. *Cells* 126, 543–558. doi: 10.1016/j.cell.2006.05.049

Ling, S. C., Polymenidou, M., and Cleveland, D. W. (2013). Converging mechanisms in ALS and FTD: disrupted RNA and protein homeostasis. *Neuron* 79, 416–438. doi: 10.1016/j.neuron.2013.07.033

Liu, J., Xia, H., Kim, M., Xu, L., Li, Y., Zhang, L., et al. (2011). Beclin1 controls the levels of p53 by regulating the deubiquitination activity of USP10 and USP13. *Cells* 147, 223–234. doi: 10.1016/j.cell.2011.08.037

Mackenzie, I. R., Nicholson, A. M., Sarkar, M., Messing, J., Purice, M. D., Pottier, C., et al. (2017). TIA1 mutations in amyotrophic lateral sclerosis and frontotemporal dementia promote phase separation and alter stress granule dynamics. *Neuron* 95, 808–816.e9. doi: 10.1016/j.neuron.2017.07.025

Markmiller, S., Soltanieh, S., Server, K. L., Mak, R., Jin, W., Fang, M. Y., et al. (2018). Context-dependent and disease-specific diversity in protein interactions within stress granules. *Cells* 172, 590–604.e13. doi: 10.1016/j.cell.2017.12.032

Martinez-Macias, M. I., Moore, D. A. Q., Green, R. L., Gomez-Herreros, F., Naumann, M., Hermann, A., et al. (2019). FUS (fused in sarcoma) is a component of the cellular response to topoisomerase I-induced DNA breakage and transcriptional stress. *Life Sci. Alliance* 2:e201800222. doi: 10.26508/lsa.201800222

Mateju, D., Franzmann, T. M., Patel, A., Kopach, A., Boczek, E. E., Maharana, S., et al. (2017). An aberrant phase transition of stress granules triggered by misfolded protein and prevented by chaperone function. *EMBO J.* 36, 1669–1687. doi: 10.15252/embj.201695957

Matsuo, T., Adachi-Tominari, K., Sano, O., Kamei, T., Nogami, M., Ogi, K., et al. (2021). Involvement of ferroptosis in human motor neuron cell death. *Biochem. Biophys. Res. Commun.* 566, 24–29. doi: 10.1016/j.bbrc.2021.05.095

Maziuk, B., Ballance, H. I., and Wolozin, B. (2017). Dysregulation of RNA binding protein aggregation in neurodegenerative disorders. *Front. Mol. Neurosci.* 10:89. doi: 10.3389/fnmol.2017.00089

Monahan, Z., Ryan, V. H., Janke, A. M., Burke, K. A., Rhoads, S. N., Zerze, G. H., et al. (2017). Phosphorylation of the FUS low-complexity domain disrupts phase separation, aggregation, and toxicity. *EMBO J.* 36, 2951–2967. doi: 10.15252/embj.201696394

Murray, D. T., Kato, M., Lin, Y., Thurber, K. R., Hung, I., McKnight, S. L., et al. (2017). Structure of FUS protein fibrils and its relevance to self-assembly and phase separation of low-complexity domains. *Cells* 171, 615–627.e16. doi: 10.1016/j.cell.2017.08.048

Nagai, T., Ibata, K., Park, E. S., Kubota, M., Mikoshiba, K., and Miyawaki, A. (2002). A variant of yellow fluorescent protein with fast and efficient maturation for cell-biological applications. *Nat. Biotechnol.* 20, 87–90. doi: 10.1038/nbt0102-87

Naumann, M., Pal, A., Goswami, A., Lojewski, X., Japtok, J., Vehlow, A., et al. (2018). Impaired DNA damage response signaling by FUS-NLS mutations leads to neurodegeneration and FUS aggregate formation. *Nat. Commun.* 9:335. doi: 10.1038/s41467-017-02299-1

Neumann, M., Rademakers, R., Roeber, S., Baker, M., Kretzschmar, H. A., and Mackenzie, I. R. A. (2009). A new subtype of frontotemporal lobar degeneration with FUS pathology. *Brain* 132, 2922–2931. doi: 10.1093/brain/awp214

Nogami, M., Ishikawa, M., Doi, A., Sano, O., Sone, T., Akiyama, T., et al. (2021a). Identification of hub molecules of FUS-ALS by Bayesian gene regulatory network analysis of iPSC model: iBRN. *Neurobiol. Dis.* 155:105364. doi: 10.1016/j.nbd.2021.105364

Nogami, M., Miyamoto, K., Hayakawa-Yano, Y., Nakanishi, A., Yano, M., and Okano, H. (2021b). DGCR8-dependent efficient pri-miRNA processing of human pri-miR-9-2. *J. Biol. Chem.* 296:100409. doi: 10.1016/j.jbc.2021.100409

Okano, H., and Morimoto, S. (2022). iPSC-based disease modeling and drug discovery in cardinal neurodegenerative disorders. *Cell Stem Cell* 29, 189–208. doi: 10.1016/j.stem.2022.01.007

Okano, H., Yasuda, D., Fujimori, K., Morimoto, S., and Takahashi, S. (2020). Ropinirole, a new ALS drug candidate developed using iPSCs. *Trends Pharmacol. Sci.* 41, 99–109. doi: 10.1016/j.tips.2019.12.002

Rhoads, S. N., Monahan, Z. T., Yee, D. S., Leung, A. Y., Newcombe, C. G., O'Meally, R. N., et al. (2018). The prionlike domain of FUS is multiphosphorylated following DNA damage without altering nuclear localization. *Mol. Biol. Cell* 29, 1786–1797. doi: 10.1091/mbc.E17-12-0735

Spannl, S., Tereshchenko, M., Mastromarco, G. J., Ihn, S. J., and Lee, H. O. (2019). Biomolecular condensates in neurodegeneration and cancer. *Traffic* 20, 890–911. doi: 10.1111/tra.12704

Tada, M., Coon, E. A., Osmand, A. P., Kirby, P. A., Martin, W., Wieler, M., et al. (2012). Coexistence of Huntington's disease and amyotrophic lateral sclerosis: a clinicopathologic study. *Acta Neuropathol.* 124, 749–760. doi: 10.1007/s00401-012-1005-5

Tsuiji, H., Iguchi, Y., Furuya, A., Kataoka, A., Hatsuta, H., Atsuta, N., et al. (2013). Spliceosome integrity is defective in the motor neuron diseases ALS and SMA. *EMBO Mol. Med.* 5, 221–234. doi: 10.1002/emmm.201202303

Vance, C., Rogelj, B., Hortobágyi, T., de Vos, K. J., Nishimura, A. L., Sreedharan, J., et al. (2009). Mutations in FUS, an RNA processing protein, cause familial amyotrophic lateral sclerosis type 6. *Science* 323, 1208–1211. doi: 10.1126/science.1165942

Wolozin, B., and Ivanov, P. (2019). Stress granules and neurodegeneration. *Nat. Rev. Neurosci.* 20, 649–666. doi: 10.1038/s41583-019-0222-5

Wu, J., Zhou, L., Tonissen, K., Tee, R., and Artzt, K. (1999). The quaking I-5 protein (QKI-5) has a novel nuclear localization signal and shuttles between the nucleus and the cytoplasm. *J. Biol. Chem.* 274, 29202–29210. doi: 10.1074/jbc.274.41.29202

frontiers | Frontiers in Molecular Neuroscience

TYPE Original Research
PUBLISHED 05 January 2023
DOI 10.3389/fnmol.2022.1068019

OPEN ACCESS

EDITED BY
Philip Washbourne,
University of Oregon,
United States

REVIEWED BY
Sadie A. Bergeron,
West Virginia University,
United States
Suresh Sundram,
Monash University,
Australia

*CORRESPONDENCE
Kewen Jiang
✉ jiangkw_zju@zju.edu.cn

†These authors have contributed equally to this work

SPECIALTY SECTION
This article was submitted to Methods and Model Organisms, a section of the journal Frontiers in Molecular Neuroscience

RECEIVED 13 October 2022
ACCEPTED 12 December 2022
PUBLISHED 05 January 2023

CITATION
Wu J, Lin X, Wu D, Yan B, Bao M, Zheng P, Wang J, Yang C, Li Z, Jin X and Jiang K (2023) Poly(I:C)-exposed zebrafish shows autism-like behaviors which are ameliorated by *fabp2* gene knockout. *Front. Mol. Neurosci.* 15:1068019. doi: 10.3389/fnmol.2022.1068019

Poly(I:C)-exposed zebrafish shows autism-like behaviors which are ameliorated by *fabp2* gene knockout

Jing Wu[1†], Xueting Lin[1†], Dian Wu[1†], Binhong Yan[2], Mengyi Bao[1], Peilei Zheng[2], Jiangping Wang[1], Cuiwei Yang[3], Zhongxia Li[4], Xiaoming Jin[5,6] and Kewen Jiang[1,2*]

[1]Department of Child Psychology, The Children's Hospital, Zhejiang University School of Medicine, National Clinical Research Center For Child Health, Hangzhou, China, [2]Department of Biobank Center, The Children's Hospital, Zhejiang University School of Medicine, National Clinical Research Center For Child Health, Hangzhou, China, [3]Department of Neurology, The Children's Hospital, Zhejiang University School of Medicine, National Clinical Research Center For Child Health, Hangzhou, China, [4]Department of Pediatrics, The Seventh Affiliated Hospital of Guangxi Medical University (Wuzhou GongRen Hospital), Wuzhou, Guangxi, China, [5]Indiana Spinal Cord and Brain Injury Research Group, Stark Neurosciences Research Institute, Department of Anatomy, Cell Biology and Physiology, Indiana University School of Medicine, Indianapolis, IN, United States, [6]Stark Neuroscience Research Institute, Department of Neurological Surgery, Indiana University School of Medicine, Indianapolis, IN, United States

Introduction: Autism spectrum disorder (ASD) is a group of neurodevelopmental disorders mainly representing impaired social communication. The etiology of ASD includes genetic and environmental risk factors. Rodent models containing ASD risk gene mutations or environmental risk factors, such as exposure to maternal inflammation, show abnormal behavior. Although zebrafish conserves many important brain structures of humans and has sophisticated and fine behaviors in social interaction, it is unknown whether the social behaviors of their offspring would be impaired due to exposure to maternal inflammation.

Methods: We exposed zebrafish to maternal immune activation (MIA) by injection with polyinosinic:polycytidylic acid [poly(I:C)], and screened their behaviors through social behavioral tests such as social preference and shoaling behavior tests. We compared phenotypes resulted from different ways of poly(I:C) exposure. RNA sequencing was performed to explore the differential expression genes (DEGs). Gene ontology (GO), Kyoto Encyclopedia of Genes and Genomes (KEGG) and protein–protein interaction (PPI) network analysis was performed with the detected DEGs to find the concentrated pathways. Finally, we knocked out the *fatty acid-binding protein 2 (fabp2)*, a key node of the concentrated PPI network, to find its rescues on the altered social behavior.

Results: We reported here that MIA offspring born to mothers injected with poly(I:C) exhibited impaired social approach and social cohesion that mimicked human ASD phenotypes. Both maternal exposure and direct embryo exposure to poly(I:C) resulted in activations of the innate immune system through toll-like receptors 3 and 4. RNA-sequencing results from MIA brain tissues illustrated that the numbers of overexpressed genes were

significantly more than that of underexpressed genes. GO and KEGG analyses found that MIA-induced DEGs were mainly concentrated in complement and coagulation cascade pathways. PPI network analyses suggested that *villin-1* (*vil1*) pathway might play a key role in MIA-induced ASD. Knockout of *fabp2* in F0 zebrafish rescued the social behavior deficits in MIA offspring.

Conclusions: Overall, our work established an ASD model with assessable behavior phenotype in zebrafish and provided key insights into environmental risk factor in ASD etiology and the influence of *fabp2* gene on ASD-like behavior.

KEYWORDS

autism, F0 knockout, zebrafish, social interaction, shoaling, *fabp2*

1. Introduction

Autism spectrum disorder (ASD) is a group of neurodevelopmental disorders with genetic and clinical heterogeneity characterized by altered social communication, unusually restricted interests, and repetitive behavior (Lai et al., 2014). The etiology of ASD includes environmental and genetic risk factors (Lyall et al., 2017). Next-generation sequencing approaches have found a large number of high-risk genes in ASD (O'Roak et al., 2012; Yuen et al., 2017). Mice containing ASD risk gene mutations showed abnormal behavior, including social disorder (Ey et al., 2011; Crawley, 2012). Similar behavioral abnormalities were observed in mouse models of environmental risk factors for ASD, such as exposure to maternal inflammation (Patterson, 2011). These models deepen our understanding of the mechanisms underlying ASD at both molecular and neural levels. However, preparing mouse models of ASD is time-consuming and laborious, and the yield is limited, especially when a large number of disordered animals are needed such as for targeted drug screening.

The zebrafish (Danio rerio) is an easy-to-handle vertebrate model for neuroscience research (Kalueff et al., 2014). Recent evidence suggests that it conserves many important human brain structures, such as the amygdala, hippocampus and hypothalamus (Parker et al., 2013) and that it has a sophisticated and fine behavior in social interaction, anxiety, aggression, learning and cognition (Kalueff et al., 2014). Since zebrafish and human genomes are highly conserved with more than 80% of human disease genes presenting in zebrafish (Howe et al., 2013), zebrafish has been widely used as a useful tool to clarify the functions of human candidate genes for ASD. However, after knockout of human high-risk genes of ASD, zebrafish offspring does not always show an autism-like phenotype, which limits its use for testing novel treatment and for drug screening. Although it is possible to knockout multiple genes with a single embryo microinjection in this model (Parvez et al., 2021), the low success and high mortality rate is a significant challenge. On the other hand, immune alterations are shown to play key roles in the mechanism of ASD. Immune abnormalities are associated with increased risk of ASD in children (Atladóttir et al., 2010), occurrence of psychiatric and non-psychiatric comorbidities of ASD (Wakefield, 2002; Wakefield et al., 2005; Ashwood and Wakefield, 2006), and many other features of ASD including mood and sleep disturbances. In rodents, exposing to maternal inflammation, i.e., maternal immune activation (MIA; Patterson, 2011), impairs sociability in offspring and serves as an environmental risk factors-ASD model. Although zebrafish has multiple advantages for ASD research as mentioned above, it is unknown whether sociability would also be impaired in MIA offspring.

A zebrafish model of ASD that involves environmental risk factors and immune alterations would be valuable not only for studying the pathology, comorbidity, and underlying mechanisms of ASD, but also for treatment development and drug screening. Here, we established that the social behavior is impaired in zebrafish offspring exposed to MIA by comparing them with those of direct embryo exposure of environmental risk factor. Since the mechanisms underlying MIA-induced ASD has not been fully understood, we analyzed differential gene expressions (DEGs) and protein interactions in MIA-induced ASD zebrafish. Finally, we identified a gene [*fatty acid-binding protein 2* (*fabp2*)] that was the only one of the top 10 co-expressed differential genes of both MIA and *in vitro* exposure of environmental risk factor and interacted with the key node [*villin-1* (*vil1*), a gene encoding actin-binding proteins] of protein–protein interaction (PPI) network. It was upregulated in MIA offspring but downregulated in offspring with direct embryo

Abbreviations: ASD, Autism spectrum disorders; DEG, Differential expression genes; DNB, DNA nanoball; dpf, Days post-fertilization; E3, Embryonic media; Fabp2, Fatty acid-binding protein 2; GO, Gene ontology; i.p., Intraperitoneal injection; IFABP, Intestinal fatty acid binding protein; KEGG, Kyoto Encyclopedia of Genes and Genomes; LC50, Half-maximal lethal concentrations; MIA, Maternal immune activation; mpf, Months post-fertilization; NTT, Novel tank test; OFT, Open field test; PBS, Phosphate buffered solution; PIVE, Polyinosinic:polycytidylic acid in vitro exposure; PPI, Protein–protein interactions; Poly(I:C), Polyinosinic:polycytidylic acid; RT-qPCR, Reverse transcription quantitative PCR; SEM, Standard error of the mean; SS, Social stimulus; TLR, Toll-like receptor; TS, Test subject; Vil1, villin-1; WT, Wild type.

exposure to environmental risk factor. Importantly, knockout of this gene rescued the social behavior deficits in both MIA and *in vitro* exposure of environmental risk factor offspring.

2. Materials and methods

2.1. Zebrafish care and husbandry

All experiments and animal handling were performed according to the Guide for the Care and Use of Laboratory Zebrafish by the China Zebrafish Resource Center and were approved by the Animal Care and Use Committee at Zhejiang University School of Medicine (16779). Wild-type (WT) zebrafish (*Danio rerio*) AB strain was housed in a modular zebrafish system (Haisheng, China), and all fish were kept in a 10-h dark / 14-h light cycle, and 28 ± 0.5°C filtered and UV sterilized water. For breeding, after keeping adult female and male fish separate overnight in a 1-L crossing tank, we released them by removing the divider at 8–9 am the next morning and collected the fertilized embryos within 1 h after their releasing. After being maintained in embryonic media E3 for 24 h, healthy embryos were selected and raised regularly (See Additional file 1: File S1).

2.2. MIA and polyinosinic:polycytidylic acid (poly(I:C)) *in vitro* exposure (PIVE)

Poly(I:C) was used to establish MIA in zebrafish as previously reported in pregnant dams (Kim S. et al., 2017). For PIVE, we evaluated the toxicity of poly(I:C) by using embryos of 1–6 days post-fertilization (dpf; Aspatwar et al., 2019). In brief, healthy fertilized embryos (1 dpf) were randomly placed into a 200 µl volume of E3 or E3 with gradient concentrations of poly(I:C) (528,906, Millipore; 10, 50, 100, 250, 500, 750, or 1,000 µM) for the next consecutive 5 days. The embryos/larvae were carefully checked daily and the numbers of death, morphological defects of individuals such as absence of swim bladder, skeletal abnormality, pericardial edema and unhatched embryo, as well as the individuals of abnormal movement pattern were checked with a stereo microscope and recorded. The half-maximal lethal concentrations (LC50) were calculated based on above evaluation (Additional file 2: Figure S1).

A modified MIA by poly(I:C) injection without infections of segmented filamentous bacteria was used (Chow et al., 2016; Kim S. et al., 2017). In brief, a healthy adult female zebrafish received a single intraperitoneal injection (i.p.) of poly(I:C) (20 µg/g or 50 µg/g; about 5 µl) or received an injection of the same volume of vehicle (phosphate buffered solution (PBS)) as control. Basing on our results of poly(I:C)-indued immune response (Tsukada et al., 2021), we chose to mate the fish in 24 h after Poly(I:C) injection. For injection (i.p.), after a fish was hypothermic anesthetized, a needle (tip 0.1 µm) was gently inserted into the midline of the abdomen behind the pectoral fins to a depth of 3 mm. After injection, it was put back into reproductive water (28°C). Normally, the fish would recover free swimming within 1 min; otherwise, the fish was not used for mating (Samaee et al., 2017). We collected fertilized embryos within 1 h after mating and the healthy embryos were collected the next morning and raised normally. For PIVE, after establishing the LC50 (200.7 µM) of poly(I:C), we used concentrations lower than LC50 in our experiments, which resulted in little visible morphological defects and low mortality. The fertilized embryos (1 dpf) from the wild type (WT) strain were raised in E3 with poly(I:C) (10, 50, or 100 µM separately; final volume of 200 µl for each embryo by using 96-well plate) for the next consecutive 5 days or in E3 with the same volume of vehicle. Embryos/larvae were examined daily under a stereo microscope, and the numbers of death, morphological defects and abnormal movement-pattern were recorded. The fish were raised under normal husbandry from 6 dpf.

2.3. Measurement of immune response parameters

For maternal immune response induced by poly(I:C) at 24 h after injection, the fish were anesthetized by low-temperature, and the liver, brain, spleen and intestine tissues were collected, quickly frozen and stored at −80°C. There were 1–2 biological repeat samples in each group (n = 1–2), which was a mixture of tissue samples of 7 zebrafish individuals (20 mg) (Figure 1A). For immune response of MIA offspring or PIVE larvae, the fish were anesthetized at 3, 7, 14, and 21 dpf, respectively. There were two biological repeat samples in each group (n = 2), which was a mixture of 10–15 zebrafish individuals (20 mg) (Figure 1A). The frozen samples were thawed in ice, homogenized in ice-cold RIPA (200 µl per 20 mg tissue), and then centrifuged to obtain the supernatant (15,000 rpm, 4°C, 30 min) for further measurement. The immunoglobulin M (IgM), complement C4 (C4) and immunoglobulin A (IgA) levels were analyzed by using the kits (Nanjing Jiancheng Bioengineering Institute, Nanjing, China) according to the manufacturer's protocols. An immunoturbidimetric assay method was used to measure the agglutinate produced by the reaction at 340 nm wavelength (Hitachi 7180 biochemical analyzer).

Poly(I:C) can activate host immune defense through toll-like receptor (TLR). To determine immune response to the MIA/PIVE treatment, TLR3, TLR4ba and TLR4bb genes were detected by a reverse transcription quantitative PCR (RT-qPCR) (see detail in 2.7 section). At 24 h after the poly(I:C) injection, 3–5 maternal fish, as well as at 1 dpf, 3–5 offspring were collected from the MIA-PBS and MIA-50 µg/g groups. For PIVE, 3–5 offspring were collected from the PIVE-E3 and PIVE-100 µM groups at 1 dpf (PIVE-1) or 2 dpf (PIVE-2) after a 24 h poly(I:C) treatment (Figure 1A).

2.4. Behavioral analysis

During a light cycle, the fish were transferred to a testing room equipped with a high-definition digital camera at least 1 h

10.3389/fnmol.2022.1068019

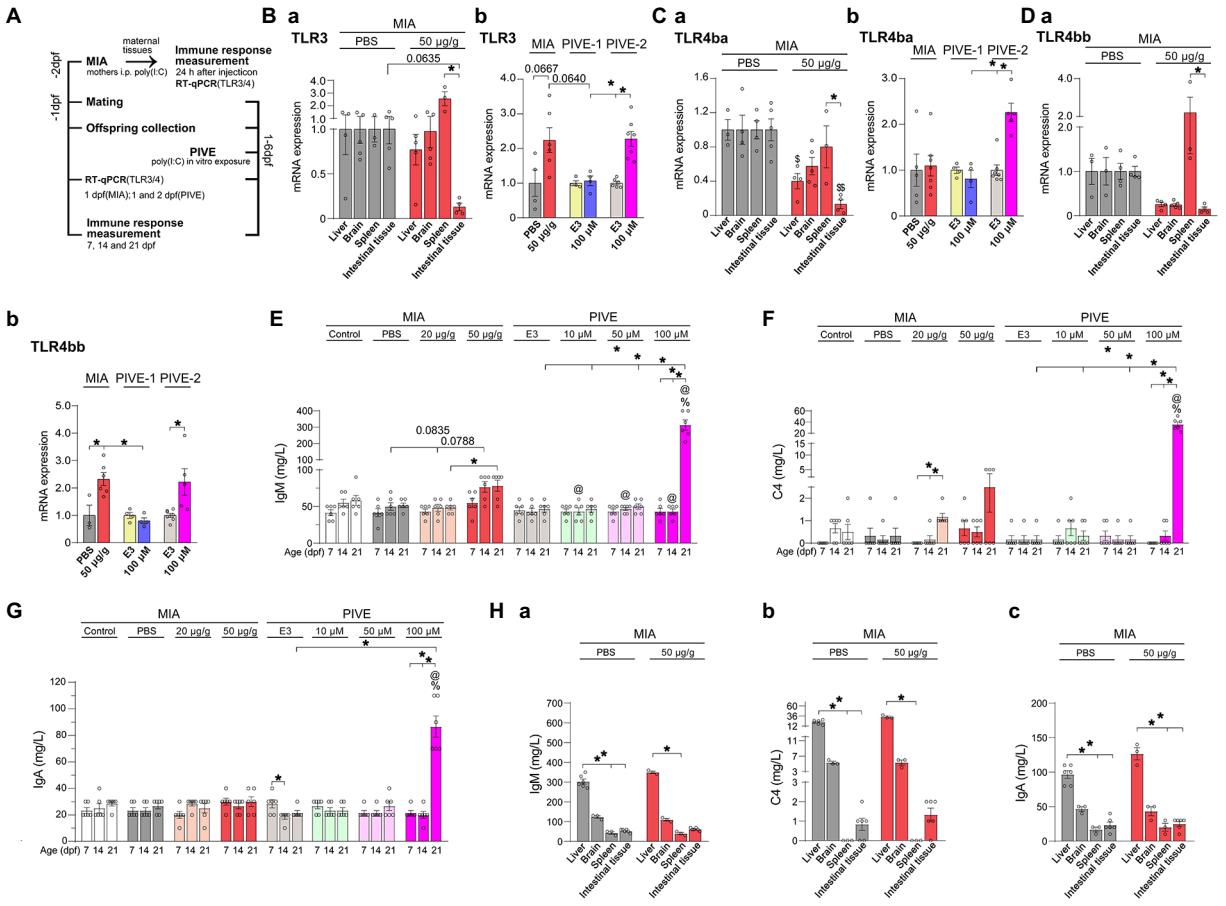

FIGURE 1

MIA offspring born to mothers injected with poly(I:C) showed an immune response. **(A)** For the maternal immune response induced by poly(I:C) (MIA-50μg/g), 24h after injection, TLR3, TLR4ba, and TLR4bb genes were selected and detected by quantitative RT-PCR, and the immunoglobulin M (IgM), complement C4 (C4) and immunoglobulin A (IgA) levels were analyzed by the immunoturbdimetric assay method. For MIA offspring TLR3, TLR4ba, and TLR4bb gene levels and IgM, C4 and IgA levels were checked at 1dpf; as well as for PIVE, TLR3, TLR4ba and TLR4bb gene levels and IgM, C4, and IgA levels were tested at 1dpf (PIVE-1) or 2dpf (PIVE-2) after a 24h poly(I:C) treatment. **(Ba)** TLR3 mRNA expression was up-regulated in spleen of maternal fish of MIA-50μg/g group (U=0, p=0.0635) compared to that of MIA-PBS group; TLR3 mRNA expression was significantly down-regulated in intestinal tissue compared to that in spleen of maternal fish of MIA-50μg/g group (Z=3.37, p<0.05). **(Bb)** TLR3 mRNA expression was up-regulated of MIA offspring (U=3.30, p=0.0667) compared to that of MIA-PBS group; For PIVE, there was no significant change in TLR3 mRNA expression of the offspring collected at 1dpf after a 24h poly(I:C) treatment; while TLR3 mRNA expression of the offspring collected at 2dpf after a 24h poly(I:C) treatment was significantly up-regulated. **(Ca)** TLR4ba mRNA expression was significantly down-regulated in intestinal tissue and liver of maternal fish of MIA-50μg/g group compared to that of MIA-PBS group (Two-way ANOVA, F=32.07 for MIA and F=2.40 for Tissue; multiple comparisons test: t=5.04 and 3.06, p<0.01 and 0.05, in intestinal tissue and liver, respectively). TLR4ba mRNA expression was significantly down-regulated in intestinal tissue compared to that in spleen of maternal fish of MIA-50μg/g group (t=3.41, p<0.05). **(Cb)** TLR4ba mRNA expression did not changed of MIA offspring compared to that of MIA-PBS group; For PIVE, there was no significant change in TLR4ba mRNA expression of the offspring collected at 1dpf after a 24h poly(I:C) treatment; while TLR4ba mRNA expression of the offspring collected at 2dpf after a 24h poly(I:C) treatment was significantly up-regulated (U=0.00, p<0.05). **(Da)** TLR4bb mRNA expression was significantly down-regulated in intestinal tissue compared to that in spleen of maternal fish of MIA-50μg/g group (Z=2.89, p<0.05). **(Db)** TLR4bb mRNA expression was up-regulated of MIA offspring (U=1.00, p<0.05) compared to that of MIA-PBS group; For PIVE, there was no significant change in TLR4bb mRNA expression of the offspring collected at 1dpf after a 24h poly(I:C) treatment; while TLR4bb mRNA expression of the offspring collected at 2dpf after a 24h poly(I:C) treatment was significantly up-regulated (U=1.00, p<0.05). **(E)** The levels of IgM were increased of MIA-50μg/g offspring at 14dpf (Z=2.46, p=0.08, compared to that of MIA-PBS group). The levels of IgM were significantly increased of PIVE-100μm larvae at 21dpf (Z=3.14, p<0.05, compared to that of PIVE-E3 group). **(F)** The levels of C4 were not changed significantly of MIA-50μg/g offspring. The levels of C4 were significantly increased of PIVE-100μm larvae at 21dpf (Z=3.43, p<0.05, compared to that of PIVE-E3 group). **(G)** The levels of IgA were not changed significantly of MIA-50μg/g offspring. The levels of IgA were significantly increased of PIVE-100μm larvae at 21dpf (Z=3.58, p<0.05, compared to that of PIVE-E3 group). **(Habc)** IgM, C4 and IgA levels were not changed significantly of maternal fish of MIA-50μg/g group compared to that of MIA-PBS group. Data are presented as mean±SEM. *p<0.05; $^{\$}$ p<0.05 compared with the MIA-PBS group of the same age; $^{\%}$ p<0.05 compared with the MIA-20μg/g group of the same age; $^{@}$ p<0.05 compared with the MIA-50μg/g group of the same age. Detail about the n and descriptive data for each group and statistical analysis results could be found in Additional file 11: File S4.

before the initiation of experiments. Tracking of fish behavior was done by using the ImageJ with a wrMTrck plugin (Selvaraj et al., 2019). We analyzed the developmental changes of fish behavior for both MIA and PIVE. For larvae, the social preference test, shoaling behavior and inattentive behavior test were used at 7, 14, and 21 dpf; for juvenile and adult zebrafish,

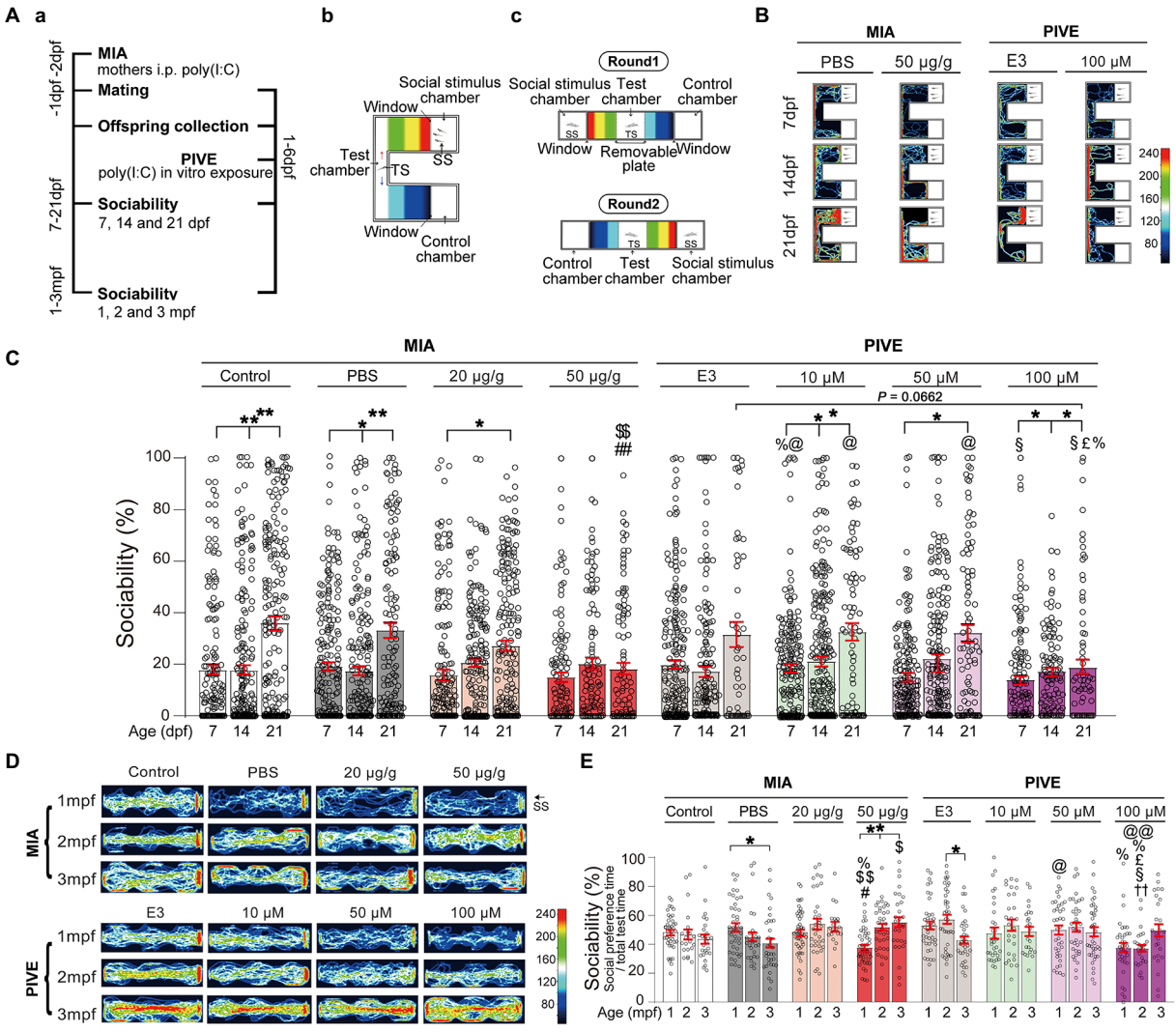

FIGURE 2
MIA offspring exhibited impaired social approach. **(Aa)** Zebrafish were tested for sociability (percentage of time spent investigating social object/total test time spent) at 7, 14, and 21dpf **(Ab)**, and 1, 2, and 3mpf **(Ac)** after maternal poly(I:C) injection (MIA) or PIVE to fertilized embryos. **(B)** Video tracking of movements of MIA and PIVE larvae at 7, 14, and 21dpf, showing the social interaction with social cue. **(C)** Sociability of MIA and PIVE larvae at 7, 14, and 21dpf. MIA impaired the sociability at 21dpf in 50μg/g group (Z=4.16 and 4.06, p<0.01, compared to that of MIA-Control and MIA-PBS group, respectively); PIVE impaired the sociability at 21dpf of 100μM group (Z=2.54, p=0.07, compared to that of PIVE-E3 group). **(D)** Video tracking of movements of MIA and PIVE larvae at 1, 2, and 3mpf, showing the social interaction with social cue. **(E)** Sociability of MIA and PIVE larvae at 1, 2, and 3mpf. MIA decreased the sociability levels at 1mpf of 50μg/g group (Z=3.59 and 3.99, p<0.05 and 0.01, compared to that of MIA-Control and MIA-PBS group respectively); PIVE impaired the sociability at 2mpf of 100μM group (Z=3.74, p<0.01, compared to that of PIVE-E3 group). Data are presented as mean±SEM. * p<0.05, ** p<0.001; $^{\#}$ p<0.05, $^{\#\#}$ p<0.001 compared with the MIA-control group of the same age with social stimulus; § p<0.05, §§ p<0.001 compared with the MIA-PBS group of the same age with social stimulus; $^{\%}$ p<0.05 compared with the MIA-20μg/g group of the same age; $^{@}$ p<0.05, $^{@@}$ p<0.001 compared with the MIA-50μg/g group of the same age. †† p<0.001 compared with the PIVE-E3 group of the same age with social stimulus. § p<0.05 compared with the PIVE-10μM group of the same age; $^{£}$ p<0.05 compared with the PIVE-50μM group of the same age. TS, Test subject; SS, Social stimulus. Detail about the n and descriptive data for each group and statistical analysis results could be found in Additional file 11: File S4.

the social preference test, shoaling behavior, open field test (OFT), novel tank test (NTT) and mirror test were used at 1, 2, and 3 month(s) post-fertilization (mpf) (Figures 2Aabc, 3Aab, 4A, 5Aabcd). Detailed information about the test tools is provided in Additional file 3: File S2. For all behavioral analysis, the test fish must be healthy. Those with obvious deformities or immobility within the test time were excluded from further analysis.

2.4.1. Social preference test

The social preference test for larvae was carried out as described in Dreosti et al. (2015). We used a transparent U-shaped plastic tank containing three compartments: a central area (bottom of U-shaped tank), the left side and the right side of the U-shaped tank, which were separated by two glass barriers located at both side of U-shaped tank (3 cm away from the bottom). Briefly, a single fish was introduced into the central area for 1 min and permitted to interact with a group of

three fish placed in one of two side compartments for another 6 min. The sociability wherein the social preference was an index based on subtracted non-social exploration, i.e., the time of the fish spent closest to the group of strangers divided by total test time (Figures 2Ab,C) or total interaction time (the time spent closest to social stimulus + the time near the empty area diagonally opposite; Additional file 2: Figure S2) and expressed as a percentage. For juvenile and adult zebrafish, we used a transparent plastic tank containing five compartments (separated by transparent plastic plates): the stimulus-fish area, near stimulus-fish area, central area, away from stimulus-fish area and reference area (Ogi et al., 2021; Figure 2Ac). Briefly, after a single fish was introduced into the central area for 30 s, the plates between the near/away stimulus-fish area was removed and let the fish stay in the area for another 30s (for acclimation). Then it was permitted to interact with a single strange fish placed in stimulus-fish area for another 10 min. To avoid moving direction preference, we randomly put a stimulus fish into the stimulus area on one side (Round 1). After 10-min behavioral recording, the same fish's behavior was checked with the stimulus fish put on the opposite side (Round 2). The sociability was defined as the time of the fish spent in the near stimulus-fish area averaged from round 1 and 2, divided by total test time (Figures 2Ac,E) or total interaction time (the time spent closest to social stimulus + the time near the empty area diagonally opposite; Additional file 2: Figure S2) and expressed as a percentage.

2.4.2. Shoaling behavior

The shoaling behavior was estimated with/without acclimation with slight modifications (Kim O. H. et al., 2017; Dwivedi et al., 2019). For larvae, four fish were released into the center of a transparent disk, and their behaviors were immediately recorded for 10 min (without acclimation) and for another 10 min (with acclimation). For juvenile and adult zebrafish, four fish were released in the center of the transparent tank, and their behaviors were immediately recorded for 10 min (without acclimation) and for another 10 min (with acclimation). A camera was fixed to the top of the swimming tanks. The distances between the four fish were estimated every 30 s (Figure 3Ab).

2.4.3. Inattentive behavior test

Inattentive behavior test was done as previously reported (Dwivedi et al., 2019) to examine the response of larvae to an aversive stimulus, as well as their cognition. A moving red bar projected using a PowerPoint slide was used as an aversive stimulus. In brief, a plate was kept at the center on a digital display, 10 larvae were put into each lane for acclimation (30 min) on a blank white background, and followed by aversive stimulation (30 min) with a moving red bar on the lower half of the plate (Additional file 2: Figure S3A). The number of larvae in the upper half of plate (i.e., avoiding the lower half) was counted after every 2 min. Inattentive attitude was quantified by normalizing the number of aversive stimulus period over acclimatization period using the following formula:

$$Larvae\ in\ upper\ half\ over\ acclimatization\,(\%) = \frac{Aversive\ stimulus - Acclimatization}{Acclimatization} \times 100\%$$

2.4.4. OFT

OFT utilizes the innate avoidance of a fish to novel open space to measure anxiety. An OFT was performed using a previously described method with slight modifications (Zakaria et al., 2021), by designing a tank that was virtually divided into a peripheral area and a central area (6 × 4 mm) (Figure 5Ab). For testing, a single fish was introduced into the central area for 1 min and video-tracked for 10 min. The time spent in the central zone was evaluated.

2.4.5. NTT

In this test, a fish was placed into a novel experimental tank for acclimation (10 min) and recorded for 12 min (Audira et al., 2018). The time spent in the upper zone was recorded (Figure 5Ac).

2.4.6. Mirror test

The test was conducted according to a previous study (Vaz et al., 2019), with slight modifications. A tank with a mirror placed on one side was used. A fish was placed at the center of the tank for 6 min. The behavior of the fish was recorded for 10 min using a digital video camera positioned directly above the tank. The area within 3 cm of the mirror was defined as the approach zone. The time spent in the approach zone was recorded (Figure 5Ad).

2.5. Library construction and high-throughput sequencing

Total RNA was isolated from brain tissue of zebrafish (1 mpf; MIA: PBS and 50 μg/g groups, PIVE: E3 and 100 μM groups; $n = 15$; about 60 mg of brain tissue; three replicates each group) by the TRIzol (Dingguo, China) according to the manual instruction. The total RNA was qualified and quantified using a Nano Drop and Agilent 2100 Bioanalyzer (Thermo Fisher Scientific, United States). RNA-Seq sequencing library was prepared using TruSeq™ RNA sample preparation kit (Illumina, United States). Briefly, purified mRNA was fragmented, then first-strand cDNA was generated using random hexamer-primed reverse transcription, followed by a second-strand cDNA synthesis and end repairing. The cDNA fragments were amplified by PCR to gain double stranded PCR products, which were then heated denatured and circularized by splint oligo sequence to get single strand circle DNA (ssCir DNA), the final library. The final library was amplified with phi29 to make DNA nanoball (DNB), which had more than 300 copies. The DNBs were loaded into a patterned nanoarray and single end 50 bases reads were generated on a BGIseq500 platform (BGI-Shenzhen, China).

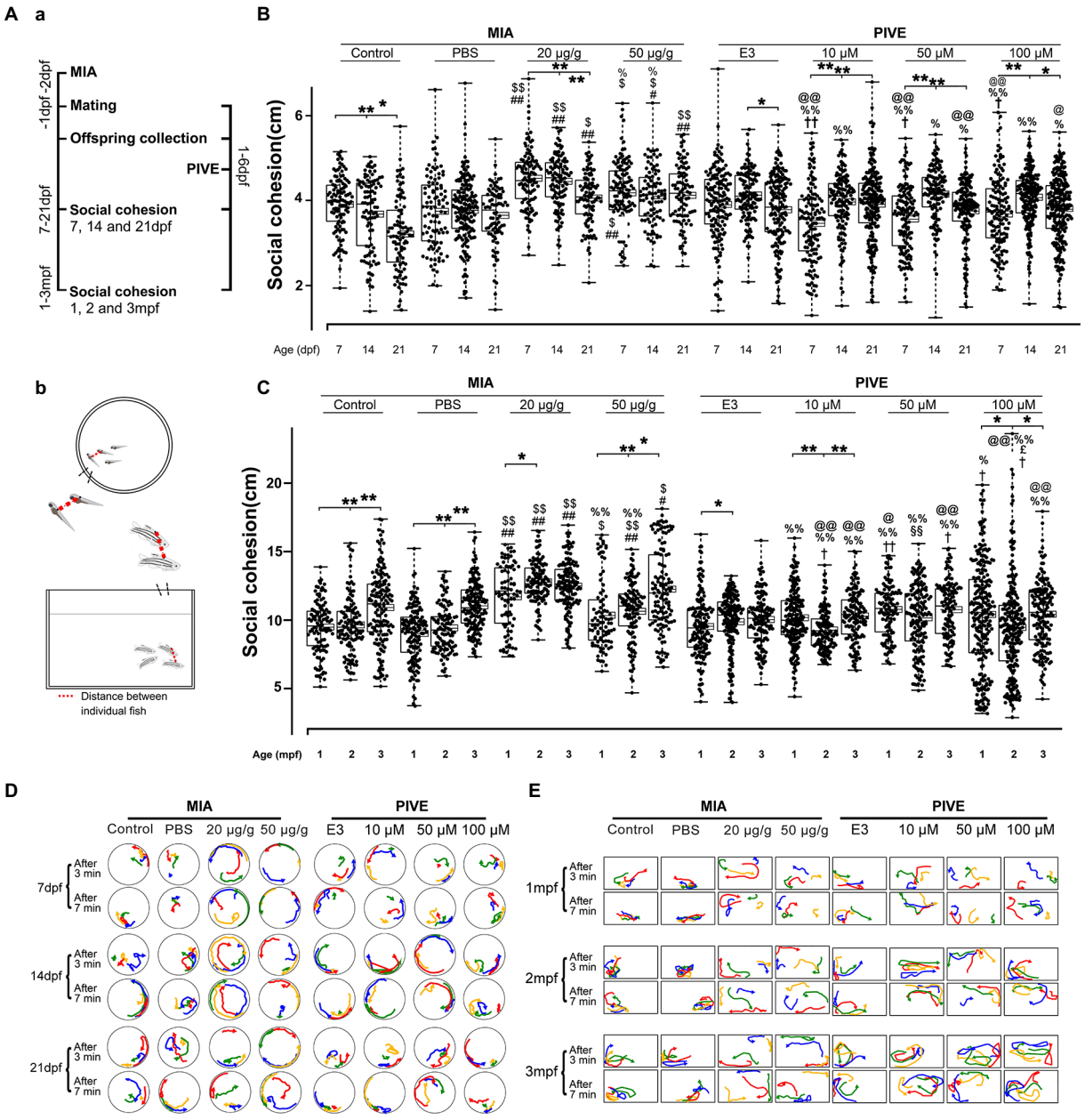

FIGURE 3
MIA offspring exhibited decreased social cohesion. **(Aa)** Zebrafish were tested for social cohesion (distance between individual fish) at 7, 14, and 21dpf, and 1, 2, and 3mpf **(Ab)** after maternal poly(I:C) injection (MIA) or PIVE to fertilized embryos. **(B)** Both MIA-20 and 50μg/g induced a decreased social cohesion at 7, 14, and 21dpf (MIA-20μg/g: Z=5.66, 6.31, and 5.57, p all <0.01 for 7, 14, and 21dpf vs. MIA-Control; Z=6.66, 7.45, and 3.59, p<0.01, 0.01, and 0.05, respectively, for 7, 14, and 21dpf vs. MIA-PBS. MIA-50μg/g: Z=2.54, 2.68 and 5.95, p=0.07, <0.05 and 0.01, respectively, for 7, 14, and 21dpf vs. MIA-Control; Z=3.69, 3.30, and 4.01, p<0.05, 0.05, and 0.01, respectively, for 7, 14, and 21dpf vs. MIA-PBS) but not for PIVE fish. **(C)** Both MIA-20 and 50μg/g induced a decreased social cohesion at 1, 2, and 3mpf (MIA-20μg/g: Z=5.76, 10.93, and 7.72, p all <0.01 for 1, 2, and 3mpf vs. MIA-Control; Z=Z=7.46, 11.63, and 5.77, p all <0.01 for 1, 2 and 3mpf vs. MIA-PBS. MIA-50μg/g: Z=1.60, 4.06 and 3.48, p>0.05, <0.01 and 0.05, respectively, for 1, 2, and 3mpf vs. MIA-Control; Z=3.15, 4.85, and 3.51, p<0.05, 0.01, and 0.05, respectively, for 7, 14, and 21dpf vs. MIA-PBS), but not for PIVE fish. **(D,E)** Tracking of individual fish in a group of four fish shows impaired social cohesion in MIA fish. The movement of each group of fish was analyzed after video tracking. The positions of individual fish in 3s periods at two different time windows (3 and 7min, respectively) were traced, and their paths were presented in different colors (#1 fish in red, #2 fish in yellow, and so on). Aggregation of MIA-control/PBS and PIVE-E3 fish groups in a corner of tank is apparent, in comparison with MIA fish. Data are presented as mean±SEM (right side of the histogram), median±75% confidence interval (left side of the histogram), and maximum and minimum. * p<0.05, ** p<0.001; $^{\#}$ p<0.05, $^{\#\#}$ p<0.001 compared with the MIA-control group of the same age with social stimulus; $^{\$}$ p<0.05, $^{\$\$}$ p<0.001 compared with the MIA-PBS group of the same age with social stimulus; $^{\%}$ p<0.05, $^{\%\%}$ p<0.001 compared with the MIA-20μg/g group of the same age; $^{@}$ p<0.05, $^{@@}$ p<0.001 compared with the MIA-50μg/g group of the same age.† p<0.05, †† p<0.001 compared with the PIVE-E3 group of the same age with social stimulus. §§ p<0.001 compared with the PIVE-10μM group of the same age; $^{£}$ p<0.05 compared with the PIVE-50μM group of the same age. Detail about the n and descriptive data for each group and statistical analysis results could be found in Additional file 11: File S4.

2.6. Sequencing data processing, and gene ontology (GO) enrichment and Kyoto Encyclopedia of Genes and Genomes (KEGG) analysis of DEGs

The sequencing data was filtered with SOAPnuke (v1.5.2)[1] by removing reads containing sequencing adapter, reads whose low-quality base ratio (base quality less than or equal to 5) is more than 20%, and reads whose unknown base ("N" base) ratio is more than 5%. Then, the clean reads were mapped to the reference genome using HISAT2 (v2.0.4).[2] Bowtie2 (v2.2.5)[3] was applied to align the clean reads to the reference coding gene set, then expression level of gene was calculated by RSEM (v1.2.12).[4] The heatmap was drawn by pheatmap (v1.0.8)[5] according to the gene expression in different groups. Essentially, differential expression analysis was performed using the DESeq2 (v1.4.5)[6] with Q value ≤0.05. To learn more about the biological role of these DEGs, GO[7] and KEGG[8] enrichment analysis of annotated DEGs was performed by Phyper[9] based on Hypergeometric test. The significant levels of terms and pathways were corrected by *Q* value with a rigorous threshold (*Q* value ≤0.05) (Bonferroni correction for multiple comparisons). The STRING database[10] was used to infer PPIs in DEGs' enrichment pathways (Szklarczyk et al., 2017) (Figure 6).

2.7. Validation of selected genes by RT-qPCR

The most differential co-expressed genes of two groups (MIA-50 μg/g and PIVE-100 μM) were selected and detected by quantitative RT-PCR. At 1 mpf, 5–6 fish were collected from the MIA-PBS, MIA-50 μg/g, PIVE-E3 and PIVE-100 μM groups, and total RNA was extracted by TRIZOL reagent (Dingguo). Reverse transcription was performed with PrimeScriptTM RT Reagent Kit (RR036A, TaKaRa, Japan), according to the manufacturer's protocol. RT-qPCR was performed using a StepOnePlusTM apparatus (ABI, United States) and TB Green Premix Ex TaqTM (RR420A, TaKaRa, Japan). The thermal cycle was as follows: pre-denaturation at 95°C for 30 s, then 40 cycles at 95°C for 5 s, 60°C for 15 s, and 60°C extension for 30 s. The relative gene expression was normalized to an endogenous housekeeping gene (β-actin) and the formula $2^{-\triangle\triangle Ct}$ was calculated using the comparative Ct method (three replicates for each sample) (Figures 6J, 7Hab). The primer sequences used in this study are listed in Additional file 4: File S3.

2.8. F0 knockout of *fabp2* and screens

F0 knockout of *fabp2* gene in zebrafish was carried out as previously reported, using an approach including two rounds of embryo injections: a validation round followed by a phenotyping round (Selvaraj et al., 2019; Figure 7A).

2.8.1. Cas9/gRNA preparation

Synthetic gRNA consisting of two components was bought from Integrated DNA Technologies (IDT, United States): the crRNA (Alt-R CRISPR-Cas9 crRNA) and tracrRNA (Alt-R CRISPR-Cas9 tracrRNA, #1072532). The *fabp2* crRNA was predesigned by IDT (more information sees Additional file 4: File S3).[11] The crRNA was annealed with the tracrRNA to form the gRNA by mixing each crRNA of the set separately with an equal molar amount of tracrRNA and diluting to 57 μM in Duplex buffer (IDT, #11–01–03-01). For gRNA/Cas9 assembly, Cas9 protein (IDT, Alt-R S.p. Cas9 Nuclease V3, 61 μM, #1072533) was diluted to 57 μM in Cas9 buffer: 20 mM Tris–HCl, 600 mM KCl, 20% glycerol, and then equal volumes of gRNA and Cas9 solutions were mixed (typically 1 μl gRNA; 1 μl Cas9), incubated at 37°C for 5 min then cooled on ice, generating a 28.5 μM RNP solution. The three RNP solutions were pooled in equal amounts before injections. The concentration of each RNP was thus divided by three (9.5 μM each), leaving the total RNP concentration at 28.5 μM. Approximately 1 nl of the three-RNP pool was injected into the yolk at the single-cell stage before cell inflation. This amounts to around 10.0 fmol of RNP (10.0 fmol [1,646 pg] of Cas9 and 10.0 fmol [333 pg] of total gRNA). Each unique RNP was present in equal amounts in the pool. Therefore, in the case of three RNPs, 3.3 fmol of each RNP was co-injected. Three *scrambled* crRNAs (Alt-R CRISPR-Cas9 Negative Control crRNA #1, #2, #3) were prepared into RNPs and injected following the same steps as above (more information sees Additional file 4: File S3).

2.8.2. Unviability

The percentage of unviable embryos/larvae was evaluated as previously reported (Selvaraj et al., 2019), based on the total number of embryos/larvae that died or were dysmorphic (not associated with the expected phenotype) after 1 dpf. This death/dysmorphic count was divided by the total number of larvae at 1 dpf to get a percentage of unviable embryos/larvae. Percentages of unviable embryos/larvae in the uninjected or scrambled controls were usually low (<9%) (Figure 7Gab).

1 https://github.com/BGI-flexlab/SOAPnuke
2 http://www.ccb.jhu.edu/software/hisat/index.shtml
3 http://bowtiebio.sourceforge.net/%20Bowtie2%20/index.shtml
4 https://github.com/deweylab/RSEM
5 https://cran.r-project.org/web/packages/pheatmap/index.html
6 http://www.bioconductor.org/packages/release/bioc/html/DESeq2.html
7 http://www.geneontology.org/
8 https://www.kegg.jp/
9 https://en.wikipedia.org/wiki/Hypergeometric_distribution
10 https://string-db.org/
11 eu.idtdna.com

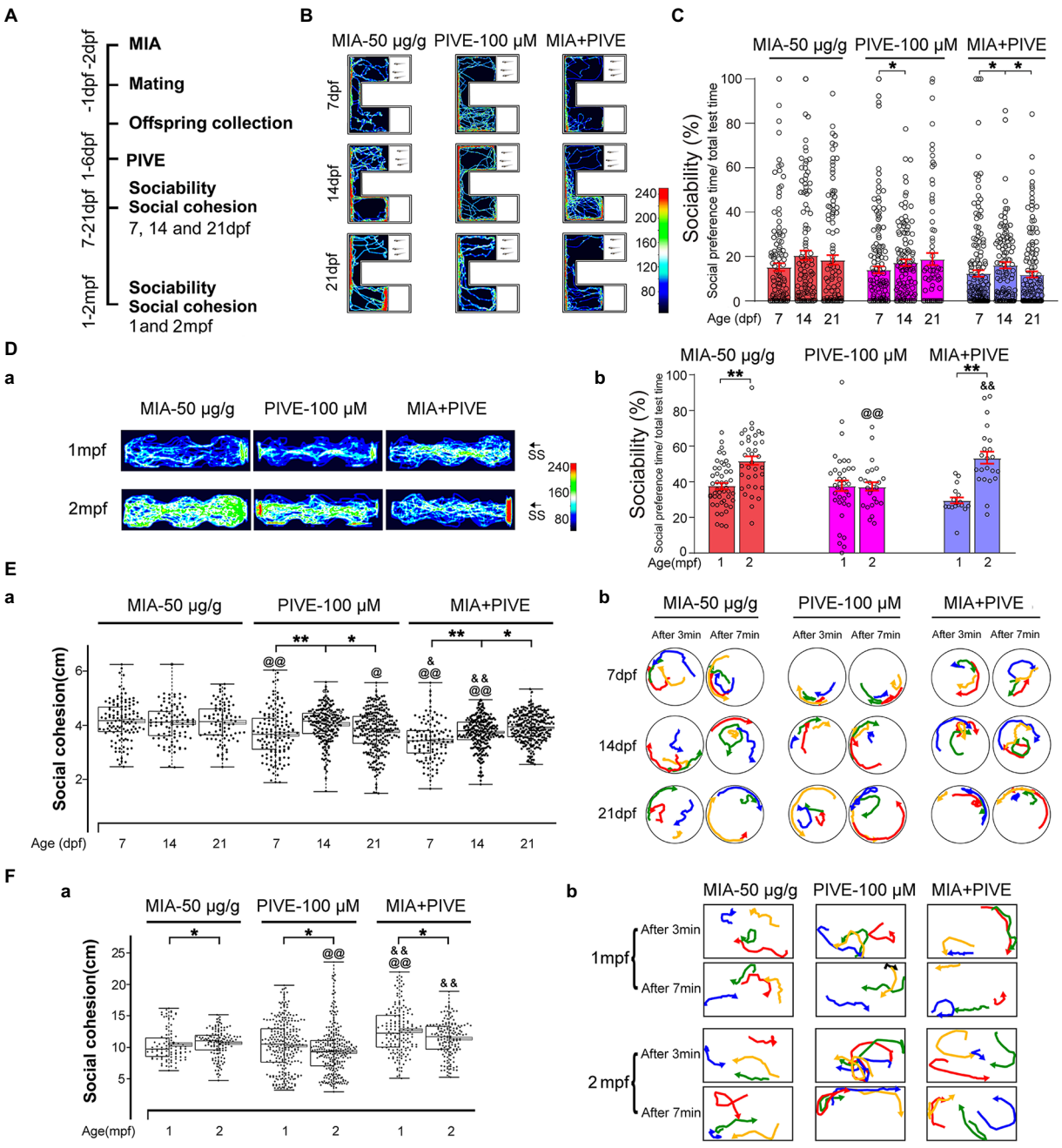

FIGURE 4
MIA combined with PIVE impaired social approach and decreased social cohesion. **(A)** Zebrafish were tested for sociability and social cohesion at 7, 14, and 21dpf, and 1 and 2mpf after MIA+PIVE. **(B)** Video tracking of movements of MIA+PIVE larvae at 7, 14, and 21dpf, showing the social interaction with the social cue. **(C)** Sociability of MIA+PIVE larvae at 7, 14, and 21dpf. MIA+PIVE did not further impair the sociability at 7, 14, and 21dpf. **(Da)** Video tracking of movements of MIA+PIVE fish at 1 and 2mpf, showing the social interaction with the social cue. **(Db)** Sociability of MIA+PIVE fish at 1 and 2mpf. Although the sociability in the MIA+PIVE group decreased at 1mpf, but not statistically significant. **(Ea,Fa)** MIA+PIVE induced an increased social cohesion at 7 and14dpf (Z=4.73, 4.32, and 3.16, p<0.01, 0.01 and 0.05, respectively, for 7, 14, and 21dpf vs. MIA-50μg/g; Z=2.55 and 5.55, p<0.05 and 0.01, respectively, for 7 and 14dpf vs. PIVE-100μM), and a decreased social cohesion at 1 and 2mpf (Z=4.61, p<0.01 for 1mpf vs. MIA-50μg/g; Z=5.40 and 6.89, p all <0.01 for 1 and 2mpf vs. PIVE-100μM). **(Eb,Fb)** Tracking of individual fish in a group of four fish show impaired social cohesion in MIA+PIVE fish. Data are presented as mean±SEM. * p<0.05, ** p<0.001; $^{@}$ p<0.05, $^{@@}$ p<0.001 compared with the MIA-50μg/g group of the same age. $^{\&}$ p<0.05, $^{\&\&}$ p<0.001 compared with the PIVE-100μM group of the same age. Detail about the n and descriptive data for each group and statistical analysis results could be found in Additional file 11: File S4.

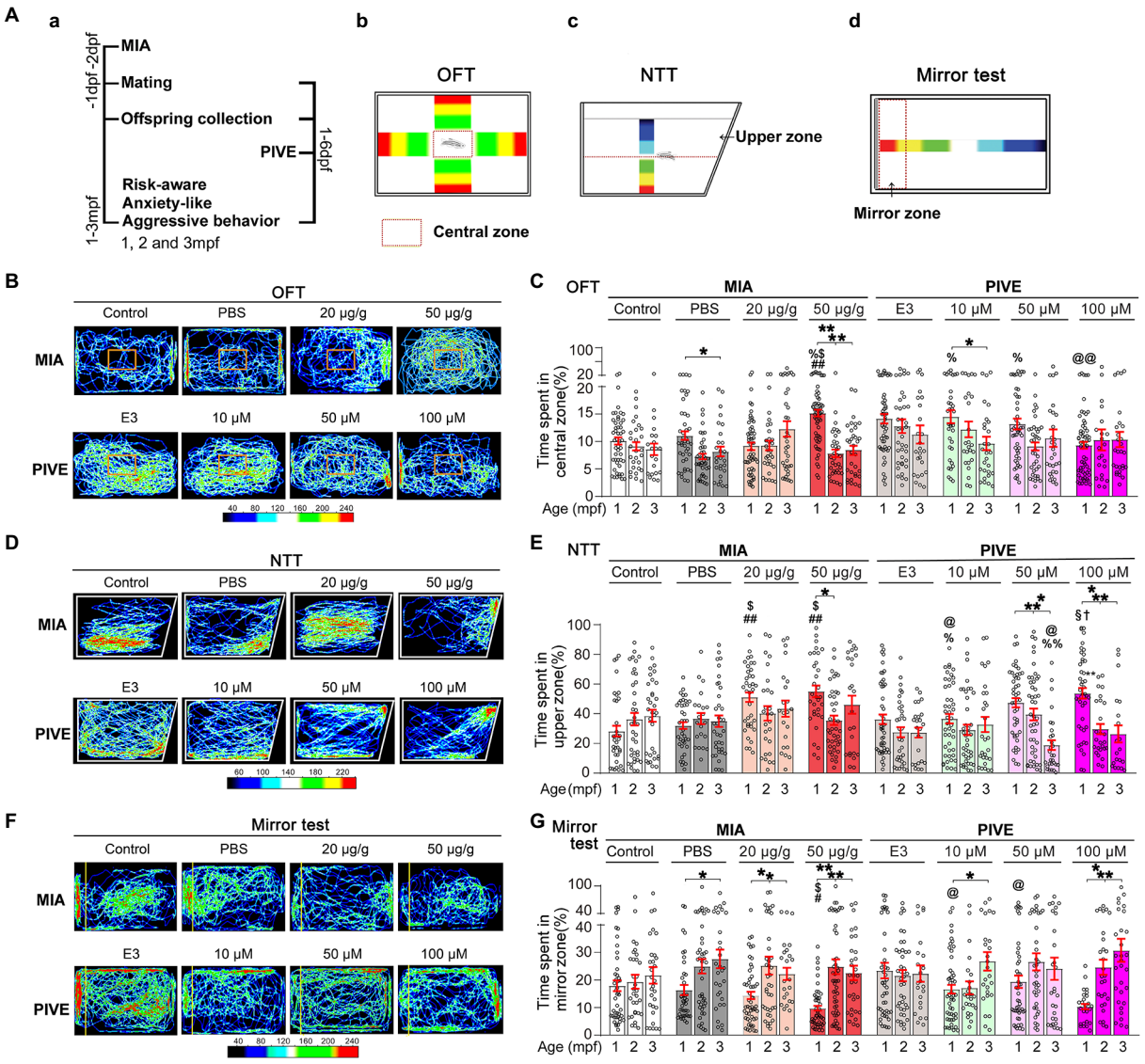

FIGURE 5
MIA offspring exhibited a decreased risk-aware, anxiety-like and aggressive behavior. **(Aa)** OFT **(Ab)**, NNT **(Ac)**, and mirror **(Ad)** tests were used to evaluate the risk-awareness, anxiety-like and aggressive behavior at 1, 2, and 3 mpf of MIA or PIVE fish. **(B)** Video tracking of movements of MIA or PIVE fish during OFT. **(C)** Only MIA-50μg/g exhibited a decreased risk-awareness at 1mpf (MIA-50μg/g: Z=4.41 and 3.48, p<0.01 and 0.05 vs. MIA-Control and MIA-PBS respectively), as they spent more time in the central zone of the tank. **(D)** Video tracking of movements of MIA or PIVE fish during NNT. **(E)** MIA-20 and 50μg/g exhibited a decreased anxiety-like behavior at 1mpf as they spent more time in upper zone of the tank (MIA-20μg/g: Z=4.17 and 3.46, p<0.01 and<0.05 vs. MIA-Control and MIA-PBS, respectively. MIA-50μg/g: Z=4.45 and 3.77, p<0.01 and<0.05 vs. MIA-Control and MIA-PBS, respectively); as well as observed at 1mpf in PIVE-100μM group (Z=3.21, p<0.05 vs. PIVE-E3 group). **(F)** Video tracking of movements of MIA or PIVE fish during mirror test. **(G)** MIA-50μg/g exhibited a decreased aggressive behavior at 1mpf as they spent less time in mirror zone of the tank during mirror test (Z=3.17 and 2.96, p all <0.05 vs. MIA-Control and MIA-PBS respectively); similar change was not observed in PIVE-100μM group. Data are presented as mean±SEM. * p<0.05, ** p<0.001; # p<0.05, ## p<0.001 compared with the MIA-control group of the same age with social stimulus; $ p<0.05 compared with the MIA-PBS group of the same age with social stimulus; % p<0.05, %% p<0.001 compared with the MIA-20μg/g group of the same age; @ p<0.05, @@ p<0.001 compared with the MIA-50μg/g group of the same age.† p<0.05 compared with the PIVE-E3 group of the same age with social stimulus. § p<0.05 compared with the PIVE-10μM group of the same age. Detail about the n and descriptive data for each group and statistical analysis results could be found in Additional file 11: File S4.

2.8.3. Genomic DNA extraction

After individual larvae were transferred to 0.2 ml PCR tubes separately, excess liquid was removed from each tube and 50 μl of 1× base solution (25 mM KOH, 0.2 mM EDTA in water) was added. The tubes were incubated at 95°C for 30 min, then cooled to room temperature before the addition of 50 μl of 1× neutralization solution (40 mM Tris–HCL in water). Genomic DNA was stored at 4°C.

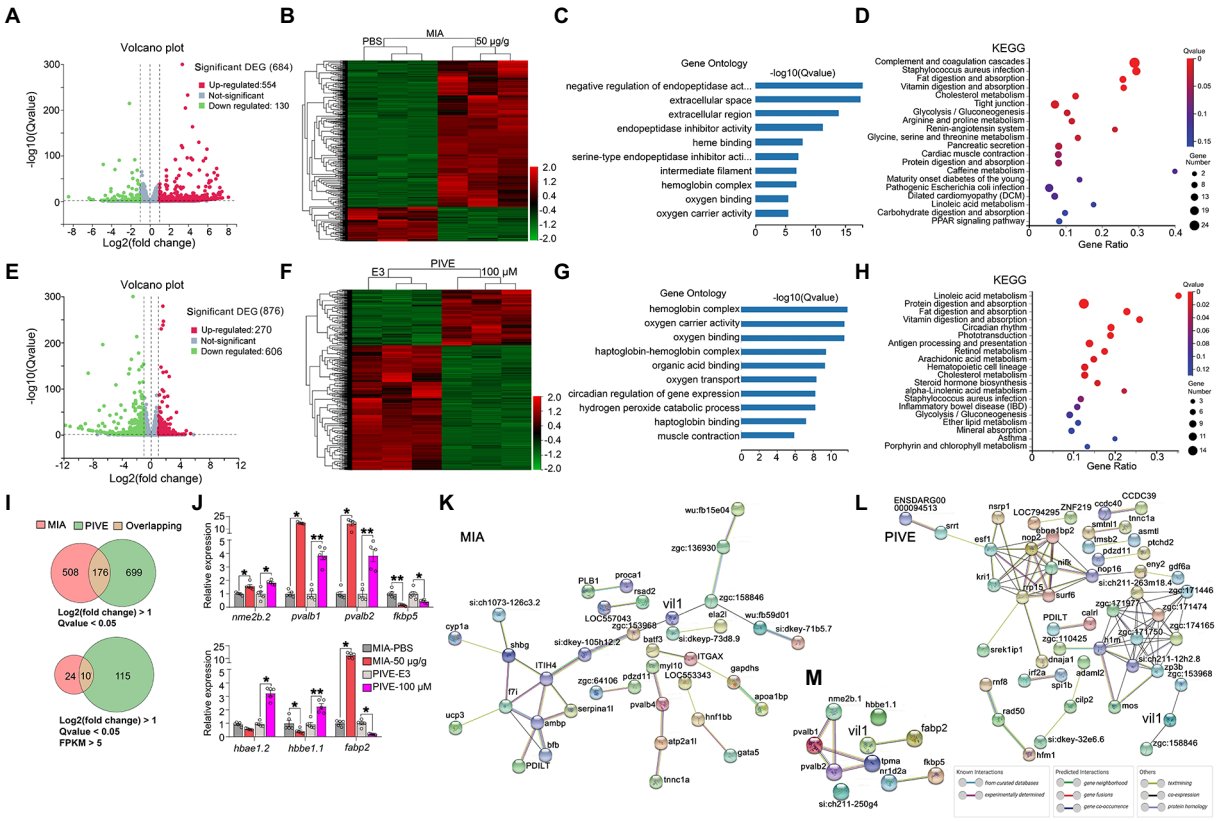

FIGURE 6
Clustering, GO enrichment and KEGG signaling pathway analysis of DEGs. **(A)** A volcano graph shows DEGs in MIA-50μg/g zebrafish brain. The red dots indicate up-regulated genes and the green dots indicate down-regulated genes. **(B)** The overall distribution of DEGs between the MIA-50μg/g group and MIA-PBS group at 1mpf. Red and green represent up-regulated and down-regulated changes, respectively, in the clustering analysis. The color intensity is directly proportional to the levels of changes. **(C)** GO analysis of MIA-induced DEGs; bar plot shows the top 10 enrichment score [−log10 (*Q*-value)] of DEGs involving biological process, cellular component, and molecular function. **(D)** Significant changes in the KEGG pathway of MIA-induced DEGs. The bubble graph shows enrichment score [−log10 (*Q*-value)] of the significant pathway. The size of the circle represents the number of enriched DEGs. *Q*-value is represented by a color scale, and the statistical significance increases from blue (relatively lower significance) to red (relatively higher significance). **(E)** A volcano graph shows DEGs in PIVE-100μM zebrafish brain. **(F)** The overall distribution of DEGs in the PIVE-100μM group and PIVE-E3 group at 1mpf. **(G)** A GO analysis of PIVE-induced DEGs. **(H)** Significant changes in the KEGG pathway of MIA-induced DEGs. **(I)** Venn diagram denoting the number of all DEGs by two thresholds that are affected in MIA or PIVE offspring. **(J)** Quantitative RT-PCR validation of top 7 co-expressed differential gens in brain of MIA-50μg/g and PIVE-100μM group at 1mpf [MIA-50μg/g: t=4.33, 25.00(U), 25.00(U), 1.78, 2.50 and 25.00(U), p<0.05, 0.05, 0.05, 0.01, 0.05, and 0.05 for *nme2b.2*, *pvalb1*, *pvalb2*, *fkbp5*, *hbbe1.1*, and *fabp2*, respectively, vs. MIA-PBS. PIVE-100μM: t=4.18, 7.63, 5.62, 3.04, 25.00(U), 5.13 and 25.00(U), p<0.05, 0.01, 0.01, 0.05, 0.05, 0.01, and 0.05 for *nme2b.2*, *pvalb1*, *pvalb2*, *fkbp5*, *hbbe1.2*, *hbbe1.1*, and *fabp2*, *respectively*, vs. PIVE-E3.]. PPI network of DEGs of MIA-50μg/g group **(K)** and PIVE-100μM group **(L)**. **(M)** PPI network of *fabp2*. Nodes represent genes, lines represent the interaction of proteins with genes, and the results within the nodes represent the structure of proteins. Line colors represent evidence of interactions between proteins. Data are presented as mean±SEM. * p<0.05, ** p<0.001. Detail about the *n* and descriptive data for each group and statistical analysis results could be found in Additional file 11: File S4.

2.8.4. PCR and sanger sequencing

Each PCR well contained: 2 μl 5× Phusion HF buffer, 0.2 μl dNTP (10 mM), 0.1 μl Phusion High-Fidelity DNA Polymerase, 1.0 μl genomic DNA, 0.05 μl forward primer (10 μM), 0.05 μl reverse primer (10 μM), and 6.6 μl dH_2O; for a total of 10.0 μl. The PCR plate was sealed and placed into a thermocycler. The PCR program was: 95°C for 5 min, then 35 cycles of: 95°C for 20 s, 70°C for 20 s, 72°C for 20 s, then 72°C for 7 min then cooled to 4°C until collection. PCR primers are provided in Additional file 4: File S3. The concentration of PCR product was quantified by Qubit, and the length of the product was verified on 2.5% agarose gel. The samples were sent to Tsingke Biotechnology Co., Ltd. (Hangzhou, China) for Sanger sequencing. Briefly, the PCR products were purified and secondary verified on a 1% agarose gel. The BigDye® Terminator v3.1 (Thermo Fisher Scientific) and 3,730 sequencer was used for sequencing.

2.8.5. Headloop PCR

Headloop PCR was done as previously described (Rand et al., 2005; Selvaraj et al., 2019). Assessment of PCR products on agarose gel is sufficient to determine whether the target loci were effective mutants in F0 embryos. The headloop PCR primer pairs and the headloop tags are provided in Additional file 4: File S3. For headloop PCR, each well

10.3389/fnmol.2022.1068019

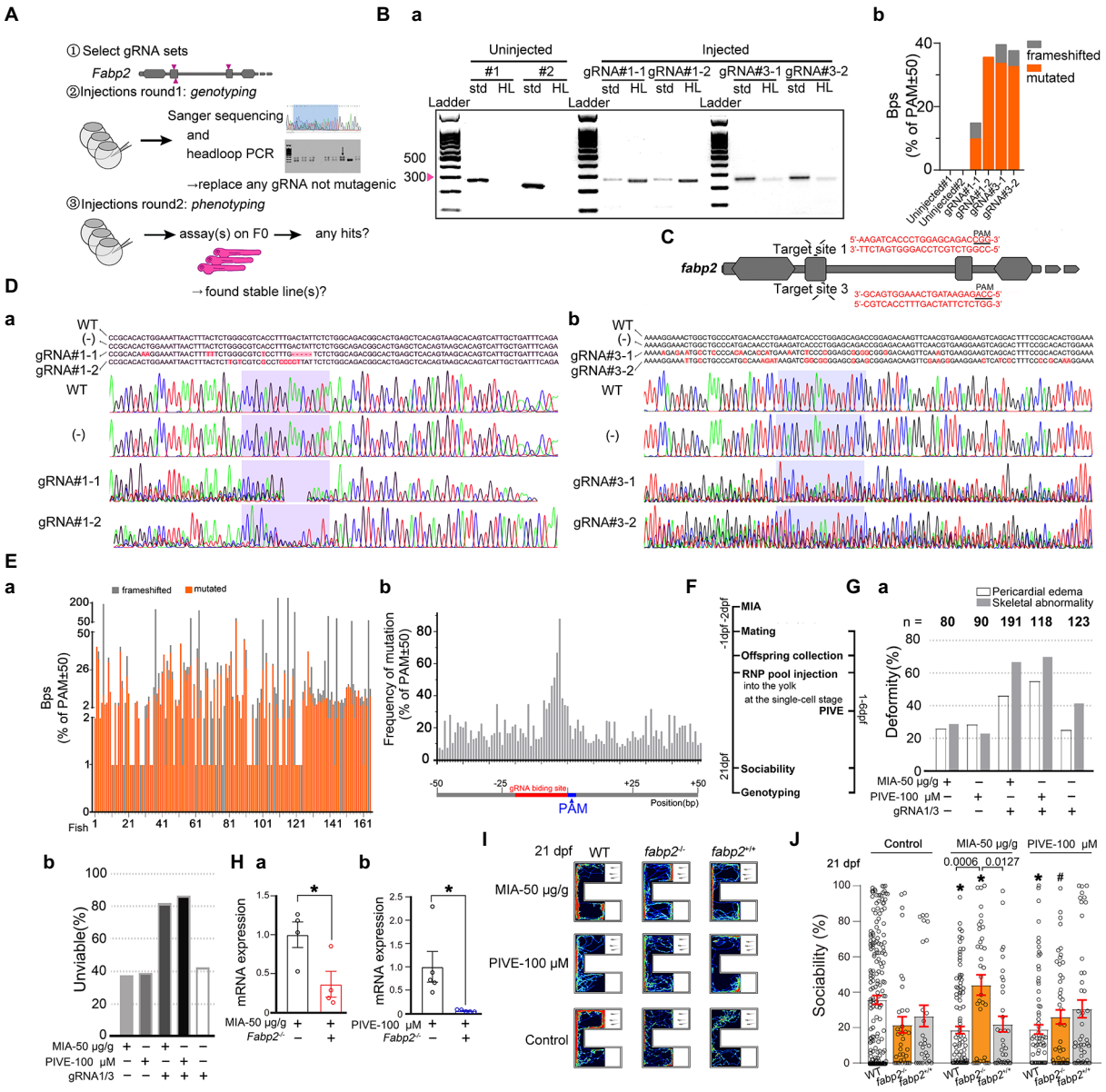

FIGURE 7
Fabp2 gene F0 knockout ameliorated MIA-induced autism-like behaviors. **(A)** Two rounds F0 knockout of *fabp2* gene including selection of gRNAs, verification of mutagenic gRNAs and phenotyping. **(Ba)** Target loci of *fabp2* amplified with the PCR primes used for sequencing (std, standard) or with headloop primer (HL). **(Bb)** Frameshifted and mutated bps (Sanger sequencing) of the same samples as showed in **(Ba)**. **(C)** Schematic diagram of the target site in the zebrafish *fabp2* genome. **(Dab)** Sequencing maps of WT and *fabp2*$^{-/-}$ zebrafish. (–): gRNA not mutagenic. **(Ea)** Frameshifted and mutated bps (Sanger sequencing) of all samples (83 fish at 21dpf; 46 fish at 1mpf which for finding stable lines). **(Eb)** Frequency of mutations of R50-PAM-F50 (83 fish at 21dpf; 46 fish at 1mpf which for finding stable lines). **(F)** After maternal poly(I:C) injection (MIA), two-RNP pool was injected into the yolk at the single-cell stage before cell inflation; or two-RNP pool was injected into the yolk at the single-cell stage followed by PIVE to these embryos, and zebrafish were tested for sociability at 21dpf followed by verification of genotyping. **(Ga)** Deformity of gRNA injection with MIA or PIVE. **(Gb)** Unviability of gRNA injection with MIA or PIVE. **(Hab)** mRNA expressions of *fabp2* with MIA or PIVE (MIA: t=2.72, p<0.05; PIVE: U=0.00, p<0.05). **(I)** Video tracking of movements of WT or *fabp2*$^{-/-}$ larvae with MIA or PIVE at 21dpf. **(J)** Sociability of WT or *fabp2*$^{-/-}$ larvae with MIA or PIVE at 21dpf. *Fabp2* F0 knockout ameliorated MIA-induced autism-like behaviors (*fabp2*$^{-/-}$+MIA: Z=4.06, p<0.01 vs. *fabp2*$^{-/-}$ without MIA). Data are presented as mean±SEM. * p<0.05 compared with Control group of the same zebrafish line. $^{\#}$ p<0.05 compared with MIA-50μg/g group of the same zebrafish line. Detail about the *n* and descriptive data for each group and statistical analysis results could be found in Additional file 11: File S4.

contained: 2 μl 5× Phusion HF buffer, 0.2 μl dNTPs (10 mM), 0.05 μl forward primer (10 μM), 0.05 μl reverse primer (10 μM), 0.1 μl Phusion Hot Start II polymerase, 1 μl genomic DNA, 6.6 μl dH_2O; for a total of 10.0 μl. PCR program was: 98°C for 30 s; then 30 cycles of: 98°C for 10 s, 72°C for 20 s; then 72°C for 7 min. Amplification was assessed by agarose gel

electrophoresis (Figure 7Da). To calculate the headloop PCR score, GelDoc Go gel imaging system (Bio-Rad) was used to imaging the gel. Then, Quantity One software (Bio-Rad) was used to quantify band intensity.

2.8.6. F0 screens in two rounds of injections

In the first round, each *fabp2* gRNA was injected separately, followed by headloop PCR to confirm mutagenesis, thereby controlling the false negative rate of a screen. If a gRNA was found not to generate enough mutations, it was replaced with a new one and the experiment was repeated; or directly abandoned. The second round of injection used mixed *fabp2* gRNA sets to generate the F0 knockouts for phenotyping. The control larvae were injected with a set of scrambled RNPs, which controlled for any potential effect caused by the injection of Cas9 and exogenous RNA.

2.9. Statistical analysis

We used ImageJ software to analyze the behavior tracking data. SPSS 23.0 (IBM, Armonk, NY, United States) were used for statistical analysis. All continuous data conformed to the normal distribution (according to the Kolmogorov–Smirnov test) were analyzed using One/Two-way ANOVA followed by Šídák'sor Tukey's multiple comparisons test under the condition of a significant F value ($p < 0.05$). Those data with non-normal distribution were analyzed using Kruskal-Wallis test followed by Bonferroni's multiple comparisons test; or using Multiple Mann–Whitney tests with Bonferroni's correction under the condition of a significant H value ($p < 0.05$). Prior to testing, we had performed several pilot experiments identifying the best concepts for our experimental paradigms. To obtain convincing statistical power, we included all samples produced from several batches/crosses for MIA and PIVE paradigm only discarding fishes with obvious deformities or immobility within the test time. Since we did not find any batch/cross effects on our behavior results in statistical tests, no multiple testing corrections were made. Data were expressed as mean ± standard error of the mean (M ± SEM). $p < 0.05$ were considered as statistically significant.

3. Results

3.1. MIA offspring born to mothers injected with poly(I:C) showed an immune response

In rodents, exposing to MIA (Patterson, 2011) serves as an environmental risk factors-ASD model. At 24 h after maternal poly(I:C) injection, TLR4ba mRNA expressions were significantly down-regulated in intestinal tissue and liver of maternal fish (Figure 1Ca), which can be seen in TLR3 and TLR4bb, but there was no statistical significance. TLR3 and TLR4bb, but not TLR4ba, mRNA expressions were up-regulated in spleen of maternal fish (Figures 1Ba,Ca,Da), which was not statistically significant when compared to those injected with PBS. Compared with the expressions in spleen, TLR3, TLR4ba and TLR4bb mRNA expressions were significantly down-regulated in intestinal tissue of maternal fish (Figures 1Ba,Ca,Da). Considering zebrafish do not have a placenta and are external fertilizers, it is unknown whether mothers injected with poly(I:C) would also induce an immune reaction in MIA offspring. We found that TLR3 ($p = 0.0667$) and TLR4bb mRNA expressions were significantly up-regulated but that of TLR4ba of MIA offspring at 1 dpf was not (Figures 1Bb,Cb,Db). For PIVE, there were no significant changes in TLR3 and TLR4ba/b mRNA expressions of the offspring collected at 1 dpf after a 24 h poly(I:C) treatment (Figures 1Bb,Cb,Db); while both TLR3 and TLR4ba/b mRNA expressions of the offspring collected at 2 dpf after a 24 h poly(I:C) treatment were significantly up-regulated (Figures 1Bb,Cb,Db). Furthermore, we measured the immune response parameters after the poly(I:C) treatment. We found that the levels of IgM were increased in MIA-50 μg/g offspring at 14 dpf ($p = 0.0835$, compared to those injected with PBS). Although the levels of C4 were increased in MIA-20 μg/g and MIA-50 μg/g offspring at 21 dpf the change was not significant when compared with the controls (Figures 1E,F). Interestingly, the levels of IgM, C4 and IgA were significantly increased in PIVE-100 μm larvae only at 21 dpf (Figures 1E–G). At 24 h after poly(I:C) injection, the levels of IgM, C4 and IgA were increased in maternal liver, which were not statistically significant, and it could not be found in brain, spleen and intestinal tissues (Figures 1Ha,Hb,Hc).

3.2. MIA offspring born to mothers injected with poly(I:C) exhibited impaired social approach

The offspring produced by pregnant rodents with MIA have abnormal behavior that is reminiscent of autism, which makes MIA a useful disease model (Smith et al., 2007). However, whether this type of autism phenotype can be replicated in zebrafish has not been reported. Normally, zebrafish showed a development of social approach behavior from 7 to 21 dpf (Figures 2B,C). The levels of sociability (as a ratio of either total test time or total interaction time) were significantly lower in MIA-50 μg/g group at 21 dpf compared to the MIA-Control and MIA-PBS group, respectively, (Figures 2B,C; Additional file 2: Figure S2A; Additional file 5: Movie S1). We examined whether directly exposing embryos to poly(I:C) could also impair the social approach behavior and found that PIVE-10, 50, and 100 μM did not impair the sociability (as a ratio of either total test time or total interaction time) at 7 and 14 dpf (Figures 2B,C and Additional file 2: Figure S2A). Only PIVE-100 μM impaired the sociability (as a ratio of total test time) when being compared with the PIVE-E3 group ($p = 0.0662$) at 21 dpf (Figures 2B,C; Additional file 6: Movie S2).

Sociability was also tested for these fish at 1, 2, and 3 mpf. Only MIA-50 μg/g offspring exhibited impaired social approach behavior at 1 mpf (Figures 2D,E; Additional file 2: Figure S2B; Additional file 7: Movie S3). PIVE-100 μM also impaired social approach behavior at 2 mpf (Figures 2D,E; Additional file 2: Figure S2B; Additional file 8: Movie S4). Poly(I:C) exposure also induced changes of total distance moved and average velocity during the social preference test of larvae (Additional file 2: Figure S4) and juvenile/adult zebrafish (Additional file 2: Figure S5). We did not find any sex differences at 3 mpf of these poly(I:C) exposure-induced sociability and movement changes (Additional file 2: Figure S6).

3.3. MIA offspring born to mothers injected with poly(I:C) exhibited had decreased social cohesion

We next tested group behavior of the poly(I:C) treated fish using the shoaling assay. The distances between individual fish can indicate their social interaction or impaired social behavior among conspecifics. Zebrafish larvae showed a development of social cohesion from 7 to 21 dpf (Figures 3B,D) and remained stable from 1 to 3 mpf (Figures 3C,E). Comparing MIA and control/PBS fish revealed that MIA groups had significantly larger mean distances between individual fish at 7, 14, and 21 dpf, and 1, 2, and 3 mpf (Figures 3B,D). We plotted the path of individual fish after video tracking (Figures 3D,E). Social cohesion, aggregation, or shoaling behaviors were apparent in the control/PBS fish groups. However, individual fish of the MIA groups moved independently from one another, suggesting a deficit in social interaction (Additional file 9–110: Movies S5, S6). In contrast, this pattern of activity was not detected in PIVE groups (Figures 3B–E). Poly(I:C) exposure also induced changes of total distance moved and average velocity during social cohesion test in zebrafish (Additional file 2: Figure S7).

3.4. MIA offspring born to mothers injected with poly(I:C) combined with PIVE exhibited impaired social approach and decreased social cohesion

Since our results found that either MIA or PIVE at least partially impaired social approach and decreased social cohesion, we further tested the effects of MIA combined with PIVE on social approach and cohesion. In the MIA-50 μg/g + PIVE-100 μM group, the offspring did not exhibit impaired social approach behavior during the social stimulating test at 7, 14, and 21 dpf when compared to that of MIA-50 μg/g and PIVE-100 μm groups, respectively, (Figures 4A,B,C). Although the sociability in the MIA-50 μg/g + PIVE-100 μM group decreased (Figures 4B,C), similar to that observed at 1 mpf compared to that of MIA-50 μg/g group (Figures 4Da,Db), but not statistically significant. This group recovered to the normal levels and was significantly higher than that of PIVE-100 μM group at 2 mpf (Figures 4Da,Db; Additional file 2: Figure S2C). For social cohesion, the MIA + PIVE group had significantly shorter mean distances between individual fish at 7 and 14 dpf than the MIA-50 μg/g or PIVE-100 μM group (Figures 4Ea,Eb). However, the MIA + PIVE group did have markedly longer mean distance between individual fish at 1 mpf than the MIA-50 μg/g group (Figures 4Fa,Fb).

3.5. MIA offspring born to mothers injected with poly(I:C) exhibited a decreased risk-aware, anxiety-like and aggressive behavior

ASD children often have less risk awareness. Therefore, we use OFT to evaluate risk-awareness of poly(I:C)-treated zebrafish. We found that only MIA-50 μg/g group exhibited a decreased risk-awareness at 1 mpf (Figures 5B,C), as they spent more time in the central zone of the tank. Conversely, PIVE did not affect this behavior (Figures 5B,C). Similarly, MIA-20 and 50 μg/g groups exhibited a decreased anxiety-like behavior at 1 mpf (Figures 5D,E) as they spent more time in upper zone of the tank during NNT; similar changes were observed in PIVE-100 μM group at 1 mpf (Figures 5D,E). We also found that MIA-50 μg/g group exhibited a decreased aggressive behavior at 1 mpf (Figures 5F,G) as they spent less time in mirror zone of the tank during the mirror test; a similar change was observed in PIVE-100 μM group at 1 mpf, which was not statistically significant when compared to the PIVE-E3 group (Figures 5F,G). To determine whether this decreased awareness of risk and new environment and decreased social interaction in fish with poly(I:C) exposure is due to impaired cognition, we used an inattentive behavior test to check their cognition of "aversive" stimulus. We found that only MIA-50 μg/g group did exhibit a decreased cognition at 14 dpf, as the larvae of MIA-50 μg/g were less responsive to "aversive" stimulus and stayed longer in "aversive" stimulus area. Such changes were not observed at 7 and 21 dpf (Additional file 2: Figure S3B). The larvae of PIVE-100 μM did not show a reduced response to "aversive" stimulus compared with PIVE-E3 group at 7, 14, and 21 dpf (Additional file 2: Figure S3B). Therefore, the decreased awareness of risk, new environment and social interaction in fish (1 to 3 mpf) with poly(I:C) exposure might not result from poly(I:C) induced cognition impairment.

3.6. Transcriptomic characterization of the brains of MIA fish

Given the striking behavioral abnormalities after poly(I:C) exposure, we performed a transcriptomic survey of the brain of 1 mpf fish (MIA: PBS and 50 μg/g group, PIVE: E3 and 100 μM group; $n = 15$). RNA-sequencing analysis of brain RNA from the MIA group identified 684 DEGs (threshold: $p < 0.05$; Log_2 (Fold Change) > 1.0 or Log_2 (Fold Change) < −1.0; Additional file 4: File S3), which are summarized in a volcano plot (Figure 6A). The volcano plot illustrates that the numbers of overexpressed genes were

significantly more than that of underexpressed genes (up vs. down: 554 vs. 130 genes). Moreover, a hierarchical clustering of DEGs was conducted (Figure 6B). To gain an insight into the biology of the expression changes observed in the MIA brain, we performed a GO enrichment analysis and a KEGG pathway annotation. These analyses were performed to identify GO enrichment in the categories of cellular components, biological processes, and molecular functions. For GO enrichment, the DEGs were plentiful in negative regulation of endopeptidase activity, extracellular space, extracellular region, endopeptidase inhibitor activity, heme binding, etc. (Figure 6C). The KEGG pathway found that DEGs were mainly enriched in complement and coagulation cascades, fat digestion and absorption, cholesterol metabolism, and tight junction, etc. (Figure 6D). For PIVE, RNA-sequencing analysis of brain RNA identified 876 DEGs (threshold: $p < 0.05$; Log_2 (Fold Change) > 1.0 or Log_2 (Fold Change) < −1.0), which are summarized in a volcano plot (Figure 6E). The volcano plot also illustrates that the numbers of underexpressed genes were significantly more than that of overexpressed genes (under vs. over: 606 vs. 270 genes). A hierarchical clustering of DEGs was conducted (Figure 6F). For GO enrichment, the DEGs were plentiful in hemoglobin complex, oxygen carrier activity, oxygen binding, haptoglobin-hemoglobin complex, and organic acid binding (Figure 6G). The KEGG pathway found that DEGs were mainly enriched in the linoleic acid metabolism, protein digestion and absorption, fat digestion and absorption, phototransduction, antigen processing and presentation (Figure 6H).

The top 10 co-expressed differential genes of two groups (MIA-50 μg/g and PIVE-100 μM) were selected and detected by RT-qPCR. Testing on one gene (*hbae1.3*) was not made due to its homology to *hbae1.2*, and two genes (*tpma* and *nr1d2a*) failed in our experiment. The results showed that expressions of the remaining top 7 co-expressed differential genes were similar to that of RNA sequencing (Figures 6I,J and Additional file 2: Figure S8).

To determine the interaction between DEGs related to social behavior deficits in GO enrichment and KEGG signaling pathways, we identified a potential PPI network for these DEGs (Figure 6K for MIA; Figure 6L for PIVE). The PPI network integrated these DEGs using STRING analysis; both PPI enrichment *p*-value was statistically significant ($p < 0.001$). From the PPI network, we found that *vil1* forms a more complicated network with other genes in MIA than in PIVE. We speculated that *vil1* mediated pathways might play an important role in the MIA-induced ASD in zebrafish. Furthermore, using STRING analysis involves the top 10 co-expressed differential genes of the MIA-50 μg/g and PIVE-100 μM groups and *vil1*, we found only *fabp2* interacted with *vil1* (Figure 6M), exactly representing that MIA has the tendency of overexpression and PIVE has the tendency of underexpression.

Next, we searched on SFARI Gene[12], an evolving online database designed to permit tracking the ever-expanding genetic risk factors that emerge in the literature https://www.sfari.org/resource/sfari-gene/ – bottom for ASD, and got a total of 991 ASD scored genes. We analyzed the RNA-sequencing results for these genes. The MIA group identified 10 DEGs (threshold: $p < 0.05$; Log2 (Fold Change) > 1.0 or Log2 (Fold Change) < −1.0), which are summarized in a volcano plot (Additional file 2: Figure S9A). Moreover, a hierarchical clustering of DEGs was conducted (Additional file 2: Figure S9B). The GO enrichment analysis and a KEGG pathway annotation were performed. For GO enrichment, the DEGs were plentiful in fibrinogen complex, semaphoring receptor complex, lamellipodium, etc. (Additional file 2: Figure S9C). The KEGG pathway found that DEGs were mainly enriched in complement and coagulation cascades, tryptophan metabolism, cGMP-PKG signaling pathway, etc. (Additional file 2: Figure S9D). For PIVE, RNA-sequencing identified 18 DEGs (threshold: $p < 0.05$; Log2 (Fold Change) > 1.0 or Log2 (Fold Change) < −1.0), which are summarized in a volcano plot (Additional file 2: Figure S9E). A hierarchical clustering of DEGs was conducted (Additional file 2: Figure S9F). For GO enrichment, the DEGs were plentiful in RNA polymerase II transcription factor complex, FACT complex, host cell nucleus, etc. (Additional file 2: Figure S9G). The KEGG pathway found that DEGs were mainly enriched in circadian rhythm, endocrine and other factor-regulated calcium reabsorption, mineral absorption, etc. (Additional file 2: Figure S9H). From the PPI network, we found that only *vil1-fabp2* and *atp1a1a.4* co-incidenced in both MIA and PIVE (Additional file 2: Figures S9J,K).

3.7. *Fabp2* gene F0 knockout ameliorated MIA-induced autism-like behaviors

In the first round, three gRNAs were injected separately followed by headloop PCR, and we found that two gRNAs generated enough mutations. In the second round of injections, we used two confirmed *fabp2* gRNA sets to generate F0 knockouts for phenotyping (Figures 7A,Bab,C). The rates of deformity and unviability were high with *fabp2* gRNA1/3 set injections (Additional file 2: Figures S10B,C). All headloop PCR results were identical with that of Sanger sequencing. The ratios of mutated and frameshifted events were 89.09% (147/165) and 70.30% (116/165) of the total occurrence, respectively. The mutated and frameshifted base pairs (bps) were 43.20% (1,389/3,215) and 56.80% (1,826/3,215) of the total variation numbers (bps) respectively (Figures 7Da,Db,Ea). Frequency of mutations of R50-PAM-F50 did not show any distribution patterns (Figure 7Eb). We found that the sociability in *fabp2*$^{-/-}$ zebrafish was not significantly impaired at 21 dpf when compared to WT (Figures 7F,I,J). However, *fabp2*$^{-/-}$ rescued the sociability of MIA-induced social behavior deficits (Figures 7I,J), as the sociability was enhanced significantly in *fabp2*$^{-/-}$ zebrafish treated with MIA. (Additional file 2: Figure S2D); *fabp2*$^{-/-}$ also ameliorated the sociability of PIVE-induced social behavior deficits but without a statistical significance compared to the *fabp2*$^{-/-}$-Control group (Figures 7I,J).

12 https://www.sfari.org/resource/sfari-gene

4. Discussion

Although several environmental risk factor-ASD models such as the MIA-induced model have been established in rodent, so far there have been no reported MIA-induced ASD model with behavioral features in zebrafish. In this study, we established a MIA-induced ASD zebrafish model by demonstrating the involvement of immune activations and characterizing its ASD-like phenotypes.

Studies on rodent models have shown that MIA is sufficient to cause ASD independently, with the offspring showing abnormal brain morphology as well as ASD-like phenotypes (Shi et al., 2003; Shin Yim et al., 2017; Garcia-Valtanen et al., 2020; Haddad et al., 2020). Since zebrafish do not have a placenta and are external fertilizers that do not have induced maternal immune response to affect developing fetus during pregnancy, establishing an MIA-induced ASD zebrafish model is relatively hard. Previous studies have established that TLRs detect exogenous and endogenous threats through pathogen-associated molecular patterns (PAMPs) and damage-associated molecular patterns (DAMPs) and then activate the innate immune system to produce pro-inflammatory cytokines (Han et al., 2021). TLRs are expressed on peripheral immune cells and CNS cells, including microglia and neurons. Classic rodent animal models of MIA use the PAMPs poly(I:C) to stimulate TLR3 and trigger a maternal inflammatory response (Meyer, 2014). DAMPs, such as self RNA, self DNA, high mobility group protein B1 (HMGB1) and heat shock proteins, are normal cell constituents that are released from endogenous damaged cells, which stimulate TLR4 to trigger a maternal inflammatory response (Akira and Takeda, 2004; Tang et al., 2012). Here, we showed that poly(I:C) exposure activated the maternal innate immune system not only by TLR3 but also by TLR4. Furthermore, TLR3 and TLR4bb mRNA expressions were significantly up-regulated in MIA offspring as well as the levels of IgM/C4 were increased in MIA offspring (Figures 1Bb,Cb,Db); while there were no significant changes in TLR3 and TLR4ba/b mRNA expressions in PIVE offspring after a 24 h poly(I:C) exposure (Figures 1Bb,Cb,Db). It suggested that the effects of one-dose maternal poly(I:C) injection is stronger than that of 24 h direct poly(I:C) exposure on eggs, indicating that maternal poly(I:C) exposure did activate innate immune system of their offspring and these effects on the eggs in the MIA model were likely a result of MIA but not a direct effect of poly I:C on the eggs penetrating the placenta. The proposed immune mechanisms of transmitting the effects of MIA to the developing fetus include dysregulated maternal innate, adaptive and complement pathways, and maternal autoantibodies (Knuesel et al., 2014). In rodent animal models, an underlying mechanism of MIA-induced behavioral abnormalities in offspring may involve an imbalance of pro-and anti-inflammatory cytokines in the maternal-placental-fetal axis (Horváth et al., 2019; Lammert and Lukens, 2019; Garcia-Valtanen et al., 2020; Haddad et al., 2020; Reed et al., 2020; Jaini et al., 2021). RNA-sequencing analysis of brain cytokine RNA from the MIA group identified 1 DEG (ccl19b) (Additional file: Figures S12A,B), indicating potential roles of cytokines in mediating the effects of MIA on the developing offspring. Testing cytokine expressions in early developing offspring might get more interesting results. Comparing with MIA, the increased numbers of DEGs of brain cytokine RNA from RNA-sequencing analysis suggest that PIVE larvae have a stronger immune activation with upregulated TLR expressions and increased levels of complement and autoantibodies. We proposed that MIA offspring did not have a continuous effect of the maternal immune response on the developing larvae. Our results indicated that poly(I:C) exposure (both MIA and PIVE) activated the innate immune system through both PAMPs and DAMPs.

ASD is characterized by altered social communication (Lai et al., 2014). In this study, we found that if zebrafish mothers were exposed to poly(I:C) before mating, their offspring exhibited social impairments, especially in social cohesion, as indicated by the significantly larger mean distance between individual fish during the whole study periods (Figures 3B,D). A tendency of moving independently from one another of the fish suggests a likely deficit in social interaction (Additional file 9–10: Movies S5, S6). A comparison among maternal exposure, *in vitro* exposure to embryos, and maternal exposure combined with *in vitro* exposure to embryos (Additional file 2: Figure S11) reveals obviously differences in the degree of social behavioral deficits. For example, the MIA-50 μg/g offspring showed impaired sociability at early larvae stage, decreased social cohesion during whole study age periods, and decreased risk-aware, anxiety-like and aggressive behavior; but PIVE-100 μM zebrafish did not exhibit the same pattern (Meshalkina et al., 2018). Our results indicated that the social behavior tests in this study were sensitive and that different exposures led to different phenotypes. Consistently, PIVE group with a stronger immune activation had a more severely impaired social approach and social cohesion. MIA + PIVE group also had a more severely impaired social approach and social cohesion than MIA or PIVE, but not in social cohesion at 7, 14, and 21 dpf. In comparisons with control/PBS group, the social cohesion of MIA + PIVE group impaired gradually from 7 to 21 dpf as the distance between individuals was lowest at 7 dpf, and highest at 21 dpf; while the distance between individuals of control/PBS group gradually decreased from 7 to 21 dpf. Why did the social cohesion of MIA + PIVE group show inconsistent results? The reason is unknown. We speculate that part of the reason may be related to the weakening of juvenile activities and the reduction of their moving distance caused by MIA + PIVE treatment, thus masking the impact on social cohesion. With the continuous growth, the side effects of this treatment gradually subside. A meta-analysis of 15 studies found that common maternal bacterial infections during pregnancy increased the odds of offspring ASD by 13% (Jiang et al., 2016). The present results provided evidences that immune activation was directly correlated with the phenotypic variety/severity of ASD (Ashwood and Wakefield, 2006; Atladóttir et al., 2010).

Poly(I:C) is a synthetic dsRNA that is recognized by TLR3 and can activate host immune defense. Systemic administration of poly(I:C) induces viral-like acute inflammatory response (Tsukada

et al., 2021). Our results as mentioned above indicated that maternal poly(I:C) exposure activated the innate immune system in zebrafish through not only TLR3 but also TLR4.The presence of behavioral anomalies and immune activations of poly(I:C)-exposed offspring (both MIA and PIVE) provides a unique opportunity for identifying molecular correlates of resilience and susceptibility to poly(I:C) exposure [28]. Therefore, we performed RNA sequencing to compare genome-wide transcriptional changes in these poly(I:C)-exposed offspring. Our GO and KEGG analyses of RNA-sequencing results showed that the pathways of DEGs were different between MIA and PIVE-offspring brain tissues. The KEGG analysis showed that MIA-offspring brain tissues were plentiful in complement and coagulation cascades. Similar results were observed in those with poly(I:C) exposure to zebrafish embryos except complement and coagulation cascades. We found overexpression of complement genes in MIA brain tissues, including *si:dkey-105 h12.2*, *si:dkey-32n7.4*, *f7*, cfb, *c3a.1*, *serpinc1*, *plg*, *f2*, *f5*, *fgb*, *fga*, *proca*, *c8g*, *fgg*, *c8a*, *kng1*, *c3a.6*, *cfh*, *c9*, *serpinf2a*, *serpinf2b*, *c3a.3*, *c5*, and *serping1*. However, the expression levels of these genes in the brain tissues in PIVE-100 μM group did not change or even decreased. As observed in this study, different immune alterations are associated with different phenotypes, which is consistent with the existence of various characteristics or subgroups of human ASD phenotypes (Ashwood and Wakefield, 2006; Atladóttir et al., 2010). Meanwhile, the results indicate that complement activation played an important role in MIA-induced ASD. Accumulating evidence suggests that the pathogenesis of ASD involves a dysregulated complement pathway (Fagan et al., 2017), which includes increased frequencies of C4B alleles in ASD patients and their mothers (Warren et al., 1991), increased levels of C1q and C3 and C3 fragments in the plasma of ASD children (Corbett et al., 2007; Momeni et al., 2012), and hyper-activation of the complement system in postmortem brain tissue from ASD patients (Hutsler and Zhang, 2010; Tang et al., 2014). The abnormal complement signaling as a result of inflammatory insult during pre-and postnatal development may lead to alterations of cerebral connectivity resulting from diminished complement-mediated synaptic pruning, and may contribute to ASD pathophysiology (Schafer et al., 2012). According to previous observation in rodent MIA-model, the top identified canonical signaling pathways range from altered neuronal signaling pathways such as dopamine-and cAMP-regulated phosphoprotein 32 kDa (DARPP-32) signaling, γ-aminobutyric acid receptor signaling, and opioid signaling, to mitochondrial oxidative phosphorylation and translation initiation by eukaryotic initiation factor 2 signaling, which was dependent on brain region and markedly differed between subgroups (Mueller et al., 2021). Although we were not able to stratify MIA/PIVE-exposed offspring into resilient and susceptible subgroups by the cluster analysis and to correlate DEGs to these subgroups, the different phenotypes and patterns of DEGs between MIA and PIVE we have found indicate that poly(I:C)-exposed zebrafish was a useful ASD model for studying phenotypes and molecular mechanisms. We further analyzed the RNA-sequencing results for 991 ASD scored genes. From PPI network, we found that only *vil1-fabp2* and *atp1a1a.4* appeared simultaneously in MIA and PIVE groups (Additional file 2: Figures S9J,K), indicating that these genes may be key mediators of poly(I:C) exposure behavior changes from MIA and PIVE in zebrafish. This result is different from what have been observed in rodent MIA models relating multiple cell signaling pathways, such as opioid signaling, G-protein-coupled receptor signaling, CXCR4 signaling, CREB signaling in neurons, MTOR signaling, oxidative phosphorylation, EIF2 signaling, camp-mediated signaling, DARRP-32 signaling, and GABA receptor signaling, which contained more ASD-risk genes in their observed DEGs (Mueller et al., 2021).

The different phenotypes and patterns of DEGs between MIA and PIVE groups and the results of PPI network analysis suggest that *vil1* forms a more complicated network with other genes in MIA than in PIVE. In the top 10 co-expressed differential genes of two groups (MIA-50 μg/g and PIVE-100 μM), we found only *fabp2* interacted with *vil1* (Figure 6M). We demonstrated that MIA-induced social behavioral deficits were ameliorated by *fabp2* knockout. Similar effect was achieved in those treated with PIVE, as the sociability was enhanced significantly although the amplitude was lesser than MIA. A role of *fabp2* in ASD has not been reported previously. Only one previous study found that intestinal fatty acid binding protein (IFABP, FABP2), an index of gastrointestinal permeability, was significantly increased in serum of ASD patients (Saresella et al., 2016). A relevant result showed that the plasma *fabp2* level in patients with anxiety and depression was significantly higher than that in the control group (Stevens et al., 2018). *Fabp2* is a biomarker of barrier integrity of gut epithelium tight junction, which is upregulated and released by the presence of dysbiotic microbiota. Altogether, *fabp2* can be considered as a novel biomarker or target for psychiatric diseases including ASD, anxiety, and depression. On the other hand, *Vil1* is altered following an induction of cell stress in intestinal epithelial cells. Acute changes in actin dynamics increased intestinal epithelial cell survival, whereas long-term changes in actin dynamics lead to intestinal epithelial cell death and intestinal inflammation (Roy et al., 2018). Thus, we proposed that *fabp2-vil1* signaling may play a pivotal role in MIA-induced ASD.

There are several studies have generated intestinal *FABP* (*FABP2*) and liver *FABP* (*FABP1*) knockout mice and their phenotypes have been characterized. Both *FABPs* are important in the net intake of dietary lipids, which have unique functions in intestinal lipid assimilation involved in systemic energy metabolism (Gajda et al., 2023). *FABP2*-knockout did not cause death of mice, but their weight would change with a hyperinsulinemia, but *FABP2* was not necessary for dietary fat absorption (Vassileva et al., 2000). Another study results showed that *FABP2*-knockout led to changes in gut motility and morphology, resulting in a relatively lean phenotype at the whole-body level (Lackey et al., 2020). Concluded, *FABP2* may participate in dietary lipid sensing and signal transduction, affect intestinal

motility, intestinal structure and nutrient absorption, and thus affect systemic energy metabolism. However, there was no mental disease-like phenotype such as ASD observed in *FABP2*-knockout mice. Zhao et al. (2020) knocking out or overexpressing of *fabp2* in zebrafish and found that *fabp2* could promote intestinal n-3 PUFA absorption to mediate TAG synthesis and CL homeostasis, by regulating the genes involved in lipid metabolism, as well as there was no mental disease-like phenotype could be observed in *fabp2*$^{-/-}$ zebrafish. In contrast, we observed that the sociability in *fabp2*$^{-/-}$ zebrafish (21 dpf) was impaired (Figures 7I,J), which was not shown in adulthood (data not shown). Furthermore, *fabp2*$^{-/-}$ rescued the sociability of MIA/PIVE-induced social behavior deficits. It is unclear how *fabp2* is related to the ASD-like behavior, and how *fabp2* $^{-/-}$ affects MIA/PIVE-induced social behavior defects in zebrafish. Recently, Wei et al. (2022) carried out a bioinformatics analysis of genomic and immune infiltration patterns in ASD. They used weighted correlation network analysis (WGCNA) to separate 5,000 DEGs into eight significant modules and two hub genes were found (one of was *FABP2*). Immune cell infiltration showed that *FABP2* was significantly associated with memory B cells and CD8 T cells and could affect multiple pathways of immunity. We hypothesize that *fabp2* may influence the immune microenvironment by regulating immune cells and immune-related pathways inducing an ASD behavior as observed in the present study that *fabp2* $^{-/-}$ larvae showed an impaired sociability. As mentioned above, MIA-offspring brain tissues were plentiful in complement and coagulation cascades, *fabp2*-knockout may also influence the immune microenvironment to rescue the social behavior deficits from the Poly(I:C) exposure. *Fabp2* not only is a candidate molecular marker for the development of ASD, but also influence the ASD behavior in both causing and ameliorating directions.

In addition, the prevalence of ASD in male is generally higher than that in female (4: 1) (Werling and Geschwind, 2013). It may be related to gene difference on X chromosome or sex hormone, epigenetic regulations which may be sex-biased. There are many ASD-related genes on the X chromosome, such as *FRM1*, *NLGN4X* (Nguyen et al., 2020; Wong et al., 2020). However, we did not find any gender difference at 3 mpf of the MIA-induced sociability and movement changes (Additional file 2: Figure S6), indicating that the immune activation involved in the MIA-induced ASD zebrafish model may not lead to phenotypic differences between gender.

5. Limitations

The major limitation of the present study is that the results are confined to a single maternal injection of poly(I:C) within 24 h before mating to induce MIA. Particularly, it is not known what the effects of longer-term treatment on behavior would be. Further studies are required to titrate the lowest dose of poly(I:C) for altering social behavior. It remains possible that a combination of different doses, injection time and / or frequency, interval and / or route of administration may result in better model generation with improved phenotype. It remains unknown whether there is any difference between genders in larvae of MIA-induced ASD. It is also not known what the phenotype of *fabp2*$^{-/-}$ fish would be and what the longer-term effects of *fabp2* knockout would be on social behavior after poly(I:C) exposures, as we only tested up to 21 dpf. Finally, the underlying molecular and neural mechanisms about how *fabp2* knockout rescues social behavior deficits require further study.

6. Conclusion

In this study, we established an environmental risk factor-ASD model in zebrafish and demonstrated its social behavior impairments that mimic human ASD phenotypes. The model replicated the phenotype of human ASD with multiple comorbidities and characteristics. Both maternal exposure and direct embryo exposure of poly(I:C) resulted in activations of the innate immune system through toll-like receptor 3/4. GO and KEGG analysis of RNA sequencing data found that the MIA-induced DEGs were mainly concentrated in complement and coagulation cascade pathways. PPI network analysis of the detected DEGs suggested that *vil1* pathways may play a key role in MIA-induced ASD. *Fabp2,* the only gene in the top 10 DEGs which interacted with the key node (*vil1*) of the concentrated PPI network, was upregulated in MIA offspring but downregulated in PIVE offspring. Knocking out *fabp2* rescued the social behavior deficits in both MIA and PIVE offspring. Overall, our work established an ASD model with assessable behavior phenotype in zebrafish and provided key insights into environmental risk factor and the influence of *fabp2* gene on ASD-like behavior.

Data availability statement

The original contributions presented in the study are included in the article/Supplementary material, further inquiries can be directed to the corresponding author.

Ethics statement

The animal study was reviewed and approved by the Animal Care and Use Committee at Zhejiang University School of Medicine (16779).

Author contributions

JWu, KJ, and XJ designed the experiments. JWu, XL, DW, BY, PZ, MB, JWa, and CY performed the main experiments. JWu, XL, and KJ created the *fabp2* knockout F0 zebrafish. JWu, ZL, and KJ performed the RNA sequencing analysis. JWu and KJ wrote the manuscript with the help of XJ. All authors read and approved the final manuscript.

Funding

KJ was supported by the National Natural Science Foundation of China (81871012 and 81571263), ZL was supported by the National Natural Science Foundation of China (81901325), and also supported by the Natural Science Foundation of Zhejiang Province (LY20H090017 and LY20H090015).

Conflict of interest

The authors declare that the research was conducted in the absence of any commercial or financial relationships that could be construed as a potential conflict of interest.

Publisher's note

Supplementary material

The Supplementary material for this article can be found online at: https://www.frontiersin.org/articles/10.3389/fnmol.2022.1068019/full#supplementary-material

References

Akira, S., and Takeda, K. (2004). Toll-like receptor signalling. *Nat. Rev. Immunol.* 4, 499–511. doi: 10.1038/nri1391

Ashwood, P., and Wakefield, A. J. (2006). Immune activation of peripheral blood and mucosal CD3+ lymphocyte cytokine profiles in children with autism and gastrointestinal symptoms. *J. Neuroimmunol.* 173, 126–134. doi: 10.1016/j.jneuroim.2005.12.007

Aspatwar, A., Hammaren, M. M., Parikka, M., and Parkkila, S. (2019). Rapid evaluation of toxicity of chemical compounds using zebrafish embryos. *J. Vis. Exp.* 150:e59315. doi: 10.3791/59315

Atladóttir, H. Ó., Thorsen, P., Østergaard, L., Schendel, D. E., Lemcke, S., Abdallah, M., et al. (2010). Maternal infection requiring hospitalization during pregnancy and autism spectrum disorders. *J. Autism Dev. Disord.* 40, 1423–1430. doi: 10.1007/s10803-010-1006-y

Audira, G., Sampurna, B. P., Juniardi, S., Liang, S.-T., Lai, Y.-H., and Hsiao, C.-D. (2018). A versatile setup for measuring multiple behavior endpoints in zebrafish. *Inventions* 3:75. doi: 10.3390/inventions3040075

Chow, K. H., Yan, Z., and Wu, W. L. (2016). Induction of maternal immune activation in mice at mid-gestation stage with viral mimic poly(I:C). *J. Vis. Exp.* 109:e53643. doi: 10.3791/53643

Corbett, B. A., Kantor, A. B., Schulman, H., Walker, W. L., Lit, L., Ashwood, P., et al. (2007). A proteomic study of serum from children with autism showing differential expression of apolipoproteins and complement proteins. *Mol. Psychiatry* 12, 292–306. doi: 10.1038/sj.mp.4001943

Crawley, J. N. (2012). Translational animal models of autism and neurodevelopmental disorders. *Dialogues Clin. Neurosci.* 14, 293–305. doi: 10.31887/DCNS.2012.14.3/jcrawley

Dreosti, E., Lopes, G., Kampff, A. R., and Wilson, S. W. (2015). Development of social behavior in young zebrafish. *Front. Neural Circuits* 9:39. doi: 10.3389/fncir.2015.00039

Dwivedi, S., Medishetti, R., Rani, R., Sevilimedu, A., Kulkarni, P., and Yogeeswari, P. (2019). Larval zebrafish model for studying the effects of valproic acid on neurodevelopment: an approach towards modeling autism. *J. Pharmacol. Toxicol. Methods* 95, 56–65. doi: 10.1016/j.vascn.2018.11.006

Ey, E., Leblond, C. S., and Bourgeron, T. (2011). Behavioral profiles of mouse models for autism spectrum disorders. *Autism Res.* 4, 5–16. doi: 10.1002/aur.175

Fagan, K., Crider, A., Ahmed, A. O., and Pillai, A. (2017). Complement C3 expression is decreased in autism spectrum disorder subjects and contributes to behavioral deficits in rodents. *Mol. Neuropsychiatry* 3, 19–27. doi: 10.1159/000465523

Gajda, A. M., Tawfeeq, H. R., Lackey, A. I., Zhou, Y. X., Kanaan, H., Pappas, A., et al. (2023). The proximal intestinal fatty acid-binding proteins liver FABP (LFABP) and intestinal FABP (IFABP) differentially modulate whole body energy homeostasis but are not centrally involved in net dietary lipid absorption: studies of the LFABP/IFABP double knockout mouse. *Biochim. Biophys. Acta Mol. Cell Biol. Lipids* 1868:159238. doi: 10.1016/j.bbalip.2022.159238

Garcia-Valtanen, P., van Diermen, B. A., Lakhan, N., Lousberg, E. L., Robertson, S. A., Hayball, J. D., et al. (2020). Maternal host responses to poly(I:C) during pregnancy leads to both dysfunctional immune profiles and altered behaviour in the offspring. *Am. J. Reprod. Immunol.* 84:e13260. doi: 10.1111/aji.13260

Haddad, F. L., Patel, S. V., and Schmid, S. (2020). Maternal immune activation by poly I:C as a preclinical model for neurodevelopmental disorders: a focus on autism and schizophrenia. *Neurosci. Biobehav. Rev.* 113, 546–567. doi: 10.1016/j.neubiorev.2020.04.012

Han, V. X., Patel, S., Jones, H. F., and Dale, R. C. (2021). Maternal immune activation and neuroinflammation in human neurodevelopmental disorders. *Nat. Rev. Neurol.* 17, 564–579. doi: 10.1038/s41582-021-00530-8

Horváth, G., Otrokocsi, L., Beko, K., Baranyi, M., Kittel, Á., Fritz-Ruenes, P. A., et al. (2019). P2X7 receptors drive poly(I:C) induced autism-like behavior in mice. *J. Neurosci.* 39, 2542–2561. doi: 10.1523/JNEUROSCI.1895-18.2019

Howe, K., Clark, M. D., Torroja, C. F., Torrance, J., Berthelot, C., Muffato, M., et al. (2013). The zebrafish reference genome sequence and its relationship to the human genome. *Nature* 496, 498–503. doi: 10.1038/nature12111

Hutsler, J. J., and Zhang, H. (2010). Increased dendritic spine densities on cortical projection neurons in autism spectrum disorders. *Brain Res.* 1309, 83–94. doi: 10.1016/j.brainres.2009.09.120

Jaini, R., Wolf, M. R., Yu, Q., King, A. T., and Frazier, T. W. (2021). Maternal genetics influences fetal neurodevelopment and postnatal autism spectrum disorder-like phenotype by modulating in-utero immunosuppression 11, 348. doi: 10.1038/s41398-021-01472-x

Jiang, H. Y., Xu, L. L., Shao, L., Xia, R. M., Yu, Z. H., Ling, Z. X., et al. (2016). Maternal infection during pregnancy and risk of autism spectrum disorders: a systematic review and meta-analysis. *Brain Behav. Immun.* 58, 165–172. doi: 10.1016/j.bbi.2016.06.005

Kalueff, A. V., Stewart, A. M., and Gerlai, R. (2014). Zebrafish as an emerging model for studying complex brain disorders. *Trends Pharmacol. Sci.* 35, 63–75. doi: 10.1016/j.tips.2013.12.002

Kim, O. H., Cho, H. J., Han, E., Hong, T. I., Ariyasiri, K., Choi, J. H., et al. (2017). Zebrafish knockout of down syndrome gene, DYRK1A, shows social impairments relevant to autism. *Mol. Autism.* 8:50. doi: 10.1186/s13229-017-0168-2

Kim, S., Kim, H., Yim, Y. S., Ha, S., Atarashi, K., Tan, T. G., et al. (2017). Maternal gut bacteria promote neurodevelopmental abnormalities in mouse offspring. *Nature* 549, 528–532. doi: 10.1038/nature23910

Knuesel, I., Chicha, L., Britschgi, M., Schobel, S. A., Bodmer, M., Hellings, J. A., et al. (2014). Maternal immune activation and abnormal brain development across CNS disorders. *Nat. Rev. Neurol.* 10, 643–660. doi: 10.1038/nrneurol.2014.187

Lackey, A. I., Chen, T., Zhou, Y. X., Bottasso Arias, N. M., Doran, J. M., Zacharisen, S. M., et al. (2020). Mechanisms underlying reduced weight gain in intestinal fatty acid-binding protein (IFABP) null mice. *Am. J. Physiol. Gastrointest. Liver Physiol.* 318, G518–G530. doi: 10.1152/ajpgi.00120.2019

Lai, M. C., Lombardo, M. V., and Baron-Cohen, S. (2014). Autism. *Lancet* 383, 896–910. doi: 10.1016/S0140-6736(13)61539-1

Lammert, C. R., and Lukens, J. R. (2019). Modeling autism-related disorders in mice with maternal immune activation (MIA). *Methods Mol. Biol.* 1960, 227–236. doi: 10.1007/978-1-4939-9167-9_20

Lyall, K., Croen, L., Daniels, J., Fallin, M. D., Ladd-Acosta, C., Lee, B. K., et al. (2017). The changing epidemiology of autism spectrum disorders. *Annu. Rev. Public Health* 38, 81–102. doi: 10.1146/annurev-publhealth-031816-044318

Meshalkina, D. A., M, N. K., E, V. K., Collier, A. D., Echevarria, D. J., Abreu, M. S., et al. (2018). Zebrafish models of autism spectrum disorder. *Exp. Neurol.* 299, 207–216. doi: 10.1016/j.expneurol.2017.02.004

Meyer, U. (2014). Prenatal poly(i:C) exposure and other developmental immune activation models in rodent systems. *Biol. Psychiatry* 75, 307–315. doi: 10.1016/j.biopsych.2013.07.011

Momeni, N., Brudin, L., Behnia, F., Nordstrom, B., Yosefi-Oudarji, A., Sivberg, B., et al. (2012). High complement factor I activity in the plasma of children with autism spectrum disorders. *Autism Res. Treat.* 2012:868576. doi: 10.1155/2012/868576

Mueller, F. S., Scarborough, J., Schalbetter, S. M., Richetto, J., Kim, E., Couch, A., et al. (2021). Behavioral, neuroanatomical, and molecular correlates of resilience and susceptibility to maternal immune activation. *Mol. Psychiatry* 26, 396–410. doi: 10.1038/s41380-020-00952-8

Nguyen, T. A., Wu, K., Pandey, S., Lehr, A. W., Li, Y., Bemben, M. A., et al. (2020). A cluster of autism-associated variants on X-linked NLGN4X functionally resemble NLGN4Y. *Neuron* 106, 759–768.e7. doi: 10.1016/j.neuron.2020.03.008

Ogi, A., Licitra, R., Naef, V., Marchese, M., Fronte, B., Gazzano, A., et al. (2021). Social preference tests in zebrafish: a systematic review. *Front. Vet. Sci.* 7:1239. doi: 10.3389/fvets.2020.590057

O'Roak, B. J., Vives, L., Fu, W., Egertson, J. D., Stanaway, I. B., Phelps, I. G., et al. (2012). Multiplex targeted sequencing identifies recurrently mutated genes in autism spectrum disorders. *Science* 338, 1619–1622. doi: 10.1126/science.1227764

Parker, M. O., Brock, A. J., Walton, R. T., and Brennan, C. H. (2013). The role of zebrafish (Danio rerio) in dissecting the genetics and neural circuits of executive function. *Front. Neural Circuits* 7:63. doi: 10.3389/fncir.2013.00063

Parvez, S., Herdman, C., Beerens, M., Chakraborti, K., Harmer, Z. P., Yeh, J. J., et al. (2021). MIC-drop: a platform for large-scale in vivo CRISPR screens. *Science* 373, 1146–1151. doi: 10.1126/science.abi8870

Patterson, P. H. (2011). Maternal infection and immune involvement in autism. *Trends Mol. Med.* 17, 389–394. doi: 10.1016/j.molmed.2011.03.001

Rand, K. N., Ho, T., Qu, W., Mitchell, S. M., White, R., Clark, S. J., et al. (2005). Headloop suppression PCR and its application to selective amplification of methylated DNA sequences. *Nucleic Acids Res.* 33:e127. doi: 10.1093/nar/gni120

Reed, M. D., Yim, Y. S., Wimmer, R. D., Kim, H., Ryu, C., Welch, G. M., et al. (2020). IL-17a promotes sociability in mouse models of neurodevelopmental disorders. *Nature* 577, 249–253. doi: 10.1038/s41586-019-1843-6

Roy, S., Esmaeilniakooshkghazi, A., Patnaik, S., Wang, Y., George, S. P., Ahrorov, A., et al. (2018). Villin-1 and gelsolin regulate changes in actin dynamics that affect cell survival signaling pathways and intestinal inflammation. *Gastroenterology* 154, 1405–1420.e2. doi: 10.1053/j.gastro.2017.12.016

Samaee, S. M., Seyedin, S., and Varga, Z. M. (2017). An affordable intraperitoneal injection setup for juvenile and adult zebrafish. *Zebrafish* 14, 77–79. doi: 10.1089/zeb.2016.1322

Saresella, M., Piancone, F., Marventano, I., Zoppis, M., Hernis, A., Zanette, M., et al. (2016). Multiple inflammasome complexes are activated in autistic spectrum disorders. *Brain Behav. Immun.* 57, 125–133. doi: 10.1016/j.bbi.2016.03.009

Schafer, D. P., Lehrman, E. K., Kautzman, A. G., Koyama, R., Mardinly, A. R., Yamasaki, R., et al. (2012). Microglia sculpt postnatal neural circuits in an activity and complement-dependent manner. *Neuron* 74, 691–705. doi: 10.1016/j.neuron.2012.03.026

Selvaraj, V., Venkatasubramanian, H., Ilango, K., and Santhakumar, K. (2019). A simple method to study motor and non-motor behaviors in adult zebrafish. *J. Neurosci. Methods* 320, 16–25. doi: 10.1016/j.jneumeth.2019.03.008

Shi, L., Fatemi, S. H., Sidwell, R. W., and Patterson, P. H. (2003). Maternal influenza infection causes marked behavioral and pharmacological changes in the offspring. *J. Neurosci.* 23, 297–302. doi: 10.1523/JNEUROSCI.23-01-00297.2003

Shin Yim, Y., Park, A., Berrios, J., Lafourcade, M., Pascual, L. M., Soares, N., et al. (2017). Reversing behavioural abnormalities in mice exposed to maternal inflammation. *Nature* 549, 482–487. doi: 10.1038/nature23909

Smith, S. E., Li, J., Garbett, K., Mirnics, K., and Patterson, P. H. (2007). Maternal immune activation alters fetal brain development through interleukin-6. *J. Neurosci.* 27, 10695–10702. doi: 10.1523/JNEUROSCI.2178-07.2007

Stevens, B. R., Goel, R., Seungbum, K., Richards, E. M., Holbert, R. C., Pepine, C. J., et al. (2018). Increased human intestinal barrier permeability plasma biomarkers zonulin and FABP2 correlated with plasma LPS and altered gut microbiome in anxiety or depression. *Gut* 67, 1555–1557. doi: 10.1136/gutjnl-2017-314759

Szklarczyk, D., Morris, J. H., Cook, H., Kuhn, M., Wyder, S., Simonovic, M., et al. (2017). The STRING database in 2017: quality-controlled protein-protein association networks, made broadly accessible. *Nucleic Acids Res.* 45, D362–D368. doi: 10.1093/nar/gkw937

Tang, G., Gudsnuk, K., Kuo, S. H., Cotrina, M. L., Rosoklija, G., Sosunov, A., et al. (2014). Loss of mTOR-dependent macroautophagy causes autistic-like synaptic pruning deficits. *Neuron* 83, 1131–1143. doi: 10.1016/j.neuron.2014.07.040

Tang, D., Kang, R., Coyne, C. B., Zeh, H. J., and Lotze, M. T. (2012). PAMPs and DAMPs: signal 0s that spur autophagy and immunity. *Immunol. Rev.* 249, 158–175. doi: 10.1111/j.1600-065X.2012.01146.x

Tsukada, T., Shimada, H., Sakata-Haga, H., Shoji, H., Iizuka, H., and Hatta, T. (2021). Decidual cells are the initial target of polyriboinosinic-polyribocytidylic acid in a mouse model of maternal viral infection. *Biochem. Biophys. Rep.* 26:100958. doi: 10.1016/j.bbrep.2021.100958

Vassileva, G., Huwyler, L., Poirier, K., Agellon, L. B., and Toth, M. J. (2000). The intestinal fatty acid binding protein is not essential for dietary fat absorption in mice. *FASEB J.* 14, 2040–2046. doi: 10.1096/fj.99-0959com

Vaz, R., Hofmeister, W., and Lindstrand, A. (2019). Zebrafish models of neurodevelopmental disorders: limitations and benefits of current tools and techniques. *Int. J. Mol. Sci.* 20:1296. doi: 10.3390/ijms20061296

Wakefield, A. J. (2002). The gut-brain axis in childhood developmental disorders. *J. Pediatr. Gastroenterol. Nutr.* 34, S14–S17. doi: 10.1097/00005176-200205001-00004

Wakefield, A. J., Ashwood, P., Limb, K., and Anthony, A. (2005). The significance of ileo-colonic lymphoid nodular hyperplasia in children with autistic spectrum disorder. *Eur. J. Gastroenterol. Hepatol.* 17, 827–836. doi: 10.1097/00042737-200508000-00009

Warren, R. P., Singh, V. K., Cole, P., Odell, J. D., Pingree, C. B., Warren, W. L., et al. (1991). Increased frequency of the null allele at the complement C4b locus in autism. *Clin. Exp. Immunol.* 83, 438–440. doi: 10.1111/j.1365-2249.1991.tb05657.x

Wei, R. Q., Guo, W. L., Wu, Y. T., Alarcon Rodriguez, R., Requena Mullor, M. D. M., Gui, Y. C., et al. (2022). Bioinformatics analysis of genomic and immune infiltration patterns in autism spectrum disorder. *Ann. Transl. Med.* 10:1013. doi: 10.21037/atm-22-4108

Werling, D. M., and Geschwind, D. H. (2013). Sex differences in autism spectrum disorders. *Curr. Opin. Neurol.* 26, 146–153. doi: 10.1097/WCO.0b013e32835ee548

Wong, H., Hooper, A. W. M., Niibori, Y., Lee, S. J., Hategan, L. A., Zhang, L., et al. (2020). Sexually dimorphic patterns in electroencephalography power spectrum and autism-related behaviors in a rat model of fragile X syndrome. *Neurobiol. Dis.* 146:105118. doi: 10.1016/j.nbd.2020.105118

Yuen, R. K. C., Merico, D., Bookman, M., J, L. H., Thiruvahindrapuram, B., Patel, R. V., et al. (2017). Whole genome sequencing resource identifies 18 new candidate genes for autism spectrum disorder. *Nat. Neurosci.* 20, 602–611. doi: 10.1038/nn.4524

Zakaria, F., Akhtar, M. T., Wan Ibrahim, W. N., Abu Bakar, N., Muhamad, A., Shohaimi, S., et al. (2021). Perturbations in amino acid metabolism in reserpine-treated zebrafish brain detected by (1)H nuclear magnetic resonance-based metabolomics. *Zebrafish* 18, 42–54. doi: 10.1089/zeb.2020.1895

Zhao, Y., Cao, X., Fu, L., and Gao, J. (2020). N-3 PUFA reduction caused by fabp2 deletion interferes with triacylglycerol metabolism and cholesterolhomeostasis in fish. *Appl. Microbiol. Biotechnol.* 104, 2149–2161. doi: 10.1007/s00253-020-10366-9

frontiers | Frontiers in Molecular Neuroscience

TYPE Review
PUBLISHED 13 March 2023
DOI 10.3389/fnmol.2023.1133209

OPEN ACCESS

EDITED BY
William C. Cho,
QEH, Hong Kong SAR, China

REVIEWED BY
Greta Pintacuda,
Broad Institute, United States
Luis R. Hernandez-Miranda,
Charité Universitätsmedizin Berlin, Germany

*CORRESPONDENCE
Monika Piwecka
✉ mpiwecka@ibch.poznan.pl

SPECIALTY SECTION
This article was submitted to Molecular Signalling and Pathways, a section of the journal Frontiers in Molecular Neuroscience

RECEIVED 28 December 2022
ACCEPTED 06 February 2023
PUBLISHED 13 March 2023

CITATION
Piwecka M, Fiszer A, Rolle K and Olejniczak M (2023) RNA regulation in brain function and disease 2022 (NeuroRNA): A conference report. *Front. Mol. Neurosci.* 16:1133209. doi: 10.3389/fnmol.2023.1133209

RNA regulation in brain function and disease 2022 (NeuroRNA): A conference report

Monika Piwecka*, Agnieszka Fiszer, Katarzyna Rolle and Marta Olejniczak

Institute of Bioorganic Chemistry, Polish Academy of Sciences, Poznań, Poland

Recent research integrates novel technologies and methods from the interface of RNA biology and neuroscience. This advancing integration of both fields creates new opportunities in neuroscience to deepen the understanding of gene expression programs and their regulation that underlies the cellular heterogeneity and physiology of the central nervous system. Currently, transcriptional heterogeneity can be studied in individual neural cell types in health and disease. Furthermore, there is an increasing interest in RNA technologies and their application in neurology. These aspects were discussed at an online conference that was shortly named NeuroRNA.

KEYWORDS

RNA biology, transcriptomics, RNA processing, miRNA, non-coding RNAs, neurodegenerative disorders, RNA therapeutics, brain tumors

Introduction

Modern molecular and cellular biology are more and more fostered by high-throughput approaches and jointly provide novel research tools to accelerate our understanding of how biological systems are built and regulated. Neuroscience is propelled by quickly advancing genomics, transcriptomics, and other -omics technologies; CRISPR-based gene-editing technology; the development of new models such as induced pluripotent stem cells (iPSCs)-derived brain organoids; high-resolution structural and functional deep brain imaging methods; among others. Interdisciplinary approaches advance the knowledge of basic regulatory processes in neural cells, re-visit their heterogeneity and connectivity, and eventually, give promise for developing better treatment strategies for patients suffering from neurological disorders.

RNA biology bestows a rich resource for neuroscience. It provides methods for studying gene expression in space and time, across different genotypes/phenotypes, and among different neural cell types. RNA biology also provides research tools for perturbing gene expression, which is used to perform basic research and is increasingly tested for biomedical translational purposes. Neural cells possess highly complex and multi-level gene expression regulation mechanisms and appear evident both for the transcriptional and post-transcriptional regulatory processes. Cell type-specific subsets of genes are being recognized to be regulated and coordinated at the RNA level, e.g., in response to activity inputs, injuries, or neuroinflammation. Transcriptional heterogeneity of neural cells within individual populations (e.g., interneurons) is studied in depth with single-cell RNA sequencing (scRNA-seq) and reveals unprecedented intra-populational differences (Romanov et al., 2017; Mayer et al., 2018; Muñoz-Manchado et al., 2018; Polioudakis et al., 2019; La Manno et al., 2021; Perez et al., 2021; Kamath et al., 2022), which

are revolutionizing traditional classifications of neural cells based on morphology and physiology (e.g., neurotransmitter release). RNA processing is being steadily more integrated into nuclear, axonal, and synaptic signaling networks in neurons (Wong et al., 2017; Holt et al., 2019). RNA localization and subcellular modes of action of different RNA-binding proteins as well as localized translation are still under intensive investigation not only in neurons but also in other neural cell types in health and disease (Nussbacher et al., 2019; Koester and Dougherty, 2022). Moreover, aberrant RNA processing has been associated with many neurological dysfunctions. Neuropathologies, as well as neuromuscular disorders, are scrutinized, e.g., for targeting RNA splicing as a novel treatment option. RNA represents not only a target but may also serve as a source of biomarkers (Drew, 2019; Fyfe, 2021). Importantly, RNA technologies are applied for designing RNA-based therapeutics; e.g., RNA interference (RNAi) and CRISPR/Cas13 technologies are tested for providing treatment interventions in rare neurological disorders (Duarte and Déglon, 2020; Morelli et al., 2022). In fact, contemplation about how contemporary RNA biology aligns with neuroscience may come in many flavors and fascinating directions.

A virtual conference *RNA Regulation in Brain Function and Disease* was organized to discuss the state-of-the-art research at the interface of RNA biology and neuroscience, with the focus on five themes arranged in five conference sessions (Figure 1); each session is briefly summarized in the following paragraphs. The organizing committee aimed to integrate and discuss novel insights into the central nervous system (CNS) and its dysfunctions from the systems biology perspective to finer molecular and cellular scales. To do that, we brought together a panel of experts in the field and young principal investigators who shared with attendees' novel results, views, expertise, and insights into cutting-edge methods. The NeuroRNA Conference (https://neurorna2022.com/) took place from 28 to 30 September 2022. There were over 200 participants from 17 countries, 17 invited talks, 13 selected talks, and 33 poster presentations.

Living in an exciting era of single-cell transcriptomics: Impressions on the keynote lecture

The opening keynote lecture entitled "*Cellular architecture of the human brain*" was given by *Sten Linnarsson* from the Karolinska Institute, Stockholm, Sweden. ScRNA-seq technologies are gaining momentum in neuroscience, and *Sten Linnarsson* has contributed to both the inception and development of these technologies. Importantly, in the Linnarsson lab, scRNA-seq has been continuously used to uncover the complexity of the mammalian brain. During the conference, the participants had a chance to hear about two new studies, which, shortly after the meeting, became publicly available as preprints (Braun et al., 2022; Siletti et al., 2022). The first study's aim has been to map the cellular composition of the adult human brain with single-nucleus transcriptomics to obtain a highly resolved molecular atlas. The project has been run in collaboration with the Allen Institute for Brain Science within the BRAIN Initiative Cell Census Network (BICCN) and sampled over 100 anatomically distinct locations from three adult brains (each run in technical duplicate), to perform analysis of an impressive number of >3.3 million of high-quality cells. That large-scale effort revealed a great transcriptomic diversity across the adult human brain cell types and subtypes that have been defined on the more general level by 31 super-clusters. Super-clusters represent the main categories of cells and reflected the anatomical distribution and developmental origin of cells. Some neuronal super-clusters corresponded to cortical layers and projection patterns of pyramidal neurons, whereas others clearly corresponded to the neuron's developmental origin (MGE and CGE interneuron clusters corresponding to medial and caudal ganglionic eminences-origin, respectively) or distinct non-neuronal populations. Cells within super-clusters have been assigned to >3,300 individual clusters that correspond to specific individual cell types as defined based on their transcriptomes. One surprising super-cluster named "splatter" neurons was mainly found in subcortical brain regions and was composed of 92 different clusters. These cells seemed very heterogeneous when it comes to neurotransmitter identity and yet formed a complex 'family' of transcriptionally related neurons. The breadth and wealth of the data enabled further inspection including sub-clustering into plausible cell subtypes. The data also give additional insight into the spatial region-specific distribution of glial cells, e.g., mature oligodendrocytes and their progenitors (OPCs), and astrocytes. Switching to the cell atlas of the human developing brain, >1.6 million cells were analyzed from 26 embryos (Braun et al., 2022). The study disentangles region specificity of different cell types, including radial glia, neuroblasts, and glioblasts. That dataset was used, among others, to re-visit corticogenesis. Altogether, both studies represent the most comprehensive resources available to date of individual cell transcriptomes derived from the adult and developing human brain. These resources will benefit future comparative studies, e.g., focusing on neuropathologies.

Single-cell and spatial transcriptomics in brain research

Single-cell technologies are becoming very popular these days, and the rapid evolution of scRNA-seq methods has led to manifold discoveries over a short time. Numerous scRNA-seq studies have been reported to date, including resources of single-cell transcriptomes from different brain regions and developmental time points from human, primate, and rodent samples, from both homeostatic and multiple pathological conditions, form cell type-enriched samples (e.g., FACS-sorted), or obtained from unsorted single-cell or single-nuclei suspensions. In turn, spatial transcriptomic methods bypass tissue dissociation and retain spatial information. This allows for the assessment of gene expression across thousands of cells within the context of the entire structural organization of tissue in normal physiology or under perturbation. In the first scientific session of the conference "*Single-cell and Spatial Transcriptomics in Brain Research*," the state-of-the-art and future perspectives of the single-cell field in the context of neuroscience have been discussed.

10.3389/fnmol.2023.1133209

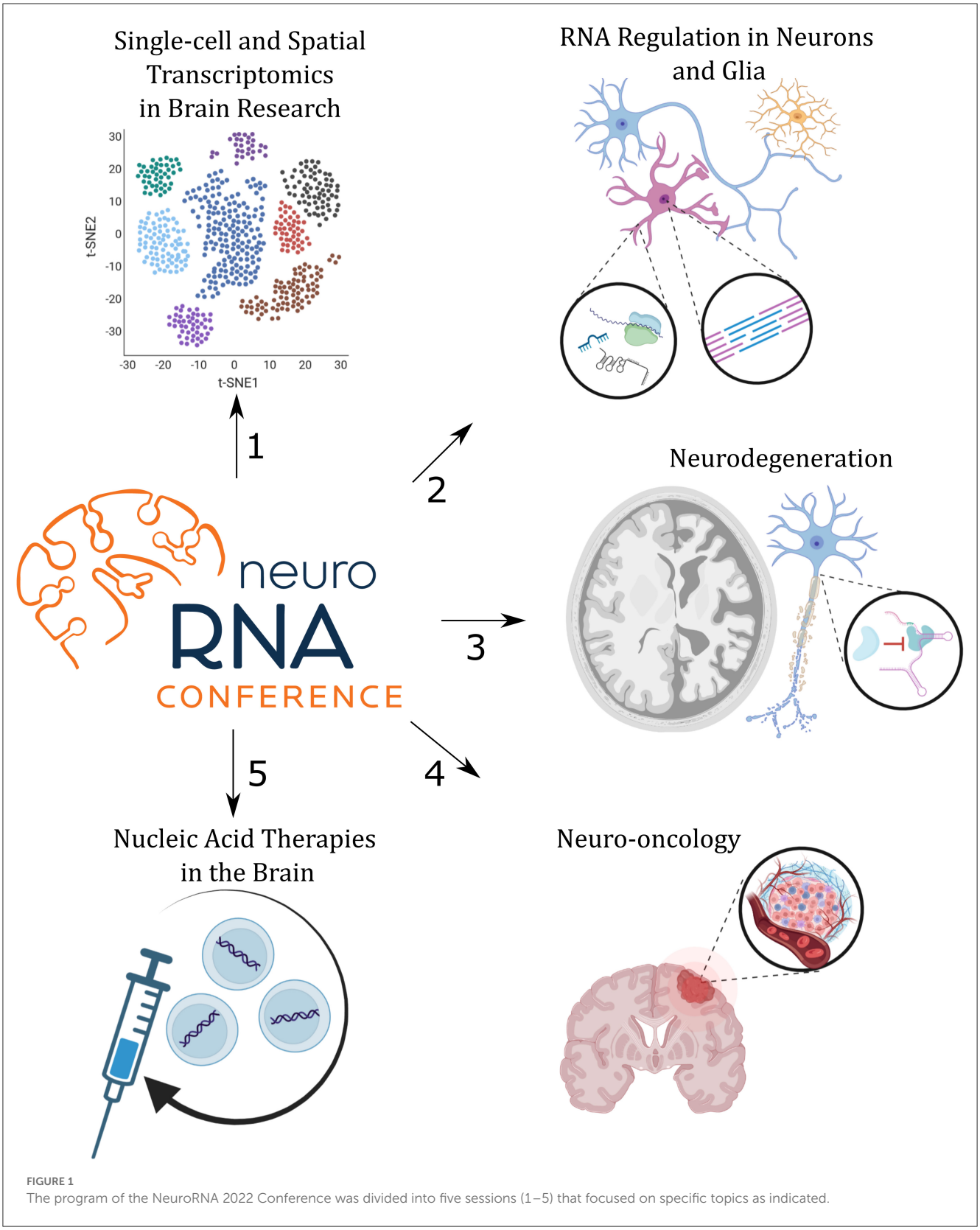

FIGURE 1
The program of the NeuroRNA 2022 Conference was divided into five sessions (1–5) that focused on specific topics as indicated.

Single-cell RNA sequencing (scRNA-seq) has become revolutionary in expanding our understanding of complex biological systems such as brain tumors and their microenvironment. *Bozena Kaminska* (Nencki Institute of Experimental Biology, Polish Academy of Sciences, Warsaw, Poland) and her lab apply scRNA-seq and most recently spatial

transcriptomics in order to study gliomas, with the main focus on glioma-associated brain macrophages and microglia and their heterogeneity in mouse glioma models. They observed a subpopulation of so-called glioma-activated microglia and were able to detect marker genes that clearly distinguish these cells from homeostatic microglia, resident macrophages, and macrophages that infiltrate the tumor. However, both macrophages and microglia shared the signatures of signaling-associated genes, and at this level, these different myeloid cells were indistinguishable. Further application of CITE-seq [Cellular Indexing of Transcriptomes and Epitopes by sequencing (Stoeckius et al., 2017)] that takes the advantage of transcriptomics and a panel of surface protein markers helped to dissect the differences between mRNA and protein abundance for a panel of genes with the single-cell resolution. The presented results were in line with the notion that monocytes/myeloid cells in the tumor microenvironment are often immunosuppressive (Munn and Bronte, 2016), additionally showing that the phenotypes can transit from proinflammatory monocytes to tumor-supportive macrophages in the brain tumor microenvironment. Interestingly, the early results show that the frequency of the switch between monocytes and tumor-associated macrophages tends to be sex-dependent or sex-biased.

A strong trend in neuroscience, and also other disciplines, has been shifting toward determining high-throughput information from multiple experimental modalities within individual cells. *Ozgun's Gokce* (Ludwig Maximilian University, Munich, Germany) illustrated how spatial transcriptomics may be combined with the measurement of morphological features afforded by electron microscopy. Gokce lab studies dementia and focuses on the identification of the cellular responses associated with the loss of white matter (WM) volume, which is one of the hallmarks of a dementing brain (Bethlehem et al., 2022). White and gray matter aged rodent brains were dissected with scRNA-seq which allowed the identification of white matter-associated microglia (WAMs) along with three subpopulations of homeostatic and activated microglia (Safaiyan et al., 2021). Careful examination of microglia transcriptomes in WM of aged brain and cross-comparison with known signatures of microglia showed that WAMs share some features with disease-associated microglia (DAM), especially when it comes to activation of genes implicated in phagocytic activity and lipid metabolism. Another observation is that there is a great loss of oligodendrocytes in WM of 24-month-old mice (Kaya et al., 2022) and that these cells are also changing their phenotypes, e.g., a subpopulation of "interferon response" oligodendrocytes was noticed in the white matter of aged brains. A new development from Gökçe lab, spatial transcriptomics-correlated electron microscopy (Androvic et al., 2022) combines multiplex error-robust FISH [MERFISH (Chen et al., 2015)] information with EM. It was applied to study the spatial context of glial cells in WM. In the proof-of-principle study, it enabled to provide a link between the morphology of "foamy" microglia (featuring lipid droplets inside the cell) and a tiny population of interferon-response microglia with their transcriptional signatures and proximity to T-cells (Androvic et al., 2022). The application of single-cell technologies and spatially resolved molecular approaches gives the opportunity to provide unprecedented depth into many physiological states of glial cells in a high-throughput data-driven fashion. It can also provide new clues to the relevance of the co-existence of different cell types/subtypes in spatial proximity. How about single-cell chromatin profiling? *Marek Bartosovic* (Karolinska Institute, Stockholm, Sweden) switched gears to "*Multimodal profiling of the epigenome at single-cell resolution*", particularly focusing on the application of CUT&Tag in single nuclei obtained from juvenile (P15, P25) mouse brain. That setup enabled the study of multiple histone marks and transcription factors Olig2 and Rad21 at single-cell resolution and cluster cells according to their chromatin profile (Bartosovic et al., 2021). These datasets allowed also the prediction of cell-type-specific promoter-enhancer interactions. In addition to the measurement of open chromatin regions, now it is possible to capture multimodal epigenetic marks in single cells. To achieve that, the new nanobody-Tn5 fusions are being used to target and barcode two distinct active and repressive histone marks (Bartosovic and Castelo-Branco, 2022). This new method termed nano-CUT&Tag is of much better sensitivity as compared with scCUT&Tag and allows for the discrimination of more cell types/states together with the possibility to infer chromatin velocity to predict differentiation trajectories of distinct cell types. Dissection of the oligodendrocyte population with nano-CUT&Tag revealed the presence of two sequential waves of H3K27me3 repression at distinct gene groups during the lineage differentiation. A recent introduction of a cutting-edge method combining spatial co-profiling of gene expression (RNA) and spatial chromatin profiling was also mentioned (Deng et al., 2022).

Agnieszka Rybak-Wolf (Berlin Institute for Medical Systems Biology, Berlin, Germany) presented an article on herpes simplex virus (HSV)-driven encephalitis. HSV-1 infection was evoked in human brain organoids and studied at the molecular and physiological levels. The study recapitulated known features of HSV-1 infection (such as diminished synaptic gene expression and decreased synaptic firing) and delivered novel insights into perturbed gene expression due to infection, e.g., activation of antisense transcription and global increase in the length in poly(A) tails in mRNA (Rybak-Wolf et al., 2021). Single-cell RNA-seq in HSV-1-infected organoids revealed an overall changed cellular composition of organoids upon infection and a few clusters of cells (aka cell types) that were more susceptible to infection ("highly infected" cells). In turn, acyclovir (ACV)-treated organoids featured low virus load, yet their transcriptomes were not back to normal "pre-infection" profiles. In particular, the TNF-α signaling pathway was still upregulated post-ACV treatment in certain cell types. Attenuation of inflammatory response with anti-inflammatory drug rescued some infection effects in organoids, such as recovered neuroepithelial integrity. The presented work provided robust evidence for the relevance of brain organoids as a model system for studies on brain infections and the usefulness of scRNA-seq in tracing therapeutic outcomes of new therapies and drug re-purposing. Another study that took advantage of brain organoids as a model system was presented in a short talk by *Ivano Legnini* (Berlin Institute for Medical Systems Biology, Berlin, Germany) who showed the validity of the new optogenetic method for programmable silencing or activation of target genes. Light-inducible CRISPR/Cas9 construct and gRNAs were used to target and activate transcription from *Sonic Hedgehog* (SHH) promoter in a proof-of-concept experiment (Legnini et al., 2022).

Importantly, such a system allows the programming of gene expression only in intended cells. By light-controlled activation of a morphogen (such as *SHH)* in 3D brain organoids, one can provide a stimulus to develop an organoid with a certain spatial patterning mimicking *in vivo* situation, i.e., developing neural tube-like in case of *SHH* activation. The analysis of optogenetically patterned brain organoids was performed both with single-cell and spatial transcriptomic methods.

The following short talks in this session provided a transition to the second scientific session about the mechanisms of gene expression regulation in brain cell types. *Franz Ake* (Bellvitge Institute for Biomedical Research IDIBELL, Barcelona, Spain) discussed the insights into the challenges and importance of detecting alternative polyadenylation (APA) in individual cells. Is differential APA attributed to neurological conditions and can that be investigated from the single-cell transcriptomic datasets generated with currently available platforms? To tackle that question, Mireya Plass lab applies single-cell isoform quantification in iPSC-derived neurons from patients with Alzheimer's disease (AD) and isogenic controls using an in-house developed workflow. Preliminary results show a subset of genes that switch mRNA isoforms in AD pathology as compared with controls and that it occurs in a cell type-specific manner in heterogeneous neuronal cells differentiated from iPSCs. In turn, *Rotem Ben Tov Perry* from the Weizmann Institute of Science (Rehovot, Israel) presented a study about long-non-coding RNA (lncRNA) called *Silc1*. *Silc1* RNA has been previously shown to be important for cis-activation of the transcription factor *Sox11* during neuroregeneration in the peripheral nervous system (Perry et al., 2018), and now its role has been dissected in the CNS. In the presented unpublished results [now available as a preprint (Perry et al., 2022)], the authors highlighted transcriptional induction of *Silc1* upon stimulation in the hippocampus and evidenced its role in neural plasticity and memory formation in spatial learning.

RNA regulation in neurons and glia

In the second scientific session, a few timely subjects regarding RNA regulation in neural cells have been discussed. RNA splicing, the choice of transcription start site (TSS), and poly(A) site have fundamental roles in mRNA maturation, stability, and localization, and all of these ultimately influence the gene expression programs, oftentimes in a cell type-specific manner. *Hagen Tilgner* (Weill Cornell Medicine, New York, USA) provided a comprehensive overview of the current understanding of alternative splicing and mRNA isoform usage in the brain that is now being dissected with single-cell resolution. The application of single-cell isoform RNA sequencing (Gupta et al., 2018) highlighted a cell type specificity at the isoform level for a subset of mRNAs as well as brain-region specificity of different isoforms (Joglekar et al., 2021). That phenomenon has functional consequences on the occurrence of different protein isoforms and may impact distinct subcellular localization patterns of either RNA or the protein. Tilgner lab is moving forward with single-nuclei RNA sequencing (snRNA-seq) and isoform identification that enables analysis of frozen tissue material (i.e., the majority of clinical samples). The key methodological development in SnISOr-seq (single-nuclei isoform RNA sequencing) is the addition of two steps in cDNA library preparation: an asymmetric PCR to amplify barcoded cDNA and an enrichment step using exon-targeting probes to filter out purely intronic molecules (Hardwick et al., 2022). As alternative exon inclusion/skipping event is relatively common in the brain and cell type-specific phenomenon, more interestingly, there is cell type-specific coordination of exons, TSS, and poly(A) patterns that can be noticed from snRNA-seq datasets (Hardwick et al., 2022).

Joseph Dougherty (Washington University School of Medicine, St. Louis, USA) talked about alternative translation and local translation in glia, and it was a very valuable contribution to discussions regarding the regulation of alternative mRNA isoforms in brain cells. Local translation in neurons is nowadays an intensively studied and well-recognized phenomenon (Holt, Martin, and Schuman 2019). The recognition of local translation in other neural cells, such as astroglia, has been emerging recently. From the Dougherty lab's earlier work, we have learned that translation exists in distal astrocytic processes (Sakers et al., 2017), and that line of research has been extended to microglia (Vasek et al., 2021). Microglia have been shown to perform local protein synthesis in peripheral microglial processes, particularly at the perisynaptic and phagocytic structures. In fact, a specific subset of mRNAs is being translated at the peripheral process of microglia as shown by profiling of the ribosome-bound mRNAs from processes and the enrichment of phagocytosis-related transcripts. From the other angle, it was evidenced that translation is required for phagocytic cup formation and sufficient to enable phagocytosis in microglia processes that were severed from the cell somas. Switching to alternative translation, that process depends on differential usage of translation initiation sites on one transcript. Similarly to alternative splicing, alternative translation diversifies proteome and allows for greater biological complexity. The Dougherty lab showed that the choice of translation initiation site might be activity-dependent in neurons (Sapkota et al., 2019). Another interesting observation coming from translating ribosome affinity purification to ribosome footprinting is a cell type-specific mechanism for translational stop codon readthrough in the mouse brain (Sapkota et al., 2019).

In recent years, the community has made substantial progress toward the detection and profiling of non-coding RNAs (ncRNAs) in the mammalian brain and multiple pathological conditions, e.g., in the past 10 years, numerous studies have informed about changes in microRNA (miRNA) levels in the different brain regions of patients suffering from neurological disorders and in neural tissues from animal models of respective conditions. Functions and mechanism of actions of newly annotated ncRNAs in the majority of cases remain unclear, albeit there is still a growing interest in research focusing on disentangling ncRNA impact on gene expression, as some of them have been evidenced to possess important regulatory functions. Functional studies in animal models provide evidence that certain miRNAs influence pathogenesis, e.g., genetic deletion of miR-128, a crucial regulator of neuronal excitability, leads to fatal epilepsy in mice (Tan et al., 2013). During the conference, *Jeroen Pasterkamp* from the University Medical Center Utrecht introduced his lab's work on ncRNAs in neurological disease, namely, miRNAs and circular

RNAs (circRNAs) and their association with temporal lobe epilepsy (TLE). miRNAs and miRNA-binding proteins Argonautes are mainly localizing to the cytoplasm in cells, yet there are exceptions from that commonly accepted rule (Leung, 2015). What are the function and the mechanism beyond nuclear miRNAs, still remains unclear. Abnormal nuclear localization of a subset of miRNA in TLE was observed and now gets dissected to provide new knowledge about the mechanism of nuclear miRNA action. The recent insight into circRNAs in neurons and their newly evidenced role in the regulation of dendritic spine morphology was also highlighted (Gomes-Duarte et al., 2022). The subject of ncRNA in brain research was continued with the selected talks. *Mollie K. Meffert* (The Johns Hopkins University School of Medicine, Baltimore, USA) presented her group's ongoing work on the abundant let-7 family of miRNAs and its molecular targets and function in the brain. *Fmr1* KO mice have been used in the study, and they showed an activity-dependent reduction of let-7 levels in behavioral studies. *Orna Issler* (Icahn School of Medicine at Mount Sinai, New York, USA) introduced the topic of sex-specific lncRNAs in the context of depression, and more generally — mood. A previous study highlighted that a substantial part of the differentially expressed genes in the brains of depressed humans (∼1/3) belong to lncRNA-encoding genes and that these transcripts display region- and sex-specific patterns of the regulation (Issler et al., 2020). Her current project focused on one particular lncRNA called FEDORA, which was found to be positively correlated with depression susceptibility in women (Issler et al., 2021). Last but not the least, a new insight into circRNA Cdr1as association with brain homeostasis over daily light–dark (LD) cycles was introduced by *Andranik Ivanov* (Berlin Institute of Health, Berlin, Germany). Cdr1as is one of the best studied to date brain-enriched circRNAs. It has the unique property of possessing multiple binding sites for miRNA, in mice >120 binding sites for miR-7 and one binding site for miR-671. Cdr1as was previously shown to be involved in the regulation of miR-7 and its mRNA targets in excitatory neurons in multiple regions of the mouse brain. *Cdr1as* KO mice were identified with behavioral abnormalities, namely, sensorimotor gating phenotype that is associated with neuropsychiatric disorders and dampened neural activity in *in vitro* autaptic neuronal cultures (Piwecka et al., 2017). However, the study by Ivanov et al., brings another layer of complexity to *Cdr1as* functions in neurons and circRNA stability, as it clearly implies that Cdr1as undergoes dynamic turn-over in the suprachiasmatic nucleus over the LD cycles (Ivanov et al., 2022).

RNA in brain pathology: Neurodegeneration

This session was focused on recent findings and challenges in studying RNA molecules in neurodegenerative disorders. Mutant forms of RNAs can trigger disruptions in molecular pathways that specifically affect neurons, which further contribute to neurodegeneration. Global deregulation of the transcriptome is a common observation in the diseased brain and its investigation with RNA-seq helps to understand the pathology at the molecular level. The presentations in this session covered some of these aspects in Parkinson's disease (PD) and Alzheimer's disease (AD), and repeat expansion diseases such as Huntington's disease (HD).

Gracjan Michlewski (International Institute of Molecular and Cell Biology, Warsaw, Poland) presented insights into specific RNA–protein interaction networks. RNA-binding protein HuR — pri-miR-7 — α-synuclein (*SNCA*) mRNA has been investigated in the context of PD. This regulatory network provides an option for therapeutic intervention in PD, as increased levels and aggregation of α-synuclein are a hallmark of this disease, and miR-7 biogenesis *via* HuR might be targeted to impact *SNCA* expression (Poewe et al., 2017). The RNA Pull-Down COnfocal NAnoscanning (RP-CONA) method was used to identify compounds that may disrupt pri-miR-7–HuR interaction (Zhu et al., 2021) and that line of research is further developed in Michlewski lab.

Evgenia Salta (Netherlands Institute for Neuroscience, Amsterdam, the Netherlands) referred to the cellular and molecular complexity of AD pathology, including complex miRNA regulation and challenges in the use of miRNAs as therapeutics (Walgrave et al., 2021b). The focus of current research in the Salta lab is on revealing coding and non-coding regulators of adult hippocampal neurogenesis in AD. Based on previous results regarding miR-132 downregulation in AD (Walgrave et al., 2021a) and its role in neurogenesis, miR-132 has been further studied in the context of impaired neurogenesis in AD. More details of this process are expected to emerge from ongoing scRNA-seq of AD patients' brains, specifically regions containing neurogenic niches. Interestingly, samples from non-demented patients with AD are included in these analyses.

Pawel Switonski (Institute of Bioorganic Chemistry, Polish Academy of Sciences, Poznan, Poland) is studying neuronal vulnerability to degeneration in the spinocerebellar ataxia type 7 (SCA7), one of the CAG repeat expansion diseases. Purkinje cells (PCs) represent the main cell type that undergoes degeneration in SCA7. They constitute approximately 2% of cells in the cerebellum and are one of the biggest and most highly structured neurons in the adult brain, thus it is impossible to isolate them without losing the integrity of neuronal processes. In the presented study, the author described the challenges and eventually the method on how to specifically enrich single nuclei of PCs from the mouse cerebellum. The nuclei have been subjected to snRNA-seq. Based on the established PC isolation method, further studies are being conducted to unravel PC-specific molecular mechanisms leading to neuronal death (Switonski et al., 2021).

In the two following short talks, insights into RNA biology in the context of the other repeat expansion diseases have been presented. First, *Katarzyna Tutak* (Institute of Molecular Biology and Biotechnology, Adam Mickiewicz University, Poznan, Poland) presented details of the mechanism of repeat-associated non-AUG (RAN) translation occurring at repeated expanded tracts in fragile X-associated tremor/ataxia syndrome (FXTAS) (Baud et al., 2022). RAN translation results in the production of toxic glycine-rich protein (polyG) derived from expanded CGG repeats (Guo et al., 2022). Attempts to identify the modifiers of this process have been discussed, as the new knowledge may open up novel possibilities for designing of therapeutic strategy for FXTAS. In another presentation, *Pawel Joachimiak* (Institute of Bioorganic Chemistry, Polish Academy of Sciences, Poznan, Poland) referred to the allele-specific analysis of transcript levels for selected

polyglutamine (polyQ) diseases. Patients suffering from polyQ diseases usually possess both normal and mutant alleles of the affected gene (Bunting et al., 2022). Investigating mRNAs from genes implicated either in HD or spinocerebellar ataxia type 3 (SCA3) provides information about disproportions in allelic expression, as well as changes in expression levels during neuronal differentiation. This is a starting point for detailed analyses of mutant mRNA-specific processes (Ciesiolka et al., 2021; Joachimiak et al., 2022), which are important for a precise description of molecular mechanisms underlying polyQ diseases. In the last short talk in this session, *Sambhavi Puri* (Boston University School of Medicine, Boston, USA) shared the results on circRNAs deregulation in AD. Altogether, 48 circRNAs have been identified to be associated with AD conditions based on RNA-seq data generated from the hippocampus and the cortex of patients' brains. Moreover, circRNA expression was shown to differ by dementia subtype. The importance of impaired circRNA expression patterns and their association with pathogenesis are still emerging topics in the AD field.

RNA in brain pathology: Neuro-oncology

Brain tumors are complex diseases resulting from the disruption of key cellular pathways, including those regulating cell survival and division. Genetic mutations, perturbed RNA profiles, and epigenetic alterations contribute to tumorigenesis. It is already known that all these changes are heterogeneous on a cell type basis within an individual tumor and between patients, which is increasingly appreciated as a determinant of treatment failure and disease recurrence in the case of brain tumors. During this conference session, we discussed the intratumor heterogeneity, new mechanisms of regulatory interactions between ncRNAs, and the possibilities for the identification of new RNA and epigenetics-oriented therapeutics and diagnostic approaches.

Itay Tirosh (Weizmann Institute of Science, Rehovot, Israel) presented a single-cell transcriptomic analysis of glioblastoma samples that recapitulated the high intratumoral heterogeneity of the most aggressive brain tumor. The presented scRNA-seq data showed that glioblastoma cells exist in four main cellular states. The authors found that these states might be affected by the tumor microenvironment and exhibit plasticity, i.e., multiple possible transitions between states can be observed per transcriptome level. The relative frequency of cells in each state also varies between glioblastoma samples, and it is influenced by copy number amplifications of the *CDK4*, *EGFR*, and *PDGFRA* loci and by mutations in the *NF1* locus (Neftel et al., 2019). Further analyses of pan-cancer data regarding intratumoral heterogeneity of the different cancer types revealed that transcriptomic profiles appear to be inherently variable when it comes to gene expression related to oncogenic signaling, proliferation, complement/immune response, and hypoxia (Gavish et al., 2021).

The presence of glioblastoma stem-like cells (GSCs) within the tumor mass, hypoxic microenvironment, and poor infiltration of immune cells to the core of the tumor is perceived to be the other reasons why anti-tumor therapies fail to be efficient. *Agnieszka Bronisz* (Mossakowski Medical Research Institute, Polish Academy of Sciences, Warsaw, Poland) presented an interesting therapeutic approach designed to target GSCs with the oncolytic herpes virus (oHSV)-based immunotherapy. It was illustrated in the talk that oHSV infection alone may activate the host antitumor immune system by triggering "immunosecretion", i.e., the release of antigens and cytokines that stimulate the immune response. The presented data showed that upon infection with oHSV and the transcriptome- and secretome-associated proteins are regulated in GSC. The observed changes have been linked to T-cell-mediated cytotoxicity and B-cell-dependent immune response memory. On the other hand, detailed downstream analyses identified the presence of stress-resistant and oHSV-resistant GSCs located in the hypoxic niche. Transcriptome-wide data revealed that the tumor microenvironment shapes two distinguishing characteristics of GSCs: increased cell-to-cell communication with immune cells and metabolic shift toward hypoxic adaptation, both with signatures predictive of glioblastoma patent survival. One of the antisense lncRNAs has been identified as a sensor of response and adaptation of GSCs to hypoxia. Further analyses pointed out that it might be a promising therapeutic target for glioblastoma therapy, especially in combination with oncolytic virus immunotherapy.

The relevance of ncRNAs for tumorigenesis, tumor progression, and relapse was commented on in *Anna's Krichevsky* (Brigham and Women's Hospital and Harvard Medical School, Boston, USA) talk (Brigham and Women's Hospital and Harvard Medical School, HMS Initiative in RNA Medicine, Boston, USA). In particular, the role of the network is composed of a few distinct ncRNAs including a miRNA, enhancer-associated RNA, promoter-associated RNA, and snRNA. The central part of that network is miR-10b, a miRNA that remains silent in the brain cortex and becomes upregulated in gliomas where it is known to serve a tumor-promoting role. The two mentioned lncRNAs are involved in the chromatin folding and concordant regulation of miR-10b and other co-transcribed genes. The network remains inactive in homeostatic astrocytes and becomes activated during neoplastic transformation. In addition, Krichevsky's group evidenced that direct binding between miR-10b and U6 has a strong impact on downstream U6 interaction with splicing factors SART3 and PRPF (El Fatimy et al., 2022). These results shed new light on the nuclear function of one of the major cancer-associated miRNAs.

Zaneta Zarebska (Institute of Bioorganic Chemistry, Polish Academy of Sciences, Poznan, Poland) presented results on circRNAs and their role in gliomagenesis and GBM progression. RNA-seq results obtained from GBM samples revealed the differential expression patterns within the tumor samples compared with the normal brain. Specific circRNAs have been found to correlate with the GBM molecular subtypes, which is another attempt for providing better stratification that may underlie the future personalized treatment of patients with GBM.

Katarzyna Leszczynska (Nencki Institute of Experimental Biology, Warsaw, Poland) shifted the attention to the pediatric high-grade gliomas (pHGG) and one of the recognized mutations in histone H3 that is specific for these tumors: H3F3A variant. Chromatin-modifying agents, including histone deacetylase (HDAC) inhibitors, have been identified as promising candidate therapeutics against pHGG. The treatments of HDAC inhibitors provided also new directions in targeting H3K27M-expressing cells. However, the precise correspondence between the efficiency and chromatin response of that treatment is still not completely

understood. The presented data focused on the chromatin alterations induced by HDAC inhibitors and the role of histone variants in response to these therapies. With the multiple cellular models expressing the H3K27M histone variant, several new drugs with sub-micromolar efficacy in killing H3K27M-expressing cells were identified. The results pointed out that direct analysis of the chromatin landscape, and particularly the expression of histone variants in pHGG, and provide new insights into chromatin response to specific epigenetic treatments.

Nucleic acid therapies in the brain

Many nucleic acid-based therapeutics, mainly antisense oligonucleotides (ASOs), have recently entered the clinical trial phase. This progress is particularly evident in the field of neurodegenerative diseases, such as HD, where the strategies for lowering the level of mutant protein with ASO or RNAi appear to be very promising. Unfortunately, despite many years of research and the positive results of preclinical studies, some clinical trials had to be terminated prematurely due to ASO ineffectiveness or unexpected side effects. The main problem is still the effective and minimally invasive delivery of the therapeutic to the brain and its specificity. One line of research is the development of new gene therapy constructs and viral vectors for the targeted delivery of therapeutic molecules such as RNAi triggers or CRISPR-Cas system components. Our speakers raised all these important issues in their speeches.

Leontien van der Bent (uniQure biopharma B.V., Amsterdam, the Netherlands) demonstrated recent advances in the development of miRNA-based gene therapies for the treatment of various CNS disorders, including HD, temporal lobe epilepsy, amyotrophic lateral sclerosis, synucleinopathies, and AD. MiQure technology relies on vector-based RNAi triggers, also known as artificial miRNAs (Kotowska-Zimmer et al., 2021), to specifically knockdown target RNAs. The advantage of this approach, as compared with ASO-based technology, is the possibility of obtaining a long-term therapeutic effect after a single administration of the viral vector. It is worth mentioning that uniQure is currently conducting Phase I–II clinical trials of the first AAV gene therapy for HD in which rAAV5-miHTT is delivered directly to the brain by MRI-guided stereotactic infusion (https://clinicaltrials.gov/ct2/show/NCT04120493). This stage of research was preceded by numerous preclinical studies in rodents, mini pigs, and non-human primate models, which demonstrated the effectiveness and safety of the approach (Spronck et al., 2021).

Undoubtedly, the last decade was the time of genome editing technology, which gave great hope in the context of gene therapy. Still, the biggest problem is the safety of the technology. *Nicole Deglon* (Neuroscience Research Center and Department of Clinical Neuroscience, Hospital and University of Lausanne, Switzerland), an expert in the field of viral gene transfer, presented her research on the development of the second-generation AAV-KamiCas9 self-activating system for the efficient and safe editing of CNS disease genes. Transient expression of the Cas9 protein decreases the risk of off-target effects, while optimized AAV vectors ensure efficient transduction of specific brain circuits affected in neurodegenerative disorders (Merienne et al., 2017).

Another class of therapeutics showing a wide spectrum of applications is ASOs. The therapeutic potential of short antisense oligonucleotide steric blockers and small compounds targeting expanded CGG repeats in FMR1 5'UTR was demonstrated by *Krzysztof Sobczak* (Institute of Molecular Biology and Biotechnology, Adam Mickiewicz University, Poznan, Poland). CGG repeat expansion reaching 55–200 triplets leads to the development of FXTAS syndrome. The toxicity of the RNA containing expanded CGG repeats results in the sequestration of nuclear proteins involved in RNA metabolism, the initiation of non-canonical translation of the polyglycine-containing protein which forms nuclear insoluble inclusion, and the formation of the R-loop structure. ASO LNA designed by the Sobczak group is specific to bind and disrupt the RNA structure formed by CGG repeats during transcription, thereby abolishing all these toxic effects. These ASOs have been shown to improve motor behavior and rescue gene expression abnormalities associated with FXTAS in a mouse model of the disease (Derbis et al., 2021). Interestingly, the authors observed non-specific upregulation of other CGG repeat transcripts; however, protein levels remained unchanged.

A careful evaluation of the effects induced by ASO was the topic presented by *Savani A. Anbalagan* (Institute of Molecular Biology and Biotechnology, Adam Mickiewicz University, Poznan, Poland) (Adam Mickiewicz University, PL). He showed that ASO targeting the splicing site of a protein-coding gene embedded in ncRNA may influence the expression and function of the ncRNA. In this study, ASO-inducing intron retention events and increased gene expression resulted in defects in axonal morphogenesis in zebrafish larvae. Without careful evaluation of this phenomenon and the application of appropriate controls, it could have been misinterpreted as an effect of the protein-coding gene.

Lorea Blazquez (Biodonostia Health Research Institute, San Sebastian, Spain) studies aberrant regulation of RNA processing in neurological disorders and her talk focused on frontotemporal dementia. A non-coding mutation in the *GRN* gene leads to an abnormal splicing pattern that causes *GRN* mRNA degradation and progranulin haploinsufficiency. She showed that the CRISPR-dCas13 system can not only be used to identify a target sequence in a pre-mRNA for RNA-based therapeutic strategies but also can be used as a therapeutic approach to restore the GRN open reading frame. RNA-targeting CRISPR-dCas13 has some advantages over ASO or the traditional CRISPR-Cas9 system. It can be expressed from viral vectors without the need for repeated administration and appears to be at least theoretically safer than DNA targeting Cas9. However, more research is needed to confirm its therapeutic potential.

Conclusion

The increasing synergy between RNA biology and neuroscience brings the research in the interface of both disciplines to a new level that enables us to look into physiology with a molecular resolution and in a high-throughput manner. The first edition of the NeuroRNA conference illustrated how rapidly developing new technologies focused on RNA can enrich our understanding

of the basic molecular processes in neural cells and contribute to the formulation of new research hypotheses that aim to bring us closer to unraveling the complexity of the human brain and to find cures for complex neurological conditions. In his biography, Santiago Ramón y Cajal penned "It is commonplace fact that scientific discoveries are a function of the methods used." That notion definitely holds true when contemplating NeuroRNA 2022.

A few summary points on the presented and discussed insights that are worth highlighting as follows:

1. The repertoire of neural cell types and subtypes in the adult human brain, both neurons and glia, is much more heterogenous when considering transcriptome-based classification, i.e., >3,000 cell types discovered in the adult human brain as based on RNA single-nuclei sequencing.
2. Plasticity of certain neural cells, i.e., the possibility to acquire new states and transit between states. It is more often evidenced with scRNA-seq and trajectory inference methods (e.g., for oligodendrocytes, microglia, glioblastoma tumor cells, and glioblastoma stem cells).
3. Alternative transcript isoforms and 3'UTR usage (including APA) are commonplace in neural cells, cell type-specific, and likely context-dependent (i.e., isoform switch may occur depending on the condition). This phenomenon will be surely investigated further delivering new knowledge on how RNA isoforms influence the diversification of proteome on a cell type basis.
4. Local translation is not restricted to neurons. Other polarized and highly structured cell types feature regulated the transport of a specific subset of transcripts to perform local synthesis of specific proteins in cell peripheries, that is, evidenced by microglia and the production of phagocytosis-related factors in microglial processes, and astrocytes and local synthesis of proteins with roles in regulating synapses in astrocyte peripheral processes.
5. Subcellular localization of regulatory RNAs is one of the determinants of their versatility, e.g., miRNAs may function in a non-canonical way in the nucleus, and re-localization of regulatory RNAs might be associated with the pathology (epilepsy and tumorigenesis).
6. The landscape of non-coding RNAs which is functional in the brain is quickly progressing with many newly identified molecular roles that influence the physiology of the CNS on a cell type basis and oftentimes in a sex-based manner. Of note, a poster presentation by *Vittorio Padovano* (Sapienza University, Rome, Italy) on lncRNA in motor neurons supported by lncRNA knockout in the mouse model was awarded the best poster award at the conference.

Many alterations in the transcriptome, specific mutated transcripts, disease-specific transcript isoforms, mislocalized regulatory RNAs, etc., are carefully examined with the ultimate aim to find causative and treatable pathological targets in the CNS. A new generation of therapeutics that are more precise and specific in reaching the targets is on the horizon, and we hope that in the next incarnation of NeuroRNA, we will learn about the progress in that matter. Last but not the least, we would like to express our gratitude to the conference speakers for the inspiring talks and for sharing fresh, oftentimes unpublished results, the audience for the stimulating discussions, and the sponsors for their support.

Author contributions

MP conceptualized the manuscript and edited the final version of the manuscript. MP, KR, AF, and MO wrote and edited the first draft of the manuscript. All authors approved the submitted version.

Funding

The NeuroRNA Conference was supported by the Polish Ministry of Education and Science, the Excellent Science — Support for Scientific Conferences program, grant no. DNK/SP/514092/2021, sponsors and Institute of Bioorganic Chemistry PAS (https://neurorna2022.com/organisers/). The authors would also like to acknowledge their funding sources: MP — the National Agency for Academic Research, Polish Returns 2019, grant no. PPN/PPO/2019/1/00035, the National Science Centre, Sonata Bis 8, grant no. 2018/30/E/NZ3/00624, and Opus 19, grant no. 2020/37/B/NZ3/03633, AF - the National Science Centre, Opus, grant no. 2021/41/B/NZ3/03803, and KR — the National Science Centre, grant no. 2017/25/B/NZ3/02173.

Acknowledgments

The authors would like to thank the members of the conference office, i.e. Magdalena Wozna-Wysocka, Edyta Koscianska, Ewelina Kaluzna, and Marianna Pewinska for their help in organizing the event, as well as Dorota Moniuszko for the graphic design of NeuroRNA Conference logo. The conference was held under the honorary patronage of the President of the Polish Academy of Sciences, the Polish Biochemical Society, and BioTechnologia Journal. The figure presented in this study was created with BioRender.com.

Conflict of interest

The authors declare that the research was conducted in the absence of any commercial or financial relationships that could be construed as a potential conflict of interest.

Publisher's note

References

Androvic, P., Schifferer, M., Anderson, K. P., Cantuti-Castelvetri, L., Ji, H., Liu, L., et al. (2022). Spatial transcriptomics-correlated electron microscopy. *bioRxiv*. doi: 10.1101/2022.05.18.492475

Bartosovic, M., and Castelo-Branco, G. (2022). Multimodal chromatin profiling using nanobody-based single-cell CUT and tag. *bioRxiv*. doi: 10.1101/2022.03.08.483459

Bartosovic, M., Kabbe, M., and Castelo-Branco, G. (2021). Single-cell cutandtag profiles histone modifications and transcription factors in complex tissues. *Nat. Biotechnol.* 39, 825–835. doi: 10.1038/s41587-021-00869-9

Baud, A., Derbis, M., Tutak, K., and Sobczak, K. (2022). Partners in crime: proteins implicated in RNA repeat expansion diseases. *WIREs RNA* 13, e1709. doi: 10.1002/wrna.1709

Bethlehem, R. I., Seidlitz, J., White, S. R., Vogel, J. W., Anderson, K. M., Adamson, C., et al. (2022). Brain charts for the human lifespan. *Nature* 604, 525–533. doi: 10.1038/s41586-022-04554-y

Braun, E., Danan-Gotthold, M., Borm, L. E., Vinsland, E., Lee, K. W., Lönnerberg, P., et al. (2022). Comprehensive cell atlas of the first-trimester developing human brain. *bioRxiv*. doi: 10.1101/2022.10.24.513487

Bunting, E. L., Hamilton, J., and Tabrizi, S. J. (2022). Polyglutamine diseases. *Curr. Opinion Neurobiol.* 72, 39–47. doi: 10.1016/j.conb.2021.07.001

Chen, K. H., Boettiger, A. N., Moffitt, J. R., Wang, S., and Zhuang, X. (2015). Spatially resolved, highly multiplexed RNA profiling in single cells. *Science* 348, aaa6090. doi: 10.1126/science.aaa6090

Ciesiolka, A., Stroynowska-Czerwinska, A., Joachimiak, P., Ciolak, A., Kozlowska, E., Michalak, M., et al. (2021). Artificial MiRNAs targeting CAG repeat expansion in ORFs cause rapid deadenylation and translation inhibition of mutant transcripts. *Cellular Mol. Life Sci.* 78, 1577–1596. doi: 10.1007/s00018-020-03596-7

Deng, Y., Bartosovic, M., Kukanja, P., Zhang, D., Liu, Y., Su, G., et al. (2022). Spatial-CUT and tag: spatially resolved chromatin modification profiling at the cellular level. *Science* 375, 681–686. doi: 10.1126/science.abg7216

Derbis, M., Kul, E., Niewiadomska, D., Sekrecki, M., Piasecka, A., Taylor, K., et al. (2021). Short antisense oligonucleotides alleviate the pleiotropic toxicity of RNA harboring expanded CGG repeats. *Nat. Commun.* 12, 1265. doi: 10.1038/s41467-021-21021-w

Drew, L. (2019). Why rare genetic diseases are a logical focus for RNA therapies. *Nature* 574. S16–18. doi: 10.1038/d41586-019-03075-5

Duarte, F., and Déglon, N. (2020). Genome editing for CNS disorders. *Fron. Neurosci.* 14, 579062. doi: 10.3389/fnins.2020.579062

El Fatimy, F. R., Zhang, Y., Deforzh, E., Ramadas, M., Saravanan, H., Wei, Z., et al. (2022). A nuclear function for an oncogenic MicroRNA as a modulator of SnRNA and splicing. *Mol. Cancer* 21, 17. doi: 10.1186/s12943-022-01494-z

Fyfe, I. (2021). RNA biomarkers of Parkinson disease. *Nat. Rev. Neurol.* 17, 132–132. doi: 10.1038/s41582-021-00470-3

Gavish, A., Tyler, M., Simkin, D., Kovarsky, D., Castro, L. N. G., Halder, D., et al. (2021). The transcriptional hallmarks of intra-tumor heterogeneity across a thousand tumors. *bioRxiv*. doi: 10.1101/2021.12.19.473368

Gomes-Duarte, A., Venø, M. T., Wit, M. D., Senthilkumar, K., Broekhoven, M. H., Herik, J., et al. (2022). Expression of Circ_Satb1 Is decreased in mesial temporal lobe epilepsy and regulates dendritic spine morphology. *Front. Mol. Neuroscience* 15, 832133. doi: 10.3389/fnmol.2022.832133

Guo, S., Nguyen, L., and Ranum, L. P. W. (2022). RAN proteins in neurodegenerative disease: repeating themes and unifying therapeutic strategies. *Curr. Opinion Neurobiol.* 72, 160–70. doi: 10.1016/j.conb.2021.11.001

Gupta, I., Collier, P. G., Haase, B., Mahfouz, A., Joglekar, A., Floyd, T., et al. (2018). Single-cell isoform RNA sequencing characterizes isoforms in thousands of cerebellar cells. *Nat. Biotechnol.* 36, 1197–1202. doi: 10.1038/nbt.4259

Hardwick, S. A., Hu, W., Joglekar, A., Fan, L., Collier, P. G., Foord, C., et al. (2022). Single-nuclei isoform RNA sequencing unlocks barcoded exon connectivity in frozen brain tissue. *Nat. Biotechnol.* 40, 1082–1092. doi: 10.1038/s41587-022-01231-3

Holt, C. E., Martin, K. C., and Schuman, E. M. (2019). Local translation in neurons: visualization and function. *Nat. Struct. Mol. Biol.* 26, 557–566. doi: 10.1038/s41594-019-0263-5

Issler, O., Zee, Y. Y., Ramakrishnan, A., Wang, J., Tan, C., Loh, H. E., et al. (2020). Sex-specific role for the long non-coding RNA LINC00473 in depression. *Neuron* 106, 912–926. doi: 10.1016/j.neuron.2020.03.023

Issler, O., Zee, Y. Y., Ramakrishnan, A., Xia, S., Zinsmaier, A. K., Tan, C., et al. (2021). The long noncoding RNA FEDORA is a cell-type- and sex-specific regulator of depression. *bioRxiv*. doi: 10.1101/2021.11.30.470628

Ivanov, A., Mattei, D., Radscheit, K., Compagnion, A-. C., Pett, J. P., and Herzel, H., et al. (2022). Analyses of CircRNA expression throughout the light-dark cycle reveal a strong regulation of cdr1as, associated with light entrainment in the SCN. *Int. J. Mol. Sci.* 23, 12347. doi: 10.3390/ijms232012347

Joachimiak, P., Ciesiołka, A., Figura, G., and Fiszer, A. (2022). Implications of Poly(A) tail processing in repeat expansion diseases. *Cells* 11, 677. doi: 10.3390/cells11040677

Joglekar, A., Prjibelski, A., Mahfouz, A., Collier, P., Lin, S., Schlusche, A. K., et al. (2021). A spatially resolved brain region- and cell type-specific isoform atlas of the postnatal mouse brain. *Nat. Commun.* 12, 463. doi: 10.1038/s41467-020-20343-5

Kamath, T., Abdulraouf, A., Burris, S. J., Langlieb, J., Gazestani, V., Nadaf, N. M., et al. (2022). Single-cell genomic profiling of human dopamine neurons identifies a population that selectively degenerates in parkinson's disease. *Nat. Neurosci.* 25, 588–595. doi: 10.1038/s41593-022-01061-1

Kaya, T., Mattugini, N., Liu, L., Ji, H., Besson-Girard, S., Kaiji, S., et al. (2022). T cells induce interferon-responsive oligodendrocytes during white matter aging. *bioRxiv*. doi: 10.1101/2022.03.26.485917

Koester, S. K., and Dougherty, J. D. (2022). A proposed role for interactions between argonautes, MiRISC, and RNA binding proteins in the regulation of local translation in neurons and glia. *J. Neurosci.* 42, 3291–3301. doi: 10.1523/JNEUROSCI.2391-21.2022

Kotowska-Zimmer, A., Pewinska, M., and Olejniczak, M. (2021). Artificial miRNAs as therapeutic tools: challenges and opportunities. *Wiley Interdisciplinary Rev.* 12, e1640. doi: 10.1002/wrna.1640

La Manno, M. G., Siletti, K., Furlan, A., Gyllborg, D., Vinsland, E., Albiach, A. M., et al. (2021). Molecular Architecture of the developing mouse brain. *Nature* 596, 92–96. doi: 10.1038/s41586-021-03775-x

Legnini, I., Emmenegger, L., Zappulo, A., Wurmus, R., Martinez, A. O., Jara, C. C., et al. (2022). Spatio-temporal, optogenetic control of gene expression in organoids. *bioRxiv*. doi: 10.1101/2021.09.26.461850

Leung, A. K. L. (2015). The whereabouts of MicroRNA actions: cytoplasm and beyond. *Trends Cell Biol.* 25, 601–610. doi: 10.1016/j.tcb.2015.07.005

Mayer, C., Hafemeister, C., Bandler, R. C., Machold, R., Brito, R. B., Jaglin, X., et al. (2018). Developmental diversification of cortical inhibitory interneurons. *Nature* 555, 457–462. doi: 10.1038/nature25999

Merienne, N., Vachey, G., Longprez, L., Meunier, C., Zimmer, V., Perriard, G., et al. (2017). The self-inactivating KamiCas9 system for the editing of CNS disease genes. *Cell Rep.* 20, 2980–2991. doi: 10.1016/j.celrep.2017.08.075

Morelli, K. H., Wu, Q., Gosztyla, M. L., Liu, H., Yao, M., Zhang, C., et al. (2022). An RNA-targeting CRISPR–Cas13d system alleviates disease-related phenotypes in huntington's disease models. *Nat. Neurosci.* 24, 1–12. doi: 10.1101/2022.01.23.477417

Munn, D. H., and Bronte, V. (2016). Immune suppressive mechanisms in the tumor microenvironment. *Curr Opinion Immunol.* 39, 1–6. doi: 10.1016/j.coi.2015.10.009

Muñoz-Manchado, A. B., Gonzales, C. B., Zeisel, A., Munguba, H., Bekkouche, B., Skene, N. G., et al. (2018). Diversity of interneurons in the dorsal striatum revealed by single-cell RNA sequencing and patchSeq. *Cell Rep.* 24, 2179–2190.e7. doi: 10.1016/j.celrep.2018.07.053

Neftel, C., Laffy, J., Filbin, M. G., Hara, T., Shore, M. E., Rahme, G. J., et al. (2019). An integrative model of cellular states, plasticity, and genetics for glioblastoma. *Cell* 178, 835–849.e21. doi: 10.1016/j.cell.2019.06.024

Nussbacher, J. K., Tabet, R., Yeo, G. W., and Lagier-Tourenne, C. (2019). Disruption of RNA metabolism in neurological diseases and emerging therapeutic interventions. *Neuron* 102, 294–320. doi: 10.1016/j.neuron.2019.03.014

Perez, J. D., Dieck, S. T., Alvarez-Castelao, B., Tushev, G., Chan, I. C. W., and Schuman, E. M. (2021). Subcellular sequencing of single neurons reveals the dendritic transcriptome of GABAergic interneurons. *ELife*. 10, e63092. doi: 10.7554/eLife.63092

Perry, R. B. T., Hezroni, H., Goldrich, M. J., and Ulitsky, I. (2018). Regulation of neuroregeneration by long noncoding RNAs. *Mol. Cell* 72, 553–567. doi: 10.1016/j.molcel.2018.09.021

Perry, R. B. T., Tsoory, M., Tolmasov, M., and Ulitsky, I. (2022). Silc1 long noncoding RNA is an immediate-early gene promoting efficient memory formation. *bioRxiv*. doi: 10.1101/2022.11.11.516100

Piwecka, M., GlaŽar, P., Hernandez-Miranda, L. R., Memczak, S., Wolf, S. A., Rybak-Wolf, A., et al. (2017). Loss of a mammalian circular RNA locus causes mirna deregulation and affects brain function. *Science* 357, eaam8526. doi: 10.1126/science.aam8526

Poewe, W., Seppi, K., Tanner, C. M., Halliday, G. M., Brundin, P., Volkmann, J., et al. (2017). Parkinson disease. *Nat. Rev. Disease Primers* 3, 1–21. doi: 10.1038/nrdp.2017.13

Polioudakis, D., Torre-Ubieta, L., Langerman, J., Elkins, A. G., Shi, X., Stein, J. L., et al. (2019). A single-cell transcriptomic atlas of human neocortical development during mid-gestation. *Neuron* 103, 785–801. doi: 10.1016/j.neuron.2019.06.011

Romanov, R. A., Zeisel, A., Bakker, J., Girach, F., Hellysaz, A., Tomer, R., et al. (2017). Molecular interrogation of hypothalamic organization reveals

distinct dopamine neuronal subtypes. *Nat. Neurosci.* 20, 176–188. doi: 10.1038/nn.4462

Rybak-Wolf, A., Wyler, E., Legnini, I., Loewa, A., GlaŽar, P., Kim, S. J., et al. (2021). Neurodegeneration in human brain organoids infected with herpes simplex virus type 1. *bioRxiv*. doi: 10.1101/2021.03.05.434122

Safaiyan, S., Besson-Girard, S., Kaya, T., Cantuti-Castelvetri, L., Liu, L., Ji, H., et al. (2021). White matter aging drives microglial diversity. *Neuron* 109, 1100–1117. doi: 10.1016/j.neuron.2021.01.027

Sakers, K., Lake, A. M., Khazanchi, R., Ouwenga, R., Vasek, M. J., Dani, A., et al. (2017). Astrocytes locally translate transcripts in their peripheral processes. *Proc. Nat. Acad. Sci.* 114, E3830–3838. doi: 10.1073/pnas.1617782114

Sapkota, D., Lake, A. M., Yang, W., Yang, C., Wesseling, H., Guise, A., et al. (2019). Cell-type-specific profiling of alternative translation identifies regulated protein isoform variation in the mouse brain. *Cell Rep.* 26, 594–607. doi: 10.1016/j.celrep.2018.12.077

Siletti, K., Hodge, R., Albiach, A. M., Hu, L., Lee, K. W., Lönnerberg, P., et al. (2022). Transcriptomic diversity of cell types across the adult human brain. *bioRxiv*. doi: 10.1101/2022.10.12.511898

Spronck, E. A., Vallès, A., Lampen, M. H., Montenegro-Miranda, P. S., Keskin, S., Heijink, L., et al. (2021). Intrastriatal administration of AAV5-MiHTT in non-human primates and rats is well tolerated and results in MiHTT transgene expression in key areas of huntington disease pathology. *Brain Sci.* 11, 129. doi: 10.3390/brainsci11020129

Stoeckius, M., Hafemeister, C., Stephenson, W., Houck-Loomis, B., Chattopadhyay, P. K., Swerdlow, H., et al. (2017). Simultaneous epitope and transcriptome measurement in single cells. *Nat. Methods* 14, 865–868. doi: 10.1038/nmeth.4380

Switonski, P. M., Delaney, J. R., Bartelt, L. C., Niu, C., Ramos-Zapatero, M., Spann, N. J., et al. (2021). Altered H3 histone acetylation impairs high-fidelity DNA repair to promote cerebellar degeneration in spinocerebellar ataxia type 7. *Cell Rep.* 37, 110062. doi: 10.1016/j.celrep.2021.110062

Tan, C. L., Plotkin, J. L., Venø, M. T., Schimmelmann, M. V., Feinberg, P., Mann, S., et al. (2013). MicroRNA-128 governs neuronal excitability and motor behavior in mice. *Science*. 342, 1254–1258. doi: 10.1126/science.1244193

Vasek, M. J., Deajon-Jackson, J. D., Liu, Y., Crosby, H. W., Yi, J., Dougherty, J. D., et al. (2021). Microglia perform local protein synthesis at perisynaptic and phagocytic structures. *bioRxiv*. doi: 10.1101/2021.01.13.426577

Walgrave, H., Balusu, S., Snoeck, S., Eynden, E. V., Craessaerts, K., Thrupp, N., et al. (2021a). Restoring MiR-132 expression rescues adult hippocampal neurogenesis and memory deficits in Alzheimer's disease. *Cell Stem Cell* 28, 1805–1821.e8. doi: 10.1016/j.stem.2021.05.001

Walgrave, H., Zhou, L., Strooper, B. D., and Salta, E. (2021b). The promise of MicroRNA-based therapies in Alzheimer's Disease: challenges and perspectives. *Mol. Neurodeg.* 16, 76. doi: 10.1186/s13024-021-00496-7

Wong, H. W., Lin, J. Q., Ströhl, F., Roque, C. G., Cioni, J-. M., Cagnetta, R., et al. (2017). RNA docking and local translation regulate site-specific axon remodeling in vivo. *Neuron* 95, 852–868. doi: 10.1016/j.neuron.2017.07.016

Zhu, S., Choudhury, N. R., Rooney, S., Pham, N. T., Koszela, J., Kelly, D., et al. (2021). RNA pull-down confocal nanoscanning (RP-CONA) detects quercetin as Pri-MiR-7/HuR interaction inhibitor that decreases α-synuclein levels. *Nucleic Acids Res.* 49, 6456–6473. doi: 10.1093/nar/gkab484

Frontiers in
Molecular Neuroscience

Leading research into the brain's molecular structure, design and function

Part of the most cited neuroscience series, this journal explores and identifies key molecules underlying the structure, design and function of the brain across all levels.

Discover the latest Research Topics

See more →

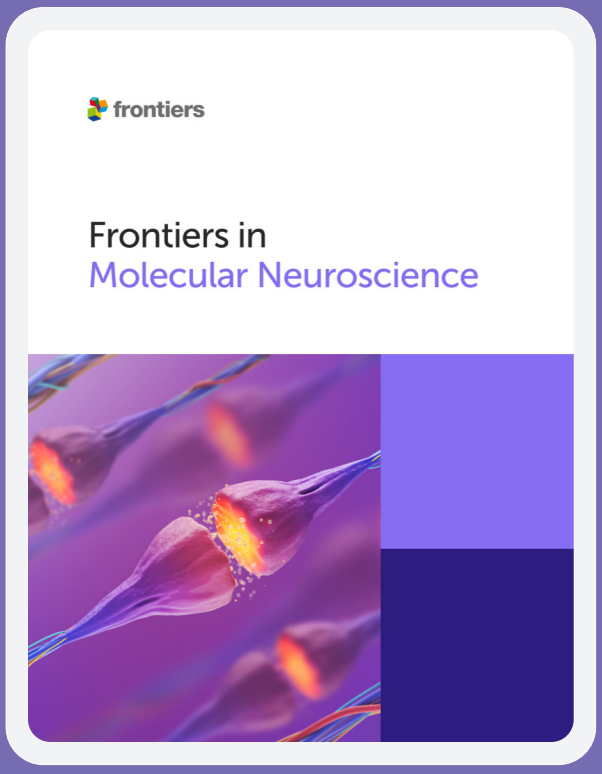

Frontiers

Avenue du Tribunal-Fédéral 34
1005 Lausanne, Switzerland
frontiersin.org

Contact us

+41 (0)21 510 17 00
frontiersin.org/about/contact